Hashemite Kingdom of Jordan

Jordan Journal of Biological Sciences

An International Peer-Reviewed Scientific Journal

Financed by the Scientific Research and Innovation Support Fund

This title is indexed in Scopus

http://jjbs.hu.edu.jo/

المجلة الأردنية للعلوم الحياتية
Jordan Journal of Biological Sciences (JJBS)
http://jjbs.hu.edu.jo

Jordan Journal of Biological Sciences (JJBS) (ISSN: 1995–6673 (Print); 2307-7166 (Online)): An International Peer- Reviewed Open Access Research Journal financed by the Scientific Research and Innovation Support Fund, Ministry of Higher Education and Scientific Research, Jordan and published quarterly by the Deanship of Scientific Research , The Hashemite University, Jordan.

Submission Address
Professor Atoum, Manar F
The Hashemite Universit y
P.O. Box 330127, Zarqa, 13115, Jordan
Phone: +962-5-3903333 ext.4147
E-Mail: jjbs@hu.edu.jo

المجلة الاردنية للعلوم الحياتية
Jordan Journal of Biological Sciences (JJBS)
http://jjbs.hu.edu.jo

International Advisory Board (Arranged alphabetically)

Instructions to Authors

Scopes

Study areas include cell biology, genomics, microbiology, immunology, molecular biology, biochemistry, embryology, immunogenetics, cell and tissue culture, molecular ecology, genetic engineering and biological engineering, bioremediation and biodegradation, bioinformatics, biotechnology regulations, gene therapy, organismal biology, microbial and environmental biotechnology, marine sciences. The JJBS welcomes the submission of manuscript that meets the general criteria of significance and academic excellence. All articles published in JJBS are peer-reviewed. Papers will be published approximately one to two months after acceptance.

Type of Papers

The journal publishes high-quality original scientific papers, short communications, correspondence and case studies. Review articles are usually by invitation only. However, Review articles of current interest and high standard will be considered.

Submission of Manuscript

Manuscript, or the essence of their content, must be previously unpublished and should not be under simultaneous consideration by another journal. The authors should also declare if any similar work has been submitted to or published by another journal. They should also declare that it has not been submitted/ published elsewhere in the same form, in English or in any other language, without the written consent of the Publisher. The authors should also declare that the paper is the original work of the author(s) and not copied (in whole or in part) from any other work. All papers will be automatically checked for duplicate publication and plagiarism. If detected, appropriate action will be taken in accordance with International Ethical Guideline. By virtue of the submitted manuscript, the corresponding author acknowledges that all the co-authors have seen and approved the final version of the manuscript. The corresponding author should provide all co-authors with information regarding the manuscript, and obtain their approval before submitting any revisions. Electronic submission of manuscripts is strongly recommended, provided that the text, tables and figures are included in a single Microsoft Word file. Submit manuscript as e-mail attachment to the Editorial Office at: JJBS@hu.edu.jo. After submission, a manuscript number will be communicated to the corresponding author within 48 hours.

Peer-review Process

It is requested to submit, with the manuscript, the names, addresses and e-mail addresses of at least 4 potential reviewers. It is the sole right of the editor to decide whether or not the suggested reviewers to be used. The reviewers' comments will be sent to authors within 6-8 weeks after submission.
Manuscripts and figures for review will not be returned to authors whether the editorial decision is to accept, revise, or reject. All Case Reports and Short Communication must include at least one table and/ or one figure.

Preparation of Manuscript

The manuscript should be written in English with simple lay out. The text should be prepared in single column format. Bold face, italics, subscripts, superscripts etc. can be used. Pages should be numbered consecutively, beginning with the title page and continuing through the last page of typewritten material.

The text can be divided into numbered sections with brief headings. Starting from introduction with section 1. Subsections should be numbered (for example 2.1 (then 2.1.1, 2.1.2, 2.2, etc.), up to three levels. Manuscripts in general should be organized in the following manner:

Title Page

The title page should contain a brief title, correct first name, middle initial and family name of each author and name and address of the department(s) and institution(s) from where the research was carried out for each author. The title should be without any abbreviations and it should enlighten the contents of the paper. All affiliations should be provided with a lower-case superscript number just after the author's name and in front of the appropriate address.
The name of the corresponding author should be indicated along with telephone and fax numbers (with country and area code) along with full postal address and e-mail address.

Abstract

The abstract should be concise and informative. It should not exceed **350 words** in length for full manuscript and Review article and **150 words** in case of Case Report and/ or Short Communication. It should briefly describe the purpose of the work, techniques and methods used, major findings with important data and conclusions. No references should be cited in this part. Generally non-standard abbreviations should not be used, if necessary they should be clearly defined in the abstract, at first use.

Keywords

Immediately after the abstract, **about 4-8 keywords** should be given. Use of abbreviations should be avoided, only standard abbreviations, well known in the established area may be used, if appropriate. These keywords will be used for indexing.

Abbreviations

Non-standard abbreviations should be listed and full form of each abbreviation should be given in parentheses at first use in the text.

Introduction

Provide a factual background, clearly defined problem, proposed solution, a brief literature survey and the scope and justification of the work done.

Materials and Methods

Give adequate information to allow the experiment to be reproduced. Already published methods should be mentioned with references. Significant modifications of published methods and new methods should be described in detail. Capitalize trade names and include the manufacturer's name and address. Subheading should be used.

Results

Results should be clearly described in a concise manner. Results for different parameters should be described under subheadings or in separate paragraph. Results should be explained, but largely without referring to the literature. Table or figure numbers should be mentioned in parentheses for better understanding.

Discussion

The discussion should not repeat the results, but provide detailed interpretation of data. This should interpret the significance of the findings of the work. Citations should be given in support of the findings. The results and discussion part can also be described as separate, if appropriate. The Results and Discussion sections can include subheadings, and when appropriate, both sections can be combined

Conclusions

This should briefly state the major findings of the study.

Acknowledgment

A brief acknowledgment section may be given after the conclusion section just before the references. The acknowledgment of people who provided assistance in manuscript preparation, funding for research, etc. should be listed in this section.

Tables and Figures

Tables and figures should be presented as per their appearance in the text. It is suggested that the discussion about the tables and figures should appear in the text before the appearance of the respective tables and figures. No tables or figures should be given without discussion or reference inside the text.

Tables should be explanatory enough to be understandable without any text reference. Double spacing should be maintained throughout the table, including table headings and footnotes. Table headings should be placed above the table. Footnotes should be placed below the table with superscript lowercase letters. Each table should be on a separate page, numbered consecutively in Arabic numerals.

Each figure should have a caption. The caption should be concise and typed separately, not on the figure area. Figures should be self-explanatory. Information presented in the figure should not be repeated in the table. All symbols and abbreviations used in the illustrations should be defined clearly. Figure legends should be given below the figures.

References

References should be listed alphabetically at the end of the manuscript. Every reference referred in the text must be also present in the reference list and vice versa. In the text, a reference identified by means of an author's name should be followed by the year of publication in parentheses (e.g.(Brown,2009)). For two authors, both authors' names followed by the year of publication (e.g.(Nelson and Brown, 2007)). When there are more than two authors, only the first author's name followed by "*et al*." and the year of publication (e.g. (Abu-Elteen *et al*., 2010)). When two or more works of an author has been published during the same year, the reference should be identified by the letters "a", "b", "c", etc., placed after the year of publication. This should be followed both in the text and reference list. e.g., Hilly, (2002a, 2002b); Hilly, and Nelson, (2004). Articles in preparation or submitted for publication, unpublished observations, personal communications, etc. should not be included in the reference list but should only be mentioned in the article text (e.g., Shtyawy,A., University of Jordan, personal communication). Journal titles should be abbreviated according to the system adopted in Biological Abstract and Index Medicus, if not included in Biological Abstract or Index Medicus journal title should be given in full. The author is responsible for the sccuracy and completeness of the references and for their correct textual citation. Failure to do so may result in the paper being withdraw from the evaluation process. Example of correct reference form is given as follows:-

Reference to a journal publication:

Bloch BK. 2002. Econazole nitrate in the treatment of *Candida vaginitis*. *S Afr Med J.* , **58**:314-323.

Ogunseitan OA and Ndoye IL. 2006. Protein method for investigating mercuric reductase gene expression in aquatic environments. *Appl Environ Microbiol*., **64**: 695-702.

Hilly MO, Adams MN and Nelson SC. 2009. Potential fly-ash utilization in agriculture. *Progress in Natural Sci.*, **19**: 1173-1186.

Reference to a book:

Brown WY and White SR.1985. **The Elements of Style**, third ed. MacMillan, New York.

Reference to a chapter in an edited book:

Mettam GR and Adams LB. 2010. How to prepare an electronic version of your article. In: Jones BS and Smith RZ (Eds.), **Introduction to the Electronic Age**. Kluwer Academic Publishers, Netherlands, pp. 281–304.

Conferences and Meetings:

Embabi NS. 1990. Environmental aspects of distribution of mangrove in the United Arab Emirates. Proceedings of the First ASWAS Conference. University of the United Arab Emirates. Al-Ain, United Arab Emirates.

Theses and Dissertations:

El-Labadi SN. 2002. Intestinal digenetic trematodes of some marine fishes from the Gulf of Aqaba. MSc dissertation, The Hashemite University, Zarqa, Jordan.

Nomenclature and Units

Internationally accepted rules and the international system of units (SI) should be used. If other units are mentioned, please give their equivalent in SI.

For biological nomenclature, the conventions of the *International Code of Botanical Nomenclature, the International Code of Nomenclature of Bacteria,* and the *International Code of Zoological Nomenclature* should be followed.
Scientific names of all biological creatures (crops, plants, insects, birds, mammals, etc.) should be mentioned in parentheses at first use of their English term.

Chemical nomenclature, as laid down in the *International Union of Pure and Applied Chemistry* and the official recommendations of the *IUPAC-IUB Combined Commission on Biochemical Nomenclature* should be followed. All biocides and other organic compounds must be identified by their Geneva names when first used in the text. Active ingredients of all formulations should be likewise identified.

Math formulae

All equations referred to in the text should be numbered serially at the right-hand side in parentheses. Meaning of all symbols should be given immediately after the equation at first use. Instead of root signs fractional powers should be used. Subscripts and superscripts should be presented clearly. Variables should be presented in italics. Greek letters and non-Roman symbols should be described in the margin at their first use.

To avoid any misunderstanding zero (0) and the letter O, and one (1) and the letter l should be clearly differentiated. For simple fractions use of the solidus (/) instead of a horizontal line is recommended. Levels of statistical significance such as: $^{*}P < 0.05$, $^{**}P < 0.01$ and $^{***}P < 0.001$ do not require any further explanation.

Copyright

Submission of a manuscript clearly indicates that: the study has not been published before or is not under consideration for publication elsewhere (except as an abstract or as part of a published lecture or academic thesis); its publication is permitted by all authors and after accepted for publication it will not be submitted for publication anywhere else, in English or in any other language, without the written approval of the copyright-holder. The journal may consider manuscripts that are translations of articles originally published in another language. In this case, the consent of the journal in which the article was originally published must be obtained and the fact that the article has already been published must be made clear on submission and stated in the abstract. It is compulsory for the authors to ensure that no material submitted as part of a manuscript infringes existing copyrights, or the rights of a third party.

Ethical Consent

All manuscripts reporting the results of experimental investigation involving human subjects should include a statement confirming that each subject or subject's guardian obtains an informed consent, after the approval of the experimental protocol by a local human ethics committee or IRB. When reporting experiments on animals, authors should indicate whether the institutional and national guide for the care and use of laboratory animals was followed.

Plagiarism

The JJBS hold no responsibility for plagiarism. If a published paper is found later to be extensively plagiarized and is found to be a duplicate or redundant publication, a note of retraction will be published, and copies of the correspondence will be sent to the authors' head of institute.

Galley Proofs

The Editorial Office will send proofs of the manuscript to the corresponding author as an e-mail attachment for final proof reading and it will be the responsibility of the corresponding author to return the galley proof materials appropriately corrected within the stipulated time. Authors will be asked to check any typographical or minor clerical errors in the manuscript at this stage. No other major alteration in the manuscript is allowed. After publication authors can freely access the full text of the article as well as can download and print the PDF file.

Publication Charges

There are no page charges for publication in Jordan Journal of Biological Sciences, except for color illustrations,

Reprints

Ten (10) reprints are provided to corresponding author free of charge within two weeks after the printed journal date. For orders of more reprints, a reprint order form and prices will be sent with article proofs, which should be returned directly to the Editor for processing.

Disclaimer

Articles, communication, or editorials published by JJBS represent the sole opinions of the authors. The publisher shoulders no responsibility or liability what so ever for the use or misuse of the information published by JJBS.

Indexing

JJBS is indexed and abstracted by:

DOAJ (Directory of Open Access Journals)	CABI
Google Scholar	EBSCO
Journal Seek	CAS (Chemical Abstract Service)
HINARI	ETH- Citations
Index Copernicus	Open J-Gat
NDL Japanese Periodicals Index	SCImago
SCIRUS	Clarivate Analytics (Zoological Abstract)
OAJSE	Scopus
ISC (Islamic World Science Citation Center)	AGORA (United Nation's FAO database)
Directory of Research Journal Indexing (DRJI)	SHERPA/RoMEO (UK)
Ulrich's	

المجلة الأردنية للعلوم الحياتية
Jordan Journal of Biological Sciences (JJBS)
ISSN 1995- 6673 (Print), 2307- 7166 (Online)
http://jjbs.hu.edu.jo

The Hashemite University

Deanship of Scientific Research

TRANSFER OF COPYRIGHT AGREEMENT

Journal publishers and authors share a common interest in the protection of copyright: authors principally because they want their creative works to be protected from plagiarism and other unlawful uses, publishers because they need to protect their work and investment in the production, marketing and distribution of the published version of the article. In order to do so effectively, publishers request a formal written transfer of copyright from the author(s) for each article published. Publishers and authors are also concerned that the integrity of the official record of publication of an article (once refereed and published) be maintained, and in order to protect that reference value and validation process, we ask that authors recognize that distribution (including through the Internet/WWW or other on-line means) of the authoritative version of the article as published is best administered by the Publisher.

To avoid any delay in the publication of your article, please read the terms of this agreement, sign in the space provided and return the complete form to us at the address below as quickly as possible.

Article entitled:----------

Corresponding author: ----------

To be published in the journal: Jordan Journal of Biological Sciences (JJBS)

I hereby assign to the Hashemite University the copyright in the manuscript identified above and any supplemental tables, illustrations or other information submitted therewith (the "article") in all forms and media (whether now known or hereafter developed), throughout the world, in all languages, for the full term of copyright and all extensions and renewals thereof, effective when and if the article is accepted for publication. This transfer includes the right to adapt the presentation of the article for use in conjunction with computer systems and programs, including reproduction or publication in machine-readable form and incorporation in electronic retrieval systems.
Authors retain or are hereby granted (without the need to obtain further permission) rights to use the article for traditional scholarship communications, for teaching, and for distribution within their institution.

☐ **I am the sole author of the manuscript**

☐ **I am signing on behalf of all co-authors of the manuscript**

☐ **The article is a 'work made for hire' and I am signing as an authorized representative of the employing company/institution**

Please mark one or more of the above boxes (as appropriate) and then sign and date the document in black ink.

Signed:_____ **Name printed:** _____
Title and Company (if employer representative) : _____
Date: _____

Data Protection: By submitting this form you are consenting that the personal information provided herein may be used by the Hashemite University and its affiliated institutions worldwide to contact you concerning the publishing of your article.

Please return the completed and signed original of this form by mail or fax, or a scanned copy of the signed original by e-mail, retaining a copy for your files, to:

Hashemite University
Jordan Journal of Biological Sciences
Zarqa 13115 Jordan
Fax: +962 5 3903338
Email: jjbs@hu.edu.jo

EDITORIAL PREFACE

Jordan Journal of Biological Sciences (JJBS) is a refereed, quarterly international journal financed by the Scientific Research and Innovation Support Fund, Ministry of Higher Education and Scientific Research in cooperation with the Hashemite University, Jordan. JJBS celebrated its 12th commencement this past January, 2020. JJBS was founded in 2008 to create a peer-reviewed journal that publishes high-quality research articles, reviews and short communications on novel and innovative aspects of a wide variety of biological sciences such as cell biology, developmental biology, structural biology, microbiology, entomology, molecular biology, biochemistry, medical biotechnology, biodiversity, ecology, marine biology, plant and animal biology, plant and animal physiology, genomics and bioinformatics.

We have watched the growth and success of JJBS over the years. JJBS has published 11 volumes, 45 issues and 479 articles. JJBS has been indexed by SCOPUS, CABI's Full-Text Repository, EBSCO, Clarivate Analytics- Zoological Record and recently has been included in the UGC India approved journals. JJBS Cite Score has improved from 0.18 in 2015 to 0.7 in 2019 (Last updated on 1 March, 2021) and with Scimago Institution Ranking (SJR) 0.18 (Q3) in 2019.

A group of highly valuable scholars have agreed to serve on the editorial board and this places JJBS in a position of most authoritative on biological sciences. I am honored to have six eminent associate editors from various countries. I am also delighted with our group of international advisory board members coming from 15 countries worldwide for their continuous support of JJBS. With our editorial board's cumulative experience in various fields of biological sciences, this journal brings a substantial representation of biological sciences in different disciplines. Without the service and dedication of our editorial; associate editorial and international advisory board members, JJBS would have never existed.

In the coming year, we hope that JJBS will be indexed in Clarivate Analytics and MEDLINE (the U.S. National Library of Medicine database) and others. As you read throughout this volume of JJBS, I would like to remind you that the success of our journal depends on the number of quality articles submitted for review. Accordingly, I would like to request your participation and colleagues by submitting quality manuscripts for review. One of the great benefits we can provide to our prospective authors, regardless of acceptance of their manuscripts or not, is the feedback of our review process. JJBS provides authors with high quality, helpful reviews to improve their manuscripts.

Finally, JJBS would not have succeeded without the collaboration of authors and referees. Their work is greatly appreciated. Furthermore, my thanks are also extended to The Hashemite University and the Scientific Research and Innovation Support Fund, Ministry of Higher Education and Scientific Research for their continuous financial and administrative support to JJBS.

Professor Atoum, Manar F.
March, 2021

JJBS

Volume 14, Number 1, March 2021
ISSN 1995-6673

Jordan Journal of Biological Sciences

CONTENTS

Original Articles

JJBS

Volume 14, Number 1, March 2021
ISSN 1995-6673
Pages 1- 6

Jordan Journal of Biological Sciences

Development of biodegradable poly (vinyl alcohol) /chitosan cross linked membranes for antibacterial wound dressing applications

Mohamed E. Hassan[1*], Hassan A. Shehata[2], Alaa Fahmy[2], Mohand Badr[2], Tamer M. Tamer[3], Ahmed M. Omer[3*]

[1]Center of Excellence, Encapsulation & Nano biotechnology Group, Chemistry of Natural and Microbial Products Department, National Research Centre, El Behouth Street, Cairo 12622, Egypt,[2]Department of Chemistry, Faculty of Science, Al-Azhar University, Cairo, Egypt,[3]Polymeric Materials Research Department, Advanced Technology & New Materials Research Institute (ATNMRI), City of Scientific Research and Technological Applications (SRTA-City), Alexandria, Egypt.

Received February 6, 2020; Revised April 11, 2020; Accepted May 5, 2020

Abstract

In this study, poly vinyl alcohol/chitosan (PVA/Cs) membranes were developed via surface crosslinking technique for advanced wound dressing applications. Fourier Transform Infrared Spectrophotometer (FT-IR) and Scanning Electron Microscope (SEM) analysis tools were conducted to illustrate the chemical structures and the morphological changes of the developed membranes. Moreover, the mechanical analysis also investigated using tensile testing machine. The obtained results showed that PVA/Cs cross linked membrane recorded maximum force of 46.2 N compared with 26.09 N for Cs, indicating that the crosslinking process improved the developed membrane. Besides, the hydrophilic character of the developed membranes was examined using water uptake studies and decreased from 187% and 142% recorded by native Cs and PVA, respectively to 115% for the cross linked membrane. Two different types of bacteria were used for studying the anti-bacterial activities of the developed cross linked membranes, namely gram-positive bacteria *(Staphylococcus aureus)* and gram-negative bacteria *(Escherichia coli)*. The anti-bacterial activity of the developed cross linked membranes was augmented compared with native PVA and Cs membranes as the maximum inhibition (%) value increased from10 and 12% to 22 and 30% after crosslinking. Besides, the cross linked membranes exhibited better bio-degradability; moreover, the mechanical strength of the cross linked membranes showed good mechanical stability. The findings suggest that the cross linked PVA/Cs membranes could be efficiently applied as anti-bacterial and bio-degradable dressers for accelerating the wound healing process.

Keywords: Poly (vinyl alcohol); Chitosan; Anti-bacterial activity; Wound dressings

1. Introduction

Retrieval of wound is a specific biological process linked with the phenomena of growth and tissue regeneration (Bowler et al., 2001; Sen 2009). Recently, modern wound dressing has been applied to care for wounds instead of the traditional wound dressing, since it offers a moist environment at the wound region and hastens the migration process of epithelial cells to replace the dead cells and reconstitute the injured tissue (Alvarez et al., 1983; Boateng et al., 2008). Various requirements should be present in the modern wound dressing such as the ability for inhibition of the bacterial attack, reducing the inflammation of wound, easy sterilization/application, bio-compatibility, water/oxygen permeability and biodegradability (Guo and Luisa 2010; Jones et al., 2002). Polymers are widely used in biomedical industries including drug delivery systems, tissue engineering and wound dressing applications (Van de Velde and Paul 2002; Mona et al., 2016). Among these polymers, polyvinyl alcohol (PVA) is an amorphous vinyl polymer and is considered one of the oldest synthetic hydrophilic polymers (Hassan and Nikolaos 2000). PVA has been receiving much interest for several applications such as food industry, resins, water treatment and cosmetics (Kamal et al. 2014; Moulay 2015). Owing to its unique advantages such as hydrophilicity, bio-safety to the human cells, film forming ability, chemical resistance, mechanical resistance, good biocompatibility and biodegradability, PVA has been also applied for advanced bio-medical applications including wound dressing, surgical sutures, drug vehicles, contact lenses and artificial organs (Baker et al. 2012; Kamoun et al., 2017; Marin et al., 2014). Numerous physic-chemical modifications such as blending, chemical crosslinking, grafting and composite formation have been adopted for PVA in order to improve its clinical features. PVA has been modified with other

* Corresponding author e-mail: mohassan81@gmail.com.

** Abbreviations: FT-IR: Fourier Transform Infrared Spetrophotometer; SEM: Scanning Electron Microscope; PVA/Cs: poly vinyl alcohol/chitosan; PMN: polymorphonuclear; DD: degree of deacetylation; LB medium: Luria-Bertani medium; DNS: dinitrosalicylic acid.

natural polymers such as alginate, dextran and chitosan biopolymers to widen its bio-medical application range (Fathi et al., 2011; Kanatt et al., 2012; Levi et al., 2011).

Chitosan (Cs) is a nitrogen contained polysaccharide, and could be easily obtained via a simple deacetylation of chitin which is the main constituent of the exoskeleton of crustacean shells such as shrimps, lobsters, and crabs (Zargar et al., 2015; Samia et al., 2020). The structure of chitosan comprises randomly distributed (1-4)-linked 2-amino-2-deoxy-β -d-glucopyranose units (Sahoo et al., 2009; Ismail et al., 2019). Moreover, chitosan has reactive amine and hydroxyl groups along its backbone, soluble in aqueous acidic conditions and possesses a high viscosity which enables it to form intermolecular hydrogen bonds (Rinaudo 2006). Furthermore, chitosan has appealing biological properties including bio-degradability, mucoadhesive character, non-toxicity, excellent bio-compatibility and bio-activity (Moutinho et al., 2019; Pokhrel and Paras 2019). Therefore, chitosan has been employed in a wide range of advanced wound dressing, tissue engineering, drug delivery systems and health-care food supplements (Rami et al., 2014; Sun et al., 2019). The bio-activity of chitosan involves blood anti-coagulants, anti-inflammatory, anti-oxidant and antibacterial activities; hence it is able to form a strong protective film and can inhibit the attack of several types of microorganisms (Elchinger et al., 2015; Tamer et al., 2018). Several studies reported that chitosan has the ability to accelerate the wound healing process through stimulation of the migration of mononuclear cells and polymorphonuclear (PMN), which enhances the re-epithelization and skin tissue regeneration (Tamer et al., 2018). Besides, several modification techniques such as blending (Murakami et al., 2010), combination with bioactive agents (Sudheesh Kumar et al., 2012), Schiff base formation (Tamer et al., 2016) and chemical crosslinking (Kenawy et al., 2019) have been conducted for chitosan in order to promote its antibacterial activity against several types of bacteria, which in turn accelerates the process of wound healing.

Herein, we aimed to develop anti-bacterial and bio-degradable cross linked membranes based on PVA and chitosan bio-polymer for wound dressing applications. FT-IR and SEM analysis tools were conducted to investigate the chemical structure and the changes in the surface morphologies of the developed membranes. Moreover, the mechanical stability and hydrophilicity were also explored. The anti-bacterial activities of the cross linked membrane against two different types of bacteria were also evaluated.

2. Materials and methods

2.1. Materials

Chitosan (DD % = 93 %) was supplied from polymer department, ATNMRI, SRTA City, Alexandria; (Egypt). Poly (vinyl alcohol); Mwt 72000; hydrolyzed) was obtained from Biochemica, Germany. Sodium hydroxide (98 %), acetone (99%), ethanol (99%) and acetic acid (98%) were brought from El-Nasr Company (Alexandria), Glutaraldehyde (25%) was obtained from Sigma-Aldrich

2.2. Experimental

2.2.1. Preparation of chitosan membrane

Chitosan solution was prepared by dissolving chitosan in acetic acid solution 2% (w/v) and distilled water for 24 h at room temperature under a gentle stirring with a final concentration of 2 % (w/v). Thereafter, chitosan solution was casted in a clean petri-dish at room temperature for 48 h to ensure complete solvent evaporation.

2.2.2. Preparation of PVA membrane

PVA solution was obtained by dissolving PVA powder in hot distilled water under a gentle stirring at 80 ^{o}C for 3 h to obtain a homogenous solution with a final concentration 5% (w/v). On a clean petri dish, PVA solution was casted at room temperature for 48 h to ensure complete solvent evaporation. The membrane was separated, rinsed with 50 mL of acetone and allowed to dry for 24 h at room temperature.

2.2.3. Preparation of PVA/Cs membrane

A fixed volume of the previously prepared PVA and Cs solutions were mixed under a constant stirring for 1 h at room temperature to obtain a homogenous blend solution with a final ratio of PVA/Cs (1:1). On a clean petri dish, the PVA/Cs solution was casted at room temperature for 48 h to ensure complete solvent evaporation. The membrane was separated and rinsed with 50 mL of acetone.

2.2.4. Surface crosslinking process

Finally, prepared Cs, PVA, and PVA/Cs membranes were surface cross linked by soaking in 0.01% of glutaraldehyde/acetone solution at room temperature under a gentle stirring overnight. Then, the crosslinked membrane was washed several times with acetone to eliminate any unreacted glutaraldehyde and followed with air-drying overnight at room temperature.

2.2.5. Physicochemical characterization

The chemical structures of the developed cross linked membranes were investigated using Fourier Transform Infrared Spectrophotometer (Shimadzu FT-IR - 8400 S, Japan), while the surface morphological changes were examined by Scanning Electron Microscope (SEM; Model Jsm 6360 LA, Joel, Japan). Furthermore, the mechanical properties were studied using a universal testing machine (AG-1S, Shimadzu, Japan). Besides, water uptake (%) estimation was performed by soaking an accurate amount of dried samples in distilled water (pH 7) for 6 h at room temperature. The swollen samples were gently separated from the swelling medium and carefully bolted between two filter papers to eliminate the excess of adherent surface water and followed by weighing in an electronic balance. The percent of water uptake was calculated according to the following equation:

$$\text{Water uptake (\%)} = [(M_1 - M_0) / M_0] \times 100 \quad (1)$$

Where, M_0 and M_1 are weights of dried and swollen sample, respectively (Mohy Eldin et al. 2015a, Mohy Eldin et al. 2015b)

2.2.6. Anti-bacterial activity assay

Anti-microbial activity of the prepared membranes was tested depending on the previously reported procedure (Hassan et al., 2018). In brief, bacteria (*Staphylococcus*

aureus and *Escherichia coli*) were incubated in LB medium containing 0.5 % yeast extract, 1 % peptone and 1 % NaCl). The inoculation was at 37 °C for 24 h under shaking conditions. The obtained bacterial suspension was diluted with the previous peptone medium. Formerly, 0.1 mL of diluted bacteria suspension was cultured in 10 mL of liquid peptone medium. 10 mg of the tested membrane sample was dissolved in the previous medium and followed with sterilization at 121°C for 30 min. The inoculated medium remained shaking at 37 °C for 24 h. The bacterial growth inhibition (%) was assayed via measuring the absorbance of the culture medium at 620 nm using visible spectroscopy. The inhibition (%) was estimated by the following equation:

Where, A_b and A_a are the absorbance of bacterial culture in absence and in presence of tested sample, respectively.

2.2.7. Bio-degradability test

Consistent with the reported method (Miller 1959), bio-degradability of the developed cross linked membranes was measured using dinitrosalicylic acid (DNS) reagent. A definite amount of samples (0.1g) was soaked for 24 h in 2 mL of phosphate buffer (pH 7.0) and 0.5 mL of lysozyme solution at 37 °C. Next, 1.5 mL of DNS reagent was added to stop the activity of lysozyme and followed with boiling in for 15 min, and finally left to cool. The generated color from the reaction of liberated reduced sugars and DNS reagent was analyzed by measuring the optical density (OD) at 540 nm using a visible spectroscopy (Hassan et al., 2019).

3. Results

3.1. FT-IR analysis

FT-IR spectra of Cs, PVA, and PVA/Cs cross linked membranes were presented in Fig.1. From the spectrum of PVA, the characteristic band at 3502 cm^{-1} associated with the presence O-H groups, while the broad C-H stretching band appeared at 1918 cm^{-1}. The spectrum of the native chitosan showed a broad band around 3355-3475 cm^{-1} which corresponded to the stretching vibration of NH_2 and O-H groups (Abeer et al., 2017). The absorption band at 2914 cm^{-1} corresponded to both methyl and methylene groups. Moreover, the peak at 1654 cm^{-1}confirmed the presence of C=O and NH-C-O groups (Mostafa et al., 2019). The band at 1580 cm^{-1} was a result of C=C stretching in the aromatic ring. In addition, the band at 1416 cm^{-1} could be related to deformation vibration of C-N. Besides, the IR spectrum of PVA/Cs cross linked membrane showed absorption band at 3416 cm^{-1} as a result of the stretching vibration of NH_2 in secondary amides and OH groups on Cs combined with the present OH groups of PVA. Band at 1585 cm^{-1} corresponded to vibration of –NH- of Cs, and C-O stretching and C-H bending were observed at 722 cm^{-1} (Wahba and Hassan 2017). The results showed also that the crosslinking process clearly decreased the intensity of bands arising from the NH bending (amide II) at 1585 cm^{-1} of chitosan.

Figure1. FT-IR spectra PVA, Cs, and PVA/Cs cross linked

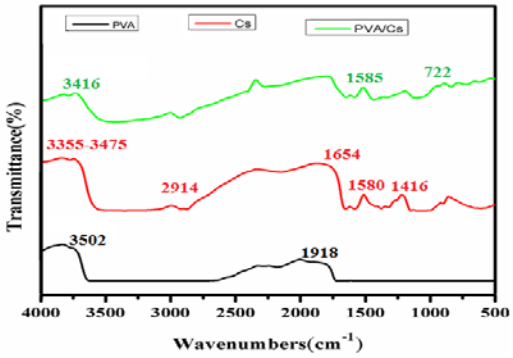

membranes.

3.2. SEM analysis

SEM images of native Cs, PVA and the cross linked PVA/Cs membranes were clarified in Fig. 2. As it can be seen, Cs showed a smooth surface with some wrinkles, while PVA exhibited more rough and un-homogenous surface. On the other hand, PVA/Cs membrane displayed a uniform surface without pores. All cross linked membranes exhibited a uniform surface without pores, which indicates the uniform distribution of PVA and PVA molecules throughout the films.

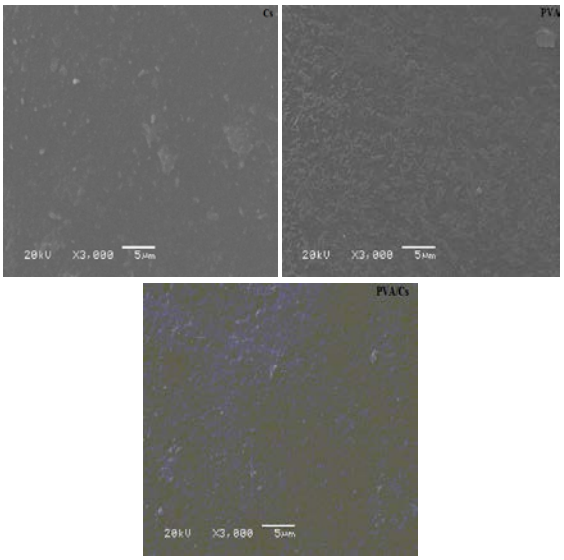

Figure2. SEM images of Cs, PVA and PVA / Cs cross linked membranes

3.3. Mechanical properties

Table 1 showed an increase in the tensile strength values for PVA membrane and associated with the strong interactions between the present ionic function groups. Moreover, the mechanical properties of Cs membrane were clearly improved after crosslinking with PVA. Where, PVA/Cs cross linked membrane recorded maximum force of 46.2 N compared with 26.09 N for neat Cs, indicating that the crosslinking process improved the developed membrane owing to the generated covalent bonds between PVA and Cs in addition to the present hydrogen bonds.

Table 1. Mechanical parameters of PVA, Cs, and PVA/Cs crosslinked membranes.

Sample	Max Force (N)	Max Dis. (mm)	Max stress (N/mm^2)	Max strain (%)	Energy (J)	Energy Max (J)
PVA	70.5	73.69	38.81	263.2	2.80	2.01
Cs	26.09	2.78	21.47	11.60	0.0548	0.0520
PVA/Cs (1:1)	46.2	41.70	34.45	129.3	1.05	1.01

3.4. Water uptake evaluation

Fig. 3 demonstrates the water uptake values of Cs, PVA and PVA/Cs cross linked membranes. The results showed that maximum water uptake values were 187% and 142% recorded by native Cs and PVA respectively, which can be attributed to the hydrophilic nature of both Cs and PVA. On the other hand, a significant decrease in water uptake value (115%) was observed in case of cross linked PVA/Cs membrane owing to the consumption of some hydrophilic groups through the crosslinking process in the membrane matrix.

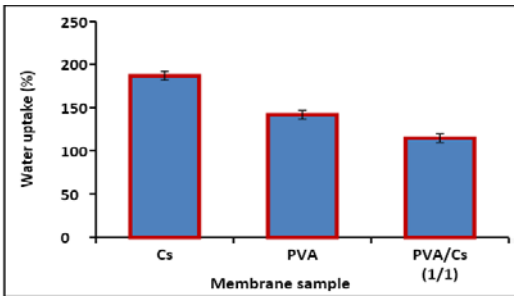

Figure 3. Water uptake values for PVA, Cs and PVA/Cs crosslinked membranes.

3.5. Anti-bacterial activity evaluation

Fig. 4 investigated the anti-bacterial activity of the developed cross linked membranes against *Staphylococcus aureus* as gram-positive bacteria and *Escherichia coli* as gram-negative bacteria. It was clear from the results that the anti-bacterial activity of the developed cross linked membranes were improved compared with native Cs and PVA membranes, whereas maximum inhibition (%) value increased from 10 and 12% for PVA membrane to 22 and 30 % after crosslinking with Cs.

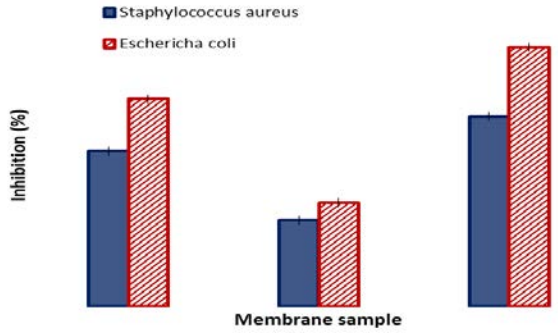

Figure 4: Anti-bacterial activity values for PVA, Cs and PVA/Cs cross linked membranes.

3.6. Bio-degradability evaluation

Fig. 5 clarified that all prepared membranes were bio-degraded in presence of lysozime. It is well known that the enzyme biodegrades polysaccharide via hydrolyzing the glycosidic bonds that existing in their structures.

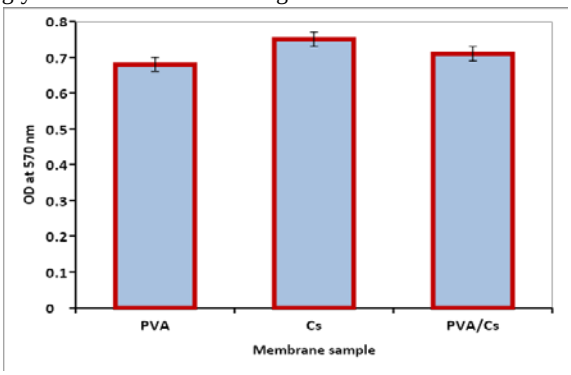

Figure 5. Bio-degradability of PVA, Cs and PVA/Cs cross linked membranes.

4. Discussion

Developing membrane to be used in wound healing process is an essential work, especially if this membrane formed from natural, biodegradable biopolymers such as polyvinyl chloride and chitosan (Balasubramaniet al., 2001).

Polyvinyl chloride/chitosan membrane shows better mechanical properties; besides, it has more function groups than the two constituents separately as shown in figure 1 (Omer et al., 2016; Hassan et al., 2019). Bio-degradability of the developed membranes could be related to the bio-degradation nature of native PVA and Cs, since both of them have hydrophilic groups such as OH groups (in case of PVA and Cs) and NH_2 group (in case of Cs) (Ueno and Toru 2001). These groups could impart the hydrophilicity of the developed membranes and offer several potentials for lysozime enzyme adsorption (Shewan and Jason 2013). Bacterial infection delays the process of wound healing and could lead to death (Dutta et al., 2009). Therefore, it is essential to evaluate the capability of the developed membranes for inhibiting the growth of different types of bacteria. The results showed that the inhibition (%) against gram-negative bacteria was higher than those against gram-positive bacteria. The interaction of positively charged amine groups present on the surface of cross linked membranes with the negatively charged cell surface that could block the feeding channels responsible for exchanging electrolytes and nutrients and, as a result, an inhibition of the normal bacteria metabolism took place and was followed with death of the bacterial cells. FT-IR, SEM and water uptake analysis concluded that the developed membrane has become more suitable for use in wound dressing with its new functional groups that make it more flexible and more antibacterial.

5. Conclusion

PVA/Cs cross linked membranes were prepared as anti-bacterial wound dressing membranes. FT-IR and SEM analysis tools were applied to investigate the chemical structure and surface morphologies of the developed membranes. Moreover, water uptake and mechanical properties were also evaluated. The developed membranes displayed a decent inhibition (%) against both gram positive and gram-negative bacteria. Results also showed

that PVA/Cs cross linked membranes were bio-degradable and could be applied for modern wound dressing applications.

Conflict of interest

The authors declare that they have no conflict of interest.

References

Abeer AA, Faten AM, Mohamed EH, Eman RH, Mona AE (2017) Covalent immobilization of *Alternaria tenuissima* KM651985 laccase and some applied aspects. *Biocatalysis and Agricultural Biotechnology* 9: 74–81.

Alvarez OM, Patricia MM, William HE (1983) The Effect of Occlusive Dressings on Collagen Synthesis and Re-Epithelialization in Superficial Wounds. *Journal of Surgical Research* 35(2):142–48.

Baker MI, Steven PW, Zvi S, Barbara DB (2012) A Review of Polyvinyl Alcohol and Its Uses in Cartilage and Orthopedic Applications. *Journal of Biomedical Materials Research Part B: Applied Biomaterials* 100(5):1451–57.

Balasubramani M, Ravi KT, Mary B (2001) Skin Substitutes: A Review. *Burns: Journal of the International Society for Burn Injuries* 27(5):534.

Boateng JS, Kerr HM, Howard NES, Gillian ME (2008) Wound Healing Dressings and Drug Delivery Systems: A Review. *Journal of Pharmaceutical Sciences* 97(8):2892–2923.

Bowler PG, Duerden BI, David GA (2001) Wound Microbiology and Associated Approaches to Wound Management. *Clinical Microbiology Reviews* 14(2):244–69.

Dutta PK, Shipra T, Mehrotra GK, Joydeep D (2009) Perspectives for Chitosan Based Antimicrobial Films in Food Applications. *Food Chemistry* 114(4):1173–82.

Elchinger P, Cédric D, Sophie F, Olivier R, Stéphanie B, Thierry B, Claude T, Philippe M (2015) Immobilization of Proteases on Chitosan for the Development of Films with Anti-Biofilm Properties. *International Journal of Biological Macromolecules* 72:1063–68.

Fathi E, Nahid A, Mohamad I, Zeinab A (2011) Physically Crosslinked Polyvinyl Alcohol–Dextran Blend Xerogels: Morphology and Thermal Behavior. *Carbohydrate Polymers* 84(1):145–52.

Guo S, Luisa AD (2010) Factors Affecting Wound Healing. *Journal of Dental Research* 89(3):219–29.

Hassan CM, Nikolaos AP (2000) Structure and Applications of Poly (Vinyl Alcohol) Hydrogels Produced by Conventional Crosslinking or by Freezing/Thawing Methods. Pp. 37–65 in *Biopolymers· PVA Hydrogels, Anionic Polymerisation Nanocomposites*. Springer.

Hassan MA, Omer AM, Abbas E, Based WMA, Tamer TM (2018) Preparation, Physicochemical Characterization and Antimicrobial Activities of Novel Two Phenolic Chitosan Schiff Base Derivatives. *Scientific Reports* 8(1):11416.

Hassan ME, Jun B, Dou DQ (2019) Biopolymers; Definition, Classification and Applications. *Egyptian Journal of Chemistry* 62(9):1725-1737.

Hassan ME, Yang Q and Xiao Z (2019) Covalent immobilization of glucoamylase enzyme onto chemically activated surface of κ-carrageenan. *Bulletin of the National Research Centre* 43:102.

Ismail SA, Hassan ME, Hashem AM (2019) Single step hydrolysis of chitin using thermophilic immobilized exochitinase on carrageenan-guar gum gel beads. Biocatalysis and Agricultural Biotechnology 21: 101281

Jones I, Lachlan C, Robin M (2002) A Guide to Biological Skin Substitutes. *British Journal of Plastic Surgery* 55(3):185–93.

Kamal H, Hegazy E, Mohamed MM, Sabaa MW, El-Dessouky MM (2014) Adsorption Properties of PVA/PAA/Clay Composite Hydrogel Synthesized by Gamma Radiation and Its Application in Removal of Crystal Violet Dye from Its Aqueous Solution. *Journal of Nuclear Technology in Applied Science* 2(5):523–37.

Kamoun EA, Kenawy E, Xin C (2017) A Review on Polymeric Hydrogel Membranes for Wound Dressing Applications: PVA-Based Hydrogel Dressings. *Journal of Advanced Research* 8(3):217–33.

Kanatt SR, Rao MS, Chawla SP, Arun S (2012) Active Chitosan–Polyvinyl Alcohol Films with Natural Extracts. *Food Hydrocolloids* 29(2):290–97.

Kenawy E, Omer AM, Tamer TM, Elmeligy MA, Mohy Eldin MS (2019) Fabrication of Biodegradable Gelatin/Chitosan/Cinnamaldehyde Crosslinked Membranes for Antibacterial Wound Dressing Applications. *International Journal of Biological Macromolecules* 139:440–48.

Levi S, Vladislav R, Verica M, Vesna R, Branko B, Teresa F, Katarzyna EK, Viktor N (2011) Limonene Encapsulation in Alginate/Poly (Vinyl Alcohol). *Procedia Food Science* 1:1816–20.

Marin E, John R, Yhors C (2014) A Review of Polyvinyl Alcohol Derivatives: Promising Materials for Pharmaceutical and Biomedical Applications. *African Journal of Pharmacy and Pharmacology* 8(24):674–84.

Miller GL (1959) Use of Dinitrosalicylic Acid Reagent for Determination of Reducing Sugar. *Analytical Chemistry* 31(3):426–28.

Mohy Eldin MS, Omer AM, Wassel MA, Tamer TM, Abd-Elmonem MS, Ibrahim SA (2015a) Novel Smart pH Sensitive Chitosan Grafted Alginate Hydrogel Microcapsules for Oral Protein Delivery: I. Preparation and Characterization. *International Journal of Pharmacy and Pharmaceutical Sciences* 7(10):320–26.

Mohy Eldin MS, Omer AM, Wassel MA, Tamer TM, Abd-Elmonem MS, Ibrahim SA(2015b) Novel smart pH sensitive chitosan grafted alginate hydrogel microcapsules for oral protein delivery: II. Evaluation of the swelling behavior. *International Journal of Pharmacy and Pharmaceutical Sciences* 7(10) 331-337.

Mona AE, Amira AG, Mohamed MIH, Mohamed EH, Naziha MH, Amal MH (2016) Enzymatic synthesis using immobilized *Enterococcus faecalis* Esawy dextransucrase and some applied studies. *Int J Biol Macromol* 92:56–62

Mostafa FA, El Aty AAA, Hassan ME, Awad GEA (2019) Immobilization of xylanase on modified grafted alginate polyethyleneimine bead based on impact of sodium cation effect. *International Journal of Biological Macromolecules* 140: 1284-1295.

Moulay S (2015) Poly (Vinyl Alcohol) Functionalizations and Applications. *Polymer-Plastics Technology and Engineering* 54(12):1289–1319.

Moutinho I, Inês CO, Mariana CS, Vasconcelos M, Ana P (2019) Different Chitosan-Based Biomaterials and Their Biomedical Applications. *Eur J Med Res Clin Trials* 1: 1-12.

Murakami K, Hiroshi A, Shingo N, Shin-ichiro N, Megumi T, Motoaki H, Satoko K, Hidemi H, Yoshihiro T, Tomoharu K (2010) Hydrogel Blends of Chitin/Chitosan, Fucoidan and Alginate as Healing-Impaired Wound Dressings. *Biomaterials* 31(1):83–90.

Omer AM, Tamer TM, Hassan MA, Rychter P, Mohy Eldin MS, Koseva N (2016) Development of Amphoteric Alginate/Aminated Chitosan Coated Microbeads for Oral Protein Delivery. *International Journal of Biological Macromolecules* 92:362–70.

Pokhrel S, Paras NY (2019) Functionalization of Chitosan Polymer and Their Applications. *Journal of Macromolecular Science, Part A* 56(5):450–75.

Rami L, Sebastien M, Samantha D, Jean-Christophe F, Robin S, Silke S, Eric L, Joëlle A, Alexandra M, Laurent D (2014) Physicochemical Modulation of Chitosan-based Hydrogels Induces Different Biological Responses: Interest for Tissue Engineering. *Journal of Biomedical Materials Research Part A* 102(10):3666–76.

Rinaudo M (2006) Chitin and Chitosan: Properties and Applications. *Progress in Polymer Science* 31(7):603–32.

Sahoo D, Sarmila S, Priyanka M, Sasmal S, Nayak PL (2009) Chitosan: A New Versatile Bio-Polymer for Various Applications. *Designed Monomers and Polymers* 12(5):377–404.

Sen CK (2009) Wound Healing Essentials: Let There Be Oxygen. *Wound Repair and Regeneration* 17(1):1–18.

Shewan HM, Jason RS (2013) Review of Techniques to Manufacture Micro-Hydrogel Particles for the Food Industry and Their Applications. *Journal of Food Engineering* 119(4):781–92.

Samia AA, Mohamed AAA, Gamal MES, Atef MI, Aliaa RES, Sherien MMA, Mohamed EH (2020) Catalytic, kinetic and thermal properties of free and immobilized Bacillus subtilis -MK1 α-amylase on Chitosan-magnetic nanoparticles. *Biotechnology Reports* 26: e00443

Sudheesh Kumar PT, Vinoth-Kumar L, Anilkumar TV, Ramya C, Reshmi P, Unnikrishnan AG, Shantikumar VN, Jayakumar R (2012) Flexible and Microporous Chitosan Hydrogel/Nano ZnO Composite Bandages for Wound Dressing: In Vitro and in Vivo Evaluation. *ACS Applied Materials & Interfaces* 4(5):2618–29.

Sun X, Chao L, Omer AM, Li-Ye Y, Xiao-kun O (2019) Dual-Layered PH-Sensitive Alginate/Chitosan/Kappa-Carrageenan Microbeads for Colon-Targeted Release of 5-Fluorouracil. *International Journal of Biological Macromolecules* 132:487–94.

Tamer TM, Valachová K, Collins MN, Hassan MA, Omer AM, Mohy Eldin MS, Švík K, Jurˇcík R, Ondruška L, Biró C, Albadarin AB, Šoltés L (2018) MitoQ Loaded Chitosan-Hyaluronan Composite Membranes for Wound Healing. *Materials* 11, 569

Tamer TM, Hassan MA, Omer AM, Based WMA, Hassan ME, El-Shafeey M, Mohy Eldin MS (2016) Synthesis, Characterization and Antimicrobial Evaluation of Two Aromatic Chitosan Schiff Base Derivatives. *Process Biochemistry* 51(10):1721–30.

Tamer TM, Valachová V, Hassan MA, Omer AM, El-Shafeey M, Mohy Eldin MS, Šoltés L (2018) Chitosan/Hyaluronan/Edaravone Membranes for Anti-Inflammatory Wound Dressing: In Vitro and in Vivo Evaluation Studies. *Materials Science and Engineering: C* 90:227–35.

Ueno H, Takashi M, Toru F (2001) Topical Formulations and Wound Healing Applications of Chitosan. *Advanced Drug Delivery Reviews* 52(2):105–15.

Van de Velde K, Paul K (2002) Biopolymers: Overview of Several Properties and Consequences on Their Applications. *Polymer Testing* 21(4):433–42.

Wahba MI, Hassan ME (2017) Agar-Carrageenan Hydrogel Blend as a Carrier for the Covalent Immobilization of ®-D-Galactosidase. *Macromol Res* 25(9):913–923

Zargar V, Morteza A, Amir D (2015) A Review on Chitin and Chitosan Polymers: Structure, Chemistry, Solubility, Derivatives, and Applications. *ChemBioEng Reviews* 2(3):204–26.

JJBS
Jordan Journal of Biological Sciences

Volume 14, Number 1,March 2021
ISSN 1995-6673
Pages 7 - 9

First record of *Lyphira heterograna* (Ortmann, 1892) from the North West of the Arabian Gulf

Tariq H.Y. Al-Maliky[1,*] and Anwar M.J. Al-Maliky[2]

[1] Marine Biology Department, Marine Science Centre, [2] Biology Department, College of Education for Pure Science , Basrah University, Iraq

Received March 2, 2020; Revised May16, 2020; Accepted May 16, 2020

Abstract

One male specimen of the species *Lyphira heterograna* (Ortmann, 1892) was recorded for the first time in October 2016 from Iraqi coast, North West of the Arabian Gulf, outside its known distribution range in the Indian and Pacific Oceans. The present specimen agrees morphologically with the original description of *L. heterograna* in key diagnostic characters and should be considered a range extension for the species and a new record for the region.

Keywords: Arabian Gulf , Crustacea, Leucosiidae, *Lyphira heterograna*.

1. Introduction

The genus *Lyphira* was described in detail by Galil (2009) based on studies of crabs of the family Leucosiidae found in the Indian Ocean. In her revision of this genus, Galil (2009) reclassified its genera from *Philyra* to *Lyphira* and established that the species had a wide distribution range across the Indian and western Pacific Ocean, including Japan, Taiwan, China, Malaysia, Indonesia, Philippines, East China Sea. In the Arabian Gulf, the genus *Lyphira* had been thought to be represented solely by the species *Lyphira perplexa* Galil, 2009 (Naderloo, 2017, Al-Maliky, 2020).

Recently, there has been a drive to identify the Leucosiid crabs from the Iraqi coast, on the North West of the Arabian Gulf (Al-Khafaji *et al*., 2017; Yasser and Naser, 2019; Al-Maliky, 2020, Al-Maliky and Luísa, 2020). In this time, six species were recorded, namely: *Ixa holthuisi* Tirmizi, 1970, *Arcania erinacea* Fabricius, 1787, *Seulocia anahita* Galil, 2005, *Hiplyra sagitta* Galil, 2009, *Lyphira perplexa* Galil, 2009 and *Hiplyra elegans* Galil, 2009.

The aim of the present paper is to confirm the identification of *Lyphira heterograna* for the first time in the Arabian Gulf, far outside its previously accepted distribution range.

2. Materials and Methods

One male specimen of *Lyphira heterograna* was collected a live in October 2016 at sampling location 29° 53’ 35.9736’’ N, 48° 35’ 28.9212’’ E (Fig. 1), by trawl net in 3-13 m of water depths. The specimen was preserved in 70-80% alcohol solution and deposited in the Department of Marine Biology, Marine Science Center, University of Basrah, Iraq. Specimen was photographed using the stereomicroscope (Carl Zeiss - Stemi 2000-C), equipped with a digital camera (Canon G 10 Wide 52 mm). The specimen was identified based on a comparison of morphological characteristics outlined for *L. heterograna* by: Ortmann (1892), Shen (1932) and Galil, (2009).

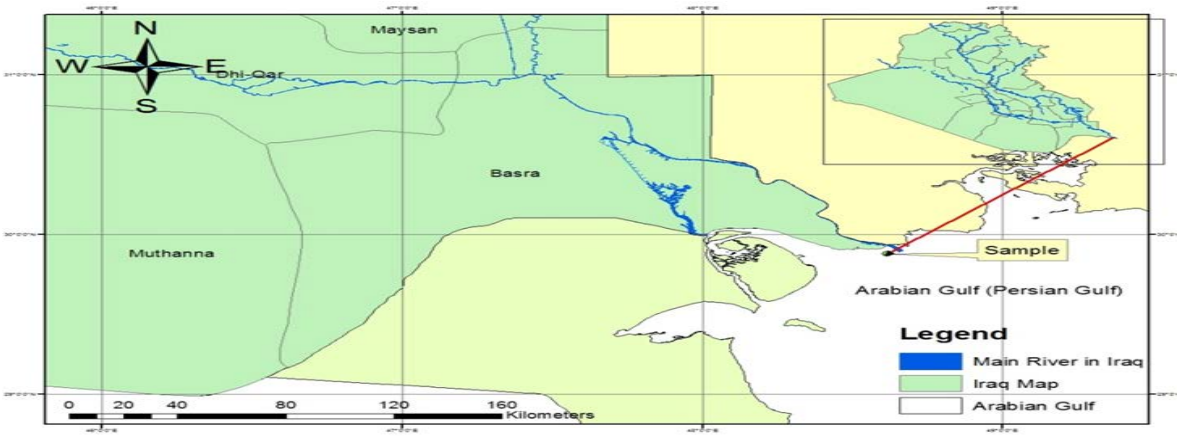

Figure 1. Map representing the study site in the Iraqi coast, Arabian Gulf.

* Corresponding author e-mail: tariq.hataab@yahoo.com.

3. Material examined

Single damaged male, (carapace only): Carapace Length 12.60 mm, Carapace Width 13.22 mm.

4. Result and Discussion

Systematic Treatment

Order Decapoda Latreille, 1802
Family Leucosiidae Samouelle, 1819
Subfamily Philyrinae Rathbun, 1937
Genus *Lyphira* Galil, 2009
Lyphira heterograna (Ortmann, 1892)

Philyra globulosa – H. Milne Edwards 1837: 132, pl. 24, fig. 4; *Philyra heterograna* Ortmann, 1892: 582, pl. 26, fig. 17; *Philyra globosa* – Lanchester 1900: 764; *Philyra peitahoensis* Shen, 1932: 18, pl. 1.1-2, text figs 10-12, 16b; *Philyra anatum* – Rathbun 1910: 312; *Philyra acutidens* Chen, 1987: 195, fig. 1.

Description of single male specimen

Carapace bearing minute granules, hepatic, branchial and intestinal regions with prominent granules (Fig. 2A); frontal margin slightly granulated; epistome slightly arcuate at anterior margin, inner angles of afferent branchial canals not prominent; external maxillipeds well granulated. Pterygostomian region prominently granulated (Fig. 2B). Anterior margin of abdominal sulcus prominently granulated. Fused abdominal segments 2-6 minutely granulated (Fig. 2B); male gonopod with a digitate apical process (Fig. 3A,B).

Note: Other appendages such as chelipeds and periopods were lost during collection.

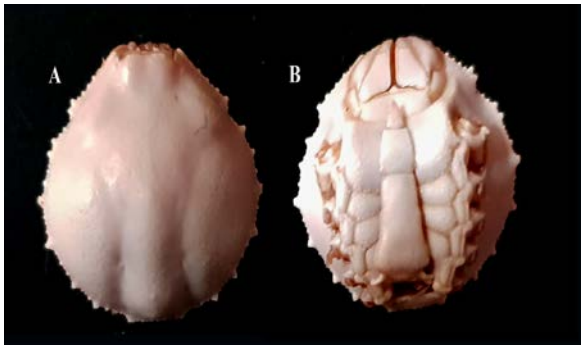

Figure 2. *Lyphira heterograna* (Ortmann, 1892) A, dorsal view; B, ventral view.

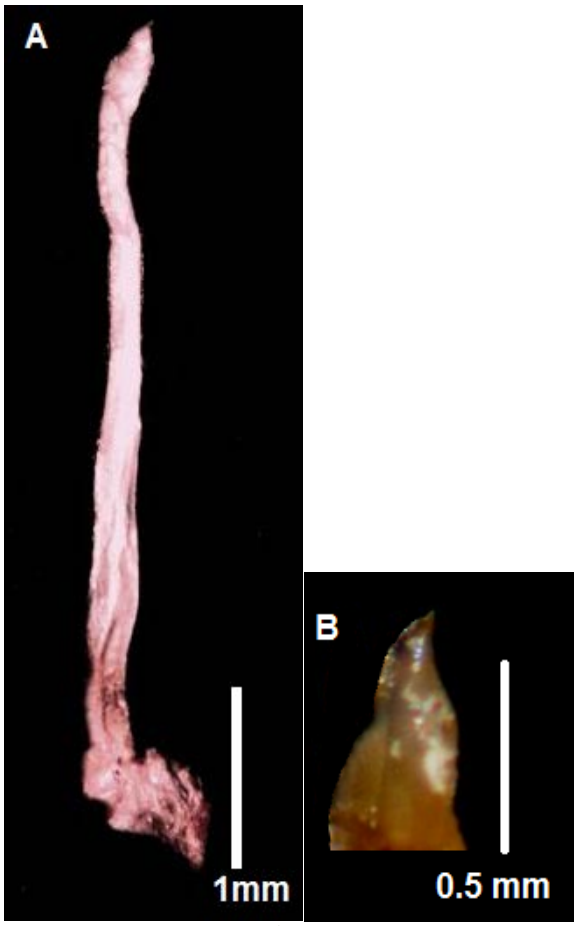

Figure 3. First male gonopod of *Lyphira heterograna* (Ortmann, 1892): A. whole gonopod; B. close-up of apical process.

5. Remarks

Only one species of the genus *Lyphira* was known from the Arabian Gulf, the species *Lyphira perplexa* (Naderloo, 2017, Al-Maliky, 2020). *Lyphira heterograna* can be easily separated from *L. perplexa* by its smaller body size and the digitate apical process of the first male gonopod. In *L. perplexa* the first gonopod has a flattened, squat, distally rounded apical process. The present specimen represents the first record of the species *L. heterograna* outside its previously known distribution range in the Indian and western Pacific Ocean and marks the first record of *L. heterograna* in the Arabian Gulf.

Distribution of *Lyphira heterograna* (Ortmann, 1837)

Japan, Taiwan, China, Malaysia, Indonesia, Philippines, East China Sea, and the **Arabian Gulf , as in the present study.**

References

Al-Khafaji, K.K.S., Abdul-Sahib, I.M. and Ajeel, S.G. 2017. First records of Leucosiid crabs: *Hiplyra sagitta* (Galil, 2009) from Iraqi Coast, NW-Arabian Gulf. International Journal of Aquaculture, 7 (22): 139-142.

Al-Maliky, T.H.Y. 2020. New records of Leucosiid crabs *Lyphira perplexa* Galil, 2009 (Crustacea; Decapoda; Leucosiidae) in the northwestof the Arabian Gulf, Iraq. OCEAN LIFE, 3 (2): 1-3.

Al-Maliky, T.H.Y. and Luísa, P. C. 2020. First record of *Hiplyra elegans* (Gravier, 1920), (Crustacea; Decapoda; Leucosiidae) in the northwestof the Arabian Gulf, Iraq. Revista Meio Ambiente e Sustentabilidade, 9(19): 8 p.

Chen H. 1987. On two new species of Leucosiidae (Crustacea, Brachyura) from the Chinese waters. Studia Marina Sinica, 28: 195-203.

Galil, B.S. 2009. An examination of the genus *Philyra* Leach, 1817 (Crustacea, Decapoda, Leucosiidae) with descriptions of seven new genera and six new species. Zoosystema, 31(2): 279-320.

Lanchester W.F. 1900. On a collection of crustaceans made at Singapore and Malacca. Part I. Crustacea Brachyura. Proceedings of the Zoological Society of London, 1900: 719-770.

Milne Edwards H. 1836-1844. Les Crustacés, in CUVIER G. (ed.), Le regne animal distribue d'apres son organisation, pour servir de base a l'histoire naturelle des animaux, et d'introduction a l'anatomie comparee. Edition accompagnee de planches gravees, representant les types de tous les genres, les caracteres distinctifs des divers groupes et les modifi cations de structure sur lesquelles repose cette classifi cation. 4e édition, 17. Fortin, Masson et Cie, Libraires, Paris: 1-278; Atlas, pls 1-80 (see Cowan [1976: 60] for details on the publication dates).

Naderloo, R. 2017. Atlas of crabs of the Persian Gulf. Springer Verlag, 1–443. DOI 10.1007/978-3-319-49374-9

Ortmann A. 1892. Die Abtheilungen Hippidea, Dromiidea und Oxystomata. Die Decapoden-Krebse des Strassburger Museums, mit besonderer Berücksichtigung der von Herrn Dr. Döderlein bei Japan und bei den LiuKiu-Inseln gesammelten und z. Z. im Strassburger Museum aufbewahrten Formen. V. eil. Zoologische Jahrbucher, Abtheilung fur Systema- tik, Geographie und Biologie deriere 6: 532-588, pl. 26.

Rathbun, M.J. 1910. — V. Brachyura, in the danish expedition to siam 1899-1900. Det kongelige danske videnskabernes selskabs Skrifter. Naturvidenskabelig og mathematisk afdeling, 5 (4): 303-367.

Shen C.J. 1932. The brachyuran Crustacea of North China. Zoologia Sinica, 9(1): 1-300.

Yasser, A. and Naser, M. 2019. First report of leucosiid crabs (Decapoda, Brachyura) from the Iraqi coast of the Persian Gulf. Journal of Biological Studies, 2(1): 25-30.

JJBS

Volume 14, Number 1,March 2021
ISSN 1995-6673
Pages 11 - 15

Jordan Journal of Biological Sciences

Morphology, Histology and Serotonin Immunoreactivity on Salivary Glands of Stick Insect, *Phobaeticus serratipes* (Phasmida: Phasmatidae)

Wan Nurul 'Ain, W.M.N and Nurul Wahida Othman*

Centre for Insect Systematics, Department of Biology and Biotechnology, Faculty of Science and Technology, Universiti Kebangsaan Malaysia, 43600 Bangi, Selangor, Malaysia.

Received November 11, 2019; Revised Feb16, 2020; Accepted June 1, 2020

Abstract

The salivary gland plays a significant role in physiological processes in insects including food lubrication, extra-oral digestion and enzyme secretion. This study was conducted to describe the morphology and histology of salivary glands of stick insect, *Phobaeticus serratipes* (Phasmida: Phasmatidae). The observation on gross morphology of salivary glands was photographed by using DSLR Canon EOS 6D camera attached to a stereo microscope. The histological study of the salivary glands involves special staining procedures of periodic Schiff's acid reagent and Alcian blue method. The immunohistochemical study of the biogenic amine serotonin distribution was observed under fluorescence microscope Zeiss AxiocamMRm Apotome.2. Results showed that the salivary glands were the acinar type that consists of two cells, parietal cell and zymogenic cell. The serotonin immunoreactivity of the salivary glands which located on the nerve fibers and might act as a neurotransmitter.

Keywords: Morphology, histology, serotonin, *Phobaeticus serratipes*, salivary gland

1. Introduction

Phasmatodea insects are herbivores that use their bodies' similarities to twigs, leaves, branches and lichen as an advantage for camouflaging themselves with vegetation (Bedford, 1978). Phasmatodea consists of 3000 species that are divided into 3 Families and 500 Genera (Whiting *et al*., 2003) including the largest insect, *Phobaeticus chani* Bragg, with the length of the female can reach up to 567 mm (Hennemen and Conle, 2008). They belong to the monophyletic group within the Orthopteroidea that is similar with Orthoptera, Blattaria, Dermaptera, Dictyoptera, Grylloblattodea and Mantophasmatodea (Flook and Rowel, 1998). The earliest described stick insects from West Malaysia were *Marmessoidea rosea* (Fabricius) in 1793 and *Heteropteryx dilatata* (Parkinson) in 1798 (Seow-Choen, 2005). To date, only five families of stick insects were recorded in Malaysia. They are Heteronemiidae, Phasmatidae, Aschiphasmatidae, Bacillidae and Phylliidae.

The salivary gland of insects is the gland associated with the nutrients intake where secretion is usually involved in the digestion and lubrication of food (Ali, 1997). There are two main types of the salivary glands of insects which are acinar as in the locust and cockroaches and tubular as in blowfly and Lepidoptera (Ali, 1997). The general function of salivary secretions is digestion but they may perform additional functions in some insects. For example, the saliva of locusts and cockroaches contains digestive enzymes (Gardiner, 1972; Kendall, 1969), the saliva of mosquitoes contains anticoagulants and irritants (Gardiner, 1972; Ribeiro, 1992) and labial on Lepidoptera can produce silk (Kafatos, 1968).

Salivation can be controlled either by direct nervous innervation or via neurohormone. Biogenic amines are one of the mediators involved in the control of insect salivation. They also act as neurotransmitters, neuromodulators or neurohormones in the nervous system and various peripheral organs of vertebrates or invertebrates (Baumann *et al*., 2003; Blenau and Baumann, 2001; Evans, 1980; Roeder, 1994). Serotonin, dopamine, octopamine and tyrosine hydroxylase are some of the biogenic amines. Salivary glands can be innervated from several sources. Most insects have salivary nerve which projects from suboesophageal ganglion but some species like *Periplaneta americana* and *Rhodnius prolixus* are also equipped with a salivary nerve that projects from stomatogastric nervous system (Baptist, 1941; Davis, 1985). Dopamine and serotonin emulate an important role in the control of salivary glands in most insects (Baines and Tyrer, 1989; Berridge, 1970; House, 1973). Salivary nerves of stick insects receive axonal projection from salivary nerve 1 (SN1) and salivary nerve 2 (SN2) in the subesophageal ganglion (Ali and Orchard, 1996). Immunohistochemistry shows that dopamine presents in SN1 whereas serotonin presents in SN2.

Not much research has been done on the salivary glands of stick insects. In this study, we report on the morphology and histology of the salivary gland of

* Corresponding author e-mail: wahida@ukm.edu.my.

Phobaeticus serratipes. We present a detailed description of the salivary gland using stereo microscope and light microscope. We also present results of the location of serotonin in the salivary gland. Stick insects are hypothesized to have an acinar type of salivary glands based on their feeding behaviour with chewing mouthpart. Salivary glands of insects have at least two different types of secretion cells such as parietal cells and zymogenic cells (Beams and King, 1932). The serotonin might be present on the nerve of the salivary gland as it is known as a monoamine neurotransmitter.

2. Material and Methods

2.1. Samples preparation

Samples were collected from Langkawi Island, Kedah, Fraser's Hill, Pahang and Gunung Ledang, Johor. Overall, 30 fresh samples were used in this study.

2.2. Gross Morphology of Salivary Glands

All stick insects were weighed before dissection. Solutions of methylene blue were injected at the jointed segment between the legs and abdomen and also between the head and thorax of the stick insects. Samples were left for an hour at room temperature. Dissections were done in phosphate-buffered saline (PBS) and images of salivary glands in-situ and ex-situ were captured using a DSLR Canon EOS 6D camera attached to a stereo microscope.

2.3. Tissue sections

The salivary glands were fixed in the formalin solution for 2-4 hours. Then, the formalin solution was removed by washing in 70% ethanol. Next, the glands were dehydrated through a series of ethanol (50%, 90%, 100%) for an hour each. Tissue was left in sub-Xylene for an hour, infiltrated with wax (3x at 58ºC) and embedded. Tissue was sectioned (3-5µm) using Leica RM2245 microtome. The slides containing tissues were stained using Alcian blue staining followed by periodic acid-Schiff's reagent (PAS). Images of the stained sections were observed under the light microscope (Zeiss Axio Scope) with iSolutionLite software.

2.4. Tissue sections immunofluorescence

The serotonin detection was performed in the tissue sections and whole mounts salivary gland tissue (Wan Nurul 'Ain and Nurul Wahida, 2015). Briefly, slides of tissue sections were rehydrated through a series of solutions (xylene and ethanol (2x100%, 95%, 70%). Then, the slides were further rehydrated with phosphate-buffered saline (PBS) for 10 minutes. The excess wash buffer was drained. Slides were partially dried after removal from PBS except for the tissue sections. After that, 2 drops of pre-blocking agent PBT (PBS of 50ml +0.2% bovine serum albumin, 25ul +0.1% TritonX-100, 5ul) was used to cover tissue sections and left for 20 minutes and then tapped off and wiped away. Tissue sections were covered with diluted primary antibody (anti serotonin) or negative control (PBT). The primary antibody was diluted 1 in 1000(1µl in 1ml of PBT + 1% normal goat serum, 100ul) (PBT+N). Slides were incubated overnight at 4ºC. Slides were rinsed with PBS to wash off excess serum and drained. Tissues were then covered with PBT plus normal goat serum (PBT+N). Then, the tissues were incubated overnight (4 °C) with secondary antibody conjugated to Dylight (dilution 1:300). The antibody was washed with PBT (30 min, 4x) before a complete inversion in PBS and further washing with series of ethanol (100%, 95%, 70%, 50%) to rehydrate it. The slides were mounted in a mixture of 50% glycerol and PBS and covered with a coverslip. The slides were then dried out on a slide warmer overnight and observed under a fluorescence microscope (Zeiss AxiocamMRm Apotome.2) with ZenPro2012 software and Olympus FSX100 microscope.

2.5. Whole mount tissue immunofluorescense

Fresh salivary glands were fixed in 4% paraformaldehyde in PBS (18 hours at 4ºC). After washing it with PBS, the tissue was permeabilized by exposing it to methanol (5 min, 70% MeOH in PBS, 60min, 100% MeOH and 5min, 70% MeOH in PBS) before washing with PBS (5min, 2x). The tissues were incubated for 30min in 100 mL of PBT+N (PBT + 5% normal goat serum) before being processed with 100 mL of diluted (1:1000) primary antibody serotonin and incubated overnight at 4ºC. The antibodies were washed off by multiple rinses with PBS (5min, 3x) and PBT (45min, 2x). Then, secondary antibody Dylight (1:300) was added to each vial, and the tissues were incubated at 4ºC overnight. The tissues were washed in PBT (5min, 3x) before a complete inversion in PBT for 2 hours. The tissues were cleared in a mixture of 50% glycerol and 50% PBS overnight before mounting on slides. The control samples were processed with similar procedure but with absence of the primary antibody. The distribution of serotonin was observed under fluorescence microscope (Zeiss Axiocam MRm Apotome.2) with ZenPro2012 software and Olympus FSX100 microscope.

3. Result and Discussion

3.1. General morphology of salivary glands

The salivary glands of *Phoebaeticus serratipes* consist of cluster of small globular types of acini. This acinar type of salivary glands had also been reported in other species of stick insect such as *Carausius morosus* (Asimakopoulos and Orchard, 1998) and other solid feeder insects such as grasshopper, *Gastrimargus musicus* (Nurul-Wahida and Cooper, 2014) and cockroach, *Periplaneta americana* (Just and Walz, 1996). Based on the gross morphology of the salivary glands that had been studied, the salivary glands of *P. serratipes* are paired glands that can be found at both sides of the lateral prothorax and extended to the metathorax (Figure1).

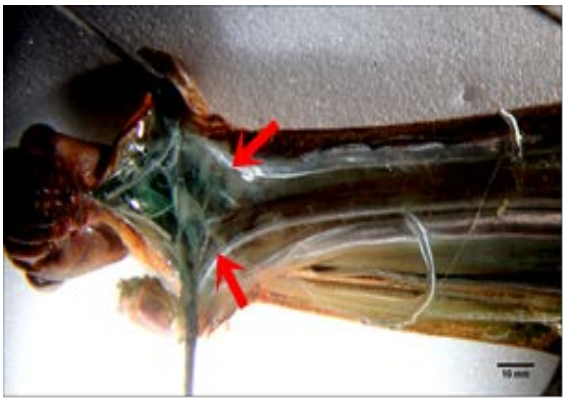

Figure 1. Image of in-situ (red arrows) along the prothorax to metathorax.

The size and distribution of salivary glands are different between the male and female stick insects due to the difference in the size of their body. The size of female is bigger than the male stick insect. The process of saliva secretion occurred at the glands of the globular acinar. The transparent and fine asinus duct canal acts as the connector between all the acini. This canal has an outlet from each of the acinus globules where it channels out the saliva from the acinus to the lower part of the labium of the mouthpart. The saliva will be collected in the collecting ducts before it is secreted. The collecting ducts from both sides of salivary glands will be fused at the head capsule and opened to become a salivary cup at the labium (Kendall, 1969), thus forming the main duct (Figure 2). The saliva is secreted from the main duct.

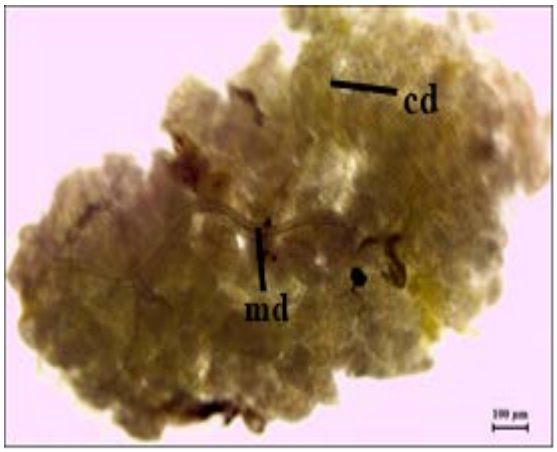

Figure 2. Ex-situ of acinar salivary glands of *P. serratipes*. md (main duct); cd (collecting duct).

Based on *ex-situ* and *in-situ* observation, no secretory gland was detected in *P. serratipes*. This secretory gland can be found in other species such as *Asceles glaber* (Dossey *et al*., 2012) and *Oreophoetes peruana* (Eisner *et al*., 1997).

3.2. Histology of salivary glands

The acinar glands of *P. serratipes* consist of two types of cells, parietal and zymogenic (Figure 3). Each acinus cell is covered by a basal membrane on the outside. Basal membrane mould acinus cell a round shape which later forms acinus globule.

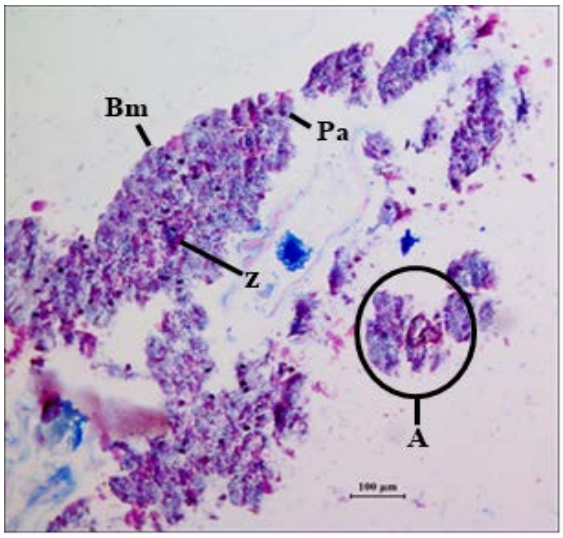

Figure 3. Tissue section of *P. serratipes* salivary gland. Tissue was stained with Alcian blue and PAS reagent. A (Acini); Bm (basal membrane); Pa (parietal cell); z (zymogenic cell).

Parietal cells are cone-shaped and have wide basal connected with basal membrane cells. They are located between zymogenic cells and extended towards the centre of each acinus. The nucleus of the parietal cell is big and oval-shaped. It is located at the centre of the cell. In contrast, zymogenic cells have an irregular shape. The basal of the cell is smaller compared to parietal cells. The nucleus is small in size and present on the side of each cell.

3.3. Serotonin distributions on salivary glands

The serotonin on the salivary glands of *P. serratipes* can be seen clearly at the axons along the ducts to the acini globules and the nerve fibers in the acini (Figure 4).

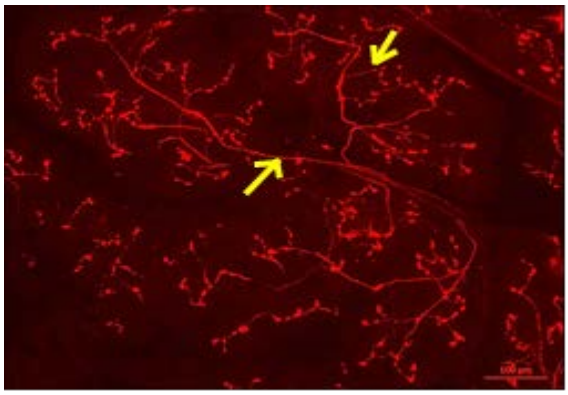

Figure 4. The serotonin distributions on the nerve fibers of *P. serratipes* salivary glands (yellow arrows).

Moreover, for the cross-section of the tissues, the serotonin was distributed on both cells in the salivary glands, parietal cells and zymogen cells (Figure 5). This result was supported by Nurul-Wahida and Cooper (2014) who reported the presence of serotonin on both parietal and zymogenic cells of yellow-winged grasshopper, *Gastrimargus musicus*. Serotonin is absent on the salivary gland of controlled stick insect (Figure 6).

The presence of serotonin will produce saliva with high protein content (Just and Walz, 1996). Electrical innervation towards the nerves or glands of the salivary ducts that superfusion with dopamine and serotonin will stimulate the secretion of saliva (Just and Walz, 1996).

Liquid secretion rate is controlled by peripheral cell (p-cell) at the base of each acinar globule and involved in the transportation of water and electrolytes as in cockroaches, *Periplaneta americana* (Kessel and Beams, 1963; Sutherland and Chillseyzn, 1968). Central cell, also known as c-cell, will react with serotonergic innervation and supply the proteinaceous components to the saliva (Just and Walz, 1994, 1996; Walz *et al*., 2006). The parietal cells of stick insects have similar function and morphology as the peripheral cells or p-cells of the cockroaches, whereas the zymogenic cells are similar to the central cells or c-cells.

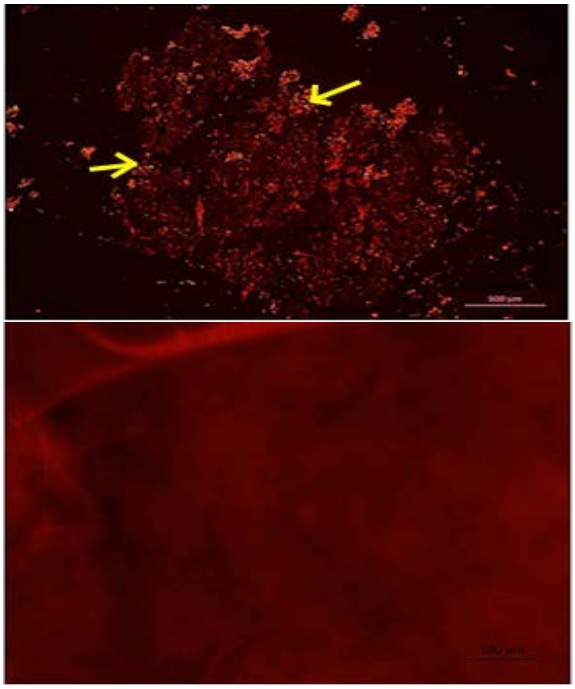

Figures 5-6. (5) Serotonin distributions on the cross section of salivary glands tissues of *P. serratipes* (yellow arrows). (6) No serotonin-like immunoreactive process on salivary glands of control stick insect.

4. Conclusion

It can be concluded that the serotonin in *P. serratipes* plays a role as a neurotransmitter that is similarly described in the *Periplaneta americana* (Ali, 1997; Ali and Orchard, 1995) due to its presence on the nerve fibers of the salivary glands. Besides, the distribution of serotonin on both parietal and zymogenic cells suggests that the serotonin also innervates the production of proteinaceous and non-proteinaceous saliva for this species.

Acknowledgements

The authors would like to thank Universiti Kebangsaan Malaysia and Ministry of Higher Education of Malaysia (MOHE) for the facilities and grant provided (Young Researcher Encouragement Grant GGPM – 2013 – 089 and FRGS/1/2015/WAB13/UKM/02/01), Nazca Scientific and Olympus from Universiti Putra Malaysia for the fluorescence microscope facility. We also would like to express our gratitude to Dr. Azman Sulaiman for helping us with the samples.

References

Ali DW. 1997. The aminergic and peptidergic innervations of insect salivary glands. *The Journal of Experimental Histology*, **200**: 1941-1949.

Ali DW and Orchard I. 1995. *J. Exp. Biol*, **199**: 699-709.

Ali DW and Orchard I. 1996. Immunohistochemical localization of tyrosine hydroxylase in the ventral nerve cord of the stick insect, *Carausius morosus*, including neurons innervating the salivary glands. *Cell Tissue Res*, **285**: 453- 462.

Asimakopoulos S and Orchard I. 1998. The aminergic control of salivary glands in the stick insect, *Carausius morosus*. *Biogenic amines*, **14**(2): 143-162.

Baines RA and Tyrer NM. 1989. The innervations of locust salivary glands. II. Physiology of excitation and modulation. *J. Comp. Physiol*, A **165**: 407-413.

Baptist BA. 1941. The morphology and physiology of the salivary glands of Hemiptera- Heteroptera. *Q.J. microsc.Sci*, **83**: 91-139.

Baumann A, Blenau W and Erber J. 2003.Biogenic Amines. In REsh VH, Carde RT, editors.Encyclopedia of Insects. San Diego: Academic Press. 91-94.

Beams HW and King RL. 1932. The architecture of the parietal cells of the salivary glands of the grasshopper, with special reference to the intracellular canaliculi, golgi bodies and mitochondria. *J. of Morph*, **53**(2).

Bedford GO. 1978. Biology and ecology of the Phasmatodea. *Annu.Rev. Entomol*, **23**:125-149.

Berridge MJ. 1970. A structural analysis of intestinal absorption. *Symp. R. Entomol. Soc. London*. **5**: 135-150.

Blenau W and Baumann A. 2001. Molecular and pharmacological properties of insect biogenic amine receptors: lessons from *Drosophila melanogaster* and *Apis mellifera*. *Arch Insect Biochem Physiol*, **48**: 13-38.

Davis NT. 1985. Serotonin-immunoreactive visceral nerves and neurohemal system in the cockroach *Periplaneta americana* (L.). *Cell Tissue Res*, **240**: 593-600.

Dossey AT, Bernier UR, Dancel MCA, Gottardo M, Meer RKV, Roush WR and Whitaker JM. 2012. Defensive Spiroketalsfrom *Asceles glaber* (Phasmatodea): Absolute Configuration and Effects on Ants and Mosquitoes. *J. Chem. Ecol*.

Eisner T, Attygalle AB, Herath KB, Jerrold MJ, Morgan RC and Smedley SR. 1997. Defensive production of quinolone by a phasmid insect (*Oreophoetes peruana*). *The Journal of Experimental Biology*, **200**: 2493– 2500.

Evans PD. 1980. Biogenic amines in the insect nervous system. *Adv Insect Physiol*, **15**:317-473.

Flook PK and Rowell CH. 1998. Inferences about orthopteroid phylogeny and molecular evolution from small subunit nuclear ribosomal DNA sequences. *Insect. Mol. Biol*, **7**: 163-78.

Gardiner MS. 1972.**The Biology of Invertebrates**, McGraw-Hill, New York.

House CR. 1973. An electrophysiological study of neuroglandular transmission in the isolated salivary glands of the cockroach. *J.exp.Biol*, **58**:29-43.

Hennemann FH and Conle OV. 2008. Revision of Oriental Phasmatodea: The tribe Pharnaciini Gunther, 1953, including the description of the world's longest insect, and survey of the Family Phasmatidae Gray. 1835 with keys to the subfamilies and tribes (Phasmatodea: "Anareolatae":Phasmatidae) *Zootaxa*, **1906**: 1-316.

Just F and Walz B. 1994. Salivary glands of the cockroach, *Periplaneta americana*: new data from light and electron microscopy. *J. Morph*, **220**: 35-46.

Just F and Walz B. 1996.The effects of serotonin and dopamine on salivary secretion by isolated cockroach salivary glands. *J. Exp. Biol*, **199**: 407-413.

Kafatos FC. 1968. The labial gland: a salt-secreting organ of saturniid moths. *J .Exp. Biol*, **48**: 435-453.

Kendall MD. 1969. The fine structure of the salivary glands of the desert locust *Schistocerca gregaria* Forskål. Z. *zellforsch. mikrosk. Anat*, **98**: 399-420.

Kessel RG and Beams HW. 1963. Electron microscope observations on the salivary gland of the cockroach, *Periplaneta arnericana*. *Z. Zellforsch.* **59**: 857- 877.

Nurul Wahida O and Cooper PD. 2014. Feeding and the salivary gland response in free-ranging yellow-winged grasshoppers (*Gastrimargus musicus*). *Australian Journal of Zoology*, **62**: 393-400.

Ribeiro JMC. 1992. Characterization of a vasodilator from the salivary glands of the yellow fever mosquito *Aedes aegypti. J. exp. Biol*, **165**: 61-71.

Roeder T. 1994. Biogenic amines and their receptors in insects. *Comp Biochem Physiol*, **107**C: 1-12.

Seow-Choen, F. 2005. **Phasmids of Peninsular Malaysia and Singapore**, Natural History Publications (Borneo) Sdn. Bhd., Kota Kinabalu.

Sutherland DJ and Chillseyzn JM. 1968. Function and operation of the cockroach salivary reservoir. *J. Insect Physiol.* **14**: 21-31.

Walz B, Baumann O, Baumann A, Blenau W and Krach C. 2006. The aminergic control of cockroach salivary glands. *Arch. Of Ins Biochem and Physiol*, **62**: 141-152.

Wan Nurul ‘Ain WMN and Nurul Wahida O. 2015. Morphology, histology and serotonin distribution on digestive tract of stick insect, *Phoebaeticus serratipes* (Phasmida: Phasmatidae).3rd International Conference on Chemical, Agricultural and Medical Sciences (CAMS-2015), Singapore.

Whiting MF, Bradler S and Maxwell, T. 2003. Loss and recovery of wings in stick insects. *Nature*, **421**: 264-276.

JJBS

Volume 14, Number 1, March 2021
ISSN 1995-6673
Pages 17 - 21

Jordan Journal of Biological Sciences

Chemical Composition and Anti-inflammatory Activity of the Essential Oil of *Echium humile* (Boraginaceae) in vivo from South-West of Algeria

Hamid Benlakhdar[1] , Nasser Belboukhari[1] , Khaled Sekkoum[1] , Abdelkrim Cheriti[2], Hatice Banu Keskinkaya[3], Salah Akkal[4,*]

[1]*Bioactive Molecules and Chiral Separation Laboratory (BMCSL), PO Box 417, University of Bechar Bechar, 08000, Algeria* ,[2]*Phytochemistry and Organic Synthesis Laboratory (POSL), PO Box 417, University of Bechar Bechar, 08000, Algeria* ,[3]*Selcuk University, Faculty of Science, Department of Biology 42130/ Keykubat Campüs, Konya, Turkey,*[4] *Valorization of Natural Resources, University of Mentouri Constantine1, Route AinElbey, 25000, Constantine, Algeria.*

Received April 9, 2020; Revised May 19, 2020; Accepted June 1, 2020

Abstract

The objective of this work is to study and analyze the chemical composition and anti-inflammatory effect of the essential oil of *Echium humile*. The essential oil of the fresh aerial parts is obtained by hydrodistillation where 37 compounds are identified by GC-MS analysis. The major constituents are bicycloelemene (15.9%), pentacosane (8.4%), p-cymen-8-ol (5.8%), β-phellandrene(4.9%), trans-thujone (4.1%). The minor constituent is camphene hydrate (0.5%). The anti-inflammatory effect of the essential oil at the doses of 150 and 200 mg/kg compared with the control and the reference drug (Diclofenac) on local inflammation by formalin-induced mouse paw edema revealed considerable anti-inflammatory properties of this oil.

Keywords: Boraginaceae , *Echium humile* , essential oil, anti-inflammatory activity

1. Introduction

The Boraginaceae family incorporates more than 2700 species and 200 genus usually found in cosmopolitan, living spaces particularly in tropic (Ceramella *et al*., 2019 ; Ahmad *et al*., 2018 ; Tarimcilar *et al*., 2015). This family is medicinally used as antimicrobial, antitumor, anti-inflammatory (Dresler *et al*., 2017), antioxidant, immomodulatory, emolient, sedative and antianxiolytic (Zarghami *et al*., 2018) . *Echium humile* Desf. (syn, *Echium pycnanthum* ssp.) (Mahklouf *et al*., 2018) (common name : Hemimiche, Ouacham(Vipérine) (Slimani *et al*., 2018 ; Laallam *et al*., 2011), is a wild plant species of Boraginaceae family, commonly found in dry spaces and desert , well-known as a traditional remedy, usually used to treat liver disease , digestive ailments and hepatitis (Chaouche *et al*., 2012 ; Miara *et al*., 2018). The *Echium humil* with several flowering stems and dense transparent bristles. (Ozenda., 1977) , The bibliography search results in a lack of studies on the chemical composition and biological evaluation of essential oil of *E. humile*, so we decided to extract the volatile oil and analyzed these chemical constituents followed by a study of its anti-inflammatory activity. The anti-inflammatory activity of the essential oil of *E. humile* is like that of *cordia verbenceae* in general (Benzie and Strain, 1996).

2. Materials and Methods

2.1. Plant material

Fresh aerial parts of *Echium humile* were collected from the region of Bechar (Latitude : 31°58′20″ N ; Longitude : 2°16′20″ W ; 949 m) in South-West Algeria in April 2017 at the flowering stage. The botanical identification and the voucher specimen are conserved at Medicinal plant encyclopedia herbarium of the bioactive molecules and chiral separation laboratory under accession number MPE14-3-E1

2.2. Animals

Albinos Swiss mice weighing 23-36g allocated in different groups (n=6 per group) were used in the experiment of acute toxicity and evaluation of anti-inflammatory activity. Animals were obtained from Pasteur Institute Algiers. They were housed at 22±2°C. The photoperiod is 12/24 hours.

2.3. Essential oil extraction

Essential oil was obtained by hydro-distillation (8h) from fresh aerial part (1200g). The oil after preparation was submitted to GC/MS analysis.

2.4. GC-MS analysis

GC/MS data of the *Echium humile* essential oil were carried out using a BRUKER Chemical Analysis, equipped with an DB-5 capillary column (25 m x 0.25 mm ; film thickness 0.25µm). The oven temperature was

* Corresponding author e-mail: salah4dz@yahoo.fr. .

held at 60°C for 5 min and then 60-220°C at 4°C/min ; carrier gas helium with a flow rate of 2ml/min., injector temperatures were set at 240°C, split ratio 1/40. Ionization energy 70 eV ; masse range 40-400 amu. Compounds of the *Echium humile* essential oil were identified by comparison of their retention indices (RI) to n-alkanes (C9 -C40) and retention indices with NIST Spectral Library and literature.

2.5. Toxicity

The acute toxicity test in mice was performed. Male and female mice weighing 23-36 g were separated into test and control groups composing sixe (n=6) animals in each group. The test was carried out using intra-planta (IP) doses of the essential oil of the *Echium humile* species :25, 50, 150 and 200 mg / kg in body weight. The control group received only physiological saline (25 µl / kg). The experimental mice were allowed to eat; all were kept under regular observation for 48 h, for any mortality or behavioral change.

2.6. Study of anti-inflammatory activity

We checked the inhibitory action of the volatile oil on the edema caused by the injection of 1% of a solution of formalin in physiological saline (NaCl 0.9%) at the dose of 0.025ml/paw, according to the method of Winter (Winter *et al*., 1962). The measurements of the volumes of the left hind paw of each mouse were carried out before the induction of the edema and every 30, 60, 120 and 180 minutes after the injection of the formalin. 30 minutes before the injection of formalin, the different groups of mice received intra-peritoneally different treatments: The control group of 6 mice received physiological saline (0.9%) at the dose of 10µl/g. The two experimental groups of 6 mice each received the oil at the dose of 150 and 200mg / kg of body weight. A group of 6 mice received diclofenac intraperitoneally as a reference product at a dose of 10µl/mg.

2.7. Statistical analysis

Data are presented as mean ± S.E.M values and analyzed by ANOVA followed by Student's *t* test. Values of $P < 0.05$ were considered statistically significant.

3. Results

3.1. Chemical analyses of essential oil

Thirty-seven compounds were identified in the light yellowish volatile oil obtained of *Echium humile* grown wild in Algeria with a yield of 1.2% (w/w). As shown in (table 1), the compounds presented about (83.5%) of total oil, where the major compounds were bicycloelemene (15.9%) and pentacosane (8.4%), p-cymen-8-ol (5.8%), β-phellanddrene (4.9%), trans-thujone (4.1%), whereas the minor component is camphene hydrate (0.5%). The oil comprises eleven monoterpenoids (22.2%), thirteen sesquiterpenoids (33.7%), three diterpenoids (6.0%), one sesterpenoids (8.4%) and nine non-terpenes (13.2%). The unidentified compounds represent (4.1%) of oil.

3.2. Toxicity

Intra-peritoneal administration (IP) of 25, 50, 150 and 200 mg / kg of essential oil to the different groups of mice did not show any particular clinical sign, and no death was observed (100% survival rate) during the 48 hours of observation. The absence of dead mice and undesirable effects during the 48 hours of observation indicates that the tested essential oil is not toxic by intra-peritoneal (IP) administration in a single dose.

3.3. Anti-inflammatory activity

The study was designed to assess the anti-inflammatory activity of the essential oil of the *Echium himule* plant. The anti-inflammatory action was carried out *in vivo* by edema formalin-induced mouse paw administration of oil at a dose of 150mg / kg significantly prevents the paw edema induced by formalin. The increase in percentage of inflammatory edema of the paw is 40±7%; 60±9%; 46.6±6.33% and 33.3±6.33% compared to the control group treated with physiological saline where the increase in edema is 60±5.17%; 80±8.67%; 86.6±8.33% and 93.3±3.83% after 30, 60, 120 and 180 minutes after injection of formalin respectively. At 200 mg / kg, the essential oil of *Echium humile* shows better prevention of paw edema formalin-induced versus dose 150 mg / kg. The increased percentages of inflammatory edema of the paw are less important. They are only 38.46±5%; 46.15±5.67%; 30.76±3.50% and 23.07±2.33% after 30, 60, 120 and 180 minutes respectively after injection of formalin (Table 2).

Assessment of percentage of inhibition shows that the essential oil of the *E. humile* has a greater anti-inflammatory activity in the fourth phase of this process. A better inhibition of inflammatory edema of the mouse paw was observed after 180mn (Figure 1) with a percentage of inhibition of 75.27±20.78%. After 120 minutes the essential oil shows an inhibition of 64.4±9.9% which is equal to the reference group treated with diclofenac. Hence the administration of the essential oil in the prevention of inflammatory edema with formalin by intra-planta administration has proved effective, in a dose-dependent manner (150 and 200 mg / kg). However this anti-inflammatory effects was weak in the initial period of edema but important later on (180mn).

Table1. Composition of the essential oil of *Echium humile*

N°	Compound	Rt	Area (%)	RI_{Expe}	RI_{Litu}	Reference
1	β-phellandrene	5.5	4.9	1041	1042	(Goodner, 2008)
2	β-Ocimene, (E)-	5.7	0.6	1047	1047	(Babushok *et al*., 2011)
3	Cis-sabinene	6.5	1.5	1067	1068	(Davies, 1990)
4	Terpinolene	7.0	0.6	1081	1081	(Davies, 1990)
5	Cis-thujone	8.0	0.8	1105	1106	(Tunalier *et al.* , 2002)
6	Menth-2-en-1-ol cis-p-	8.2	1.4	1111	1111	(Davies, 1990)
7	Trans-thujone	8.4	4.1	1116	1117	(Tunalier *et al*., 2002 ; Asta *et al.*, 2018)
8	Camphene hydrate	9.7	0.5	1148	1148	(Babushok *et al*., 2011)
9	Pinocarvone	10.2	0.8	1160	1160	(Babushok *et al*., 2011)
10	1-Nonanol	10.7	0.8	1173	1173	(Babushok *et al*., 2011)
11	Borneol	10.8	1.2	1177	1177	(Davies., 1990)
12	p-cymen-8-ol	11.1	5.8	1184	1183	(Babushok *et al*., 2011)
13	Isopulegyl acetate	13.9	1.1	1257	1258	(Davies, 1990)
14	p-Anisyl alchohol	14.9	2.8	1282	1282	(Babushok *et al*., 2011)
15	Dihydrocarvyl acétate	16.4	0.6	1319	1319	(Davies, 1990)
16	Bicycloelemene	16.8	15.9	1331	1333	(Babushok *et al*., 2011)
17	α-cubebene	17.5	1.1	1348	1348	(Goodner, 2008)
18	Longifolene	19.7	3.1	1405	1405	(Babushok *et al*., 2011 ; Santos *et al*., 2006)
19	γ-elemene	20.9	1.4	1444	1444	(Santos *et al*.,2006)
20	α-Patchoulene	21.4	0.9	1456	1457	(Babushok *et al*., 2011)
21	δ-cadinene	23.7	1.0	1526	1526	(Asta *et al*., 2018)
22	trans-Nerolidol	24.6	3.4	1552	1553	(Davies, 1990)
23	Germacrene B	24.7	1.4	1555	1554	(Deoliveira *et al*., 2007)
24	cis-Muurol-5-en-4-α-ol	24.9	2.2	1560	1560	(Khan *et al*., 2016)
25	Geranyl isovalerate	26.2	0.9	1599	1599	(Babushok *et al*., 2011)
26	Cadin-4-en-7-ol <cis->	26.5	1.3	1636	1636	(Adams, 2007)
27	Bisabolol<β->	26.7	0.9	1674	1675	(Adams, 2007)
28	Geranyl tiglate	26.9	2.5	1695	1695	(Adams, 2007)
29	β-Eudesmol, acetate	27.5	0.7	1792	1792	(Adams, 2007 ; Zito *et al*., 2013)
30	Hexadec-9-enoic acid,(Z)-	29.2	0.8	1950	1951	(Babushok *et al*., 2011)
31	α-Cadinol	33.7	0.7	2255	2255	(Tunalier *et al*., 2002)
32	Libocedrol	36.0	1.1	2345	2345	(Adams, 2007)
33	4-Epi-dehydroabietol	36.4	3.5	2357	2359	(Angelopouluo *et al*., 2001)
34	Ferruginol acetate< trans>	36.5	1.2	2362	2363	(Asuming *et al*., 2005)
35	Manoyl oxide	37.0	1.7	2379	2378	(Deoliveira *et al*., 2007)
36	Pentacosane	39.9	8.4	2498	2499	(Üçüncu *et al*., 2010)
37	5-ethylpentacosane	44.0	1.9	2669	2668	(Ramaroson *et al*., 1997)
38	Unknown	50.1	4.1	2951	-	-

Table 2. Effect of the essential oil of the aerial part of *Echium humile* on formalin-induced mouse paw edema.

Treatment groups (n =6)	Doses	30 min	60-min	120-min	180-min
Control (physiological saline)	5ml/kg	60±5.17%	80±8.67%	86.6±8.33%	93.3±3.83%
EO*Eh*	150mg/kg	40±7%	60±9%	46.6±6.33%	33.3±6.33%
EO*Eh*	200mg/kg	38.4±5%	46.1±5.67%	30.7±3.50%*	23.07±2.33%
Diclofenac	10µl/g	23.07±3.67%	35.4±6%	30.7±3.17%**	15.3±2%

EO*Eh*= essential oil of *Echium humile*; data are expressed as mean ± standard error to mean. Significance levels in comparison to control values are *p<0.01; **p= 0.001. n = 6

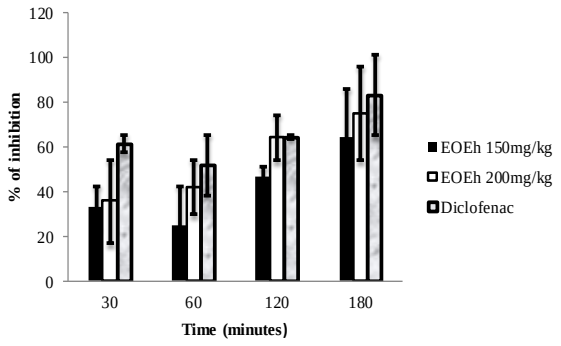

Figure 1. Percentage of inhibition of formalin-induced mouse paw edema of different doses of *Echium humile* essential oil.

Discussion

4.1. Volatile compounds composition

Essential oil of fresh flowering aerials parts of *Echium humile* has a light yellowish color and the yield was 1.2 % (w/w). This oil was averred to be rich in sesquiterpenoids and monoterpenoids. The identified sesquiterpene hydrocarbons were bicycloelemene (15.9%), longifolene (3.1%), germacrene B(1.4%) , γ-elemene (1.4%), α- cubebene (1.1%), δ-cadinene (1.0%), α-patchoulene (0.9%). The oxygenated sesquiterpens constituents in essential oil including geranyl tiglate (2.5%), cis-Muurol-5-en-4-α-ol (2.2%) , Cadin-4-en-7-ol

4.

<cis-> (1.3%) , Bisabolole<β>(0.9%), Geranyl isovalerate (0.9%), α-Cadinol (0.7%). On the other hand, the monoterpenoids with 22.2% , are mainly p-cymen-8-ol (5.8%), β-phellandrene (4.9%) and trans-thujone (4.1%). The other compounds are deterpenoids , sesterpenoids and non-terpenoids accounting for 6.0% , 8.4% and 13.2% respectively besides one unknown compound (4.1%).

4.2. Anti-inflammatory Activity

In our tests, the drug diclofenac is used as a reference substance. The anti-inflammatory potential of oil *was* evaluated in vivo on the paw of the mouse by creating an edema with formalin.

In the control animals, the sub-plantar injection of formalin produces local edema which gradually increases. The volume of the mouse paw was measured at 30, 60, 120 and 180 minutes after injection of formalin. Diclofenac, at 10 µl / kg, significantly reduces the volume of paw edema by 35.4±9.25%; 30.76±4.55% and 15.37±10.85% after 60, 120 and 180 minutes respectively.

At 150 mg / kg, the essential oil remarkably inhibited the development of formalin-induced edema of the paw from the first 60 minutes, with a maximum reduction of 64.30±21.93% after 180 minutes. However, the anti-inflammatory effect remains weaker than that of diclofenac (10 µl / kg ip) during the 180 minutes. By increasing the dose to 200 mg / kg, the essential oil showed strong anti-inflammatory activity. These effects are greater compared to those obtained with diclofenac (10 µl / kg ip).

The results obtained from anti-inflammatory tests show that the essential oil of *Echium humile* has an effect on inflammation and significantly reduces the formalin-induced paw edema, with a good dose – effect relationship, better inhibition is obtained at 200 mg / kg.

The effects of the essential oil of *Echium humile* manifested the same anti-inflammatory mechanism due to diclofenac, from the 120 minutes period. It is concluded that the essential oil of *Echium humile* contains compounds which has anti-inflammatory activity, such as diclofenac used as a reference substance in our tests. Also, the important effectiveness of this essential oil could be linked to the chemical profile, because it is rich in biologically active molecules such as sesquiterpenes, monoterpenes.

5. 5. Conclusion

The essential oil from the fresh aerial part of the *Echium humile* plant with a yield of 1.2% (w / w) and composed mainly of mono- and sesqui-terpenids. These majority constituents are bicycloelemene (15.9%); pentacosan (8.4%) p-cymen-8-ol (5.8%). The essential oil of *Echium humile* showed significant anti-inflammatory activity compared to the control and the animal reference group. It is the prime study determining the chemical composition and anti-inflammatory activity of the essential oil of the fresh aerial part of the species *Echium humile*.

Acknowledgments

The authors are grateful to the General Direction of Scientific Research of Algeria (DGRSDT).

References

Adams RP. 2007. **Identification of essential oil components by gas chromatography/mass spectrometry**. fourth ed. Carol Stream USA, Allured Publishing Corporation.

Ahmad L, He Y, Semotiuk AJ, Liu QR and Hao JC. 2018. Survey of pyrrolizidine alkaloids in the tribe Lithospermeae (Boraginaceae) from Pan-Himalaya and their chemotaxonomic significance. *Biochemical systematics and ecology*. **81**: 49-57.

Angelopoulou D, Demetzos C and Perdetzoglou D. 2001. An interpopulation study of the essential oils of Cistus parviflorus L. growing in Crete (Greece). *Biochemical systematics and ecology*. **29**: 405-15.

Asta J and Jurga B. 2018. Chemical Polymorphism of Essential Oils of Artemisia vulgaris Growing Wild inLithuania. *Chem. Biodiversity*. **15**: 1-13

Asuming WA, Beauchamp PS, Descalzo JT, Dev BC, Dev V, Frost S and Ma CW. 2005. Essential oil composition of four Lomatium Raf. species and their chemotaxonomy. *Biochemical Systematics and Ecology*. **33**: 17-26.

Babushok VI, Linstrom PJ and Zenkevich IG. 2001. Retention indices for frequently reported compounds of plant essential oils. *J. Phys. Chem. Ref. Data*. **40**: 1-47.

Benzie IF and Strain JJ. 1996. The ferric reducing ability of plasma (FRAP) as a measure of "antioxidant power": the FRAP assay. Analytical biochemistry. 239 : 70-76.

Ceramella J, Loizzo MR , Iacopetta D, Bonesi M , Sicari V, Pellicanò TM, and Sinicropi MS. 2019. Anchusa azurea Mill. (Boraginaceae) aerial parts methanol extract interfering with cytoskeleton organization induces programmed cancer cells death. *Food & function*. **10**: 4280-90.

Chaouche T, Haddouchi F and Bekkara FA. 2012. Identification of shikonin from the roots of Echium pycnanthum pomel. *Asian J. Pharm. Clin. Res.* **5** : 30-32.

Davies NW. 1990. Gas chromatographic retention indices of monoterpenes and sesquiterpenes on methyl silicon and carbowax 20M phases. *J. Chromato*. **503**: 1-24.

Deoliveira JC, Da camara C and Schwartz MO. 2007. Volatile constituents of the stem and leaves of Cordia species from mountain forests of Pernambuco (north-eastern Brazil). *J. Essen. Oil Res.* **19** : 444-48.

Dresler S, Szymczak G and Wójcik M. 2017. Comparison of some secondary metabolite content in the seventeen species of the Boraginaceae family. *Pharmaceutical biology*. 55: 691-95.

Goodner KL. 2008. Practical retention index models of OV-101, DB-1, DB-5, and DB-Wax for flavor and fragrance compounds. *LWT-Food Science and Technology*. **41**: 951-58.

Khan M, Mahmood A and Alkhathlan HZ. 2016. Characterization of leaves and flowers volatile constituents of Lantana camara growing in central region of Saudi Arabia. *Arab. J. Chem*. **9:** 764-74.

Laallam H, Boughediri L and Bissati S. 2011. Inventaire des Plantes Mellifères du Sud-Ouest Algérien. Synthèse: *Revue des Sciences et de laTechnologie*. **23**: 81-89.

Mahklouf MH, Sherif AS and Betelmal AG. 2018. Floristic Study for Tarhuna–Libya. Hacettepe *Journal of Biology and Chemistry*. **46**: 337-64.

Miara MD, Bendif H, Hammou MA and Teixidor-Toneu I. 2018. Ethnobotanical survey of medicinal plants used by nomadic peoples in the Algerian steppe. *J. ethno*. **219**: 248-56.

Ozenda P. 1977. **Flore du Sahara**. second ed. Cnrs, Paris. pp. 396.

Ramaroson-RB, Gaydou ÉM and Bombarda I. 1997. Hydrocarbons from three Vanilla bean species: V. fragrans, V. madagascariensis, and V. tahitensis. *J. Agricultural and Food Chemistry*. **45**: 2542-45.

Santos RP, Nunes EP, Nascimento RF, Santiago G MP, Menezes GHA, Silveira ER and Pessoa ODL. 2006. Chemical composition and larvicidal activity of the essential oils of Cordia leucomalloides and Cordia curassavica from the Northeast of Brazil. *J. Braz. Chem. Soc*. **17** : 1027-30.

Slimani N, Mahboub N, Chehma A, Huguenin J, Barir A and Bezza IF. 2018. Epidermal anatomic characterization of spontaneous plants belonging to Poaceae, Cistaceae and Boraginaceae families in Algerian northern sahara. *Inter. J. of Bio. and Agricu. Reas*. **1** : 41- 48.

Tarimcilar G, Yilmaz Ö and Kaynak G. 2015. Onosma demirizii (Boraginaceae), a new species from central Anatolia, Turkey. *Bangladesh journal of botany*. **44** : 261-265.

Tunalier Z, Kirimer N and Baser KHC. 2002. The composition of essential oils from various parts of Juniperus foetidissima. *Chem. Na.t Comp*. **38** : 43-47.

Üçüncü O, Cansu TB, Özdemir T, Karaoğlu ŞA and Yayli N. 2010. Chemical composition and antimicrobial activity of the essential oils of mosses (Tortula muralis Hedw., Homalothecium lutescens (Hedw.) H. Rob., Hypnum cupressiforme Hedw., and Pohlia nutans (Hedw.) Lindb.) from Turkey. *Turk. J. of Chem*. **34** : 825-34.

Winter CA, Risley EA and Nuss GW. 1962. Carrageenin-induced edema in hind paw of the rat as an assay for anti-inflammatory drugs. *Proceedings of the society for experimental biology and medicine*. **111** : 544-47.

Zarghami M, Chabra A, Khalilian A and Asghar HA. 2018. Antidepressant effect of *Asperugo procumbens* L. in comparison with fluoxetine: arandomized double blind clinical trial. *Res. J. of Pharmacognosy*. **5** : 15-20.

Zito P, Sajeva M, Bruno M, Rosselli S, Maggio A and Senatore F. 2013. Essential oils composition of Periploca laevigata Aiton subsp. Angustifolia (Labill.) Markgraf (Apocynaceae–Periplocoideae). *Nat. Prod. Res.* **27** : 255-65.

JJBS

Volume 14, Number 1, March 2021
ISSN 1995-6673
Pages 23 - 29

Jordan Journal of Biological Sciences

Comparison of different solvents for Antioxidant and Antibiogram Pattern of *Bergenia ciliata* rhizome Extract from Shimla district of Himachal Pradesh

Kanika Dulta [a] , Kiran Thakur [a] , Amanpreet Kaur Virk [a] , Arti Thakur [b] , Parveen Chauhan [a] ,Vinod Kumar [c] and P.K. Chauhan [a,*]

[a] *Faculty of Applied Sciences and Biotechnology, Shoolini University, Solan-173229, Himachal Pradesh, India,*[b] *Faculty of Sciences, Shoolini University, Solan-173229, Himachal Pradesh, India,*[c] *Department of Chemistry, Uttaranchal University, Dehradun-2480001, Uttarakhand,India*

Received March 18, 2020; Revised June 3, 2020; Accepted June 5, 2020

Abstract

Bergenia ciliata is a well-known herb commonly known as Paashaanbhed, with various pharmaceutical properties. The scientific exploration of *Bergenia ciliata* is growing in the Western Himalayas for its phytochemical and pharmacological properties. The present study aimed to evaluate the *Bergenia ciliata* rhizome extracts for total phenol content, total flavonoid content, antioxidant and antimicrobial activities. Four different solvents viz., aqueous, chloroform, methanol and ethanol were used for extraction. Among the solvents tested, methanol was found to be the best extractive solvent with the highest total phenolic content of 31.46 mg GAE g^{-1} DE and the lowest IC_{50} values for DPPH and ABTS assays, i.e 80.20 and 73.38 µg mL^{-1}, respectively. Methanol and ethanol extracts exhibited effective antimicrobial activity against *E. coli, S. typhi,* and *S. aureus* (MIC = 6.25 µg mL^{-1}). The current study suggested that the methanol extract of *Bergenia ciliata* has strong antioxidant and antimicrobial potential, which can be used in functional foods and pharmaceutical industries.

Keywords: *Bergenia ciliata*, Antioxidants, Phytochemicals, Antimicrobial

1. Introduction

Nowadays, chief concerns of food and pharmaceutical industries are microbial contamination and side effects of synthetic antioxidants. Increasing tendency for replacing synthetic antioxidant by natural one and growth of microbial resistance to existing antibiotics from the other has stimulated researchers toward considering medicinal plants for dual antioxidant and antimicrobial properties (Savoia, 2012 and Pandey *et al*., 2015). For thousands of years, plants have been used as the source of medicines by mankind. Plant derived natural products or their derivatives play an essential role in both innovation and promotion of new drugs (Mercy *et al*., 2018 and Hazra *et al*., 2010). Exploration of new antimicrobials of plant origin, as reliable source of antibiotics, is receiving attention of the scientific community. According to WHO, about 80 % of the world's population depends on traditional medication from plants. Approximately 25 % of drugs contain phytonutrients extracted from plants (Ebong, 2015) as they are factories of natural phytochemicals (Johnson *et al*., 2015). These plants synthesize bioactive chemicals (phytochemicals) as secondary metabolites (Zulfiqar *et al*., 2017) that are used directly for antibacterial, fungicidal and herbicidal purposes (Agu *et al*., 2017). Many phytochemicals possess antioxidant activity and decrease the risk of diseases (Asgharian *et al*., 2017).

Bergenia ciliata is a perennial herb which belongs to Saxifragaceae family and consists of 30 genera and 580 species (Ruby e*t al*., 2012 and Pokhrel *et al*., 2014). It grows widely in cold and temperate regions of the Himalayas (Islam *et al*., 2002). The plant species flourishes well in rocky areas and on the cliffs. Three species of *Bergenia, i.e. Bergenia ligulata, Bergenia ciliata* and *Bergenia stracheyi* are found in Indian Himalayan region. These are commonly known in Indian system of medicine as *Pashanbheda* (Asolkar *et al*., 1992). The leaves, root, rhizomes and other parts of *Bergenia ciliata* are used as a traditional medicine in Asian countries (Bhattarai, 1994 and Bagul *et al*., 2003) Juice of the rhizome is taken for urinary trouble and hemorrhoids (Manandhar, 1995). *Bergenia ciliata* rhizome is widely used in folk medicines anti-bacterial, antipyretic, analgesic, antioxidant, hypoglycemic, antiviral, anti-inflammatory and antimalarial (Sinha *et al*., 2001 and Walter *et al*., 2013) antidiabetic and anti-tussive properties (Hsieh *et al*., 2001 and Chauhan *et al*., 2012). It is also reported to be helpful for kidney and gall bladder stone, cough, fever, diarrhea and lungs diseases (Farooquee *et al*., 2004; Rai *et al*., 2000 and Pradhan *et al*., 2008). The virtues of plant are attributed to its secondary metabolites such as bergenin, β-sitosterol, arbutin, phytol, gallic acid and catechin, which are therapeutic and account for its use in traditional medicine (Dharmender *et al*., 2010 and Sajad *et al*., 2010).

* Corresponding author e-mail: chauhanbiochem084@gmail.com

The aim of present study was to determine the total phenolic, flavonoid content and their antioxidant and antibacterial activities of different solvent extracts from rhizome of *Bergenia ciliata*.

2. Materials and Methods

2.1. Collection of Plant Material

Rhizomes of *Bergenia ciliata* were collected from the Narkanda region (2700 m amsl) of Shimla district, Himachal Pradesh, India during spring season from April to June, 2018. The plant was identified at CSIR-Indian Institute of Integrative Medicine (CSIR-IIIM), Jammu and the verified sample was submitted in Herbarium at the School of Biological and Environmental Sciences, Shoolini University, Solan, India.

2.2. Morphological Evaluation

In the morphological evaluation various organoleptic characters such as color, odor, shape, fracture, texture, taste and size were determined by Kokate (Kokate, 2005).

2.3. Preparation of Extract

Firstly, the collected rhizomes of *Bergenia ciliata* were washed with water to remove soil and other foreign particles and then dried under shaded place. The dried material was then grinded into a coarse powder using grinder. For the extract preparation, 10 g of powder was soaked separately in 100 mL of different solvents-aqueous, chloroform, methanol and ethanol for 48 h with constant shaking. Extracts were then filtered using Whattman filter paper (No.1). Extracts were dried by evaporation using vacuum evaporator at 40 °C. The filtrate was stored and used for further experiments (Turner, 2006).

2.4. Extraction Yield

The percentage yield of the extraction was calculated using formula: {(V1/V2)/100}.

2.5. Qualitative Phytochemical Analysis

Phytochemical tests were done to identify the presence of chemical constituents in the rhizome extracts of *Berginia ciliata* using standard protocol (Harborne, 2012 and Das *et al*., 2010). These include tests for alkaloids, phenols, carbohydrates, flavonoids, phenols, saponins and proteins.

2.6. Total Phenolic Content (TPC)

TPC was evaluated by a Folin–Ciocalteu assay (Singleton, 1999). Each sample (1 mg/mL; 100 µL) was taken separately in test tubes. 1 mL of Folin–Ciocalteu reagent and 1 mL of sodium carbonate solution (20 %) were added. After 5 min, the mixture was incubated at 25 °C in a water bath for 60 min. Absorbance was determined at 760 nm. The phenolic content values were expressed as mg of gallic acid equivalent per gram of dry extract (mg GAE g DE).

2.7. Total Flavonoid Content (TFC)

TFC was evaluated by the aluminum chloride method (Zhishen *et al*., 1999). Each sample (1 mg/mL; 100 µL) was added to aluminum chloride solution (2 %, 0.5 mL), incubated for 15 min at 37 °C. Absorbance was determined at 510 nm. The total flavonoid content was shown as mg of rutin equivalent per gram of dry extract (mg RE g DE).

2.8. Antioxidant Activity

2.8.1. DPPH (2,2-diphenyl-1-picryl-hydrazyl-hydrate) free radical scavenging Assay

The effect of extracts on DPPH radical was determined as described (Barros *et al*., 2007). For stock solution, 20 mg DPPH was dissolved in methanol. Then, the DPPH solution was diluted with methanol to reach an absorbance of 0.68–0.76 at 517 nm. To prevent free radicals, the DPPH stock solution was coated with aluminium foil and kept in the dark for 24 h. The extract was placed in a cuvette and mixed with 2 mL of diluted DPPH solution and was kept for 30 min in the dark. Absorbance of the solution mixture was taken at 517 nm using spectrophotometrically.

DPPH scavenging effect (%) = $(A_b\text{-}As/A_b) \times 100$

where A_b= absorbance of blank

As = absorbance of extract/standard.

Ascorbic was used as standard substance. The free radical scavenging activity was expressed as IC_{50} value, which represented the inhibitory concentration of extract/standard required to scavenge 50 % of free radicals.

2.8.2. ABTS (2,2-azino-bis-3-ethylbenzothiazoline-6-sulfonic acid) radical scavenging assay

ABTS radical scavenging assay was performed as described (Re *et al*., 1999). The ABTS radical cation solution was produced by reacting 7 mM ABTS stock solution and 2.45 mM potassium persulfate solution was prepared in 100 mL methanol. These two mixtures were mixed in equal quantities and kept in dark at room temperature for 14–16 h. Then, the ABTS solution was diluted with methanol to reach an absorbance of 0.68–0.76 at 745 nm. 2 mL of solution was mixed extract and incubated for 20 min. Percent inhibition of absorbance at 745 nm was calculated using the formula:

ABTS Scavenged effect (%) = $(A_b\text{-}As/A_b) \times 100$

2.9. Antimicrobial Activitiy:

Antimicrobial activity was tested against three bacterial cultures (Gram negative, viz. *Escherichia coli* (MTCC 82) *and Salmonella typhi* (MTCC734) and Gram positive, viz. *Staphylococcus aureus* (MTCC 96). These strains were obtained from Food Technology Laboratory of Shoolini University, Solan, Himachal Pradesh, India.

2.9.1. Agar Well Diffusion Assay

Agar well diffusion method is widely used for *in vitro* antimicrobial activity (Perez *et al*., 1990). The microorganisms were first inoculated in nutrient broth at 37 °C. The bacterial density reached 0.5 of the McFarland Standard was uniformly spread on the surface of the nutrient agar plates using sterile cotton swabs. The wells were punched aseptically with the cork borer (6 mm). 100 µL of each extract (100 mg/mL) was placed in the wells made in the nutrient agar plate. Then, the petri plates were incubated at 37 °C. Positive control 10 µL of ampicillin (100 mg/mL stock) was used in the experiment; dimethyl sulfoxide (DMSO) was used as a negative control. To determine the effectiveness of extract against each organism the tests were performed in triplicates and results were recorded as mean ± SD.

2.9.2. Minimum Inhibitory Concentration (MIC)

MIC of the different extracts was evaluated by broth dilution method (CLSI, 2012). From stock (100 mg/mL) 100 µL of extract was prepared to check its activity against different bacterial strains in a 96-welled micro titer plate. 10 µL of ampicillin was taken as a positive control; 10 µL of DMSO was taken as a negative control for all the bacterial strains. Plates were incubated under normal conditions at 37 °C for 16-20 h. After 24 h, 10 µL resazurin dye was added in each well, and plates were again incubated for 2 h. The viability of bacterial cells was indicated by color change from purple to pink or colorless (Virk *et al*., 2019).

2.10. Statistical Analysis

All the experiments were done in triplicates for each sample and the results expressed as mean ± SD. IC_{50} values were calculated by linear regression.

3. Results

3.1. Morphological Features

The rhizomes of *Bergenia ciliata* were 4-12.3 cm long, 1.2-2.0 cm in diameter, yellowish brown in color, palmate, barrel shaped, with rough surface, characteristic odour and bitter in taste **(Figure 1 and Table 1).**

Figure 1. *Bergenia ciliata* rhizome.

Table 1. Morphological characteristics of *Bergenia ciliata* rhizomes

Features	Observation
Color	Yellowish brown
Odour	Characteristic and slight
Shape	Barrel shaped
Fracture	Short & fibrous
Texture	Rough
Taste	Bitter
Size	4-12.3 cm long and 1.2-2.0 cm in diameter

3.2. Extraction yield

The yield of extraction from rhizomes of *Bergenia ciliata* was determined by using the solvents of different polarity and was found different for each of the solvent used **(Table 2 and Figure 2).** Among solvents tested, the highest yield was obtained by methanol extract (16.23%), followed by aqueous (13.77%), ethanol (9.54%) and chloroform extract (2.54%).

Table 2. The total yield of different extracts

Extract type	Yield (in %)
Aqueous	13.77
Chloroform	2.54
Methanol	16.23
Ethanol	9.54

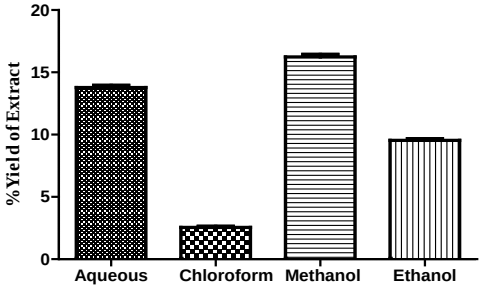

Figure 2. Effect of different solvents on extraction yield.

3.3. Bioactive compounds screening

The present results showed the presence of alkaloids, tannins, flavonoids, phenols, saponins, and carbohydrates **(Table 3).** Large amounts of both primary and secondary metabolites were observed in all the extracts. However, alkaloids were present only in methanol and ethanol extract, whereas proteins were observed only in the chloroform extract.

Table 3. Phytochemicals analysis in different extracts of *Bergenia ciliata* rhizomes

Phytochemical tests	Test Name	Aqueous	Chloroform	Methanol	Ethanol
Alkaloids	Mayer's test	-ve	-ve	+ve	+ve
Carbohydates	Benedict's test	+ve	+ve	+ve	+ve
Flavanoids	Lead acetate test	+ve	+ve	+ve	+ve
Phenol	Ferric chloride test	+ve	+ve	+ve	+ve
Saponins	Froth test	+ve	+ve	+ve	+ve
Proteins	Millon's test	-ve	+ve	-ve	-ve

+ve = present; -ve = not detected

3.4. Total phenolic and flavonoid content

Total phenolic content was calculated from the standard curve of gallic acid using the equation: y= 0.741x+0.1326, while total flavonoid content was calculated using the standard curve of quercetin using the equation: y=0.965x+0.0362 contents.

Total phenolic content obtained was in the range of 11.10 to 31.46 mg GAE g^{-1}. The highest phenolic content was achieved by methanol extract (31.46 mg GAE g^{-1} DE), followed by aqueous (24.66 mg GAE g^{-1} DE) and chloroform extract (12.86 mg GAE g^{-1} DE). The lowest phenolic content was obtained with ethanol extract (11.10 mg GAE g^{-1} DE) (**Figure 3 and Table 4**). Total flavonoid

content was in the range of 10.66 to 19.06 mg RE g^{-1}. The highest flavonoid content was found in aqueous extract (19.06 ± 0.61 mg RE g^{-1} DE), followed by methanol (18.46 mg RE g^{-1} DE), ethanol (14.97 mg RE g^{-1} DE) and chloroform extract (10.66 mg RE g^{-1} DE).

Table 4. Total phenolic and flavonoid content of different extracts of *Bergenia ciliata* rhizomes

Extract type	Total Phenolic content (mg GAE/g DE)	Total Flavonoid content (mg RE/g DE)
Aqueous	24.66 ± 0.69	19.06 ± 0.61
Chloroform	18.46 ± 0.16	10.66 ± 0.93
Methanol	31.46 ± 1.05	18.46 ± 0.16
Ethanol	11.10 ± 0.62	14.97 ± 1.49

Values represent mean ± SD of triplicates; TPC = total phenolic content; TFC = total flavonoid content; mg GAE g^{-1} DE: mg gallic acid equivalents per gram of dry extract of the sample; mg RE g^{-1} DE: mg rutin equivalents per gram of dry extract of the sample.

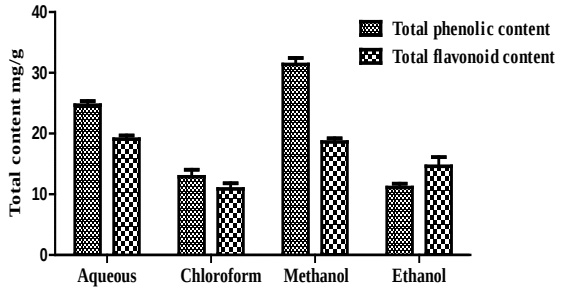

Figure 3. Phenolic and flavonoid content in different extracts of *Bergenia ciliata* rhizomes.

3.5. Antioxidant activity

All the extracts of *Bergenia ciliata* rhizomes exhibited good antioxidant properties, which varied with the type of solvents. The best activity for DPPH assay was observed in methanol extract (IC_{50} = 80.20 µg mL^{-1}), followed by aqueous (IC_{50} = 135.2 µg mL^{-1}) and chloroform extract (IC_{50} = 138.2 µg mL^{-1}), respectively **(Figure 4 and Table 5).**

Table 5. Antioxidant activity of different extracts of *Bergenia ciliata* rhizomes

Extract type	DPPH radical IC_{50} (µg mL^{-1})	ABTS radical IC_{50} (µg mL^{-1})
Aqueous	135.2	94.8
Chloroform	138.2	118.8
Methanol	80.20	73.38
Ethanol	184.6	141.4
Ascorbic acid	22.53	28.3

Each value represents the mean ± SD of triplicates. IC_{50} = half maximal inhibitory concentration; DPPH= 2,2-diphenyl-1-picrylhydrazyl; ABTS= (2,2'-azino-bis(3-ethylbenzothiazoline-6-sulfonic acid))

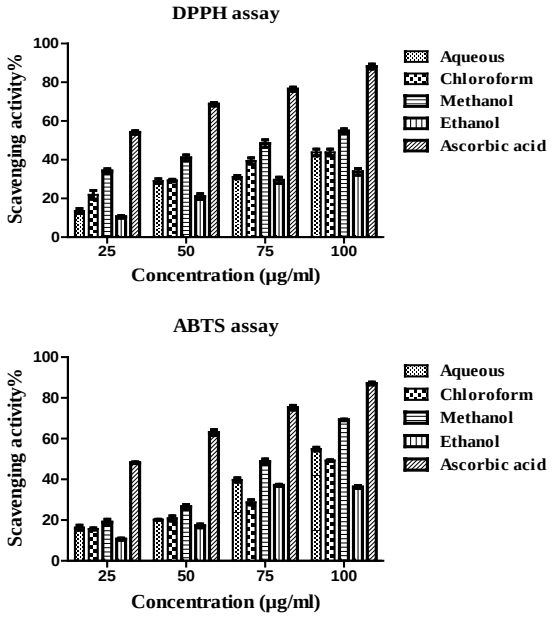

Figure 4. DPPH and ABTS assay of different extracts of *Bergenia ciliata* rhizomes.

In case of ABTS assay, the best activity was observed in methanol extract (IC_{50} = 73.38 µg mL^{-1}), followed by aqueous (IC_{50} = 94.81 µg mL^{-1}) and chloroform extract (IC_{50} = 118.8 µg mL^{-1}). The lowest activity was observed in ethanol extract with IC_{50} value of 184.6 and 141.4 mg mL^{-1} for DPPH and ABTS assay. Ascorbic acid was used as a standard, which exhibited an IC_{50} value of 22.53 and 28.30 µg mL^{-1} for DPPH and ABTS assay, respectively.

3.6. Antibacterial activity and MIC

All the extracts were active against bacterial strains and showed a range between 10.33 ± 0.47 to 17.0 ± 0.81 mm **(Table 6 and Table 7).** The methanol and ethanol extracts of rhizomes appeared to be the most active against all strains. The best activity was obtained by methanol extract of rhizome (IZD = 17 mm; MIC = 6.25 µg/mL^{-1}) against *E. coli* **(Figure 5).** The same extract was active against *S. aureus* and *S. typhi* with (Inhibition zone diameter (IZD) = 15.6 mm and 14.6 mm; MIC = 6.25 µg/mL^{-1}). The chloroform and aqueous extract exhibited the lowest effect against all the tested bacteria (IZD range of 10.3 ± 0.47 to 12.3 ± 0.94 mm, and MIC is 6.25–25 µg/mL^{-1}). However, this antibacterial activity was less than that of ampicillin.

Table 6. Antibacterial activity of different extract of *Bergenia ciliata* rhizomes

	Microorganism		
Extracts	*E. coli*	*S. aureus*	*S. typhi*
Aqueous	12.3 ± 0.94	10.3 ± 0.47	12.6 ± 0.47
Chloroform	11.3 ± 0.47	12.0 ± 0.81	11.6 ± 0.47
Methanol	17.0 ± 0.81	14.6 ± 0.94	15.6 ± 0.94
Ethanol	16.0 ± 0.81	16.3 ± 0.47	14.6 ± 0.47
Amp	27.6 ± 0.47	24.3 ± 0.81	24.3 ± 0.47
DMSO	ND	ND	ND

Zones of inhibition (mm) are presented as mean ± SD. *E. coli* = *Escherichia coli*, *S. typhi* = *Salmonella typhi*, *S. aureus* = *Staphylococcus aureus*; IZD: Inhibition zone diameter (mm); Amp =Ampicillin (positive control); DMSO = dimethyl sulfoxide (negative control); ND (not detected).

Table 7. Minimum Inhibitory Concentration against test organisms (µg/mL^{-1})

Extracts	*E. coli*	*S. aureus*	*S. typhi*
Aqueous	6.25	12.5	12.25
Chloroform	25	25	12.25
Methanol	6.25	6.25	6.25
Ethanol	6.25	6.25	6.25

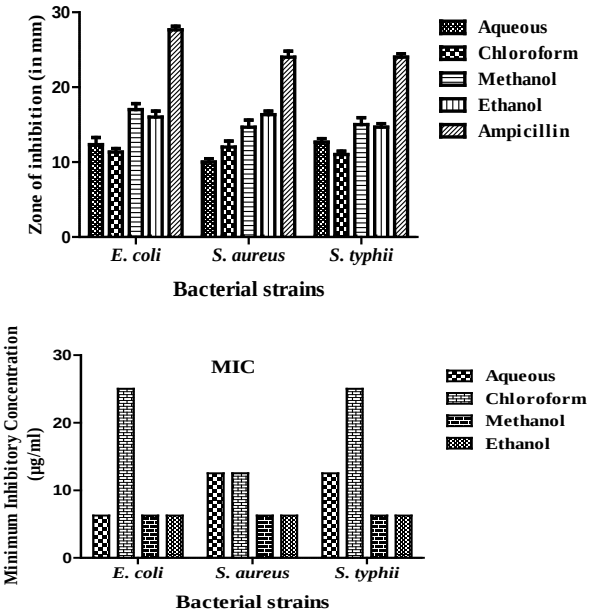

Figure 5. Antibacterial and MIC of different extracts of *B. ciliata* rhizomes.

4. Discussion

Natural products have been traditionally employed since prehistoric times for the maintenance of general health conditions and management of various ailments. They provide clues to investigate and isolate bioactive components in modern era. Results showed that methanol extract yield greater quantities of active compounds as compared to solvent extracts and also possessed good antioxidant and antimicrobial activities. The preliminary phytochemical screening tests might be helpful in the identification of the pharmacologically bioactive components in the plant material and subsequently lead to discovery and development of drugs (Bhandary *et al*., 2012). Results obtained in this study indicated the presence of alkaloids, carbohydrates, flavonoids, phenols, saponins and proteins. The presence of these secondary metabolites in rhizomes extract of *Bergenia ciliata* is in agreement with the previous reports (Uddin *et al*., 2012 and Ahmad *et al*., 2018). These differences could be attributed to the exposure to adverse conditions; parasitic or microbial infection of the plant prior to collection as most phytochemicals are secondary metabolites that are produced in response to such activities (Vila *et al*., 2016). The presence of alkaloids, anthraquinones, flavonoids, and saponins in the leaf and root extracts of *Bergenia ciliata* was similar to other reports (Pokhrel *et al*., 2014). Water also meets the definition of green solvent which has a low environment and health hazard (Li *et al*., 2008 and Welton *et al*., 2015). The extraction yield may be affected by several parameters, including temperature, time, the type of solvent, solvent to sample ratio and the number of extraction cycles (Che *et al*., 2017 and Efthymiopoulos *et al*., 2018). This study showed that total phenolic content of the solvent extracts was in the given order methanol > aqueous > chloroform > ethanol. This is due to the polarity of extracting solvent and the solubility of chemical constituents in the solvent, (Singh *et al*., 2014) which may be due to the influence of dielectric constant, organic solvent structure and chemical properties of phytochemicals (Cheok *et al*., 2012 and Jayaprakasha *et al*., 2003). The total phenolic content reported in the rhizome extract of *Bergenia ciliata* was 442 mg GAE g^{-1} which was much higher than the values obtained for the rhizome extract of *Bergenia ciliata* in this study (Singh *et al*., 2013). These findings are in good agreement with the previous study, which reported methanol as an effective solvent for extraction of antioxidant and phenolic compounds. According to the present study, no difference in the total phenolic content was observed in the rhizome extract of *Bergenia ciliata* collected from Sikkim Himalaya, and the rhizome extract of *Bergenia ciliata* collected from Shimla region. Total flavonoid content was found to be higher in the aqueous extract and the lowest in the chloroform extract. These results are not in agreement with the previous work, which reported that flavonoid content in the extracts depends on the solvent polarity (Singh *et al*., 2017 and Hajji *et al*., 2009).

Antioxidants are important defense mechanisms in preventing the harmful effects of free radicals (Birben *et al*., 2012 and Kedare *et al*., 2011). The methanol extract had high antioxidant activity, when assessed with ABTS and DPPH assay. However, the antioxidant activities were lower as compared to the positive controls. The methanol and aqueous extract of *Bergenia ciliata* rhizome possess strong antioxidant activities as compared to the n-hexane fraction (Uddin *et al.*, 2012).

Another investigation also confirmed that both methanol and aqueous solvents were found to be more active radical scavengers (Rajkumar *et al*., 2010). Our results revealed that there is a significant correlation between phytochemical and antioxidant assays that could be attributed to the different mechanism of the radical antioxidant reaction. Li et al have also reported statistical correlation between the TPC and IC_{50} values which confirmed that phenolic content contributes to the free radical scavenging activity of the plant metabolites (Li *et al*., 2009).

The present study supported strong antimicrobial activity of *Bergenia ciliata* rhizome against important pathogenic bacteria. The methanol and ethanol extract showed highest antibacterial activity and MIC against *E. coli, S. typhi* and *S. aureus.* The earlier study revealed a wide range of antimicrobial activity of different concentrations (200-1000 µg/disc) in methanol extract of *Bergenia ciliata* (Sinha *et al*., 2001). Methanolic extract shows the high antimicrobial activity due to the presence of high phenols and flavonoids content in the plant extract. These results are similar with the earliest study where similar resulted were reported in case of *B. ligulata* leaf extracts (Agnihotri *et al*., 2014).

5. Conclusion

The present study concluded that the methanolic extract of *Bergenia ciliata* rhizome contains the highest Total phenolic content and also exhibited high scavenging activity against DPPH and ABTS radicals. Methanol extract also exhibited strong antimicrobial activity against bacteria. *Bergenia ciliata* is a good source for the isolation of antioxidant and antibacterial compounds that can be a breakthrough for pharmaceutical industry.

Acknowledgment

Authors are highly thankful to the School of Bioengineering and Food Technology, Shoolini University, Solan, India.

Reference

Agnihotri V, Sati P, Jantwal A and Pandey A. 2014. Antimicrobial and antioxidant phytochemicals in leaf extract of *Bergenia ligulata*: a Himalayan herb of medicinal value. *Nat Prod Res*, **29:** 1074–1077.

Agu KC and Okolie PN. 2017. Proximate Composition, Phytochemical Analysis, and in Vitro Antioxidant Potentials of Extracts of *Annona Muricata* (soursop). *Food Sci. Nutr*, **5:** 1029–1036.

Ahmad M, Butt MA, Zhang G, Sultana S, Tariq A and Zafar M. 2018. *Bergenia ciliata*: A comprehensive review of its traditional uses, phytochemistry, pharmacology and safety. *Biomed Pharmacother*, **97:** 708-721.

Asgharian A and Ojani S. 2017. In Vitro Antioxidant Activity and Phytochemical Screening of Flowers and Leaves of *Hypericum Perforatum* L. Ethanolic Extracts from Tonekabon-Iran. *J. Phytochem. Biochem*, **1:** 1–5.

Asolkar LV, Kakkar KK and Chakre OJ. Glossary of Indian Medicinal Plants with active principles. PID, CSIR, New Delhi; 1992. p.122.

Bagul MS, Ravishankara, MN, Padh H and Rajani M. 2003. Phytochemical evaluation and freeradical scavenging properties of rhizome of *Bergenia ciliata* (Haw.) Sternb. forma *ligulata* Yeo. *J. Nat. Remed*, **3:** 83–89.

Barros L, Ferreira MJ, Queiros B, Ferreira IC and Baptista P. 2007. Total phenols, ascorbic acid, β-carotene and lycopene in Portuguese wild edible mushrooms and their antioxidant activities. *Food chem*, **103:** 413–419.

Bhandary SK, Kumari SN, Bhat VS, Sharmila KP and Bekal MP. 2012. Preliminary Phytochemical Screening of Various Extracts of *Punica Granatum* Peel, Whole Fruit and Seeds. *Nitte Univ. J. Heal. Sci*, **2:** 34–38.

Bhattarai NK. 1994. Folk herbal remedies for gynaecological complaints in Central Nepal. *Inf. J. Phrmaccog*, **32:** 13.

Birben E, Sahiner UM, Sackesen C, Erzurum S and Kalayci O. 2012. Oxidative Stress and Antioxidant Defense. *World Allergy Organ J*, **5:** 9–19.

Chauhan R, Kumari R and Dwivedi J. 2012. Pashanbheda a golden herb of Himalaya: a review. *Int J Pharm Sci Rev Res*, **15:** 24–30.

Che Sulaiman IS, Basri M, Fard Masoumi HR, Chee WJ, Ashari SE and Ismail M. 2017. Effects of Temperature, Time, and Solvent Ratio on the Extraction of Phenolic Compounds and the Anti-radical Activity of *Clinacanthus Nutans Lindau* Leaves by Response Surface Methodology. *Chem. Cent. J*, **11:** 54.

Cheok CY, Chin NL, Yusof YA and Law CL. 2012. Extraction of Total Phenolic Content from Garcinia Mangostana Linn. Hull. I. Effects of Solvents and UV–vis Spectrophotometer Absorbance Method. *Food Bioprocess. Tech*, **5:** 2928–2933.

CLSI. 2012 Methods for Dilution Antimicrobial Susceptibility Tests for Bacteria That Grow Aerobically, Approved Standard, 9th ed, Clinical and Laboratory Standards Institute, 950 West Valley Road, Suite 2500, Wayne, Pennsylvania 19087, USA, M07–A9.

Das K. Tiwari RS and Shrivastava DK. 2010. Techniques for evaluation of medicinal plants as antimicrobial agents: Current methods and future trends. J. *Med. Plant Res*, **4:** 104–111.

Dharmender R, Madhavi T, Reena A and Sheetal, A. 2010. Simultaneous quantification of bergenin, (þ)-catechin, gallicin and gallic acid; and quantification of ß-sitosterol using HPTLC from *Bergenia ciliata* (Haw.) Sternb. *Forma ligulata Yeo* (Pasanbheda). *Pharm Anal Acta*, **1:** 104.

Ebong PE. 2015. Phytomedicine: Panacea for Primary Health Care Delivery in Nigeria; Univercity of Calabar Press: Calabar, Nigeria, 63–74.

Efthymiopoulos I, Hellier P, Ladommatos N, Russo-Profili A, Eveleigh A, Aliev A, Kay A and Mills-Lamptey B. 2018. Influence of Solvent Selection and Extraction Temperature on Yield and Composition of Lipids Extracted from Spent Coffee Grounds. *Ind. Crops Prod*, **119:** 49–56.

Farooquee NA, Majila, BS and Kala CP. 2004. Indigenous knowledge systems and sustainable management of natural resources in a high-altitude society in Kumaun Himalaya India. *J Hum Eco*, **16:** 33–42.

Hajji M, Masmoudi O, Ellouz-Triki Y, Siala R, Gharsallah N and Nasri M. 2009. Chemical composition of volatiles and antioxidant and radical-scavenging activities of *Periploca laevigata* root bark extracts. *J Sci Food Agric*, **89:** 897–905.

Harborne J. 2012. Phytochemical methods: A guide to modern techniques of plant analysis, Springer Science & Business Media.

Hazra B, Sarkar R, Biswas S and Mandal N. 2010. Comparative study of the antioxidant and reactive oxygen species scavenging properties in the extracts of the fruits of *Terminalia chebula*, *Terminalia belerica* and *Emblicaofficinalis*. *BMC Complement. Altern. Med*, **10:** 1–20.

Hsieh PC, Mau JL and Huang SH. 2001. Antimicrobial effect of various combinations of plant extracts. *Food Microbiol*, **18:** 35–43.

Islam MU, Azhar I, Usmanghani K, Gill MA, Din SU and Ahmad, A. 2002. Antifungal activity evaluation of *Bergenia ciliata*. *Pak. J. Pharmacol*, **192:** 1-6.

Jayaprakasha GK, Selvi T and Sakariah KK. 2003. Antibacterial and Antioxidant Activities of Grape (*vitis Vinifera*) Seed Extracts. *Food Res. Int*, **36:** 117–122.

Johnson OO and Ayoola GA. 2015. Antioxidant activity among selected medicinal plants combinations (multicomponent herbal preparation). *Int. J. Res. Health Sci*, **3:** 526–532.

Kedare SB and Singh RP. 2011. Genesis and Development of DPPH Method of Antioxidant Assay. *J. Food Sci. Technol*, **48:** 412–422.

Kokate CK. 2005. Practical Pharmacognosy. 4th ed. Delhi, Published by Vallabh Prakashan. 22–23.

Li CJ and Trost BM. 2008. Green Chemistry for Chemical Synthesis. *Proc. Natl. Acad. Sci*. U. S. A. **105:** 13197–13202.

Li X, Wu X and Huang L. 2009. Correlation between antioxidant activities and phenolic contents of radix *Angelicae sinensis* (Danggui). *Mol*, **14:** 5349–5361.

Manandhar NP. 1995. Medicinal folk-lore about the plants used as antihelmintic agents in Nepal. *Fitoter*, **66:** 149–155.

Mercy R and David Udo E. 2018. Natural products as lead bases for drug discovery and development. *Res. Rep. Med. Sci*, **2:** 1–2.

Pandey A and Agnihotri V. 2015. Antimicrobials from medicinal plants: research initiatives, challenges and the future prospects. In: Gupta VK, Tuohy MG, O'Donovan A, Lohani M, eds. Biotechnology of Bioactive Compounds: Sources and Applications in Food and Pharmaceuticals. John Wiley & Sons Ltd. 123-150.

Perez C, Paul M and Bazerque P. 1990. Antibiotic assay by agar-well diffusion method. *Acta Biol. Med. Exp*, **15:** 113–115.

Pokhrel P, Parajuli RR., Tiwari AK and Banerjee J. 2014. A short glimpse on promising pharmacological effects of *Bergenia ciliata*. *JOAPR*, **2:** 1–6.

Pradhan B and Badola HK. 2008. Ethnomedicinal plant use by Lepcha tribe of Dzongu valley, bordering Khangchenzonga Biosphere Reserve, in North Sikkim. *India J Ethnobiol Ethnomed*, **4:** 22.

Rai LK, Prasad P and Sharma E. 2000. Conservation threats to some important medicinal plants of the Sikkim Himalaya. *Biol Conserv*, **93:** 27–33.

Rajkumar V, Gunjan Guha G, Kumar RA and Mathew L. 2010. Evaluation of Antioxidant Activities of *Bergenia ciliata* Rhizome. *Rec. Nat. Prod*, **4:** 38–48.

Re R, Pellegrini N Proteggente A, Pannala A, Yang M and Rice-Eas C. 1999. Antioxidant activity applying an improved ABTS radical cation decolorization assay. *Free Radic. Biol. Med*, **26:** 1231–7.

Ruby K, Chauhan R, Sharma S and Dwivedi J. 2012. Polypharmacological activities of Bergenia species. *Int. J. Pharm. Pharm. Sci*, **1:** 100–109.

Sajad T, Zargar A, Ahmad T, Bader GN Naime M and S Ali. 2010. Antibacterial and antiinflammatory potential of *Bergenia ligulata*. *Am J Biomed Sci*, **2:** 313–32

Savoia D. 2012. Plant-derived antimicrobial compounds: alternatives to medicines. *Future Microbiol*. **8:** 979–990.

Singh M, Jha A, Kumar A, Hettiarachchy N, Rai AK and Sharma D. 2014. Influence of the Solvents of Major Phenolic Compounds (punicalagin, Ellagic Acid and Gallic Acid) and Their Antioxidant Activities in Pomegranate Aril. *J. Food Sci. Tec*, **51:** 2070–2077.

Singh M, Pandey N, Agnihotri V, Singh KK and Pandey A. 2017. Antioxidant, antimicrobial activity and bioactive compounds of *Bergenia ciliata* Sternb.: A valuable medicinal herb of Sikkim Himalaya. *J Tradit ComplemenT Med*, **7:** 152–157.

Singh M, Roy B, Tandon V and Chaturvedi R. 2013. Extracts of dedifferentiated cultures of *Spilanthes acmella* Murr. possess antioxidant and anthelmintic properties and hold promise as an alternative source of herbal medicine. *Plant Biosyst*, **148:** 259–267.

Singleton V. 1999. Analysis of total phenols and other oxidation substrates and antioxidants by means of Folin-Ciocalteu reagent. *Methods Enzymol*, **299:** 152–178.

Sinha S, Murugesan T, Maiti K, Gayen JR, Pal M and Saha BP. 2001. Evaluation of antiinflammatory potential of *Bergenia ciliata* Sternb. rhizome extract in rats. *J Pharma Pharmacol*, **53:** 193–196.

Turner C. 2006. Overview of modern extraction techniques for food and agriculture samples. 3-19.

Uddin G, Rauf A, Arfan M, Ali M, Qaisar M, Saadiq M and Atif M. 2012. Preliminary Phytochemical Screening and Antioxidant Activity of *Bergenia ciliata. Middle-East J Sci. Res*, **11:** 1140-1142.

Vila E, López S, Johnson R, Römling U, Dobrindt U, Cantón R, Giske C, Naas T, Carattoli A and Martínez-Medina M. 2016. *Escherichia coli*: An Old Friend with New Tidings. *FEMS Microbiol. Rev*, **40:** 437–463.

Virk AK, Kumari C, Tripathia A, Kakadec A, Lic X and Kulshrestha S. 2019. Development and efficacy analysis of a *Moringa oleifera* based potable water purification kit. *J Water Process Eng*, **27:** 37–46.

Walter NS, Bagai U and Kalia S. 2013. Antimalarial activity of *B. ciliata* (Haw) Sternb against *Plasmodium berghei*. *Parasitol Res*, **112:** 3123–3128.

Welton T. 2015. Solvents and Sustainable Chemistry. *Proc. Math Phys. Eng. Sci*, **471:** 20150502.

Zhishen J, Mengcheng T and Jianming W. 1999. The determination of flavonoid contents in mulberry and their scavenging effects on superoxide radicals. *Food Chem*, **64:** 555–559.

Zulfiqar S, Abidi AI, Shakir HA and Ali SS. 2017. Preliminary Screening of Some Plants of Punjab. Pak. *Phytochem*, **63:** 179–191.

JJBS

Volume 14, Number 1, March 2021
ISSN 1995-6673
Pages 31 - 39

Jordan Journal of Biological Sciences

The one-pot synthesis of some bioactive pyranopyrazoles and evaluation of their protective behavior against extracellular H_2O_2 and SNP in *T. Thermophila*.

Boutaina Addoum[1], Bouchra El khalfi[1], Reda Derdak[1], Souraya Sakoui[1], Abdelhakim Elmakssoudi[2,] and Abdelaziz Soukri[1,*]

[1]*Laboratory of Physiopathology, Genetics Molecular and Biotechnology (PGMB), Department of Biology, Faculty of Sciences Ain Chock, Research Center of Health and Biotechnology, Faculty of Sciences Aïn Chock, Hassan II University, B.P 5366 Maarif, Casablanca, Morocco,*[2]*Laboratory of Organic Synthesis, Extraction, and Valorization (OSEV), Department of Chemistry, Faculty of Sciences Aïn Chock, Hassan II University, B.P 5366 Maarif, Casablanca, Morocco.*

Received Feb 29, 2020; Revised June 13, 2020; Accepted June 26, 2020

Abstract

This study aims to evaluate the antioxidant activity of pyranopyrazoles derivatives synthesized *via* multicomponent reaction and characterized by spectroscopic techniques (^{1}H-NMR; ^{13}C-NMR and IR). All the synthesized compounds were screened for their anti-stress properties *in vivo* by using as a test organism the eukaryotic cells "*Tetrahymena*" exposed to oxidative and nitrosative stress. Thereafter the antioxidant activity *in vitro* is performed by using the 2,2-diphenyl-1-picrylhydrazyl (DPPH) scavenging assays.

Our results clearly showed the protective behavior of the compounds studied **(5a** and **5b)**, especially against H_2O_2-induced stress. On the other hand, the *in vitro* bioassays reveal that the **5a** derivative possesses significant antioxidant activity much greater than ascorbic acid (Vitamin C). All these findings confirmed the prominent antioxidant behavior of the synthesized compounds **5a** and **5b**. However, further studies are needed to describe the mechanism action and the effect of substitution on the activity of these compounds.

Keywords: Pyranopyrazoles, *Tetrahymena*, Stress, Antioxidant Activity, Synthesis.

1. Introduction

Oxidative stress is defined as the aggression of cellular constituents associated with an unbalance between reactive species and the antioxidant system (Kumar et *al*., 2015). The cells are damaged when they are emerged by ROS and RNS, it includes nucleic acids (DNA, RNA), proteins and lipids sequestration, which play an important role in the pathogenesis of several diseases (Fourrat *et al*., 2007).

Recently, a large variety of synthetic products were aberrantly exploited as efficient antioxidant drugs, which supports the inner antioxidant defense system (SOD, GLx, Glutathione, Vitamin C) and overcomes many free radical-related diseases including cancer, diabetes, kidney failure, Alzheimer's, and Parkinson's (Pisoschi and Pop, 2015).

Among these efficient and available synthetic products, we found the pyranopyrazoles derivatives (Dove P, 2016) that are considered as primeval measuring sticks for expansive preclinical and pharmacological investigations (Debasis, Banerjee, and Mitra, 2014) due to their wide-ranging activities such as antioxidant, antibacterial, antiviral, antifungal, anti molluscoidal and analgesic behavior (Mamaghani and Hossein Nia, 2019).

This study began with the synthesis of pyranopyrazoles derivatives *via* a multicomponent reaction (MCR) approach (Zahouily *et al.*, 2005) starting from aromatic aldehyde, ethyacetoacetate, malononitrile and hydrazine hydrate in the presence of $Na_2CaP_2O_7$ (Tekale *et al*., 2013) as a catalyst in a green solvent (water) (Maleki *et al*., 2016). Then the bioactivity of these compounds was screened *in vivo* and *in vitro*. In this regard, the well-studied protozoan *Tetrahymena thermophila* (Mar *et al*., 2017; Sugimoto *et al*., 1960) was subjected to oxidative and nitrosative stress then was treated with these compounds. This protozoan can be easily cultured and maintained under laboratory conditions (Doerder and Brunk, 2012) and their sensitivity to stress (Zhang *et al*., 2015) exposure encouraged several researchers to consider this freshwater ciliate as a standard test organism to understand many cellular and molecular processes (Huang *et al.*, 2016). On the other side, these compounds were subjected also to the DPPH test to confirm their protective potential *in vitro* compared to the ascorbic acid as a potent antioxidant.

To be specific, the protective effects of pyranopyrazoles on *T. thermophila* have not been evaluated so far. Hence, we tested, examined and discussed for the first time the effects of these compounds on the physiological and kinetic parameters of *T. thermophila* cells exposed to oxidative stress, however, further studies are needed such as the evaluation of their

* Corresponding author e-mail: ab.soukri@gmail.com.

effect on the specific activity of some antioxidant enzymes like: catalase (CAT), superoxide dismutase (SOD) and GAPDH (Glyceraldehyde 3-phosphate dehydrogenase).

2. Experimental

2.1. Material and methods

2.1.1. Instruments

All the chemicals were purchased from Sigma Aldrich and used without any further purification. The ^{1}H and ^{13}C NMR spectra were recorded on a Bruker 300 MHz in DMSO-d_6 as a solvent. Chemical shifts are given in parts per million (δ-scale). The X-ray diffractometer (XRD) pattern of the diphosphate (DIPH) $Na_2CaP_2O_7$ was recorded on a Bruker D8 Advance X-ray diffractometer with Cu-Kα radiation. The simples were analyzed by FT-IR spectroscopy (using a SCHIMADZU IRAffinity-1S in the range of 4000-400cm^{-1}). Analytical thin-layer chromatography was performed with Silica on TLC Alu foils. Visualization of the developed chromatogram was performed by UV light (254nm). The melting point of the pyranopyrazoles derivatives was determined using a Buchi 510 apparatus.

*2.2. Procedure for synthesis of pyranopyrazoles derivatives **5a** and **5b**.*

The catalyst $Na_2CaP_2O_7$ (20mol %) was added to a mixture of the aromatic aldehyde **1** (salicylaldehyde **1a**, *p*-anisaldehyde **1b**) (1 mmol), ethyacetoacetate **2** (1mmol), malononitrile **3** (1.2 mmol), hydrazine hydrate **4** (2 mmol), and 1 ml of water in a flask fitted with a reflux condenser. The resulting mixture was heated to reflux (an oil bath) with stirring for 20 min. Acetone (2 ml) was added and the mixture stirred for 2 min. The catalyst was removed by filtration and then the resulting crude reaction mixture was poured onto crushed ice and precipitated solid was collected and recrystallized using 96% ethanol to afford pyranopyrazoles **5a** and **5b** (Maleki *et al.*, 2016). The products were well characterized by their melting points ^{1}H, ^{13}C NMR, and IR spectroscopy.

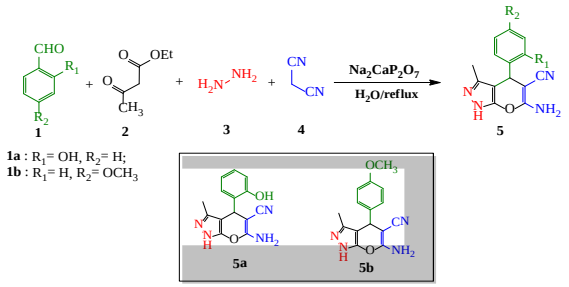

Figure 1. The synthesis reaction catalyzed by the $Na_2CaP_2O_7$.

2.3. Biological Evaluation: microorganisms' growth and toxicological bioassays

2.3.1. Reagents

Peroxide hydrogen and SNP were purchased from Himedia. The culture media such as yeast extract and Tryptone were obtained from Biokar, DPPH, and ascorbic acid were obtained from Sigma-Aldrich. The pyranopyrazoles were synthesized in the Laboratory of Organic Synthesis, Extraction and Valorization according to the references and their structures are summarized in figure 1.

2.3.2. Strains and growth conditions

Before the experiments, the strains *Tetrahymena Thermophila* (SB 1969) were grown axenically in the stock medium of PPYE (1.5% of protease peptone and 0.25% of yeast extract, autoclaved in high-pressure at 120° C for 30 min before use. The culture medium is inoculated with 1 % (v / v) of *Tetrahymena Thermophila* then incubated at 32°C (Addoum *et al.*, 2018; Mar, El Khalfi, and Soukri, 2018).

2.3.3. Cells exposed to stress

To evaluate the effect of stress on protozoan growth, the cultures of *T. thermophila* are treated respectively with 0.4 mM of H_2O_2 and 1.8mM of SNP after 24h of incubation as reported previously in our previous work (Addoum *et al.*, 2018). Each sample (treated and control) was maintained at 32°C for 72h and accompanied by an optical microscope display (A. KRÜSS Optronic) then a cell counting was performed to evaluate the time and number of generation (figure 2).

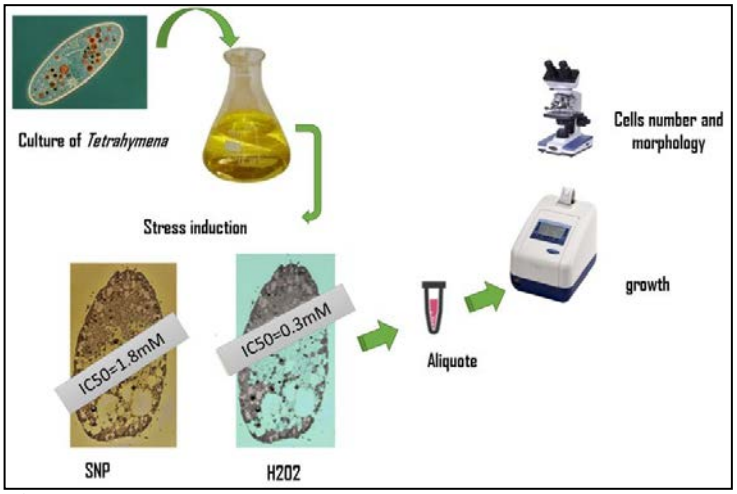

Figure 2. General protocol for stress induction. Cells were grown at 32°C in PPYE medium containing H_2O_2 reagent (0.3mM) or SNP reagent (1.8mM).

2.3.4. Growth measurement

The growth kinetics of *Tetrahymena* was established by daily monitoring of the optical density OD at a wavelength of 600 nm during 120h.

2.3.5. Morphological changes

To observe the morphology of *T. Thermophila* in different experimental conditions (treated and untreated), fresh samples were removed, examined and images were taken using the A. KRÜSS Optronic microscope (magnifications x10).

2.3.6. Cells densities

To determine the cell viability an aliquot of 1ml was taken immediately from the treated cultures and the control then supplemented with a suitable volume of formaldehyde (2-4%). After fixation, the relative cell number was determined by using a hemocytometer counting chamber (Malassez double cells).

2.3.7. Growth Curves

Growth and cell viability curves of *T. Thermophila* were produced based on time-OD and cell density-time. To produce growth curves, flasks of growth medium were inoculated with *Tetrahymena* cells and followed different treatment (stress, antioxidant treatment, and control). During the culture period, growth (OD) and cell number were measured every 24 hours up to 120h. Three biological replicates were included in this study. The obtained values were used to produce the *T. Thermophila* curves and analyzed via the GraphPad prism 8:0.

2.4. Chemicals

2.4.1. Stock solution

A stock solution of pyranopyrazoles (**10mg/mL**) was prepared in dimethylsulfoxide (**DMSO**) (0.01%) (Reddy et *al.*, 2019). Then we prepared a gamut of dilutions from 10-0.6 mg/ML. The prepared molecules were stored at ambient temperature in obscurity.

2.4.2. Toxicity assays

For each derivative two independent tests were performed; we started with the turbidity test that consists to add 5µl of each dilution separately to the culture medium, then we inoculate 1% (v/v) a calibrated inoculum ($1.5x10^5$ cells/mL) of protozoan *Tetrahymena*. Under this experimental condition, the protozoan is maintained at 32°C for 72h. Ultimately, we retain the minimum inhibitory concentration (MIC) to evaluate their protective effects against stress conditions. This concentration was referred to as the lowest concentration of the tested compound that yields a visible growth of the protozoan on the liquid medium tubes. On the other side, this test is confirmed by the investigation of total cells number via microscopic visualization (X10). Estimates of cell viability were reported as a percentage of cell numbers (individuals/ml).

2.5. Antioxidant treatment

To assess the effect of pyranopyrazoles on ROS production; the appropriate stock solution and the test dilutions were selected. Five nominal test concentrations were chosen (table1) and added to a ciliate-containing flask (100 ml of PPYE medium). The treatment with pyranopyrazoles was done at the beginning (t = 0) before the transplantation of *Tetrahymena* cells(105cell/ml). All experiments were performed with protozoan cells in the exponential growth phase. The optical densities of the protozoan are measured by a UV-visible spectrophotometer (Jenway 7315 UV) as described in the literature (Addoum *et al.*, 2018; Errafiy, Ammar, and Soukri, 2013).

Simultaneously the determination of absorbance was accompanied by microscopic imaging analysis and we calculated also the cell densities via hemocytometer technique as described previously in this paper.

In each bioassay, we used two controls: the negative control (Zero mg/mL concentration of pyranopyrazoles), and the positive control (living cells not exposed to stress but treated with pyranopyrazoles). Each concentration was conducted in triplicate.

2.6. DPPH scavenging activity

The detection of the anti-radical activity of pyranopyrazoles was performed by the method of DPPH (El-borai *et al.*, 2016). Various concentrations of selected compounds were mixed with about 1ml of methanol solution then placed in a tube which was added 4ml of DPPH prepared in methanolic solution (0.004%). Then, the tubes are maintained at obscurity for 30 min. The absorbance was screened at 517 nm *via* a UV spectrophotometer; this reduction was accompanied by the color change from purple to yellow. We used as standard various concentrations of the ascorbic acid prepared in distilled water (El-borai *et al.*, 2016).

The percentage inhibition of free radical DPPH (I%) was calculated by the following formula:

$$I\,\% = (A_{control} - A_{sample} / A_{control}) \times 100$$

Where $A_{control}$ reflected the absorbance of the ascorbic acid and A_{sample} is the absorbance of pyranopyrazoles products.

2.7. Statistical Analysis

The statistical data are expressed as mean +/- SD for three successive measurements by using Graph Pad Prism software 8.0. For statistical significance, we used Student's t-test and the P-value was fixed in ≤ 0.05 for a statistically significant difference.

3. Results

3.1. Chemistry

3.1.1. Synthesis

The current study described the catalyzed synthesis of some biologically active pyranopyrazoles by using an ecofriendly catalyst, and these compounds are prepared *via* a one-pot reaction depicted in scheme 2. Primarily, we endeavored to the catalyst four-component commercially available to condense *in situ*; aromatic aldehyde **1**, ethylacetoacetate **2**, hydrazine hydrate **3,** and malononitrile **4** in the water at reflux temperature. The pyranopyrazoles **5a** and **5b** were obtained in high yields (87% and 98 %, respectively).

The structures of the synthesized compounds were confirmed by using spectroscopic techniques.

3.1.2. Characterization Spectroscopic data of synthesized products 5a and 5b

6-Amino-3-methyl-4-(2-hydroxyphenyl)-1,4-dihydropyrano[2,3-*c*] pyrazole-5-carbonitrile 5a: White solid; m.p. 215-218 °C; ^{1}H NMR (300 MHz, DMSO-d_6, ppm): δ 1.9 (s, 3H), 4.56 (s, 1H), 6.70 (2H), 6.94-7.18 (m, 5H), 11.00 (s, 1H); ^{13}C NMR (75 MHz, DMSO-d_6, ppm): δ 9.85, 28.64, 55.06, 104.95, 115.1, 120.79, 123.53, 124.25, 127.55, 128.93, 136.52, 148.39, 159.09, 160.08; IR (KBr, cm^{-1}): 3448, 3419, 3352, 2189, 1660, 1610 (Kanagaraj and Pitchumani, 2010).

6-Amino-3-methyl-4-(4-methoxyphenyl)-1,4-dihydropyrano[2,3-*c*] pyrazole-5-carbonitrile 5b: White solid; m.p. 210-212 °C; ^{1}H NMR (300 MHz, DMSO-d_6, ppm): δ 1.78 (s, 3H), 3.72 (s, 3H), 4.54 (s, 1H), 6.83 (2H), 6.86-7.08 (m, 4H), 12.09 (s, 1H); ^{13}C NMR (75 MHz, DMSO-d_6, ppm): δ 9.66, 35.51, 55.00, 57.9, 97.89, 113.79, 120.69, 128.44, 135.64, 136.43, 154.77, 158.01, 160.68; IR (KBr, cm^{-1}): 3483, 3255, 3113, 2193, 1643, 1602 (Maleki *et al* ., 2016) .

3.1.3. Physical data of synthesized pyranopyrazoles

Table 1. Physical analytic data of synthesized compounds **5a** and **5b**

Compound	Structural Formula	Aspect	Color	R_f	m.p.(°C)	Yield (%)
5a	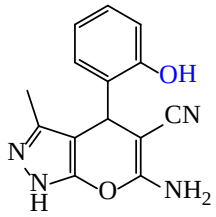		White	0.36	215-218	87
5b	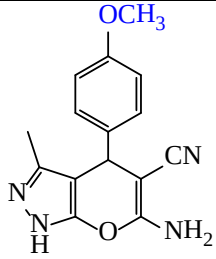		White	0.65	210-212	98

3.2. Toxicological assays

3.2.1. Strains and growth conditions

During this study, we screened the effect of the molecule on the protozoan viability to find the toxic lethal concentration. Accordingly, the results gathered in table 2 demonstrate that both products can be used at their non-toxic concentration (625µg/ml). At this concentration, the growth and viability of this protozoan are not affected.

Table 2. The evaluation of Tetrahymena response after treatment with pyranopyrazoles

Toxicological data	Compound	10mg/ml	5mg/ml	2.5mg/ml	1.25mg/ml	0.625mg/ml	0mg/ml
Turbidity	5a	+++	++++	++++	+++++	+++++	++++++
	5b	++	+++++	+++++	+++++	+++++	++++++
Density	5a	$0.8x10^5$	$1x10^5$	$1.4x10^5$	$1.6x10^5$	$1.8x10^5$	$2x10^5$
	5b	$1.6x10^5$	$1.8x10^5$	$1.9x10^5$	$2x10^5$	$2.2x10^5$	

* (+) means the growth of Tetrahymena in the PPYE medium; - means the absence of Tetrahymena growth in the PPYE medium. The four derivatives are added to the PPYE medium at a non-toxic concentration of 1.25mg/ml. The number of cells is expressed as a function of cells/ml.

3.2.2. Treatment with pyranopyrazoles

3.2.2.1. Effect on the growth of Tetrahymena

By comparing and analyzing the results reported in figure 3, we noticed that the supplementation with **5a** and **5b** derivative protected the normal growth of the protozoan especially against the oxidative stress; besides that, we found that the compound substituted with a hydroxyl group **5a** and **5b** are more active against oxidative stress (Figure 3). This effect is more pronounced and appreciated after 48 h of continuous culture.

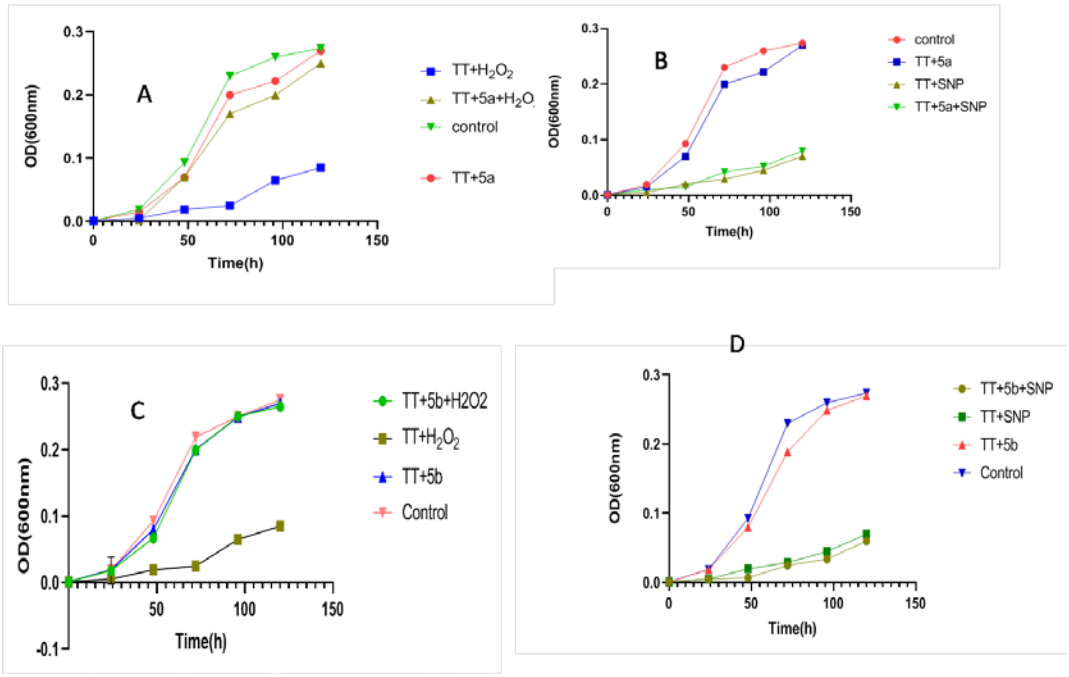

Figure 3. The anti-stress effect of pyranopyrazoles derivatives. Protozoan growth was determined by measuring the absorbance at 600 nm during 120 h. (A) reflected the protective effect of **5a** derivative against oxidative stress and (B) against nitrosative stress. The curve (C) represents the protective effect of **5b** derivative against oxidative stress and (D) against nitrosative stress.

3.2.2.2. Morphological behavior

Light microscopic analysis of treated cells in the PPYE medium showed clearly that *T. Thermophila* exposed to stress are characterized with morphological transformations such as elongated or spherical forms, the close observation demonstrates the presence of conjugation forms, as well as small dark vacuoles that appeared and increased in number with time. After the treatment of samples with **5a** and **5b** derivatives the protist keeps and preserves their normal shape (pear-shape) against stress damage (see figure 4).

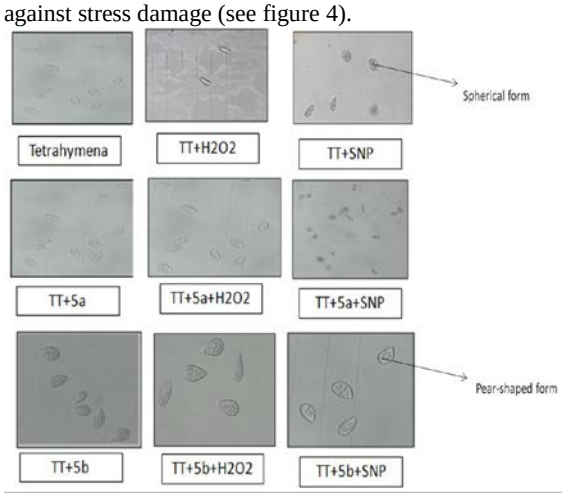

Figure 4. Microscopic analysis images of *Tetrahymena thermophila* (TT) cells. Microscopic images were taken at the objective (x10) of cells grown at 32°C in PPYE medium containing H_2O_2 or SNP as stressors. *Tetrahymena* cells cultivated without stress agents present negative control.

3.2.2.3. The speed swimming of Tetrahymena

The lowest mobility of *Tetrahymena* is recorded under the stress conditions described previously. In close observation, we noticed that some cells moved but not in straight light as the normal shapes. The protozoans exposed to stress are spinning around themselves. Accordingly, an improvement in speed swimming is observed after the addition of the derivative **5a** and **5b** product, which confirms their protective effect (table 3).

Table 3. The protective effect of pyranopyrazoles on physiological parameters of Tetrahymena.

*The density of *Tetrahymena* cells have been detected by using the light microscope and Malassez chamber.

3.2.2.4. The cells densities

Tetrahymena	Density*	Morphology	Speed swimming(motility)
TT	26.10^4 cell/ml	Pear-shaped	Rapid moving
TT+SNP	12.10^4cell/ml	Atypical form	Slight moving
TT+H202	10.10^4cell/ml	Weird form	Slight moving
TT+5a+SNP	13.10^4cell/ml	Atypical form	Slight moving
TT+5b+SNP	14.10^4cell/ml	Atypical form	Slight moving
TT+5a+H_2O_2	25.10^4cell/ml	Pear-shaped	Rapid moving
TT+5b+H_2O_2	20.10^4cell/ml	Pear-shaped	Rapid moving

The results reported in Figures 5 and 6 highlighted that the toxic effect of oxidative stress has reduced a significant number of cells, which confirms that *T. Thermophila* is more sensitive to this agent compared to SNP. The supplementation with pyranopyrazoles to the cultures has preserved a large number of cells. The highest activity was recorded after the addition of the **5a** derivative that protected a high number of *Tetrahymena* cells. As reported in Figures 5 and 6, the cell number of treated samples became similar to the control, which proved the protective potential of these compounds.

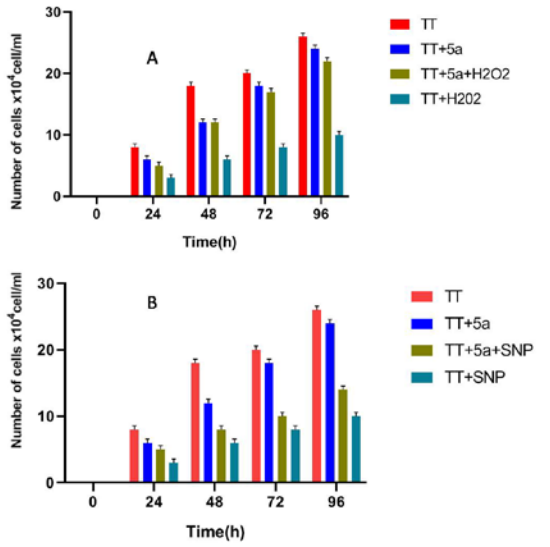

Figure 5. Relative survival of *T. Thermophila* based on cell densities. (A) reflected the protective effect of **5a** derivative against oxidative stress and nitrosative stress(B).

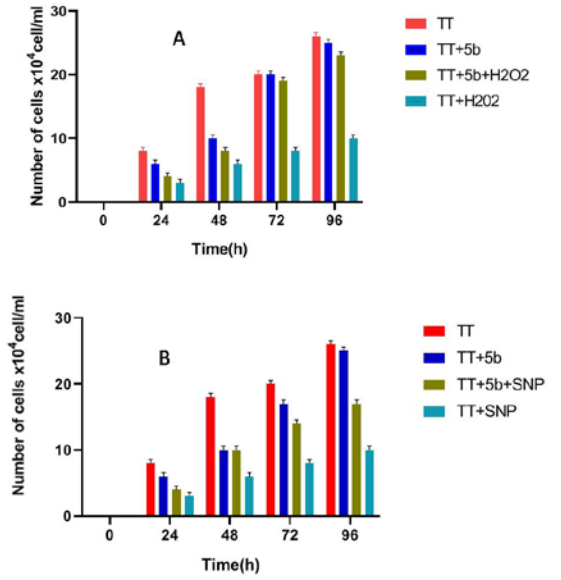

Figure 6. Relative survival of *T. Thermophila* based on cell densities. (A) The protective effect of **5b** derivative against oxidative stress and (B) against nitrosative stress. Error bars reflected the standard deviations for three independent biological replicates, with each experiment being comprised of three individual measurements.

3.2.3. Antioxidant activity in-vitro: test DPPH

By analyzing and comparing the ongoing results we emphasize that the antioxidant activity of the selected pyranopyrazoles **5a** showed an activity that can exceed the antioxidant activity of the ascorbic acid (see figure 7). By analyzing the data reported in these graphs we noticed that the IC_{50} value of **5a** is detected at 6 µg/ml ±0.05 vs. 9 µg/ml ±0.05 for ascorbic acid. In parallel, the antioxidant activity of **5b** is important and shows also a significant activity compared to the antioxidant potential of the reference (see figure 8). Indeed, the IC_{50} value is recorded at 700 µg/ml ±0.05 for **5b** compared to 500 µg/ml ±0.05 for ascorbic acid.

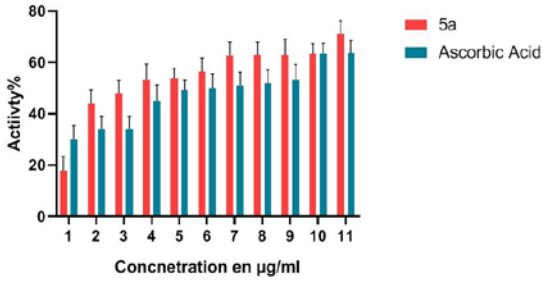

Figure 7. Antioxidant activity (% inhibition of DPPH) under different concentrations of **5a** derivative. Determination of IC50 of the pyranopyrazoles by DPPH method. Ascorbic acid was used as standard.

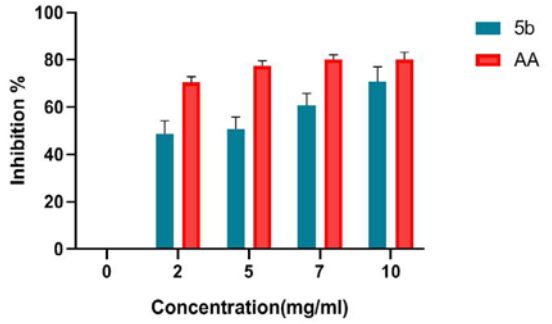

Figure 8. Evaluation of antioxidant properties of pyranopyrazoles **5b** by DPPH assay.

4. Discussion

This paper presents a preliminary study describing the protective effect of pyranopyrazoles products against oxidative and nitrosative stress on *Tetrahymena thermophile* growth, to investigate the possible use of these compounds as anti-stress agents. The evaluation of the acute toxicity of both stressors (H_2O_2 and SNP) on *Tetrahymena* cells will be considered as an important reference value for its further potential utilization to control chronic diseases. This protozoa *Tetrahymena* is characterized by three essential phases of growth (Errafiy and Soukri, 2012): a latent phase that lasts 24 h followed by an exponential phase and a stationary phase that approaches 160h (Mar, El khlafi and Soukri, 2018). When protozoa are treated with stressors, there is a disruption in protozoan growth that varies with the species and stress agent used (Mountassif *et al.*, 2007).

Our finding confirmed that Hydrogen peroxide completely inhibits the growth of *Tetrahymena Thermophila* however the nitroprusside sodium slows its growth (Mar, El khlafi and Soukri, 2018). Similar results have been reported previously by Errafy (Errafiy, Ammar, and Soukri, 2013). Some biological and molecular mechanisms in responses to stress have been examined by using many model organisms including protozoan, yeasts, and vertebrates (Errafiy and Soukri, 2012).

The Toxicities of stressors are routinely determined by analysis of some parameters such as the dynamic growth curves of T. Thermophila; the ciliary movement and the viability of the cells (Addoum *et al*., 2018). In this study,

the authors reported that the treated protozoan with peroxide hydrogen undergo some morphological and physiological transformations, and according to the literature surveys the Hydrogen peroxide acts in oxidative stress as a messenger molecule that diffuses through cells to initiate intermediate cellular effects (Ganjoor and Mehrabi, 2017) such as changes in the shape and recruitment of immune cells (Rahman et *al.,* 2012). Prompted by our finding, we confirmed that the cell densities of the Tetrahymena population were proportional to the IC50 concentration of stressors. At this lethal concentration, cell growth diminished to 50 %. Similar results were observed also by using other stressors such as ethanol (Nilsson, 1974), bromide ethidium (Ashour B, 1980), gelsemine (Ye *et al.*, 2019), and some xenobiotics. These stressors may influence a variety of physiological parameters such as the membrane fluidity, autophagic vacuolization, the rates of cell death and the main speed of *Tetrahymena* cells (Fryb and Henry, 1997)

Nitrosative stress, as well as oxidative stress, can activate a specific route of signalization via the overproduction of NO; this radical can react with ROS such as superoxide anion (O^{2-}) to form peroxynitrite ($ONOO^{-}$) (Sies, 2017). The peroxynitrite is recognized as a biological oxidant that influenced some mitochondrial functions and induced cell death by apoptosis (Sies, 2017).

In our study, we induced nitrosative stress by using the SNP, as a consequence we detected several morphological changes including the appearance of mostly elongated or spherical forms with wide gloomy vacuoles. All that, reflected the harmful effect of SNP that can damage the structure and alter some cellular constituents of the stressed protozoan (DNA; mitochondria; membrane…). On the other hand, excessive NO production can induce a reversible (or irreversible) modification of cellular proteins (Fourrat *et al.*, 2007). NO-induced stress inhibits several enzymes essential for metabolism, including the specific activity of GAPDH via S-nitrosylation correlated with a significant decrease in the growth of protozoan *Tetrahymena Thermophila*. By comparing the effect of both derivatives on the morphology and growth of protozoa in the presence of stressors, we can deduce that **5a** and **5b** compounds have a higher protective effect against the H_20_2-induced stress. The main speed of *Tetrahymena* (motility) is another physiological parameter which should be more studied to assess the cytotoxic effect of stress on the locomotion of this ciliate. The ciliary locomotion of treated protozoan is diminished, which can be an indicator of membrane toxicity; it can be also explained by an alteration of membrane potency. Several research studies indicate that toxicants alter the ion fluxes which have a direct effect on the swimming speed of *Tetrahymena* (Fryb and Henry, 1997)

To the best of our knowledge, the current study is devoted to examining the protective effects of pyranopyrazoles scaffold against stress-induced *Tetrahymena* cells. The supplementation with **5a** and **5b** compound has been improved the motility, the cell number, and the growth curve; which emphasizes the protective effect of both derivatives especially against oxidative damage (Mar *et al*., 2019). We also notified that the **5a** derivative is the most active compound that stimulates also the growth of *Tetrahymena*; this effect can be related to their basic pyranopyrazole skeleton of this compound and the nature of the substituent on the 4-phenyl ring. To remedy the damage caused by oxidative and nitrosative stress, we used two pyranopyrazoles derivatives. These compounds are characterized by several properties, such as antimicrobial, antitumoral, and antioxidant (Shahbazi *et al*. 2019). Nevertheless, these synthesized compounds own a toxic effect against the protozoa *Tetrahymena*. The non-lethal concentration of the two derivatives is used to evaluate their protective effect against stressors. The results reported herein showed clearly that **5a** and **5b** protect protozoa against extracellular H_2O_2, which can be related to the increase of SOD and glutathione peroxidase production (Mountassif et *al.*, 2007). According to the literature surveys, these synthesized products were reported to have significant antioxidant activity. For this purpose, we can say that both compounds used in our study can have a direct effect on the activity of ROS by trapping them or an indirect effect by increasing the production of intracellular antioxidant enzymes (Mar *et al*., 2019).

On the other hand, the study in vitro results reveal that **5a** derivative possesses the top of antioxidant activity compared to the antioxidant of reference. The IC 50 of this product is lower than the value of ascorbic acid (6 µg mL^{-1} for **5a** vs 9 µg mL^{-1} for Ascorbic acid). The second product **5b** besides also a good activity (IC_{50} value is recorded at 7mg/ml) compared to ascorbic (IC_{50} value is 5mg/ml). Overall, our finding established an interesting structure-activity relationship SAR. Likewise, the compound incorporating the hydroxyl group in the *meta*-position of the phenyl group (derivative **5a**) provided an impressive activity against oxidative stress. The most illustrative example has been reported by (Roghayeh, and Mahmoodi 2016), they indicated that the introduction of a hydroxyl group on the aromatic ring of pyranopyrazole can effectively modulate its mechanism of action and increase significantly their free radical scavenging activities (Jouha *et al*., 2017; Harshad G *et al*., 2012). These results are in harmony with our results reported herein.

In summary, the pyranopyrazoles are highly active compounds. Although its chemical structure and stereochemistry have been defined (Reddy *et al*., 2018), nevertheless its biological effects are poorly described.

5. Conclusion

We described herein a simple and efficient approach to synthesize some pyranopyrazoles derivatives. The results reported in this paper confirmed their antioxidant potenti*al.* We are convinced that the current study is a step to underlying the relationship between structure and biological function which will encourage to building-up a variety of motifs occurred via structural modifications onto existing bioactive pyranopyrazoles scaffolds, as a consequence we may enhance the inherent medicinal deed of these compounds or provide their drug-like proprieties.

Acknowledgment

Financial support by the National Center for Scientific and Technical Research (**CNRST**) is gratefully acknowledged. This work was supported also by University Hassan II of Casablanca. All authors wish to

thank Professor Aziz AUHMANI for NMR analysis in the Faculty of Sciences Cadi Ayyad Marrakech in Morocco.

Conflict of interest

All the authors declared that there is no conflict of interest.

Funding statement

This research did not receive any specific grant from funding agencies in the public, commercial, or non-profit sectors.

References

Addoum B, El Khalfi B, Mar PD, Filali Ansari Na, Elmakssoudi A, Soukri A. 2018. Synthesis, Characterization of Some α-Aminophosphonate Derivatives and Comparative Assessment of Their Antioxidant Potential in-Vivo and in-Vitro. *Der pharma Chemica.*,**10(12):**58-67.

Ashour B, Tribe M, and Whittaker P. 1980.The effect of chloramphenicol, ethidium bromide and cycloheximide on mortality and mitochondrial protein synthesis of adult blowflies. *Journal of Cell Science*., **41**:273-289.

Azaam M, El Refaie K, Bad A, El-din A, Khamis A, and El-Magd M. 2018. Antioxidant and Anticancer Activities of α-Aminophosphonates Containing Thiadiazole Moiety. *Journal of Saudi Chemical Society*., **22(1)**:34–41.

Debasis D, Banerjee R, and Mitra A. 2014. Bioactive and Pharmacologically Important Pyrano[2,3-c]Pyrazoles. *Journal of Chemical and Pharmaceutical Research*.,**6(11):**108–16.

Doerder FP and Brunk C. 2012. Learn More about *Tetrahymena Thermophila*. The *Zebrafish: Genetics, Genomics and Informatics*:30–50.

Dove P. 2016. Docking Studies of Hybrid Pyrazole Analogues. *Drug Design, Development and Therapy*.,**10**: 3529–3543.

El-borai M, Rizk HF, Sadek M, and El-keiy M. 2016. An Eco-Friendly Synthesis of Heterocyclic Moieties Condensed with Pyrazole System under Green Conditions and Their Biological Activity. *Green and Sustainable Chemistry*.,**06**(02):88-100.

Errafiy N, Ammar E and Soukri A. 2013. Protective Effect of Some Essential Oils against Oxidative and Nitrosative Stress on *Tetrahymena Thermophila* Growth. *Journal of Essential Oil Research*.,**25(4)**:339–47.

Errafiy N and Soukri A. 2012. Purification and Partial Characterization of Glyceraldehyde-3-Phosphate Dehydrogenase from the Ciliate *Tetrahymena Thermophila*.*Acta Biochimica Et Biophysica Sinica*.,**44(6)**:527–34.

Fourrat L, Iddar A, Valverde F, Serrano A, and Soukri A. 2007. Effects of Oxidative and Nitrosative Stress on *Tetrahymena Pyriformis* Glyceraldehyde-3-Phosphate Dehydrogenase. *The Journal of Eukaryotic Microbiology*.,**54(4):**338–46.

Fryb H and Henry JA. 1997. Membrane Toxicity of Opioids Measured by Protozoan. *Toxicology.*,**117(1):**35-44.

Ganjoor M and Mehrabi M. 2017. Inhibitory Effect of Hydrogen Peroxide and Ionic Silver on Growth of a Pathogenic Bacterium (*Vibrio Harveyi*) Isolated from Shrimp (*Litopenaeus Vannamei*). *Fish & Ocean Opj*: 2(4).

Harshad G, Ranjan G and Manish P. 2012. Microwave-Assisted Multi-Component Synthesis of Indol-3-Yl Substituted Pyrano[2,3-c] Pyrazoles and Their Antimicrobial Activity.*Journal of the Serbian Chemical Society*.,**77(8):**983–91.

Huang AG, Xiao T, Lei L, Gao X W, and Fei L. 2016. The Oxidative Stress Response of Myclobutanil and Cyproconazole on *Tetrahymena Thermophila*. *Environmental Toxicology and Pharmacology*., **41**:211–18.

Jouha J, Loubidi M, Bouali J, Hamri S, Hafid A, Suzenet F, Guillaumet G, Dagcı T, Khouili M, Aydın F, Saso L, and Armagan G. 2017. Synthesis of New Heterocyclic Compounds Based on Pyrazolopyridine Scaffold and Evaluation of Their Neuroprotective Potential in MPP+-Induced Neurodegeneration.*European Journal of Medicinal Chemistry*., **129**:41–52.

Kanagaraj K and Pitchumani K. 2010. Solvent-Free Multicomponent Synthesis of Pyranopyrazoles: Per-6-amino-bcyclodextrin as a Remarkable Catalyst and Host. *Tetrahedron Letters*., **51** :3312–3316.

Kumar KA, Verma AK, Kumar T, and Srivastava R. 2015. Oxidative Stress: A Review.*The international journal of science & Technologie.*,**3(7)**: 2321 – 919.

Mamaghani M, and Hossein Nia R. 2019. A Review on the Recent Multicomponent Synthesis of Pyranopyrazoles. *Polycyclic Aromatic Compounds*.

Maleki B, Nasiri N, Reza T, Khojastehnezhad A, and Akhlaghi HA. 2016. Green Synthesis of Tetrahydrobenzo[b]Pyrans, Pyrano[2,3-c] Pyrazoles and Spiro[Indoline-3,4′-Pyrano[2,3-c]Pyrazoles Catalyzed by Nano-Structured Diphosphate in Water .*RSC Advances*., **6** :79128-79134.

Mar PD, Otto H, El khalif B, and Soukri A. 2019. Biochemical Study of the Protective Effect of *Salvia Officinalis* Essential Oil against the Oxidative Stress Induced by Hydrogen Peroxide in *Tetrahymena Thermophila*. *Derpharma chemica*.,**11(3):**8-12.

Mar PD, El Khalfi B, and Soukri A. 2018. Protective Effect of *Oregano* and *Sage* Essentials Oils against Oxidative Stress in *Tetrahymena Thermophila* and *Tetrahymena Pyriformis*. *Journal of King Saud University - Science.*, **32** :279–287.

Mar PD, El Khalfi B, Perez-Castiñeira JR, Serrano A, Soukri A. 2017. Cell Stress by Phosphate of Two Protozoa *Tetrahymena Thermophila* and *Tetrahymena Pyriformis*. *Advances in Bioscience and Biotechnology*., **8**:451–62.

Mountassif D, Kabine M, Manar R, Bourhim N, Zaroual Z, Latruffe N, and El Kebbaj MS. 2007. Physiological, Morphological and Metabolic Changes in *Tetrahymena Pyriformis* for the in Vivo Cytotoxicity Assessment of Metallic Pollution: Impact on d-β-Hydroxybutyrate Dehydrogenase. *Ecological Indicators* **7(4)**:882–94.

Nilsson JR. 1974. Effects of DMSO on Vacuole Formation, Contractile Vacuole Function, and Nuclear Division in *Tetrahymena Pyriformis* GL. *Journal of Cell Science*., **16(1)**:39-47.

Pisoschi AM, and Pop A. 2015. The Role of Antioxidants in the Chemistry of Oxidative Stress: A Review. European Journal of Medicinal Chemistry., 97:55–74.

Rahman T, Hosen I, Towhidul IM, and Shekhar HU. 2012. Oxidative Stress and Human Health. *Advances in Bioscience and Biotechnology*., **03(07)**:997–1019.

Reddy GM, Jarem RG, Reddy VH, KumariAK, ZyryanovG V, and YuvarajaG. 2019. An Efficient and Green Approach: One Pot, Multi Component, Reusable Catalyzed Synthesis of Pyranopyrazoles and Investigation of Biological Assays. *Journal of Saudi Chemical Society.*, **23(3)**:263–73.

Reddy GM, Jarem RG, Reddy VH, KumariAK, ZyryanovG V, and YuvarajaG. 2018. Highly Functionalized Pyranopyrazoles: Synthesis, Antimicrobial Activity, Simulation Studies and Their Structure Activity Relationships (SARs). *Research on Chemical Intermediates.*,**44(12)**:7491–7507.

Roghayeh SM. 2016. Green and efficient Synthesis of Pyranopyrazoles Using [Bmim] [OH À] as an Ionic Liquid Catalyst in Water under Microwave Irradiation and Investigation of Their Antioxidant Activity. RSC *Advances*: 85877–84.

Shahbazi S, Ghasemzadeh MA, Pegah S, Zolfaghari MR, and Bahmani Ma. 2019. Synthesis and Antimicrobial Study of 1,4-Dihydropyrano[2,3-c] Pyrazole Derivatives in the Presence of Amino-Functionalized Silica-Coated Cobalt Oxide Nanostructures as Catalyst. *Polyhedron*., **170**:172–79.

Sies H. 2017. Redox Biology Hydrogen Peroxide as a Central Redox Signaling Molecule in Physiological Oxidative Stress: Oxidative Eustress. *Redox Biology*., **11**:613–19.

Sugimoto N, Watanabe H, and Ide A. 1960. The Synthesis of L-α-Amino-β-(Pyrazolyl-N)-Propionic Acid in *Citrullus Vulgaris*. *Tetrahedron*., **11(4)**:231–33.

Tekale SU, Kauthale SS, JadhavKM, and Rajendra P P. 2013. Nano-ZnO Catalyzed Green and Efficient One-Pot Four-Component Synthesis of Pyranopyrazoles. *Journal of Chemistry*.,**840954** :8.

Ye Q, Zhang C, Wang Z, Feng Y, Zhou A, Shaolin X, Qiong X, Enfeng S, and Jixing Z. 2019. Induction of Oxidative Stress, Apoptosis and DNA Damage by Koumine in *Tetrahymena Thermophila*. *PLoS ONE*.,**14(2):** e0212231

Zahouily M, Elmakssoudi A, Mezdar A, Rayadh A, Sebti S, and Lazrek H. 2005. Three Components Coupling Catalysed by $Na_2CaP_2O_7$: Synthesis of Amino Phosphonates Under Solvent-Free Conditions at Room Temperature. *Letters in Organic Chemistry*., **2(5)**:428–32.

Zhang SW, Feng JN, CaoY, Meng LP, and Wang SL. 2015. Autophagy Prevents Autophagic Cell Death in *Tetrahymena* in Response to Oxidative Stress. *Zoological Research*.,**36(1):** 167-173.

JJBS

Jordan Journal of Biological Sciences

Volume 14, Number 1, March 2021
ISSN 1995-6673
Pages 41 - 49

Antimicrobial Activities of Natural Volatiles Organic Compounds Extracted from *Dittrichia viscosa* (L.) by Hydrodistillation

Nafila Zouaghi [1], Nour El Houda Bensiradj [2], Carlos Cavaleiro [3], Boubekeur Nadjemi [1] and Ahmad Telfah [4,5,*]

[1]Laboratoire d'étude et de développement des techniques de traitement et d'épuration des eaux et de gestion environnementale. Ecole Normale Supérieure, Kouba, Algeria,[2] Laboratoire de Chimie Théorique Computationnelle et Photonique Faculté de chimie USTHB Algeirs, Algeria ,[3] Centro de Estudos Farmacêuticos / Faculdade de Farmácia, Universidade de Coimbra, Portugal,[4] Leibniz-Institut für Analytische Wissenschaften - ISAS - e.V. 44139 Dortmund, Germany,[5] Hamdi Mango Center for Scientific Research (HMCSR), The University of Jordan, Amman 11942, Jordan

Received Oct 18, 2019; Revised May 1, 2020; Accepted June 26, 2020

Abstract

The chemical characterization and antimicrobial activities of *Dittrichia viscosa* (L.) essential oils extracted by hydrodistillation technique from leaves and stems are reported in this work. *Dittrichia viscosa* (L.) samples were collected from the Bainem forest in the northwest part of Algiers (the capital). Gas chromatography-mass spectrometry (GC-MS) analytical method was employed to identify the oil's chemical composition. It was found that leaves are mainly composed of three major abundant composites, specifically, caryophyllene oxide (10.4%), fokienol (9.6%) and trans-nerolidol (7%). Moreover, the oil isolated from the stems was found to be chiefly composed of trans-totarol (18.1%), α-cedrol (16.7%), and ferruginol (16.6%). Additionally, antimicrobial activity tests were performed on the isolated essential oils using the zone of inhibition (agar disk-diffusion method) to determine the minimum inhibitory concentration (MIC) of four bacteria strains, mainly, *Bacillus subtilis, Staphylococcus aureus, Pseudomonas aeruginosa,* and *Escherichia coli*. The MIC values of leaves are found to range between 15 µg and 100 µg, whereas stems are found to exhibit MIC values ranging between 20 µg and 300 µg. Furthermore, antifungal susceptibility tests, which become important tools to dictate the treatment of fungal diseases, are conducted on two yeast strains: *Saccharomyces cerevisiae* and *Candida albicans*. The obtained antimicrobial results are correlated with the chemical composition findings of the essential oils from leaves and stem to determine the roles of the chemical composites on the antibacterial activity. Interestingly, the oil obtained from the leaves displayed a better inhibitory effect on (bacteria and yeast strains) in comparison with oil (stems). This difference in inhibitory effect can be attributed to the dominant existence of the oxygenated sesquiterpenes and trans-nerolidol compounds in leaves.

Keywords: *Dittrichia viscosa* (L.); Volatile Organic Compounds; Chemical Reactivity; Antibacterial Activity.

1. Introduction

Finding new antibiotics has gained extensive attention, taking into consideration that several existing drugs have become inefficient due to the timewise increase in antimicrobial resistance (AMR) (Prestinaci et *al*., 2015). Nowadays, natural products extracted from plants have become one of the major sources of new drugs. Plants can provide a wide range of complex and structurally diverse compounds. It is well known that plant products constitute a significant sector of the existing antimicrobial compounds (Berdy, 2005).

Many researchers have geared their investigations toward taking advantage of plant and microbial extracts such as essential oils as potential candidates for antimicrobial agents (Runyoro *et al*., 2006; Nazzaro *et al*., 2013). The comparison of the results deduced from different articles on the *in vitro* antimicrobial activities of natural products is of prime importance. However, the comparison is extremely difficult due to the non-standardization of the methodology and the insufficiency of plant products database.

Antibiotics are influential drugs used to fight diseases at large commercial scales. Any powerful antibiotic has a wide range of side effects, consequently, patients taking antibiotics, are subjected to side effects ranging from mild to severe depending on the type of antibiotic, the targeted microbes and the patient himself (Slama *et al*., 2005).

Due to their rich and diverse chemical composition, plants could be very efficient against microbes and thus provide precious sources of natural antimicrobial agents. The elements isolated from plants are important alternatives to many synthetic antimicrobial drugs because of their weak or no side effects and their better bioavailability (Roosita *et al*., 2008). Nevertheless, ensuring minimum toxicity, specific concentrations of the natural products should be considered. Antiquity plants were used as antimicrobial due to their healing and antiseptic properties. *Dittrichia viscosa* (L.) (*D. viscosa)* is a perennial herbaceous plant described as a flowering plant with viscous and glandular leaves (Quezel and Santa, 1963). It is a native of the Mediterranean basin and is

* Corresponding author e-mail: telfah.ahmad@isas.de.

widely distributed in Europe as well as Asia and Australia (Parolin *et al*., 2014). This genus of the *Asteraceae* family includes over 100 species, but only a few species have been tested for their antimicrobial properties (Brullo and Marco, 2000; Seca *et al*., 2014). Figure 1 represents the *D. viscosa* plant, which was reported to possess a high content of phenolic acids and flavonoids. (Grauso *et al*., 2019) interpreted the extensive use of its roots in the traditional Greek-Arabic medicine as an expectorant agent of the mucous membranes to treat cough and catarrh. The medicinal and pharmacological potential of *D. viscosa* plant includes, but not limited to, balsamic, healing, antipyretic, antidiabetic, antichloristic, antiviral, antifungal, antibacterial, and antiseptic applications (Alejandro *et al*., 2008).

Figure 1: Image of D. viscosa and its flowers as well as chemical structure of main volatile constituents.

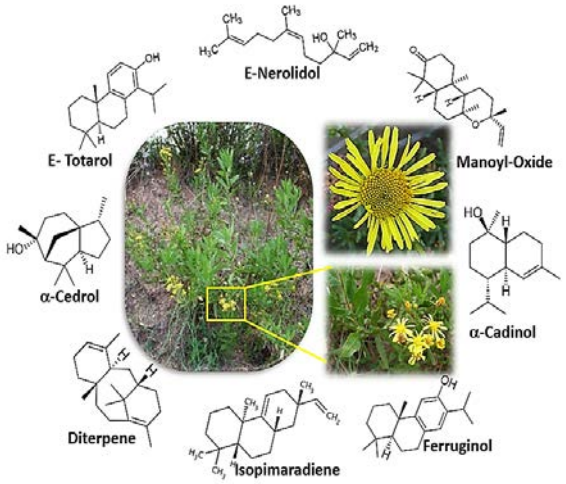

Historically, the D. viscosa was used to treat wounds and injuries, bruises, and intestinal disorders (Laurentis *et al*., 2002). *D. viscosa* extracts have shown anti-inflammatory activity and free radical-generating characteristics enabling it to be efficient in protecting against enzymatic and non-enzymatic lipid peroxidation (Schinella *et al*., 2002).

The study is focused on characterization and investigating the antimicrobial activities of the oil extracted from leaves and stems of *D. viscosa* plant collected from Bainem forest (northwest part of Algiers). Characterization and the chemical variation of the isolated essential oils (leaves and stems) were compared with results obtained from other regional parts of Algeria as well as other countries such as Italy, France, Portugal, Turkey, Tunisia, Syria, Jordan. Furthermore, the *in vitro* antimicrobial activities of the isolated essential oils (leaves and stem) are conducted using the zone of inhibition (agar disk-diffusion method) (Heatley, 1944; Hudzicki, 2009) to correlate the chemical composition of essential oils and their antimicrobial activities.

2. Materiel and Methods

2.1. Plant material and essential oil preparation

D. viscosa leaves and stems were harvested from the Bainem forest located on the northwest part of Algiers on July 27, 2012. The plant was identified by Higher National Agronomic School (E.N.S.A) in Algeria. Collected leaves and stems samples were left to dry in the dark and at ambient room temperature. Later on, the dried samples were submitted to hydrodistillation using a Clevenger type apparatus for 5 hours as described in the literature (European Pharmacopoeia 6.0., 2008).

2.2. Volatile isolation and identification using GC and GC–MS analysis

The volatile isolated were analyzed by gas chromatography (GC) Hewlett-Packard 6890, equipped with a single injector and two flame ionization detection (FID) systems and two Supelco fused silica capillary columns with different stationary phases. Particularly, SPB-1 (poly dimethyl siloxane of dimensions (30 m × 0.20 mm) and film thickness of 0.20 µm and SupelcoWax-10 (polyethylene glycol) were used. The temperature of the oven was programmed to incrementally increase from 70 to 220 ºC at a heating rate of 3 ºC/min. At a temperature of 220 °C, the system was subjected to isothermal invariance for 15 minutes. It worth mentioning that the temperature of the injector and detectors were fixed at 250 ºC. The carrier gas used was helium, and the splitting ratio was 1:40. The GC-MS was carried out in a Hewlett-Packard 6890 gas chromatograph fitted with an HP1 fused silica column (poly dimethyl siloxane (30 m × 0.25 mm (i.d.)) with the film thickness of 0.25µm). The GC parameters, as described above, were as the following: An interface temperature of 250 ºC, MS source temperature of 230 ºC and the MS quadruple temperature of 150 ºC. The ionization energy and current were 70 eV and 60 µA, respectively.

2.3. Identification

Compounds were identified by their GC retention indices on both SPB-1 and SupelcoWax-10 columns and from their mass spectra. Retention indices calculated by linear interpolation relative to retention times of C8–C23 of n-alkanes (Van den Dool and Kratz, 1963) were compared with those of reference samples included in C.E.F. / Faculty of Pharmacy, University of Coimbra laboratory database. Acquired mass spectra were compared with reference spectra from the laboratory database, Wiley (Wiley, 2007), and validated literature data (Cavaleiro *et al*., 2004; Cavaleiro *et al*., 2011). Relative amounts of individual components were calculated based on GC raw data areas without FID response factor correction.

2.4. Antimicrobial tests

2.4.1. Disc diffusion assay

The essential oils obtained from the aerial parts of *D. viscosa* were tested against four bacteria strains (reference strains) and two yeast strains. The bacteria strains used were *Escherichia coli* (ATCC 4157), *Pseudomonas aeruginosa* (ATCC 9027), *Bacillus subtilis* (ATCC 9372), *Staphylococcus aureus* (ATCC 6538). The two yeasts used were *Saccharomyces cerevisiae* (ATCC 601) and *Candida albicans* (ATCC 24433). The microbial strains were supplied by CRD (Center of research and development) of SAIDAL pharmaceutical group Algiers. To carry out the antibacterial test, the bacteria strains were inoculated into nutrient broth Mueller Hinton (MH) at 37 °C for 24 hours, and then the bacterial suspension was obtainable in the time period of 18-24 hours. The same procedure was

repeated for the yeast strains except the incubation temperature was 30 °C, and the suspension was obtained in a time span of 48 hours. Three to five different bacterial colonies from the same patch were placed individually in 6 mL of sterile physiological water. The focus of 10^6 CFU/ml for wavelength 450 nm was obtained (Hammer and Carson, 1999). The 6 mm diameter paper discs were separately impregnated with 25 µg, 100 µg and 300 µg content of the oil dissolved in dimethyl sulfoxide (DMSO) 10% (v/v) (Sigma Aldrich). The paper discs then placed on the nutrient broth, which had previously been inoculated with the selected test microorganism. The plates were left for 1 hour at 4 °C and then incubated for bacteria at 37 °C for 24 hours in the case of bacteria. For yeast strains, the plates were incubated at 30 °C for 48 hours. In addition, the DMSO solvent that was used to dissolve the extracted oil was also used as a negative control. Standard antibiotics Trimethoprim-sulfamethoxazole, Cefixime, Amoxicillin, and Lymecycline at the concentration of 25 µg/disk were employed as positive controls. Antimicrobial activities were assessed in triplicate based on the inhibition zone radius (z), taking into account the disc diameter (6 mm).

2.4.2. The minimum inhibitory concentration (MIC)

The minimum inhibitory concentration (MIC) of different bacterial samples is determined by diluting the essential oil in Mueller-Hinton-agar (MHA). A bacterial suspension of 10^6 CFU/ml is prepared from a modern bacterial culture from 18 to 24 hours. The serial dilution of essential oils in the MH, ranging from 10 to 300 µg. ml^{-1}, are placed in Petri dishes and exposed to drying, as well as Petri dishes without essential oil. Finally, 1 µl of each microbial strain was added to each Petri dish and placed in an incubator at 37 °C for 24 hours. For each concentration, three tests were carried out.

3. Results and Discussion

3.1. Comparison of the Volatiles Compounds

D. viscosa essential oil was obtained by hydrodistillation of leaves and stems in a yield of 0.15% and 0.036%, respectively. Qualitative and quantitative determinations are given in (Table 1 and Figure 2). The chromatographic profile of stems is characterized by high amounts of chief abundant compounds: diterpenoids (69.1%), cis-totarol (18.1%), α-cedrol (16.7%), ferruginol (16.6%), isoabienol (12.1%), abienol (8.3%), isopimaradiene (5.1%), abietatriene (4.0%) and manoyl-oxide (3.6%).

Investigation of the stems of the species *Inula graveolens* revealed a predominance of oxygenated monoterpenes (60.1%) with bornyl acetate (33.4%) and borneol (21.4%) (Harzallah-skhiri et *al*., 2005). A pioneering study conducted on the stems of *Inula candida* (L.) reported the concentrations of the major components to be the flavonoids composition (0.008-0.023%), phenolic acids (0.411-0.516%), total polyphenols (1.53-1.75%), non-tannin polyphenols (0.56-0.78%) and tannins (0.96-1.06%) (Maleš et *al*., 2010). To the best of our knowledge, the analysis of the chemical composition of the essential oils (stems) derived from Algerian *D. viscosa (*same family of the above examples*)* has not been investigated previously. Hence, the detailed report on the analysis of the chemical composition of the essential oils is of great value for relevant future investigations.

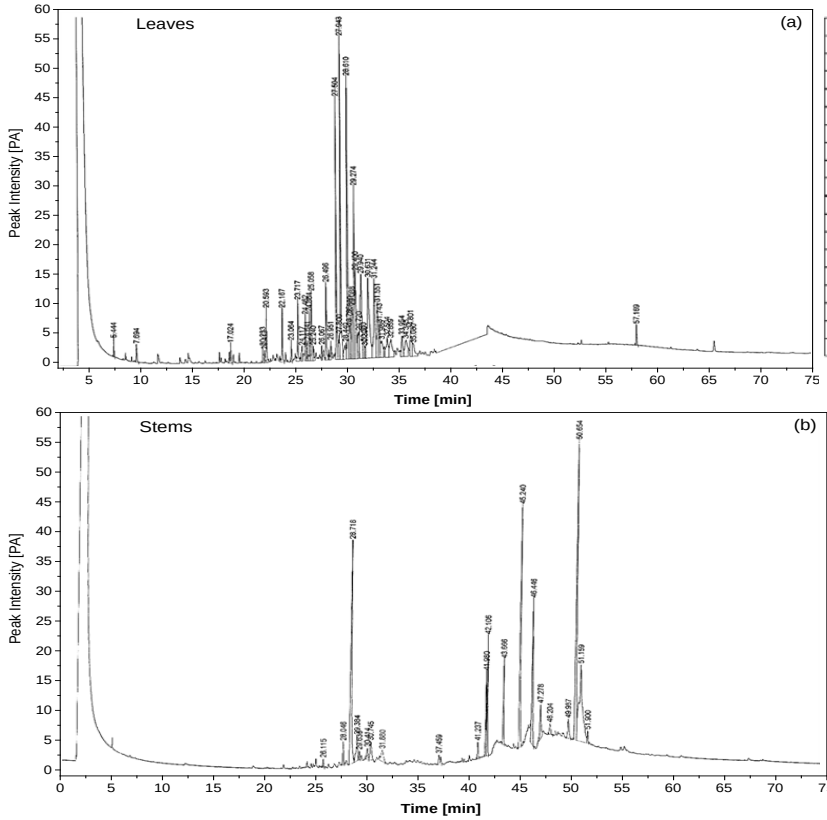

Time	Compound	RI[b]
5.444	α-pinene	929
7.694	limonene	1206
17.024	α-ylangene	1489
20.593	α-copaene	1489
22.167	trans-caryophyllene	1590
23.064	geranyl acetate	1876
23.717	allo-aromadendrene	1638
24.462	ϒ–muurolene	1684
24.641	β-selinene	1716
24.864	selina-3,5-diene	n.d
25.058	Δ-selinene	1716
25.240	α- muurolene	1724
26.067	cis-calamenene	1824
27.504	trans-nerolidol	2032
27.943	caryophyllene oxide	1974
28.610	fokienol	2160
29.940	ϒ-eudesmol	2152
30.631	α-eudesmol	22.09

Time	Compound	RI[b]
26.115	*δ-cadinene*	1747
28.046	*trans-nerolidol*	*2032*
28.715	*α-cedrol*	*2103*
29.384	*T-cadinol*	2152
30.745	*α-cadinol*	2219
41.980	*manoyl-oxide*	2343
42.106	*isopimaradiene*	2287
43.666	*abietatriene*	2469
45.240	*isoabienol*	n.d
46.446	*Abienol*	n.d
49.987	*cis-totarol*	n.d
50.654	*trans-totarol*	n.d
51.159	*Ferruginol*	n.d

Figure 2: Chromatograms and main compounds of the essential oil of **(a)** leaves and **(b)** stems from *D. viscosa* obtained by SPB-1 column.

Essential oils (leaves) are characterized by a high content of oxygenated sesquiterpenes (40.7%), caryophyllene oxide (10.4%), fokienol (9.6%), α-eudesmol (7.6%), trans-nerolidol (7.0%) and γ-eudesmol (6.2 %.) as main components. The chemical composition of leaves is found to differ drastically from that of stems, with co-dominance of trans-nerolidol (7.0%, 1.1%) and caryophyllene oxide (10.4%, 1.1%) for leaves and stems respectively.

Table 1: Chemical composition of the essential oil of *D. viscosa*: leaves and stems.

No.	Compounds	Leaves [%]	Stems (%)	RI[a]	RI[b]
	α-pinene	0.4	-	930	1027
	myrcene	-	t	980	1161
	δ-3-carene	-	t	1005	1152
	limonene	t	t	1020	1206
	terpinolene	-	t	1076	1288
	tepinene-4-ol	-	t	1158	1597
	terpinyl acetate	-	t	1328	1688
	α-ylangene	0.4	-	1364	1489
	α-copaene	1.4	-	1368	1489
	trans-caryophyllene	1.5	t	1406	1590
	geranyl acetate	0.5	-	1429	1876
	allo-aromadendrene	1.8	-	1446	1638
	germacrene D	-	t	1464	1699
	γ–muurolene	1.1	-	1465	1684
	β-selinene	0.6	-	1469	1716
	selina-3,5-diene	1.3	-	1475	n.d
	δ-selinene	2.1	t	1480	1716
	α-muurolene	0.5	t	1484	1724
	cis-calamenene	0.3	-	1506	1824
	δ-cadinene	-	0.4	1507	1747
	trans-nerolidol	7.0	1.1	1545	2032
	caryophyllene oxide	10.4	1.1	1558	1974
	fokienol	9.6	-	1573	2160
	α-cedrol	-	16.7	1576	2103
	γ-eudesmol	6.2	-	1608	2152
	T-cadinol	-	4.9	1615	2152
	α-eudesmol	7.6	-	1627	2209
	α-cadinol	-	1.8	1630	2219
	manoyl oxide	-	3.6	1964	2343
	isopimaradiene	-	5.1	1968	2287
	abietatriene	-	3.6	2018	2469
	isoabienol	-	12.1	2070	n.d
	abienol	-	8.3	2110	n.d
	cis-totarol	-	1.7	2230	n.d
	trans-totarol	-	18.1	2253	n.d
	ferruginol	-	16.6	2271	n.d
GROUPED COMPONENTS					
	Monoterpene hydrocarbons	0.4	0.0	-	-
	Oxygenated monoterpenes	0.0	0.0	-	-
	Sesquiterpene hydrocarbons	11.4	0.4	-	-
	Oxygenated sesquiterpenes	40.7	25.7	-	-
	Diterpenoids	0.0	69.1	-	-
	Geranyl acetate esters	0.5	-	-	-

- Compounds listed in the order their elution from SPB-1 column
- RI[a]: Retention indices in the SPB-1 column.
- Ri[b]: Retention indices in the Supelcowax 10 column.
- t: Traces (<0.05%).

The yields and the main constituents of the *D. viscosa* essential oil extracted from samples of other countries are reported in Table 2.

Table 2: Major compounds of essential oil of *D. viscosa* obtained from different countries and regions as long as the experimental data [(*)].

Country(region) Area	Algeria (north) (Bainem forest) [(*)]	Tunisia (Beja 2015)	Syria Al-Qadmous2014	Spain –Donadio village2000	Italy Sardinian2003	Portugal (Algarve 2008)	Jordan (Irbid 2010)	Turkey (Fethiye1996)	France (Corcia 2006)	Algeria (east) Constantine Hamma Bouziane 2012	Algeria (east) Constantine Ain El-Bey 2012
Data	Experimental	Literature	Literature	Literature	Literature	Literature	Literature	Literature	Literature	Literature	Literature
Yield of essential oil [%]	0.15	t	0.09	-	0.43	<1	0.05	0.20	0.03–0.07	8.0	10.0
Extraction method	HD	HD	HD	HD	HD	HD	HD	HD	HD	HD	HD
Part of the plant	L	L	L	AP	AP	AP	AP	FAP	FAP	FAP	FAP
α-pinene	0.4	-	-	-	-	-	-	0.7	-	-	0.1
α-ylangene	1.4	-	-	-	-	0.5	-	-	0.4	-	-
α-copaene	-	-	-	-	-	0.7	-	-	0.2	-	-
Trans-caryophyllene	1.5	-	-	-	-	-	-	-	0.7	-	-
geranylacetone	0.5	-	-	-	-	-	-	-	0,1	-	-
allo-aromadendrene	1.8	1.3	-	-	-	0.6	-	-	-	-	0.4
γ–muurolene	1.1	-	-	-	-	-	-	-	0.2	-	-
β-selinene	1.3	-	-	-	-	-	-	-	-	-	-
α- selinene	2.1	-	-	-	-	-	-	-	-	-	-
α-muurolene	0.5	-	0.2	-	-	1.3	-	0.1	0.6	-	-
cis-*calamenene*	0.3	-	-	-	-	-	-	-		-	-
trans-*nerolidol*	7.0	-	13.6	7.7	1.9	8.4	19.8	1.5	8.6	9.6	25.3
caryophylleneoxide	10.4	6.7	7.8	0.4	8.0		-	1.5	2.5	0.1	5.5
fokienol	9.6	-	-	38.8	-	-	20.9	-	21.1	7.2	4.4
γ-eudesmol	6.2	-	-	-	-	-	2.6	-	0.1	-	-
α-eudesmol	7.6	-	-	-	-	-	2.7	-	2.2	0.9	-
Oxygenated Sesquiterpenes	40.7	6.7	54.3	-	-	32.7	77.2	-	60.0	-	-

- t: Traces (<0.05%), L: Leaves, AP: Aerial parts,
- FAP: Fresh aerial parts.
- HD: Hydrodistillation technique.

The variations can be attributed to several factors such as the studied part of the plant, collection location, harvest season, and timing of extraction (Miguel et *al.*, 2005; Camacho et *al*., 2003). The major ingredients of essential oils from all regions are oxygenated sesquiterpenes (23.8% to 77.15%).

The obtained results in this work of the chemical compositions of the essential oils (leaves) indicate significant similarities with those extracted from Al-Qadmous of Syria (Nasser et *al*., 2014). Both studies report a predominance of trans-nerolidol (13.64%) with caryophyllene oxide (7.83%). It was reported that the plant extracted from Beja of Tunisia (Alalan et *al*., 2015) contains caryophyllene oxide of 6.67%, slightly smaller than the caryophyllene oxide percentage reported in our work.

Comparing the chemical composition of the aerial parts with the counterparts from samples extracted from Donadio village of Spain (Camacho et *al*., 2003) shows the presence of fokienol (38.8%) and trans-nerolidol (7.71%). The chemical composition analysis of the essential oils extracted from the samples from Irbid in Jordan (Al-Qudah et *al*., 2010) indicates similar compounds with concentrations of fokienol (20.87%), trans-nerolidol (19.75%), α-eudesmol (2.66%) and γ-eudesmol (2.57%). Moreover, plants extracted from Sardinian of Italy (Marongiu et al., 2002) were found to contain 12-carboxyeudesma-3, 11(13)-diene (43.97%), globulol (16.8%), valerianol (12.0%) and caryophyllene oxide (8.0%). Likewise, the plant extracted from Algarve of Portugal (Albano et *al*., 2012) was reported to be consisted of β-oplopenone (7.2%), δ-cadinol (5.5%) and α-cadinol (5.3%).

The analysis of the chemical composition of fresh aerial parts of the plants extracted from the Constantine: Hamma Bouziane and Ain El-Bey eastern part of Algerian (Berhail Boudouda et *al*., 2012) indicate that it contains trans-nerolidol (9.6%, 25.3%), caryophyllene oxide (0.1%, 5.5%) and fokienol (7.2%, 4.4%). Further comparison with samples extracted from Corcia of France (Blanc et *al*., 1996) indicates the presence of trans-nerolidol (8.6%),

caryophyllene oxide (2.5%), and fokienol (21.1%). In addition, the compositional investigations of the fresh aerial parts of essential oils extracted from Turkish Fethiye (Kotan et *al.*, 2007) demonstrate that they contain borneol (25.2%), bornyl acetate (22.5%) and isobornyl acetate (19.5%) as major components.

3.2. Antimicrobial Activities

Essential oils (leaves and stems) exhibit antimicrobial activity that can be basically determined from the size variation of the inhibiting zone. The diameter of the DMSO solvent used as a negative control is 6 mm (diameter of a paper disk). The antimicrobial effect was improved by increasing the essential oil concentration. Concentration of 300 µg is found to exhibit the best antimicrobial activity (Figures 3 and 4).

Remarkably, the essential oil (leaves) showed better inhibitory effect (on bacteria and yeast strains) as compared with oil (stems). This could be interpreted in terms of the existence of a high concentration of the oxygenated sesquiterpenes group (40.7%), as well as the presence of trans-nerolidol (7%). The existence of trans-nerolidol in isolated oil (leaves) is found to play a significant role against *C. albicans* yeast strain only. However, the cis-nerolidol isomer is found to exhibit inhibitory activity against two *C. albicans* strains (Curvelo et *al.*, 2014). The microbial inhibitory role of oil (stems) can be attributed to the existence of diterpenoids (69.1%) (Núñez et *al.*, 2018).

The four bacterial strains were selected deliberately from Gram-positive and Gram-negative strains, to confirm the anticipated fact that Gram-positive bacteria are the most susceptible bacteria to oil extract from *D. viscosa*.

It should also be mentioned that a synergy between the essential oil compounds can contribute to antimicrobial activity (Marino et *al.*, 2001 and Amorim et. *al.*, 2013). (Seca et *al.*, 2013) confirming the importance of the genus *Inula* as a medicines source for humans.

The antimicrobial activities of the essential oil (leaves and stems) were compared with the antibacterial activities of standard antibiotic agents (trimethoprim-sulfamethoxazole, amoxicillin, and lymecycline). The antibacterial efficacy of oil extracted from *D. viscosa* leaves was fair on *Escherichia coli*, *Bacillus subtilis*, and *Staphylococcus aureus* and almost 40-60 % of the average efficacy of the selected standard antibacterial (Figure 5). Interestingly, at concentration of 25 µg, all antibiotics except Bacillus subtilis show higher inhibition with compare to the essential oil.

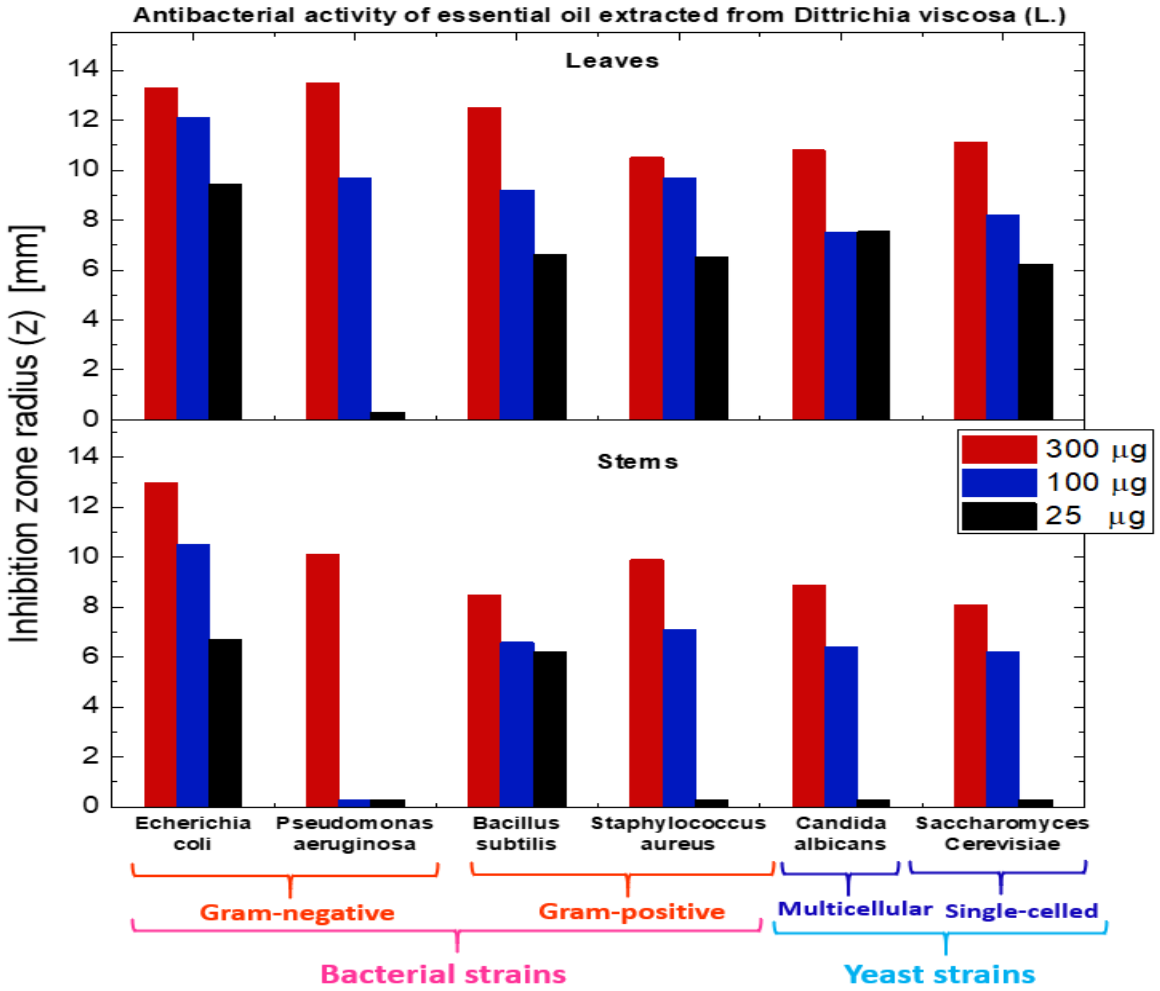

Figure 3: Antimicrobial activities of the essential oil (leaves and stems) of *D. viscosa.* Concentrations of 25 µg, 100 µg and 300 µg were applied on two Gram-negative bacteria strains (*Escherichia coli* and *Pseudomonas aeruginosa*) and other two Gram-positive strains (*Bacillus subtilis* and *Staphylococcus aureus*) as well as two yeast strains (*Saccharomyces cerevisiae* and *Candida albicans*), that are single-celled and multicellular, respectively.

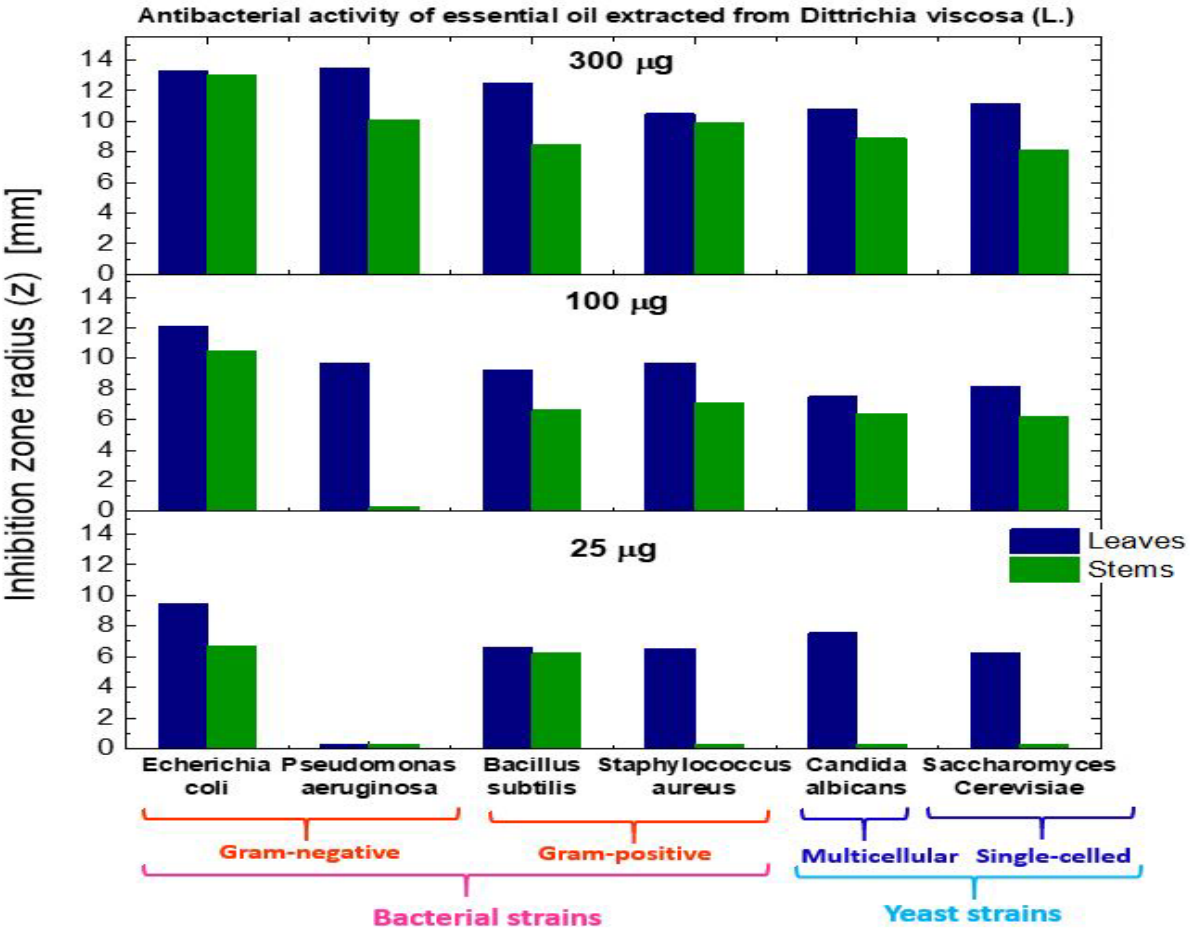

Figure 4: Comparing the concentration effect of isolated essential oil concentration from the leaves and stems of *D. viscosa* on antimicrobial activities. The concentrations are 25 µg, 100 µg and 300 µg applied on two Gram-negative bacteria strains (*Escherichia coli* and *Pseudomonas aeruginosa*) and other two Gram-positive strains (*Bacillus subtilis* and *Staphylococcus aureus*) as well as two yeast strains (*Saccharomyces cerevisiae* and *Candida albicans*), that are single-celled and multicellular, respectively.

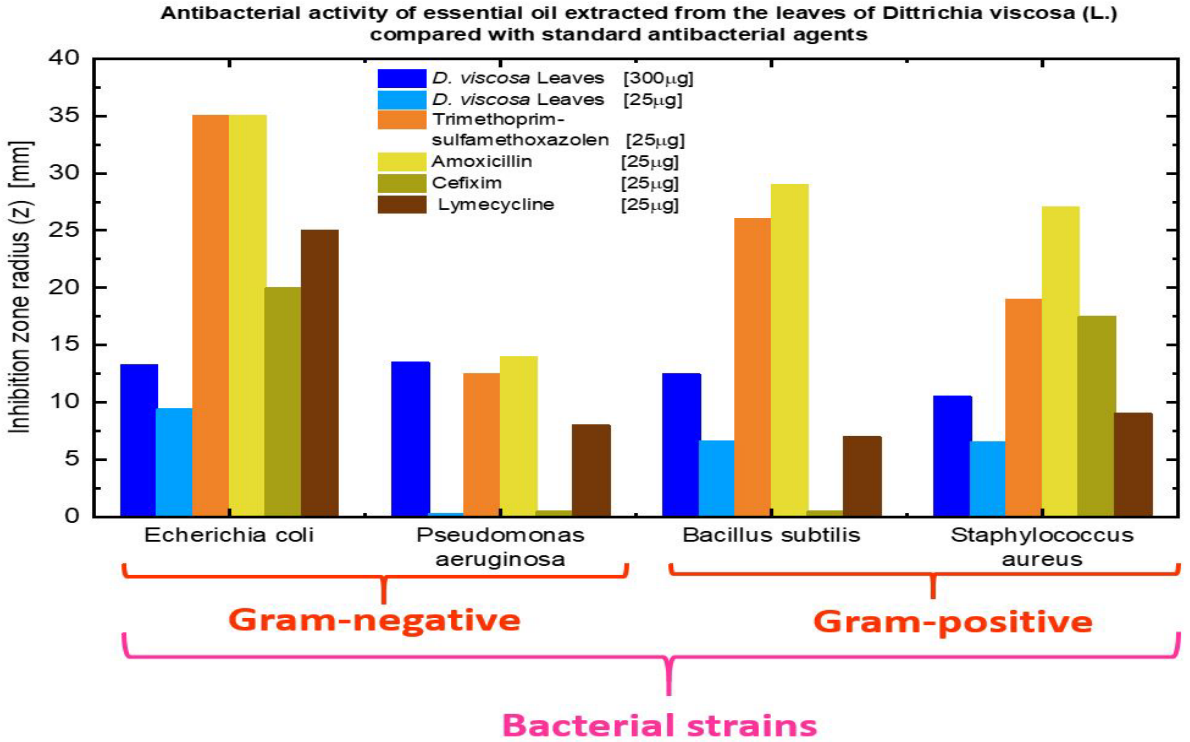

Figure 5: The Antimicrobial activities of isolated essential oil of *D. viscosa* (leaves and stems) at 25 µg concentration as well as standards antibiotics (TRS: Trimethoprim-sulfamethoxazole; CF: cefixime; AMC: Amoxicillin; LE: Lymecycline).

As tabulated in Table 3, the MIC value of the oil on Gram-positive bacteria is 20 µg/ml. However, On Gram-negative bacteria, the MIC values of the oil vary, depending on the strain tested.

Table 3: Minimal inhibitory concentration (MIC) of *D. viscosa* essential oils (leaves and stems).

Minimum Inhibitory Concentration (MIC) [µg.ml^{-1}]		
Microorganism	Leaves	Stems
Gram-negative bacteria		
Echerichia coli	15	20
Pseudomonas aeruginosa	100	300
Gram-positive bacteria		
Bacillus subtilis	20	20
Staphylococcus aureus	20	20
Yeast strains		
Saccharomyces cerevisiae	20	100
Candida albicans	20	100

The MIC values are in the range between 20 and 100 µg/ml. The oil strongly inhibits the growth of *Escherichia coli*. The MIC values indicate that our samples exhibit better antimicrobial activities than that obtained using the oil of leaves of *D. viscosa*, harvested in Tunisia (250 µg/ml) (Gharred et *al.* 2019). A study of antibacterial activity against Staphylococcus aureus ATCC 25923 yields a MIC of 32 µg/ml (Aissa et *al*., 2019). On the contrary, the MIC generated by oil on *Pseudomonas aeruginosa*, is found to be higher and equal to 300 µg/ml and 100 µg/ml for stems and leaves, respectively.

4. Conclusions

In conclusion, the chemical composition of the essential oils extracted from *Dittrichia viscosa* (L.) by hydrodistillation indicates the predominance of the oxygenated sesquiterpenes (40.7 %) in the oil extracted from leaves. The extracted oil from stems is found to contain the diterpenoids (69.1%) substantially. The chemical compositions of the essential oils (leaves and stems) are in good agreement with literature, nonetheless the differences between some results of this work and previous works are mostly due to difference in plant located region, harvest season and timing of extraction.

Essential oils (leaves and stems) exhibit antimicrobial activities which were deduced from the size variation of the inhibiting zone. Furthermore, the antimicrobial activity is found to enhance by increasing the concentration of essential oil. Concentration of 300 µg is found to yield optimum antimicrobial activity.

The oil (leaves) demonstrates a better inhibitory effect against all bacterial and fungal strains compared to oil (stems). This is due to the significant presence of trans-nerolidol (7%), caryophyllene oxide (10.4%) and fokienol (9.6%) in the leaves with compare to stems. Additionally, the trans-nerolidol was observed in isolated oil extracted from leaves only which plays a significant role against *C. albicans* yeast strain.

The antibacterial efficacy of *D. viscosa* leaves oil was found to be fair on *Escherichia coli*, *Bacillus subtilis*, and *Staphylococcus aureus* and almost 40-60 % of the average efficacy of the selected standard antibacterial.

Despite the fact that trimethoprim-sulfamethoxazole, amoxicillin, and lymecycline are more effective than oil extracted from *D. viscosa* leaves, it is still natural and can be used at higher doses allowed to compensate for the difference inefficiency. However, the toxic doses of the essential oil should be avoided. The essential oil can also be added to standard antibiotics for synergistic therapy since antibiotic combinations are frequently used to treat serious Gram-negative infections.

Acknowledgments

The scientific and the financial support provided by the Fundaçãopara a Ciência e Tecnologia (FCT), POCI 2010/FEDER is acknowledged.

References:

Alalan L, AL-Shammaa I and Al-Nouri AS. 2015. Analysis of the chemical composition of essential oil extracted from Syrian Inula viscosa (L.). J Chem Pharma Res. 7 (12): 861-864.

Albano MS, Lima AS, Miguel MG, Pedro GL, Barroso JG and Figueiredo AC. 2012. Antioxidant, Anti-5-lipoxygenase and Antiacetyl cholinesterase Activities of Essential Oils and Decoction Waters of Some Aromatic Plants. Rec Nat Prod. 6 (1): 35-48.

Alejandro F, Barrero M, Mar Herrador, Pilar Arteaga, Julieta V and Catalán. 2008. *Dittrichia viscosa* L. Greuter: Phytochemistry and Biological Activity. Nat Prod Commun. 3: 11.

Al-Qudah MA, Al-Jaber AS, Mayyas HI, Abu-Orabi ST and Abu Zarga MH. 2010. Chemical Compositions of the Essential Oil from the Jordanian Medicinal Plant *Dittrichia Viscosa*. Jordan J. Chem. 5: 343-348.

Amorim MHR, Gil-Da-Costa RM, Lopes C and Bastos MMSM. 2013. Sesquiterpene lactones: adverse health effects and toxicity mechanisms. Critical Reviews Toxicology 43: 559–579.

Aissa I, Nimbarte VD, Zardi-Bergaoui A, Znati M, Flamini G, Ascrizzi R, and Ben Jannet H. 2019. Isocostic Acid, a Promising Bioactive Agent from the Essential Oil of *Inula viscosa* (L.): Insights from Drug Likeness Properties, Molecular Docking and SAR Analysis. Chem. Biodiversity. 1-16. https://doi.org/10.1002/cbdv.201800648.

Berdy J. 2005. Bioactive microbial metabolites, J Antibiot. 58: 1–26.

Berhail Boudouda H, Benmerache A, Chibani S, Kabouche A, Abuhamdah S, Semra Z and Kabouche Z. 2012. Antibacterial Activity and Chemical Composition of Essential Oils of *Inula viscosa* (L.) Ait. (*Asteraceae*) from Constantine, Algeria. Der Pharmacia Lettre. 4 (6) : 1878-1882. http://scholarsresearchlibrary.com/archive.html.

Blanc MC, Bradesi P, Gonçalves MJ, Salgueiro L and Casanova J. 1996. Essential oil of Dittrichia viscosa ssp. viscosa: analysis by 13C-NMR and antimicrobial activity. Flavour Fragr J. 21: 324–332.

Brullo S and De Marco G. 2000. Taxonomical revision of the genus *Dittrichia* (*Asteraceae*). Portugaliae Acta Biology. 19: 341–354.

Camacho A, Fernández A, Fernández C, Altarejos J and Laurent R. 2003. Composition of the essential oil of *Dittrichia viscosa* (L.) W. Greuter. Riv Ital EPPOS. 29: 3-8.

Cavaleiro C, Gonçalves MJ, Serraa D, Santoroa G, Tomi F, Bighelli A, Salgueiroa L and Casanova J. 2011. Composition of a volatile extract of *Eryngium duriaei* subsp. juresianum (M. Laínz) M. Laínz, signalised by the antifungal activity. J Pharm Biomed Anal. 54 (3): 619 - 622.

Cavaleiro C, Salgueiro LR, Miguel MG and Proença da Cunha A. 2004. Analysis by gas chromatography–mass spectrometry of the volatile components of *Teucrium lusitanicum* and *Teucrium algarbiensis*. J Chromatogr A. 1033 (1): 187 - 190.

Curvelo JAR, Marques M, Barreto ALS, Romanos MTV, Portela MB, Kaplan MAC and Soares RMA. 2014. A novel Nerolidol-rich essential oil from *Piper clausseniánum* modulates *Candida albicans* biofilm. J Med Microbiol. 63: 697–702.

European Pharmacopoeia 6.0. 2008. Determination of essential oils in herbal drugs. 2,8,12.

Gharred N, Dbeibia A, Falconieric D, Hammamia S, Pirasc A and Dridi-Dhaouadi S. 2019. Chemical composition, antibacterial and antioxidant activities of essential oils from flowers, leaves and aerial parts of Tunisian *Dittrichia Viscosa*. J Essent Oil Res. 1-8. https://doi.org/10.1080/10412905.2019.1612789

Grauso L, Cesarano G, Zotti M, Ranesi M, Su W, Bonanomi G and Lanzotti V. 2019. Exploring *Dittrichia viscosa* (L.) Greuter phytochemical diversity to explain its antimicrobial, nematicidal and insecticidal activity. Phytochem Rev. doi:10.1007/s11101-019-09607-1.

Hammer KA and Carson CF. 1999. Riley TV Antimicrobial activity of essential oils and other plant extracts. J Appl Microbiol. 86: 985-990.

harzallah-skhiri F, Chéraif I, Ben Jannet, H and Hammami M. 2005. Chemical Composition of Essential Oil from Leaves-stems, flowers and Roots of *Inula graveolens* Tunisia. Pak J Biol Sci. 8 (2): 249-254.

Heatley NG. 1944. A method for the assay of penicillin. Biochem J. 38: 61–65.

Hudzicki J. 2009. Kirby- Bauer disk diffusion susceptibility test protocol. ML Microbe Library, ASM. http://www.microbelibrary.org/component/resource/laboratory-test/3189-kirby-bauer-disk-diffusion-susceptibility-test-protocol.

Kotan R, Kordali S and Cakir A. 2007. Screening of antibacterial activities of twenty-one oxygenated monoterpenes. Z Naturforsch C. 62 (7-8): 507-13.

Laurentis, Nicolino, Losacco, V, Milillo MA, Lai and Olimpia, 2002. Chemical investigations of volatile constituents of *Inula viscosa* (L.) Aïton (Asteraceae) from different areas of Apulia, Southern Italy. Delpinoa. 44: 115-119.

Maleš Ž, hazler pilepić k, petrović l and Bagarić, i. 2010. Quantitative analysis of phenolic compounds of *Inula Candida* (l.) Cass. PERIOD BIOL. 112 (3): 307–310.

Marino M, Bersani C, Comi G. 2001. Impedance measurements to study the antimicrobial activity of essential oils from *Lamiaceae* and *Compositae*. Int J Food Microbiol. 67: 187-195.

Marongiu B, Piras A, Pani F, Porcedda S and Ballero M. 2002. Extraction, separation and isolation of essential oils from natural matrices by supercritical CO2. Flavour Fragr J. 18: 505.

Miguel MG, Duarte J, Figueiredo, AC, Barroso JG and Pedro LG. 2005. *Thymus carnosus* Boiss.: Effect of harvesting period, collection site and type of plant material on essential oil composition. J Essent Oil Res. 17: 422-426.

Nasser M, Housheh S, Kourini A and Maala N. 2014. Chemical composition of essential oil from leaves and flowers of *Inula viscosa* (L.) in Al- Qadmous region, Syria. Int J Pharm Sc and Res. 5 (12): 5177-5182.

Nazzaro F, Fratianni F and De Martino L. 2013. Effect of essential oils on pathogenic bacteria. Pharm J. 6: 1451–1474.

Núñez S, San-Martín A and Corsini G. 2018. Antimicrobial activities of diterpenoids and semisynthetic derivatives from *Azorella compacta*. J Chil Chel Soc. 63: 4200-4204. 10.4067/S0717-97072018000404200.

Parolin P, Scotta MI and Bresch C. 2014. Biology of *Dittrichia viscosa*, a Mediterranean ruderal plant: a review. Φyton. 83: 251–262.

Prestinaci F, Pezzotti P and Pantosti A. 2015. Antimicrobial resistance: a global multifaceted phenomenon. Pathog Glob Health. 109: 309 – 318.

Quezel P and Santa S. 1963. Nouvelle flore de L'Algérie et des régions désertiques Méridionales. Editions du Centre National de la recherche scientifique. Tome II.

Roosita K, Kusharto CM, Sekiyama M, Fachrurozi Y and Ohtsuka R. 2008. Medicinal plants used by the villagers of a Sundanese commty in West Java, Indonesia. J Ethnopharmacol. 115: 72-81.

Runyoro DK, Matee MI and Ngassapa OD. 2006. Screening of Tanzanian medicinal plants for anti-Candida activity. BMC Complement Altern. Med. 6: 11.

Schinella GR, Tournier HA, Prieto JM, Mordujovich DBP and Rios JL. 2002. Antioxidant activity of anti-inflammatory plant extracts. Life Sci. 18: 1023-1033.

Seca AML, Grigore A, Diana CGA, Pinto, and Silva AMS. 2014. The genus *Inula* and their metabolites: From ethnopharmacological to medicinal uses. J Ethnopharmacol. 154: 286–310.

Slama TG, Amin A, Brunton SA, File TM, Milkovich G. Rodvold KA, Sahm DF, Varon J and Weiland D. 2005. A clinician's guide to the appropriate and accurate use of antibiotics: the Council for Appropriate and Rational Antibiotic Therapy (CARAT) criteria. Am J Med. 117 Suppl 7A. 7: 1– 6.

Side Larbi K, Meddah B, Tir Touil Meddah A and Sonnet P. 2016.The antibacterial effect of two medicinal plants Inula viscosa, Anacyclus valentinus (Asteraceae) and their synergitic interaction with antibiotics. J Fundam Appl Sci. 8(2): 244-255.

Van den Dool H and Kratz PD. 1963. A generalization of the retention index system including linear temperature programmed gas liquid partition chromatography. J Chromatogr. 11: 463–471.

Wiley. 2007. Registry 8th Edition with NIST 05 MS Spectra, Revision (2005) D.06.00. Agilent Technologies.

JJBS

Jordan Journal of Biological Sciences

Volume 14, Number 1, March 2021
ISSN 1995-6673
Pages 51 - 64

Identification and characterization of antimicrobial peptide genes in *Clarias gariepinus* and *Chelon ramada*

Karima F Mahrous*, Dalia M Mabrouk, Mohamad M Aboelenin, Heba AM Abd El kader and Mohamed S Hassanane

Cell Biology Dept., Division of Genetic Engineering and Biotechnology Research- National Research Centre, 33 El Bohouth St., Dokki, Giza, P.O.12622, Egypt.

Received Feb 28, 2020; Revised June 13, 2020; Accepted June 28, 2020

Abstract

Antimicrobial peptides (AMPs) are small molecular weight proteins that play an important role in the innate immune response against pathogenic invasions. In the present study, the coding sequences (CDs) of four AMPs were characterized and analyzed. NK-lysin (Cgnkl) and hepcidin (Cghep) coding sequences were obtained from *Clarias gariepinus* (North African catfish), while two hepcidin paralogs (Crhep1 and Crhep2) coding sequences were identified from *Chelon ramada* (thin-lipped mullet). Cgnkl coding sequence consists of 128 amino acids with predicted signal peptide cleavage site between codons 17 and 18 and six conserved cysteine residues that are held together by three disulfide bonds. On the other hand, Cghep, Crhep1, Crhep2 coding sequences consist of 91, 85 and 90 amino acids, respectively, and show the similar predicted signal cleavage site between codons 24 and 25 as well as eight characteristic cysteine residues. Several synonyms and non-synonyms SNPs were detected within Cghep and Crhep1 CDs. Finally, phylogenetic and conservation analyses were carried out on the amino acid sequences of the discovered AMPs and the 3D structures of their propeptides was predicted.

K*eywords*: Antimicrobial peptides, Hepcidin, NK-lysin, *Clarias gariepinus, Chelon ramada*

1. Introduction

Although AMPs have been recognized in the middle of the 20th century, they have gained increasing attention in recent years. AMPs are small size peptides that have a great diversity in amino acid composition, structural organization, and mechanism of action (Bruno *et al*., 2019). They display antimicrobial activity against several microorganisms and viruses and participate in the innate host defense of each eukaryotic species (Masso-Silva and Diamond, 2014). Generally, all AMPs are able to disrupt microbes lipidic membranes to kill or inhibit proliferation (Lai and Gallo, 2009; Mahrous *et al*, 2020a; Mahrous *et al*, 2020c).

Fish is a great source of AMPs, as it mainly relies on humoral primary immune defense mechanism to succeed in the highly dynamic and challenging external environment rich with microorganisms (Sathyan *et al*., 2013). A large number of AMPs has been identified from different fish species, including hepcidin and NK-lysin.

Hepcidin, a small cysteine-rich AMP, plays an essential role in host iron metabolism regulation and immunological processes. Its amphipathic structure is similar to other AMPs, such as defensins. It has the ability to defend against pathogenic bacteria in an indirect way through decreasing iron in the plasma and extracellular fluids and, as a result, limiting its proliferation (Drakesmith & Prentice, 2012; Huang *et al*., 2019). Unlike many other AMPs displaying a high degree of sequence variability among closely related organisms, hepcidin is highly conserved from teleosts to mammals (Masso-Silva and Diamond, 2014). Most mammals present only one copy of the hepcidin gene, but in fish, multiple copies exist. Hepcidin antimicrobial peptides (HAMPs) of fish are divided into two groups, HAMP1 and HAMP2. HAMP1 is present in all fish while, HAMP2 is present only in acanthopterygian (Neves *et al*., 2017).

NK-lysin, a member of the Saposin-like protein family, is orthologous with human granulysin. It is larger (74–78 amino acids) than the classical AMPs (Kim *et al*., 2016). It is released from the natural killer cells and cytotoxic T lymphocytes (Zhou *et al*., 2016) with remarkable broad-spectrum activities against fungi (Stenger *et al*., 1998), protozoa (Lama *et al*., 2018) and bacteria (Pereiro *et al*., 2017), and tumor cells (Fan *et al*., 2016). Its sequence is rich in positively charged amino acids and the sulfide bond-forming cysteines (Wang *et al*., 2018).

Egypt is one of the top seven aquaculture producers by quantity. Its average annual production is 3.3 tons (FAO, 2017). With the continued expansion of cultured fish species, aquaculture became a key component of the animal production industry. *Chelon ramada* (Thin-lipped mullet) is a potential species for fish culture in Egypt due to its temperature tolerance, superior growth, wide salinity tolerance range and high-quality flesh (Mehanna *et al*., 2019). Also, *Clarias gariepinus* (North African catfish), is an important catfish species for aquaculture purposes due to its rapid growth and the high protein content (Shourbela *et al*., 2014).

* Corresponding author e-mail: l_fathy@yahoo.com.

In the present study, we analyze the coding sequence of Cgnkl,Cghep, Crhep1 and Crhep2. We provide the predicted conserved domains, post-transcriptional modification motifs, signal peptides cleavage sites and the propeptides 3D structure. Further, we compare their deduced amino acid sequences with orthologous peptides of other bony fish species and construct phylogenetic trees.

2. Materials and Methods

2.1. Tissue Collection

Seven North African catfish (*C. gariepinus*) and five thin-lipped mullet (*C. ramada)* fish were collected from Lake Manzala and liver tissues were isolated and stored directly in -80°C for RNA extraction.

2.2. RNA isolation and cDNA synthesis

Liver tissue was homogenized in Trizol reagent (Invitrogen, Germany) and total RNA was extracted according to the manufacturer's instructions. RNA yield and purity were measured using NanoDrop™ 1000 Spectrophotometer (Thermo Fisher Scientific, USA). RNase-free DNase kit (Promega) was used to remove any DNA contamination. One microgram (1 µg) of RNA was reverse transcribed into cDNA using Revert Aid First-strand synthesis cDNA kit (Thermo Fisher Scientific, USA) as described previously (Sroor *et al.*, 2020).

2.3. Pre-processing and de novo assembly of transcriptome data

Since some genes are tissue-specific and or inducible, we assembled RNA-seq datasets (which belong to the same or closely relates species) in order to maximize the chance of identifying the target AMPs. Moreover, assembly of RNA-seq from several datasets helps in designing primers primer pairs within the mRNA conserved regions without SNPs which may prevent amplification due to mismatching. The transcriptome raw RNA-Seq data of *C. gariepinus* (Sequence Read Archive (SRA) accession # SRX4609822- SRX4609825, ERX538457 and ERX2104803) were assembled. For *C. ramada*, the transcription raw RNA-Seq data of *Chelon labrosus* (Thicklip grey mullet; SRA accession # SRX1672957) *and Mugil cephalus* (Grey mullet; SRA accession # SRX1817285 - SRX1817288) were assembled. FastQC (Andrews, 2010) assessment reports of sequence reads were performed to evaluate read quality before pre-processing. Adapter clipping, trimming reads based on quality, and removing sequences with ambiguous bases (N) were conducted using Trimmomatic (Bolger *et al*., 2014). Bases at both ends of reads were removed within a sliding window of 10 base pairs when the average quality in this window was lower than Q20 score. To verify the integrity of the remaining raw sequence reads, FastQC was performed again. Upon completion, the quality assessed reads were then ready to be used as the input for the various assembly strategies and all subsequent analyses were conducted using clean reads. Trinity RNA-Seq de novo transcriptome assembly version 2.0.4 was run using the default parameters (Haas *et al*., 2013). Reference transcripts were generated by combining all clean reads of the sequencing data sets. To represent the assembled component from each cluster, only the longest transcript was selected to prevent redundancy. All the data processing steps were performed online depending on Galaxy project (Enis *et al.*, 2018).

Geneious Software version 10 (Biomatters, Ltd., New Zealand) was used to perform batch Basic Local Alignment Search Tool (BLAST) for the assembled mRNA sequences against NCBI databases to find homologues sequences based on blastn and blastx tools. The assembled mRNA sequences found to be homologues to the target antimicrobial peptides gene (NK-Lysin and Hepcidin) were used to design specific primers (Table 1) using Primer-BLAST software (www.ncbi.nlm.nih.gov/tools/primer-blast) to amplify the CDs of each gene.

2.4. Amplification and sequencing of the Coding sequence (CDs) within the target genes

The designed primers (Table 1) were synthetized by Macrogen (South Korea). Polymerase chain reaction (PCR) were performed in a 25 µl of reaction volume, which included a 1 µl of cDNA, a 50 ng of each primer, a 200 µM of each dNTP, a 2.5 µl of 10X PCR buffer and a 0·5 U of Taq DNA polymerase (Promega, Madison, WI, USA). Amplification was carried out in a thermocycler programmed as follows: an initial start separation cycle at 94°C for 2 min, 35 cycles including a denaturation step at 94°C for 30 sec, an annealing of each gene (Table 1) for 30 sec, a polymerization step at 72°C for 45 sec and a final extension cycle at 72°C for 10 minutes. The PCR products were screened by electrophoresis on a 2% agarose gel in a 0.5X of TBE buffer stained with ethidium bromide and visualized with an UV transilluminator as described previously (Mahrous *et al.*, 2020b). The PCR products were purified using GeneJET *Gel Extraction* Kit (Thermo Fisher Scientific, USA) according to the manufacture instructions and sent for sequencing (Macrogen, South Korea).

2.5. Amino acids sequence analysis

The CDs of each gene were translated into amino acids sequence and analyzed using CD-Search software (https://www.ncbi.nlm.nih.gov/Structure/cdd/wrpsb.cgi) to identify the conserved domains. SignalP-5.0 (http://www.cbs.dtu.dk/services/SignalP/) software was used to identify the cleavage sites of the signal peptide. The amino acid sequences were scanned using MOTIF online software (https://www.genome.jp/tools/motif/) to compute the potential motifs within them. The 3D tertiary structure of the peptide (without the signal peptide) was predicted using I-TASSER server (Yang *et al*., 2015) **a**nd the secondary structure assignment was performed using STRIDE a web server (http://webclu.bio.wzw.tum.de /cgi-bin /stride/stridecgi.py). The conservation score of the amino acids within the target proteins was computed using ConSurf server (https://consurf.tau.ac.il/). UCSF Chimera software- version 1.14 (https://www.cgl.ucsf.edu/ chimera/) was used for 3D structure visualization and secondary structure assignment. MEGA-X software-version 10.16 (Kumar *et al*., 2018) was used to align the selected sequences by MUSCLE algorithm based in neighbor joining clustering method while the phylogenetic tree was constructed using Maximum Likelihood (ML) algorithm.

Table 1: The designed primer sequences used for PCR amplification

Species	Gene name		Primer sequence	Annealing temp
Clarias gariepinus	NK-lysin (*cgnkl*)	*cgnkl-F* *cgnkl-R*	AACTATCTTTCCCATCTTTAAC AGAAAAGCATCAATCAGTTC	50
Clarias gariepinus	Hepcidin (*cghep*)	*cghep-F* *cghep-R*	ACTTGCTTTTAAACGACGACTA ACGTCCCATCTCATGTCTGA	53
Chelon ramada	Hepcidin-1 (*crhep1*)	*crhep1-F* *crhep1-R*	CACAAAGATCAGGAGAAAAC GTGGTCATTTTGTCACATG	52
Chelon ramada	Hepcidin-2 (*crhep2*)	*crhep2-F* *crhep2-R*	AGAAGACCTATCAACTCTAATC GATGAAGGAAGGGTCTTTAG	53

3. Results

The total RNA was isolated from *C. gariepinus* and *C. ramada* and converted into cDNA, then the target regions within the mRNA of the studied genes were amplified using specific primers. The resultant PCR products of Crhep1, Crhep2, Cghep and Cgnkl genes had molecular weights of 520, 408, 362 and 459 bp, respectively (Figure 1A). The PCR products were purified and sequenced then the nucleotides sequences were analyzed using several bioinformatics tools to predict the biological characteristics of these peptides.

3.1. Characterization of C. gariepinus NK-lysin (Cgnkl)

The determined sequence of *C. gariepinus* NK-lysine gene complete CDs consisted of 387 nucleotides coding for 128 aa (Figure 1B). The mRNA CDs sequence was deposited into GenBank under accession number MH674388. Saposin (B) SapB domain (aa position 56–128) which is a characteristic for saposin-like proteins (*SAPLIPs*) superfamily was detected within Cgnkl peptide (Figure 2A) Four N-Myristoylation sites (MYRISTYL; 13-GSACAI-18, 34-GSLDSV-39, 54-PGACMAC-59, 71-GNNSNQ-76), a N-glycosylation site (ASN GLYCOSYLATION; 72-NNSN-75), a Casein kinase II phosphorylation site (CK2 PHOSPHO SITE; 27-SDEE-30) and a Protein kinase C phosphorylation site (PKC PHOSPHO SITE; 78-TIR-80) motifs were found in the full length peptide sequence (Figure 2B). The first 17 amino acids represented a signal peptide with a putative cleavage site between Ala17 and Ile18 (Figure 2C).

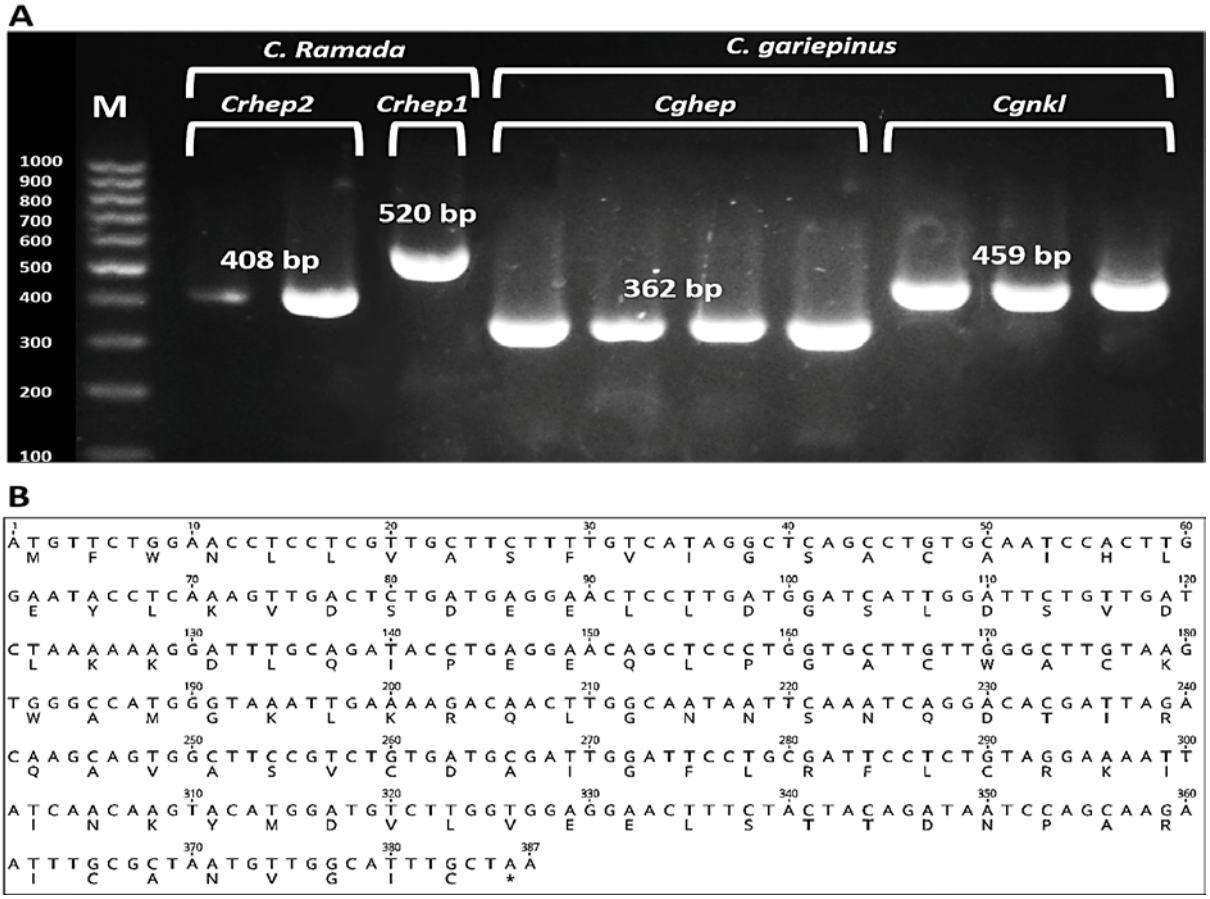

Figure 1: (A) Agarose gel electrophoresis for the PCR product of the amplified region within antimicrobial peptides Crhep1, Crhep2, Cghep and Cgnkl cDNA. M: 100 bp molecular marker (B) The nucleotides and translated amino acids sequences of Cgnkl prepropeptide.

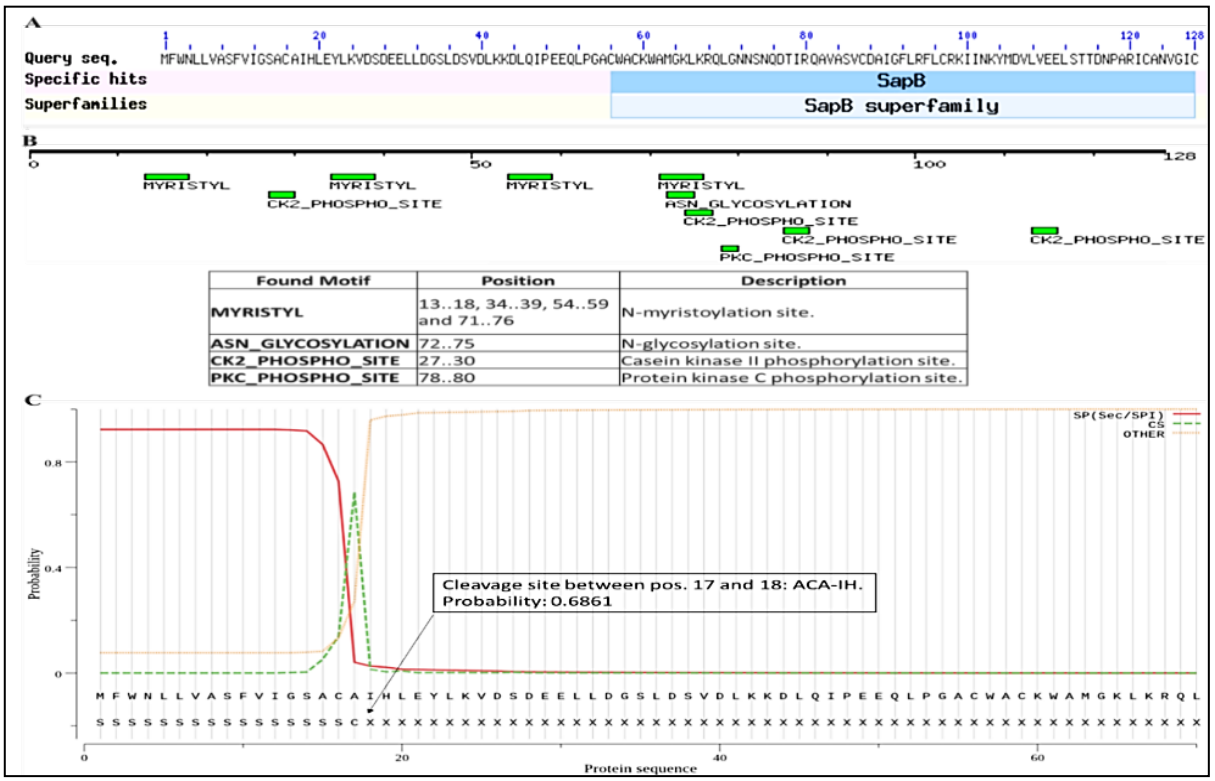

Figure 2. Predicted motifs and domains within Cgnkl prepropeptide. A) The detected conserved domain for SapB superfamily within the amino acids sequence. B) The predict motifs within the prepropeptide. C) The predicted signal peptide cleavage site. SP(Sec/SPI): standard secretory signal peptides transported by the secretory translocon and cleaved by Signal Peptidase I, CS: cleavage site, Other, Other: the sequence does not have any kind of signal peptide.

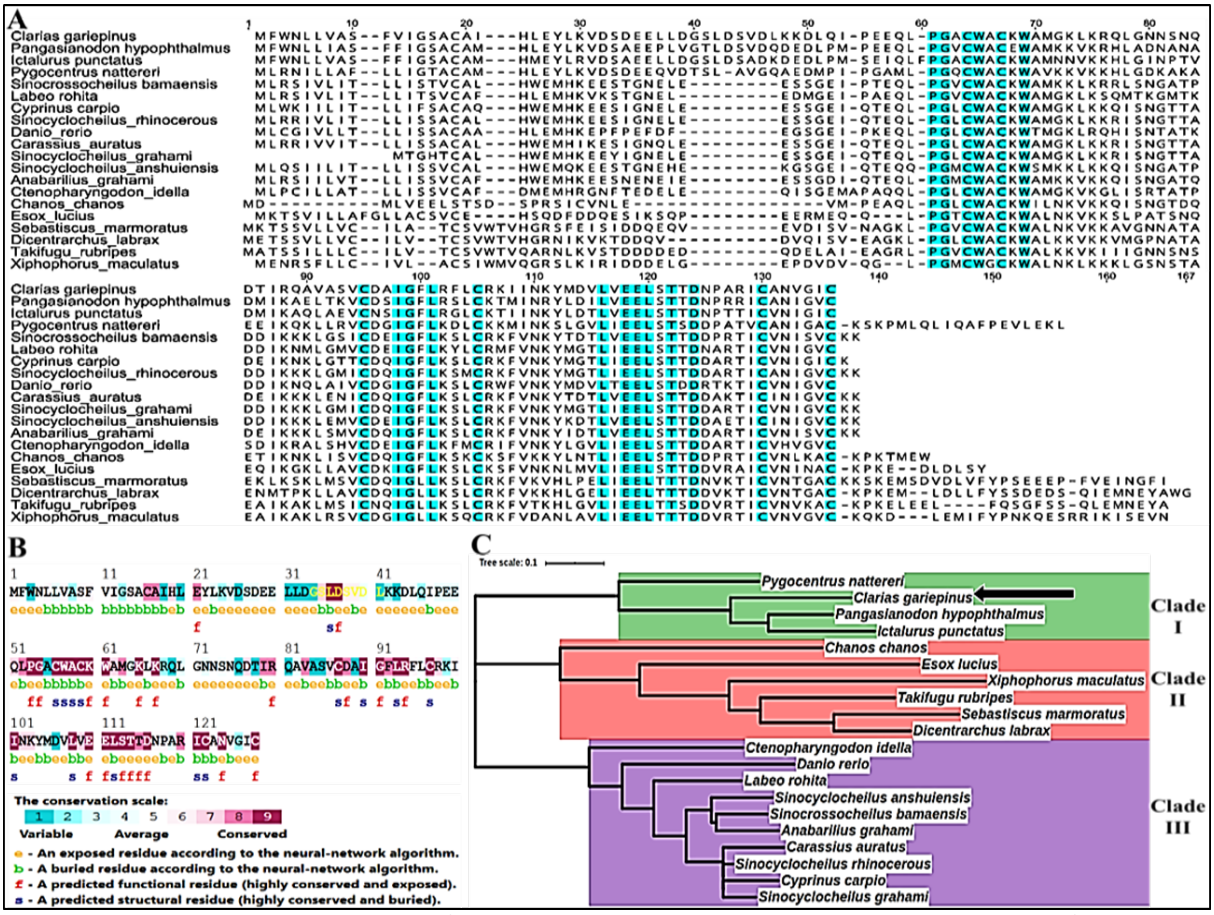

Figure 3. Phylogenetic and conservation analysis of the relationship Cgnkl and its orthologous prepropeptide in some bony fish species. (A) multiple sequence alignment (conserved residues highlighted in cyan). (B) conservation analysis. (C) phylogenetic tree.

Alignment of Cgnkl amino acid sequence with the NK-lysine prepropeptides from 19 species belong to bony fish (Figure 3A and B) displayed that 19 aa were conserved of which, 13 aa were positioned at the last 35 residues in the Cgnkl C-terminus. Moreover, 10 conserved residues could be exposed whereas the remaining 9 conserved residues might be buried. The constructed phylogenetic tree was composed of 3 main clades (Figure 3C). Cgnkl existed in clade I with *P. nattereri*, *P. hypophthalmus* and *I. punctatus*. The distance between *C. gariepinus* and *P. hypophthalmus* (Iridescent shark fish) NK-lysin sequences is the smallest distance and *C. gariepinus* and *X. maculatus* (Southern flatfish) NK-lysine sequences is largest distance.

The predicted 3D structure of Cgnkl propeptide was constructed of 57.7% alpha helix,7.2% beta sheet, 0.9% isolated beta bridge,25.2% turn and 9% coil. Six conserved cysteine (Cys) residues forming three disulfide bonds (Cys39-Cys111, Cys42-Cys105, and Cys70-Cys80) were detected (Figure 4). There were differences in the secondary structure assignment between the results of UCSF Chimera software which consist of (Figure left) and stride results which contain additional beta-sheets and isolated beta bridge (Figure right). These differences in the secondary structure assignment results could be explained by the fact that each tool uses a different secondary structure assignment algorithm, and the different secondary structure assignment algorithms could lead to several alterations in the assignment results (Martin *et al.*, 2005).

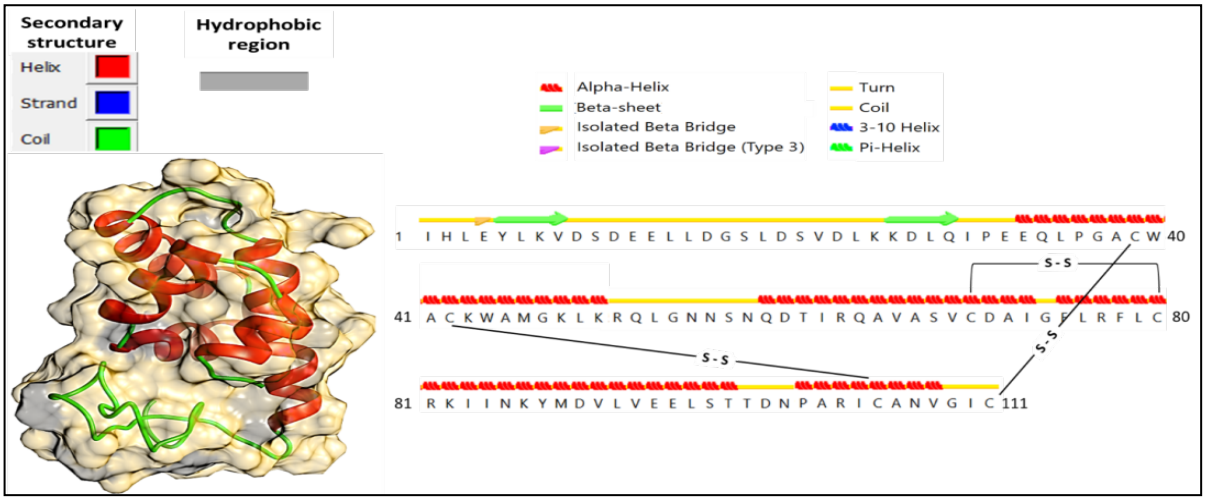

Figure 4. The predicted 3D structure of Cgnkl propeptide shows the secondary structures and molecular surface of the peptides (left) and description for the secondary structure and disulfide bonds within the peptides (right**).**

3.2. Characterization of C. gariepinus Hepcidin (Cghep)

The coding sequence of Cghep is 276 bp coding for 91 aa residues (Figure 5A). The amplified mRNA coding sequences was deposited into GenBank under accession numbers from MH674372 to MH674387. Four SNPs were identified in Cghep prepropeptide containing two synonyms SNPs (C78T and A195G) and two non-synonyms SNPs (A67G and T144G). The non-synonymous SNP (A67G) leads to threonine/alanine while the non-synonymous SNP (T144G) leads to glutamic acid/aspartic acid variation (Figure 5A and B). A segment from Phe62 to Phe91 was found to be a conserved domain belonging to hepcidin super family (Figure 6A). A Casein kinase II phosphorylation site (56-TGPE-59), a N-myristoylation site (84-GCGYCC-89),a cAMP- and cGMP-dependent protein kinase phosphorylation site (65-KRQS-68), a Microbodies C-terminal targeting signal (89-CRF-91) and Cysteine-rich region (73-CRYCCNCCKNKGCGYCC-89) motifs were found within the amino acid sequence (Figure 6B). The predicted signal peptide cleavage site is located between Ala24 and Val25, and the predicted signal peptide spanned from position 1 to 24 (Figure 6C).

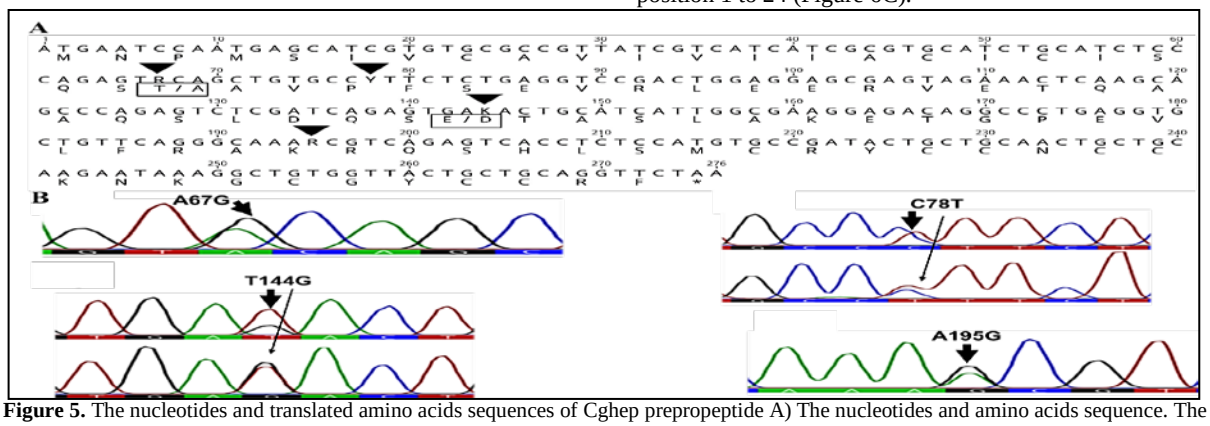

Figure 5. The nucleotides and translated amino acids sequences of Cghep prepropeptide A) The nucleotides and amino acids sequence. The solid arrows indicate the SNPs position while the boxes indicate the amino acids substitutions. R= G or A, Y=T or C and K= G or T. B) The detected SNPs within hepcidin CDs. A67G non-synonyms SNP, C78T synonyms SNP, T144G non-synonyms SNP and A195G synonyms SNP.

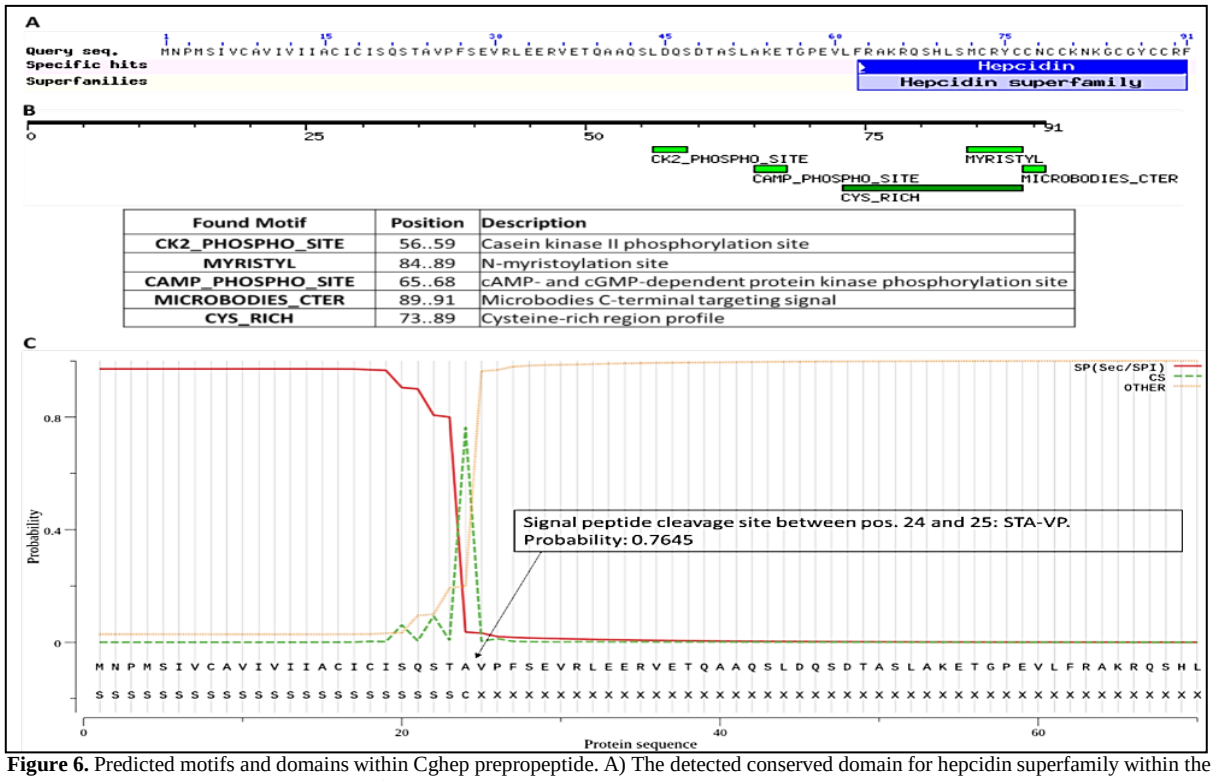

Found Motif	Position	Description
CK2_PHOSPHO_SITE	56..59	Casein kinase II phosphorylation site
MYRISTYL	84..89	N-myristoylation site
CAMP_PHOSPHO_SITE	65..68	cAMP- and cGMP-dependent protein kinase phosphorylation site
MICROBODIES_CTER	89..91	Microbodies C-terminal targeting signal
CYS_RICH	73..89	Cysteine-rich region profile

Figure 6. Predicted motifs and domains within Cghep prepropeptide. A) The detected conserved domain for hepcidin superfamily within the amino acids sequence. B) The predict motifs within the prepropeptide. C) The predicted signal peptide cleavage site. SP(Sec/SPI): standard secretory signal peptides transported by the secretory translocon and cleaved by Signal Peptidase I, CS: cleavage site, Other, Other: the sequence does not have any kind of signal peptide.

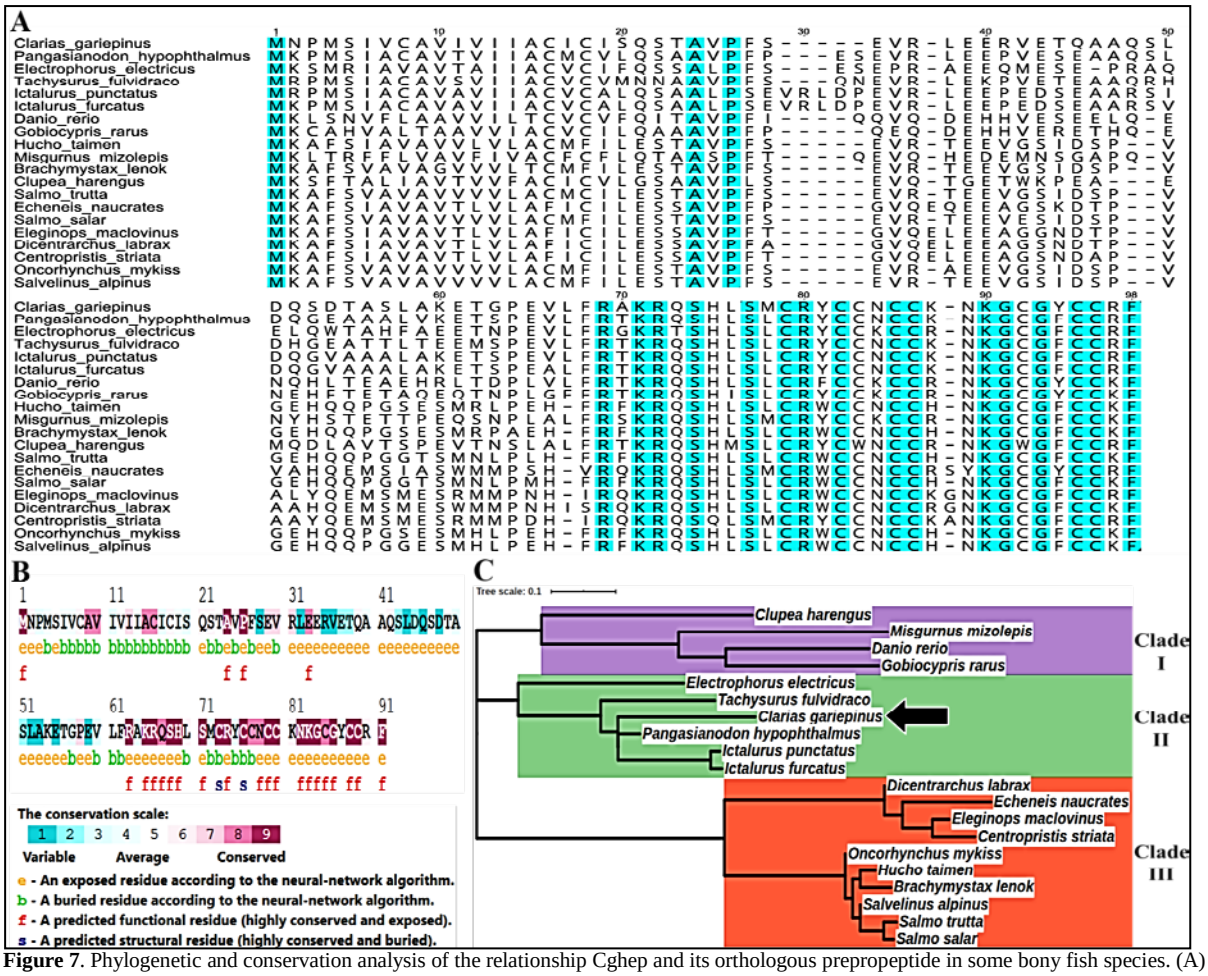

Figure 7. Phylogenetic and conservation analysis of the relationship Cghep and its orthologous prepropeptide in some bony fish species. (A) multiple sequence alignment (conserved residues highlighted in cyan). (B) conservation analysis. (C) phylogenetic tree.

Amino acid sequence alignment of Cghep with the orthologous prepropeptide from 19 bony fish species (Figure 7A and B) showed that there were 19 highly conserved amino acids among these species, and 16 amino acids among them were located within the last 29 amino acids of Cghep. 17 amino acids out of the total highly conserved amino acids were predicted to be exposed which means that they could have roles in the antimicrobial peptide function or processing while, highly conserved 2 cysteine residues were buried and could have a role in the stabilization of the hepcidin polypeptide 3D structure in these species. The phylogenetic tree of the aligned sequences (Figure 7C) showed that the tree divided to 3 main clades. Cghep is located in clade II which consists of six species. Cghep formed a subclade contains *P. hypophthalmus, I. punctatus and I. furcatus* hepcidin prepropeptides while the hepcidins from the last 2 species hepcidin are clustered together faraway from Cghep. Among the investigated species the distance between *C.gariepinus and P. hypophthalmus* (Iridescent shark fish) hepcidins is the smallest within the tree while the distance between *C. gariepinus and E. naucrates (Live sharksucker)* hepcidins in clade III *is the largest.* The predicted structure of polypeptide was constructed of 22.4% alpha helix,53.7% turn,14.9% coil and 9% 3-10 helix. Eight cysteine residues were identified in C-terminal of Cghep two residues were predicted to form one disulfide bond (Cys55-Cys56) as evident from the secondary structure (Figure 8).

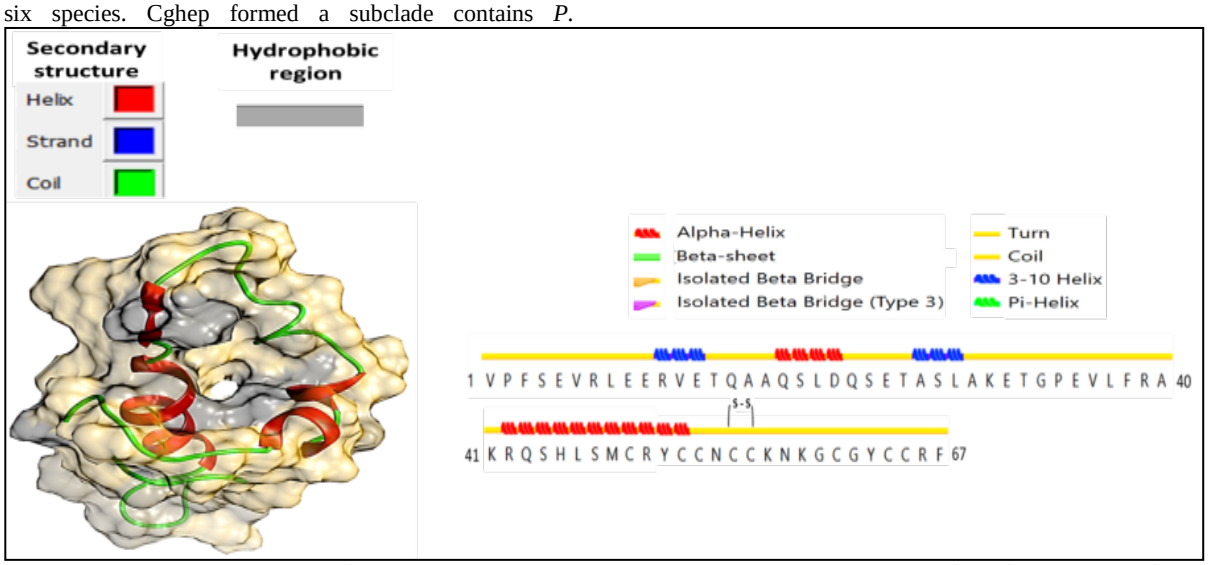

Figure 8. The predicted 3D structure of Cghep propeptide shows the secondary structures and molecular surface of the peptides (left) and description for the secondary structure and disulfide bonds within the peptides (right).

3.3. Characterization of C. ramada Hepcidin-1 (Crhep1) and Hepcidin-2 (Crhep2)

The coding sequence of Crhep1 mRNA (GenBank accession numbers from MH674362 to MH674369) consisted of 258 nucleotides (nt) coding for 85 aa (Figure 9). Three SNPs were identified in Crhep1 prepropeptide, containing one synonyms SNP (C196A C/A) and two non-synonyms SNPs (C194A and T205C). The C194A caused non-synonymous SNP alanine/aspartic acid variation while the T205C SNP caused phenylalanine/leucine variation (Figure 9A and B). Both of Crhep1 and Crhep2 have hepcidin conserved regions (which are characteristic for hepcidin superfamily members) were identified between the amino acids positions 37-85 and 38-91, respectively. A potential cleavage site for the signal peptide was predicted between Ala24 and Val25, resulting in a 24-aa signal peptide (Figure 10C). Two Crhep2 isoforms, Crhep2A and Crhep2B, were identified and deposited in GenBank under accession number MH674370 and MH674371, respectively. The nucleotide sequence of Crhep2A CDs consisted of 276 nt coding for 91 aa while Crhep2B lacked a codon coding for the amino acid number 30 (Glutamine or Q) resulting in 273 nt coding for 90 aa (Figure 13). Crhep2 prepropeptide contains a 24-aa signal peptide where its cleavage site was predicted between Ala24 and Val25 (Figure 14C). In Crhep1 prepropeptide, the ferredoxin-type iron-sulfur binding region (74-CGPGICGVC-82), Microbodies C-terminal targeting signal (83-CRF-85), Casein kinase II phosphorylation site (48-TSVD-51), and Cysteine-rich region (67-CRLCCGCCEPGICGVCC-83) motifs were found (Figure 10B). In Crhep2A prepropeptide, the cAMP- and cGMP-dependent protein kinase phosphorylation site (64-KRQS-67), Cysteine-rich region (72-CRWCCNCCRGNKGCGFCC-89), Two N-myristoylation site (81-GNKGCG-86, 84-GCGFCC-89), Microbodies C-terminal targeting signal (89-CKF-91) and motifs were found (Figure 14 B).

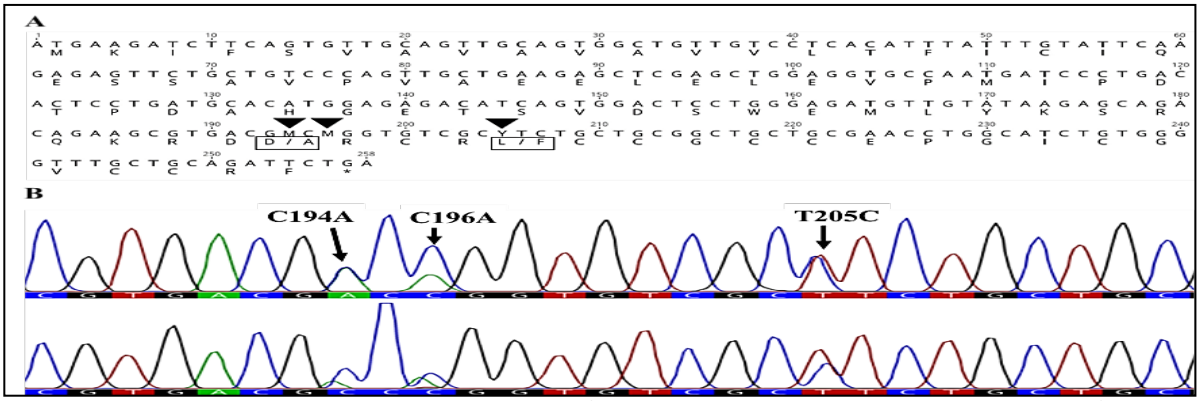

Figure 9. The nucleotides and translated amino acids sequences of Crhep1 A) The nucleotides and amino acids sequence of hepcidin-1 CDS. The solid arrows indicate the SNPs position while the boxes indicate the amino acids substitutions. M= C or A. Y=T or C. B) The detected SNPs within H1 CDS. C194A non-synonyms SNP, C196A synonyms SNP and T205C non-synonyms SNP.

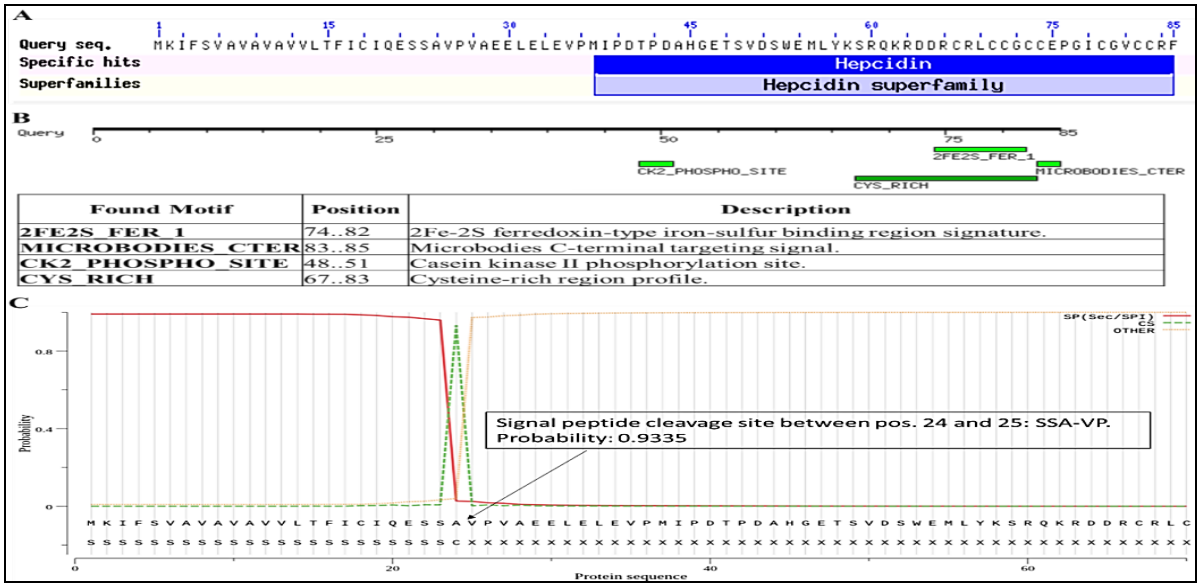

Found Motif	Position	Description
2FE2S_FER_1	74..82	2Fe-2S ferredoxin-type iron-sulfur binding region signature.
MICROBODIES_CTER	83..85	Microbodies C-terminal targeting signal.
CK2_PHOSPHO_SITE	48..51	Casein kinase II phosphorylation site.
CYS_RICH	67..83	Cysteine-rich region profile.

Figure 10. Predicted motifs and domains within Crhep1 prepropeptide. A) The detected conserved domain for hepcidin superfamily within the amino acids sequence. B) The predict motifs within the prepropeptide. C) The predicted signal peptide cleavage site. SP(Sec/SPI): standard secretory signal peptides transported by the secretory translocon and cleaved by Signal Peptidase I, CS: cleavage site, Other, Other: the sequence does not have any kind of signal peptide.

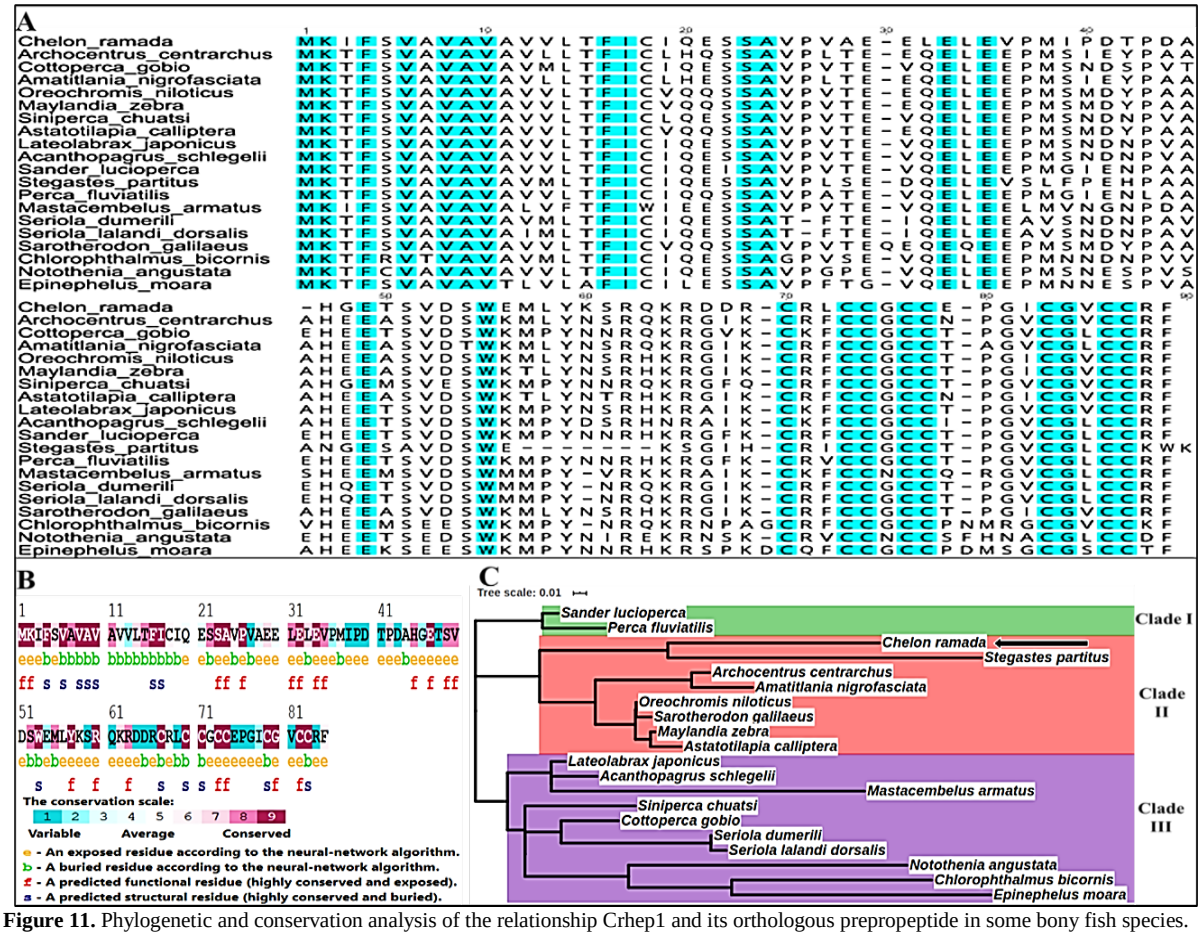

Figure 11. Phylogenetic and conservation analysis of the relationship Crhep1 and its orthologous prepropeptide in some bony fish species. (A) multiple sequence alignment (conserved residues highlighted in cyan). (B) conservation analysis. (C) phylogenetic tree.

The Crhep1 was aligned with orthologous prepropetides of 19 bony fish and about 28% from Crhep1 amino acids (24 aa) were found to be conserved among all the studied sequences (Figure 11A). Furthermore, Figure (11B) indicated that 11 conserved residues were predicted to be exposed and 13 conserved residues were predicted to be buried. The aligned sequences were used to build a phylogenetic tree which had 3 main clades (Figure 1C). Crhep1 was clustered with hepcidins from 7 species in clade II and form a subclade with *S. partitus*. The hepcidin sequences of O. niloticus (Nile tilapia) (within Clade II) and E. moara (Longtooth grouper fish) (within Clade III) had the shortest and longest distances within the tree from Crhep1 sequence. The predicted structure of the propeptide was constructed of 19.7% alpha helix, 3.3% isolated beta bridge, 52.5% turn, 13% coil and 11.5% 3-10 helix. Eight conserved cysteine residues were detected from which, four residues form two disulfide bonds (Cys43-Cys55, Cys46-Cys50) (Figure 12).

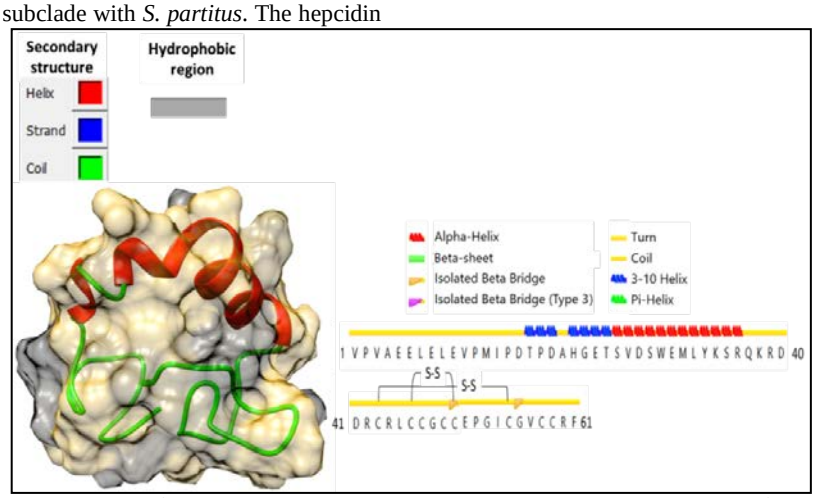

Figure 12. The predicted 3D structure of Crhep1 propeptide shows the secondary structures and molecular surface of the peptides (left) and description for the secondary structure and disulfide bonds within the peptides (right).

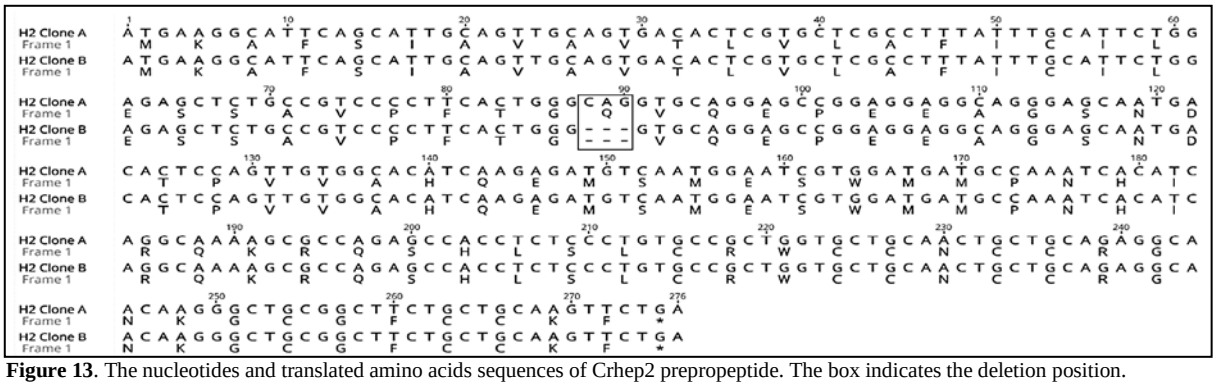

Figure 13. The nucleotides and translated amino acids sequences of Crhep2 prepropeptide. The box indicates the deletion position.

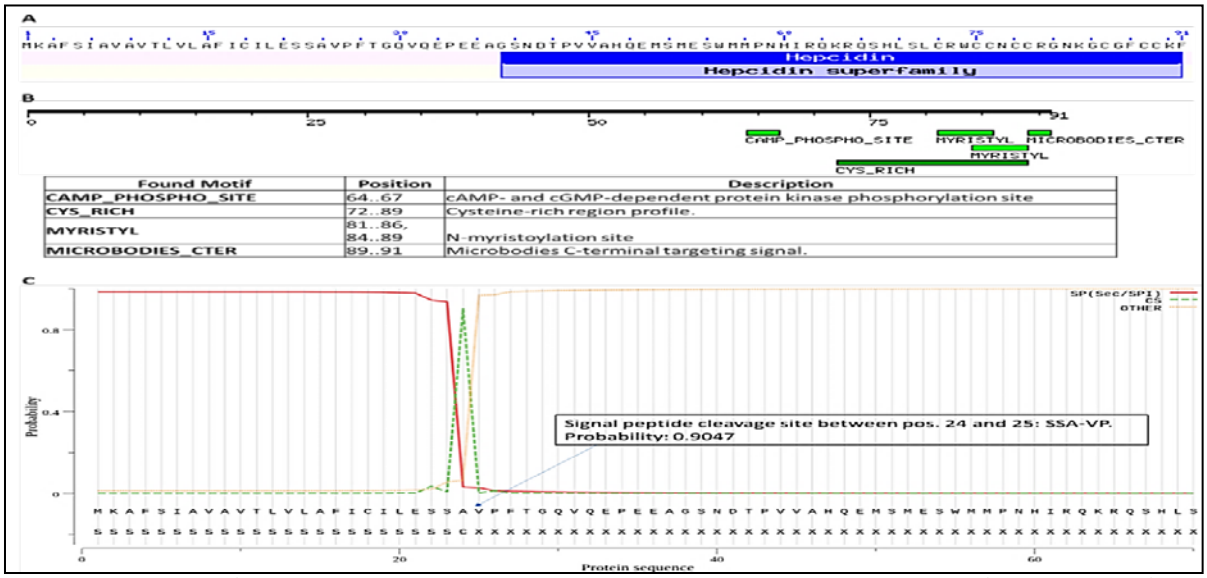

Found Motif	Position	Description
CAMP_PHOSPHO_SITE	64..67	cAMP- and cGMP-dependent protein kinase phosphorylation site
CYS_RICH	72..89	Cysteine-rich region profile.
MYRISTYL	81..86, 84..89	N-myristoylation site
MICROBODIES_CTER	89..91	Microbodies C-terminal targeting signal.

Figure 14. Predicted motifs and domains within Crhep2A prepropeptide. A) The detected conserved domain for hepcidin superfamily within the amino acids sequence. B) The predict motifs within *the* prepropeptide. C) The predicted signal peptide cleavage site. SP(Sec/SPI): standard secretory signal peptides transported by the secretory translocon and cleaved by Signal Peptidase I, CS: cleavage site, Other, Other: the sequence does not have any kind of signal peptide.

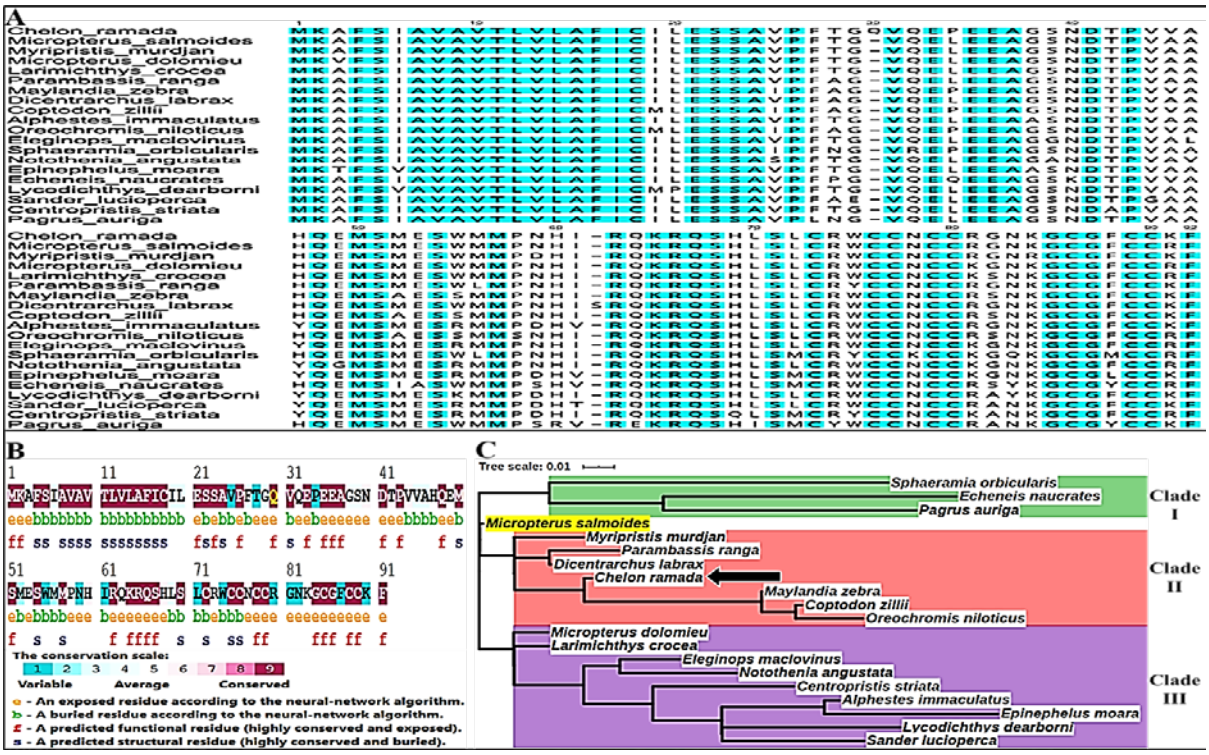

Figure 15. Phylogenetic and conservation analysis of the relationship Crhep2A and its orthologous prepropeptide in some bony fish species. (A) multiple sequence alignment (conserved residues highlighted in cyan). (B) conservation analysis. (C) phylogenetic tree.

Interestingly, about 55% (50 amino acids) of Crhep2A were highly conserved when the sequence was aligned with 19 orthologous prepropeptides from 19 bony fish species (Figure 15A and B). The 26 conserved amino acids could be exposed in the folded polypeptide, while 24 could be buried (Figure 15B). The amino acid in the position 30 (Glutamine or Q) was characteristic for Crhep2A and was not found in Crhep2B or the aligned sequences. The aligned data were used to make a phylogenetic tree and the results showed that the investigated hepcidins sequences were clustered in 3 main clades in addition to isolated branch which contained only the *M. salmoides* hepcidins (Figure 15C). Crhep2A was positioned in Clade II which contained hepcidins of 7 species. *C. ramada, M. zebra, C. zillii* and *O. niloticus* hepcidins were connected to the same node and form a subclade in which the last 3 prepropeptides grouped together. Regarding the distances between Crhep2A and the other hepcidin sequences in the tree, the *D. labrax* (European bass) and *E. moara* (Longtooth grouper fish) hepcidin sequences were estimated to have the smallest and the largest distances, respectively. The predicted structure of Crhep2A propeptide was constructed of 77% turn and 23% coil while, Crhep2B was constructed of 13.1% alpha helix,65.5% turn,14.8% coil and 6.6% 3-10 helix. Conserved eight cysteine residues were detected in both isoforms of Crhep2. In Crhep2A, four cysteine residues formed two disulfide bonds (Cys48-Cys64, Cys52-Cys61) (Figure 16A) while, in Crhep2B two cysteine residues formed one disulfide bond (Cys54-Cys60) (Figure 16B).

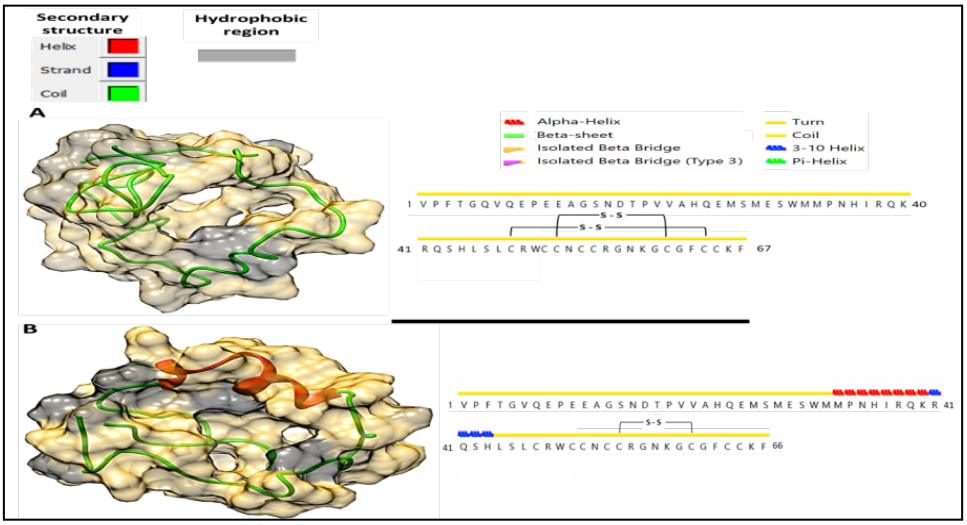

Figure 16. The predicted 3D structure of Crhep2 clone A (A) and clone B (B) propeptides shows the secondary structures and molecular surface of the peptides (left) and description for the secondary structure and disulfide bonds within the peptides (right).

4. Discussion

NK-lysin has been identified in many fish species, such as Japanese flounder (*Paralichthys olivaceus*) (Hirono *et al*., 2007), half-smooth tongue sole (*Cynoglossus semilaevis*) (Zhang *et al*., 2013), zebrafish (*Danio rerio*) (Pereiro *et al*., 2015), channel catfish (*Ictalurus punctatus*) (Wang *et al*., 2006a and 2006b), common carp (*Cyprinus carpio*) (Wang *et al*.,2018), Nile tilapia (*Oreochromis niloticus*) (Huang *et al*., 2018), turbot (*Scophthalmus maximus*) (Pereiro *et al*., 2017), Atlantic salmon (*Salmo salar*) (Acosta *et al*., 2019), and large yellow croaker (*Larimichthys crocea*) (Zhou *et al*.,2016), mudskipper (*Boleophthalmus pectinirostris*) (Ding *et al*., 2019). In contrast to the single copy gene in human, some fish have several copies of Nk-lysins, for example, zebrafish showed the highest score as it possesses four copies.

Deduced amino acid sequence of Cgnkl contains 128 aa. A signal peptide (17aa) was predicted as well as the characteristic surfactant-associated protein B (SapB) domain of the SAPLIPs (saposin-like protein family). Saposins have been reported to increase the level of intracellular ceramide, a molecule involved in the induction of apoptosis, via activating lipid-degrading enzymes, such as glucosylceramidase and sphingomyelinases. Saposin-like polypeptides are known to be greatly resistant to thermal denaturation; however, such property is abolished after reduction of the disulfide bonds (Gonzalez *et al*., 2000). One N-glycosylation site was identified in Cgnkl at 72-75aa, which is needed for the intracellular transport mechanism (Martınez *et al*., 2001). Also, four N- myristoylation sites at 13-18, 34-39, 54-59 and 71-76aa were detected. Lately, Krishnakumari *et al* (2018) indicated that myristoylation enhances antibacterial activity and modulates hemolytic activity to different extents.

The amino acid sequence of Cgnkl contains six well conserved cysteines residues that form three disulfide bonds. Cgnkl consisted of five-helices, spaced by three loops, as evident from the predicted 3D structure. As previously reported by Pereiro *et al*. (2015), this structure allows the interaction with biological membranes and the ability to altering the membrane integrity. The second and third α-helices in NK-lysin define a helix-loop-helix motif that is similar to the structural patterns of smaller anti-bacterial peptides such as bactenecin (coil-loop-coil) or protegrins (sheet-loop-sheet) (Andreu *et al*., 1999). NK-lysin is known to be extremely stable polypeptide, as its structure remains conserved after the interaction with their target cell membranes. This stability is due to its amphipathic character of 3 of its 5 helices and the disulfide bridges (Waring *et al*., 2016). Phylogenetic tree analysis showed that Cgnkl was grouped with bony fish from the same order (*siluriforms*) and was closely related to *P. hypophthalmus* (Iridescent Shark fish).

Hepcidin, a small cysteine-rich antimicrobial peptide, plays an important role in host immunological process and

iron regulation (Ke *et al*., 2015). The genomic copies of hepcidin differ notably depending on the organism. There are multiple copies of hepcidin in fish unlike most mammals which possess a single copy. It has been reported that at least five copies of hepcidin genes are found in winter flounder (Douglas *et al*., 2003) and seven copies in black porgy (Yang *et al*., 2007). In the present study, all identified hepcidins showed the characteristic features of fish hepcidins. The predicted cleavage site for the signal peptide was between Ala24 and Val25.

Fish HAMPs are divided into HAMP1 and HAMP2 groups. HAMP2 presents only in acanthopterygians, while HAMP1 presents in both acanthopterygians and non-acanthopterygians (Kim *et al*., 2019). *C. gariepinus* is a non-acanthopterygian species. Thus, the identified Cghep belongs to the HAMP1 group. The hypothetical iron regulatory sequence, QSHLS that is found in the N–terminus prior to the first Cysteine residue in the mature peptide, is not found in HAMP2 (Kim *et al*., 2019). Crhep2 lacks QSHLS motif indicating that it belongs to HAMP2 group. Consequently, Crhep2 could be more involved in iron regulation, whereas Crhep1 could be involved in the immune defense.

Sequence alignment of Cghep, Crhep1 and Crhep2 with other fish species showed a high degree of conservation, particularly the eight cysteine residues. These residues are involved in the formation of four disulfide bonds, which may stabilize hairpin-like structure. This structure is believed to be essential for proper antimicrobial and cytotoxic properties (Álvarez *et al*., 2014). Nevertheless, hepcidins of some fish have been found to have less than eight cysteine residues and still likely to be fully functional (Nemeth *et al*., 2006). Hirono *et al*. (2005) reported only six cysteine residues in Japanese Flounder (*P. olivaceus*).

Interestingly, as evident from the structure of prohepcidins identified in this study, not all of eight cysteine residues participated in formation of disulfide bonds. In Cghep and Crhep2B, only two residues formed one disulfide bond while, in Crhep1 and Crhep2A, four residues formed two bonds. Previous studies reported that Cysteine residues may serve different functions including: structural stabilization through forming stable disulfide-bonded, Metal-binding, catalytic activity and regulatory roles as they serve as sites of post translational modifications (Tu *et al*., 2004; De Domenico *et al*., 2008; Marino and Gladyshev, 2011; Marino and Gladyshev, 2012).

In Cghep, four SNPs were detected. C78T and A195G were synonyms SNPs while A67G and T144G were non-synonyms SNPs which caused threonine/alanine and glutamic acid/aspartic acid variations, respectively. In Crhep1, one synonyms SNP (C196A) and two non-synonyms SNPs (C194A and T205C) were detected. The non-synonymous SNPs C194A and T205C leads to alanine/aspartic acid and phenylalanine/leucine variations, respectively. Fernandes *et al* (2010) suggested that this genetic variation due to accelerated evolutionary rates might be directed when the host is exposed to pathogens. In our previous study, two SNPs were detected in hepcidin-1 that was identified from Nile tilapia species (*S. galilaeus*). 108 A/G was synonyms SNP and 101 A/T was non-synonyms SNP that caused Glutamine / Leucine variation. Also, one synonyms SNP (86 T/C) and one non-synonyms SNP (101 G/T) were detected in hepcidin-2. In hepcidin 2 identified from *T. Zilli*, one synonyms SNP (213 C/T) and one non-synonyms SNP (101 G/T) were found (Karima *et al*., 2020). In the present study, two Crhep2 isoforms were detected due to the absence of amino acid, Glutamine or Q, in the position 30. Pereiro *et al.* (2012) suggested that the different isoforms help fish to develop their innate immune recognition capabilities.

The post-translational modifications, such as phosphorylation, myristoylation and microbodies targeting motifs, are important for both structure and function of AMPs. They have the ability to tune peptide activities and lead to diverse structural scaffolds (Wang *et al*., 2012). Maurer-Stroh and Eisenhaber (2004) observed that N-myristoylation mediates the viral infectivity and eukaryotic infections. Recently, Latendorf *et al* (2019) demonstrated that the extent of post-translational modification and the peptide chain length are the major factors that control the antimicrobial output.

Sequence alignment with different bony fish species showed that about 55% of the deduced amino acid of Crhep2A is highly conserved. The higher variability in the amino acid sequence of Crhep1 might be an evolutionary mechanism for the recognition of a diverse range of microbes and the longer half-life with regard to Crhep2 could favor the elimination of pathogens (Pereiro *et al*., 2012). *C. ramada* hepcidins placed it with species from orders cichliformes and perciforms. Phylogenetic analysis showed that Crhep2 is highly homologous with *D. labrax* (European seabass), while Crhep1 is highly homologous with *O. niloticus* (Nile tilapia). Furthermore, the Cghep is highly homologous with *P. hypophthalmus* (Iridescent shark fish) from the same order (*Siluriformes*) and less homologous with *E. naucrates* (slender shark sucker) from order *carangiform*.

5. Conclusion

In the present study, coding sequences of Cgnkl, Cghep, Crhep1 and Crhep2 were analyzed. Cgnkl was found to possess all characteristic features of previously identified NK-lysins. The coding sequences of Cghep, Crhep1 and Crhep2 show the similar predicted signal cleavage site as well as eight characteristic cysteine residues. Further studies will be required to analyze the basal expression of the identified AMPs mRNA in different tissues.

Acknowledgement

The work was funded by the Science and Technology Development Fund (STDF), Egypt (Grant number: 15153).

References

Acosta J, Roa F, Gonzalez-Chavarria I, Astuya A, Maura R, Montesino R, Munoz C, Camacho F, Saavedra P and Valenzuela A. 2019. In vitro immunomodulatory activities of peptides derived from Salmo salar NK-lysin and cathelicidin in fish cells. *Fish Shellfish Immunol*, 88:587–594. d.

Álvarez CA, Guzmán F, Cárdenas C, Marshall S H and Mercado L. 2014. Antimicrobial activity of trout hepcidin. *Fish and ShellfishImmunology*, **41**:93–101.

Andreu D, Cristina C, Charlotte L, Hans G B and Mats A. 1999. Identification of an anti-mycobacterial domain in NK-lysin and granulysin. *Biochem J* ,344: 845-849.

Andrews S. 2010. FastQC: a quality control tool for high throughput sequence data. Available online at: http://www.bioinformatics.babraham.ac.uk/projects/fastqc

Bolger AM, Lohse M and Usadel B. 2014 . Trimmomatic: a flexible trimmer for Illumina sequence data. *Bioinformatics*, 30(15):2114-2120.

Bruno R, Maresca M and Canaan S. 2019. Worms' Antimicrobial Peptides. *Mar Drugs*.17:512.

De Domenico I, Nemeth E, Nelson JM, Phillips JD, Ajioka RS and Kay MS. 2008.The hepcidin-binding site on ferroportin is evolutionarily conserved. *Cell Metab*, 8:146–56. doi.org/10.1016/j.cmet.2008.07.002.

Ding FF, Li CH and Chen J. 2019. Molecular characterization of the NK-lysin in a teleost fish, Boleophthalmus pectinirostris: Antimicrobial activity and immunomodulatory activity on monocytes/macrophages**.** *Fish Shellfish Immunol*, 2:256-264. d

Douglas SE, Gallant JW, Ryan SL, Andrew D and Stephen CMT. 2003. Identification and expression analysis of hepcidin-like antimicrobial peptides in bony fish. *Developmental and Comparative Immunology*, 27 :589–601.

Drakesmith H and Prentice AM. 2012. Hepcidin and the iron-infection axis. *Science*, 338:768–772.

Enis A, Dannon B, Bérénice B, Marius B, Dave B, Martin Č, John C, Dave C, Nate C, Björn G,AG, Jennifer H, Vahid J, Helena R, Nicola S, Jeremy G, James T, Anton N, and Daniel B. *Nucleic Acids Research*, 46(W): W537–W544.

Fan K, Li H, Wang Z, Du W, Yin W, Sun Y and Jiang J. 2016. Expression and purification of the recombinant porcine NK-lysin in Pichia pastoris and observation of anticancer activity in vitro. *Pre. Biochem Biotechnol*, 46: 65–70.

FAO**.** 2017. Global aquaculture production dataset 1950–2015 (FishstatJ). Available at :SSSSSSSSSSSSSSSSSSSSSSSSSSSSS www.fao.org/fishery/statistics/software/fishstatj/e.

Fernandes JMO, Ruangsri J and Kiron V. 2010. Atlantic cod piscidin and its diversification through positive selection. *PloS One*, **5**: 9501.

Gonzalez C, Langdon GM, Bruix M, Galvez A, Valdivia E, Maqueda M and Rico M. 2000. Bacteriocin AS-48, a microbial cyclic polypeptide structurally and functionally related to mammalian NK-lysin. *Proceedings of the National Academy of Sciences*, 97(21):11221-11226.

Haas BJ, Papanicolaou A, Yassour M, Grabherr M, Blood PD and Bowden J. 2013. *De novo* transcript sequence reconstruction from RNA-seq using the Trinity platform for reference generation and analysis. *Nat Protoc*, 8:1494–512.

Hirono I, Hwang JY, Ono Y, Tomofumi K, Ohira T, Nozaki R, et al. Two different types of hepcidins from the Japanese flounder. Paralichthys olivaceus FEBS J. 2005;272:5257-64.

Hirono I, Kondo H, Koyama T, Arma NR, Hwang JY, Nozaki R, Midorikawa N and Aoki T. 2007. Characterization of Japanese flounder (Paralichthys olivaceus) NK-lysin, an antimicrobial peptide. *Fish Shellfish Immunol.* 22:567–575.

Huang T, Wei G, Bingqian W, Yuyong Z, Lili C, Zuochun Y, Cheng Z, Gefeng X. 2019. Identification and expression of the hepcidin gene from brown trout (Salmo trutta) and functional analysis of its synthetic peptide. *Fish Shellfish Immunol*, 87:243–253

Huang X, Hu B, Yang X, Gong L, Tan J, and Deng L. 2018. The putative mature peptide of piscidin-1 modulates global transcriptional profile and proliferation of splenic lymphocytes in orange-spotted grouper (*Epinephelus coioides*). *Fish Shellfish Immunol*. 86:1035–1043.

Karima FM, Dalia MM, Aboelenin MM and Heba AM. 2020. Molecular characterization and expression analysis of hepc1 and hepc2 in three tilapia species collected from Lake Manzala. *Bulletin of National Research Centre*, accepted.

Ke F, Yun W, Chuan-Shun Y and Chen X. 2015. Molecular cloning and antibacterial activity of hepcidin from Chinese rare minnow (Gobiocypris rarus). *Electronic Journal of Biotechnology,18:* 169–174.

Kim C, Eun J and Yoon K N. 2019. Chondrostean sturgeon hepcidin: An evolutionary link between teleost and tetrapod hepcidins. *Fish Shellfish Immunol*,88 :117–125.

Kim WH , Lillehoj HS and Gay CG. 2016. Using genomics to identify novel antimicrobials. *Rev Sci Tech Off Int Epiz*, 35 (1): 95-103.

Krishnakumari V , Ankeeta G , Harikrishna A and Ramakrishnan N. 2018. Effects of increasing hydrophobicity by N-terminal myristoylation on the antibacterial and hemolytic activities of the C-terminal cationic segments of human-β-defensins. *J Chem Biol Drug Des*, 92:1504–1513.

Kumar S, Stecher G, Li M, Knyaz C, and Tamura K. 2018. Molecular Evolutionary Genetics Analysis across computing platforms. *Molecular Biology and Evolution*, 35:1547-1549.

Lai Y and Gallo R L. 2009. AMPed up immunity: how antimicrobial peptides have multiple roles in immune defense. *Trends Immunol*, 30:131–141.

Lama R, Pereiro P, Costa MM, Encinar JA, Medina-Gali RM, Perez L, Lamas J, Leiro J, Figueras A and Novoa B. 2018. Turbot (*Scophthalmus maximus*) NK-lysin induces protection against the pathogenic parasite philasterides dicentrarchi via membrane disruption. *Fish Shellfish Immunol*,82:190–199.

Latendorf T, Ulrich G and Zhihong W. 2019. Antimicrobial Peptides (CIDAMPs) Represent a New Paradigm of Innate Defense with a Potential for Novel Anti-Infectives. *Scientific Reports, 9:3331.*

Mahrous KF, Aboelenin MM, Abd El-kader HA, Mabrouk DM, Gaafar AY, Younes AM, Mahmoud MA, Khalil WKB and Hassanane MS. 2020a. Piscidin 4: Genetic expression and comparative immunolocalization in Nile tilapia (Oreochromis niloticus) following challenge using different local bacterial strains. *Developmental & Comparative Immunology*, 112: 103777.

Mahrous KF, Aboelenin MM, Rashed MA, Abd El-Hafiez MA and Rushdi HE. 2020b. Detection of polymorphism within leptin gene in Egyptian river buffalo and predict its effects on different molecular levels. *Journal of Genetic Engineering and Biotechnology*, 18: 6.

Mahrous KF, Mabrouk DM, Aboelenin MM, Abd El-kader HA, Gaafar AY, Younes AM, Mahmoud MA, Khalil WKB and Hassanane MS. 2020c. Molecular characterization and immunohistochemical localization of tilapia piscidin 3 in response to Aeromonas hydrophila infection in Nile tilapia. *Journal of Peptide Science*, 26 (11): e3280.

Marino S. M. and Gladyshev VN. 2011. Redox biology: computational approaches to the investigation of functional cysteine residues. *Antioxid Redox Signal*, 15: 135–146

Marino S. M. and Gladyshev VN. 2012. Analysis and Functional Prediction of Reactive Cysteine Residues. *The Journal Of Biological Chemistry*, 287(7):4419–4425.

Martin J, Letellier G and Marin A .2005 Protein secondary structure assignment revisited: a detailed analysis of different assignment methods. *BMC Struct Biol*, 5: 17.

Martınez M, Irene P, Beatriz L, Enrique N, Cecilio G, Francisco Z, and Carmen A. 2001.The Role of N-Glycosylation in Transport

to the Plasma Membrane and Sorting of the Neuronal Glycine Transporter, *The Journal Of Biological Chemistry*. 276(3):2168 – 2173.

Masso-Silva JA and Diamond G. 2014. Antimicrobial peptides from fish. *Pharmaceuticals*, 7:265–310.

Maurer-Stroh S and Eisenhaber F . 2004. Myristoylation of viral and bacterialproteins. *Trends in Microbiology*,12:178–185,.

Mehanna SF, Desouky MG, Makkey AF. 2019. Some Targeted Reference Points for Thin Lip Grey Mullet Liza Ramada Management in Bardawil Lagoon, North Sinai, Egypt. *Fish Aqua J* 10:263.

Nemeth E, Preza GC, Jung CL, Kaplan J, Waring AJ, Ganz T. 2006. The N-terminus of hepcidin is essential for its interaction with ferroportin: structure-function study. *Blood*,107:328-333.

Neves JV, Migue F R, Ana CM, Tânia S, Maria SG and Pedro NS.2017. Rodrigues Hamp1 but not Hamp2 regulates ferroportin in fish with twofunctionally distinct hepcidin typesHepcidin is a small cysteine rich peptide. *Scientific Reports*, 7: *14793*.

Pereiro P, Figueras A and Novoa B. 2012. A novel hepcidin-like in turbot (*Scophthalmus maximus L*.) highly expressed after pathogen challenge but not after iron overload. Fish Shellfish Immunol, 32 : 879-889.

Pereiro P, Romero A, Diaz-Rosales P, Estepa A, Figueras A and Novoa B. 2017. Nucleated teleost erythrocytes play an NK-lysin-and autophagy-dependent role in antiviral immunity. *Front Immunol*. 8:1458.

Pereiro P, Varela M, Diaz-Rosales P, Romero A, Dios S, Figueras A and Novoa B. 2015. Zebrafish NK-lysins: First insights about their cellular and functional diversification. Dev. Comp. Immunol. 51:148–159.

Sathyan N, Philip R, Chaithanya ER, Kumar PR, Sanjeevan VN and Singh IS. 2013. Characterization of Histone H2A Derived Antimicrobial Peptides, Harriottins, from Sicklefin Chimaera Neoharriotta pinnata (Schnakenbeck, 1931) and Its Evolutionary Divergence with respect to CO1 and Histone H2A. *ISRN Molecular Biology*,2013:1-10.

Shourbela R. M. 1; Ashraf, M. Abd El-latif 2 and Abd-El-Azem. 2014. Induced spawning of african catfish , *clarias gariepinus* using (gnrha) combined with dopamine antagonist. *Veterinary Medical Journal*, 27:25-35.

Sroor FM, Aboelenin MM, Mahrous KF, Mahmoud K, Elwahy AHM and Abdelhamid IA. 2020. Novel 2-cyanoacrylamido-4,5,6,7-tetrahydrobenzo[b]thiophene derivatives as potent anticancer agents. *Arch Pharm (Weinheim)*, 353(10): e2000069.

Stenger S, Hanson DA, Teitelbaum R, Dewan P, Niazi KR, Froelich CJ, Ganz T, Thoma-Uszynski S, Melian A and Bogdan C. 1998. An antimicrobial activity of cytolytic T cells mediated by granulysin. *Science*, 282:121–125.

Tu, B P, and Weissman, J S. 2004. Oxidative protein folding in eukaryotes :mechanisms and consequences. *J Cell Biol*, 164: 341–346.

Wang GL, Wang MC, Liu YL, Zhang Q, Li CF, Liu PT, Li EZ, Nie P, Xie HX. 2018. Identification, expression analysis, and antibacterial activity of NK-lysin from common carp *Cyprinus carpio*. *Fish Shellfish Immunol*, 73:11–21.

Wang Q, Bao B, Wang Y, Peatman E and Liu Z, 2006b. Characterization of a NK-lysin antimicrobial peptide gene from channel catfish. *Fish Shellfish Immunol*, 20 (3):419–426.

Wang Q, Wang Y, Xu P and Liu Z. 2006a. NK-lysin of channel catfish: gene triplication, sequence variation, and expression analysis. *Mol Immunol*, 43 (10): 1676–1686.

Wang Y, Liu X, Ma L, Yu Y, Yu H, Mohammed S, Chu G, Mu L, and Zhang Q. 2012. Identification and characterization of a hepcidin from half smooth tongue sole Cynoglossus semilaevis. *Fish Shellfish Immunol*, 33: 213–219.

Waring AJ, Gupta M, Gordon LM, Fujii G and Walther FJ. 2016. Stability of an amphipathic helix-hairpin surfactant peptide in liposomes. *Biochim Biophys Acta*, 1858(12):3113–3119.

Yang M, Wang K, Chen J, Qu H and Li S. 2007. Genomic organization and tissue-specific expression analysis of hepcidin-like genes from black porgy (*Acanthopagrus schlegelii* B). *Fish Shellfish Immunol*, 23:1060-1071.

Yang, J, Yan R, Roy A, Xu D, Poisson J and Zhang Y. 2015. The I-TASSER Suite: protein structure and function prediction. Nat. Methods, 12(1): 7-8.

Zhang M, Long H and Sun L. 2013. A NK-lysin from *Cynoglossus semilaevis* enhances antimicrobial defense against bacterial and viral pathogens. *Dev Comp Immunol*, 40:258–265.

Zhou QJ, Wang J, Liu M, Qiao Y, Hong WS, Su YQ, Han KH, Ke QZ and Zheng WQ. 2016. Identification, expression and antibacterial activities of an antimicrobial peptide NK-lysin from a marine fish *Larimichthys crocea*, 55:195-202.

JJBS

Jordan Journal of Biological Sciences

Volume 14, Number 1, March 2021
ISSN 1995-6673
Pages 65 - 74

Genetic relationship of some *Pisum sativum* subspecies using different molecular markers

Samira A. Osman* and Hoda B. M. Ali

Genetics and Cytology Department, Genetic Engineering and Biotechnology Division, National Research Centre, Giza, P.O. 12622, Egypt
Received April 4, 2020; Revised June 26, 2020; Accepted June 28, 2020

Abstract

Field pea (*Pisum sativum*) is a member of Viciae tribe and considers the basic model of modern plant genetics because it has been utilized in Mendel's laws of inheritance. Different molecular markers such as Random Amplified Polymorphic DNA (RAPD), Inter-Simple Sequence Repeats (ISSR) and Start Codon Targeted (SCoT) were utilized for determining the genetic relationships among six *Pisum sativum* subspecies (subsp. *asiaticum*, subsp. *abyssinicum*, subsp. *elatus*, and three subsp. *sativum* convarietes *axiphium*, *medullare* and *speciosum*). It was found that SCoTs marker gave the maximum values of polymorphism (75.24%) and gene diversity (0.29), while minimum values of polymorphism (62.7%) and gene diversity (0.23) were reported in RAPD markers. It has been observed that the dendrogram (UPGMA) results of combined data were identical to SCoT dendrogram (UPGMA) results. Therefore, SCoT was the most informative marker compared to ISSR and RAPD markers for discrimination and identification of studied *P. sativum* subspecies. It could be concluded from this study that the genetic relationship among the studied subspecies was as follows: subsp. *sativum* covariates, *speciosum, medullare* and *axiphium* are the most closely related to each other, then subsp. *elatus* which is more related to subsp. *abyssinicum* than subsp. *asiaticum*

Keywords:*Pisum sativum,* Genetic relationships, molecular markers, RAPD, ISSR, SCoT

1. Introduction

Fabaceae family is one of the largest families in higher plant after Gramineae and Brassicaceae and it is commonly called legumes or pulses. This family has more than 727 genera and 20,000 species (Gepts *et al.,* 2005). Legumes have an economic importance; they have some of beneficial food crops such as soybeans, peas, beans, lentils and peanuts. Other genera of this family are significant sources of green compost or animal nutrition such as cassia, lupins, soybean, alfalfa and clover. Some genera like Laburnum, Gleditsia, Robinia, Mimosa, Acacia and Delonix are ornamental trees and shrubs. Still, other genera of this family have medicinal or insecticidal properties (for insect Derris) or yield valuable substances like tannin dyes, gum arabic, or resins. The tribe Vicieae includes three genera such as *Vicia* L., *Lathyrus* L., and *Pisum* L. (Young *et al.,* 2003).

Field pea (*Pisum sativum*) was found in the Middle East and cultivated from 10,000 years ago (Blixt, 1972; Zohary, 1996; Mithen, 2003). Cultivated *Pisum* is prevailed by *P. sativum*, but *P. sativum* ssp abyssinicum (referred to as *P. abyssinicum*) is an independently derived cultivated type. *Pisum sativum* is perhaps considered as a species complex with multiple subspecies (Vershinin *et al.,* 2003; Tar'an *et al.,* 2005). Pea is considered the basic model of modern plant genetics because it has been utilized in Mendel's laws of inheritance discover. It has a chromosome number of 2n = 14. The climate changes and the recent technologies make pea breeders perform more effective selection methods and take benefit of the large genetic diversity present in the *Pisum sativum* (Smýkal *et al.,* 2012).

Modern gene technological methods based upon induced mutants are becoming widespread in *P. stivum* subsp *sativum*. The induced variations in flower, pod, seed, leaf and stem characters have led to various attempts to classify the intraspecific diversity (Govorov, 1937; Makaševa, 1979; Lehmann and Blixt, 1984). Many convarieties and botanical varieties had been produced and described, a few like: convar. *speciosum* (Dierb.) Alef., the field peas, used now mainly as grain forage, convar. *axiphium* Alef., is known as the sugar pea with edible pods, convar. *sativum*, common pea, the dry and green seeds used, and convar. *medullare* Alef., only the green seeds useful.

Molecular markers were considered powerful tools to determine the genetic diversity through DNA sequence variations. These markers have an advantage by requiring a little amount of DNA and are fast to analyze (Sharma *et al.,* 2008). Molecular markers based on DNA assist plant breeders to directly estimate genetic variation among the relative plants without effect of environmental factors (Nguyen *et al.,* 2004). Several molecular markers were used to evaluate the extent of genetic variability, such as Random amplified polymorphic DNA (RAPD) (Pérez de la Vega, 1997, which has been widely applied for examining genetic diversity and genetic relationships among several legumes including pea (Simioniuc *et al.,* 2002; Baranger *et al.,* 2004; Tar'an *et al.*, 2005; Yadav *et al.,* 2010; Kwon *et al.,* 2012). Inter-simple sequence

* Corresponding author e-mail: s_nrc82@yahoo.com..

repeats (ISSR) marker is more reliable than the RAPD marker because it is simple, fast, cheap and highly discriminating, so it is considered an informative tool for estimating genetic relationships (Ci *et al.*, 2008; Crespe *et al.*, 2009; Zhang and Dai, 2010; Uysal *et al.*, 2010). Nowadays, Start codon targeted (SCoT) markers are considered novel alternative and reproducible tools. SCoT-PCR technique depends on the short conserved region surrounding the ATG translation start (or initiation) codon in plant genes. (Collard and Mackill, 2009; Amirmoradi *et al.*, 2012; Hamidi *et al.*, 2014). SCoTs are used due their importance as constructing markers helping in breeding programs than RAPDs, ISSRs. These markers have some properties as being fast, easy to use and cheap (Mulpuri *et al.*, 2013).

The purpose of the current study is to figure out the genetic relationships among different *Pisum sativum* subspecies based on polymorphism of RAPD, ISSR and SCoT markers.

2. Materials and Methods

2.1. Plant materials:

Seeds of *Pisum sativum* subspecies, *asiaticum* Gov, *abyssinicum* (A. Braun) Berger, *elatus* (M. Bieb) schmalb, and three convarities of subsp. *sativum* (*axiphium* Alef "Dvargsabel", *medullare* and *speciosum* (Dieb) Alef) were received from Leibniz Institute of Plant Genetics and Crop Plant Research (IPK, Gatersleben, Germany).

2.2. DNA extraction and purification:

Young leaves from each seedling plant of studied *P. sativum* subspecies were collected and genomic DNA was extracted and purified. Plant Genomic DNA Purification Kit (Gene Jet Mini Kit, Cat no. K0791, Thermo- Fisher Scientific, Germany) was used for extraction and purification of genomic DNA. The extracted DNA was checked on agarose gel (1%) using horizontal electrophoresis and diluted to working concentration 50 ng/µl by nuclease-free water and stored at -20 °C.

2.2.1. RAPD-PCR Amplification:

Six 10 bp random primers (Table 1) were used for performing RAPD-PCR. Amplification of purified DNA was achieved in PCR microtubes (Eppendorf 0.2 ml) containing 12.5 µl PCR Master Mix 2X (Dream Taq Green, Thermo-Fisher Scientific, Germany), 1 µl primer (Metabion, Germany) 10 pmol and 1 µl purified DNA (50 ng/µl) with total volume 25 µl of the reaction mixture. Thermocycler (Bio-Rad, USA) was programmed as follows: one cycle (94 °C for 5 min), 35 cycles (94 °C for 1 min, 38 °C for 45 sec and 72 °C for 45 sec), one cycle (72 °C for 5min) and finally held at 4°C. Afterward, 5µl of each PCR product were loaded in agarose gel (1%) in TAE buffer, together with 3 µl DNA Ladder 100 bp (H3 RTU, Cat No. DM003-R500, GeneDirex) in horizontal electrophoresis (Cleaver, UK) for about 2 hours at 100 V. The gel was stained with ethidium bromide and photographed by gel documentation (Bio-Rad, USA).

Table 1. Represented RAPD, ISSR and SCoT primers sequence.

Ser. No.	RAPD primers sequence			ISSR primers sequence			SCoT primers sequence		
	Primers	Sequence (5-3)	Tm (°C)	Primers	Sequence (5-3)	Tm (°C)	Primers	Sequence (5-3)	GC%
1	OPA1	CAGGCCCTTC	38	ISSR2M	(CA)8 AAGCT	61	SCoT-1	CAACAATGGCTACCACCA	50
2	OPA4	AATCGGGCTG	38	807	(AG)8 T	55	SCoT-3	CAACAATGGCTACCACCG	56
3	OPA11	CAATCGCCGT	38	812	(GA)8 A	54	SCoT-6	CAACAATGGCTACCACGC	56
4	OPB3	CATCCCCCTG	38	818	(CA)8 G	55	SCoT-9	CAACAATGGCTACCAGCA	50
5	OPH7	CTGCATCGTG	38	842	(GA)8 CTG	58	SCoT-10	CAACAATGGCTACCAGCC	56
6	OPH12	ACGCGCATGT	38	848	(CA)8AAGG	61	SCoT-11	AAGCAATGGCTACCACCA	50
7	-	-	-	857	(AC)8 CTG	54	SCoT-14	ACGACATGGCGACCACGC	67
8	-	-	-	866	(CTC)6	61	SCoT-15	ACGACATGGCGACCGCGA	67

2.2.2. ISSR-PCR Amplification:

ISSR-PCR was carried out by using eight ISSR primers (Table 1). Amplification of purified DNA was achieved in PCR microtubes (Eppendorf 0.2 ml) containing 12.5 µl PCR Master Mix 2X (Dream Taq Green, Thermo-Fisher Scientific, Germany), 1 µl primer (Metabion, Germany) 10 pmol and 1 µl purified DNA (50 ng/µl) with total volume 25 µl of the reaction mixture. Thermocycler (Bio-Rad, USA) was programmed as follows: one cycle (93°C for 20 sec), 40 cycles (94 °C for 20 sec, Tm (54-61) °C for 1 min and 72 °C for 20 sec), one cycle (72 °C for 6 min) and finally held at 4°C. Afterward, 5µl of each PCR product was loaded in agarose gel (1.5%) in TAE buffer and electrophoresis was run as described above.

2.2.3. SCoT-PCR Amplification:

SCoT-PCR was achieved by using eight SCoT primers (Table 1). Amplification of purified DNA was achieved in PCR microtubes (Eppendorf 0.2 ml) containing 12.5 µl PCR Master Mix 2X (Dream Taq Green, Thermo-Fisher Scientific, Germany), 1 µl primer (Metabion, Germany) 10 pmol and 1 µl purified DNA (50 ng/µl) with total volume 25 µl of the reaction mixture. Thermocycler (Bio-Rad, USA) was programmed as follows: one cycle (94 °C for 3 min), 35 cycles (94 °C for 1 min, 50 °C for 1 min and 72 °C for 2 min), one cycle (72 °C for 5 min) and finally held at 4 °C. Afterward, 5µl of each PCR product was loaded in agarose gel (1.2%) in TAE buffer and electrophoresis was run as described above.

2.2.4. Data analysis and molecular dendrograms construction:

Total Lab program was used to analyze images of RAPD, ISSR and SCoT assays for detecting the molecular size of each fragment and compare their presence or absence among studied species, and these data were analysed using MVSP (Multi-Variant Statistical Package, Kovach, 1998). The similarity matrix was studied and dendrogram (UPGMA, using Jaccard's coefficient) was constructed to indicate the genetic relationships between the studied species.

Polymorphic information content (PIC) values reflected gene diversity of studied species; it could be calculated with the following equation (Anderson *et al.*, 1993):

$$PICi = 1 - \sum_{f=1}^{n} (Pij)^2$$

Where, n is the number of marker alleles for marker *i* and *Pij* is the frequency of the *j* the allele for marker *i*.

The summary statistics including the number of alleles per locus, major allele frequency, gene diversity, polymorphism information content (PIC) values were calculated using Power Marker version 3.25 (Liu and Muse, 2005).

3. Results

The genetic relationships of the studied six *Pisum sativum* subspecies were determined by RAPD, ISSR and SCoT markers, the patterns of the amplified DNA products by their primers are shown in Figures 1, 2 and 3, respectively. The phylogenetic dendrograms by UPGMA of RAPD, ISSR, SCoT and combined data of three markers together were illustrated in Figure 4.

3.1. Random amplified polymorphic DNA (RAPD) analysis

The results of RAPD amplification are present in Table 2. The six RAPD primers produced good reproducible patterns, that screened the polymorphisms between the different *Pisum sativum* subspecies (Figure 1).

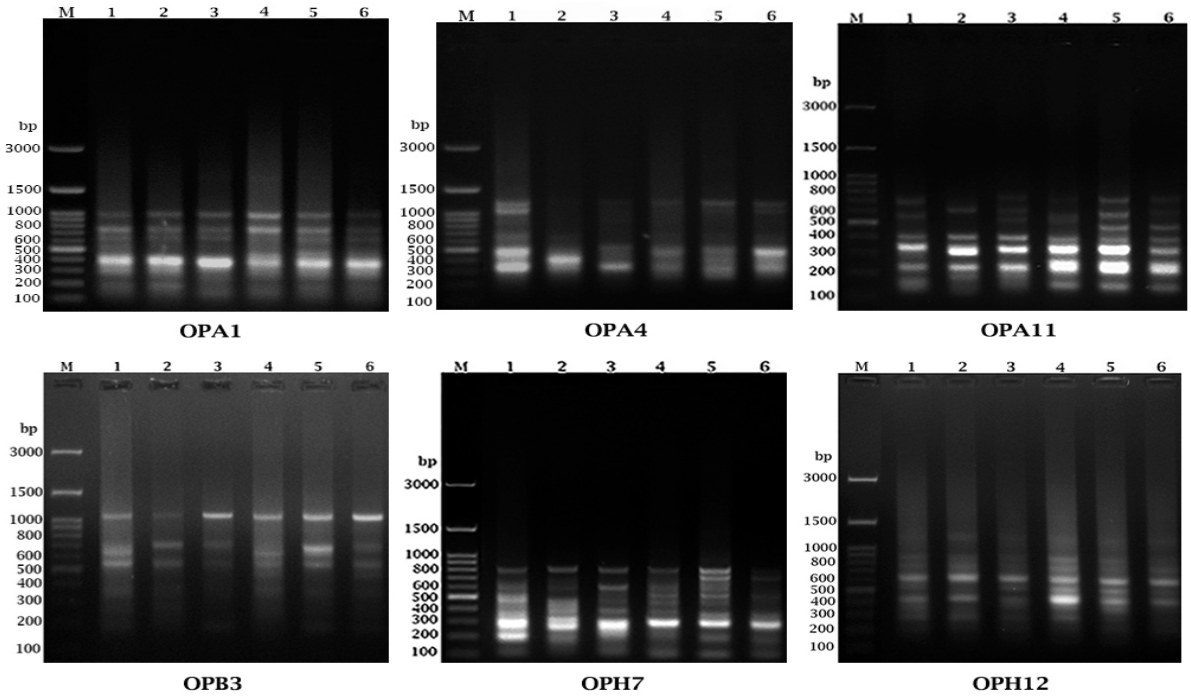

Figure 1. Electrophoresis of RAPD-PCR amplification for *Pisum sativum* subspecies.

M: DNA ladder 100 bp

1- *P. sativum* subsp. asiaticum 2- *P. sativum* subsp. abyssinicum 3- *P. sativum* subsp. elatus 4- *P. sativum* subsp. sativum con var. axiphium" 5- *P. sativum* subsp. sativum con var. medullare 6- *P. sativum* subsp. sativum con var. speciosum

A total number of 59 amplicons were produced, among them 37 bands were polymorphic. The polymorphism ranged between 33.33% with primer OPH12 and 80% with primer OPA1 with an average 62.71%. Polymorphic information content (PIC) and Gene diversity ranged from 0.11 and 0.14 in primer OPH12 to 0.14 and 0.32 in primer OPA1 with an average of 0.18 and 0.23, respectively. All of the studied subspecies had 9 positive unique bands (band present only in one subspecies while absent in others) and 8 negative unique bands (band absent only in one subspecies while present in others) (Table 2). The phylogenetic dendrogram showed two main clusters. The first cluster split into two sub-clusters, (A) contained subsp. *sativum* convar. *medullare* and convar. *speciosum* while the second sub-cluster (B) contained convar. *axiphium* only. The second cluster split into two sub-clusters, (C) contained subsp. *asiaticum* and subsp. *elatus* while the second sub-cluster (D) contained only subsp. *abyssinicum* (Figure 4a).

The highest similarity value 0.79 was found between subsp. *sativum* convar. *medullare* and *speciosum* then 0.75 between convar. *axiphium* and *medullare*, which indicates that these three convarities are more closely related. It has been observed that subsp. *elatus* is more related to subsp. *asiaticum* than subsp. *Abyssinicum*, while the lowest value observed was 0.50 between subsp. *abyssinicum* and subsp. *sativum* convar. *Speciosum* (Table 3).

Table 2. Total number of bands polymorphism, gene diversity and PIC as revealed by RAPD-PCR amplification of *Pisum sativum* subspecies.

Primer	Total of fragments	Polymorphic fragments	Monomorphic fragments	Polymorphism (%)	+ve Unique band	-ve Unique band	Gene Diversity	PIC	Allele size range (bp)
OPA1	10	8	2	80.00%	1	1	0.32	0.26	170-1000 bp
OPA4	8	5	3	62.50%	2	2	0.20	0.17	280-1185 bp
OPA11	11	7	4	63.63%	3	2	0.21	0.17	140-720 bp
OPB3	12	9	3	75.00%	3	0	0.30	0.24	190-1040 bp
OPH7	9	5	4	55,55%	0	2	0.22	0.17	100-800 bp
OPH12	9	3	6	33.33%	0	1	0.14	0.11	185-1100 bp
Total	59	37	22	-	9	8	-	-	-
Average	9.83	6.166	3.66	62.71%	-	-	0.23	0.18	-

Table 3. Similarity matrix among examined *Pisum sativum* subspecies estimated based on Jaccard' Coefficient as revealed by RAPD marker.

***P. sativum* subsp. asiaticum**	1					
***P. sativum* subsp. abyssinicum**	0.70	1				
***P. sativum* subsp. elatus**	0.71	0.70	1			
***P. sativum* subsp. sativum con var. axiphium**	0.67	0.59	0.67	1		
***P. sativum* subsp. sativum con var.medullare**	0.71	0.61	0.61	0.75	1	
***P. sativum* subsp. sativum con var. speciosum**	0.633	0.50	0.60	0.60	0.79	1
	***P. sativum* subsp. asiaticum**	***P. sativum* subsp. abyssinicum**	***P. sativum* subsp. elatus**	***P. sativum* subsp. sativum con var. axiphium**	***P. sativum* subsp. sativum con var.medullare**	***P. sativum* subsp. sativum con var. speciosum**

3.2. Inter-simple sequence repeats (ISSR) analysis

The amplified products of eight ISSR primer are present in Table (4). The primers gave a reproducible patterns that showed the polymorphisms among studied *P. sativum* subspecies (Figure 2).

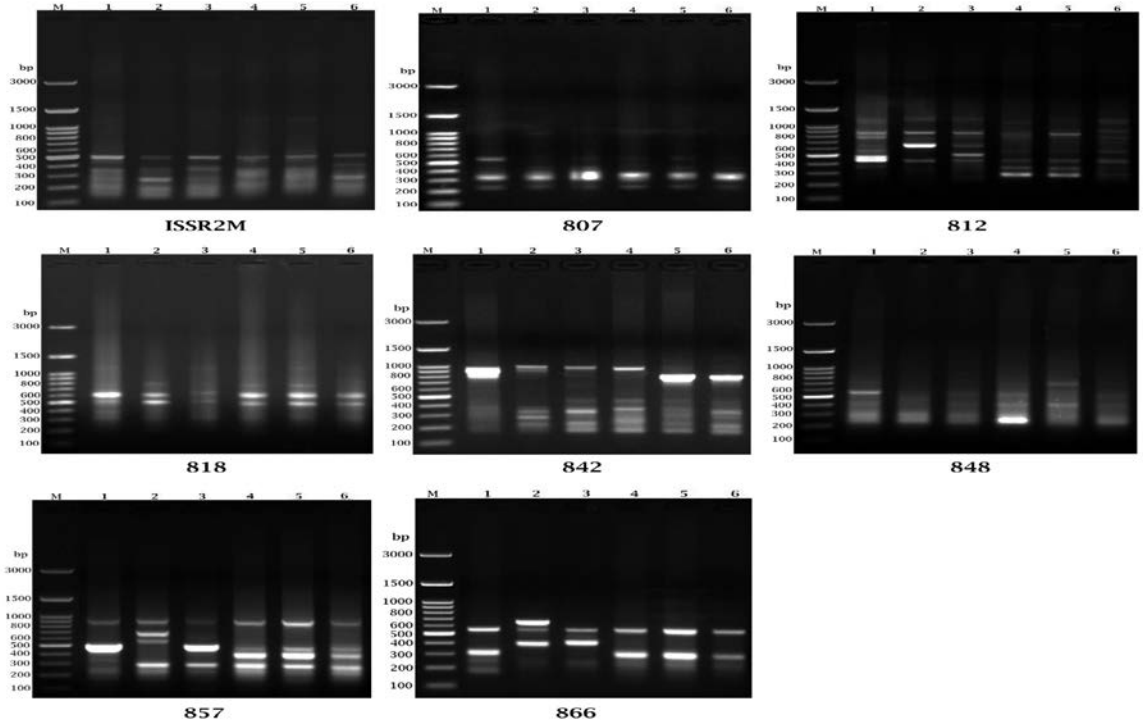

Figure 2. Electrophoresis of ISSR-PCR amplification for *Pisum sativum* subspecies.

M: DNA ladder 100 bp

1- *P. sativum* subsp. asiaticum 2- *P. sativum* subsp. abyssinicum 3- *P. sativum* subsp. elatus 4- *P. sativum* subsp. sativum con var. axiphium 5- *P. sativum* subsp. sativum con var. medullare 6- *P. sativum* subsp. sativum con var. speciosum

Table 4. Total number of bands polymorphism, gene diversity and PIC as revealed by ISSR-PCR amplification of *Pisum sativum* subspecies.

Primer	Total of fragments	Polymorphic fragments	Monomorphic fragments	Polymorphism (%)	+ve Unique band	-ve Unique band	Gene Diversity	PIC	Allele size range (bp)
ISSR2M	12	10	2	83.33%	6	3	0.27	0.23	140-1220 bp
807	5	1	4	20.00%	0	0	0.09	0.07	210-1050 bp
812	14	12	2	85.71%	3	4	0.30	0.24	290-1200 bp
818	7	3	4	42.86%	0	0	0.19	0.15	320-1100 bp
842	12	11	1	91.66%	3	3	0.32	0.26	210-1000 bp
848	6	5	1	83.33%	0	0	0.38	0.29	240-680 bp
857	8	5	3	62.5%	1	2	0.26	0.21	230-900 bp
866	7	5	2	71.43%	2	0	0.27	0.22	190-650 bp
Total	71	52	19	-	15	12	-	-	-
Average	8.875	6.5	2.375	73.24	-	-	0.26	0.21	-

A total number of 71 amplified amplicons was obtained, among which 52 amplicons were polymorphic. The polymorphism ranged from 20 % with primer 807 and 91.66 % with primer 842. The average percentage of polymorphism was 73.24 %. The maximum polymorphic information content (PIC) and Gene diversity were 0.29 and 0.38, respectively with primer 848 while the minimum PIC and Gene diversity were 0.07 and 0.09, respectively with primer 807. The average of PIC and Gene diversity were 0.21 and 0.26, respectively. All investigated *Pisum sativum* subspecies had 15 positive and 12 negative unique bands. (Table 4). The phylogenetic dendrogram showed two main clusters; (A) contained only subsp. *asiaticum*, while the second cluster (B) contained all other subspecies which was subsequently split into two sub-clusters; (C) contained subsp. *abyssinicum* and subsp. *elatus*, while the second sub-cluster (D) contained the other three subspecies which is subsequently split into two groups, (E) contained only subsp. *sativum* convar. *speciosum*, and the second group (F) contained convar. *axiphium* convar. *medullare* (Figure 4b).

The highest similarity value 0.69 was reported between subsp. *abyssinicum* and subsp. *elatus*, then 0.68 between subsp. *sativum* convar. *axiphium* and convar. *medullare*, and between convar. *medullare* and convar. *speciosum* as well. While, the lowest value observed was 0.48 between subsp. *asiaticum* and subsp. *sativum* convar. *axiphium* (Table 5).

Table 5. Similarity matrix among examined *Pisum sativum* subspecies estimated based on Jaccard' Coefficient as revealed by ISSR marker.

***P. sativum* subsp. asiaticum Gov**	1					
***P. sativum* subsp. abyssinicum**	0.52	1				
***P. sativum* subsp. elatus**	0.55	0.69	1			
***P. sativum* subsp. sativum con var. axiphium**	0.48	0.62	0.68	1		
***P. sativum* subsp. sativum con var.medullare**	0.54	0.57	0.66	0.68	1	
***P. sativum* subsp. sativum con var. speciosum**	0.49	0.57	0.61	0.62	0.67	1
	***P. sativum* subsp. asiaticum**	***P. sativum* subsp. abyssinicum**	***P. sativum* subsp. elatus**	***P. sativum* subsp. sativum con var. axiphium**	***P. sativum* subsp. sativum con var.medullare**	***P. sativum* subsp. sativum con var. speciosum**

3.3. Start codon targeted Polymorphism (SCoT) analysis

The results of SCoT amplification were shown in Table (6). The eight primers gave reproducible patterns that screened the polymorphisms among the studied *Pisum sativum* subspecies (Figure 3).

A total of 105 bands were obtained, out of which 79 bands were polymorphic bands. The polymorphism ranged from 50% with SCoT-3 and 100% with SCoT-15. The average percentage of polymorphism was 75.24 %. The maximum polymorphic information content (PIC) and Gene diversity were 0.32 and 0.40, respectively with SCoT-15, while the minimum PIC and gene diversity were 0.15 and 0.19, respectively with SCoT-3. The average of PIC and Gene diversity were 0.23 and 0.29, respectively. All investigated subspecies had 20 positive unique and 10 negative unique bands. (Table 6). The phylogenetic dendrogram showed two main clusters; (A) contained subsp. *abyssinicum* and subsp. *elatus*, while the second cluster (B) contained all other subspecies. The second cluster was split into two sub-clusters; (C) contained only subsp. *asiaticum*, while the second sub-cluster (D) contained the other three species. The second sub-cluster split into two groups, (E) contained only subsp. *sativum*

convar. *axiphium*, while the second group (F) contained subsp. *sativum* convar. *medullare* and convar. *speciosum* (Figure 4c).

The highest similarity value 0.70 was reported between subsp. *sativum* convar. *medullare* and convar. *speciosum*, then subsp. *sativum* convar. *medullare* and convar. *axiphium* (0.66), and it was observed that subsp. *abyssinicum* and subsp. *elatus* are more related to each other (0.67) than to subsp. *asiaticum*. While the lowest value observed was 0.42 between subsp. *asiaticum* and subsp. *abyssinicum* (Table 7).

Table 6. Total number of bands polymorphism, gene diversity and PIC as revealed by SCoT-PCR amplification of *Pisum sativum* subspecies.

Primer	Total of fragments	Polymorphic fragments	Monomorphic fragments	Polymorphism (%)	+ve Unique band	-ve Unique band	Gene Diversity	PIC	Allele size range (bp)
SCoT-1	10	7	3	70.00%	2	1	0.27	0.22	420-1700 bp
SCoT-3	10	5	5	50.00%	2	0	0.19	0.15	320-1965 bp
SCoT-6	16	12	4	75.00%	3	3	0.28	0.23	400-2470 bp
SCoT-9	12	10	2	83.33%	1	2	0.33	0.26	440-1575 bp
SCoT-10	13	7	6	53.85%	2	0	0.24	0.18	400-2720 bp
SCoT-11	11	8	3	72.73%	2	1	0.29	0.23	260-1320 bp
SCoT-14	13	10	3	76.92%	2	2	0.30	0.24	250-1215 bp
SCoT-15	20	20	0	100%	6	1	0.40	0.32	125-2850 bp
Total	105	79	26	-	20	10	-	-	-
Average	13.125	9.875	3.25	75.24%	-	-	0.289	0.228	-

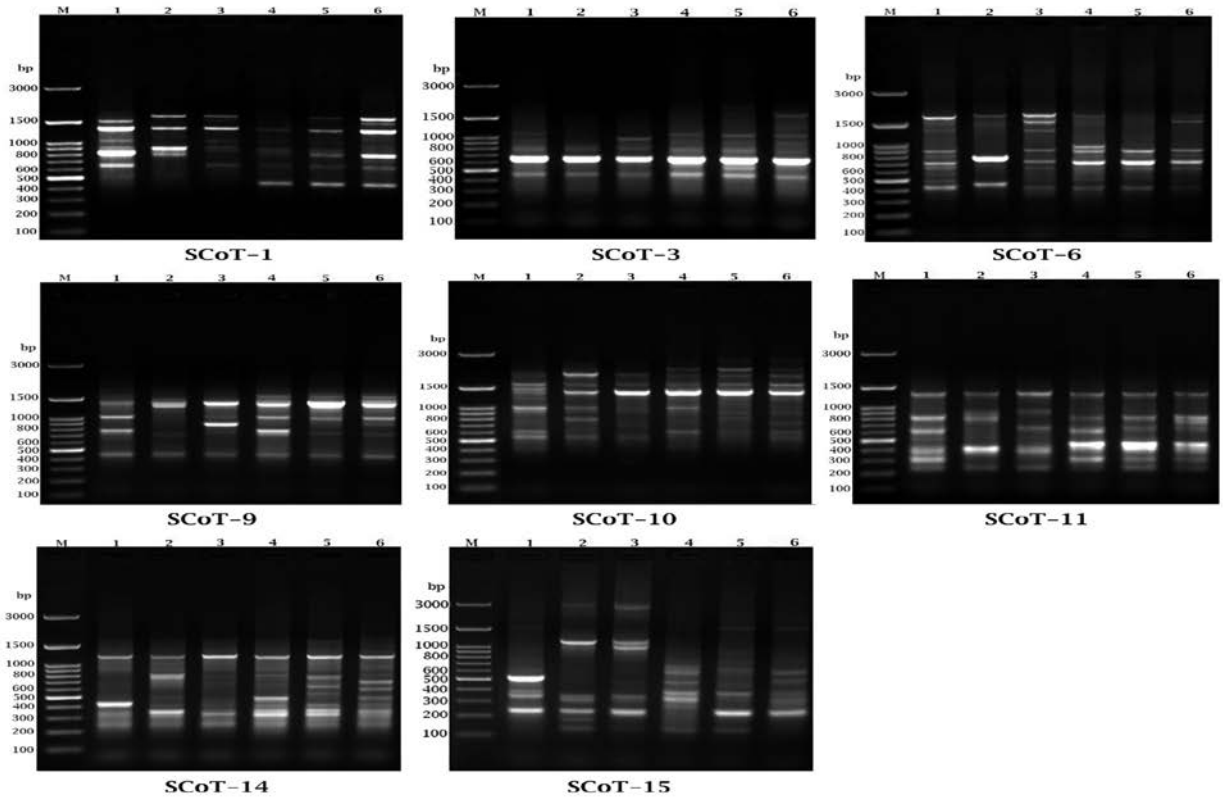

Figure 3. Electrophoresis of SCoT-PCR amplification for *Pisum sativum* subspecies.

M: DNA ladder 100 bp

1- *P. sativum* subsp. asiaticum 2- *P. sativum* subsp. abyssinicum 3- *P. sativum* subsp. elatus 4- *P. sativum* subsp. sativum con var. axiphium 5- *P. sativum* subsp. sativum con var. medullare 6- *P. sativum* subsp. sativum con var. speciosum

Table 7. Similarity matrix among examined *Pisum sativum* subspecies estimated based on Jaccard' Coefficient as revealed by SCoT marker.

***P. sativum* subsp. asiaticum**	1					
***P. sativum* subsp. abyssinicum**	0.42	1				
***P. sativum* subsp. elatus**	0.57	0.67	1			
***P. sativum* subsp. sativum con var. axiphium"**	0.58	0.44	0.53	1		
***P. sativum* subsp. sativum con var. medullare**	0.52	0.42	0.49	0.66	1	
***P. sativum* subsp. sativum con var. speciosum**	0.52	0.43	0.51	0.65	0.70	1
	***P. sativum* subsp. asiaticum**	***P. sativum* subsp. abyssinicum**	***P. sativum* subsp. elatus**	***P. sativum* subsp. sativum con var. axiphium**	***P. sativum* subsp. sativum con var.medullare**	***P. sativum* subsp. sativum con var. speciosum**

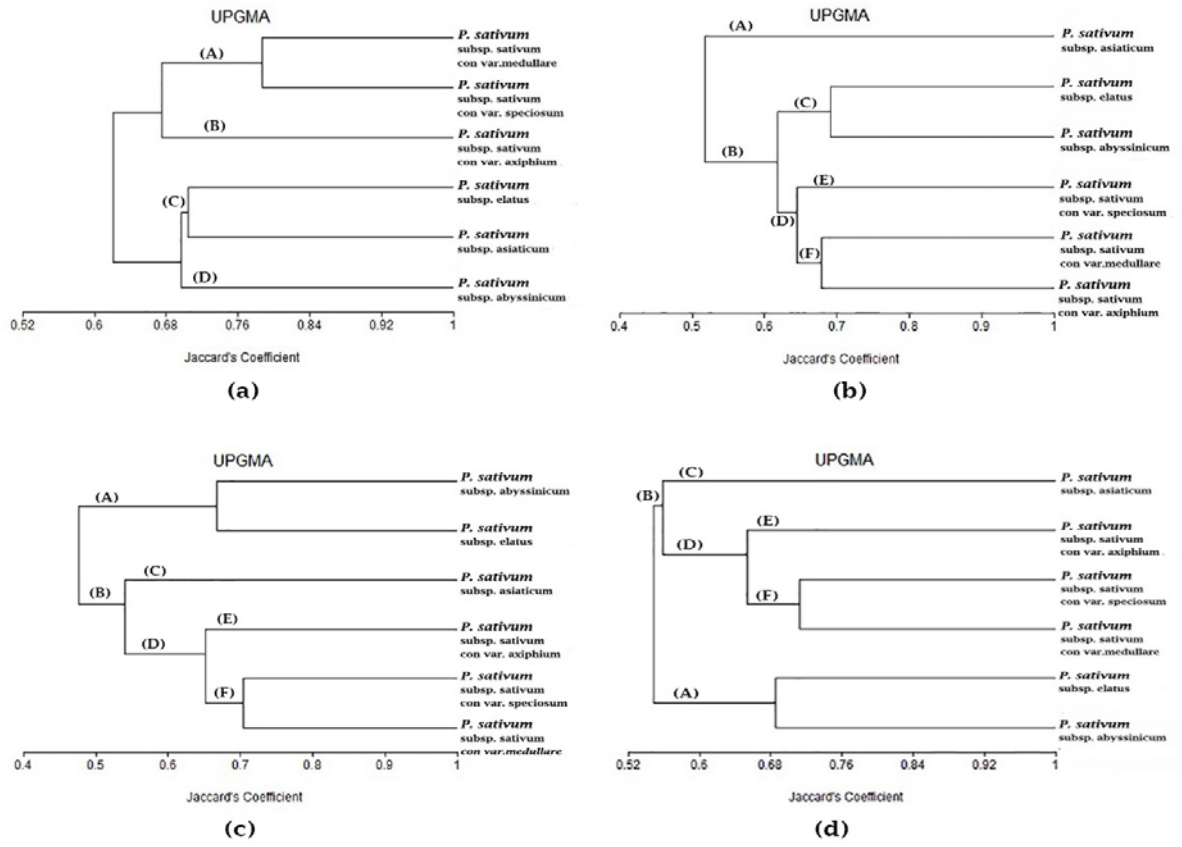

Figure 4. The constructed dendrogram by UPGMA and similarity matrix depending on Jaccard' Coefficient using (a) RAPD, (b) ISSR, (c) SCoT and (d) combined data from the *Pisum sativum* subspecies

3.4. Genetic similarity based on the combined data of RAPD, ISSR and SCoT markers:

It was observed by combining the obtained data from the three markers RAPD, ISSR and SCoT that the maximum polymorphism, PIC and Gene Diversity were detected with SCoT marker, while the minimum polymorphism, PIC and Gene Diversity were detected with RAPD marker (Table 8). The dendrogram showed two main clusters; (A) contained subsp. *abyssinicum* and subsp. *elatus*, while the second cluster (B) contained all other. The second cluster was split into two sub-clusters; (C) contained subsp. *asiaticum*, while the second sub-cluster (D) contained the other three subspecies. The second sub-cluster split into two groups, (E) contained only subsp. *sativum* convar. *axiphium* and the second group (F) contained subsp. *sativum* convar. *medullare* and convar. *speciosum* (Figure 4d). Likewise, it was observed that UPGMA results of combined data are similar to the

UPGMA of SCoT marker; this indicates that SCoT marker is an informative marker for discrimination and identification of different studied subspecies.

The highest similarity value (0.71) was reported between subsp. *sativum* convar. *medullare* and convar. *speciosum*, then subsp. *sativum* convar. *medullare* and convar. *axiphium* (0.69), and subsp. *abyssinicum* and subsp. *elatus* are more related to each other (0.69) than to subsp. *Asiaticum*,while the lowest value observed was 0.50 between subsp. *abyssinicum* and both of subsp. *sativum* convar. *speciosum* and convar. *axiphium* (Table 9).

Table 8. Comparison of genetic parameters between RAPD, ISSR and SSR analysis.

Molecular Parameter	Value		
	RAPD	ISSR	SCoT
Total number of amplicon	59	71	105
Number of polymorphic amplicon	37	52	79
+ve Unique Bands	9	15	20
% of polymorphism per assay	62.71%	73.24%	75.24%
PIC	0.19	0.21	0.23
Gene Diversity	0.23	0.26	0.30

Table 9. Similarity matrix between studied *Pisum sativum* subspecies estimated based on Jaccard' Coefficient as revealed by combined data.

***P. sativum* subsp. asiaticum**	1					
***P. sativum* subsp. abyssinicum**	0.52	1				
***P. sativum* subsp. elatus**	0.59	0.69	1			
***P. sativum* subsp. sativum con var. axiphium**	0.57	0.50	0.60	1		
***P. sativum* subsp. sativum con var.medullare**	0.57	0.52	0.57	0.69	1	
***P. sativum* subsp. sativum con var. speciosum**	0.54	0.50	0.56	0.62	0.71	1
	***P. sativum* subsp. asiaticum**	***P. sativum* subsp. abyssinicum**	***P. sativum* subsp. elatus**	***P. sativum* subsp. sativum con var. axiphium**	***P. sativum* subsp. sativum con var.medullare**	***P. sativum* subsp. sativum con var. speciosum**

4. Discussion

There are various types of markers as RAPD, ISSR and SCoT, which have been used for the proper characterization and management of germplasm to detect the genetic diversity and genetic relationships among plant taxa. RAPD marker is considered a useful molecular tool because of its simplicity and low cost; however, this technique could have problems with reproducibility (Waugh and Powell, 1992). ISSR marker target microsatellite regions, does not need information about gene sequence; it is more reproducible than RAPD as it can be performed with higher stringency (high annealing temperature). ISSR markers have been used widely for genetic diversity analyses of black gram, chick pea and jojoba plants (Souframanien and Gopalakrishna, 2004) and both types of marker (RAPD and ISSR) were useful for identifying relationships at the cultivar and species level (Karuppanapandian *et al.*, 2007; Rao *et al.*, 2007; Sharma *et al.*, 2008). Therefore, RAPD and ISSR techniques are widely used because they are fast, cheap and do not need more knowledge about DNA sequence but need a small amount of template DNA. Start Codon Targeted (SCoT) Polymorphism was designed dependent on the short conserved region next to the ATG start codon in plant genes (Collard and Mackill, 2009). Commonly SCoT markers are reproducible; however, it is proposed that annealing temperature and primer length are not the only considerations controlling reproducibility. SCoT markers were used in this study due to a number of advantages compared to other molecular markers. They provide easier development of species-specific primers than SSR and are cheaper than AFLP (Jiang *et al.*, 2014) and offer higher reproducibility than RAPD (Xiong *et al.*, 2011). Many studies were performed to evaluate the genetic diversity and relationship using SCoT markers with different plants as Egyptian *Glycine max* cultivars, *Elymus sibiricus* and *Vigna unguiculata* (Zhang *et al.*, 2015; Igwe *et al.*, 2017; Rayan and Osman, 2019). Also, Teshome et al., (2015) used EST-SSR markers in resolving the inconsistency in the taxonomic status of the different subspecies of genus *Pisum*. Stavridou *et al*. (2020) documented in their results that different landraces are more closely related to *P. sativum* subsp. *elatius* than *P. abyssinicum* and *P. fulvum* species using ISSR markers and DNA barcoding.

It was observed that high level of genetic variability among the studied pea subspecies using RAPD, ISSR and SCoT markers. SCoT markers gave maximum values of polymorphism (75.24%), PIC (0.23) and gene diversity (0.29) while ISSR markers had a polymorphism (73.24%), PIC (0.21) and gene diversity (0.26). The minimum values of polymorphism (62.7%), PIC (0.18) and gene diversity (0.23) were reported in RAPD markers. The results of molecular dendrogram (UPGMA) of combined data gave two main clusters; the first cluster included *P. sativum* subsp. *abyssinicum* and subsp. *elatus*, while the second cluster included all other subspecies. The second cluster was split into two sub-clusters; the first sub-cluster contained only *P. sativum* subsp. *asiaticum*, whereas the second sub-cluster contained the other three subspecies. The second sub-cluster was split into two groups; the first group contained only *P. sativum* subsp. *sativum* convar. *axiphium* and the second group contained subsp. *sativum*

convar. *medullare* and convar. *speciosum*. This result was identical with the results of SCoT molecular dendrogram (UPGMA). So, we can conclude that SCoT markers are more informative markers than ISSR and RAPD markers for discrimination and identification of studied species, this agreed with Zeng *et al.* (2014) and Tiwari *et al.* (2016) who mentioned that SCoT marker has a greater capability than other markers to polymorphism, for identification and discrimination among species and subspecies.

The fingerprinting and genetic relationships among studied *Pisum sativum* subspecies was performed using three types of molecular markers, RAPD, ISSR, and SCoT. It was found from RAPD, SCoT and combined observation that the most genetically related subspecies were subsp. *sativum* convar. *medullare* and convar. *speciosum* (0.79, 0.70 and 0.71, respectively); this relationship has not been verified by ISSR (subsp. *abyssinicum* and subsp. *elatus* by 0.69).

By combining the similarity matrix between the studied *Pisum sativum* subspecies as computed by Jaccard' Coefficient from these three markers (Table 14), it could be concluded that the most related subspecies are subsp. *sativum* convar. *medullare* and convar. *speciosum* (0.71), then comes subsp. *sativum* convar. *axiphium* and convar. *medullare* (0.69), Afterword comes subsp. *abyssinicum* and subsp. *elatus* (0.69). According to these observations, the genetic relationship among the studied subspecies in an order is as follows: subsp. *sativum* convar. *speciosum* is more related to convar. *medullare*, then comes convar. *axiphium*, followed by the three *P. sativum* subspecies, subsp. *abyssinicum*, subsp. *elatus* then subsp. *asiaticum*, where subsp. *elatus* has high relationship with subsp. *sativum* convar. *axiphium* (0.60%).

5. Conclusion

The genetic relationships among the six *Pisum sativum* subspecies were studied using three types of molecular markers, RAPD, ISSR and SCoT. It was found that SCoT marker is the most informative marker for the discrimination of the studied *P. sativum* subspecies. It could be concluded that the genetic relationships among the studied subspecies in an order is as follows: subsp. *sativum* convar. *speciosum* is more related to convar. *medullare* then comes convar. *axiphium* and followed by subsp. *elatus* which is more related to subsp. *abyssinicum* than subsp. *asiaticum* .

References

Amirmoradi B., Talebi R. and Karami E. 2012. Comparison of genetic variation and differentiation among annual *Cicer* species using start codon targeted (SCoT) polymorphism, DAMDPCR, and ISSR markers. Plant Syst Evol. **298:** 1679-1688. https://doi.org/10.1007/s00606-012-0669-6.

Anderson J.A., Churchil G.A., Autrique J.E., Tanksley S.O. and Sorrels M.E. 1993. Optimizing parent selection for genetic linkage maps. Genome **36:** 181-186. DOI: 10.1139/g93-024.

Baranger A., Aubert G., Arnau G., Laine A.L., Deniot G., Potier J., Weinachter C., Lejeune-Hénaut I., Lallemand J. and Burstin J. 2004. Genetic diversity within Pisum sativum using protein and PCR-based markers. Theoretical and Applied Genetics **108 (7):** 1309-1321. https://doi.org/10.1007/s00122-003-1540-5.

Blixt S (1972) Mutation genetics in *Pisum.* Agri Hort Genet. **30:** 1-293.

Ci X-Q., Chen J-Q., Li Q-m. and Li J. 2008. AFLP and ISSR analysis reveals high genetic variation and inter population differentiation in fragmented populations of the endangered *Litsea szemaois* (Lauraceae) from Southwest China. Plant Systematics and Evolution **273 (3-4):** 237-246. https://doi.org/10.1007/s00606-008-0012-4.

Collard B.C.Y. and Mackill D.J. 2009. Start codon targeted (SCoT) polymorphism: a simple, novel DNA marker technique for generating gene-targeted markers in plants. Plant Mol. Biol. Rep. **27(1):** 86-93. DOI: 10.1007/s11105-008-0060-5.

Crespe L., Pernet A., Le Bris M., Gudin S. and Oyant L. H-S. 2009. Application of ISSRs for cultivar identification and assessment of genetic relationships in rose. Plant Breeding **128 (5):** 501-506. DOI: 10.1111/j.1439-0523.2008.01600.x.

Gepts P., Charles E.B., Randy C., Stalker H., Norman F. and Young D. **2005.** Legumes as a model plant family. genomics for food and feed report of the cross-legume advances through genomics conference. Plant Physiol. **137:** 1228-1235. DOI: 10.1104/pp.105.060871.

Govorov L.I. 1937. P*isum* Tourn., Goroch (pp 231-336) - In: E. V. Vul'f (ed.) - Kul'turnaja flora SSSR; 4. Zernovye bobovye Gos. Izd. sovchoznoj kolchoznoj Lit. Moskva-Leningrad: 680pp. (http://mansfeld.ipk-gatersleben.de/apex/f? p = 185: 46: 13039378138980: NO: module, source, taxid: mf, botnam, 30772)

Hamidi H., Talebi R. and Keshavarzi F. 2014. Comparative efficiency of functional gene-based markers, start codon targeted polymorphism (SCoT) and conserved DNA-derived polymorphism (CDDP) with ISSR markers for diagnostic fingerprinting in wheat (*Triticum aestivum* L.). Cereal Res Commun. **42(4):** 558-567.

https://doi.org/10.1556/CRC.2014.0010.

Igwe D.O., Afiukwa C.A., Ubi B.E., Ogb K.I., Ojuederie O.B. and Ude G.N. 2017. Assessment of genetic diversity in *Vigna unguiculata* L. (Walp) accessions using inter-simple sequence repeat (ISSR) and start codon targeted (SCoT) polymorphic markers. BMC Genetics **18 (1):** 98. DOI: 10.1186/s12863-017-0567-6.

Jiang L.F., Qi X., Zhang X.Q., Huang L.K., Ma X. and Xie W.G. 2014. Analysis of diversity and relationships among orchard grass (*Dactylis glomerata* L.) accessions using start codon-targeted markers. Genet. Mol. Res. **13(2):** 4406–4418. http://dx.doi.org/10.4238/2014.June. 11.4.

Karuppanapandian T., Karuppudurai T., Sinha P.B., Kamarul Haniya A. and Manoharan K. 2007. Random amplified polymorphic DNA markers variability and relationships among black gram (*Vigna mungo* L. Hepper) landraces. J. PlantBiol. **34:** 79-85.

Kovach W.L. 1998. MVSP_ Multi-Variant Statistical Package for windows, ver. 3.0 Kovach computing services: Pentraeth, Wales.

Kwon S., Brown A.F., Hu J., McGee R., Watt C., Kisha T., Timmerman-Vaughan G., Grusak M., McPhee K.E. and Coyne C.J. 2012. Genetic diversity, population structure and genome-wide marker-trait association analysis emphasizing seed nutrients of the USDA pea (*Pisum sativum* L.) core collection. Genes and Genomics **34:** 305-320.

https://doi.org/10.1007/s13258-011-0213-z.

Lehmann C. and Blixt S. 1984. Artificial infraspecific classification in relation to phenotypic manifestation of certain genes in *Pisum.* - Agri Hort. Genet. **42:** 49-74.

Liu K. and Muse S.V. 2005. Power Marker: Integrated analysis environment for genetic marker data. Bioinformatics **21(9):** 2128-2129. https://doi.org/10.1093/bioinformatics/bti282.

Makaševa R.Ch. 1979. Zernovye bobovye kul'tury. I. Goroch. - D. D. Brežnev (ed.) - Kul'turnaja flora SSSR 20 Gos. Izd. Sel'skochoz. Lit. Moskva: 531 pp. 4, 1 Kolos Leningrad: 321 pp.

Mithen S. 2003. After the Ice: A Global Human History 20,000-5,000 BC. London: Weidenfield & Nicholson.

Mulpuri S., Muddanuru T. and Francis G. 2013. Start codon targeted (SCoT) polymorphism in toxic and non-toxic accessions of *jatropha curcas* L. and development of a codominant SCAR marker. Plan Sci. **207:** 117-127.

https://doi.org/10.1016/j.plantsci.2013.02.013.

Nguyen T.T., Taylor P.W.J., Redden R.J. and Ford R. 2004. Genetic diversity estimates in *Cicer* using AFLP analysis. Plant Breeding **123(2):** 173–179. https://doi.org/10.1046/j.1439-0523.2003.00942.x.

Pérez de la Vega M. 1997. El uso de marcadores moleculares en Genética Vegetal y Mejora. Invest Agr: Prod Prot Veg. **12:** 33-60.

Rao L.S., Usha Rani P., Deshmukh P.S., Kumar P.A. and Panguluri S.K. 2007. RAPD and ISSR fingerprinting in cultivated chickpea (*Cicer arietinum* L.) and its wild progenitor Cicer reticulatum Ladizinsky. Genet. Resour. Crop. Evol. **54(6):** 1235_1244. https://doi.org/10.1007/s10722-006-9104-6.

Rayan W.A. and Osman S.A. 2019. Phylogenetic relationships of some Egyptian soybean cultivars (*Glycine max* L.) using SCoT marker and protein pattern. Bulletin of national research centre **43(161):** pp.10. https://doi.org/10.1186/s42269-019-0197-4.

Sharma K., Agrawal V., Gupta S., Kumar R. and Prasad M. 2008. ISSR marker-assisted selection of male and female plants in a promising dioecious crop: jojoba (*Simmondsia chinensis*). PlantBiot echnol. Rep. **2:** 239-243. https://doi.org/10.1007/s11816-008-0070-7.

Simioniuc D., Uptmoor R., Friedt W. and Ordon F. 2002. Genetic diversity and relationships among pea cultivars revealed by RAPDs and AFLPs. Plant Breeding **121:** 429-435. https://doi.org/10.1046/j.1439-0523.2002.733320.x.

Smýkal P., Aubert G., Burstin J., Coyne C.J., Ellis N.T.H., Flavell A.J., Ford R., Hýbl M., Macas J., Neumann P., McPhee K.E., Redden R.J., Rubiales D., Weller J.L. and Warkentin T.D. 2012. Pea (*Pisum sativum* L.) in the Genomic Era. Agronomy **2(2):** 74–115.

https://doi.org/10.3390/agronomy2020074.

Souframanien J. and Gopalakrishna T. 2004. A comparative analysis of genetic diversity in blackgram genotypes using RAPD and ISSR markers. Theor. Appl. Genet. **109:** 1687-1693. https://doi.org/10.1007/s00122-004-1797-3.

Stavridou E., Lagiotis G., Karapetsi L., Osathanunkul M. and Madesis P. 2020. DNA Fingerprinting and Species Identification Uncovers the Genetic Diversity of Katsouni Pea in the Greek Islands Amorgos and Schinoussa. Plants **9:** 479

Tar'an B., Zhang C., Wankertin T., Tullu A. and Vandenberg A. 2005. Genetic diversity among varietis and wild species accessions of pea (*Pisum sativum* L.) based on molecular markers, and morphological and physiological characters. Genome **48(2):** 257-272. DOI: 10.1139/g04-114.

Teshome A., Bryngelsson T., Dagne K. and Geleta1 M. 2015. Assessment of genetic diversity in Ethiopian field pea (*Pisum sativum* L.) accessions with newly developed EST-SSR markers. BMC Genetics **16:** 102

Tiwari G., Singh R., Singh N., Choudhury D.R., Paliwal R., Kumar A. and Gupta V. 2016. Study of arbitrarily amplified (RAPD and ISSR) and gene targeted (SCoT and CBDP) markers for genetic diversity and population structure in Kalmegh [*Andrographis paniculata* (Burm. f.) Nees].Ind. Crops Prod. **86:** 1-11. https://doi.org/10.1016/j.indcrop.2016.03.031.

Uysal H., Fu Y-B., Kurt O., Peterson G.W., Diederichsen A. and Kusters P. 2010. Genetic diversity of cultivated flax (*Linum usitatissimum* L.) and its wild progenitor pale flax (*Linum bienne* Mill.) as revealed by ISSR markers. Genetic Resources and Crop Evolution **57(7):** 1109-1119. https://doi.org/10.1007/s10722-010-9551-y.

Vershinin A.V., Alnutt T.R., Knox M.R., Ambrose M.R. and Ellis T.H.N. 2003. Transposable elements reveal the impact of introgression, rather than transposition, in *Pisum* diversity, evolution and domestication. Mol Biol Evol. **20(12):** 2067-2075. https://doi.org/10.1093/molbev/msg220.

Waugh R. and Powell W. 1992. Using RAPD markers for crop improvement. Trends Biotechnol. **10:** 186-191. https://doi.org/10.1016/0167-7799 (92)90212-E.

Xiong F.Q., Zhong R.C., Han Z.Q., Jiang J., He L.Q., Zhuang W.J. and Tang R.H. 2011. Start codontargeted polymorphism for evaluation of functional genetic variation and relationships in cultivated peanut (*Arachis hypogaea* L.) genotypes. Mol. Biol. Rep. **38:** 3487-3494. https://doi.org/10.1007/s11033-010-0459-6.

Yadav K., Singh B.D., Srivastava C.P., Chand R. and Yadav A. 2010. Analysis of genetic divergence in pea (*Pisum sativum* L.) using quantitative traits and RAPD markers. Indian Journal of Genetics **70(4):** 363-369.

Young N.D., Mudge J. and Ellis T.H.N. 2003. Legume genomes: more than peas in a pod. Current Opinion in Plant Biology **6(2):** 199-204. https://doi.org/10.1016/S1369-5266(03)00006-2**.**

Zeng B., Zhang Y., Huang L., Jiang X., Luo D. and Yin G. 2014. Genetic diversity of orchardgrass (*Dactylis glomerata* L.) germplasms with resistance to rust diseases revealed by Start Codon Targeted (SCoT) markers. Biochem. Syst. Ecol. **54:** 96-102. http://dx.doi.org/10.1016/j.bse.2013.12.028.

Zhang J., Xie W., Wang Y. and Zhao X. 2015. Potential of start codon targeted (SCoT) markers to estimate genetic diversity and relationships among chinese *Elymus sibiricus* accessions. Molecules **20(4):** 5987-6001. https://doi.org/10.3390/molecules20045987.

Zhang L-J. and Dai S-L. 2010. Genetic variation within and among populations of *Orychophragmus violaceus* (Cruciferae) in China as detected by ISSR analysis. Genetic Resources and Crop Evolution **57(1):** 55-64. https://doi.org/10.1007/s10722-009-9450-2.

Zohary D. 1996. The mode of domestication of the founder crops of near east agriculture. The Origin and Spread of Agriculture and Pastoralism in Eurasia London: University College London PressHarris pp. 142-158.

JJBS

Volume 14, Number 1, March 2021
ISSN 1995-6673
Pages 75 - 82

Jordan Journal of Biological Sciences

In Silico Screening for Inhibitors Targeting 4-diphosphocytidyl-2-C-methyl-D-erythritol Kinase in *Salmonella typhimurium*

Mohammed Zaghlool Al-Khayyat*

Biology Deaprtment, College of Education for Pure Sciences, University of Mosul, Mosul city, Iraq.

Received Feb 28, 2020; Revised July 5, 2020; Accepted July 7, 2020

Abstract

In bacteria, enzymes of the isopreniod biosynthetic pathway can serve as molecular targets for developing new antibiotics in combating infections caused by resistant microbes. The amino acid sequence of the enzyme 4-diphosphocytidyl-2-C-methyl-D-erythritol kinase (IspE) was used to construct a tertiary structure via homology modeling, and its binding site was predicted by RaptorX and GalaxyWEB servers. The quality of the model was checked by three evaluation tools online. In Ramachandran plot, 99.3% of the residues were in the favoured region. The Z-plot of ProSA indicates that the model is in the range of X-ray experimentally solved proteins, and the overall quality by ERRAT is 90.2% so it is a reliable model for molecular docking. A total of 50 compounds from drug bank data base were docked using this model and ten experimental compounds were found to have binding affinities higher than the control, ADP (-8.0 Kcal/mol) in both iGEMDOCK and AutoDOCK Vina docking tools. The highest two compounds, bentiromide and Fluocinolone acetonide (-10.1 Kcal/mol) show probabilities of intestinal absorption but may cross the blood brain barrier. Although not inhibitory to the P-glycoproteins and cytochromes, these compounds can bind androgen and estrogen receptors. Therefore, investigating the pharmacodynamics and pharmacokinetics is essential in developing drugs. The compounds obtained in this study could be useful as lead-like agents in antibiotic design.

Keywords: Homology modeling, Molecular docking, Isopreniod biosynthesis, Molecular targets.

1. Introduction

Antibiotic resistance is a global issue that has serious consequences on life of patients since it negatively affects drug design projects. Many factors play role such as poverty, inadequate dosage, unregulated dispense of drugs, and untrusted drug suppliers (Hart and Kariuki, 1998; Okeke *et al*., 1999; WHO, 2000). In USA, it is estimated that 23000 people die of infections by resistant microbes each year in addition to increasing the cost from 6000-30000$ as compared to infections in patients with antibiotic-sensitive microbes (Cosgrove, 2006; CDC, 2019).

Due to antibiotic resistance, scientists are investigating alternative molecular targets to develop new antibiotics such as quorum sensing pathway, Shikimate biosynthesis pathway, Isoprenoid synthesis, bacterial cytoskeleton, divisome complex and antimicrobial peptides (Al-khayyat, 2019; Tanhaeian *et al*., 2020). Docking experiments were used for this purpose such as the study of Al-Khayyat, (2017) and Al-Khayyat *et al*., (2019).

Isoprenoids are a large diverse group of 50000 produced by living orgainsmsms. Isoprenoids are important in many functions like electron transport, cell signaling, production of glycoprotein, breakdown of protein and cell division (Hunter, 2007 Heuston *et al*., 2012; Zhao *et al*., 2013). Docking experiments were used for this purpose such as the studies of Al-Khayyat, (2017), Nasab *et al*., (2018) and Al-Khayyat *et al*., (2019).

Bacteria use the non-mevalonate pathway for producing isoprenoids. The enzyme 4-diphosphocytidyl-2-C-methyl-D-erythritol kinase (IspE) catalyzes the phosphorylation 4-diphosphocytidyl-2-C-methyl-D-erythritol by using ATP (Tidten-Luksch *et al*., 2012). In this study, homology modeling and molecular docking approaches were carried out on IspE to find inhibitors that may interfere with the non-mevalonate pathway as a preliminary screening method in the antimicrobial drug design process.

2. Materials and methods

2.1. Sequence retrieval, Binding site prediction and Homology modeling

Amino acid sequence of IspE of *Salmonella typhimurium* LT2 (Post *et al*., 1993) was obtained from Uniport database having ID: sp|P30753. Binding site was predicted by RaptorX maintained by Xu Group at University of Chicago. It is an online server, (Källberg *et al*., 2012), at (http://raptorx.uchicago.edu/). GalaxyWEB web server (Shin *et al*., 2014) was also used which is maintained by Computational Biology Lab., Department of Chemistry, Seoul University. This binding site prediction tool can be accessed at: (http://galaxy.seoklab.org/cgi-bin/submit.cgi?type=SITE). The three dimensional structure of the enzyme was built by RaptorX (Källberg *et al*., 2012).

* Corresponding author e-mail: mohammed72@uomosul.edu.iq.

2.2. Quality assessment of the Model

The accuracy of the model was assessed by three online tools: Ramachandran plot analysis by RAMPAGE (Lovell *et al*., 2003). The site is maintained by Crystallography and Bioinformatics Group at Department of Biochemistry, School of Biological Sciences, University of Cambridge, available at: (http://mordred.bioc.cam.ac.uk/~rapper/rampage. php). PROSA (Wiederstein and Sippl, 2007) determines if the protein model lies within the range of experimentally determined protein folds. It can be accessed at (https://prosa.services.came.sbg.ac.at/prosa.php). The site is maintained by Center of Applied Molecular Engineering, Department of Biosciences, University of Salzburg. ERRAT (Colovos and Yeates, 1993) computes and compares the interaction of non-bound heavy atom pairs with standards statistically. It is available at (http://servicesn.mbi.ucla.edu/ERRAT/) at Molecular Biology Institute, University of California, Los Angeles.

2.3. Ligand selection, Molecular docking

The chemical structure of the control, ADP was downloaded from ZINC database (Irwin *et al*., 2012). A total of 50 experimental structures were obtained from Drugbank database (Wishart *et al*., 2008). Molecular docking was performed by AutoDock Vina (Trott and Olson,2010) designed by Oleg Trott from Molecular graphics Laboratory at the Scripps Research Institute, La Jolla, California. The Autogrid tool was employed to pre-calculate a grid. This grid has a size of 60×60 and a box center of 2.238, -1.631 and 19.862 for x, y and z respectively. Interactions between ligand and the enzyme model were visualized by LIGPLOT+ (Wallace *et al*., 1996). Results were redocked again in iGEMDOCK, a second tool by Hsu *et al*. (2011). It was developed at National Chiao Tung University, Taiwan.

2.4. Pharmacologic properties of the compounds

The pharmacokinetics and toxicity profiles (ADMET) of the compounds were predicted by admetSAR 2 (Yang, 2019). The computed parameters were: (i) human intestinal absorption (HIA), (ii) blood-brain barrier (BBB) penetration, (iii) plasma glycoprotein (P-gp) substrate and inhibition probabilities, (iv) Cytochromes (CYP P450), substrate and inhibition probabilities (v) Ames mutagenesis test (AT), (vi) Hepatotoxicity (Hep.), (viii) Androgen receptor binding (ARB), (ix) Estrogen receptor binding (ERB), and (x) thyroid receptor binding (TRB).

3. Results and Discussion

The three dimensional structure of IspE was built by RaptorX using a template of 2.01A° X-ray diffraction of ternary complex of 4-diphosophocytidyl-2-C-methyl-D-erythritol kinase, belongs to *Escherchia coli*. The model (Fig. 1) consists of 283 amino acids and contains disordered region about14%. 31% of the molecule appears as α-helices, 27% β-sheets and 41% as coils. RaptorX predicted the binding residues for ADP. These are V^{66}, N^{65}, L^{66}, I^{94}, K^{96}, M^{100}, G^{101}, G^{103}, L^{104}, G^{105}, G^{106}, G^{107} and N^{110}. GalaxyWEB server predicted that ADP binds V^{57}, V^{60}, $N^{65,}$ L^{66}, I^{67}, K^{96}, M^{100}, G^{101}, G^{105}, G^{106}, G^{107}, Ser^{108} and N^{110}.

Shan *et al*. (2011) studied the crystal structure of the enzyme in *Mycobacterium tuberculosis* and found that it is composed of two domains; ATP binding domain at the N-terminal which extends from M^{1} to G^{148}. It is composed of four β stands β1, β4-β6 and four α-helices: α1-α4 in addition to $I3_{10}$ helix. The substrate binding domain is located at C-terminal and consists of ten β-strands β2, β3, β5-β13 and six α-helices. These are α5-α10. Mutagenesis at A^{100}, G^{102}, M^{103} and A^{104} blocked ATP binding sites and mutants of Y^{28} and Y^{185} reduced the interaction of the enzyme with the substrate. Part of the substrate enter the catalytic region, where the amino acids K^{13} and D^{140} are important in catalysis. Almuqri *et al*. (2016) stated that adenine of ADP makes contact with N^{70}, L^{71} and D^{109}. The phosphate makes H-bonds with A^{100}, G^{102}, G^{105} and G^{106}. L^{56}, L^{64}, P^{98}, V^{99}, G^{101}, M^{103} and A^{104} form hydrophobic interactions.

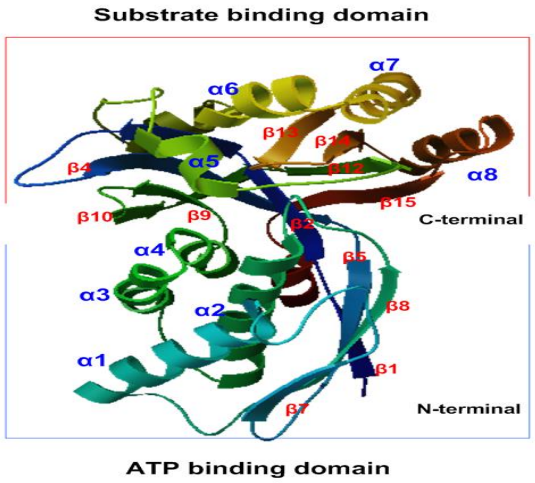

Figure 1. The three dimensional structure of IspE visualized by Python molecular viewer (Sanner, 1999).

Quality assessment was performed and found that is a reliable model. In Ramachandran plot 99.3% of the residues are within the favoured region where only E^{154} and N^{193} lie on the allowed region. It is proposed that good reliable model should have more than 90% of their residues in favored region (Laskowski *et al*., 1993). In ProSA the Z-score is -8.67 within the normal range of experimentally solved structures. In ERRAT, the overall quality of the model is 90.1% (Figs. 2 and 3).

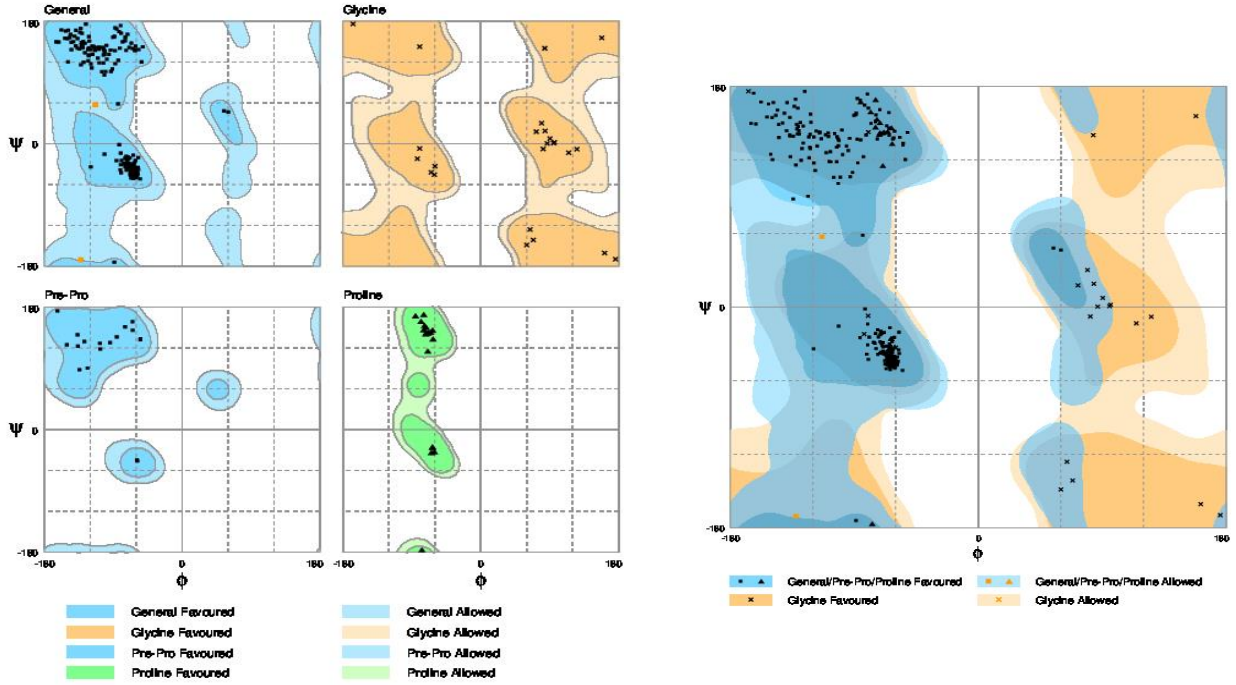

Figure 2. Ramachandran plot of IspE as predicted by Rampage.

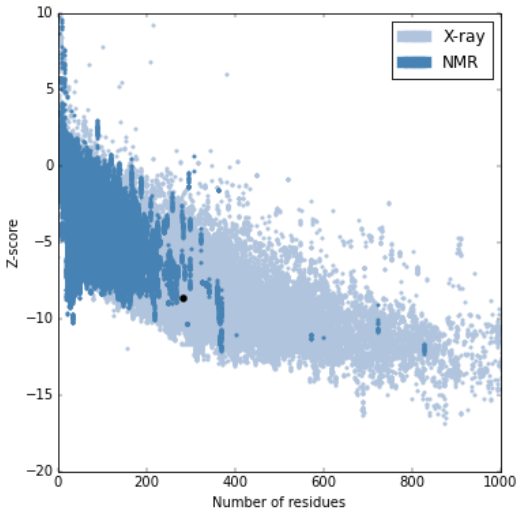

(A)

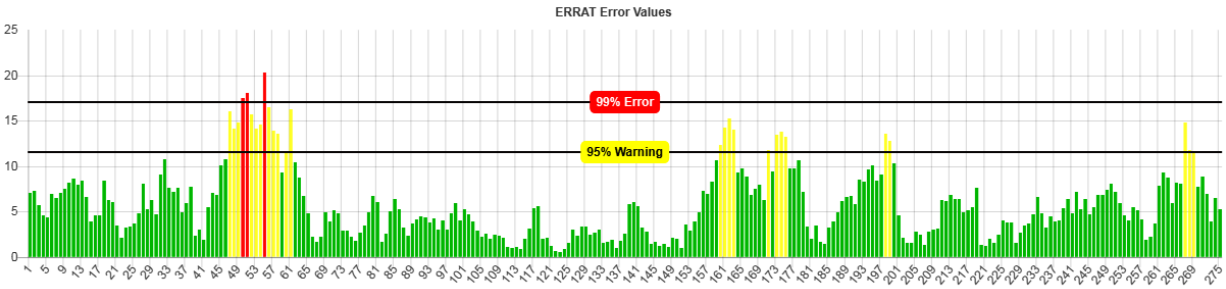

(B)

Figure 3. (A) Z-plot by ProSA of the model (black dot). The constructed model lies within normal range of X-ray determined experimental structures. (B) ERRAT analysis of the model. Black bars represent misfolded regions. On the vertical error axis, the two lines determine the confidence in which it is possible to reject region.

A total of 50 compounds were obtained from Drug bank database according to Lipinski rule of five which states that for a compound to be easily absorbed it should have molecular weight less than 500, hydrogen bond donors less than 5, hydrogen bond acceptors less than 10 and logP (measurement of lipophilicity) less than 5

(Lipinski *et al*., 2001). The compounds were docking by two softwares to get more accurate estimations of binding. Table (1) shows the results with the interactions presented. Table (2) shows the characteristics of the compounds. Figs. 4 and 5 show the interactions with ADP, control and the compound Fluocinolone acetonide respectively, while Fig. 6 shows the chemical structures of ligands. These ligands had their binding affinity higher than control so may be useful as lead compounds to design new antibiotics since it occupies the active site and interacts with its amino acid residues.

Table 1. Docking scores of IspE against experimental compounds with the interactions

Compounds	Binding affinity (Kcal/mol) by AutoDock Vina	Residues of the model forming:		Estimated ΔG (Kcal/mol) by iGEMDOCK
		Hydrogen bonds	Hydrophobic interactions	
ADP (control)	-8.0	K^{10},H^{26},V^{56}, G^{103}, G^{105}, T^{240}	L^{28}, Y^{25}, G^{101},T^{181} , $F^{185,}$ G^{239}	-69.8
Fluocinolone acetonide	-10.1	H^{26}, S^{108}, D^{141}	K^{10},Y^{25}, G^{139}, A^{140}, V^{156},T^{181}, F^{185}	-74.0
Bentiromide	-10.1	H^{26}, G^{107}, ,T^{181}, T^{240}	K^{10},Y^{25}, L^{28}, G^{101}, G^{105}, G^{106}, S^{108}, F^{185}	-73.2
Amsacrine	-9.7	G^{107}, S^{108},T^{181}	H^{26},Y^{25}, L^{28}, G^{105}, V^{156}, F^{185}	-74.6
Isradipine	-9.6	A^{140}, D^{141}	N^{12}, L^{28}, F^{32}, G^{139}, V^{156},T^{181}, F^{185}	-72.4
Troglitazone	-9.2	G^{103}, G^{107}, S^{108}	K^{10},Y^{25}, H^{26}, G^{105}, D^{141}, V^{156}, P^{182}, F^{185}	-80.2
Entacapone	-9.1	G^{103}, G^{105}	Y^{25}, L^{28}, G^{101}, S^{108}, T^{181}, F^{185}	-85.5
Betamethasone	-9.0	H^{26}, D^{141}	K^{10},Y^{25}, L^{28}, F^{32} ,G^{105}, S^{108}, A^{140}, V^{156}, T^{181}, F^{185}	-75.4
Diflorasone	-8.9	H^{26}, D^{141}	K^{10},Y^{25}, L^{28}, G^{105}, S^{108}, A^{140}, D^{141}, T^{181}, F^{185}	-77.7
Revatio	-8.6	A^{140}	L^{15},H^{26}, Y^{25}, G^{101}, G^{103},G^{105}, G^{106}, G^{107}, T^{181}, $F^{185,}$ G^{239}, T^{240}	-86.6
Doxazosine	-8.6	K^{10}, T^{240}	N^{65}, L^{66}, K^{96}, M^{100}, G^{101}, G^{103}, N^{110}, D^{141}, T^{181}, G^{239}	-82.6

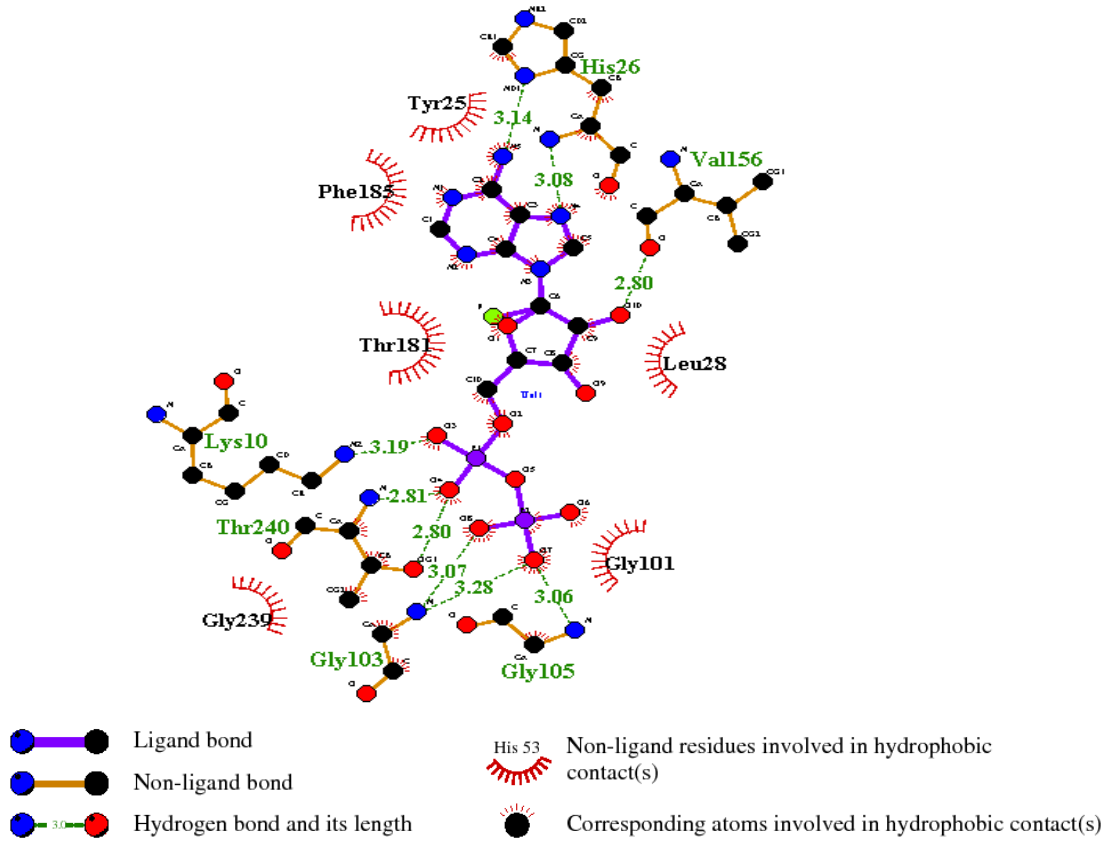

Figure 4. Docking result of ADP with the model, visualized by LIGPLOT+ (Wallace *et al*., 1996).

Table 2. Molecular properties of the best selected compounds obtained from Drug bank database

Compounds	Database ID	Mass (g/mol)	LogP[1]	HBD[2]	HBA[3]
Fluocinolone acetonide	DB00591	452.48	2.47	2	6
Bentiromide	DB00522	404.41	2.99	4	5
Amsacrine	DB00276	393.45	4.66	2	5
Isradipine	DB00270	371.14	3.00	1	5
Troglitazone	DB00197	441.54	4.16	2	5
Entacapone	DB00494	305.28	2.50	2	6
Betamethasone	DB00443	392.46	1.93	3	5
Diflorasone	DB00223	410.45	1.91	3	5
Revatio	DB00203	474.57	2.35	1	8
Doxazosine	DB00590	451.47	2.53	1	9

LogP: the logarithm of the partition coefficient in an octanol/water system, HBD: hydrogen bond donors, HBA: hydrogen bond acceptors.

Docking programs uses different algorithms to measure scores. The scoring function of AutoDock Vina (Trott and Olson, 2010) is: $c=\sum_{i<j} f t_i t_j (r_{ij})$.....(1)

Where the summation is: overall of the pairs of atoms that can move relative to each other, normally excluding 1–4 interactions, which means atoms separated by 3 consecutive covalent bonds. Each atom i is assigned a type t_i, and a symmetric set of interaction functions ft_it_j of the interatomic distance r_{ij} must be defined. This value represents the sum of intermolecular and intramolecular contributions:

$$c = c_{inter} + c_{intra}$$.....(2)

iGEMDOCK is a virtual screening software environment using post screening analysis with pharmacological interactions. iGEMDOCK gives interactive interfaces to prepare both the binding site of a given target and the ligands that are docked into the binding site by GEMDOCK docking tool. After that, iGEMDOCK will make protein-compound interactions of electrostatic (E), hydrogen-bonding (H), and van der Waals (V) energies (Yang and Chen, 2004) and the pharmacological scoring function is:

$E_{pharma}= E_{GEMDOCK}+E(E)_{pharma}+ 2E(H)_{pharma} + 0.5\ E(V)_{pharma}$ .....(3)

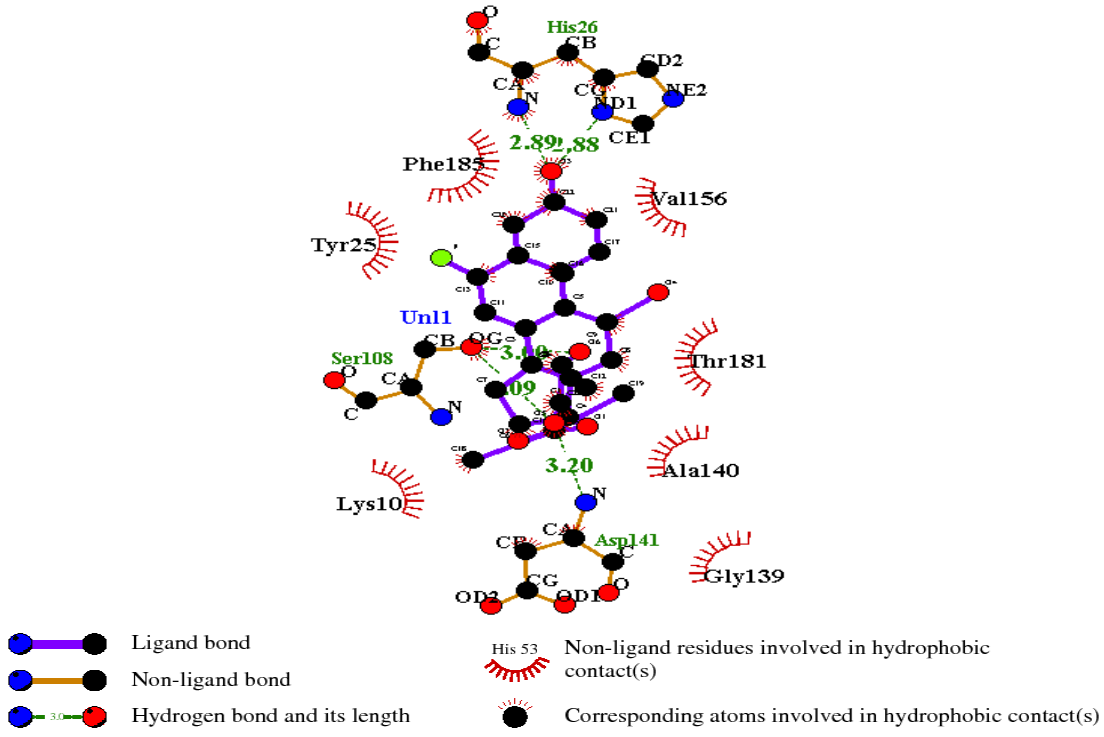

Figure 5. Docking result of Fluocinolone acetotonide with the model, visualized by LIGPLOT+ (Wallace *et al*., 1996).

Previous approaches exploited cytidine or phosphate –sugar moieties of the substrate then non substrate-like inhibitors were used in screening for lead compounds (Tidten-Luksch *et al*., 2012; Tang *et al*., 2011). By Molecular docking, Almuqri *et al*. (2016) identified five novel compounds that may act as inhibitors of IspE in *M. tuberculosis* acting on ATP binding site. These were downloaded from ZINC database and designated as ZINC33113258, ZINC21040510, ZINC33113258, ZINC89917226 and ZINC1471760. In the study of Hirsch *et al*. (2008), compounds were investigated as inhibitors of IspE by structure-designed approaches. The compounds occupied the cytidine binding pocket (i.e. substrate active site) of this enzyme and resulted in lower micromolar activities.

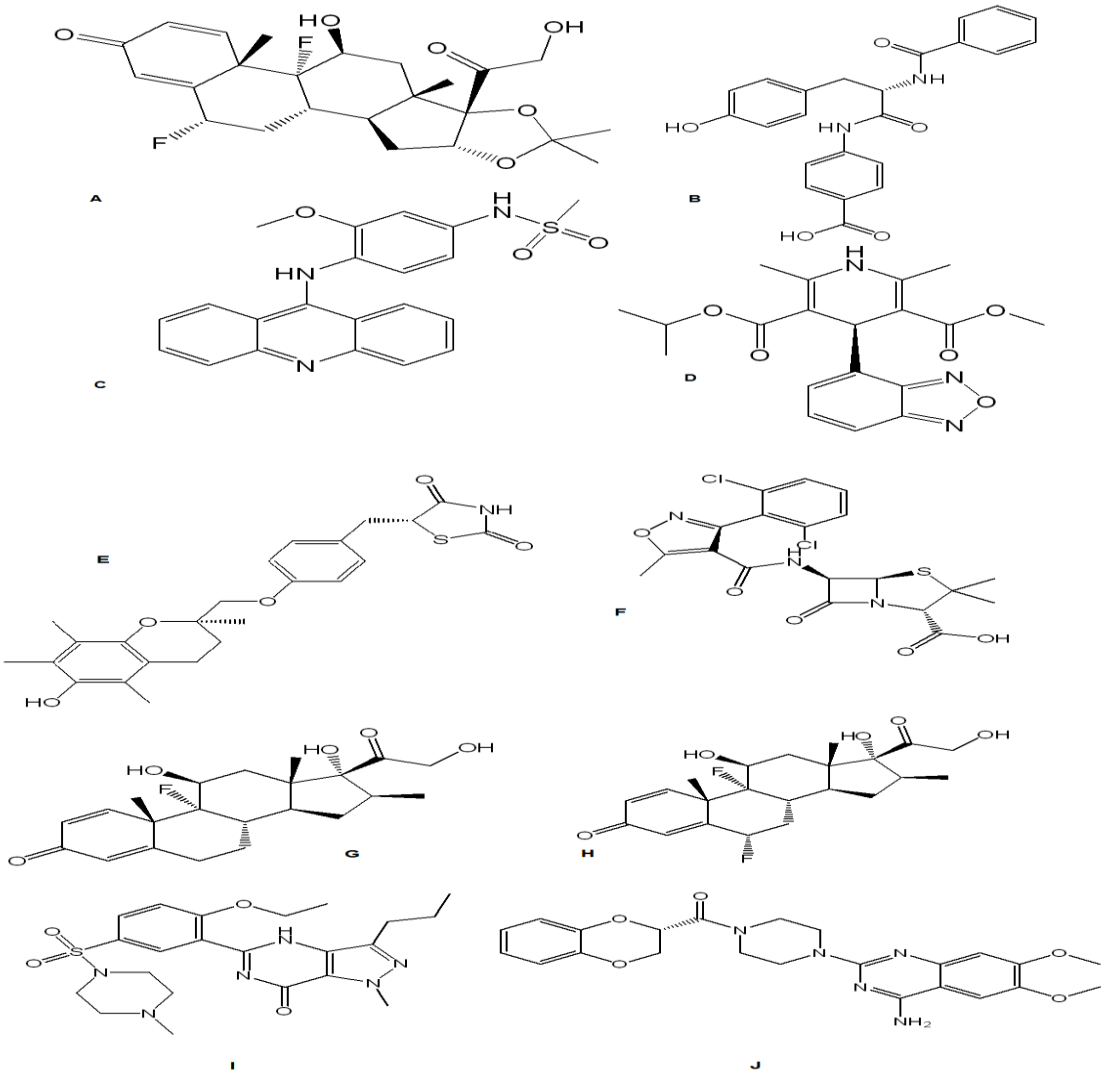

Figure 6. Chemical structures of ligands: A: Fluocinolone acetonide, B: Bentiromide, C: Amsacrine, D: Isradipine, E: Troglitazone, F: Entacapone, G: Betamethasone, H: Diflorasone, I:Revatio, J: Doxazosine.

Pharmacokinetics and dynamics were studied using AdmetSAR version 2 and results are shown in Table (3). All compounds can be absorbed from intestine but all except entacapone may cross blood brain barrier. This is preferred when the drug has to work centrally in brain but side effects can occur if the drug is required to act peripherally (van de Waterbeemd and Gifford, 2003).

Five ligands were shown to be inhibitors of P-glycoproteins. P-glycoproteins are membrane transporters functioning to pump drugs out of cells; hence, any drug that inhibit P-glycoprotein may exhibit drug interactions with other drugs co-administered (Finch and Pillans, 2014). Isradipine, revatio, amsacrine and entacapone are inhibitory to cytochromes. Different classes of cytochromes are responsible for oxidative metabolism of drugs, so their inhibition will accumulate the drugs inside human body resulting in toxicity (Zuber *et al*., 2002).

Table 3. Pharmacokinetics and pharmacodynamics of the compounds

Compounds	HIA	BBB	P-gp		CYP 3A4	CYP 2C9	CYP 2D6	CYP 3A4	CYP 2C9
			Sub.[1]	Inh.[2]	Sub.	Sub.	Sub.	Inh.	Inh.
Fluocinolone acetonide	+	+	+	-	+	-	-	-	-
Bentiromide	+	+	-	-	+	-	-	-	-
Amsacrine	+	+	-	+	+	-	-	-	-
Isradipine	+	+	-	+	+	-	-	+	+
Troglitazone	+	+	-	+	+	-	-	-	-
Entacapone	+	-	+	-	+	-	-	-	-
Betamethasone	+	+	+	-	+	-	-	-	-
Diflorasone	+	+	+	-	+	-	-	-	-
Revatio	+	+	+	+	+	+	-	+	-
Doxazosine	+	+	+	+	+	-	-	-	-

[1]Sub.: substrate, [2] Inh.: inhbition

Table 3. Continued

Compounds	CYP 2C19	CYP 2D6	CYP 1A2	AT	Hep.	ERB	ARB	TRB
	Inh.	Inh.	Inh.					
Fluocinolone acetonide	-	-	-	+	-	+	+	+
Bentiromide	-	-	-	-	+	+	+	-
Amsacrine	-	-	+	+	+	+	+	+
Isradipine	+	-	+	-	+	+	-	+
Troglitazone	-	-	-	-	+	+	+	+
Entacapone	-	-	+	-	+	-	-	+
Betamethasone	-	-	-	-	-	+	+	+
Diflorasone	-	-	-	-	-	+	+	+
Revatio	-	-	-	-	+	+	+	+
Doxazosine	-	-	-	-	+	+	-	+

4. Conclusion

This enzyme, IspE is an excellent target for drug design approaches since its inhibition may affect isoprenoid biosynthesis in bacteria. The study of pharmacokinetics is essential before considering these experimental structures as lead compounds due to side effects. Chemical modification may improve their binding to ATP binding site and may also reduce their adverse effects.

Acknowledgment

The author is very grateful to the University of Mosul/ College of Education for Pure Sciences for their provided facilities which helped to improve the quality of this work

References

Al-Khayyat MZ.2017. *In silico* screening for inhibitors targeting bacterial shikimate kinase. *Jordan J. Biol. Sci*., 10(4):273-280.

Al-Khayyat MZ.2019. Molecular targets to develop future antimicrobials. *BioTechnologia*, **100**(2):185-194.

Al-Khayyat MZ, Ameen A Gh and Abdulla YA.2019. Virtual screening for inhibitors targeting the rod shape determining protein in *Escherichia coli*. *Jordan J. Biol. Sci*., 12(2):183-189.

Almuqri EA, Teimouri M and Muhammad J.2016. *In Silico* identification of lead compounds for the inhibition of *Mycobacterium tuberculosis* IspE using complex based pharmacophore mapping, virtual screening and molecular dynamics simulation. *Inter J Life Sci Res*., **4**(2): 253-262.

Antibiotic reistance threats in the United States.2013. Centers for disease control and Prevention (CDC). http://www.cdc.gov/drugresistance/threat-report-2013/index.html. (Jul 14, 2019).

Colovos C and Yeates TO.1993. Verification of protein structures: Patterns of non-bonded atomic interactions. *Protein Sci*., **2**:1511-1519.

Cosgrove SE.2006. The relationship between antimicrobial resistance and patients outcomes: mortality, length, of hospital stay, and health care costs. *Clin Infect Dis*., **42**(S2): S82-89.

Finch A and Pillans P.2014. P-glycoprotein and its role in drug-drug interactions. *Aust Prescr*., **37**(4): 137-139.

Hart CA and Kariuki S.1998. Antimicrobial resistance in developing countries. *BMJ*., **317**:647-650.

Heuston S, Begley M, Gahan CG and Hill C.2012. Isoprenoid biosynthesis in bacterial pathogens. *Microbiology*, **158**:1389-1401.

Hirsch AKH., Alphey M S, Lauw S, Seet M, Barandun L, Eisenreich W, Rohdich F, Hunter WN, Bacher A and Diederich F.2008. Inhibitors of the kinase IspE: structure-activity relationships and co-crystal structure analysis. *Org Biomol Chem*., **6**: 2719-2730.

Hsu K-C, Chen Y-F, Lin S-R and Yang J-M.2011. iGEMDOCK: A graphical environment of enhancing GEMDOCK using pharmacological interactions and post-screening analysis. *BMC Bioinform*., **12**(S1):S33.

Hunter WN.2007. The non-mevalonate pathway of isoprenoid precursor biosynthesis. *J Biol Chem*., **282**(30): 21573–21577.

Irwin JJ, Sterling T, Michael MM, Bolstad ES and Coleman RG.2012. ZINC: A free tool to discover chemistry for biology. *J Chem Inf Model*., **52**:1757-1768.

Källberg M, Wang H, Wang S, Peng J, Wang Z, Lu H and Xu J.2012. Template-based protein structure modeling using the RaptorX web server. *Nat Protocols*., **7**:1511-1522.

Laskowski RA, MacArthur MW, Moss D and Thornton JM.1993. PROCHECK: A program to check the stereochemical quality of protein structures. *J Appl Crystal*., **26**:283-291.

Lipinski CA, Lombardo F, Dominy BW, Feeney PJ.2001. Experimental and computational approaches to estimate solubility and permeability in drug discovery and development settings. *Adv Drug Delivery Rev*., **46**:3-26.

Lovell SC, Davis IW, Arendall 3rd WB, de Bakker PI, Word JM, Prisant MG, Richardson JS and Richardson DC.2003. Structure validation by Cα geometry: Phi, psi and Cβ deviation. *Proteins: Struct Funct Genet*., **50**(3):437-450.

Nasab RR, Mansourian M and Hassanzadeh F.2018. Synthesis, antimicrobial evaluation and docking studies of some novel quinazolinone Schiff base derivatives. *Res Pharm Sci*. **13**(3):213–221.

Okeke IN, Lamikanra A and Edelman R.1999. Socioeconomic and behavioral factors leading to acquired bacterial resistance to antibiotics in developing countries. *Emerg Infect Dis*., **5**:18-27.

Post DA, Hove-Jensen B and Switzer RLJ.1993. Characterization of the hemA-prs region of the *Escherichia coli* and *Salmonella typhimurium* chromosomes: Identification of two open reading frames and implications for prs expression. *Gen Microbiol*., **139**:259-266

Sanner MF.1999. Python: A programming language for software integration and development. *J Mol Graphics Mod*., **17**:57-61.

Shan S, Chen X, Liu T, Zhao H, Rao Z and Lou Z.2011. Crystal structure of 4-diphosphocytidyl-2-C-methyl-Derythritol kinase (IspE) from *Mycobacterium tuberculosis. The FASEB J*., **25**:1577-1584.

Shin W-H, Lee GR, Heo L, Lee H and Seok C.2014. Prediction of protein structure and interaction by GALAXY protein modeling programs. *BioDesign*., **2(**1): 1-11.

Tang M, Odejinmi SI, Allette YM, Vankayalapati H and Lai K.2011. Identification of novel small molecule inhibitors of 4-diphosphocytidyl-2-C-methyl-D-erythritol (CDP-ME) kinase of Gram-negative bacteria. *Bioorg Med Chem*., **19**:5886-5895.

Tanhaeian A, Azghandi M, Mousavi Z and Javadmanesh A. 2020. Expression of Thanatin in HEK293 cells and investigation of its antibacterial effects on some human pathogens. *Protein Pept Lett*., **27(1):**41-47.

Tidten-Luksch N, Grimaldi R, Torrie LS, Frearson JA, Hunter WN and Brenk R.2012. IspE inhibitors identified by a combination of *in silico* and *in vitro* high-throughput screening. *PLoS ONE*, **7**(4): e35792.

Trott O and Olson AJ. 2010. AutoDock Vina: Improving the speed and accuracy of docking with a new scoring function, efficient optimization and multithreading. *J Comput Chem*., **31**:455-61.

van de Waterbeemd H and Gifford E. 2003. ADMET *in silico* modeling: Towards prediction paradise? *Nature*, **2**: 192-204.

Wallace AC, Laskowaski RA and Thornton JM. 1996. LIGPLOT: A program to generate schematic diagrams of protein-ligand interactions. *Protein Eng*., **8**:127-34.

Wiederstein M and Sippl MJ. 2007. ProSA-web: Interactive web service for the recognition of errors in three-dimensional structures of proteins. *Nucleic Acids Res*., **35**:W407-410.

Wishart DS, Knox C, Guo AC, Cheng D, Shrivastava S, Tzur D, Gautam B and Hassanali M..2008. Drug Bank: A knowledgebase for drugs, drug actions and drug targets. *Nucleic Acids Res*., **36**: 901-906.

World Health Organization.2000. Overcoming antimicrobial resistance. World Health Organization report on infectious diseases. World Health Organization.

Yang H, Lou C, Sun L, Li J, Cai Y, Wang Z, Li W, Liu G and Tang Y.2019. admetSAR 2.0: Web-service for prediction and optimization of chemical ADMET properties. *Bioinformatics*, **35**(6):1067-1069.

Yang J-M and Chen C-C.2004. GEMDOCK: A generic evolutionary method for molecular docking. *Proteins*, **55**: 288-304.

Zhao L, Chang W-C, Xiao Y, Liu H-W and Liu P. 2013.Methylerythritol phosphate pathway of isoprenoid biosynthesis. *Annu Rev Biochem*., **82**:497-530.

Zuber R, Anzenbacherová E and Anzenbacher P.2002. Cytochromes P450 and experimental models of drug metabolism. J Cell Med., **6**(2):189-198.

JJBS

Volume 14, Number 1, March 2021
ISSN 1995-6673
Pages 83 - 90

Jordan Journal of Biological Sciences

Nutritional evaluation, Phytochemicals, Antioxidant and Antibacterial activity of *Stellaria monosperma* Buch.-Ham. Ex D. Don and *Silene vulgaris* (Moench) Garcke: wild edible plants of Western Himalayas

Arti Thakur*, Somvir Singh, Sunil Puri

School of Biological and Environmental Sciences, Faculty of Basic Sciences, Shoolini University of Biotechnology and Management Sciences, Solan-173229, Himachal Pradesh, India

Received June 6, 2020; Revised July 10, 2020; Accepted July 14, 2020

Abstract

Wild plants of Western Himalayas occupy an essential role to the inhabitant's livelihood. The present study evaluates the nutritional composition, phytochemicals and antioxidant activity of *Stellaria monosperma* and *Silene vulgaris*, used commonly as food and medicine by folks of Western Himalayas. These two species are facing extinction as per the IUCN Red List. The present study focused on these two plants which are used by the Gaddis (shepherds) of Western Himalayas as food. Major findings revealed that the aerial parts had high amount of carbohydrate, proteins, sodium, potassium, crude fibre and crude fat. Phytochemicals like phenols, flavonoids, tannins, terpenoids, amino acids, ascorbic acid, tocopherols, carotenoids, alkaloids and phytates were in sufficient amount, helping to deactivate and absorb free radicals. Thus, both the plants have high antioxidant activity and are good radical scavengers. These plants also exhibited antibacterial potential. Amount of nutrition, phytochemicals, antioxidant and antibacterial activity was observed more in *Silene vulgaris* as compared to *Stellaria monosperma*. The need is to bring under control these plants species for harnessing their potentials of nutrition and pharmaceutical industry.

Keywords: Antioxidant, Nutritional, Phytochemicals, *Stellaria monosperma*, *Silene vulgaris*.

1. Introduction

Constantly increasing population pressure and fast reduction of natural resources has become more important to diversify the present-day agriculture yield (Deb, 2013). Utilization of wild edibles, mainly those recognized as under-utilized, are known to improve health and nutrition, livelihoods and environmental sustainability. These plants provide vitamins, trace elements and minerals, which are the source of nutraceuticals (Leonti, 2012). Wild edible plants play significant role in the functioning of the body and suitable growth (Afolayan and Jimoh, 2009; Ali-Shtayeh *et al.*, 2008). According to FAO information, in developing countries about 1billion population depend on wild plants for their food (Taylor, 2015). Traditionally, these edible plants are used as food as well as medicines (Ubwa, 2014). Many ethnobotanical studies suggested that these plants play major role in maintenance of life, especially of the rural community as they are used wild plants as drugs and food (Verma and Kaushal, 2014). Researcher's enthusiasm lies to re-examine each plant with a new approach regarding their probable use for food and medicine. Primary metabolites such as carbohydrate, proteins, vitamins, sterols and lipids occurs in plants and provides food with nutrition (Verma and Kaushal, 2014), while secondary metabolites, such as phenols, flavonoids, tannins, alkaloids, terpenoids, lignin, quinones, coumarins and amines are the best antioxidants (Zheng and Wang, 2001; Cai *et al.*, 2003). Similarly, many wild plants provide essential biochemical and energy besides supplementary resources of vitamins and minerals that sustain the suitable physiological equilibrium of the body. It has been seen that sometimes nutritional potential of uncultivated plant species is superior compared to the cultivated variety (Ebert, 2014). Recently, several researches focused on wild edibles as a source of nutraceuticals, used for the cure of several diseases such as jaundice, diabetes, wounds, cancer etc. as recognized from various ethno pharmacological studies (Mir, 2014). Foods which are obtained from plant are abundant resources of bioactive compounds, which have been found to possess a great variety of biological activities including antioxidant potential. Epidemiological studies revealed that the utilization of fruits and vegetables as food is coupled with decline possibility of chronic and neurodegenerative diseases, mostly due to the occurrence of antioxidants (phenolic compounds and tocopherols) that are concerned in the interruption or prevention of oxidative reactions (Gerber *et al.*, 2002; Di Matteo and Esposito, 2003). The occurrence of diseases caused by microbes are constantly increasing on the entire earth and mostly are cured by the use of antimicrobials. Antibacterials, which are obtained from plants, are safer as compare to synthetic drugs due to

* Corresponding author e-mail: artithakur758@gmail.com.

their natural source. Secondary metabolites of plants such as tannins, flavonoids, quinones, coumarins, terpenoids, alkaloids and polypeptides are frequently responsible for their antimicrobial activity (Savoia, 2012).

Stellaria monosperma Buch.-Ham. ex D. Don, and *Silene vulgaris* (Moench) Garcke are the wild, herbaceous plant of the *Caryophyllaceae* family which are used as vegetable (aerial parts) by the people of Western Himalayas (Fig. 1). *Stellaria monosperma* is perennial herb about 10-60 cm tall, erect stem, leaves simple and opposite. *Silene vulgaris* is a perennial herb up to 10-60 cm length and occurred in weedy areas, semi-dry and open dry areas (Karamian and Ghasemlou, 2013). The present study planned to analyze the nutritional composition; phytochemicals, antioxidant and antimicrobial analysis of these two species from the wild, keeping in mind its importance and lack of literature.

Stellaria monosperma Silene vulgaris

Figure 1. Plants of two species in wild growing in Bharmour region of Chamba district in **Himachal Pradesh**

2. Materials and methods

The aerial parts of *Stellaria monosperma* and *Silene vulgaris* were collected in June 2018 from the Bharmour region of district Chamba, Himachal Pradesh. This area lies at 32°11' 35" to 32° 41' 54" N latitude 76° 31' 35" to 76° 53' 71" E longitude. Collected plants were cleaned with distilled water, dried with blotting paper, chopped to small pieces before drying at 60°C for 72 hours until constant weight was obtained. The dried chopped pieces were ground into powder by mortar pestle and put in the glass bottle and kept at 4°C in refrigerator and used for the further analysis.

2.1. Extract preparation

2 g of the fine powder of each sample was soaked in 20 ml methanol/water (50:50, v/v) and kept at orbital shaker for 48 hrs, filtered and filtrate evaporated and dried at 40°C at water bath and used for extract to evaluate antioxidant and antibacterial activity.

2.2. Nutritional composition

2.2.1. Determination of Carbohydrate content

Weighed 100 mg of sample, homogenized by 2 ml of 2.5 N HCl in test tube, and boiled in water bath for two hours, cooled at room temperature. In 200µl of supernatant added 500µl of distilled water and 3 mL of anthrone reagent. The reaction mixture was heated in water bath for 10 minutes and cooled. UV /visible spectrophotometer read mixture of green color at 630 nm. The carbohydrate content was calculated by calibration curve equation ($y=1.297x-0.050$; $R^2=0.998$) of glucose and results are expressed as 1g of glucose/mg of sample (Hedge and Hofreiter, 1962).

2.2.2. Determination of Protein content

Weighed 100 mg of sample and ground it with a pestle and mortar in 2mL of phosphate buffer. Centrifuged and used the supernatant for protein estimation. In 200µl, added 3 mL of $CuSO_4$ mixed well and kept for 10 minutes and then added 500µl of Folins-Ciocalteau's reagent and mixed properly. Total mixture was kept at room temperature under dark condition for 30minutes. Reaction mixture of blue colour was observed at 660nm by UV/visible spectrophotometer. The protein content of sample was calculated by calibration curve equation ($y=1.041x+0.080$; $R^2=0.999$) of Bovine Serum Albumin (BSA) and the results are expressed as 1g of BSA /mg of sample (Lowry *et al.,* 1951).

2.2.3. Estimation of Sodium and Potassium

Potassium and sodium in the acid-digest of plant sample was determined using flame photometer. A 500mg of the plant sample was weighed and put into 100 ml of conical flask containing 10 ml of concentrated HNO_3. It was kept for about 24hrs in a covered place for pre-digestion. After pre-digestion the solid sample was no more visible. A 10 ml of concentrated HNO_3 and 2-3 ml of $HClO_4$ were added. The mixture was heated, in acid proof chamber having fume exhaust system, at about 100°C for first 1 hr and then raised the temperature to 200°C. Digestion was continued until the mixture became colorless and only white dense fumes appeared. The acid contents were reduced to about 2-3 ml, by continuing heating at the same temperature and filtered through Whattman No. 42 filter paper into a 100 ml volumetric flask. Gave 3-4 washings of 10-15 ml distilled water and made volume 100 ml. Measured Na^+ and K^+ concentrations in the supernatant by flame photometer. Readings were recorded of the standards of Na and K after adjust blank to zero and then drawn a standard curve (Chikhale and Chikhale, 2017).

2.2.4. Determination of Crude Fibre

Sample (2g) was digested by boiling with50 mL of 1.25% H_2SO_4 solution for 30 min, and then filtered under pressure. The residue was rinsed three times with boiled water. This process was repeated using 50 mL of 1.25% Sodium hydroxide. The deposit was dehydrated at 100°C, cooled in room temperature and weighed. It was thereafter crucible put on muffle furnace at 550°C, for 3 h, then cooled at room temperature and reweighed (Aina *et al.,* 2012). The percentage crude fibre was calculated as:

% Crude fibre = Weight of residues – weight of ash / Weight of original sample× 100

2.2.5. Determination of Crude Fats

Sample (5g) was extracted in 25 mL of diethyl ether and placed on shaker for 24 h. The extract was filtered and put into a formerly weighed (W1) beaker. Then 100 mL of diethyl ether was added and shaken for 24 hours. The filtrate was collected in the same beaker (W1). Ether containing beaker was put on the water bath to dry at 40–60°C and the beaker was again weighed (W2) (Unuofin, 2017). The crude fat content was calculated as:

% Crude fat = W2−W1/Weight of original sample× 100

2.3. Determination of Phytochemical content

2.3.1. Determination of Phenols

100 mg of sample was homogenized by 2ml of methanol. Centrifuged for 10 minutes, at 10,000 rpm, collected the supernatant. Took 200 µl of supernatant, added 1ml of Folin-Ciocalteau reagent and kept for 2 min. After that 1000µl of 35% Na_2CO_3 solution added to the mixture and made 10 ml of final volume by distilled water. Reaction mixture was kept for 30 min in dark and OD was observed at 750nm against reagent blank. The amount of phenol was calculated by calibration curve equation (y=0.741x+0.132; R^2=0.995) by expressed in terms of mg of gallic acid (GAE)/g of sample (Jia *et al.,* 1998).

2.3.2. Determination of Flavonoids

100 mg of sample was homogenized by 2ml of methanol and centrifuged for 10 minutes at 10,000 rpm and and the supernatant was collected. 200µl of the plant extracts were made up to 1.5 ml using distilled water and added 75µl of 5% NaNO2. The reaction mixture was kept to stand for 5 min and 150 µl of 10% AlCl3 was added to it. The mixture was mixed well and allowed to stand for 5 minutes at room temperature. Thereafter, 0.5ml of 1M NaOH was added and the OD observed against to reagent blank at 510nm. Results are expressed as mg of rutin equivalents (RE) /g of sample by calibration curve equation (y=0.965x+0.036; R^2=0.999) (Jia *et al.,* 1998).

2.3.3. Determination of Tannins

100 mg of sample was homogenized by 2ml of methanol. Centrifuged for 10 minutes at 10,000 rpm and collected the supernatant. To 1ml of supernatant mixed with 0.5 ml Folin's phenol reagent and 35% Na_2CO_3 of 5ml added and the mixture was kept at room temperature for 5 minutes. The blue color of reaction mixture was observed at 640 nm by UV/visible spectrophotometer. Content of tannin was calculated by calibration curve equation (y=1.501x+0.102; R^2=0.996) of gallic acid and the results expressed as (mg/g) (Schanderl, 1970).

2.3.4. Determination of Terpenoids

100 mg of sample was homogenized by 2ml of methanol. Centrifuged for 10 minutes at 10,000 rpm, collected the supernatant. In 100µl of supernatant, added 3ml of the chloroform. Added 200µl of the concentrated sulphuric acid and solution kept at room temperature for 1.5-2hour in dark, for the duration of incubation a reddish-brown color precipitate was formed. Supernatant was decanted without disturbing the precipitate. 3ml of the 95% methanol added and vortex thoroughly until all the precipitate completely mix in methanol. The absorbance was observed at 538 nm against blank, i.e. 95% methanol. Linalool was used as the standard for estimation. Terpenoid content was calculated by the calibration curve equation (y=1.018x+0.047; R^2=0.997) of linalool and results expressed in mg/g (Ghorai *et al.,* 2012).

2.3.5. Determination of Amino acid

Weighed 500mg of plant sample and ground it in pestle and mortar with 5-10ml of 80% ethanol. Centrifuged and to 0.1 ml of extract, added 1 ml of ninhydrin solution and made the volume to 2ml with distilled water. Heated the tube for 20 minutes in water bath. Add 5ml propanol and mixed the contents. After 15 minutes read the absorbance of purple color against a blank in a spectrophotometer at 570 nm. Standard was prepared using 50mg leucine dissolved in 50ml of distilled water. Took 10 ml of this stock and diluted to 100 ml in another flask for working standard solution. Standard solution of 0.2. 0.4, 0.6, 0.8 and 1.0 ml gave concentration range of 20, 40, 60, 80 and 100 mg. Proceeded as that of the sample and read the colour. Determined the concentration of amino acid in the sample by calibration curve equation (y=0.748x+0.063; R^2=0.988) and expressed as mg/g equivalent of leucine (Moore and Stein, 1948).

2.3.6. Determination of Ascorbic acid

Ascorbate was extracted into 4% TCA by homogenizing 1g of sample in it, and total volume was made 10 ml with 4% Tri-carboxylic acid. The supernatant obtained after centrifugation for 10 min at 2000 rpm was treated with a pinch of activated charcoal, shaken well and kept for 10 min. Centrifugation process was continual for removing the residue of charcoal. 1ml of supernatant was taken for the assay. Total volumes were made to 2 ml with 4% Tri-carboxylic acid. 0.2 to 1.0 ml of the working standard were pipetted into clean test tubes, the total volumes made in test tube to 2ml with 4% Tricarboxylic acid. 500 µl DNPH reagent was added in all test tubes, by addition of 2 drops of 10% solution of thiourea. Formation of osazones after incubation at 37°C for 3 hours was seen. These osazones dissolve in 2.5ml of 85%H_2SO_4, after 30 minutes of incubation, absorbance of samples observed at 540 nm and the content of ascorbic acid in the samples was calculated using calibration curve equation (y=0.988x-0.028; R^2=0.996) and expressed as ascorbate mg/g (Roe and Kuether, 1943).

2.3.7. Determination of Carotenoids

Plant sample was taken 5-10g for saponification in a shaking water bath at 37°C for about 30 minutes. After extracting the KOH transferred, the saponified extract was transferred into a separating funnel contained 10 to 15ml of petroleum ether and mixed well which took carotenoid pigments into the layer of petroleum ether. The lower aqueous layer was decanted to one more separating funnel. Repeated the extraction of the aqueous phase with petroleum ether until it was colorless. After that the aqueous layer was discarded and added a pinch of Na_2SO_4 in petroleum ether layer to eliminate turbidity. The final volume of the petroleum ether extract was recorded. The OD at 450nm was noted in a spectrophotometer by petroleum ether as a blank. (Zakaria *et al.,* 1979).

Carotenoids (µg) = P x 4x V x 100 W

P= Sample optical density

V= Sample volume

W=Weight of the sample

2.3.8. Determination of Tocopherol

100 mg sample was mixed slowly with 0.1 N sulphuric acid and kept for overnight at room temperature, then filtered. To 1.5 ml of tissue extract, 1.5 ml of xylene was added and centrifuged. Then 1.0 ml of xylene was separated and mixed with 1.0 ml of 2, 2-pyridyl and the OD was noted at 460 nm. In the beginning, 0.33 ml $FeCl_3$ added with blank and mixed well. After 15 min, the test and standard solution read against the blank at 520 nm (Rosenberg, 1992). The tocopherol content in the sample was determined by the formula.

Tocopherol (µg) = Reading at 520nm – Reading at 450nm / Reading of standard at 520nm X 0.29 X 15

2.3.9. Determination of Alkaloid

5g of sample was mixed with 25 ml of 10% acetic acid in ethanol. The mixture was enclosed and kept for 2 h. Mixture was filtered and filtrate placed on water bath to a quarter of its original volume. Concentrated NH_4OH was added in drops to the extract when precipitation was finished. The solution was allowed to stand, washed with diluted NH_4OH, filtered, and the collected dehydrated residue was weighed (Omoruyi *et al.,* 2012). Alkaloid content was determined by:

% Alkaloid =Weight of precipitate/Weight of original sample ×100

2.3.10. Determination of Phytate

2g sample was weighed and added 50 mL of 2% HClkept for 2 h and then filtered. 25 ml of the filtrate was put in a 250 ml conical flask with 5 ml of 0.3% NH_4SCN used as indicator and added 53.5 ml of distilled water. This was then titrated with standard iron III chloride solution (0.001 95 g of iron per ml) until a brownish yellow colour developed for 5 min. (Damilola *et al.,* 2013).

Phytic acid was calculated as:

Phytic acid (%) = titer value × 0.001 95 × 1.19 × 100

2.4. Antioxidant activity

2.4.1. 2, 2-diphenyl-1-picrylhydrazyl (DPPH) assay

In order to know radical scavenging behavior of the extract, DPPH solution was prepared by dissolving 20 mg 2, 2-diphenyl-1-picrylhydrazyl in 100 ml (stock solution) methanol. 3ml was taken from this solution, and its absorbance at 515 nm (control solution) was set to 0.75.To prevent free radicals, the DPPH stock solution was coated with aluminum foil and kept in dark condition for 24 hours. A 5mg of extract was weighed and dissolved in a 5ml methanol for stock solutions preparation. Different dilutions (25, 50, 75 and 100 µl/ml) were prepared from stock solutions by serial dilution. Approximately 2 ml of each dilution was mixed with a solution of 2 ml DPPH and kept at darkness for 15 minutes. Ascorbic acid was used as a typical antioxidant compound in all the assays for comparative analysis. The inhibition percentage of DPPH free radical by extracts was determined by following formula (Barros *et al.,* 2007).

% Inhibition = (Ac-As/Ac) x 100

Where Ac is the OD of the control and As is the OD of the extract/standard. The scavenging activity of samples was expressed as IC_{50} value, which represented the inhibitory concentration of extract/standard essential to scavenge 50% of DPPH radicals.

2.4.2. 2,2-azinobis (3-ethylbenzthiazoline)-6-sulfonic acid (ABTS) assay

The 2,2-azinobis (3-ethylbenzthiazoline)-6-sulfonic acid (ABTS) free radicals scavenging activity by determine the antioxidant potential of extracts. Solutions in 100 ml methanol were prepared for ABTS (7 mM) and potassium persulphate (2.45 mM). These two solutions were thoroughly mixed for the preparation of free radicals and kept in the dark overnight. Around 3 ml of stock solution was taken and its absorbance at 745 nm was set to 0.76 (control solution). Approximately 300µl of the test sample was mixed with 3ml of 2,2-azino-bis(3-ethylbenzothiazoline-6-suplhhonic acid solution and kept at 25°C for 15 min. The optical density of the solution was read at 745 nm. For the preparation of various ascorbic acid dilutions, same method was used as for sample (Re *et al.,*1999). The data was collected in triplicates, and the formula used to measure the percentage of ABTS free radicals scavenging activity was:

% Inhibition = (Ac-As/Ac) x 100

2.4.3. Ferric reducing antioxidant power (FRAP) assay

The antioxidant potential of the edible plants was estimated by procedure of (Benzie and Strain, 1996). The process is based on the reduction of Fe3+ TPTZ complex (colorless complex) to Fe2+-tripyridyltriazine (blue colored complex) formed by the action of electron donating antioxidants at low pH. Freshly prepared FRAP reagent and 2-3 ml was added to the sample and properly mixed. Blue color complex formed when ferric tripyridyltriazine (Fe3+ TPTZ) complex was reduced to ferrous (Fe2+) form and the absorbance read at 593 nm against reagent blank. Solution was kept at 37°C for 30 minutes. The calibration curve was prepared by plotting the absorbance against concentrations of ferrous sulphate. The antioxidant activity of extract was determined by linear calibration curve ($y=0.091x+0.062$; $R^2=0.960$) of $FeSO_4$ and expressed as mM $FeSO_4$ equivalents/g of extract.

2.5. Antibacterial activity

2.5.1. Collection of test organisms

The bacterial strains used such as *Escherichia coli* (MTCC 82), *Staphylococcus aureus* (MTCC 96) were obtained from parasitology laboratory of Shoolini University of Biotechnology and Management Sciences, Solan, India. These strains were grown in nutrient broth and were incubated at 37 °C for 14-16 h.

2.5.2. Antibacterial activity of plants extract

The disk diffusion method is used to evaluate antimicrobial activity of each plant extract (Razmavar *et al.,* 2014)**.** Methanolic plant extracts (50mg) were dissolved in 1 ml of 10% DMSO, then loaded on sterile filter paper discs (8 mm in diameter) to obtain final concentration of 50µl/disc. Filter paper discs loaded with 10µl of streptomycin were used as positive control. The plates were kept in the fridge at 4°C for 2 hr to permit plant extracts diffusion then incubated at 37°C for 24 hrs. The occurrence of inhibition zones was recorded by measuring scale and showed as antibacterial activity of extract.

2.5.3. Statistical analysis

At the end of the experiment, data were subjected to analysis of variance (ANOVA) and mean separation. The statistical analysis was done using Graph Pad Prism® 5.2.The least significant difference (LSD) at 5% level was used to compare the means of two species. Data are mean±SD, of three replicates (n=3) were examined by two way ANOVA followed by Bonferroni multiple comparison post-test.

3. Results

3.1. Nutrition composition

The results of nutrition composition in *Stellaria monosperma* and *Silene vulgaris* are shown in Table 1.Carbohydrate content in *S.vulgaris* was higher by 12% compare to the *S.monosperma*. Protein content in *S.vulgaris* was higher by 71% from the *S.monosperma*. Sodium and potassium content was also higher in the *S.vulgaris* by 12% and 7% respectively. Similarly, crude fibre and crude fat were high in the *S.vulgaris* by 13% and 35% from the *S.monosperma.* It is evident from the above results that *Silene vulgaris* had high nutritional properties as compared to *Stellaria monosperma*.

Table 1. Nutrition composition of *Stellaria monosperma* Buch.-Ham. ex D. Don, *Silene vulgaris* (Moench) Garcke. Data as mean ± SD, of three replicates (n=3) were analyzed using graph pad prism 5.2 by Two way Anova followed by Bonferroni multiple comparison post-test P<0.001*** significance level. Different lower case letters between columns in a table indicate significant difference between two species.

Parameters	*S.monosperma*	*S.vulgaris*
Carbohydrate (mg/g)	5.51±0.065a	6.15 ± 0.234a
Protein (mg/g)	4.53±0.393a***	7.73±0.113b***
Sodium (mg/g)	2.85±0.507a	3.18±0.025a
Potassium (mg/g)	31.11±0.862a***	33.37±0.682b***
Crude fibre (%)	3.23±0.251a	3.66 ± 0.152a
Crude fats (%)	0.34±0.030a	0.46±0.020a

3.2. Phytochemicals determination

The presence of phytochemicals in *Stellaria monosperma* and *Silene vulgaris* studied is shown in Table 2. Phenol and flavonoid content were high by 14% and 15% in *S. vulgaris* respectively. The tannin and terpenoid content was higher by 38% and 82% in *S. vulgaris* from *S.monosperma*. The quantity of amino acid and ascorbic acid was higher by 74% and 25% in *S. vulgaris* as compared to the *S.monosperma*. Tocopherol and carotenoids content was also high in the *S. vulgaris* by 23% and 19% respectively. Alkaloid and phytate content was higher in *S.monosperma* by 7% and 26% as compared to the *S.vulgaris*.

Table 2. Phytochemical composition of *Stellaria monosperma* Buch.-Ham. ex D. Don and *Silene vulgaris* (Moench) Garcke. Data as mean ± SD, of three replicates (n=3) were analyzed using graph pad prism 5.2 by Two way Anova followed by Bonferroni multiple comparison post-test P<0.001*** significance level. Different lower case letters between columns in a table indicate significant difference between two species.

Parameters	*S. monosperma*	*S. vulgaris*
Phenols (mg/g)	8.20 ± 0.434a***	9.33 ± 0.056b***
Flavanoids (mg/g)	1.63 ± 0.110a	1.87 ± 0.073a
Tannins (mg/g)	0.84 ± 0.019a	1.16 ± 0.004a
Terpenoids (mg/g)	2.691 ± 0.074a***	4.91 ± 0.098b***
Amino acids (mg/g)	0.939 ± 0.109a***	3.37 ± 0.172b***
Ascorbic acid (mg/g)	0.546 ± 0.033a	0.68 ± 0.048a
Tocopherol (µg/g)	7.52 ± 0.554 a***	9.27 ± 0.543b***
Carotenoids (µg/g)	205.95±0.563a***	245.60 ± 0.687b***
Alkaloid (%)	0.28±0.05a	0.26±0.03a
Phytate (%)	1.17±0.11a	0.87±0.10a

3.3. Antioxidant assay

Methanolic extract of *S.vulgaris* showed the strongest ABTS activity with low IC_{50} value 4.0375µg/ml while *S.monosperma* showed lower antioxidant activity with high IC_{50} value 5.483 µg/ml. Similarily, *S.vulgaris* showed the strongest DPPH activity with low IC_{50} value 2.303 µg/ml while *S.monosperma* showed lower antioxidant activity with high IC_{50} value4.152 µg/ml.IC_{50} value of FRAP assay of *S.monosperma* was high 129.855 µM as compared to *S.vulgaris* 71.760µM. IC_{50} value of ascorbic acid was low as compared to studied species shown in Table 3. High IC_{50} value indicates low antioxidant activity while lower IC_{50} value means higher antioxidant activity of plant extract. Therefore, the antioxidant activity of the *S. vulgaris* was higher as compared to *S. monosperma*.

Table 3. IC50 value of *Stellaria monosperma* Buch.-Ham. ex D. Don, *Silene vulgaris* (Moench) Garcke by ABTS, DPPH and FRAP assay.

Parameters	Ascorbic acid	*S. monosperma*	*S. vulgaris*
ABTS (IC50 µg/ml)	0.682	5.483	4.0375
DPPH (IC50 µg/ml)	0.851	4.152	2.303
FRAP (IC50 µM)	42	129.855	71.760

Inhibitory concentration at which 50% of ABTS and DPPH radicals scavenged.

3.4. Antibacterial activity

Antibacterial activity of methanolic extracts of *Stellaria monosperma* and *Silene vulgaris* against *E.coli* and S.aureus was shown in Table 4. Zone of inhibition observed in the *S. monosperma* and *S.vulgaris* against *E.coli* was 13.4±0.1 and 23.166±0.152mm, while against *S.aureus* was 14.133±0.152 and 13.533±0.057mm respectively. Streptomycin was used as positive control and zone of inhibition observed against *E.coli* and *S.aureus* was 32.166±0.208 and 28.233±0.208 mm respectively.

Table 4. Antibacterial activity of *Stellaria monosperma* Buch.-Ham. ex D. Don, *Silene vulgaris* (Moench).Data as mean ± SD, of three replicates (n=3) were analyzed using graph pad prism 5.2 by Two way Anova followed by Bonferroni multiple comparison post-test P<0.001*** significance level. Different lower case letters in a table indicate significant difference between control and species.

Bacterial strain	Positive control	*S. monosperma*	*S. vulgaris*
E.coli	32.166±0.208a	13.4±0.1b***	23.166±0.152c***
S.aureus	28.233±0.208a	14.133±0.152b***	13.533±0.057c***

4. Discussion

The present study investigated the nutritional, phytochemical, antioxidant and antimicrobial capacity of two underutilized wild edible plants, i.e. *Stellaria monosperma* and *Silene vulgaris.* These species are threatened and facing extinction as per the IUCN Red List (http://www.iucnredlist.org). Both species, besides food value, have medicinal value (Chopra *et al.*, 1986). *Stellaria monosperma* is known as a folk remedy for asthma, blood disorder, conjunctivitis, constipation, inflammation, skin ailments and obesity. In food it is eaten in salads or served as cooked greens. *Silene vulgaris* is known as emollient and is used in baths or as a fumigant. Aerial parts are eaten

raw as salad or cooked like spinach. Juice obtained from *Silene vulgaris* is used in cure of ophthalmia and is a general antidote in the remedy of poisoning and a remedy against constipation and intestinal pains. The present studies indicate that for the properties studied, *Silene vulgaris* is better than the other species. The high carbohydrate content makes it a rich source of energy, and this could be used to enrich the energy content of diets (Anital *et al.,* 2006). The carbohydrate content of *Stellaria monosperma* were comparatively less than *Silene vulgaris*. The total carbohydrates in the two species ranged between 5.5 to 6.5 mg/g. The recommended carbohydrate values for humans are 130g (Datta *et al.,* 2019). It implies that daily requirement could be reached when nearly 200g of those dried plants are consumed. Amount of protein ranged between 4.5 to 7.7 mg/g and amount studied in these species was nearly same to some leafy vegetables that are underutilized (Datta *et al.,* 2019). Proteins are essential in the manufacturing and defense of certain organic materials necessary for the proper functioning of the human body (Hayat *et al.,* 2014). The rich protein content of *Silene vulgaris* could provide necessary supplement to diets. Sodium and potassium content are considered to play an important role in human diet for physical and mental growth, as well as essential constituents of teeth, bones, muscles and blood (Unuofin *et al.,* 2017). Sodium plays a central role in the transportation of metabolites and potassium necessary for its diuretic nature. In the present study, in both species sodium content was comparatively high compared to cultivated vegetables and fruits where it ranged between 0.03-1.2 (Gopalan *et al.,* 2004). Similarly, the content of potassium was quite high in our study. The ratio of Na and K in any diet constitutes an important role in hypertension and arteriosclerosis. Sodium enhances the blood pressure whereas potassium decreases blood pressure (Saupi *et al.,* 2009). The ratio of potassium/sodium in our study occurred to quite low (10.9 in *Stellaria monosperma* and 10.49 in *Silene vulgaris*) compared to *Amaranthus viridis* (32.4), *Achyranthes aspera* (67.0). In addition, some common fruits like Papaya (11.5) tomato (11.3), and Amla (45.0) have very high ratio as reported by Sundriyal and Sundriyal (2004) and Datta et al. (2019). High fiber contained food help to reduce diseases related with metabolic disorders (Ikewuchi and Ikewuchi, 2009). *Stellaria monosperma* and *Silene vulgaris* have the rich amount of crude fibre (3.23 and 3.66% respectively) indicating that these plants decline the risk of several diseases as well as provide good supplement to human diet.

Excess intake of fat in diet is a main reason of cancer, aging and cardiovascular diseases, (Aruah *et al.,* 2011). In this context, the low content of crude fat in both the species studied (0.34 and 0.46% respectively) revealed that it could avoid certain chronic ailments in humans. Phenols are important aromatic secondary metabolite in plants, which hold ROS scavenging capability and have many biological properties like antioxidant, anti-aging, anti-inflammation, anti-cancer, and anti-atherosclerosis (Han *et al.,* 2007). Phenol content in *Stellaria monosperma* and *Silene vulgaris* was 8.2 and 9.3 mg/g, respectively, in contrast to Prasad and Chandra (2018) who reported 3.3 mg/g in *Euphorbia thymifolia* and 2.5 mg/g in *Pouzolzia hirta*, both edible medicinal plants of Western Himalayas. Total polyphenols present in the leaves of *Silene vulgaris* was 3.35 mg/g as reported by Smahane et al. (2015). Mamadalieva *et al.* (2014) reviewed the genus *Silene* whereby they isolated more than 450 compounds important classes include phytoecdysteroids (which mimic insect molting hormones), triterpene saponins (with detergent properties), volatiles, other phenolics and terpenoids. Similarly, flavonoids have been reported as antioxidants, scavengers of a large variety of free radicals and lipid peroxidation inhibitor (Williams *et al.,* 2004). The flavonoids content recorded in *Stellaria monosperma* and *Silene vulgaris* was 1.63 and 1.87mg respectively, which is in sufficient amount and provides added advantage to these species. Tannins are beneficial for the remedy of cancer and ulcerated tissues (Sun *et al.,* 2012). The tannin content in leaves of *Silene vulgaris* was 0.28 mg/g (Smahane *et al.,* 2015). The occurrence of tannins 0.48 and 1.16mg in both the species seems to be beneficial in the curing of several diseases. Presence of ascorbic acid (0.546 and 0.680mg), tocopherols (7.52 and 9.27µg) which is in sufficient quantity in these wild edible plants plays a significant role in deactivating and absorbing free radicals and protects the human body (Islary *et al.,* 2016). Alkaloid is a capable remedial bioactive substance in plants. Consumption of high alkaloids containing food may cause paralysis and rapid heartbeat which is not good for health. Intake of a high dose of alkaloids will lead to the damage of blood vessels, muscles and other soft tissues and death (Gemede and Ratta, 2014). The alkaloid content recorded in *Stellaria monosperma* and *Silene vulgaris* was of low amount, which justifies its uses by folks. The alkaloids and phytic acids are considered as anti-nutrition. The phytate content of *Stellaria monosperma* and *Silene vulgaris* was low, 1.17% in former and 0.87% in later species. Phytate content in diet of 1-16% over a long time decreases the bioavailability of mineral elements (Oke, 1969). Excessive consumption of phytic acid contained food causes diseases, e.g. osteomalacia rickets. However, the small quantity of anti-nutrient that is alkaloid and phytate could decrease by boiling, soaking and frying (Ekop, 2005). IC_{50} value of methanolic extracts of *P. esculenta* and *S. nigrum* by DPPH and ABTS was 1.37±0.02, 1.03±0.001 mg/g and 0.18±0.01, 0.19±0.001 mg/g (Seal, 2015). The IC_{50}value in studied species by ABTS, DPPH and FRAP in *S.monosperma* and *S.vulgaris* was high as compared to that reported by previous studies. Antibacterial activity of ethanolic extract of the *Catunaregam spinosa* against *E.coli* and *Klebseila pneumonia* was 18mm and 24mm, respectively. It is a wild edible fruit used by people of Tamil Nadu, India (Anand *et al.,* 2017). Zone of inhibition observed in present study was relatively similar to the previous study. Therefore, *Stellaria monosperma* and *Silene vulgaris* can be considered plants with free radical scavengers, besides a great potential in the food, nutritional and pharmaceutical industries. Further studies related to their cultivation (domestication) practices need to be taken up.

5. Conclusion

Wild edible plants *Stellaria monosperma* and *Silene vulgaris* collected from Bharmour region of District Chamba, Himachal Pradesh, were found to have an appreciable amount of carbohydrate, protein, sodium,

potassium, crude fiber and crude fats. These wild plants are rich in phytochemicals, alkaloid, phenol, flavonoids, tannins, terpenoids, amino acid, ascorbic acid, tocopherols and carotenoids, which have the antioxidant capacity. In addition, the present study revealed that the *Silene vulgaris* has a high amount of nutritional, phytochemical and antioxidant potential was observed as compared to *Stellaria monosperma*. The antibacterial activity of the *Silene vulgaris* was high as compared to the *Stellaria monosperma* against *Escherichia coli* and antibacterial activity of *Stellaria monosperma* was high as compared to the *Silene vulgaris* against *Staphylococcus aureus.* Both studied plants showed lowest antibacterial activity as compared to the streptomycin. Therefore, these plants are recommended for their domestication, food industry and biomedicical application.

Acknowledgement

The authors thank Prof. P.K. Khosla, Vice Chancellor of Shoolini University of Biotechnology and Management Sciences, Solan (H.P), India for providing research facilities.

References

Afolayan AJ and Jimoh FO. 2009 Nutritional quality of some wild leafy vegetables in South Africa. *Int J of Food Sci and Nut*, **60:** 424-431.

Aina VO, Sambo B, Zakari A, Haruna MH, Umar H, Akinboboye RM and Mohammed A. 2012. Determination of nutritional and anti-nutrient content of *Vitis vinifera* (Grapes) grown in Bomo (Area C) Zaria, Nigeria. *Adv Journal of Food Sci and Tech*, **4:** 445-448.

Ali-Shtayeh MS, Jamous RM, Al-Shafie JH, Elgharabah WA, Kherfan FA and Qarariah KH. 2008. Traditional knowledge of wild edible plants used in Palestine (NorthernWest Bank): a comparative study. *J of Ethno and Ethnome*, **4:** 13.

Anand SP, Deborah S and G Velmurugan. 2017. Antimicrobial activity, nutritional profile and phytochemical screening of wild edible fruit of Catunaregam spinosa (Thunb.) Tirveng. *The Pharma Innov J*, **6:** 106-109.

Antial BS, Akpanz EJ, Okonl PA and Umorenl IU. 2006. Nutritive and anti-nutritive evaluation of sweet potatoes (*Ipomoea batatas*) leaves. *Pak J of Nut*, **5:** 166-168.

Aruah BC, Uguru, MI and Oyiga BC. 2011. Nutritional evaluation of some Nigerian pumpkins (Cucurbita spp.). *Fruit,Veg and Cereal Sci and Biotech*, **5 :** 64-71.

Barros L, Joao FM, Queiros B, Ferreira IC and Baptista P. 2007. Total phenol, ascorbic acid, β-carotene and lycopene in Portuguese wild edible mushroom and their antioxidant acitivities. *Food Chem*, **103:** 413-419.

Benzie IF and Strain JJ. 1996. The ferric reducing ability of plasma (FRAP) as a measure of "antioxidant power": the FRAP assay. *Anal Bio*, **239:** 70-76.

Cai YZ, Sun M and Corke H. 2003. Antioxidant activity of betalains from plants of the Amaranthaceae. *J of Agri and Food Chem*, **51:** 2288-2294.

Chikhale HU and Chikhale PU. 2017. Flame Photometric Estimation of Sodium and Potassium Ion Present In Water Sample of Darna and Godavari River. *Int J of Sci & Eng Res*, **8**:131-136.

Chopra RN, Nayar SL and Chopra IC.1986. Glossary of Indian Medicinal Plants (Including the supplement). CSIR Publisher Publisher New Delhi.

Damilola O, Joseph OB, Olufemi A and Amoo I. 2013. Chemical composition of red and white cocoyam (*Colocosia esculenta*) leaves. *Int J of Sci and Res*, **1:** 121-125.

Datta S, Sinha BK, BhattachaejeeS and Seal T. 2019. Nutritional composition, mineral content, antioxidant activity and quantitative estimation of water soluble vitamins and phenolics by RP-HPLC in some lesser used wild edible plants. *Heliyon*, **5:** 1431.

Deb CR, Jamir NS and Sungkumlong O. 2013. A study on the survey and documentation of underutilized crops of three districts of Nagaland, India. *J of Glo Bio*, **2:** 67-70.

Delgado-Pelayo R, Gallardo-Guerrero L and Hornero-Méndez D. 2014. Chlorophyll and carotenoid pigments in the peel and flesh of commercial apple fruit varieties. *Food Res Int*, **65:** 272-281.

Di Matteo V and Esposito E. 2003. Biochemical and therapeutic effects of antioxidants in the treatment of Alzheimer's disease, Parkinson's disease, and amyotrophic lateral sclerosis. *CNS Neurological Disorder*, **2:** 95-107.

Ebert AZ. 2014. Potential of underutilized traditional vegetables and legume crops to contribute to food and nutritional security, income and more sustainable production systems. *Sustainability*, **6:** 319-335.

Ekop AS and Eddy NO. 2005. Comparative studies of the level of toxicants in the seed of Indian almond (*Terminalia catappa*) and African walnut (*Coula edulis*). *Chem Cl J*, **2:** 74-76.

Gemede, H.F. and Ratta, N. 2014. Antinutritional factors in plant foods: potential health benefits and adverse effects. *International Journal of Nutrition and Food Science*, **3:** 284-289.

Gerber M, Boutron-Ruault MC, Hercberg S, Riboli E, Scalbert A and Siess MH. 2002. Food and cancer: state of the art about the protective effect of fruits and vegetables. *Bull. du Cancer*, **89:** 293-312.

Ghorai N, Chakraborty S, Gucchait S, Saha SK and Biswas S. 2012. Estimation of total Terpenoids concentration in plant tissues using a monoterpene, Linalool as standard reagent. *Nat Protocol Exc*, **5:** 1038.

Gopalan C, Ramashastri BV and Balasubramanium SC. 2004 (Eds.), Nutritive Value of Foods. ICMR, New Delhi.

Han X, Shen T and Lou H. 2007. Dietry polyphenols and their biological significance. *Int J of Mole Sci*, **8:** 950-988.

Hayat I, Ahmad A, Khalil S and Gulfraz M. 2014. Exploring the potential of red kidney beans (*Phaseolus vulgaris* L.) to develop protein-based product for food applications. *J of Animal and Plant Sci*, **24:** 860-868.

Hedge JE and Hofreiter BT. 1962. In: Carbohydrate Chemistry, 17 (Eds.), Whistler RL and Be Miller JN), Academic Press, New York.

Ikewuchi CC and Ikewuchi JC. 2008. Chemical profile of *Pleurotus tuberregium* (Fr) Sing's sclerotia. *Pac J of Sci and Tech*, **10:** 295-299.

Islary A, Sarmah J and Basumatary S. 2016. Proximate composition, mineral content, phytochemical analysis and in vitro antioxidant activities of a wild edible fruit (*Grewia sapida* Roxb. ex DC.) found in Assam of North-East India. *American J of Phys Biochem and Pharma*, **5:** 21-31.

Jia Z, Tang M and Wu J. 1998. Total Phenolic, Flavonoid contents and Antioxidant.

Karamian R and Ghasemlou F. 2013. Screening of total phenol and flavonoid content, antioxidant and antibacterial activities of the methanolic extracts of three Silene species from Iran. *Int J of Agric and Crop Sci*, **5:** 305-312.

Leonti M. 2012. The co-evolutionary perspective of the food-medicine continuum and wild gathered and cultivated vegetables. *Genetic Res and Crop Evol*, **59:** 1295-1302.

Lowry OH, Rosebrough NJ, Farr AL and Randall RJ. 1951. (The Original Method). *J of Bio Chem*, **193:** 265.

Mamadalieva NZ, Lafont R and Michael M. 2014. Diversity of Secondary Metabolites in the Genus *Silene* L. (Caryophyllaceae)-Structures, Distribution, and Biological Properties. *Div*, **6:** 415-499.

Mir MY. 2014. Documentation and ethnobotanical survey of wild edible plants used by the tribals of Kupwara, J & K, India. *Int J of Herbal Med*, **2:** 11-18.

Moore S and Stein WH. 1948. Photometric Ninhydrin method for use in the chromatography of amino acid. *J of Bio Chem*,**176:** 1516-1526.

Oke OL.1969. Chemical studies on the more commonly used vegetables in Nigeria. *Afr. Sci. Ass*, **11:** 42-48.

Omoruyi, BE, Bradley G and Afolayan AJ. 2012. Antioxidant and phytochemical properties of *Carpobrotus edulis* (L.) bolus leaf used for the management of common infections in HIV/AIDS patients in Eastern Cape Province. *BMC Complementary and Alternative Medicine*, **12:** 215.

Prasad K and Chandra D. 2018. Amino acid and antioxidant composition of some wild edible medicinal plants of Uttarakhand Himalayas. J of Chem and Pharmac Res, **10:** 40-48.

Razmavar S, Abdulla MA, Ismail SB and Hassandarvish P. 2014. Antibacterial activity of leaf extracts of *Baeckea frutescens* against methicillin-resistant *Staphylococcus aureus*. *Bio Res Int*, **2014:** 1-5.

Re R, Pellegrini N, Proteggente A, Pannala A, Yang M and Rice-Evans C. 1999. Antioxidant activity applying an improved ABTS radical cation decolorization assay. *Free Rad Bio and Med*, **26:** 1231-1237.

Roe JH and Kuether CA. 1943. The determination of ascorbic acid in whole blood and urine through the 2, 4-dinitrophenylhydrazine derivative of dehydroascorbic acid. *J of Bio chem*, **147:** 399-407.

Rosenberg HR. 1992. Chemistry and physiology of the vitamins. Interscience Publishers, Inc. NewYork. 452-453.

Saupi N, Zakaria MH and Bujang JS. 2009. Analytic chemical composition and mineral content of yellow velvet leaf (*Limnocharis flava* L. Buchenau)'s edible parts. *J of Appl Sci*, **9:** 2969-2974.

Savoia D. 2012. Plant-derived antimicrobial compounds: Alternatives to antibiotics. *Future Microbio*, **7:** 979-990.

Schanderl SH. 1970. Methods in food analysis. New York: Academic Press 709.

Seal T and Chaudhuri K. 2015. Antioxidant Activities of Some Selected Wild Edible Plants of Arunachal Pradesh State in India and Effect of Solvent Extraction System. *Am J Pharm Tech Res*, **5.**

Smahane B, Dalila B, El Mansouri Latifa NA, El Youbi H and Amal DA. 2015. Phytochemical Studies, Antioxidant Activity and Protective Effect on DNA Damage and Deoxyribose of Silene Vulgaris Extract from Morocco. *Int J of Pharma and Phyto Res*, **7:** 1172-1178.

Sun Y, Zhang T, Wang B, Li H and Li P. 2012. Tannic acid, an inhibitor of poly (ADP-ribose) glycohydrolase, sensitizes ovarian carcinoma cells to cisplatin. *Anti-can D*, **23:** 979-990.

Sundriyal M. and Sundriyal RC.2004. Wild edible plants of the Sikkim Himalaya: Nutritive values of selected species. *Eco Bot*, **58:** 286-299.

Taylor M, Kambuou R, Lyons GH, Hunter D, Morgan EH and Quartermain A. 2015. Realizing the potential of indigenous vegetables through improved germplasm information and seed systems. *Acta Hort*, **1102:** 29-42.

Ubwa ST, Tyohemba RL, Oshido BA and Amua QM. 2014. Chemical analysis of some wild underutilized mucilaginous vegetables and a domesticated vegetable in Benue State, Nigeria. *J of App Sci and Tech*, **4:** 4566-4574.

Unuofin JO, Otunola GA and Afolayan AJ. 2017. Nutritional evaluation of *Kedrostis africana* (L.) Cogn: An edible wild plant of South Africa. *Asian Pac J of Trop Biomed*, **7:** 443-449.

Verma KS and Kaushal VS. 2014. Nutritive assessment of different plant parts of *Carica papaya* Linn of Jabalpur region. *J of Nat Pro and Plant Res*, **4:** 52-56.

Williams RJ, Spencer JP and Rice-Evans C. 2004. Flavonoids: Antioxidants or signalling molecules? *Free Rad Bio and Med*, **36:** 838-849.

Zakaria H, Sinpson K, Brown PR and Krotatin A. 1979. Use of reversed phase high performance liquid chromatographic analysis for the determination pro vitamin A in tomatoes. *J of Chrom*, **176:** 109-117.

Zheng W and Wang SY. 2001. Antioxidant activity and phenolic compounds in selected herbs. *J. Agric. Food Chem*, **49:** 5165-5170.

JJBS

Volume 14, Number 1, March 2021
ISSN 1995-6673
Pages 91 - 95

Jordan Journal of Biological Sciences

Assessment of genetic variability among Jordanian tomato landrace using inter-simple sequence repeats markers

Mohammad H. Brake[1,*], Moath A. Al-Gharaibeh[2], Hassan R. Hamasha[3,1], Nuha S. Al Sakarneh[2], Ibrahim A. Alshomali, Hussein M. Migdadi[4], Muien M. Qaryouti[5], Nizar J. Haddad[2]

[1] Science department, science faculty, Jerash University, Jerash, Jordan; [2] National Agriculture Research Center, Al-Baqah, Jordan; [3] Department of biology, faculty of science, Taibah University, Saudi Arabia; [4] Department of Plant production, college of food and Agriculture sciences, King Saud University, Saudi Arabia; [5] National research and development center for sustainable agriculture (ESTIDAMAH), Riyadh Technology Valley, King Saud University, Saudi Arabia.

Received: April 25, 2020; Revised: August 18, 2020; Accepted: August 31, 2020

Abstract

Twenty-nine Jordanian tomato landraces (*Solanum lycopersicum* L.) were characterized using inter-simple sequence repeats marker (ISSRs). Seven primers of ISSR could generate 77 markers; 51 of which were polymorphic. The lowest genetic similarity value (0.46) was found between landraces Jo964 and Jo955, while the highest (0.94) was obtained between landraces Jo983 and 29. The dendrogram shows that the samples are clustered in two main groups. The first group includes 4 landraces, and there are 25 landraces in the second group, which comprises one subgroup containing 13 landraces. Accessions collected from the Irbid region reported more mean values for the effective alleles (1.64), Shannon index (0.49), and heterozygosity (0.34). This study highlighted the diversity among Jordanian tomato landraces conserved in the National gene bank. These results will help in the establishment of a core collection for conserving collected landraces. The precise molecular characterization will help in efficient management and genetic improvement of local landraces.

Keywords:*Solanum lycopersicum*, landrace, ISSR, genetic diversity

1. Introduction

Tomato (*Solanum lycopersicum* L.) is an essential vegetable crop that is grown worldwide. The worldwide production of tomato and world area harvested was 182 million tonnes and 4.76 million hectares in 2018, respectively (FAOSTAT, 2018). Jordan produced 0.84 million tonnes in 2018. Because of it is economic importance as a food source, the tomato is considered one of the best genetically studied crops.

Tomatoes were probably domesticated for the first time in the Peruvian region or Mexico, according to De Candolle (1886) and Bauchet and Causse (2012), respectively. McCue (1952) reported that tomato was introduced first to Spain by Cortes and reached Italy through Naples, which was controlled by the Spanish at that time. From Europe, the tomato spread worldwide. During four centuries of cultivation, large numbers (7500) of landraces and varieties have been grown worldwide (Korir et al., 2014).

Landraces include local varieties, local populations, traditional cultivars, farmer varieties, and populations (Zeven, 1998), and traditional and primitive varieties (Negri *et al.*, 2009). Landrace are varieties with a high capacity to tolerate biotic and abiotic stress, resulting in high yield stability and an intermediate yield level under a low-input agricultural system (Zeven, 1998). In Jordan, a large number of tomato landraces were found. Since 1983, the National Agricultural Research Center collected seed samples of tomato landraces from local farmers throughout the country and maintained these samples in the seed bank (Qaryouti *et al.*, 2007).

Different DNA-based markers used to study the genetic variability among tomato varieties and landraces. These markers include random amplified polymorphic DNA (RAPD) (Salunke *et al.*, 2012, Foolad *et al.*, 1993), inter-simple sequence repeat polymorphic (ISSR) (Aguilera *et al.*, 2011, Sharifova *et al.*, 2017, Vargas-Ponce *et al.*, 2011), amplified fragment length polymorphism (AFLP) (Cebolla-Cornejo *et al.*, 2013, Ojha, 2003), simple sequence repeats (SSR) (Benor *et al.*, 2008, Saravanan *et al.*, 2014), and single nucleotide polymorphism (SNP) (Sim *et al.*, 2012, Cortés-Olmos *et al.*, 2015). The inter-simple sequence repeat markers in comparison with other molecular markers are powerful tools to assess the genetic diversity in tomato germplasm (Terzopoulos and Bebeli, 2008). ISSRs are simple, fast, and do not use radioactive materials. To the best of our knowledge, nothing has been done regarding the characterization of Jordanian tomato landraces using molecular markers. This work aims to study the genetic variability among 29 Jordanian tomato landraces using ISSR molecular marker.

* Corresponding author e-mail: m.break@jpu.edu.jo..

2. Materials and methods

2.1. Plant material

Twenty-nine Jordanian tomato landraces were investigated in this study. Seeds for landraces were obtained from the National Seed Bank belonging to the National Agricultural Research Center (NARC). Seeds were sown, and young and healthy leaves were harvested and stored at -20 °C until use. Figure 1 shows the collection sites of all landraces.

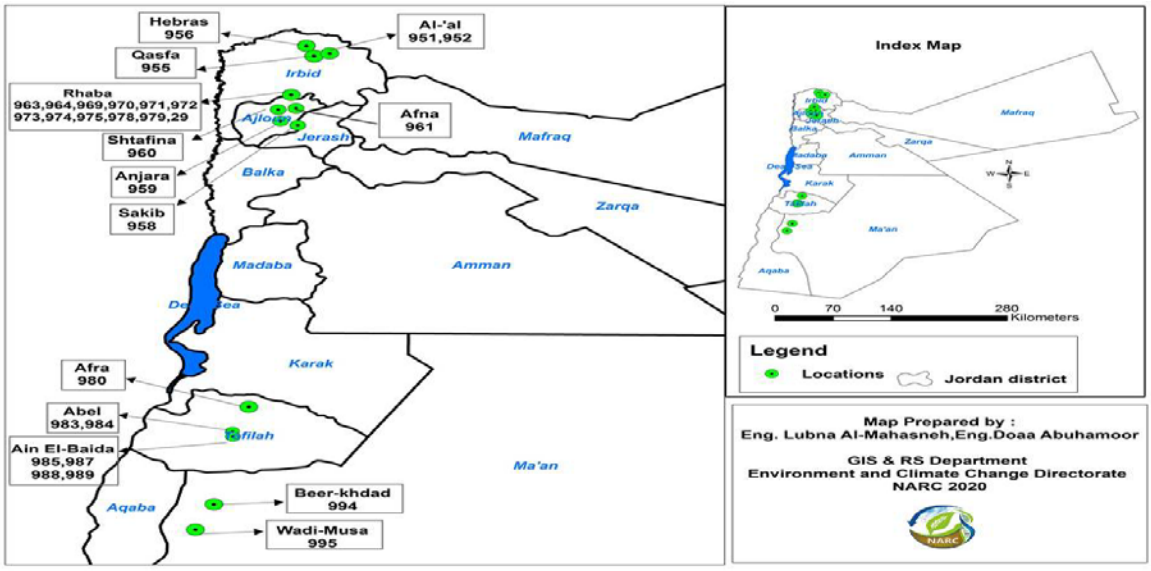

Figure 1. Map of Jordan showing collection sites of tomato landraces.

2.2. DNA extraction

Leaves were ground using a homogenizer. Total genomic DNA was extracted according to Doyle and Doyle (1987), the quality and quantity were determined using a spectrophotometer (NanoDrop 2000) and 1% agarose gel electrophoresis, respectively.

2.3. ISSR fingerprinting

Based on preliminary analysis, seven ISSR primers (Alpha DNA) (Table 1) were chosen and used for PCR amplification. According to Bornet and Branchard (2001), 25 µl reaction mixture containing 3µL of genomic DNA (10ng/µL), 0.3 µM of the primer, 1X Taq polymerase reaction buffer, 1.5 unit of Taq DNA polymerase and 0.2 mM of each dNTP were used in the amplification. Amplifications were performed using PTC-100 thermal cycler (MJ Research Inc., USA) programmed as follow, 5 min at 94 °C as an initial denaturation, followed by 40 cycles composed of 30 s at 94 °C, 45 s annealing at 52 °C, and 90 s at 72 °C and 72 °C for 5 min as a final extension. Using 1.5% agarose and 1X TBE buffer, the ISSR products were electrophoresed. Gene Ruler 100 bp DNA marker (ThermoFisher Scientific, USA) was used to estimate the fragment size and the gel stained using ethidium bromide (10 mg/ml), visualized by UV-transilluminator and photographed using an AlphaImager gel-documentation system according to Sambrook et al. (1989).

Table 1. Primers and their sequence, number of amplified bands, % prime efficiency, polymorphic markers, polymorphism, and discrimination power percentages.

Primer	Sequence 5'-3'	Total # of amplified bands	% primer fficiency	Polymorphic bands	% Polymorphism	% Discrimination power
UBC 807	$(AG)_8T$	12	16	11	92	22
UBC 809	$(AG)_8G$	15	19	11	73	22
UBC 810	$(GA)_8T$	11	14	1	9	2
UBC 811	$(GA)_8C$	12	16	11	92	22
UBC 817	$(CA)_8A$	6	8	4	67	8
UBC 823	$(TC)_8C$	11	14	8	73	16
UBC 825	$(AC)_8T$	10	13	13	50	10
Total		77		51		

2.4. Data analysis

For statistical analysis, the DNA profile for each landrace/primer was scored visually, and clear amplified bands were chosen. The presence of the band donated 1 and 0 for absence (Khierallah et al., 2014; Brake et al., 2014; Ng and Tan, 2015). Primer efficiency (the number of markers produced by primer/total number of markers obtained) was estimated and discrimination power according to Khierallah et al. (2011) for each primer was determined. The binary data collected by scoring ISSR profiles were used to calculate a similarity matrix using Jaccard's coefficients. Jaccard genetic similarity values were used to build the dendrogram based on the UPGMA method analyzed using NTSYSpc 2.02 software (Rohlf, 2000). Accessions were grouped into four main populations according to their origin. Irbid, Ajloun, Raba and Tafila with Ma'an. The total number of alleles, genetic diversity (He), and Shannon index for each population, and

the number of private alleles per population were calculated using GenAlex (Peakall and Smouse, 2012).

3. Results

The genetic diversity for 29 Jordanian tomato landraces was assessed in this study using molecular markers. Seven ISSR primers were used. Figure (2) is an example of the banding profile generated by ISSR primer UBC 823. The ISSR primers amplified 77 scorable markers (Table 1). The number of markers generated per primer varied from 6 (UBC 817) to 15 (UBC 809) and averaged 11 markers per primer. The size of the amplification products ranged from 200 to 1,900 bp. Fifty-one markers out of 77 were polymorphic with a percentage equal to 66% and an average of 7.3 polymorphic markers generated per primer. The primers UBC 807 and UBC 809 showed 11 polymorphic markers, while UBC 817 showed 4 polymorphic markers. The highest primer efficiency was obtained using the primer UBC 809, while the lowest obtained using the primer UBC 817 (Table 1). The highest value of discrimination power was observed using the primers UBC 807, UBC 809, and UBC 811, while the lowest was obtained by the primer UBC 810.

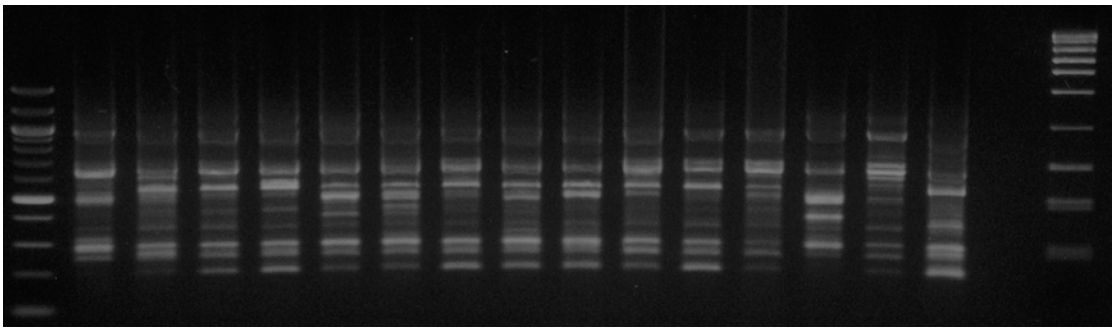

Figure 2. ISSR amplification profiles of 15 tomato landraces with primer UBC 823.

Based on Jaccard's genetic similarity coefficient, a dendrogram showing the relatedness between the landraces was constructed (figure 3). The lowest genetic similarity value (0.46) was found between landraces Jo964 and Jo955, while the highest (0.94) was obtained between landraces Jo983 and 29. The landraces are clustered into two subgroups, the first one comprises the landraces Jo964, Jo955, Jo969, and Jo78, and the second contains the other landraces. All landraces but one in the second subgroup are clustered in one main group with a genetic similarity value of 72.2%; this group is subdivided into further groups. At about 0.84 of genetic similarity, one interesting group contains 45% of the landraces (13) are formed and subdivided into two subgroups. The first contains 7 landraces, all but one from north Jordan and the second comprises 6 landraces, 4 of them from the southern part of Jordan.

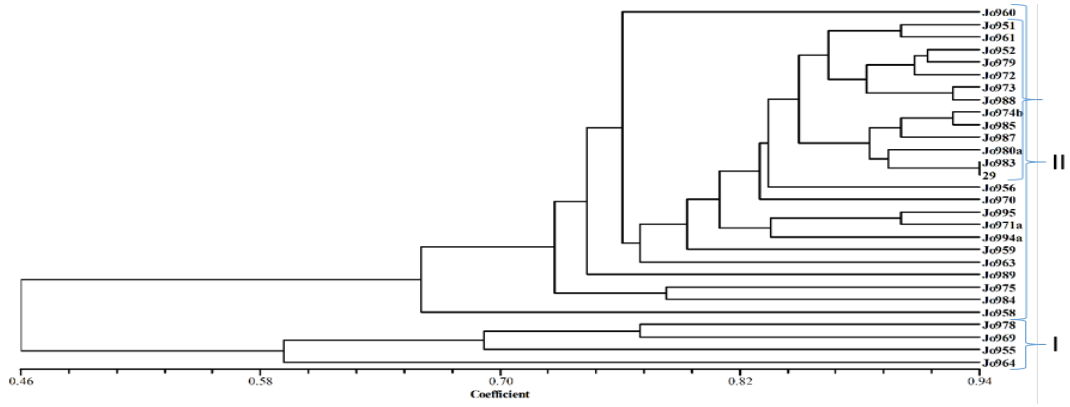

Figure 3. Dendrogram of 29 Jordanian tomato landraces generated by UPGMA cluster analysis of the genetic similarity values.

Table 2. Diversity parameters, of tomato landraces obtained from the analysis of ISSR alleles

Population	Number of samples	Na	Ne	I	H	%P	Private alleles
Irbid	4	1.64	1.64	0.49	0.34	76.62%	0.0
Ajloun	4	1.61	1.46	0.37	0.26	63.64%	0.0
Rhaba	12	1.75	1.61	0.48	0.33	80.52%	0.0
Tafila and Ma'an	9	1.52	1.38	0.32	0.22	57.14%	1.0
Mean		1.63	1.52	0.42	0.29	69.48%	

Na= Average No. of alleles, Ne = No. of effective alleles, I = Shannon index, H = diversity, P% percent of polymorphism. No. private alleles = No. of unique alleles for a single population.

The genetic diversity parameters analyzed among populations is present in Table (2). The average number of alleles (Na) varied between 1.52 for landraces collected from Tafila and Ma'an to 1.75 that collected from Rhaba. Accessions collected from the Irbid region reported more mean values for the effective alleles (1.64), Shannon index (0.49), heterozygosity (0.34). Tafila and Ma'an region showed 57.14% polymorphic percentage, and 80.52% was

reported for accessions collected from the Rhaba region. One private allele was recorded from the collection of Tafila and Ma'an.

4. Discussion

Molecular markers used in tomato including genetic variability, phylogenetic relationships, varietal fingerprinting, the marker-based selection, and the map-based cloning or QTLs (Ruiz et al., 2005, Sharifova et al., 2017, Kiani and Siahchehreh, 2018) .

In the last decades, the value of tomato landraces as gene source in many countries in the world has been explored (Cebolla-Cornejo *et al*., 2013, Corrado *et al*., 2014, Comlekcioglu *et al*., 2010); however, Jordanian tomato landraces were underrepresented. The evaluation of genetic variability is considered the first step toward effective utilization of crop genetic resources. In the presented work, molecular markers are used for the first time to evaluate the genetic variability among Jordanian tomato landraces.

The results reveal high percent of polymorphism (66%), which is consistent with results from previous analysis for tomato landraces using multilocus molecular markers in Turkey and Iran (Henareh et al., 2016, Kiani and Siahchehreh, 2018), Egypt (Hassan et al., 2013), Greece (Terzopoulos and Bebeli, 2008), Azerbaijan and other countries (Sharifova et al., 2017), Italy (Corrado et al., 2014), and Spain (Ruiz et al., 2005). Shahlaei et al. (2014) have used 10 ISSR primers to study genetic diversity for 10 tomato accessions and observed 23.25% of polymorphism percentage and 1.55 of an average resolving power value of markers was recorded. However, Mansour et al., (2010) reported high polymorphism in ISSR analysis (100%). In our study, polymorphism percentage ranged from 9 to 92% with an average polymorphic band of 7.3 per primer observed, which is more in other research. Edris et al., (2014) who reported a 62% polymorphism and a polymorphic band of 3.5 per primer. In contrary, 34% in Brazilian tomato cultivar using ISSR was reported (Aguilera et al., 2011).

The high polymorphism obtained could be explained by the nature of self-pollinating in tomato. Self-pollinating decrease intraspecific diversity while increasing interspecific diversity.

There is no clear clustering according to the collection site of landraces; however, some evidence was observed in the relationship with the site of collection. The first group in the dendrogram includes four landraces from north Jordan (Rhaba and Irbid), and the landraces Jo985, Jo987, Jo980a, and Jo983 which are collected from Tafila are clustered together. Furthermore, the landraces Jo961, Jo972, Jo973, and Jo979 are from closely related sites. This results are consistent with results of previous studies and explained that the accessions from different regions might have the similar genetic background and those from the same origin might also have different genetic background (Keneni et al., 2005; Gashaw et al., 2007; Celka et al., 2010; Comlekcioglu et al., 2010, Aguilera et al., 2011; Sharifova et al., 2013 and 2017) and in disagreement with other studies (Terzopoulos and Bebeli, 2008). Factors behind increasing the number of alleles, and increased gene diversity, varied among genetic diversity studies could be different molecular markers uses, i.e. dominant vs codominant markers, resolution of marker alleles using different electrophoresis system in fragmentation of amplified products and size and geographic composition of the tested germplasm. The presented study confirms that ISSR molecular markers are powerful tools to assess genetic diversity among Jordanian tomato landraces.

5. Conclusion

This study investigated the genetic variability of 29 Jordanian tomato landraces was investigated using ISSR molecular-based DNA marker. Nevertheless, using different types and more polymorphic molecular markers (SSRs, SNPs) could be necessary to distinguish the accessions with unknown origin and biological status. These results will help in the establishment of core collection and better conservation of Jordanian tomato landraces. The DNA-based characterization will help in efficient management and maintenance in the genetic improvement approaches. Furthermore, evaluation of these landraces under abiotic stress could be useful to produce new tomato varieties coping with climate change.

References

Aguilera J, Pessoni L, Rodrigues G, Elsayed A, da Silva D and Barros E. 2011. Genetic variability by ISSR markers in tomato (Solanum lycopersicon Mill.). Revista Brasileira de Ciências Agrárias, **6(2):** 243-252.

Bauchet G and Causse M. 2012. Genetic diversity in tomato (*Solanum lycopersicum*) and its wild relatives. Genetic Diversity in Plants, Prof. Mahmut Caliskan (Ed.). InTech, France, pp. 133-162.

Benor S, Zhang M, Wang Z and Zhang H. 2008. Assessment of genetic variation in tomato (Solanum lycopersicum L.) inbred lines using SSR molecular markers. Journal of Genetics and Genomics, **35(6):** 373-379.

Bornet B and Branchard M. 2001. Nonanchored Inter Simple Sequence Repeat (ISSR) markers: reproducible and specific tools for genome fingerprinting. Pant Mol Biol Rep, **19:** 209–215.

Brake M, Migdadi H, Al-Gharaibeh M, Ayoub S, Haddad N and El Oqlah A. 2014. Characterization of Jordanian olive cultivars (Olea europaea L.) using RAPD and ISSR molecular markers. Sci. Hortic., **176:** 282–289.

Cebolla-Cornejo J, Roselló S and Nuez F. 2013. Phenotypic and genetic diversity of Spanish tomato landraces. Sci. Hortic., **162:**150-164.

Celka Z, Buczkowska K, Baczkiewicz A, Drapikowska M. 2010. Genetic differentiation among geographically close populations of Malva alcea. Acta Biologica Cracoviensia. Series Botanica. **52**(2): 32-41.

Comlekcioglu N, Simsek O, Boncuk M and Aka-Kacar Y. 2010. Genetic characterization of heat tolerant tomato (Solanum lycopersicon) genotypes by SRAP and RAPD markers. Genetics and Molecular Research, **9(4):** 2263-2274.

Corradoa G, Caramante M, Piffanelli P and Rao R. 2014. Genetic diversity in Italian tomato landraces: Implications for the development of a core collection. Sci. Hortic., **168:**138-144.

Cortés-Olmos C, VilanovaaL S, Pascual L, Roselló J and Cebolla-Cornejo J. 2015. SNP markers applied to the characterization of Spanish tomato (Solanum lycopersicum L.) landraces. Sci. Hortic., **194:**100-110.

De Candolle A. 1886. Plants Cultivated for Their Seeds. In: Origin of Cultivated Plants. 2nd Edition, International Scientific Series Vol. XLIX, Kegan Paul Trench & Co., London, 376-384.

Doyle JJ and Doyle JL. 1987. A rapid DNA isolation procedure for small quantities of fresh leaf tissue. Phytochem. Bull., **19:** 11-15.

Edris S, Abo-Aba S, Algandaby MM, Ramadan AM, Gadalla NO, Al-Kordy MA, Sabir JS, Eldomyati FM, Alzhairy AM, Bahieldin A. 2014. Molecular characterization of tomato cultivars grown in Saudi Arabia and differing in earliness of fruit development as revealed by AFLP and ISSR. Life Sci. J. **11(8):**602-612.

Foolad MR, Jones RA and Rodriguez RL. 1993. RAPD markers for constructing intraspecific tomato genetic maps. Plant Cell Rep., **12(5):** 293-297.

Gashaw A, Mohammed H, Singh H. 2007.Genetic divergence in selected durum wheat genotypes of Ethiopian plasm. Afr. Crop Sci. J. **15(2)**: 67-72.

Hassan N, Mostafa S and Twfik A. 2013. Assessment of genetic diversity of tomato (Lycopersicon esculentum L.) germplasm using molecular markers (RAPD AND ISSR). Egypt. J. Genet. Cytol., **42:**163-182.

Henareh M, Dursun A, Abdollahi-Mandoulakani B and Haliloğlu K. 2016. Assessment of genetic diversity in tomato landraces using ISSR markers. Genetika, **48(1):** 25-35.

Keneni G, Jarso M, Wolabu T, Dino G. 2005. Extent and pattern of genetic diversity for morpho-agronomic traits in Ethiopian highland pulse landraces II. Faba bean (Vicia faba L.). Gen. Res.Crop Evol. **52(5):**551-561.

Khierallah H, Al-Sammarraie S and Mohammed H. 2014. Molecular characterization of some Iraqi date palm cultivars using RAPD and ISSR markers. Asian J. Sci. Res., **4(9):** 490-503.

Khierallah H, Bader S, Baum M and Hamwieh A. 2011. Genetic Diversity of Iraqi Date Palms Revealed By Microsatellite Polymorphism. J. Amer. Soc. Hort. Sci., **136(4):** 282-287.

Kiani G and Siahchehreh M. 2108. Genetic Diversity in Tomato Varieties Assessed by ISSR Markers. International Journal of Vegetable Science, **24(4):** 353-360.

Korir NK, Diao W, Tao R, Li X, Kayesh E, Li A, Zhen W and Wang S. 2014. Genetic diversity and relationships among different tomato varieties revealed by EST-SSR markers. Genet. Mol. Res., **13(1):** 43–53.

Mansour A, Teixeira da Silva JA, Edris S, Younis RA. 2010. Comparative assessment of genetic diversity in tomato cultivars using IRAP, ISSR and RAPD molecular markers. Focus on Tree Genetics and Genomics. Genes, Genome and Genomics **4:**41-47.

McCue G. 1952. The History of the Use of the Tomato: An Annotated Bibliography. Ann. Missouri Bot. Gard., 39(4): 289-348.

Negri V, Maxted N and Veteläinen M. 2009. European landrace conservation: an introduction. European landraces: on-farm conservation, management and use. Bioversity International, Italy. pp. 1–22.

Ng W and Tan S. 2015. Inter-Simple Sequence Repeat (ISSR) markers: are we doing it right?. ASM Sci. J., **9(1):** 30–39.

Ojha B. 2003. Amplified Fragment Length Polymorphism Mapping of Tomato Backcross Populations. J. Inst. Agric. Anim. Sci., **24:** 21-28.

Peakall R, Smouse P.E. 2012. GenAIEx 6.5: genetic analysis in Excel. Population genetic software for teaching and research an update. Bioinformatics **28(19):** 2537–2539.

Qaryouti M, Hamdan H, Edwan M, Hurani O and Al-Dabbas M. 2007. Evaluation and Characterization of Jordanian Tomato Landraces. Dirasat, Agri. Scien., **34(1+2):** 44-56.

Rohlf FJ. NTSYS-pc. 2000. Numerical Taxonomy and Multivariate Analysis System. Version 2.02 Exeter Software, Setauket, N.Y.

Ruiz J, García-Martínez S, Pció B, Gao M and Quiros C. 2005. Genetic Variability and Relationship of Closely Related Spanish Traditional Cultivars of Tomato as Detected by SRAP and SSR Markers. J. Amer. Soc. Hort. Sci., **130(1):** 88-94.

Salunke D, Jadhav A, Pawar B, Kale A and Chimote V. 2012. Diversity Analysis of Tomato Genotypes Using RAPD Markers and High-Performance Liquid Chromatography In Relation To β - Carotene Content. VEGETOS, **25(2):** 95-101.

Sambrook J, Fritsh EF and Maniatis T. 1989. **Molecular cloning: a laboratory manual**. Cold Spring Harbor, New York.

Saravanan KR, Rajaram R and Renganathan P. 2014. Studies on genetic diversity using SSR marker associated traits in tomato genotypes (Lycopersicum esculentum L.). European journal of biotechnology and bioscience, **1(5):** 26-29.

Shahlaei A, Torabi S, Khosroshahli M. 2014. Efficacy of SCoT and ISSR markers in assessment of tomato (Lycopersicum esculentum Mill.) genetic diversity. International Journal of Biosciences. **5(2):**14-22.

Sharifova S, Mehdiyeva S, Theodorikas K, Roubos K. 2013. Assessment of genetic diversity in cultivated tomato (Solanum lycopersicum L.) genotypes using RAPD primers. Journal of Horticultural Research**. 21(1):**83-89.

Sharifova S, Mehdiyeva S and Abbasov M. 2017. Analysis of genetic diversity among different tomato genotypes using ISSR DNA marker. Genetika, **49(1):** 31-42.

Sim AC, Deynze A, Stoffel K, Douches D, Zarka D, Ganal M, Chetelat R, Hutton S, Scott J, Gardner R, Panthee D, Mutschler M, Myers J and Francis D. 2012. High-Density SNP Genotyping of Tomato (Solanum lycopersicum L.) Reveals Patterns of Genetic Variation Due to Breeding. PLOS ONE, 2012. https://doi.org/10.1371/journal.pone.0045520

Terzopoulos P and Bebeli P. 2008. DNA and morphological diversity of selected Greek tomato (Solanum lycopersicum L.) landraces. Sci. Hortic., **116(4):** 354-361.

Vargas-Ponce O, Pérez-Álvarez L, Zamora-Tavares P and Rodríguez A. 2011. Assessing Genetic Diversity in Mexican Husk Tomato Species. Plant Mol Biol Rep, **29:** 733–738.

Zeven AC. 1998. Landraces: A review of definitions and classifications. Euphytica, **104:** 127-139.

JJBS

Volume 14, Number 1, March 2021
ISSN 1995-6673
Pages 97 - 104

Jordan Journal of Biological Sciences

In vitro antioxidant and inhibitory potential of leaf extracts of *Varthemia sericea* against key enzymes linked to type 2 diabetes

Abdelouahab Dehimat [1,2,*] Ines Azizi[2] Véronique Baraggan-Montero[3] Bachra Khettal[1]

[1] *Laboratoire de Biotechnologies Végétales et Ethnobotanique, Faculté des Sciences de la Nature et de la Vie, Université de Bejaia, Bejaia 06000, Algérie.* [2] *Département des Sciences de la Nature et de la Vie, Faculté des Sciences exactes et des Sciences de la Nature et de la Vie, Université de Biskra, Biskra 07000, Algérie.* [3] *LBN, Université de Montpellier, Montpellier, France*

Received Feb 17, 2020; Revised July 15, 2020; Accepted July 15, 2020

Abstract

Diabetic disease is a chronic metabolic disease characterized by postprandial and fasting hyperglycemia. It is believed that inhibition of α-amylase and α-glucosidase enzymes can be an important strategy in the administration of postprandial hyperglycemia linked to type 2 diabetes. The aim of this study was to evaluate the α-amylase and α-glucosidase inhibitory and antioxidant of leaf extracts from *Varthemia sericea* (Batt. et Trab.) Diels. Methanol extract and its fractions, cold water and ethanol extracts of *Varthemia sericea* leaves were initially screened for phytochemical class, antioxidant properties and α-amylase and α-glucosidase inhibitory activities. Furthermore, all extracts of *Varthemia sericea* were found to be potent inhibitors of α-amylase with IC_{50} values range of 37.98±2.26 and 119.89±0.89 µg/ml. The methanol extracts of *Varthemia sericea* had both the strongest inhibitory effect against the α-amylase and the α-glucosidase with IC_{50} values of 55.63±1.51 and 113.33±1.59 µg/ml, respectively. Besides, all leaf extracts from *Varthemia sericea* showed a good antioxidant activity. Whereas, the observed effects were associated with the determination of phytochemical class such as alkaloids, coumarin, and tannins, etc. Overall, our findings suggest that extract from *Varthemia sericea* leaves may be useful for diabetic care.

Keywords: *Varthemia sericea*, α-Amylase, α-Glucosidase, Antioxidant, Phytochemical screening.

1. Introduction

Diabetes mellitus is a chronic metabolic disease characterized by postprandial and fasting hyperglycemia (Jain and Saraf, 2010). A sudden rise in the blood glucose levels, causing hyperglycemia in type 2 diabetes patients happens due to hydrolysis of starch by pancreatic α-amylase and uptake of glucose by intestinal α-glucosidase (Gray, 1995).

Subsequently, it is assumed that inhibition of these hydrolytic enzymes can significantly diminish the postprandial increase of blood glucose level after different starch diet, and in this way can be a significant technique in the administration of hyperglycemia linked to type 2 diabetes (Kwon *et al.*, 2008).

Currently, there are some antidiabetic drugs, namely, acarbose, continuous use of these latter is often associated with undesirable side effects, such as liver toxicity and adverse gastrointestinal symptoms (van de Laar, 2008; Etxeberria *et al.*, 2012).

Experimental data demonstrated that oxidative stress, through the production of reactive oxygenic spices (ROS), contributes to the progression of diabetes causing damage to insulin action and increased incidence of complications (Giacco and Brownlee, 2010). Natural antioxidants from plants offer a substitute source of dietary ingredients; for example, α-amylase and α-glucosidase inhibitors are considered as one of the effective approaches for regulating type 2 diabetes by controlling glucose uptake and increasing the secretion of insulin hormone (Visweswara *et al.*, 2013).

Existent studies, along with numerous others (Apostolidis and Lee, 2010; Nwosu *et al.*, 2011), add to the increasing body of evidence, that members of the class Asteraceae are an excellent source of enzymes inhibitors.

Varthemia genus extracts are known to contain a wide array of bioactive substances with diverse health benefits (Afifi *et al.*, 1997; Al-Dabbas *et al.*, 2006b). It is also known as one of the most common plant species which has long been used as an anti-diabetic herb.

However, reports show that the extracts of Varthemia species possessed a strong effect in fasting plasma glucose concentrations reduction in diabetic patients with poor glycemic control. In addition, it has a lowering effect on the blood glucose level in hyperglycemic rats (Afifi *et al.*, 1997).

Due to the increasing attention in the valorization of endemic plants to support their use, the leaf extracts from *Varthemia sericea* (*V. sericea)* were studied herein. *V. sericea* is an endemic plant growing wild in the center of Algerian Sahara. The aqueous extract of *V. sericea* is commonly used as an Algerian folk-medicine for the treatment of gastrointestinal disorders (Hammchich and Maiza, 2006). To the best of our knowledge, this study

* Corresponding author e-mail: abdelouahab.dehimat@univ-biskra.dz.

is the first to undertake *V. sericea* leaves extracts that may be useful for diabetic care. To this end, methanol extract and its fractions, cold water, and ethanol based extracts from *V. sericea* leaves were screened for potential α-amylase and α-glucosidase inhibitory activity and antioxidant proprieties.

2. Materials and methods

2.1. Chemicals

All chemicals were of analytical grade and purchased from Sigma Aldrich.

2.2. Preparation of the methanol extract and its fractions

The extractions were carried out according to the method of Markham, (1982). The leaves of *V. sericea* powder were soaked in 75 % aqueous-methanol (V/V) with a ratio of plant material and extracting solvent of 1:10 (W/V), under agitation over three nights. The extract was filtered on filter paper to obtain the first filtrate. This procedure was repeated on the residue using 50% aqueous-methanol (V/V) under agitation to obtain the last filtrate. The first and the last filtrates were combined then the methanol was removed under reduced pressure on a rotavapor below 40 °C.

The methanol extract was subjected to fractionation using liquid extraction; it was successively extracted with different solvents of increasing polarity: Petroleum ether, chloroform, ethyl acetate. The obtained organic layer of each partition was evaporated under reduced pressure on a rotavapor below 40 °C to dryness and to afford petroleum ether, chloroform, and ethyl acetate fractions. The methanol and its fractions were stored at 4°C prior to use.

2.3. Cold water and ethanol extracts preparation

30 g of plant material was extracted with 300 ml of 50% aqueous-ethanol (V/V); the same quantity was extracted with 300 ml of distilled water as mentioned in Alimpić et al. (2015a). In both cases, extraction was performed under agitation during 72 h at room temperature.

This process was repeated twice in the same conditions and each of the extracts was gathered and then filtered through a filter paper (Whatman No.1), evaporated under reduced pressure and stored at 4 °C for further experiments.

2.4. Phytochemistry screening

Each extract of the leaves (2–3 mg/ml) of *V. sericea* was subjected to a different primer phytochemical investigation for the identification of various chemical groups (Harborne, 1998), using different tests (Alcaloïdes, steroïdes, quinones, coumarins, tannins, anthocyanes, saponins, terpenoids, anthraquinones and cardiac glycosodiques).

2.5. Antioxidant capacity determination

2.5.1. ABTS scavenging activity

The spectrophotometric analysis of 2,2′- azinobis-3-ethylbenzothiazoline-6-sulfonic acid ABTS+ scavenging activity was determined according to the method of Re et al. (1999). The ABTS• + was produced by reacting 2 mM ABTS in H_2O with 2.45 mM potassium persulfate [$K_2S_2O_8$], stored in the dark at room temperature for 16 h. The ABTS•+ solution was diluted with distilled water to give an absorbance of 0.700 ± 0.025 at 734 nm. 160 µl of this solution was mixed with 40 µl of the sample in methanol and the absorbance was recorded at 734 nm after 10 min. BHT and BHA were used as antioxidant standards.

2.5.2. Galvinoxyl radical (GOR) scavenging assay

Galvinoxyl radical (GOR) scavenging assay was determined according to the method of Shi, (2001) where Galvinoxyl was reduced by hydrogen-donation free radical scavengers. Briefly, 160 µl of GOR (0.1 mM Galvinoxyl) (4 mg in 100 ml methanol) was mixed with 40 µl of the sample in methanol and the absorbance was recorded at 428 nm after 120 min. The given results as an absorbance were compared to those of standards (BHT and BHA).

2.5.3. Hydroxyl (•OH) radical scavenging activity

Hydroxyl radical scavenging activity was measured by the adapted method of Smirnoff and Cumbes (1989). Briefly, 40 µl extract was mixed with 80 µL salicylic acid (3 mM), 24 µL $FeSO_4$ (8 mM) and 20 µL H_2O_2 (20 mM). After incubation for 30 min at 37°C, 36 µL H_2O was added and the absorbance of the mixtures was measured at 510 nm. Ascorbic acid used as a positive control.

2.5.4. Cupric reducing antioxidant capacity (CUPRAC)

Cu^{2+} ion reduction was assessed by the cupric reducing antioxidant capacity (CUPRAC) method (Apak *et al.*, 2004) by mixing 10 mM of copper chloride [$CuCl^2$] (50 µl), 7.5 mM of neocuproine in ethanol (50 µl), and 1 M ammonium acetate [CH_3COONH_4] (60 µl) with 40 µl of the sample at diverse concentrations in a microplate of 96 wells. The absorbance was measured at 450 nm after 40 min of incubation. The $A_{0.5}$ values were calculated from the absorbance curves. BHA and quercetin were used as standards.

2.5.5. O-phenanthroline reduction assay

The reaction mixture consisted of 30 µl O-phenanthroline (0.5% in methanol), 50 µl [$FeCl^3$] (0.2%), 110 µl methanol, and 10 µl of different concentrations of the extract. The combination was incubated for 20 min at 30°C, the absorbance of an orange-red solution was measured at 510 nm against a reagent blank (50 µl of [$FeCl^3$] (0.2%) and 30 µl of O-phenanthroline (0.5%) made up to 200 µl with methanol) and the percentage inhibition was calculated. The BHA and BHT were used as a positive standard (Szydlowska-Czerniaka *et al.*, 2008).

2.5.6. Ferrous ions chelating activity

The iron-chelating activity of the extracts was measured by the ferrozine method (Hennessy *et al.*, 1984) with some modifications. To 40 µl of each sample (dissolved in methanol) was added 40 µl of methanol and 40 µl 0.2 mM [$FeCl_2$ $4H_2O$]. Ferrozine (80 µl, 0.5 mM) was then added. The combination was agitated vigorously and left at room temperature for 10 min. The absorbance was measured at 593 nm. EDTA was used as a standard.

2.6. Enzyme assay

2.6.1. α-Amylase inhibitory assay

Screenings for α-amylase inhibition by extracts were carried out according to Zengin et al. (2014) with slight modification based on the starch-iodine color method. 25 µl of extracts at different concentration were added to 50 µl solution α- amylase 1U and were incubated for 10 min at 37°C. Then, 50 µl of starch 0.1% was added to each test tube and incubated at 37 °C for 10 min. 25 µl of HCl (1M) was added to stop the enzymatic reaction followed by the addition of 100 µl IKI solution. The color change was noted and the absorbance was read at 630 nm. The results were definite as % inhibition calculated using the formula:
%INH=1-[(Ac-Ae)-(As-Ab)/(Ac-Ae)]

Ac=Absorbance [Starch +IKI +HCl +Vol of the solvent of extract +Vol of Enzyme buffer] Ae=Absorbance [Enzyme + Starch +IKI +HCL + Vol of extract solvent]

As=Absorbance [Enzyme+Extract+ Starch +IKI+HCl]

Ab=Absorbance [Extrait+IKI+125µl Buffer]

2.6.2. α-Glucosidase inhibitory assay

10 µl of the sample (extracts or acarbose) solution was added to 120 µl of phosphate buffer (pH 6.9) (0.2 M), 20 µl α-glucosidase (0.5 unit/mL) from Baker's yeast (in phosphate buffer) was added to each test tube, then 50 µl of 5 mM p-Nitrophenyl-α-D-glucopyranoside solution (prepared in phosphate buffer) was mixed and incubated for 15 min at 37°C. 80 µl of Sodium carbonate solution (0.2 M) was then added. The lecture of absorbances was measured at 405 nm using a microplate reader set to 37 °C against a blank (Asghari *et al.*, 2018).

2.7. Statistics Analysis

All data points are mean values ± standard error (SE) of at least three independent experiments. Where appropriate, data were analyzed by one-way analysis of variance (ANOVA) followed by Dunnett's Multiple Comparison test and Tukey's Multiple Comparison Test. The software employed for statistical analysis was SPSS IBM 20.0

3. Results

3.1. Determination of phytochemicals classes

The results of the phytochemical screening of leaf extracts from *V. sericea* were presented in **Table 1**. Various types of bioactive compounds were detected such as alkaloids, coumarins, and tannins, etc.

Table 1. Results of phytochemical screening presenting in leaf extracts of *Varthemia sericea.*

Phytochemical Groups	Ethanol	Cold water	Methanol	Petroleum ether	Chloroform	Ethyl acetate	Aqueous residue
Alcaloïdes	++	+	++	+	+	+++	-
Steroïdes	+	-	-	-	-	-	-
Quinones	-	++	-	NT	-	-	-
Coumarines	+++	++	+++	NT	+	+++	+++
Tannins	+++	+	+	NT	+	++	+++
Anthocyanes	-	++	-	-	-	-	-
Saponins	-	+++	-	NT	-	-	-
Terpenoides	+++	++	NT	NT	NT	NT	NT
Anthraquinones	-	+	NT	NT	NT	NT	NT
Cardiaque glycosodiques	+	+	NT	NT	NT	NT	NT

+++: Very abundant, ++: Abundant, +: Rare,-: Not detected. NT: Not tested.

3.2. Determination of Antioxidant properties of leaf extracts of V. sericea

The results of antioxidants activities of leaf extracts of *V. sericea* were presented in IC_{50} values in **Table 2**.

Based on the outcomes, the ethyl acetate fraction exhibited a high potential effect against ABTS scavenging assay followed by methanol and ethanol extracts with IC_{50} of 53.72 ± 2.22, 83.22 ± 0.33 and 87.20 ± 1.33 µg/ml, respectively.

For the Galvinoxyl radical (GOR) aqueous residue fraction exhibited a scavenging capacity with an IC_{50} value of 32.44 ± 4.73 µg/ml, while ethyl acetate fraction, methanol extract, ethanol extract and chloroform fraction exhibited a similar scavenging activity with IC_{50} values of 137.96 ± 3.06, 137.38 ± 2.47, 146.62 ± 4.01 and 156.41 ± 2.42 µg/ml, respectively. Lowest values were recorded with petroleum ether fraction and cold water extract that exhibited close capacities with no significant difference ($P \leq 0.05$).

Furthermore, the hydroxyl radical scavenging activity was increased significantly after hydrolysis and the highest activity was observed with IC_{50} values (288.08±2.08 and 360.40±1.57µg/ml) for ethanol and methanol extracts, respectively (Table 2). These results were compared against ascorbic acid (IC_{50}= 13.86 ± 0.47 µg/ml). Moderate activity was observed with cold water extract, aqueous residue and chloroform fraction (IC_{50}= 523.70±0.96, 638.06±1.69 and 696.61±2.18 µg/ml, respectively).

In the same context, the methanol extract showed a potential O.phenanthroline reduction with $A_{0.5}$ of 117.63±1.97 µg/ml, followed by chloroform, ethanol, ethyl acetate and aqueous residue 163.55±2.25, 166.85±1.4, 182.48±1.10 and 184.22±2.78µg/ml, respectively. Cold water and petroleum ether had a slight effect with $A_{0.5}$ 438.26±2.17 and 501.5±0.57 µg/ml, respectively, compared to the standards (BHA and BHT) where they exhibited a strong effect against O.phenantroline assay with $A_{0.5}$ 0.93±0.07 and 2.24±0.17µg/ml, respectively.

Table 2. Antioxidant activity of leaf extracts of *Varthemia sericea* (IC50 and A0.5) µg/ml ±SD.

Extracts	Radical scavenging activity IC_{50} (µg/mL)			Reducing power $A_{0.5}$ (µg/mL)		Metal chelating assays IC_{50} (µg/mL)
	ABTS	GOR	OH	CUPRAC	O-phen	FIC
Ethanol	87.20±1.33^{d}	156.41±2.42^{c}	288.08±2.08^{e}	94.39±1.47^{d}	166.85±1.47^{d}	Na
Cold Water	150.30±1.62^{c}	342.56±4.22^{b}	523.70±0.96^{c}	167.83±1.22^{a}	438.26±2.17^{b}	Na
Methanol	83.22±0.33^{e}	137.38±2.47^{e}	360.40±1.57^{d}	66.39±0.89^{e}	117.63±1.97^{e}	Na
Petroleum ether	155.07±0.63^{b}	715.68±1.97^{a}	Na	137.17±1.58^{b}	501.5±0.57^{a}	Na
Chloroform extract	153.57±1.63^{b}	146.62±4.01^{d}	696.61±2.18a	114.72±2.01^{c}	182.48±1.10^{c}	Na
Ethyl acetate	53.72±2.22^{f}	137.96±3.06e	Na	52.17±1.04^{f}	163.55±2.25^{d}	Na
Aqueous Residue	279.10±2.24^{a}	32.44±4.^{73f}	638.06±1.69^{b}	45.99±2.34^{j}	184.22±2.78^{c}	Na
Standards						
BHA	1.81±0.10^{j}	5.38 ±0.06^{j}	NT	5.35±0.71^{l}	0.93±0.07^{j}	NT
BHT	1.29±0.30^{h}	3.32±0.18^{k}	NT	8.97±3.94^{k}	2.24±0.17^{f}	NT
EDTA	NT	NT	NT	NT	NT	12.11 ± 0.32
Ascorbic Acid	NT	NT	13.86 ± 0.47^{f}	NT	NT	NT

• Na: No activity (>800 µg/ml), NT: Not tested. Values expressed were means ± S.D. of three parallel measurements ($P \leq 0.05$).

• Results with different superscript letters are significantly different ($P \leq 0.05$) and the decrease order (a>b>c>d>e>f>j>h>..).

• (ABTS·+ radical scavenging, Galvinoxyl radical (GOR) scavenging antioxidant capacity assay, Hydroxyl Radical Scavenging Assay, Cupric reducing antioxidant capacity (CUPRAC), O-phenanthroline reduction assay (O-phen), Ferrous iron chelating (FIC) assay.

In addition, the capacity of different extracts to reduce copper ions property was assessed using CUPRAC assay. The different extracts and fractions exhibited an interesting reduction of copper ions at the tested concentrations. The aqueous residue fraction was the most efficient in the reduction of copper ions, followed with the ethyl acetate fraction, methanol, and ethanol extracts with $A_{0.5}$ values of 45.99 ± 2.34, 52.17 ± 1.04, 66.39 ± 0.89 and 94.39±1.47 µg/ml respectively. Chloroform and petroleum ether fractions, as well as the cold water extract, exhibited the lowest reducing capacity of copper ions

Moreover, all extracts did not show any capacity to chelate iron ions (IC_{50}>800µg/ml). Interestingly, EDTA used as standard showed a strong chelating property (IC_{50} = 12.11 ± 0.32 µg/ml) ($P \leq 0.05$).

These results show that the leaf extracts of *V. sericea* exhibited a dose-dependent antioxidant activity.

3.3. Determination of enzymes inhibitory activity of leaf extract from Varthemia sericea

The extracts of interest, methanol extract and its fractions, cold water, and ethanol extracts of the leaf of *V. sericea* were examined at lower concentrations (10-500µg/ml) and initially screened for α-amylase and α-glucosidase inhibitory effects.

The results of the determination of α-amylase and α-glucosidase inhibitory by the exhibition of *V. sericea* leaves extracts were presented in **Figure 1**, and compared to the quercetin and ascarbose as positive standards.

3.3.1. Determination of α-amylase inhibitory activity

The effect of the inhibitory enzyme showed that all the extracts exhibited a significant potential activity more than 50% of inhibition against α-amylase, at a concentration of 125 µg/ml (**Figure 1. A**).

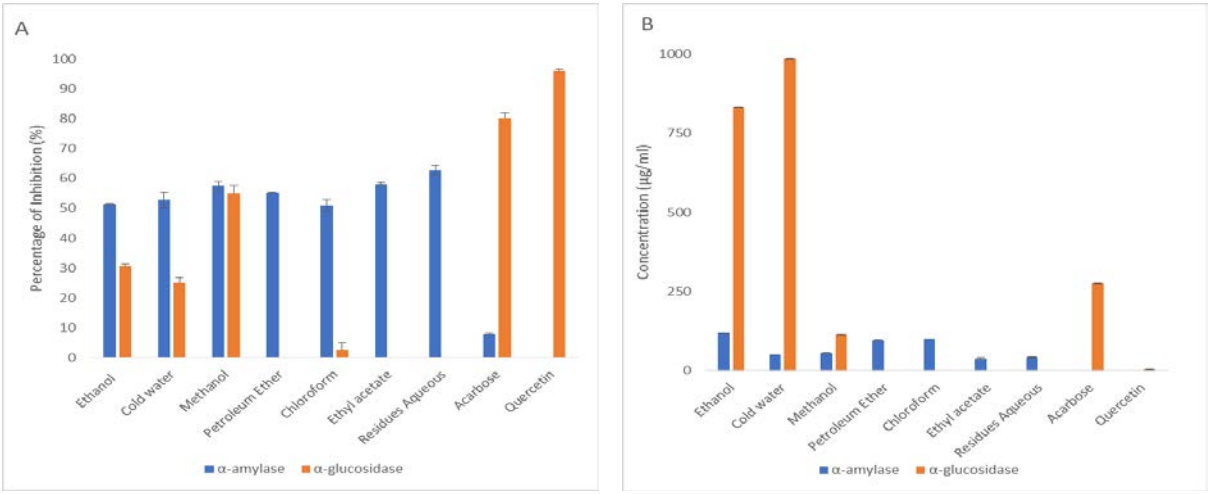

Figure 1. Activities of anti-amylase and anti-glucosidase of various extracts of leaves of *Varthemia sericea*. A) The percentage of inhibition of extracts and the positive standards at a concentration of 125µg/ml. B) Values of IC50 (µg/ml).

- Inhibition effect of Acarbose against α-glucosidase is not mentioned (IC50 = 3650.93±10.70 µg/ml).
- Values expressed are means ± S.D. of three parallel measurements ($p<0.05$).

Where the aqueous residue fraction had the best inhibition with amylase 62.70 %, followed by the ethyl acetate and methanol extracts with 58.13 and 57.52 %, respectively.

The IC_{50} values were obtained from the dose–response curves. The IC_{50} of the inhibitory effect of extracts of *V. sericea* was significantly stronger than the acarbose, represented in Figure 1. B. As a result, ethyl acetate, residue aqueous, cold water and methanol extracts acted as α-amylase inhibitory effect with IC_{50} of 37.98±2.26, 41.87±1.46, 50.54±0.68 and 55.63±1.51 µg/ml, respectively. Followed by petroleum ether, chloroform, ethanol extracts with IC_{50} of 95.89±0.89, 99.79±0.46 and 119.89±0.89 µg/ml, respectively. We can say that all leaf extracts from *V. sericea* showed a strong effect compared to the acarbose (IC_{50}= 3650.93±10.70 µg/ml).

3.3.2. Determination of α-glucosidase inhibitory activity

The results of the α-glucosidase inhibitory effect of leaf extracts of *V. sericea* are mentioned in Figure 1.

At a concentration of 125 µg/ml, the methanol extract had a percentage inhibition of 54.90 % followed by ethanol and cold water extract of 25.13 and 39.56 %, respectively. These results were lower than the quercetin inhibitory percentage (72.58%) at the same concentration, whereas they were still greater than the percentage inhibition of acarbose (54.86%), at a concentration of 312.5µg/ml (Figure 1. A).

For the inhibitory of α-glucosidase, the methanol extract inhibited the 50% of the α-glucosidase enzyme at a concentration of 113.33±1.59 µg/ml, which is more effective than acarbose (IC_{50}=275.43±1.59µg/ml) and closer to the quercetin (IC_{50}= 4.26±0.24 µg/ml). However, a slight effect was shown for the cold water and ethanol extracts (Figure 1. B).

Based on the outcomes, the methanol extract from leaves of *V. sericea* had a dual inhibitory effect against the two enzymes, which should have a specific inhibitor compound for each enzyme.

4. Discussion

V. sericea is a medicinal plant from the pharmacopeia of the central Sahara of Algeria, used to treat a wide range of diseases. The leaves of this plant have been reported to possess antispasmodic and analgesic effects used as a therapy in traditional medicine (Hammiche and Maiza, 2006).

To our knowledge, no detailed study of *V. sericea* has been delivered earlier. In the present study, we reported the inhibition effect of different leaf extracts of *V. sericea* on the two key enzymes linked to type 2 diabetes and the antioxidant activities due to the presences of bioactive molecules.

Qualitative phytochemical screening of different chemical classes in extracts of *V. sericea* revealed the presence of the alkaloids, tannins, and coumarin, which contributes to the antioxidant and anti-diabetic activities of the plant (Table 1). We can explain the presence, the absence, and the abundant or a rare presence of that chemical class by the solvent system extract which was verified by Ogbuanu et al. (2014).

Previous studies on the chemistry of Varthemia species, (Jasonia = Varthemia), *Jasonia glutinosa, Jasonia berosa, Jasonia montana,* and *Jasonia candicans,* had shown the presence of differnts phtochmical classes such us sesquiterpenes and sesquiterpene lactone derivatives 1 eudesmanoic acids, eudesmanolides,2 guaianolides and pseudoguaianolides, 2 together with various polymethoxylated flavonoids and coumarins (De Pascuai *et al.,* 1980; Ahmed *et al.,* 1993; 1994). *Jasonia montana* is considered as a rich plant in polyphenols which are used as antioxidants (Al-Howiriny *et al.,* 2005).

The existence of secondary metabolites such as the flavonoids adds value to this herb since they are a group of compounds that are known to exhibit antioxidant, and thereby anti-diabetic activities (Halliwell and Gutteridge, 1999; Ng *et al.,* 2000), which are caused by exposure to oxidative stress (Liu, 2003; Caillet *et al.,* 2006).

Subsequently, the leaf extracts of *V. sericea* were evaluated for their biological potentialities.

It is significant to use different assays to take in consideration the composition of extracts which act through several mechanisms like the inhibition of chain initiation, binding of transition metal ion catalysts, breakdown of peroxides, avoidance of continued hydrogen abstraction, reductive ability and radical quenching (Li *et al.,* 2008).

For this reason, the antioxidant ability of *V. sericea* was evaluated using six complementary -*in vitro*- tests: free-radical scavenging (ABTS, GOR, and OH.), reducing power (CUPRAC, phenanthroline) and metal chelating assays.

The results are summarized in Table 2. Free radical scavenging is thought to be one of the main mechanisms exhibited by antioxidants to delay oxidative processes. ABTS is stable free radical used to determine the ability of antioxidants to donate a hydrogen atom by converting it to the non-radical species (Alam *et al.,* 2013).

One mechanism of protecting consequence may be radical-scavenging which is via offering hydrogen atom (H·), donating electron (e). Its antioxidant ability can be mainly attributed to the existence of phytochemicals such as flavonoids or total phenolic (Li *et al.,* 2013).

The ethanol and aqueous extracts from the aerial part of *V. iphionoides* showed a pronounced 1,1-diphenyl-2-picrylhydrazyl (DPPH) radical-scavenging activity, with inhibition of about 90%, at a concentration of 100 µg/ml (Al-Dabbas *et al.,* 2006a).

In a study carried out by Kaiser et al. (2011), the aqueous extract of *Ficus racemosa* (Family of Moraceae) seed revealed a strong free radical scavenging activity having an IC 50 value of 22.10 µg/ml.

As a reducer agent, CUPRAC and the red O-phenanthroline, is widely applied in the classical spectrophotometric method for the determination of iron. The reduction can be used as an indicator of electron-donating activity, which reflects an important mechanism of antioxidant action (Hajji *et al.,* 2019).

However, the chelation of ferrous ions can be due to the presence of the nitrogen groups explaining the activity of alkaloids (Hennessy *et al.,* 1984).

The hydroxyl groups in polyphenols are responsible for their antioxidant properties, which is manifested by canceling the effect of free radicals such as peroxo, oxo, and hydroxo (Teodora *et al.,* 2020). The results of several recent studies have demonstrated that the hydroxyl groups in polyphenolic compounds may perform a crucial function in promoting inhibitory activity (Stern *et al.,* 1996; Kim *et al.,* 2008).

As it has been suggested, the phenolic content of plant materials is correlated with their antioxidant activity; the

antioxidant potentials of natural compounds are referred to as their capacity to scavenging radicals and by chelating metal ions via functional groupement of their structure. Besides, it has been suggested that the antioxidant and lipid peroxidation-inhibiting potential of flavonoid predominantly resides in the radical-scavenging capacity rather than the chelation of metals (Iraga *et al.,* 1987; Ratty and Das, 1988).

Solvents are a key step for extracting antioxidants from natural sources. Ethanol was with the highest frequency as a solvent for extraction purposes. These results suggested that the phenolic compounds that existed in these extracts are mainly flavonoids with different methoxyl and hydroxyl substitutions. The hydroxyl substitution is mainly responsible for hydrogen donations to the free radicals (Alam *et al.,* 2013).

Antioxidant activity contributes a part in the administration of diabetes mellitus (Raphael *et al.,* 2002). Some plant species have been reported to account for both antidiabetic activities as well as antioxidant activity. Phenolic from tea is found to manage both α-amylase and sucrase, which have an antioxidant effect (Matsumato *et al.,* 1993; Tchinda *et al.,* 2008).

Antioxidants from plants offer a substitute source of dietary ingredients, For example, α-amylase, α-glucosidase inhibitors are considered as one of the effective measures for regulating type 2 diabetes by controlling glucose uptake and increasing the secretion of insulin hormone (Kim *et al.,* 2009).

Enzyme inhibition is a common and important method for the discovery of new drugs and the treatment of public human health disorders. There are several enzymes whose inhibition is considered as a target for the treatment or prevention of related diseases (Asghari *et al.,* 2018), including glucosidase and amylase (Diabetes Mellitus).

According to numerous *in vitro* studies, inhibition of α-amylase and α-glucosidase is believed to be one of the most effective approaches for diabetes care (Etxeberria *et al.,* 2012; van de Laar, 2008).

Based on the finding in **Figure 1**, the methanol extract of *V. sericea* exhibited both potential inhibitory effect against the two enzymes tested (α-amylase and α-glucosidase). Interestingly, all extracts played a strong inhibitory effect against α-amylase.

The phytochemical such as polyphenol compounds in plants inhibit the activities of carbohydrate hydrolyzing enzymes, such as α-amylase and α-glucosidase, due to their ability to bind with proteins (Mai *et al.,* 2007).

The α-amylase inhibitors are also called starch blockers, as they contain substances that prevent dietary starch from being absorbed into the body system, which can be convenient within the management of diabetes. α-amylase may exert a blood-glucose-lowering effect through inhibition of salivary and pancreatic amylase (Kazeem *et al.,* 2013; Harrison *et al.,* 2014).

In a study carried out by Al-Dabbas et al. (2006b), two methods were tested, the ethanol and water extracts had a weak but substantial inhibitory effect on α-amylase in the iodine-starch assay, whereas they had a pronounced effect with inhibition of about 70% at a concentration of 200 mg/ml in the 2-chloro-4-nitrophenyl alpha-maltotrioside (CNP-G3) assay. The differrant results of α-amylase inhibition by the two methods might be attributable to the differrant substrates used. As a result, the cleavage of short-chain substrates, such as CNP-G3 was reduced by inhibitory substances to a larger extent than with longer sequence substrates in the Iodo-starch method, and this probably clarifies the complete inhibition of the α-amylase activity by the CNP-G3 method even at a low concentration (100 mM) (Al-Dabbass *et al.,* 2006b).

In other veins, α-glucosidase inhibitors are suppressor of postprandial hyperglycaemia in diabetic Mellitus patients by inhibiting the activity of α-glucosidase in the intestine, which reduces glucose absorption by delaying carbohydrate digestion and increases digestion time (Johnston *et al.,* 2010).

The genus of Vathemia (also named Jasonia) has long been used as an anti-diabetic herb, and it has a lowering effect on the blood glucose level in hyperglycemic rats (Al-Dabbas *et al.,* 2006b).

Reports show that *Varthemia iphionoides* extract possessed a moderate effect in fasting plasma glucose concentrations reduction in diabetic patients with poor glycemic control (Abu-Zaiton *et al.,* 2018).

Results of the study carried out by Afifi and colleagues (1997) revealed the decreasing of blood glucose level by *Varthemia iphionoides* essential oil, maybe due to its numerous bioactive compounds such as phenols, flavonoids, saponins, triterpenoids and tannins; these compounds may play their role in hypoglycemic effects by increasing release and decreasing glucagon's secretion, decreasing insulin resistance, slowing the absorption of glucose or by reducing hepatic glucose production (Abu-zaiton *et al.,* 2018).

Numerous studies on plant extracts of Chrysanthemum genus (Asteraceae) that may contribute to diabetes management have focused on the inhibition of α-glucosidase which catalyzes carbohydrate consumption into glucose (Yang *et al.,* 2011; Thi Luyen *et al.,* 2013; Ben Sassi *et al.,* 2018).

Indeed, these findings demonstrate that the leaf extracts are able to inhibit the oxidative reactions by free radical scavenging and by acting as reducing and chelating power agents as well as the α -amylase and α-glucosidase inhibitory activities. These therapeutic promises can be ascribed to their phenolic constituents; although, other phytochemicals could have acted synergistically (Ademiluyi *et al.,* 2015).

5. Conclusion

To sum up, the results showed that all leaf extract of *V. sericea* presented different phytochemical classes such as alkaloid, tannins, and coumarin, well known for their antioxidants and anti-diabetic effects. These leaf extracts exhibited potential inhibition effects against the two key enzymes linked to type 2 diabetes and antioxidant activities. Further works are needed to isolate and identify the bioactive molecules from the leaves of *V. sericea.*

Conflicts of interest

None.

Acknowledgments:

The authors would like to thank BENSOUICI Chawki from Biotechnology Research Center (CRBT), Constantine, Algeria for the help.

Reference

Ademiluyi A, O, Ganiyu O, Funmi P, Aragbaiye M, Sunday I. Oyeleye M, Opeyemi B and Ogunsuyi B. 2015. Antioxidant properties and in vitro a-amylase and a-glucosidase inhibitory properties of phenolics constituents from different varieties of Corchorus spp. *Journal of Taibah University Medical Sciences*, **10(3):** 278-287.

Afifi F, Saket M, Jaghabir M and Al-Eisawi D. 1997. Effect of *Varthemia iphionoides* on blood glucose level of normal rats and rats with streptozocin-induced diabetes mellitus. *Curr. Ther. Res*, **58**: 888–892.

Abu-Zaiton A, Alsohaili S, Abu-Zaitoon Y, Trad B and Wardat A. 2018. Anti-hyperglycemic Effect and Liver Enzymes Activity of *Varthemia iphionoides* essential Oil in Diabetic Rats. *International Journal of Advanced Biotechnology and Research (IJABR)*, **9(4):** 549-554.

Ahmed AA, Mahmoud AA, Tanaka T and Iinuma M. 1994. Two methylated flavonols from *jasonia candicans*. *Phytochemistry*, **35:** 241-243.

Ahmed AA, Mahmoud AA, Williams HJ, Scott AI, Reibenspies JH and Mabry TJ. 1993. New sesquiterpene alpha-methylene lactones from the Egyptian plant *Jasonia candicans*. *Journal of Natural Products*, **56:** 1276-1280.

Alam NM, Bristi NJ and Rafiquzzaman M. 2013. Review on *in vivo* and *in vitro* methods evaluation of antioxidant activity. *Saudi Pharmaceutical Journal*, **21:** 143–152.

AL-Dabbas MM, Suganuma T, Kitahara k, Hou D and Fujii M. 2006a. Cytotoxic antioxidant and antibacterial activities of *Varthemia iphionoides* Boiss. Extracts. *Journal of Ethnopharmacology*, **108:** 287-293.

Al-Dabbas MM, Kitahara K, Suganuma T, Hashimoto F and Tadera k. 2006b. Antioxidant and α-amylase inhibitory compounds from aerial parts of *Varthemia iphionoides*. Boiss. *Bioscience Biotechnology and Biochemistry*, **70:** 2178-2184

Al-Howiriny TA, Al-Rehaily AJ, Pols JR, Porter JR and Mossa JS. 2005. Three new diterpenes and the biological activity of different extracts of *jasonia montana*. *Nat. Prod. Res*, **19:** 253-265.

Alimpić A, Kotur N, Stanković B, Marin PD, Matevski V, Al Sheef NB and Laušević DS. 2015a. The in vitro antioxidant and cytotoxic effects of selected Salvia species water extracts. *Journal of Applied Botany and Food Quality*, **88**: 115–119.

Apak R, Guclu K, Ozyurek M and Karademir SE. 2004. Novel total antioxidant capacity index for dietary polyphenols and vitamins C and E, using their cupric ion reducing capability in the presence of neocuproine: CUPRAC method. *Journal of Agricultural and Food Chemistry*, **52:** 7970–7981.

Apostolidis E and Lee CM. 2010. In vitro potential of Ascophyllum nodosum phenolic antioxidant-mediated a-glucosidase and a-amylase inhibition. *Journal of Food Science*, **75:** 97–102.

Asghari B, Zengin G, Bahadori MB, Abbas-Mohammadi M and Dinparast L. 2018. Amylase, glucosidase, tyrosinase, and cholinesterases inhibitory, antioxidant effects, and GC-MSanalysis of wild mint (*Mentha longifolia* var. *calliantha*) essential oil: A natural remedy. *European Journal of Integrative Medicine*, **22:** 44–49.

Ben Sassi A, Amroussi S, Besbes M, Aouni M and Skhir F. 2018. Antioxidant and α-glucosidase activities and phytochemical constituents of Chrysanthoglossum trifurcatum (Desf.). *Asian. Pac. J. Trop. Med.* **11:** 285–291.

Caillet, S, Salmieri S and Lacroix M. 2006. Evaluation of free radical-scavenging properties of commercial grape phenol extracts by a fast colorimetris method. *Food Chemistry*, **95:** 1-6.

De Pascuai, TJD, Barrero AF, Feliciano AS, Grand M and Medarde M. 1980. *Phytochemistry*, **19:** 2155-2157.

Etxeberria U, de la Garza AL, Campion J, Martinez JA and Milagro FI. 2012. Antidiabetic effects of natural plant extracts via inhibition of carbohydrate hydrolysis enzymes with emphasis on pancreatic alpha amylase. *Expert Opinion on Therapeutic Targets*, **16:** 269–297.

Giacco F and Brownlee M. 2010. Oxidative Stress and Diabetic Complications. *Circ. Res*, **107(9):** 1058 – 1070.

Zengin G, Sarikurkcub C, Aktumseka A, Ceylana R and Ceylanc OA. 2014. comprehensive study on phytochemical characterization of Haplophyllum myrtifolium Boiss. endemic to Turkey and its inhibitory potential against key enzymes involved in Alzheimer, skin diseases and type II diabetes. *Industrial Crops and Products Industrial Crops and Products*, **53:** 244– 251

Gray DM. 1995. Carbohydrate Digestion and Absorption Role of Small Intestine. *The New England Journal of Medicine*. **29:** 1225-30.

Hajji M, Hamdi M, Sellimi S, Ksouda G, Laouer H, Li S and Nasri M. 2019. Structural characterization, antioxidant and antibacterial activities of a novel polysaccharide from Periploca laevigata root barks. *Carbohydrate Polymers*, **206:** 380–388.

Halliwell B and Gutteridge JMC. 1999. Free Radicals in Biology and Medicine, third ed. Oxford University Press, Oxford.

Hammiche V and Maiza K. 2006. Traditional medicine in Central Sahara: Pharmacopoeia of Tassili N'ajjer. *Journal of Ethnopharmacology*, **105:** 358–367.

Harborne JB. 1998. Text book of Phytochemical Methods. A Guide to Modern Techniques of Plant Analysis, 5th Edition, Chapman and Hall Ltd, London, pp. 21-72.

Harrison DE, Strong R, Allison DB, Ames BN, Astle CM and Atamna H. 2014. Acarbose, 17-a-estradiol, and nordihydroguaiaretic acid extend mouse lifespan preferentially in males. *Aging Cell*, **13:** 273-82.

Hennessy DJ, Reid GR, Smith FE and Thompson LS. 1984. Ferene - a new spectrophoto- metric reagent for iron. *Canadian Journal of Chemistry*, **62:** 721–724.

Iraga CG, Martino VS, Ferraro GE, Coussio J E and Boveris A. 1987. *Biochemical Pharmacology*, **36:** 717.

Jain S and Saraf S. 2010. Type 2 diabetes mellitus—Its global prevalence and therapeutic strategies. *Diabetes & Metabolic Syndrome: Clinical Research & Reviews*, **4(1):** 48–56.

Johnston CS, Steplewska I, Long CA, Harris LN and Ryals RH. 2010. Examination of the antiglycemic properties of vinegar in healthy adults. *Ann Nutr Metab*, **56:** 74-9.

Kaiser H, Shapna S, Kaniz F, Urmi M, Obayed U, Abu Hasanat M. Zulfiker M and Afzal H. 2011. In vitro Free Radical Scavenging and Brine Shrimp Lethality Bioassay of Aqueous Extract of *Ficus racemosa* Seed. *Jordan J of Bio Scie*,.**4(1):** 51 – 54.

Kazeem MI, Raimi OG, Balogun RM and Ogundajo AL. 2013. Comparative study on the a-amylase and a-glucosidase inhibitory potential of different extracts of Blighia sapida Koenig. *Am J Res Commun*, **1(7):** 178-92.

Kim GN, Shin JG and Jang H.D. 2009. Antioxidant and antidiabetic activity of Dangyuja (Citrus grandis Osbeck) extract treated with Aspergillus saitoi. *Food Chem*, **117:** 35–41.

Kim KY, Nam KA, Kurihara H and Kim SM. 2008. Potent α-glucosidase inhibitors purified from the red alga Grateloupia elliptica. *Phytochemistry*, **69:** 2820–5.

Kwon YI, Apostolidis E and Shetty K. 2008. In vitro studies of eggplant (Solanum melongena) phenolics as inhibitors of key enzymes relevant for type 2 diabetes and hypertension. *Bioresource Technology*, **99:**2981–2988.

Liu R. 2003. Health benefits of fruit and vegetables are from additive and synergistic combinations of phytochemicals Am. *J. Clin. Nutr*, **78:** 517S–520.

Li HB, Wong CC, Cheng KW and Chen F. 2008. Antioxidant Properties in Vitro and Total Phenolic Contents in Methanol Extracts From Medicinal Plants. *Lebens-Wizs Techonologie*, **41:** 385–390.

Teodora LR, Vãruþ RM, Amzoiu E, Mormoe M, Oana N, Amzoiu MO and Udrescu L. 2020. Determination Of The Antioxidant Capacity Of *Tragopogon Pratensis* Species And Testing Their Pancreatic And Hepatic Regenerative Activity. *Pharmaceutical Chemistry Journal*, **53(10).**

Mai TT, Thu NN, Tien PG and Chuyen N.V. 2007. Alpha-glucosidase inhibitory and antioxidant activities of Vietnamese edible plants and their relationships with polyphenol contents. *J. Nutr. Sci. Vitaminol*, **53:** 267–276.

Markham KR. 1982. Techniques of Flavonoid Identification. Academic Press, London.

Matsumato M, Ishigaki F, Ishigaki A, Iwashina H and Hara Y. 1993. Reduction of blood glucose levels by tea catechin. *Bioscience, Biotechnology and Biochemistry*, **57:** 525–527.

Ng TB, Liu F and Wang ZT. 2000. Antioxidant activity of natural products from plants. *Life Sciences*, **66:** 709–723.

Nwosu F, Morris J, Lund VA, Stewart D, Ross HA and McDougall GJ. 2011. Anti-proliferative and potential anti-diabetic effects of phenolic-rich extracts from edible marine algae. *Food Chemistry*, **126:** 1006–1012.

Ogbuanu CC, Ehiri RC and Ogah SPI. 2014. Phytochemical Screening and Preliminary TLC Characterization of Alkaloids in Sabicea brevies Root. *Research Journal of Phytochemistry*, **8:** 1-8.

Raphael KR, Sabu MC and Khuttan R. 2002. Hypoglycemic effect of methanol extract of Phyllanthus amarus Schum&Thonn on alloxan induced Diabetes mellitus in rats and its relaxation with antioxidant potential. *Indian Journal of Experimental Biology*, **40:** 905–909.

Ratty AK and Das NP. 1988. Effects of flavonoids on nonenzymatic lipid peroxidation: Structure-activity relationship. *Biochemical Medicine and Metabolic Biology*, **39:** 69-79.

Re R, Pellegrini N, Proteggente A, Pannala A, Yang M and Rice-Evans C. 1999.Antioxidant activity applying an improved ABTS radical cation decolorizationassay. *Free Radical Biology and Medicine*, **26:** 1231–1237.

Shi H, Noguchi N and Niki E. 2001. Galvinoxyl method for standardizing electron and proton donation activity. *Methods Enzymology*, **335:** 157-66.

Smirnoff N and Cumbes QJ. 1989. Hydroxyl radical scavenging activity of compatible solutes. *Phytochemistry*, **28:**1057–1060.

Stern JL, Hagerman AE, Steinberg PD and Mason PK. Phlorotannins–protein interactions. *J Chem Ecol*, **22:**1877–99.

Szydlowska-Czerniaka A, Dianoczki C, Recseg K, Karlovits G and Szlyk E. 2008. Determination of antioxidant capacities of vegetable oils by ferric-ion spectrophotometric methods. *Talanta*, **76:** 899-905.

Tchinda AT, Tchuendem Khan SN, Omar I, Ngandeu F, Nkeng PEA and Choudhary IM. 2008. Antioxidant activity of the crude extract of the fruits of Pycnanthus angolensis and α-glucosidase inhibitory activity of its constituents. *Pharmacology*, **1:** 422–431.

Thi Luyen, N, Hoang Tram L, Hong Hanh TT, Thanh Binh, T, Hai Dang N and Van Minh C. 2013. Inhibitors of α-glucosidase, α-amylase and lipase from Chrysanthemum morifolium. *Phytochem. Lett*, **6:** 322–325.

van de Laar FA. 2008. Alpha-glucosidase inhibitors in the early treatment of type 2 diabetes. *Vascular Health and Risk Management*, **4:** 1189–1195.

Visweswara RP, Madhavi K, Dhananjaya NM and Gan SH. 2013. Rhinacanthus nasutus improves the levels of liver carbohydrate, protein, glycogen, and liver markers in streptozotocin-induced diabetic rats. *Evid Based Complement Altern Med*; **2013:**1-7.

Li X, Chen W and Chen D. 2013, Protective Effect against Hydroxyl-induced DNA Damage and Antioxidant Activity of Radix Glycyrrhizae (Liquorice Root). *Advanced Pharmaceutical Bulletin*, **3(1):** 167-173

Yang J, Kim JS, Jeong HJ, Kang HH, Cho JC, Yeom HM and Kim MJ. 2011. Determination of antioxidant and α- glucosidase inhibitory activities and luteolin contents of Chrysanthemum morifolium Ramat extracts. *Afr. J. Biotechnol*, **10:** 19197–19202.

JJBS

Volume 14, Number 1, March 2021
ISSN 1995-6673
Pages 105 - 110

Jordan Journal of Biological Sciences

Protective effect of *Ferula hermonis* root extract against cycram-induced DNA, biochemical and testicular damage in rats

Shenouda M. Girgis*, Amira Abd ElRaouf and Halima S. Abdou

Department of Cell Biology, National Research Centre, 33 El-Bohouth St. (former El Tahrir St.) -Dokki, Giza, P.O. 12622, Affiliation ID: 60014618, Egypt

Received May 1, 2020; Revised July 5, 2020; Accepted July 19, 2020

Abstract

Cycram (CYC), or cyclophosphamide is an alkylating drug that has been widely used in the acute treatment of various neoplastic diseases and in the chronic treatment of autoimmune disorders. The major limitation of CYC chemotherapy is the injury of normal tissue, leading to multiple organ toxicity and alter male fertility in mice, rats and human, leading to testicular damage and decreasing in RNA, DNA and protein synthesis. The present study aims to evaluate the protective role of methanol extract of *Ferula hermonis* (FH) against CYC induced changes in testicular RNA, DNA and protein content as well sperm morphology, count and motility, blood levels of testosterone (T) and hemoglobin (Hb) in adult male albino rats. Ninety adult albino male rats were divided into 3 main treated groups (30 animals each) according to treatment periods (15, 30 and 60 days), every one divided to 3 subgroups according to CYC dose (50, 100 and 200 mg/kg bw/day, 10 animals each), and each subgroup divided to 2 sub-sub groups treated with CYC and CYC+ FH 0.025 ml/100 g bw/day by gavage, respectively, (5 animals each), besides the control (10 animals). Animals were sacrificed, sperm morphology with its count and motility, as well RNA, DNA and protein content, and testosterone and hemoglobin levels were determined. The results revealed that CYC treatment induced alterations in RNA, DNA and protein synthesis, as well as affected T and Hb levels and sperm abnormalities of male rats. However, supplementation of FH extract protects these parameters against CYC toxicities. The protective actions of FH extract seem to be closely involved with the suppressing of plasma lipid peroxidation and increasing of antioxidant enzyme activities. Therefore, FH extract might be used in combination with CYC in cancer patients' therapy, transplantation and autoimmune diseases as a protective agent against CYC-induced reproductive toxicity.

Keywords: *Ferula hermonis*, protect, Cycram, DNA, Damage, Testicular, Biochemical, Rats.

1. Introduction

Cycram (CYC) or cyclophosphamide is a cytotoxic alkylating drug that has been widely used in the acute treatment of various neoplastic diseases and in the chronic treatment of autoimmune disorders. The major limitation of CYC chemotherapy is the injury of normal tissue, leading to multiple organ toxicity mainly in the heart, testes and urinary bladder (Fraiser *et al*., 1991; Ghobadi *et a*l., 2017). CYC was reported to alter human fertility and is cytotoxic to rapidly dividing cells, which makes the highly proliferative testes a target for the damaging effects of this drug. Use of CYC for the treatment of cancer in male patients increases the incidence of oligo- and azoospermia and results in male infertility (Howell and Shalet, 1998). Previous studies have demonstrated that chronic administration of CYC to male rats/mice leads to decreased testicular weight, transitory oligospermia, decreased DNA synthesis in spermatogonia and protein synthesis in spermatids (Anderson *et al.*, 1995; Meistrich *et al*., 1995; Kaur *et al*., 1997).

Molecular components of sperm like RNA have the potential to be important indicators of reproductive toxicity. This is especially important for long-term exposures, such as those experienced in chemotherapeutic regimens, in which cytotoxic drugs are often given for months rather than days. Exposures that target germ cells for extended periods of time, as chemotherapy drugs do, may produce changes in the molecular contents of the sperm that can serve as biomarkers of testicular dysfunction (Dere *et al*., 2013). Rats treated with CYC were displayed lowest weight of testicles and epididymis (reproductive organs) and the lowest motility, progression, viability, and sperm count (Shabanian *et al.*, 2017), a decrease in serum hormone levels (testosterone [T], follicle stimulating hormone [FSH], and luteinizing hormone [LH]) (Johari *et al.*, 2011), as well as 20 % reduction in the hemoglobin (Hb) level were found (Cengiz, 2018).

Numerous studies have shown that CYC exposure can disrupt the redox balance of tissues to suggest that biochemical and physiological disturbances may result from oxidative stress (Selvakumar *et al.*, 2004). It is, therefore, important to continue the search for an effective natural compound that will protect against CYC-induced reproductive toxicity associated with chemotherapy. These studies suggest that natural compounds with antioxidative

* Corresponding author e-mail: shenoudag2009@hotmail.com.

** **Abbreviations :** FH: Ferula hermonis; CYC: Cycram; ANOVA: Analysis of variance; T: testosterone; Hb: hemoglobin; FSH: follicle stimulating hormone; LH: luteinizing hormone.

properties may have the potential to ameliorate CYC-mediated testicular injury. In the past decade, the bioactivities of flavonoids on human health have given rise to much attention, especially the antioxidant activity (Zhang, 2005). The protective role of flavonoids involves several mechanisms of action: direct antioxidant effect, inhibition of enzymes of oxygen-reduction pathways and sequestration of transient metal cations (Rice-Evans, 2001).

To prevent these toxic side effects, there is a need for novel agent or natural product such as *Ferula hermonis* (FH) that may protect against CYC-induced reproductive toxicities in male rat. FH is a medicinal plant and a known natural antioxidant that belongs to the apiaceae family and grows abundantly in the Mediterranean region and Middle East (Naguib, 2003; Auzi *et al*., 2008), and used as a tonic, stimulant and aphrodisiac and as an anti-impotency medication for both sexes, as well as increasing the "stamina" of animals. Other traditional uses for FH are cauterizing wounds, curing animal infections and increasing the milk production of cows (Canogullari *et al*., 2009). Ferula hermonis (FH) is reported to have diverse therapeutic effects (Abutaha *et al.*, 2019). Pharmacological reports have revealed that FH has several bioactivities which are useful to treat reproductive dysfunction, menopausal disturbances, neurological disorders (Zanoli *et al*., 2005) and diabetes (Raafat and El-Lakany, 2015). The plant is also reported to have antimicrobial, anti-inflammatory (Saab *et al.*, 2012; Al-Ja'fari *et al.*, 2013), anticancer activities (Saab *et al.*, 2012; Galal *et al.*, 2001) and antioxidant effect due to its flavonoid composition (Abarikwu *et al.*, 2012).

There are a little studies about effects of FH on the reproductive system and sexual appetite. The ethanolic extract of seeds and roots of FH called "masculine" was examined on male fertility and sexual functioning in rats and humans and was exhibits a high level of safety in rats, humans and cultured human fibroblasts and increases erection in rats. In addition; consumption of one tablet of masculine daily for 3 months could increase sperm number and sperm motility in men (Kassisa *et al.*, 2009). In addition, Rajeh and Al-Shehri (2019), found that FH ameliorates sperm count and T serum level due to its antioxidant activity against testicular toxicity in male rats. Another study reported that a single oral dose of FH extract can increase serum T concentration in adult male rat up to three-folds (Gunes and Fetil, 2000).

Therefore, the present study was designed to evaluate the protective effects of FH extract against CYC-induced reproductive toxicities which include sperm morphology, count and motility; RNA, DNA and protein content in rat testes as well measurement of testosterone and hemoglobin levels has been attempted.

2. Materials and Methods

2.1. Animals and treatment

Adult male albino rats (weighing 200–220 g), were obtained from animal house of National Research Centre, Dokki, Cairo, Egypt. They were housed in a standard conditions of temperature (22 ± 2°C), relative humidity (55 ± 10%), and 12/12 h light/dark cycle, and fed with a standard rat feed and water *ad libitum.* The experimental designs and protocols for study conform the requirement of Ethics Committee of our Institute in accordance with the standard guide for the care and use of laboratory animals. Animals were divided into 3 main treated groups (30 animals each) according to treatment periods (15, 30 and 60 days every one divided to 3 subgroups according to CYC dose (50, 100 and 200 mg/kg bw/day, dissolved in distilled water following pretreatment with olive oil by gavage, 10 animals each), and each subgroup divided to 2 sub-sub groups treated with CYC and CYC+ FH (0.025 ml/100 g bw/day dissolved in olive oil by gavage), nd5 animals each, besides the control group (10 animals).

2.2. Drug and chemicals

CYC was purchased from Baxter Oncology GmbH, Frankfurt, Germany. All other chemicals used were of the highest purity and analytical grade.

2.3. The herbal remedy

Roots of FH were obtained from the Experimental Station of Medicinal Plants, Ministry of Agriculture, Cairo, Egypt. Sample extract was obtained by stirring 3 g of dry organ powder with 30 ml of methanol for 24 h at 120 rpm using a magnetic stirrer plate. Extract obtained was kept at 4 °C, filtered through a Whatman filter paper (No. 4) and freed of solvent under reduced pressure at 45 °C using a rotary evaporator. The dried crude concentrated extract was stored at −20 °C until further use for analyses (Rahali *et al*., 2018). Phenolic compounds of plant sample were extracted according to the method outlined by (Duke *et al.*, 2003). The identification of the individual phenolic compounds was performed on high liquid chromatography (JASCO HPLC) (Table 1), using hypersil C18 reversed place column (250x4.6mm) with 5 µ particle size.

The herb was given to the treated animals orally (using oral tube), twice weekly as prescribed by herbalist (0.025 ml/ 100 g bw from plant water extract 50%) prepared in the form of water extract (by soaking in boiled water over night) for 8 successive weeks.

Table 1. HPLC of polyphenols in methanol extract of FH.

Ingredients	mg/100 g
Phenol	30
Resorcinol	670
Protocatchuic acid	340
Catchines	8380
Parahydroxy benzoic	3260
Caffeic acid	420
Daidzin	26
Ferulic acid	880
Coumarine	440
Paracoumaric acid unhydrate	290
Rutin	380
Myricetin	1100
Eugenol	1700
3,5 Dihydroxyisoflavon	1500
Quercedin	220
Caumpherol	3840
Pinostrobin	1810

HPLC= High pressure liquid chromatography. FH= Ferula hormones.

2.4. Sampling

At the end of the specified treatment (2, 4 and 8 weeks), the animals were euthanized by ethyl ether exposure and were killed by decapitation. Blood samples were collected in vials containing heparin. The plasma was separated for analysis of testosterone and hemoglobin using specific kits purchased from Rocky Mountain Diagnostic, Inc. 2139 Chuckwagon Road Suite 20. Colorado Springs, CO 80919, USA. Testis were obtained for RNA, DNA and protein analysis.

2.5. Sperm characteristics

Epididymal sperms were collected for sperm count and motility according to (WHO, 2010). Briefly, sperm count and motility within semen should be assessed as soon as possible after scarification, preferably at 30 minutes, but in any case within 1 hour, to limit the deleterious effects of dehydration, pH or changes in temperature on motility. Mix the semen sample well. Remove an aliquot of semen immediately after mixing, allowing no time for the spermatozoa to settle out of suspension. Remix the semen sample before removing a replicate aliquot. For each replicate, prepare a wet preparation approximately 20 m deep. Wait for the sample to stop drifting (within 60 seconds). Examine the slide with phase-contrast optics at ×200 or × 400 magnifications. Assess approximately 200 spermatozoa per replicate for the percentage of different motile categories.

For the analysis of morphological abnormalities such as head (hook less and banana shape), or abnormal tails (coiled and divided), the standard protocol for sperm morphology assay (Wyrobek *et al.,* 1983) was used. Briefly, after the treatment, the animals were sacrificed by cervical dislocation. Both of the cauda epididymises were dissected out, cut into pieces in 5 mL of saline, filtered, and smears were made. The smears were fixed in methanol and stained with 10 % Giemsa in Sörensen buffer for 10 min. A total of 1000 sperms per animal were scored under a microscope (Olympus CX21®, Japan) with 100x10 magnifications. Sperm head and tail abnormalities were determined as having either normal or abnormal morphology.

2.6. Determination of Nucleic Acids and protein

Nucleic acids (DNA and RNA) were determined using a simplified method for determination of specific DNA and RNA using quantitative PCR and an automatic DNA sequencer (Porcher *et al.*, 1992). Total protein is estimated using commercial kits (Peter, 1968).

2.7. Biochemical investigations

At the end of each experimental period and 24 h after the last dose of protective treatment, rats were sacrificed by cervical decapitation after an overnight fast. Blood was collected after 2, 4 and 8 weeks of treatment, and the separated serum was used for assaying the testosterone (T) level. Serum level of T was measured using an enzyme-linked immunosorbent assay (ELISA) purchased from Rocky Mountain Diagnostic, Inc. 2139 Chuckwagon Road Suite 20. Colorado Springs, CO 80919, USA. Hemoglobin level was determined using specific kits purchased from Crystal Chem, 955 Busse Rd, Elk Grove Village, IL 60007 USA .

2.8. Statistical analysis

The values are expressed as mean ± standard deviation (S.D). Differences between groups were assessed by one-way analysis of variance (ANOVA). Statistical analysis was performed using the SPSS for Windows 9.05 package program. Multiple comparisons were carried out by least significant difference (LSD) test. Significance at P-values <0.001, <0.01 and <0.05 have been considered in the tables.

3. Results

3.1. Effect of CYC and FH extract on RNA, DNA and protein content

The results of the present study revealed that CYC treatment significantly (P <0.01) decreased RNA, DNA and protein content in male rat testes compared to control (Table 2). RNA and DNA levels decreased specially with the high dose (200 mg/kg bw of CYC) for 15 days of treatment up to the largest dose (200 mg /kg bw) for 60 days of treatment, while protein level decreased gradually in a time and dose dependent manner. However, FH administration in combination with CYC ameliorate these levels compared to CYC only treated groups.

Table 2. Effect of CYC and FH extract on RNA, DNA and protein content in rat testes.

Treatment period	Dose	RNA mg/g tissue		DNA mean ± S.D		g/dl protein	
		CYC	CYC+FH	CYC	CYC+ FH	CYC	CYC+ FH
15 days	50	0.336± 0.030	0.403± 0.029	0.478± 0.019	0.491± 0.020	11.289**± 0.692	12.393± 0.690
	100	0.289± 0.015	0.387± 0.015	0.465± 0.013	$0.482^{N.S}$± 0.018	9.341**± 0.672	11.323*± 0.875
	200	0.268± 0.016	0.369± 0.027	0.430**± 0.039	0.474± 0.016	8.014***± 0.216	10.221**± 0.730
30 days	50	0.320± 0.030	0.392± 0.015	0.464*± 0.019	0.488± 0.030	8.745***± 0.565	10.940**± 0.644
	100	0.278± 0.018	0.376± 0.022	0.446**± 0.030	0.470± 0.025	8.035***± 0.190	9.996**± 1.005
	200	0.252± 0.021	0.330± 0.027	0.398± 0.021	0.398± 0.021	7.47***± 0.420	8.168***± 0.488
60 days	50	0.298± 0.007	0.377± 0.024	0.441**± 0.30	0.463± 0.019	8.243***± 0.547	9.168**± 0.488
	100	0.247± 0.014	0.340± 0.030	0.429± 0.034	0.456± 0.038	7.199***± 0.544	8.273***± 0.538
	200	0.230± 0.012	0.292± 0.050	0.379± 0.018	0.436**± 0.037	6.771***± 0.3199	7.917***± 0.323
Control		0.415± 0.617		0.511± 0.018		13.323± 0.757	

Data are presented as means ± SD. * Significant at P≤ 0.05; ** Significant at P ≤ 0.01;

*** Significant at P ≤ 0.001. CYC= Cycram; FH= Ferula hormones.

3.2. Serum testosterone and hemoglobin levels

Table (3) showed that CYC administration caused significant reductions ($P < 0.001$), in serum testosterone (T) level (9.308±0.399) and hemoglobin (9.393±0.505) ($P < 0.001$), when compared with the control group, especially with the high dose of CYC (200 mg/kg bw) and long period treatment (60 days) in a dose and time dependent manner (9.308±0.399 ng/l and 9.393±0.505 g/dl vs. 15.052±0.841and15.813±0.622 for T and Hb levels in treated and control groups, respectively). However, supplementation of FH improved these parameters compared to CYC only treated groups. FH was able to produce marked effects in CYC-treated rats, as demonstrated by the restoration of the levels of serum T and hemoglobin, to almost normal levels when compared with the control group.

Table 3. Effect of CYC and FH extract on serum testosterone and hemoglobin levels in male rats.

Treatments period	Dose	Testosterone hormone (ng/l)		Hemoglobin g/dl	
		CYC	CYC + FH	CYC	CYC + FH
15 days	50	11.776±0.671***	14.372±0.701	12.566± 0.783***	14.872± 0.584
	100	11.462±0.510***	13.668±0.559*	11.593± 0.525***	13.958± 0.867*
	200	11.03±0.424***	13.24±0.567*	10.114***± 0.280	13.017± 0.719**
30 days	50	11.289±0.760***	13.862±0.298*	12.304± 0.651***	14.375± 0.542*
	100	10.346±0.521***	13.526±0.417*	11.359± 0.525***	13.913± 0.655**
	200	10.037±0.292***	12.46±0.515**	9.758± 0.516***	12.755± 0.623**
60 days	50	10.39±0.502***	13.19±0.372**	11.958± 0.893***	13.997± 0.740**
	100	9.734±0.529***	12.728±0.505**	10.662± 0.526***	13.396± 0.543**
	200	9.308±0.399***	12.270±0.830**	9.393± 0.505***	12.708± 0.483**
Control		15.052±0.841		15.813±0.622	

Data are presented as means ± SD. * Significant at P≤ 0.05; ** Significant at P ≤ 0.01;

*** Significant at P ≤ 0.001. CYC= Cycram; FH= Ferula hormones.

3.3. Sperm abnormality in CYC and FH extract treated rats

Sperm abnormality rates in response to various treatments for 8 weeks of treatment are presented in table (4). CYC administration caused statistically significant ($P < 0.01$) increases in tail, head and total abnormality of sperm in comparison with the control group. A significant ($P < 0.01$) decrease in these abnormalities was observed in CYC+ FH groups as compared with alone CYC group. The values of head abnormality were brought near values to control by FH administrations to CYC-treated rats, especially with the low dose of CYC; these administrations could significantly improve this parameter when compared with the alone CYC group.

A significant decrease ($P < 0.01$) in total count and motility was found in CYC treated groups. However, the treatment with FH in combination to CYC ameliorates these parameters compared to alone CYC treated groups and brought these values near to control especially with the low dose of CYC.

Table 4. Sperm abnormality in CYC and FH extract treated rats.

Treatment	Dose	Tail abnormality		Head abnormality		Total Abnormality	Total Count	Motility %
		Divided	Coiled	Without hock	Banana shape			
CYC	50	3.0± 0.581**	2.2± 0.924**	2.0± 0.581**	1.8± 0.924**	9.0± 0.581**	26.522x10^6± 1.476	41.35% ±2.53
	100	3.4± 0.302**	3.0± 0.225**	3.6± 0.789**	2.4± 0.342**	12.4± 0.302**	24.478x10^6± 3.288	39.44% ±3.06
	200	5.0± 0.581**	4.6± 0.140**	4.0± 0.581**	3.2± 0.304**	16.4± 0.140**	22.980x10^6± 1.110	33.59% ±2.75
CYC+ FH	50	1.4± 0.401	1.2± 0.837	1.0± 0.710	0.6± 0.894	4.2± 0.837*	31.124x10^6± 1.755	68.75% ±4.57
	100	2.2± 0.837*	1.6± 0.581*	1.4± 0.140	1.0± 0.707*	6.2± 0.280**	28.100x10^6± 0.945	59.35% ±5.78
	200	3.0± 0.581**	1.2± 0.836	1.6± 0.40*	2.0± 0.837**	7.8± 0.28**	27.85x10^6± 1.069	54.69% ±4.41
Control		0.4± 0.548	0.6± 0.548	0.8± 0.095	0.4± 0.394	2.2± 0.924	32.5 x10^6± 1.714	82.42% ±4.36

Data are presented as means ± SD. * Significant at P≤ 0.05; ** Significant at P ≤ 0.01;

*** Significant at P ≤ 0.001. CYC= Cycram; FH= Ferula hormones.

4. Discussion

The present work was performed to evaluate the protective role of FH against CYC induced changes in testicular RNA, DNA and protein content, sperm morphology, count and motility, as well as blood levels of T and Hb in adult male albino rats. The main findings of this study indicated that CYC induced deleterious effect on these parameters. That is in accordance with those of (Anderson *et al.*, 1995; O'Flaherty *et al.*, 2010; Bujan *et al.*, 2013) who found that administration of CYC leads to decreased RNA, DNA and protein synthesis in male rats/mice.

Oxidative DNA damage is caused by hydroperoxide derivative of CYC through generation of H_2O_2 (Murata *et al.*, 2004). Also, acrolein has been found to interfere with

the tissue antioxidant defense system (Arumugam *et al*., 1997) and produces highly reactive oxygen free-radicals (Mythili *et al.*, 2004) that are mutagenic to mammalian cells (Kawanishi *et al*., 1998). From these studies, it is clear that the administration of a potent and safe antioxidant such as FH extract might reduce CYC-induced reproductive toxicity.

The reduction in T and Hb levels in rats exposed to CYC, especially with the high dose coincides with those of (Motawi *et al*., 2010; Mohammadi *et al*., 2014). The decline in serum T level after CYC treatment in consistent with previous reports, and this decline could be due to CYC-induced membrane lipid peroxidation (Das *et al*., 2002). The decrease in serum T level in CYC-treated rats demonstrates defect in the testis. The decreased level of Hb observed in the CYC-treated group in our study may be due to the interaction of CYC with sulfhydryl-containing proteins and/or testicular Ca^{+2} overload (Selvakumar *et al*., 2006).

The level of abnormalities in sperm morphology, total count and motility in CYC treated rats was high; however, FH administration improved these parameters. That is in line with the results of (Abarikwu *et al*., 2012; Watcho et al., 2019) who found that CYC-treated rats had higher abnormal sperm morphology than the control group. However, the CYC plus Rutin (one of the FH component) treated rats had lower abnormal sperm morphology rates than the CYC-treated rats only ($P < 0.05$).

Our results support those of Ilbey *et al.* (2009), who reported that CYC treatment induced irregular and diminished seminiferous tubules containing a few germ cells counted. As well with Mohammadi *et al*. (2014), who found that spermatogonia, spermatocyte, spermatid and sperm count in seminiferous tubules were decreased significantly in CYC treated rats. These results suggest that CYC inhibits spermatogenesis. The sperm abnormalities observed in CYC-treated rats are a serious problem of reproductive function, since abnormal sperm cannot reach the oviduct after intravaginal ejaculation (Izawa *et al*., 2008)**.**

The positive effects of antioxidants on human health have attracted more attention in recent times. Most of the FH component biological actions seem to be associated with its potency as an antioxidant. Administration of antioxidant FH along with CYC has been shown to prevent the testicular injury and reproductive dysfunction as revealed by restoring the normal level of sperm counts, morphology and motility, DNA, RNA and protein as well T and Hb levels. The protective role of FH involves several mechanisms of action: direct antioxidant effect, inhibition of enzymes of oxygen-reduction pathways and sequestration of transient metal cations (Rice-Evans, 2001).

5. Conclusion

In conclusion, this study suggests that CYC treatment induced a significant alteration in RNA, DNA and protein synthesis and affected T and Hb levels and sperm (morphology and motility) abnormalities of male rats. However, supplementation of FH protects morphological structure of sperms and RNA, DNA, protein content as well blood Hb and T levels against CYC toxicities. These protective actions of FH seem to be closely involved with the suppressing of plasma lipid peroxidation and increasing of antioxidant enzyme activities. Therefore, FH might be considered as an alternative drug in combination with CYC in cancer patients, transplantation and autoimmune diseases to prevent CYC-induced reproductive toxicity in patients receiving CYC chemotherapy.

Competing interests

The authors declare that they have no competing interests.

References

Abarikwu SO, Otuechere CA, Ekor M, Monwuba K and Osobu D. 2012. Rutin Ameliorates Cyclophosphamide-induced Reproductive Toxicity in Male Rats. *Toxicol Int.*, **9(2)**: 207-214.

Abutaha N, Nasr FA, Al-zharani M, Alqahtani AS , Noman OM, Mubarak M, Abdelhabib S and Wadaan MA. 2019. Effects of Hexane Root Extract of Ferula hermonis Boiss. on Human Breast and Colon Cancer Cells: An In Vitro and In Vivo Study. *BioMed Res Int*, Volume **2019**, Article ID 3079895, 12 pages.

Al-Ja'fari A, Vila R, Freixa B, Costa J and Canigueral S. 2013. Antifungal compounds from the rhizome and roots of Ferula hermonis. *Phytother Res.*, **27(6)**: 911-915.

Anderson D, Bishop JB, Garner RC, Ostrosky-Wegman P and Selby PB. 1995. Cyclophosphamide: review of its mutagenicity for an assessment of potential germ cell risks. *Mutat Res.*, **330**: 115-181.

Arumugam N, Sivakumar V, Thanislass J and Devaraj H. 1997. Effects of acrolein on rat liver antioxidant defense system. *Indian J Exp Biol.*, **35**: 1373–1374.

Auzi AA, Gray AI, Salem MM, Badwan AA and Sarker SD. 2008. Feruhermonins A-C: three daucane esters from the seeds of Ferula hermonis (Apiaceae). *J Asian Nat Prod Res.*, **10**: 711-717.

Bujan L, Walschaerts M, Moinard N, Hennebicq S, Saias J and Brugnon F. 2013. Impact of chemotherapy and radiotherapy for testicular germ cell tumors on spermatogenesis and sperm DNA: a multicenter prospective study from the CECOS network. *Fertil Steril.*, **100(3)**: 673-680.

Canogullari S, Baylan M, Copur G and Sahin A. 2009. Effects of dietary Ferula elaeochytris root powder on the growth and reproductive performance of Japanese quail (*Coturnixcoturnix japonica*): it is not recommended in a breeder diet. *Arch Geflugelk.*, **73 (1):** S. 56-60.

Cengiz M. 2018. Hematoprotective effect of boron on cyclophosphamide toxicity in rats. *Cell Mol Biol (Noisy le Grand)*, **64 (5)**: 62-65.

Das UB, Mallick M, Debnath JM and Ghosh D. 2002. Protective effect of ascorbic acid on cyclophosphamide induced testicular gametogenic and androgenic disorders in male rats. *Asian J Androl.*, **4**: 201-207.

Dere E, Anderson LM, Hwang K and Boekelheide K. 2013. Biomarkers of Chemotherapy-Induced Testicular Damage. *Fertil Steril.*, **100(5)**: 1192-1202.

Duke SO, Imando AM, Pace PF, Reddy KM and Semeda KJ. 2003. Isoflavone, glycophosate and amino methyl phosphoric acid levels in seeds of glyphosate treated, glyphosate-resistant soybean. *J Agric Food Chem.*, **51**: 344-350.

Fraiser LH, Kanekel S and Kehrer JP. 1991. Cyclophosphamide toxicity. Characterizing and avoiding the problem. *Drugs*, **42**: 781–795.

Galal AM, Abourashed EA, Ross SA, ElSohly MA, Al-Said MS and El-Feraly FS. 2001. Daucane sesquiterpenes from Ferula hermonis. *J Nat Prod.*, **64(3)**: 399-400.

Ghobadi E, Moloudizargari M, Asghari MH and Abdollahi M. 2017. The mechanisms of cyclophosphamide-induced testicular toxicity and the protective agents. *Expert Opin Drug Metab Toxicol.*, **13(5):** 525-536.

Gunes AT and Fetil E. 2000. Hormones: androgens, antiandrogns, anabolic steroids, estrogens - unapproved uses or indications. *Clin Dermatol.*, **18(1)**: 55-61.

Howell S and Shalet S. 1998. Gonadal damage from chemotherapy and radiotherapy. *Endocrinol Metab Clin North Am.*, **27(4):** 927–943.

Ilbey YO, Ozbek E, Simsek A, Otunctemur A, Cekmen M and Somay A. 2009. Potential chemoprotective effect of melatonin in cyclophosphamide-and cisplatin-induced testicular damage in rats. *Fertil Steril.*, **92**: 1124-1132.

Izawa H, Kohara M, Aizawa K, Suganuma H, Inakuma T and Watanabe G. 2008. Alleviative effects of quercetin and onion on male reproductive toxicity induced by diesel exhaust particles. *Biosci Biotechnol Biochem.*, **72**: 1235-1241.

Johari H, Mahmoudinejad F and Amjad G. 2011. An evaluation of the effect of the hydroalcoholic extract of ginger on the hypothalamus-pituitary-gonadal axis in adult female rats (Rat) treated with cyclophosphamide. *Pejoda.*, **6**: 62-70.

Kassisa E, Fuldera S, Khalilb K, Hadiehc B, Nahhasb F and Saad B. 2009. Efficacy and safety assessments of *ferula assa‐foetida* L., traditionally used in greco‐arab herbal medicine for enhancing male fertility, libido and erectile function. *Open Complement Med J.*, **1**: 102−109.

Kaur F, Sangha GK and Bilaspuri GS. 1997. Cyclophosphamide-induced structural and biochemical changes in testis and epididymidis of rats. *Indian J Exp Biol.*, **35**: 771-775.

Kawanishi M, Matsuda T, Nakayama A, Takebe H, Matsui S and Yagi T. 1998. Molecular analysis of mutations induced by acrolein in human fibroblast cells using supF shuttle vector plasmids. *Mutat Res.*, **417**: 65-73.

Meistrich ML, Parchuri N, Wilson G, Kurdoglu B and Kangasniemi M. 1995. Hormonal protection from cyclophosphmide-induced inactivation of rat stem spermatogonia. *J Androl.*, **16**: 334-341.

Mohammadi F, Nikzad H, Taghizadeh M, Taherian A, Azami-Tameh A, Hosseini SM and Moravveji A. 2014. Protective effect of *Zingiber officinale* extract on rat testis after cyclophosphamide treatment. *Andrologia.*, **46**: 680-686.

Motawi TMK, Sadik NAH and Refaat A. 2010. Cytoprotective effects of DL-alpha-lipoic acid or squalene on cyclophosphamide-induced oxidative injury: An experimental study on rat myocardium, testicles and urinary bladder. *Food Chem Toxicol.*, **48**: 2326-2336.

Murata M, Suzuki T, Midorikawa K, Oikawa S and Kawanishi S. 2004. Oxidative DNA damage induced by a hydroperoxide derivative of cyclophosphamide. *Free Radic Biol Med.*, **37**: 793–802.

Mythili Y, Sudharsan PT, Selvakumar E and Varalakshmi P. 2004. Protective effect of DL-alpha-lipoic acid on cyclophosphamide induced oxidative cardiac injury. *Chem Biol Interact.*, **30**: 13-19.

Naguib YM. 2003. Pharmaceutically active composition extracted from Ferula hermonis and process of its extraction. United States Patent 6623768.

O'Flaherty C, Hales BF, Chan P and Robaire B. 2010. Impact of chemotherapeutics and advanced testicular cancer or Hodgkin lymphoma on sperm deoxyribonucleic acid integrity. *Fertil Steril.*, **94**: 1374–1379.

Peter T. 1968. Protein colorimetric method. *Clinical Chem.*, **14**: 1147-1159.

Porcher C, Malinge MC, Picat C and Grandchamp B. 1992. A simplified method for determination of specific DNA or RNA copy number using quantitative PCR and an automatic DNA sequencer. *Biotechniques*, **13(1)**: 106-114.

Raafat K and El-Lakany A. 2015. Acute and subchronic in-vivo efects of Ferula hermonis L. and Sambucus nigra L. and their potential active isolates in a diabetic mouse model of neuropathic pain. *BMC Complement Altern Med.*, **15:** 257.

Rahali FZ, Kefi S, Rebey IB, Hamdaoui G, Tabart J, Kevers C, Franck T, Mouithys-Mickalad A and Sellami IH. 2018. Phytochemical composition and antioxidant activities of different aerial parts extracts of Ferula communis L. *Plant Biosyst*, DOI: 10.1080/11263504.2018.146169.

Rajeh NA and Al-Shehri AM. 2019. Antioxidant effect of Ferula hormones Boiss on acrylamide induced testicular toxicity in male rats. *Indian J Exp Biol.*, **57**: 139-144.

Rajeh NA, Al-Shehri AM (2019) Antioxidant effect of *Ferula hermonis* Bioss on acrylamide induced testicular toxicity in male rats. *Indian J Exp Biol.*, **57**: 138-144.

Rice-Evans C. 2001. Flavonoid antioxidants: Review. *Curr Med Chem.*, **8(7):** 797-807.

Saab AM, Lampronti I and Borgatti M, et al. 2012. Invitro evaluation of the anti-proliferative activities of the wood essential oils of three Cedrus species against K562 human chronic myelogenous leukaemia cells. *Nat Prod Res.*, **26(23)**: 2227-2231.

Selvakumar E, Prahalathan C, Mythili Y and Varalakshmi P. 2004. Protective effect of DL-alpha-lipoic acid in cyclophosphamide induced oxidative injury in rat testis. *Reprod Toxicol.*, **19(2)**: 163-167.

Selvakumar E, Prahalathan C, Sudharsan PT and Varalakshmi P. 2006. Protective effect of lipoic acid on cyclophosphamide-induced testicular toxicity. *Clin Chim Acta.*, **367 (1–2)**: 114-119.

Shabanain S, Farahbod F, Rafieian M, Ganji F and Adib A. 2017. The effects of Vitamin C on sperm quality parameters in laboratory rats following long-term exposure to cyclophosphamide. *J Adv Pharm Technol Res.*, **8**: 73-79.

Watcho P, Mpeck I, Deeh Defo P, Wankeu-Nya M, Ngadjui E, Bonsou Fozin G, Kamtchouing P and Kamanyi A. 2019. Cyclophosphamide-induced reproductive toxicity: Beneficial effects of Helichrysum odoratissimum (Asteraceae) in male Wistar rats. *J Integ Med.*, **17(5):** 366-373.

World Health Organization. 2010. **WHO laboratory manual for the examination and processing of human semen**. 5th ed., WHO Press, Switzerland.

Wyrobek AJ, Gordon LA, Burkhart JG, Francis MW, Kapp Jr, RW and Letz G. 1983. An evaluation of the mouse sperm morphology test and other sperm tests in nonhuman mammals. A report of the U.S. Environmental Protection Agency Gene-Tox Program. *Mutat Res.*, **115**: 1-72.

Zanoli P, Rivasi M, Zavatti M, Brusiani F, Vezzalini F and Baraldi M. 2005. Activity of single components of Ferula hermonis on male rat sexual behavior. *Int J Impot Res.*, **17(6)**: 513-518.

Zhang YM. 2005. Protective effect of quercetin on aroclor 1254-induced oxidative damage in cultured chicken spermatogonial cells. *Toxicol Sci.*, **88(2)**: 545-550.

JJBS

Volume 14, Number 1, March 2021
ISSN 1995-6673
Pages 111 - 119

Jordan Journal of Biological Sciences

Genetic diversity of seagrass *Thalassia hemprichii* and *Enhalus acoroides* in coastal area of East Java

Hery Purnobasuki*, Sucipto Hariyanto and Putut Rakhmad Purnama

Biology Department, Faculty of Sciences and Technology, Airlangga UniversitySurabaya – INDONESIA

Received Mar 13, 2020; Revised July 19, 2020; Accepted July 25, 2020

Abstract

Seagrass degradation occurring worldwide in the last few decades led scientists and governments to take a role in saving this ecosystem. Seagrass transplantation is a direct action to increase seagrass density or recover damaged seagrass habitats. Regrettably, transplantation does not guarantee the success of coastal restoration. The transplants were not resistant against environmental stress at its new habitats. One factor that should be considered when sourcing plant donor materials is genetic diversity. In this paper, we assessed a donor site, Labuhan Beach, where the seagrass species of *Thalassia hemprichii* and *Enhalus acoroides* occur. RAPD (Random Amplified Polymorphism DNA) was performed to discover polymorphic fragments in order to interprete variation genetic of these species. Genetic diversity of the donor population was compared with the same species inhabiting an undisturbed conservation area (Baluran National Park). The data revealed that genetic diversity (allelic richness) of *T. hemprichii* of Labuhan population (0.19) was higher than the population in Baluran (0.15). Equally, for *E. acoroides* genetic diversity of the Labuhan population (0.21) was higher than at Baluran (0.16; t-test p=0.037). A phylogenetic analysis of the MatK region verified that the seagrass samples taken from Labuhan Beach were indeed *T. hemprichii* and *E. acoroides* based on identity with sequences in the GenBank database. This finding suggested that the seagrass population in Labuhan could be used as donor material; however, geographic distance and differing environmental conditions must also be considered.

Keywords: polymorphic, seagrass, transplantation, RAPD, MatK, Labuhan, Baluran.

1. Introduction

Seagrasses are seashore vegetation inhabiting in marine environment area on a wide-ranged substrate content of mud, sand, clay, gravel, or a mixture of them. In general, seagrass is known to have an essential role in aspects of coastal biodiversity, economic function, and the provision of environmental services for coastal ecosystems (Spalding *et al*., 2003). Ecosystem formed by seagrasses is as a habitat provider for coastal organisms, reducing waves of sea, stabilizing sediments, introducing oxygen into water bodies, providing sources of nitrogen, phosphorus in the food chain, also contributing to the supply of organic carbon in significant quantities (Beck *et al*., 2001; Duffy, 2006).

Unfortunately, seagrass habitat is one of the unfavorable habitats on this global ecosystem (Waycott *et al*., 2009; Short *et al*., 2011). The rate of decline in seagrass beds has been estimated at 7% per year since 1990, an alarming rate compared to coral reefs, mangroves, and tropical rain forests (Waycott *et al*., 2009). Environmental changes in Indonesia impact to wide degradation of seagrass, especially due to human activities disturbances such as building development, tourism activity, polluted runoff and mining (Riani *et al*., 2012). One of the efforts to conserve seagrass habitat is seagrass transplantation and restoration. This method has been tried in various types of seagrasses and planted at multiple depths (van Katwijk *et al*. 2009). Many environmental projects and various improvement schemes have been conducted as mitigation effort for seagrass losses. In Indonesia, restoration programs for seagrass have been developed (Riani *et al*., 2012). Seagrass transplantation has been attempted in species *Enhalus acoroides* at Ambon (Irawan, 2017) and Bintan (Harnianti *et al*., 2017) as well as *Thalassia hemprichii* at Jepara (Wulandari *et al*., 2013) and Bintan (Seprianti *et al*., 2017). To improve this condition, therefore, projects of transplantation have been conducted successfully just only for few seagrass species and, at some locations, have no success to outstandingly recover seagrass meadows (Paling *et al*., 2009). Stress associated with transplantation such as transplant shock and environmental changes induced a loss of shoot in the early stage of the transplantation period (Hughes and Stachowicz, 2004). Hence, seagrass transplantion must have the good opportunity and adaptation capability to face the changing conditions in the future (Kettenring *et al*., 2014).

* Corresponding author e-mail: hery-p@fst.unair.ac.id.

** **Abbreviation:** N: Number of amplification band, P: Number of polymorphic band, %: Percentage of polymorphic band, Na: Number of Observed Allele, Ne: Number of Effective Allele, Nm: Gene Flow, Gst: Genetic differentiation between Population, H: Heterozygosity / Ne'i Genetic diversity, Ht: Total population heterozygosity, Hs: Value of Heterozygosity in the Population, I: Shannon's Information index.

Genetic diversity is an essential aspect of ensuring the resilience of transplants in adapting to environmental changes. Genetic evaluation and genotypes identification of population variations have important role to genetic protection and plant breeding programs (Tahir *et al*, 2018). Procaccini and Piazzi (2001) explained that the increase in heterozygosity in donor plant populations was positively correlated with the success of *Posidonia oceanica* seagrass transplants. Furthermore, the similarity in the level of genetic diversity is also significantly associated with the growth and reproduction rate of seagrass *Posidonia australis* and *Zostera marina* (Williams, 2001; Sinclair *et al*., 2013).

T. hemprichii and *E. acoroides* seagrasses are described from Indonesia coast (Purnama *et al*., 2019). *T. hemprichii* is a dominant species for meadow-forming on sediments associated with coral reefs. This species is recognized by ribbon-like and curved leaves, up to 40 cm long often with tannin cells that prominent look red, purple or dark brown. The stem is short and erect, bearing 2-6 leaves. The rhizome is thick and covered with triangular-shaped leaf scars (Waycott *et al*., 2004; El Shaffai, 2011). While *E. acoroides* are considered to be the most extensive tropical seagrass species, leaf lamina is like a ribbon and has a length of up to 200 cm and a width of almost 2 cm. This species can be identified by the specific character such as sickle-shaped leaves, the tips of leaf are usually rounded and smooth. The leaves may appear colors spot due to tannin cells that appear red, purple or dark brown. The leaves of this species develop directly from the rhizome. The rhizome is covered in thick, usually, dark-colored bristles that are the persistent remains of the leaves. The rhizome is around 1.5 cm in diameter with numerous pale-colored roots (Waycott *et al*., 2004; El Shaffai, 2011). These seagrass species were also found in the coastal area of Labuhan Beach, Lamongan (Purnama *et al.,* 2018,). Otherwise, the high human activity on Labuhan Beach fishing activities, shellfish collection and the entry of domestic waste through rivers, is thought to have an anthropogenic impact on the seagrass population of seagrass population there. On the other hand, the seagrass population on Labuhan Beach looks quite dense even though it is outside the conservation area. This unique phenomenon is considered to be suspected as the genotypic diversity of seagrass populations, which depends on age, maturity of the meadows ecosystem, and the spatial structure (Reusch *et al*., 2000).

Random Amplified Polymorphic DNA (RAPD) is a popular molecular marker for detecting genetic diversity of plants at interspecific and intraspecific levels (Arif *et al*., 2010; Rawashdeh, 2011; Priya *et al*., 2005). A genetic marker was used also as tools of identification of varieties of plants (Zhao, et al., 2011). This RAPD marker has also succeeded in uncovering a decrease in genetic diversity of *Posidonia oceanica* due to anthropogenic disturbance in the Mediterranean Sea region (Micheli *et al*., 2005). The marker could show genetic and clonal diversity among the population (Reusch, 2001).

In this paper, we notice genetic diversity among the population of two species of seagrass T. hemprichii and E. acoroides in 2 different locations, Labuhan Beach (representing the area near the port) and the Bama Coast of Baluran National Park (represents a conservation area). This finding is comparison data of the genetic diversity of the same species in those different location. Another popular barcode, Matk region, also performed to dig up the presence of nucleotide polymorphism in two different habitats and to verify the identity of these two seagrass species. We also compare the environmental parameters such as sediment and seawater in both habitats. Finally, this finding can later be used to consider the feasibility of seagrass in Labuhan Beach as a donor site for a transplantation project.

2. Materials and Methods

A total of 20 individual seagrass samples from two localities were collected in May-June 2019. Sampling was carried out in Labuhan Coastal waters in Lamongan (6°52'40.8"S 112°12'50.5"E) and Bama Coastal Waters of Baluran National Park (7°50'39.8"S 114°27'39.8"E) province of East Java, Indonesia (Figure 1). At each location, five individuals of *T. hemprichii* and *E. acoroides* (taxonomy identification refer to den Hartog and Kuo, 2006) were taken from different patches within > 10 meters from each other to avoid samples from the same clone. All plants that have already collected then were rinsed carefully with fresh water in order to remove detritus and attached epiphytic algae. Each of primordial leaf from shoot was dried with silica gel and then preserved at the cold condition. The genetic diversity of seagrass samples were analyzed by RAPD-PCR analysis for the molecular data in the Laboratory of Molecular Genetics, Department of Biology Airlangga University. Whereas the sediment and seawater samples were analyzed and observed in the Laboratory of Environmental and Ecology, Department of Biology Airlangga University for environmental condition data.

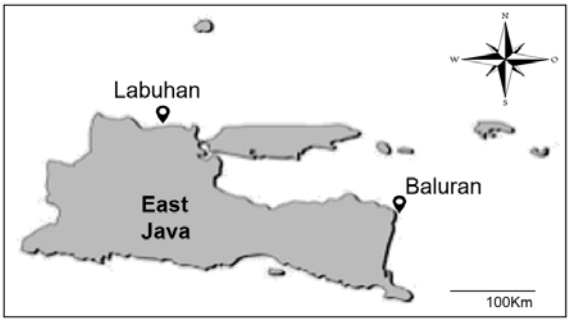

Figure 1. Map of sampling set location. Labuhan Beach and Baluran National Park.

The frozen leaves from the samples were crushed and mashed using a mortar and pestle. The genomic DNA from this leaves was extracted and analyzed using the Plant Genomic DNA Kit (New sera-Xtracta) refer to the protocols of DNA extraction.

The RAPD process was carried out using 25 ng DNA sample templates and using a two × GoTaq Green Mastermix (Promega) with a total reaction volume of 20 µl. A total of six RAPD primers were used in this study UBC127 (5'-ATCTGGCAGC-3'), OPA2(5'-TGCCGAGCTG-3 '), OPA4 (5'- AATCGGGCTG-3'), OPB12 (5'- CCTTGACGCA-3 '), OPD11 (5'-TGCCCGTCGT-3'), and OPH6 (5'- ACGCATCGCA- 3) 3 '). The PCR cycle was carried out by initiating denaturation at 95 ° C for 1 minute, followed by 38 cycles with 1 minute at 94 ° C, 1 minute at 37 ° C and 1.5

minutes at 72 ° C, and followed by a final extension of 10 minutes at 72 ° C.The PCR product from RAPD was visualized using 1.5% agarose gel in the 0.5x TBE buffer, while the MatK gene PCR product was visualized using 1% agarose gel in the 0.5x TBE buffer. A 100 bp DNA marker (Promega) was used on each of the electrophoretic gels.

MatK barcode amplification was performed using P646 5'-TAATTTACGATCAATTCATTC-3 'primer pairs and P647 5′-GTTCTAGCACAAGAAAGTCG-3 ′ (Lucas et al., 2012). The Cycle PCR used to amplify the Matk gene was 95 ° C for 5 minutes and followed by 35 cycles of 95 ° C for 1 minute, 54 ° C for 2 minutes, and 72 ° C for 2 minutes. The final extension was carried out at 72 ° C for 7 minutes. DNA sequences from the P646 primary strand Forward were carried out using Macrogen Inc. sequencing facilities (South Korea). The phylogenetic tree was generated by MEGA 7 using the Neighbor-Joining method.

Electropherograms were made manually by converting them into binary matrices that reflect the presence (1) and absence (0) of the allele. The matrix was tested using POPGENE 3.2 software.

Chemical and physical parameters of sediments are carried out to ammonium, phosphate, carbon, and size of sediment. Meanwhile, seawater samples are measured for mperature, salinity, turbidity, TDS, pH, hardness, heavy metals, and organic matters.

3. Results

As seen in Figure 2 that all primers can be well amplified on the *T. hemprichii* sample and generated a variety number of the band in both populations. Primer UBC 127 (Fig.2F) produced the most bands in *T. hemprichii,* which are 17 bands ranged from 300 bp up to 1500 bp. OPA2, OPA4, and OPB12 primers produce the same number of amplification bands by 12 bands (Fig2A-B-E). They were followed by OPD 11 by ten bands (Fig. 3D). Moreover, primer OPH 6 only produced five bands (Fig.2C).

Primer OPA2, OBP12 and UBC127 generated the same number of amplification band by 15 bands (Fig. 3A-E-F) Then, primer OPD11 and OPH6 produced 13 and 4 bands (Fig. 3D-C). The least produced primer was OPA 4, which produced only four bands (Fig. 3B). Moreover, consider to the least producing bands in this study, it shows that seagrass *E. acoroides* has a smaller number of locus then *T. hemprichii.*

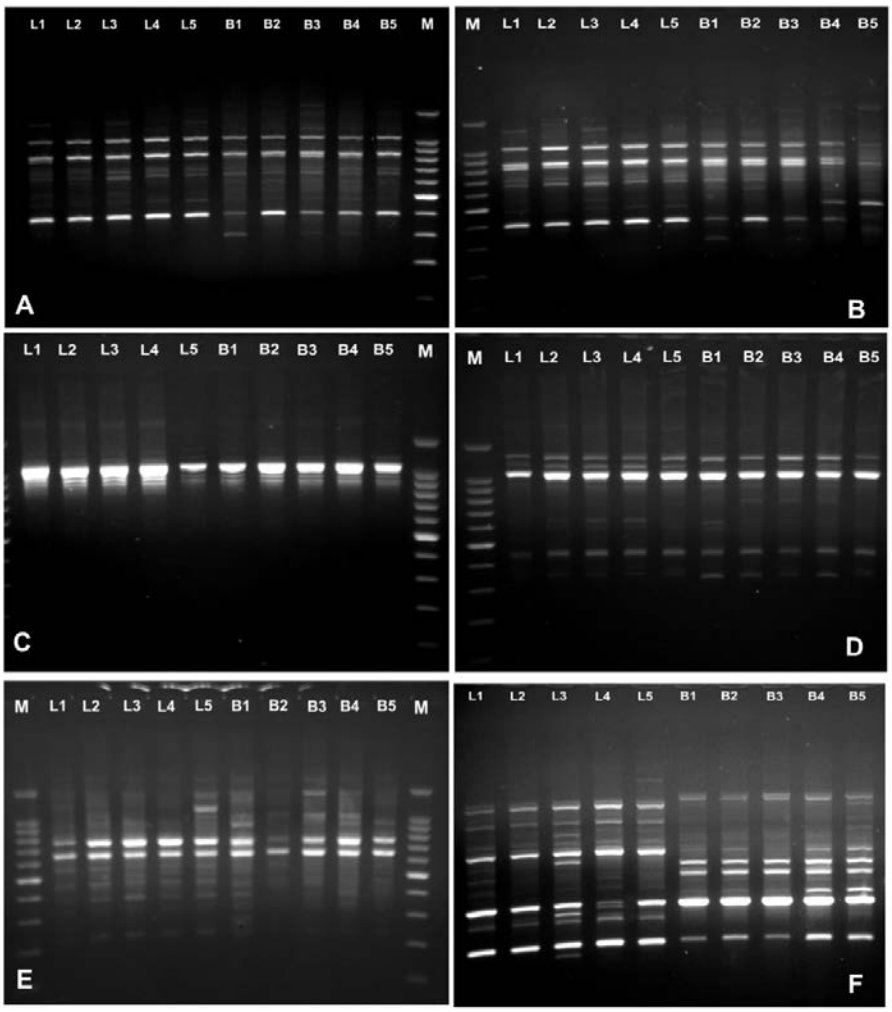

Figure 2. RAPD result from *T. hemprichii* using six primers. A. OPA2; B.OPA 4; C.OPH 6; D. OPD 11; E. OPB 12; F. UBC 127.

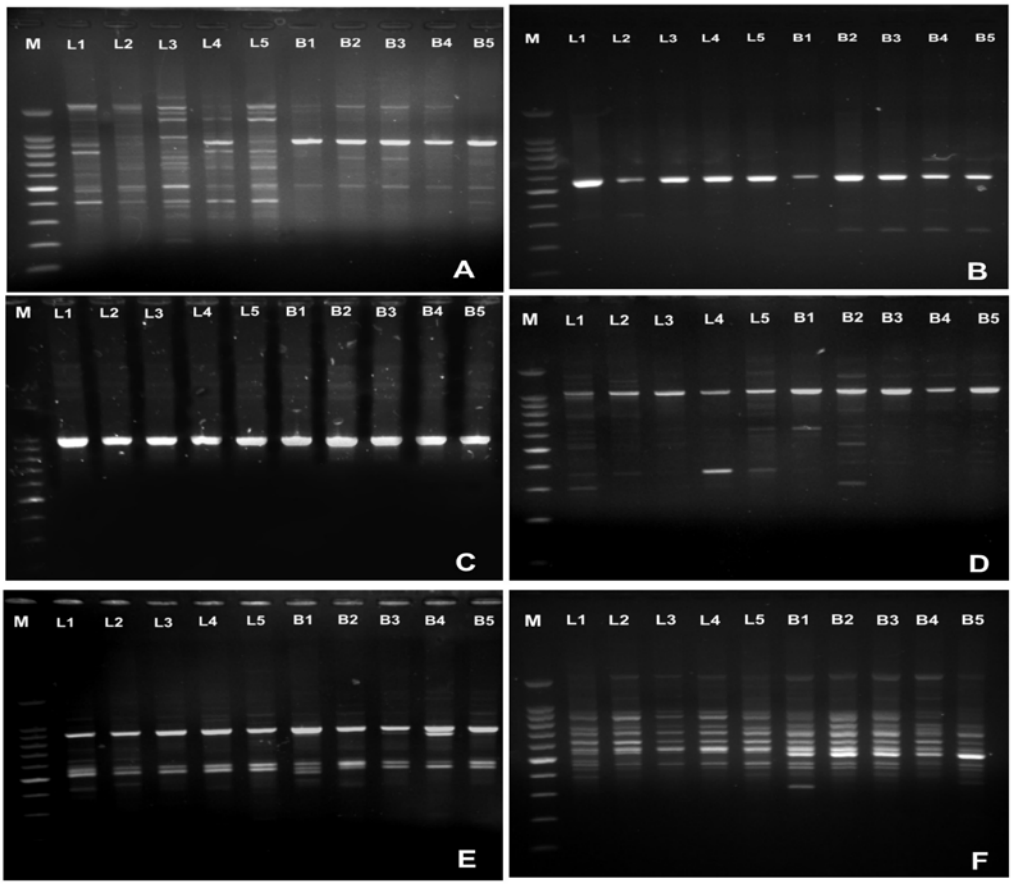

Figure 3. RAPD results from *E. Acoroides* using six primers. A. OPA2; B.OPA 4; C.OPH 6; D. OPD 11; E. OPB 12; F. UBC 127.

Table 1. Genetic diversity of *T. hemprichii* and *E. acoroides* population in Labuhan Beach and Baluran National Park.

Population	N	P	%	Na	Ne	H	I	Ht	Hs	Gst	Nm
Thalassia hemprichii											
Labuhan	68	35	51.47	1.5147	1.3266	0.1864	0.2772	0.1864	0.1864		
Baluran	68	29	42.65	1.4265	1.2683	0.1546	0.2302	0.1546	0.1546		
	68	**52**	**76.47**	**1.7647**	**1.4371**	**0.2585**	**0.3897**	**0.2585**	**0.1705**	**0.3405**	**0.9682**
Enhalus acoroides											
Labuhan	65	39	60.00	1.6000	1.3653	0.2116	0.3168	0.2116	0.2116		
Baluran	65	30	46.15	1.4615	1.2575	0.1550	0.2354	0.1550	0.1550		
	65	**50**	**76.92**	**1.7692**	**1.3882**	**0.2377**	**0.3657**	**0.2377**	**0.1833**	**0.2290**	**1.6831**

The seagrass population in Labuhan has a more extensive number of polymorphic bands and a percentage of the polymorphic band than the population in Baluran (Table 1). Other genetic parameters such as number of effective alleles, number of observed alleles, heterozygosity or Ne'i genetic diversity, total population heterozygosity, Shannon's information index, and value of heterozygosity in the population show the same condition in both seagrass species. Furthermore, genetic differentiation between the population of *T. hemprichii* is higher than the population of *E. acoroides*. In contrast, the population of *T. hemprichii* has fewer gene flow value than the population of *E. acoroides*.

Phylogenetic analysis from MatK barcode describes that species of *T. hemprichii* and *E. acoroides* taken from both locations. They are identically similar to the same species in the GenBank database (Fig.4). The barcoding analysis show that the identity of the seagrass sample from sampling locations are suitable. It also shows that the seagrass species from the different population was identic based on data in MatK region. Figure 4 also compares our sample to other seagrass species based on MatK sequence. *E. acoroides*, *T. hemprichii* together with *Halophila* spp. are clustered from single root Family Hydrocharitaceae. This data revealed that the samples of species are separated from other clusters from family Zosteraceae, Posidoniaceae, and Cymodoceae based on various seagrass accession numbers from GenBank.

The Nei genetic diversity (H) of the *T. hemprichii* population in Labuhan was slightly higher than the population in Baluran (t-test, $p = 0.173$). While the Ne'i genetic diversity of *E. acoroides* population in Labuhan was remarkably higher than the population in Baluran (t-test, $p = 0.036$); this finding indicated that the genetic differentiation in both populations was low rate.

The chemical-physical parameters of the environment are divided into sediment and seawater. The results of observing sediment parameters are in Table 2 below.

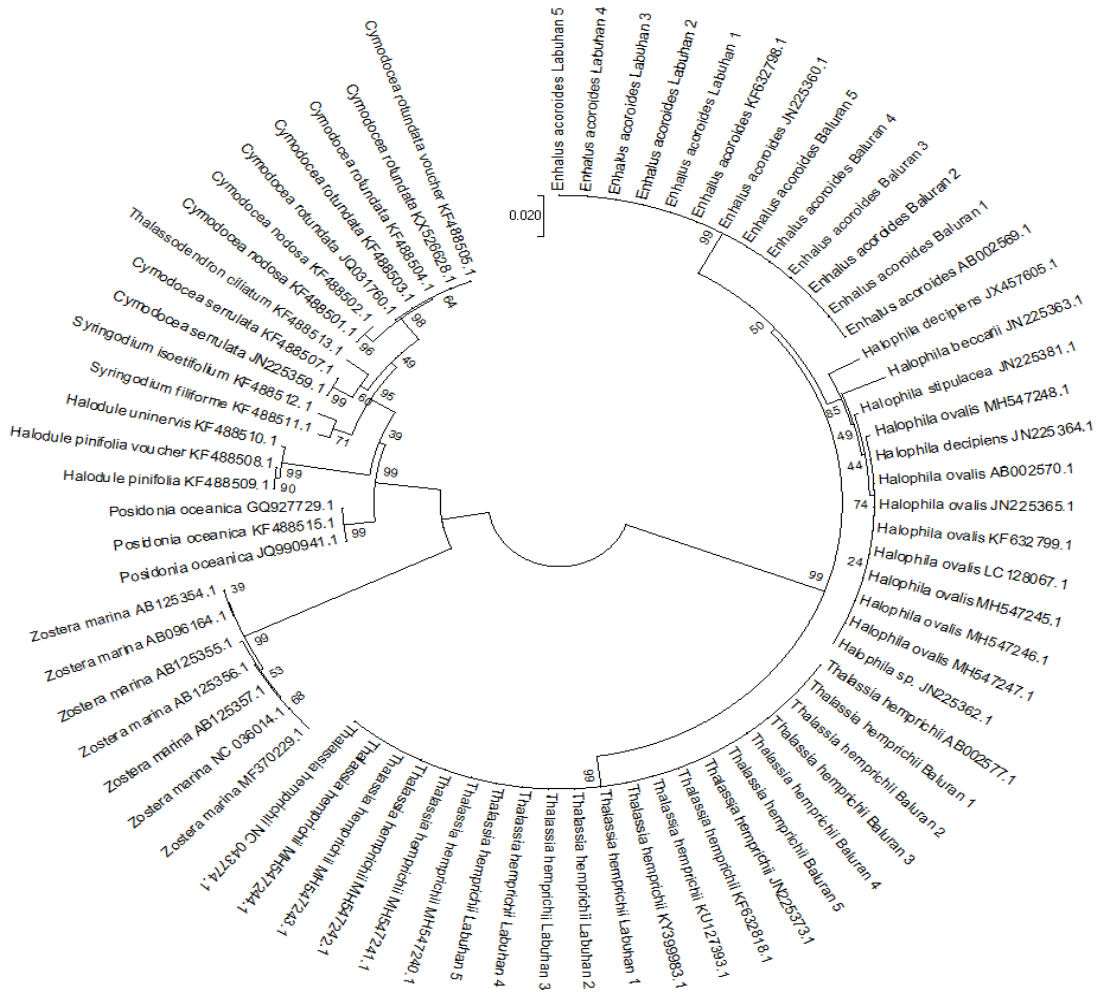

Figure 4. Phenogram of MatK region of the population of *T. hemprichii* and *E. acoroides* taken from two different sampling sites compared with various seagrass accession numbers from GenBank. The number in each branch indicated the percent of data coverage for internal nodes.

Table 2. The results of chemical-physical analysis from sediment of Labuhan and Baluran waters

		Locations	
Parameters	Units	Labuhan	Baluran
NH_3-N	%	0.057	0.087
P_2O_5	%	0.246	0.510
Carbon (C)	%	1.170	1.980
Gravel	%	0.14	13.70
Sand	%	60.94	84.74
Silt and Clay	%	38.92	1.56

Table 3. Result of chemical-physical analysis of seawater in Labuhan and Baluran waters

Parameters	Units	Locations	
		Labuhan	Baluran
Temperature	°C	28	26
Salinity	‰	34.5	35.1
Odour	-	No Odour	No Odour
TDS	mg/L	31078	31758
Turbidity	FTU	40.65	18.41
Colour	PtCo	0.38	0.06
pH	-	8.42	7.58
Hardness ($CaCO_3$)	mg/L	1870.36	2053.99
Iron (Fe)	mg/L	0.024	0.024
Fluoride (F)	mg/L	5.08	1.20
Cadmium (Cd)	mg/L	0.124	0.146
Chloride (Cl^-)	mg/L	17976.42	17140.68
Chromium (Cr_6^+)	mg/L	0.086	0.058
Manganese (Mn)	mg/L	0.133	0.132
Nitrate (NO_3^-)	mg/L	0.260	0.000
Nitrite (NO_2^-)	mg/L	0.000	0.000
Zinc (Zn)	mg/L	3.832	3.364
Cyanide (CN)	mg/L	0.000	0.000
Sulphate (SO4)	mg/L	2605.68	2736.66
Lead (Pb)	mg/L	1.537	0.159
Detergent (LAS)	mg/L	0.031	0.028
Potassium Permanganate (KMnO4)	mg/L	45.51	36.66

Based on Table 2, it can be seen that the nutrient content represented by the elements nitrogen, phosphate, and carbon shows that the sediments of Baluran waters are more abundant than Labuhan sediments. The sediment type of the two regions is dominated by sand substrates. However, the second-highest proportion of Labuhan sediments is in the form of silt and clay(38.92%), while in Baluran sediments is gravel (13.70%). The least proportion sediment of Labuhan is gravel (0.14%), while in Baluran it is silt and clay (1.56%).

The results of the analysis of seawater parameters in both regions was presented in Table 3. Labuhan waters temperature measured at the same time range shows higher results than Baluran waters, whereas salinity of seawater in Baluran has higher salt content. Seawater in Labuhan tends to be more turbid and has a higher pH, but the value is lower than Baluran waters. Some chemical materials such as fluoride, chloride, chromium, manganese, nitrate, zinc, detergent, and organic substances in the form of $KMnO_4$ in Labuhan waters are higher than Baluran, but not in cadmium, lead, and sulphate content. While the parameter data of iron, cyanide, and nitrite, both pools showed the same results.

4. Discussions

The genetic attribute of seagrass populations represented the relations of various progressions including a long-term changes related to species evolution (habitat fragmentation, population isolation, and shifts in distribution), gene flow, genetic drift, mutation, selection, and mating system (Slatkin, 1987; Schaal *et al*., 1998). In the present research RAPD survey of the two populations of tropical seagrass *E. acoroides* and *T. hemprichii* revealed that these seagrasses have a wide range of clonal diversity.

Four primers (OPA2, OPD 11, OPB 12, and UBC 127) are considered to be a potential marker to produce constant polymorphic bands pattern, clearness, amplification, and then used for further analysis for all samples. The other two primers (OPA4 and OPH6) did not well perform in the seagrass sample, especially in the DNA template extracted from *E. acoroides*, which provided a low number of PCR fragments. The DNA fragment was determined as polymorphic when some of them are available; however, it missing in different samples. Polymorphisms of RAPD markers are well-known and widely performed in population genetic research (Yang and Quiros, 1995).

Both *T. hemprichii* and *E. acoroides* of the Labuhan population have higher polymorphic fragments as well as the number of observed alleles than the Baluran population. It indicated that the seagrass population in Labuhan has high genetic variation. The Nei genetic diversity (H) of the *T. hemprichii* population in Labuhan was slightly higher than the population in Baluran (t-test, $p = 0.173$). While the Ne'i genetic diversity of *E. acoroides* population in Labuhan was remarkably higher than the population in Baluran (t-test, $p = 0.036$), this finding indicated that in both populations there is a low rate of genetic differentiation. The low rate of genetic differentiation in RAPD analysis has a higher tolerance of mutation due to RAPD amplification performed both in coding and non-coding region (Williams *et al*., 1990).

Genetic differentiation between populations (Gst) explains the proportion of genetic diversity in the entire population of each species. The Gst value of the *T. hemprichii* population was 0.3405, indicating 34% of total genetic variation was in the entire population, and 66% of total genetic variation was in each population, whereas the Gst value of *E. acoroides* was slightly fewer than *T. hemprichii* which is 0.229. So that 23% of total genetic variation represent in the entire population of two species. While 77% of total genetic variation was in each population of species.

Pharmawati *et al*. (2015) noted the number of observed heterozygosity of *E. acoroides* seagrass in Pramuka Island, Lembongan Island and Waigeo Island was 0.767; 0.436 and 0.582, respectively. That study employed five different primer pairs (Eaco1, Eaco9, Eaco19, Eaco51, Eaco55). Another study of *E. acoroides* in Aceh, Riau, Bangka Belitung, SeribuIsland, Banten, and Central Java, found the observed heterozygosity was 0.111-0.852 (Putra et al., 2018). Genetic diversity of *T. hemprichii* population in Indonesia also reported in a variety of Ne'i genetic diversity value range 0.184-0.534 (Hernawan, 2016).

Gene flow (Nm) of *E. acoroides* populations (1.6831**)** was higher than the population of *T. hemprichii* (0.9682). The genetic structure of marine organisms in Indonesia

coastal area is also influenced by oceanic condition such as ocean current of the Java Sea (Lind, 2009). Fruits of *E. acoroides* have capability to float for up to 10.2 days (Lacap *et al*., 2002) and have wide-distance dispersal (>1,000 km; Nakajima *et al*., 2017) while fruits of *T. hemprichii* stop floating after the fourth day (Wu *et al*., 2016). This finding suggested the increase in gene flow of *E. acoroides* between locations.

Seagrasses in favourable habitat inclined the genetic diversity (Larkin *et al*., 2006). In contrast, the present study revealed that both population seagrass of *E. acoroides* and *T. hemprichii* in the conservation area (Baluran National Park) has lower genetic diversity than the population in a disturbed area. This finding agrees with Putra *et al*. (2018) indicated that the population of E. acoroides with the lowest heterozygosity also found in the undisturbed area such as conservation area. A potential indicator of inbreeding through clonal reproduction can be shown by the excess of homozygosity. Small populations of organism can also multiply inbreeding and decrease genetic variation due to initiator impacts, deleterious mutations, and genetic drift which cause detrimental effects to genetic diversity (Procaccini *et al*. 2007. All those adverse effects reduce the fitness of the seagrass populations to ajust to environmental changes and lead them to extinction (Spielman *et al*., 2004; Leimu *et al*. 2006).

In this study, some immature fruit of *E. Acoroides* are found in the male and female flower of *T. hemprichii* during the sampling period (May-June) in Labuhan beach. Whereas, in the Baluran site, we only found male and female fruit of *T. hemprichii* and no reproductive organ of *E. acoroides* found there. This finding suggested that both generative and vegetative reproduction occur in Labuhan. Restricted flowering frequency and high-level inbreeding in the Baluran populations was one of the factors that influencing low clonal diversity. A complex combination of vegetative and generative reproduction support seagrass populations survives in fluctuate environmental conditions (Arriesgado *et al*., 2015).

Phylogenetic analysis of MatK barcode shows identical sequence among seagrass population in Labuhan, the population in Baluran, and sequence database obtained from GenBank. The sequence of MatK barcode of *E. acoroides* from both populations is identically similar to Enhalus acoroides AB002569.1; JN225360.1; KF632798.1. The MatK sequences of *T. hemprichii* from both populations is identically the same with *T. hemprichii* JN225373.1; KF632818.1; KF632818.1; KF632818.1; KF632818.1; KF632818.1; KF632818.1; KF632818.1; KF632818.1; KF632818.1. Another seagrass from Family Hydrocharitaceae *Halophila* spp. is closer to *E. acoroides* then *T. hemprichii*. It can be seen in Figure 4, E. acoroides and Halophila spp. are clustered in one group. The same result was also reported by Tanaka *et al*. (1997) that put genus *Enhalus* and *Halophila* in one branch based on the MatK region. However, in different barcode region, RbcL, genus *Enhalus* is closer to *Thalassia* instead of Halophila. Furthermore, using a combined barcode with a matrix of 2388bp MatK and RbcL, genus of Enhalus and Thalassia were put in one branch (Tanaka *et al*. 1997). In the marine area, one of the largest families of aquatic angiosperms is Hydrocharitaceae, with a total of 135 known species of 16 known genera. The member of Hydrocharitaceae including both freshwater and marine aquatics (Christenhusz and Byng, 2016). Seagrasses themselves are regarded as an ecological group, not a taxonomical group. This condition indicates that many seagrass family members do not necessarily show a closely related relationship. Others seagrass families are Cymodoceae, Zosteraceae and Posidoniaceae (den Hartog and Kuo, 2006).

Seagrasses are a sensitive indicator of environmental changes especially in sediment loading, water quality, and other changes of ecosystem (Dennison *et al*. 1993). Water quality is potentially degraded due to some environmental quality degradation (Ruiz *et al*., 2001). The present study revealed different conditions in which sediments of undisturbed areas (Baluran) have a higher level of nutrient (ammonium, phosphate, and carbon). Run-off water from estuaries nearby suggested did not bring many nutrients to the coastal region. The high proportion of silt and clay of Labuhan sediment associated to the high level of turbidity in the water environment. While the different constituent elements of sediment of Labuhan and Baluran was contributed by fluctuate environmental condition. It seemed that both seagrass species were adaptable to a widerange of substrate types.

The most polymorphic donor material leads to increase in the genetic diversity of transplanted seagrass. It can be beneficial for transplantation achievement (Williams, 2001). Nevertheless, reducing the effects of restoration and improvement strategies on local gene pool is vital because of transplanting plants collected from far range of locations (Williams and Davis, 1996). Management and science-based protection approach supporting a consensus planning and legal authorities must be considered to minimize the effect of environmental stressors and put up wide range of effects on seagrass beds to protect these plants from fatal damage (Coles and Fortes, 2001; Kenworthy *et al*., 2006).

Another benefit of genotype diversity for ecosystems is supports stability of environmental and is also related to morphological plasticity of plants (Williams and Heck, 2001; Lewontin 1964). Increase of shoot density was beneficial for epiphytic invertebrates or other epifaunal organisms to refuge against a predator (Williams and Heck, 2001). Procaccini and Piazzi (2001) also reported that seagrass rhizome with higher elongation and ramification value was obtained from the population with higher genetic polymorphism. Thus, a high density of seagrass not only provides high productivity of the tidal zone but also serves as carbon sequestration, especially for *E. acoroides* and moreover, reduced impact of climate changes (Williams, 2001).

5. Conclusion

Seagrass *T. hemprichii* and *E. acoroides* were identified and verified, and they inhabited in Labuhan Beach, Lamongan Regency. Even though inhabiting anunfavorable area, the population of seagrass in Labuhan Beach provides high genetic diversity. The astonishing result indicates that genetic diversity of seagrass population in Labuhan is higher than in Baluran National Park, which is a conserved region. Therefore, the population of seagrasses in Labuhan beach is ideal to be a donor material for coastal restoration. Nonetheless, the

sourcing ecosystem should be kept maintained for the sustainability of seagrass ecosystem.

Acknowledgement

PUF Grant Research program from FST Airlangga University. Ir. Bambang Sukendro, M.M as Head of Baluran National Park and Setyo Hutomo,S.H., M.Si as Head of Region III KSDA Jember for permission to study in the conservation area and take the samples for this study.

Conflict of interest

The Authors declare that there is no conflict of interest with this work and the preparation of the manuscript.

References

Arif IA, Bakir MA, Khan HA, Al Farhan AH, Al Homaidan AA, Bahkali AH, Al Sadoon M and Shobrak M. 2010. Application of RAPD for molecular characterization of plant species of medicinal value from an arid environment. *Genet Mol Res.,* **9**: 2191-9198

Arriesgado DM, Kurokochi H, Nakajima Y, Matsuki Y, Uy W H, Fortes MD, Nadaoka L, Campos WL and Lian C. 2015. Genetic diversity and structure of the tropical seagrass *Cymodocea serrulata* spanning its central diversity hotspot and range edge. *Aqua Ecol.,* **49**(3): 357-372.

Beck MW, Heck KL, Ablem KW and Childers DL. 2001. The identification, conservation, and management of estuarine and marine nurseries for fish and invertebrates. *Bios.,* **51**: 633−641

Christenhusz MJ and Byng JW. 2016. The number of known plant species in the world and its annual increase. *Phytotaxa*, **261**: 201-217.

Coles R and Fortes M. 2001. Protecting seagrass- approaches, and methods. In. Short, F. T., and Coles, R. G. (Eds). *Global Seagrass Research Methods* (Vol. 33). Elsevier.

den Hartog C and Kuo J. 2006. Taxonomy and Biogeography of Seagrasses. In Larkum, A. W., Orth, R. J., and Duarte, C. M. (Eds). *Seagrasses: Biology, Ecology, and Conservation* (p. 1-23). Dordrecht, The Netherlands: Springer.

Dennison WC, Orth RJ, Moore KA, Carter V, Kollar S, Bergstrom PW and Batiuk RA. 1993. Assessing water quality with submersed aquatic vegetation. *BioScience*, **43:** 86-95.

Duffy JE .2006. Biodiversity and the functioning of seagrass ecosystems. *Mar Ecol Prog Ser* **311**: 233−250

El Shaffai A. 2011. Field guide to seagrasses of the Red Sea. *IUCN, Gland, Switzerland and Total Foundation, Courbevoie,* France.

Harnianti N, Karlina I and Irawan H. 2017. Laju pertumbuhan jenis lamun *Enhalus acoroides* dengan teknik transplantasi polybag dan Sprig Anchor pada jumlah tunas yang berbeda dalam rimpang di perairan Bintan. *Intek Akua.,* **1**: 15-26.

Hernawan UE. 2016. Gene flow and genetic structure of the seagrass *Thalassia hemprichii* in the Indo-Australian Archipelago. Edith Cowan University, Australia (Ph.D. Thesis).

Hughes AR and Stachowicz, J. J. 2004. Genetic diversity enhances the resistance of a seagrass ecosystem to disturbance. *Proceedings of the National Academy of Sciences*, **101**: 8998-9002.

Irawan A. 2018. Transplantation of *Enhalus acoroides* on a sedimentary beach in Ambon Bay. In *IOP Conference Series: Earth and Environmental Science* **118**:. 012054). IOP Publishing.

Kenworthy WJ, Wyllie-Echeverria S, Coles RG, Pergent G and Pergent-Martini C. 2006. Seagrass conservation biology: an interdisciplinary science for protection of the seagrass biome. In *SEAGRASSES: BIOLOGY, ECOLOGY AND CONSERVATION* (pp. 595-623). Springer, Dordrecht.

Kettenring KM, Mercer KL, Reinhardt AC and Hines J. 2014. EDITOR'S CHOICE: Application of genetic diversity–ecosystem function research to ecological restoration. *J App Ecol.,* **51**: 339-348.

Lacap CDA, Vermaat JE, Rollon RN and Nacorda HM. 2002. Propagule dispersal of the SE Asian seagrasses *Enhalus acoroides* and *Thalassia hemprichii*. *Mar Ecol Prog Ser.,* **235**: 75-80.

Larkin P, Quevedo E, Salinas S, Parker J, Storey K and Hardegree B. 2006. Genetic structure of two *Thalassia testudinum* populations from the south Texas Gulf coast. *Aqua Bot.,* **85**: 198-202.

Leimu R, Mutikainen PIA, Koricheva J and Fischer M. 2006. How general are positive relationships between plant population size, fitness and genetic variation? *J Ecol.,* **94**: 942-952.

Lewontin RC. 1964. The interaction of selection and linkage. I. General considerations; heterotic models. *Genetics*, **49**: 49.

Lind CE. 2009. *Population genetics, phylogeography and the effects of aquaculture on genetic diversity of the silver-lipped pearl oyster, Pinctada maxima (Jameson)* (Doctoral dissertation, James Cook University).

Lucas C, Thangaradjou T and Papenbrock J. 2012. Development of a DNA barcoding system for seagrasses: successful but not simple. *PLoS One*, **7**: e29987.

Micheli C, Paganin P, Peirano A, Caye G, Meinesz A and Bianchi CN. 2005. Genetic variability of *Posidonia oceanica* (L.) Delile in relation to local factors and biogeographic patterns. *Aqua Bot*., **82**: 210-221.

Nakajima Y, Matsuki Y, Arriesgado DM, Campos WL, Nadaoka K and Lian C. 2017) Population genetics information for the regional conservation of a tropical seagrass, *Enhalus acoroides*, around the Guimaras Strait, Philippines. *Cons Gen.,* **18**: 789-798.

Paling EI, Fonseca M, van Katwijk MM and van Keulen M. 2009. Seagrass restoration. In: Perillo GME, Wolanski E, Cahoon DR, Brinson MM (eds) *Coastal Wetlands*: an integrated ecosystems approach. Elsevier, Amsterdam, p 687−713

Pharmawati M, Putra I, Syamsuni YF and Mahardika IGNK. 2015. Genetic diversity of *Enhalus acoroides* (L.) Royle from coastal waters of Pramuka Island, Lembongan Island, and Waigeo Island, Indonesia, based on microsatellite DNA. *Adv Sci Lett.,* **21**: 199-202.

Priya TA, Manimekalai V and Ravichandran P. 2015. Intra specific genetic diversity studies on *Calotropis gigantean (*L) R. Br. - using RAPD markers. *European J Biotech Biosci.,* **3**: 7-9

Procaccini G and Piazzi L. 2001. Genetic polymorphism and transplantation success in the Mediterranean seagrass *Posidonia Ocean Restor Ecol.,* **9**: 332−338

Procaccini G, Olsen JL and Reusch TB. 2007. Contribution of genetics and genomics to seagrass biology and conservation. *J of Exp Mar Biol Ecol.,* **350**: 234-259.

Purnama PR, Purnama ER, Manuhara YS, Hariyanto S and Purnobasuki H. 2018. Effect of high-temperature stress on changes in morphology, anatomy and chlorophyll content in tropical seagrass *Thalassia hemprichii*. *AACC Bioflux,* **11**: 1825-1833.

Purnama PR, Hariyanto S, Manuhara YSW and Purnobasuki H. 2019. Gene expression of antioxidant enzymes and heat shock proteins intropical seagrass *Thalassia hemprichii* under heat stress. *Taiwania*, **64**: 117-123.

Putra ING, Syamsuni YF, Subhan B, Pharmawati M, and Madduppa H. 2018. Strong genetic differentiation in tropical seagrass *Enhalus acoroides* (Hydrocharitaceae) at the Indo-Malay archipelago revealed by microsatellite DNA. *Peer J.,* **6**: e4315.

Rawashdeh IM. 2011. Genetic diversity analysis of *Achillea fragrantissima* (Forskal) Schultz Bip Populations Collected From Different Regions of Jordan Using RAPD Markers. *Jor J Biol Sci.*, **4**: 21-28.

Reusch TB. 2001. New markers old questions: population genetics of seagrasses. *Mar Ecol Prog Ser.*, **211**: 261-274.

Reusch TBH, Stam WT and Olsen JL. 2000. A microsatellite based estimation of clonal diversity and population subdivision in *Zostera marina*, a marine flowering plant. *Molr Ecol*., **9**: 127-140.

Riani E, Djuwita I, Budiharsono S, Purbayanto A and Asmus H. 2012. Challenging for seagrass management in Indonesia. *J Coast Dev.*, **15**: 234-242.

Ruiz JM, Perez M and Romero J. 2001. Effects of fish farm loadings on seagrass (Posidoniaoceanica) distribution, growth that and photosynthesis. *Mar Pollut Bull.,* **42**:749–760.

Schaal BA, Hayworth DA, Olsen KM, Rauscher JT and Smith WA. 1998. Phylogeographic studies in plants: problems and prospects. *Mol Ecol.,* **7**: 465-474.

Seprianti R, Karlina I and Irawan H. 2017. Laju pertumbuhan jenis lamun *Thalassia hemprichii* dengan teknik transplantasi sprig anchor dan polybag pada jumlah tegakan yang berbeda dalam rimpang di Perairan Kabupaten Bintan. *Intek Akua.*, **1**: 56-70.

Short FT, Polidoro B, Livingstone SR and Carpenter KE .2011. Extinction risk assessment of the world's seagrass species. *Biol Conserv.*, **144**: 1961−1971

Sinclair EA, Verduin J, Krauss SL, Hardinge J, Anthony J and Kendrick GA .2013. A genetic assessment of a successful seagrass meadow (*Posidonia australis*) restoration trial. *Ecol Manage Restor*., **14**: 68−71

Slatkin M. 1987. Gene flow and the geographic structure of natural populations. *Science*, **236**: 787-792.

Spalding M, Taylor M, Ravilious C, Short F and Green E. 2003. The distribution and status of seagrasses. World atlas of seagrasses. University of California Press, Berkeley, California, 5-26.

Spielman D, Brook BW and Frankham R. 2004. Most species are not driven to extinction before genetic factors impact them. *Proc Nat Acad Sci.,* **101**: 15261-15264.

Tahir NAR, Lateef DD, Omer DA, Kareem SHS, Ahmad DA and Khal LH. 2018. Genetic diversity and structure analysis of pea grown in Iraq using microsatellite markers. *Jor J Biol Sci.,* **12**: 201-207.

Tanaka N, Setoguchi H and Murata J. 1997. Phylogeny of the family hydrocharitaceae inferred from rbcL and matK gene sequence data. *J Plant Res.,* **110**: 329-337.

Van Katwijk MM, Bos AR, De Jonge VN, Hanssen LSAM, Hermus DCR and De Jong DJ. 2009. Guidelines for seagrass restoration: importance of habitat selection and donor population, spreading of risks, and ecosystem engineering effects. *Mar Poll Bull*., **58**: 179-188.

Waycott M, Duarte CM, Carruthers TJB and Orth RJ. 2009. Accelerating loss of seagrasses across the globe threatens coastal ecosystems. *Proc Natl Acad Sci.,* USA **106**: 12377−12381

Waycott M, McMahon K, Mellors J, Calladine A and Kleine D. 2004. A guide to tropical seagrasses of the Indo-West Pacific.

Williams SL. 2001. Reduced genetic diversity in eelgrass transplantations affects both population growth and individual fitness. *Ecol Appl.*, **11**: 1472−1488

Williams JGK, Kubelik AR, Livak KJ, Rafalski JA and Tingey SV. 1990. DNA polymorphisms amplified by arbitrary primers are useful as genetic markers. *Nuc Acids Res.*, **18**: 6531–6535

Williams SL and Davis CA. 1996. Population genetic analyses of transplanted eelgrass (*Zostera marina*) beds reveal reduced genetic diversity in southern California. *Rest Ecol.*, **4**: 163-180.

Williams SL and Heck KL. 2001 Seagrass community ecology. In: Bertness MD, Gaines SD, Hay ME (eds) Marine community ecology. Sinauer Associates, Sunderland, MA, p 317–337.

Wu K, Chen CNN and Soong K. 2016. Long distance dispersal potential of two seagrasses *Thalassia hemprichii* and *Halophila ovalis*. *PloS one*, **11**: e0156585.

Wulandari D, Riniatsih I and Yudiati E. 2013. Transplantasi lamun *Thalassia hemprichii* dengan metode jangkar di Perairan Teluk Awur dan Bandengan, Jepara. *J Mar Res.,* **2**: 30-38.

Yang X and Quiros CF. 1995. Characterizing the celery genome with DNA-based genetic markers. *J Amer Soc Hort Sci.*, **120**: 747-751.

Zhang J, Zhou F, Chen C, Sun X, Shi Y, Zhao H and Chen F. 2018. Spatial distribution and correlation characteristics of heavy metals in the seawater, suspended particulate matter and sediments in Zhanjiang Bay, China. *Plos One,* **13**: e0201414.

Zhao MZ, Zhang YP, Wu WM, Wang C, Qian YM, Yang G and Fang JG. 2011. A new strategy for complete identification of 69 grapevine cultivars using random amplified polymorphic DNA (RAPD) markers. *African J Plant Sci*., **5**: 273–280.

JJBS

Volume 14, Number 1, March 2021
ISSN 1995-6673
Pages 121 - 128

Jordan Journal of Biological Sciences

Effectivity of Curcumin and Thyroxine Supplementations for Improving Liver Functions to Support Reproduction of African Catfish (*Clarias gariepinus*)

Livana D Rawung[1,*], Damiana R Ekastuti[1] , Ade Sunarma[2], Muhammad Z Junior[3], Min Rahminiwati[1], Wasmen Manalu[1]

[1]*Department of Anatomy, Physiology, and Pharmacology, Faculty of Veterinary Medicine, Bogor Agricultural University, Dramaga Campus, 16680 Bogor, West Java, Indonesia,*[2]*National Freshwater Aquaculture Center, Ministry of Marine Affairs and Fisheries, Republic of Indonesia, Jalan Selabintana 37, 43114 Sukabumi, West Java, Indonesia,*[3]*Department of Aquaculture, Faculty of Fisheries and Marine Sciences, Bogor Agricultural University, Dramaga Campus, 16680 Bogor, West Java, Indonesia*

Received Mar 30, 2020; Revised July 11, 2020; Accepted July 25, 2020

Abstract

This experiment was designed to study the effect of curcumin and thyroxine supplementations on liver functions during the reproductive period of catfish. One hundred and twenty-eight African catfish (Clarias gariepinus) were assigned into a completely randomized design with a 2x2 factorial arrangement with four replications and each replication consisted of eight fish. The first factor was dose of curcumin supplementation which consisted of 2 levels i.e., 0 and 5 g kg-1feed. The second factor was dose of thyroxine supplementation consisting of 2 levels i.e., 0 and 0.1 mg.kg-1feed. The supplementation of curcumin and thyroxine hormone in catfish was given for 12 weeks. Results showed that the levels of serum vitellogenin concentrations, serum glutamic oxaloacetic transaminase (SGOT), and deoxyribonucleic acid (DNA from liver tissue in all groups did not show a significant difference ($p>0.05$). However, the concentration of malondialdehyde (MDA) in the liver tissue, the serum glutamic pyruvic transaminase (SGPT), and the ribonucleic acid (RNA) concentration in the liver tissue showed a significant difference ($p<0.05$). The supplementation of curcumin and thyroxine protect the liver, and increase the productivity of catfish liver function during the reproductive period.

Keywords: *curcumin; thyroxine; oxidative damage; Liver; vitellogenin*

1. Introduction

In oviparous animals such as fish, the liver has a very important role in reproduction to synthesize and produce vitellogenin (Cerda *et al.* 1996; Tata, 1979). Vitellogenins are major precursors to the egg yolk protein, which provides essential nutrients and other materials required by the developing embryo (Sullivan and Yilmaz, 2018). During gonad maturity, the liver cells work harder to synthesize and produce a higher number of vitellogenin to fulfill the requirements of vitellogenin by thousands of developing oocytes at the same time (Arukwe and Goksoyr, 2003).

High activities of hepatocytes during the gonad maturity process can cause the lowering functions and synthetic capacities of hepatocytes. The higher metabolic activities of hepatocytes can produce a higher number of intermediate products and free radicals (Watson, 2002; Kasiyati *et.al*. 2016a). The normal process of metabolism in the body can produce free radicals as an intermediate product (Valko *et al*. 2007). According to Rahman (2007), if there is no balance between an endogenous antioxidant system and free radicals, or if there is excess of free radicals and lipid peroxidation it will cause oxidative damages to the organ or tissue. The occurrence of lipid peroxidation is related to the high production of free radicals exceeding the availability of endogenous antioxidant (Rahman, 2007). Malondialdehyde (MDA) is the final product of lipid peroxidation; it can be used as an indicator of liver damage (Sewerynek *et al* .1996). In the conditions of liver disorders, the serum glutamic pyruvic transaminase enzyme (SGPT) and serum glutamic oxaloacetic transaminase enzyme (SGOT) also increase in the plasma (Li *et al*. 2014).

Curcumin has an antioxidant activity, and it can inhibit the activity of inflammation enzymes and lipid peroxidation (Kohli *et al.* 2005; Akram *et al.* 2010; Abdulbaqi *et al.* 2018). Curcumin also has activity as a hepato-protector agent, and this compound can prevent liver damages and optimize the liver physiological function (Manju *et al.* 2012; Negi *et al.* 2007) to synthesize vitellogenin (Lubzens *et al.* 2010). Protection of hepatocyte cells is expected to optimize liver productivity in synthesizing the metabolites needed during the period of vitellogenesis.

One of the main functions of thyroxine hormone is to increase the amount and activity of mitochondria, which in turn increases the speed of formation of adenosine triphosphate (ATP) for cellular energy (Guyton and Hall, 2006). Researches on the process of vitellogenesis in fish show the involvement of thyroid hormone (Syano *et* al.

* Corresponding author e-mail: livana83@yahoo.com.

1993; Nowell *et al.* 2001). Research conducted by Dewi (2018) showed that supplementation of thyroxine in combination either with turmeric or oodev can reduce oxidative stress in Siam catfish.

The present experiment was designed to study the effect of curcumin and thyroxine supplementations on the liver productivity, health, and physiological functions during the maturity of gonads in African catfish.

2. Materials and Methods

2.1. Location and time of study

The experiment was conducted during August-December 2018. The catfish were maintained in National Freshwater Aquaculture Center, Sukabumi, West Java, Indonesia. The concentration of malondialdehyde (MDA) concentrations in the liver tissue, SGPT, SGOT, liver DNA, and liver RNA concentrations were analyzed in the Laboratory of Physiology, Department of Anatomy, Physiology, and Pharmacology, Faculty of Veterinary Medicine, Bogor Agriculture University. Vitellogenin concentrations were analyzed and estimated in the Primate Animal Study Center, Bogor Agriculture University.

2.2. Experimental design

The experimental design used was a completely randomized design with 2x2 factorial arrangement. The first factor was a dose of curcumin supplementation consisting of two levels i.e., 0 and 5 g kg^{-1}feed. The second factor was a dose of thyroxine supplementation of two levels i.e., 0 and 0.1 mg. kg^{-1}feed. A total of 128 catfish were divided into four groups, each group had four replicates (8 fish for each replication); the first group (A) consisted of catfish without curcumin and thyroxine supplementation as a control; the second group (B) consisted of catfish supplemented with curcumin at a dose of 5.0 g kg^{-1}feed (Manju *et al.* 2012) without thyroxine supplementation, the third group (C) consisted of catfish without curcumin supplementation but with thyroxine supplementation at a dose of 0.1 mg.kg^{-1} feed (Agusnimar and Rosyadi, 2015), and the fourth group (D) consisted of catfish supplemented with curcumin at a dose of 5.0 g kg^{-1}feed and thyroxine at a dose of 0.1 mg kg^{-1}feed.

2.3. Experimental procedure

The experimental animals used in this study were female catfish with an initial body weight ranging from 250-350 g. The experimental catfish were reared in the rearing pond in 16 nets each with the size of 2x1x1 m^3 and each net contained eight catfish. The catfish were reared for 12 weeks and fed with commercial ration containing 42.70% protein. For the treatments, the required dose of curcumin and thyroxine were mixed with the commercial ration. The curcumin used in this experiment was produced by Plamed Green Science Limited (CHINA) with 93.71% concentration of curcumin. The thyroxine hormone used was a tablet of levothyroxine sodium/euthyrox (MERCK). The process of feed coating was started with the addition of carboxymethyl cellulose (CMC) powder as a binder to the commercial feed. The level of CMC addition was 10% in the commercial feed used. Further, the curcumin and/or thyroxine powder was added into the commercial feed mixed with CMC. During the rearing period, the experimental catfishes were fed daily at the level of 2% body weight.

2.4. Sample collection

Every three weeks, one catfish was taken randomly from each replication of all the treatments and sacrificed. Prior to being sacrificed, the experimental catfishes were anesthetized using clove oil with a concentration of 0.04 ml l^{-1} of water. Before being dissected, the blood was collected using a 3 ml syringe from the caudal vein. The collected blood was transferred to polyethylene tube and centrifuged at 3000 rpm for 10 minutes at 4°C to obtain serum. The serum was transferred into a new polyethylene tube and kept at -20°C until further analyses for SGPT, SGOT, and vitellogenin. The liver was divided into two parts: the first part was kept in sterile Eppendorf tube immediately immersed in liquid nitrogen and then stored at -20°C for Malondialdehyde determination (MDA), the second part of liver about 2g kept in Phospate Buffer Saline (PBS) in sterile plastic tubes was stored at -20°C for DNA and RNA assays.

2.5. Parameters measurements

2.5.1. Vitellogenin assay

Vitellogenin concentration in the serum was determined with an enzyme linked immunosorbent assay (ELISA) using the Vitellogenin Fish Kit (Korain Biotech Co.Ltd, China).

2.5.2. Malondialdehyde (MDA) assay

As much as 1 g of catfish liver was finely chopped under cold condition and dissolved in 2 ml of PBS-KCl at a pH 0f 7.4. The mixture formed was centrifuged at 10.000 rpm for 20 minutes and then the supernatant was taken for further MDA assay. The MDA concentrations of the liver to determine the peroxidation activity of liver cell membranes were measured by using the thiobarbituric acid (TBA) method (Singh *et al. 2002*). TEP (1.1.3.3-Tetraethoxy-propabe, ≥96%) MW 220.31 (Aldrich, USA) was used as a standard for MDA.

2.5.3. SGPT and SGOT assays

Kinetic method was used for the determinations of SGPT and SGOT activities according to the recommendations of the Expert Panel of the IFCC (International Federation of Clinical Chemistry). The concentrations of SGPT and SGOT were measured by using the kit of GPT (ALAT) (Human, Germany) and kit of GOT (ASAT) (Human, Germany).

2.5.4. DNA and RNA assays

Analysis of DNA and RNA concentrations of liver tissues was made by isolating 2-3 g of liver, dried in an oven at 60°C for a day, the dried liver was crushed into a mash by using a mortar and then 10 mg of the liver tissues was weighed each for analysis of liver DNA and RNA. The DNA concentration of liver tissue was determined by DNA extraction method by using genomic DNA mini kit (Geneaid Biotech Ltd, Taiwan), while the concentration of RNA was determined by RNA extraction method by using total RNA mini kit (Geneaid Biotech Ltd, Taiwan).

2.6. Statistical analyses

The data obtained were analyzed by using analysis of variance (ANOVA). The whole data analysis was conducted by general linear model procedure on MINITAB version 16 program. The differences between the means of the treatment were tested by using Tukey simultaneous test. All results significantly different were expressed with $p<0.05$.

3. Results and Discussion

3.1. Results

3.1.1. Concentrations of vitellogenin in serum of catfish

Concentrations of vitellogenin in the serum for 12 weeks of observation are shown in **Fig. 1**. Before treatment, the experimental catfish were in matured condition as it was indicated by the high serum vitellogenin concentration with an average value of 9.44 µg/ml. Serum vitellogenin concentrations as an indicator of gonad maturity slightly increased at 3 weeks of treatment and then decreased at 6 weeks of treatment, and then relatively stable at 9 and 12 weeks of treatment. There was no significant difference among the treatments ($p>0.05$). Even though there was no significant difference in serum vitellogenin concentrations among treatments, catfish treated with different doses of curcumin and thyroxine supplementations showed the dynamic changes in serum vitellogenin concentrations. At 3 and 6 weeks of treatments, the highest serum vitellogenin concentrations were found in catfish fed ration supplemented with 0 g curcumin kg^{-1}feed and 0.1 mg thyroxine kg^{-1}feed (Group C), followed by catfish fed ration supplemented with 0 g curcumin kg^{-1}feed and 0 mg thyroxine kg^{-1}feed (Group A), catfish fed ration supplemented with 5.0 g curcumin kg^{-1}feed and 0.1 mg thyroxine kg^{-1}feed (Group D), and the lowest were found in catfish fed ration supplemented with 5.0 g curcumin kg^{-1}feed and 0 mg thyroxine kg^{-1}feed (Group B). At 9 and 12 weeks of treatments, the highest vitellogenin concentrations were found in catfish fed ration supplemented with 5.0 g curcumin kg^{-1}feed and 0.1 mg thyroxine kg^{-1}feed (Group D), followed by catfish fed ration supplemented with 0 g curcumin kg^{-1}feed + 0.1 mg thyroxine kg^{-1}feed (Group C), catfish fed ration supplemented with 5.0 g curcumin kg^{-1}feed and 0 mg thyroxine kg^{-1}feed (Group B), and the lowest were in control catfish fed ration supplemented with 0 g curcumin kg^{-1}feed and 0 mg thyroxine kg^{-1}feed (Group A). At 12 weeks of treatment, serum vitellogenin concentrations did not indicate any relationship with the curcumin or thyroxine treatment. However, 9th and 12 weeks of treatments, catfish treated with curcumin and thyroxine supplementations had consistently higher serum vitellogenin concentrations compared to control catfish without curcumin and thyroxine supplements.

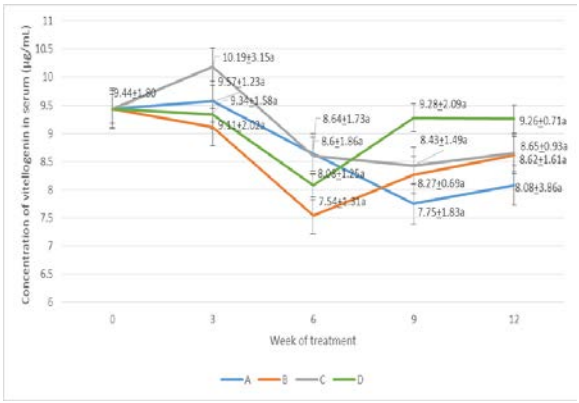

Figure 1. Concentrations of vitellogenin in serum of experimental African catfish for 12 weeks of treatment with various combinations of curcumin and thyroxine. **A** (0 g curcumin kg^{-1}feed + 0 mg thyroxine kg^{-1}feed); **B** (5.0 g curcumin kg^{-1}feed + 0 mg thyroxine kg^{-1}feed); **C** (0 g curcumin kg^{-1}feed + 0.1 mg thyroxine kg^{-1}feed); **D** (5.0 g curcumin kg^{-1}feed + 0.1 mg thyroxine kg^{-1}feed). Means ± standard deviation with different superscripts indicate a significant difference ($p<0.05$).

3.1.2. Concentrations of Malondialdehyde (MDA) in the liver tissues

The MDA concentrations in the livers of experimental catfish are presented in **Fig. 2**. Concentrations of MDA in the liver tissues were high before treatment, and decreased in three weeks of treatment, increasing during 6 weeks of treatment, and reduced at nine weeks of treatment, while increasing again at 12 weeks of treatment.

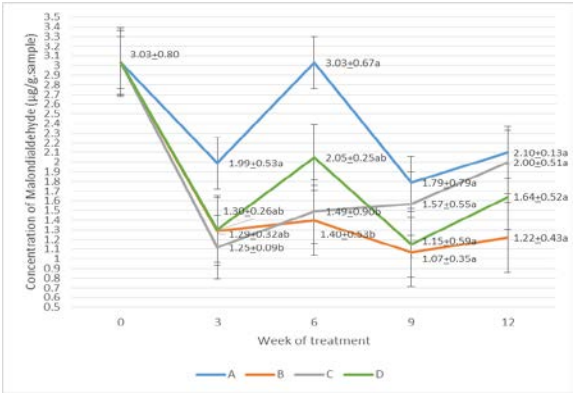

Figure 2. Concentrations of Malondialdehyde (MDA) in the liver tissues of experimental African catfish during 12 weeks of treatment with various combinations of curcumin and thyroxine. **A** (0 g curcumin kg^{-1}feed + 0 mg thyroxine kg^{-1}feed); **B** (5.0 g curcumin kg^{-1}feed + 0 mg thyroxine kg^{-1}feed); **C** (0 g curcumin kg^{-1}feed + 0.1 mg thyroxine kg^{-1}feed); **D** (5.0 g curcumin kg^{-1}feed + 0.1 mg thyroxine kg^{-1}feed). Means ± standard deviation with different superscripts indicate a significant difference ($p<0.05$).

Catfish without curcumin and thyroxine supplementations (Group A or control) had the highest liver MDA concentrations and catfish supplemented with 5.0 g curcumin kg^{-1}feed without thyroxine supplementation (Group B) and catfish supplemented with 0.1 mg thyroxine kg^{-1}feed without curcumin supplementation (Group C) had the lowest liver MDA concentrations and catfish supplemented with 5.0 g curcumin kg^{-1}feed and 0.1 mg thyroxine kg^{-1}feed (Group D) were moderate values (Fig.2). At three and six weeks of treatments, catfish of Group A had significantly the higher liver MDA concentrations compared to the other treatments ($p<0.05$). At three weeks of treatment, catfish

of Group C had the lowest liver MDA concentration ($p<0.05$). At six weeks of treatments, catfish of Group B and C had significantly lowest liver MDA concentrations ($p<0.05$) when compared to Group A. However, at 9 and 12 weeks of treatment, there was no significant difference in liver MDA concentrations among the treatments ($p>0.05$) even though catfish without curcumin supplementations (Group A and Group C) had the highest liver MDA concentrations, and catfish treated with curcumin (Group B and Group D) had the lowest liver MDA concentrations. The pattern of liver MDA concentrations during 12 weeks of treatment increased on weeks 6 and 12 of treatment. The highest liver MDA concentrations were found in control (Group A).

3.1.3. Concentrations of glutamic pyruvic transaminase (SGPT) in the serum of catfish for

Serum SGPT concentrations of experimental African catfish are presented in **Fig. 3**. The curve of serum SGPT concentrations was similar to those of liver MDA concentrations and serum SGOT concentrations. Observations in weeks 3 and 6 of treatments, serum SGPT concentrations in all groups did not differ significantly ($p> 0.05$). Further, in six weeks of treatment, serum SGPT concentrations increased compared to those at three weeks treatment. However, in weeks 9 and 12 of treatments, control catfish without curcumin and thyroxine treatment had significantly higher serum SGPT concentrations ($p<0.05$). Even though they were not always statistically significant, the highest serum SGPT concentrations were found in control catfish (Group A). Catfish of Group B, C, and D had lower serum SGPT concentrations compared to Group A. Similar to the pattern of liver MDA concentrations, the curve of liver SGPT concentrations increased on weeks 6 and 12 of treatment and the highest liver MDA concentrations in these weeks of treatments were found in control.

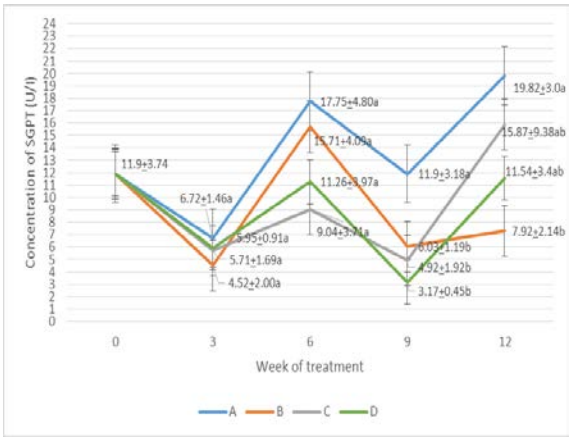

Figure 3. Concentrations of SGPT in the serum of African catfish during 12 weeks of treatment with various combinations of curcumin and thyroxine. **A** (0 g curcumin kg^{-1}feed + 0 mg thyroxine kg^{-1}feed); **B** (5.0 g curcumin kg^{-1}feed + 0 mg thyroxine kg^{-1}feed); **C** (0 g curcumin kg^{-1}feed + 0.1 mg thyroxine kg^{-1}feed); **D** (5.0 g curcumin kg^{-1}feed + 0.1 mg thyroxine kg^{-1}feed). Means ± standard deviation with different superscripts indicate a significant difference ($p<0.05$).

3.1.4. Concentrations of glutamic oxaloacetic transaminase (SGOT) in the serum of catfish

Serum SGOT concentrations of the experimental catfish during 12 weeks of treatment are presented in **Fig. 4**. Prior to the treatment, the serum SGOT concentrations were high and decreased at three weeks of treatment and maintained similar level until nine weeks of treatment and then increased after 12 weeks of treatment. Even though with dramatic changes after 12 weeks of treatment, serum SGOT concentrations in all experimental catfish groups were similar ($p> 0.05$). In the third week of treatment, serum SGOT concentrations did not differ significantly between the treatments ($p> 0.05$). The same patterns were observed in the serum SGOT concentrations sixth, ninth, and twelfth weeks of treatments. These results indicated that curcumin and thyroxine supplementations did not affect serum SGOT concentrations of catfish. However, at three weeks of treatment, catfish without curcumin and thyroxine supplementation (Group A) and catfish without curcumin supplementation but with 0.1 mg thyroxine kg^{-1}feed (Group C) had higher serum SGOT concentrations compared to catfish with 5.0 g curcumin supplementation kg^{-1}feed but without thyroxine supplementation (Group B) and catfish supplemented with 5.0 g curcumin kg^{-1}feed and 0.1 mg thyroxine kg^{-1}feed (Group D). There was a tendency that catfish without curcumin supplementation had higher SGOT compared to those supplemented with curcumin. Similar to the pattern of liver MDA and serum SGPT concentrations, the pattern of serum SGOT concentrations during 12 weeks of treatment increased after 6 and 12 weeks of treatment. However, it was not significant; the highest serum SGOT concentrations were found 6 week post treatment in catfish of Group B, followed by Group A, D and C. Even though it was not significant, the highest serum SGOT concentrations after 12 weeks of treatment were found in catfish of Group C, B, and D, followed by Group A. Similar to the curve of liver MDA concentrations, the curve of liver SGPT concentrations during 12 weeks of treatment increased after 6 and 12 weeks of treatment, and the highest liver MDA concentrations during the same period was found in catfish without curcumin and thyroxine supplements (control).

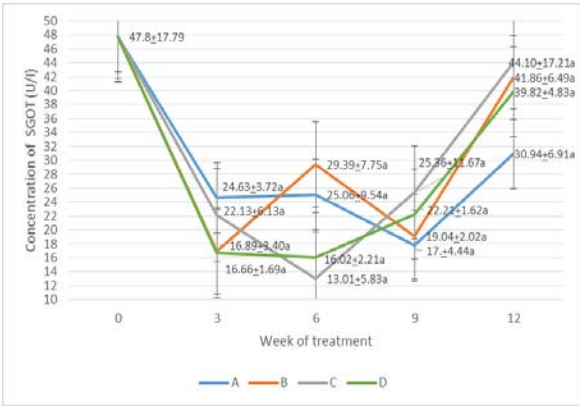

Figure 4. Concentrations of SGOT in the serum of experimental African catfish for 12 weeks of treatment with various combinations of curcumin and thyroxine. **A** (0 g curcumin kg^{-1}feed + 0 mg thyroxine kg^{-1}feed); **B** (5.0 g curcumin kg^{-1}feed + 0 mg thyroxine kg^{-1}feed); **C** (0 g curcumin kg^{-1}feed + 0.1 mg thyroxine kg^{-1}feed); **D** (5.0 g curcumin kg^{-1}feed + 0.1 mg thyroxine kg^{-1}feed). Means ±_standard deviation with different superscripts indicate a significant difference ($p<0.05$).

3.1.5. Concentrations of DNA in the liver of catfish

Concentrations of DNA in the liver of experimental catfish during 12 weeks of treatment are presented in **Fig.**

5. Statistical analysis of liver DNA concentrations at three, six, nine, and twelve weeks of curcumin and thyroxine supplementations did not differ significantly ($p > 0.05$) among the treatments. These results indicated that the supplementation of experimental catfish with curcumin and thyroxine did not affect DNA concentration in the liver tissues. The average liver DNA concentrations of experimental catfish ranged from 12.15 -12.79 $mg.g^{-1}$. In general, there were the patterns of increase and decrease in the liver DNA concentrations. However, there was an irregular pattern of fluctuation within and between the treatments. Liver DNA concentrations increased after 3 and 9 weeks of treatments. After 9 weeks of treatment, liver DNA concentration was maximum in catfish fed ration supplemented with 5.0 g curcumin kg^{-1}feed and 1.5 mg thyroxine kg^{-1}feed (Group D) followed by the Groups A, B, and C respectively.

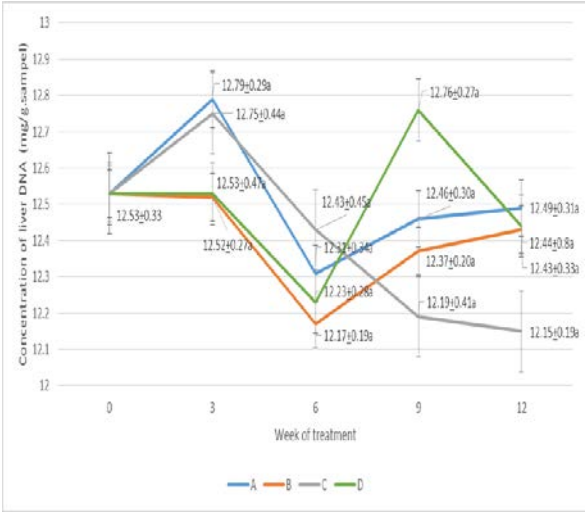

Figure 5. Concentrations of DNA in the liver tissues of experimental African catfish for 12 weeks of treatment. with various combinations of curcumin and thyroxine. **A** (0 g curcumin kg^{-1}feed + 0 mg thyroxine kg^{-1}feed); **B** (5.0 g curcumin kg^{-1}feed + 0 mg thyroxine kg^{-1}feed); **C** (0 g curcumin kg^{-1}feed + 0.1 mg thyroxine kg^{-1}feed); **D** (5.0 g curcumin kg^{-1}feed + 0.1 mg thyroxine kg^{-1}feed). Means ±_standard deviation with different superscripts indicate a significant difference ($p<0.05$).

3.1.6. Concentrations of RNA in the liver of catfish

The RNA concentrations in the liver of experimental catfish are presented in **Fig. 6**. RNA concentration in the liver cells increased after the initiation of the curcumin thyroxine treatments and reached the peak after nine weeks of treatment and later decreased to the minimum level after 12 weeks of treatment. Statistically, liver RNA concentration did not affect after three, six, and nine weeks of curcumin and thyroxine supplementation ($p > 0.05$). However, at twelve weeks of curcumin and thyroxine supplementations, there was a difference ($p<0.05$) between the treatments. The maximum RNA levels were found in catfish of Group B, followed by catfish of Group C, D, and A. Liver RNA concentrations increased after 3 and 6 weeks of treatment, and reached the peak concentration after 9th week. After 9 week of treatments, even though it was not statistically significant, the highest liver RNA concentrations were found in catfish of Group D followed by the other treatments with the order of catfish from Group C, B, and A.

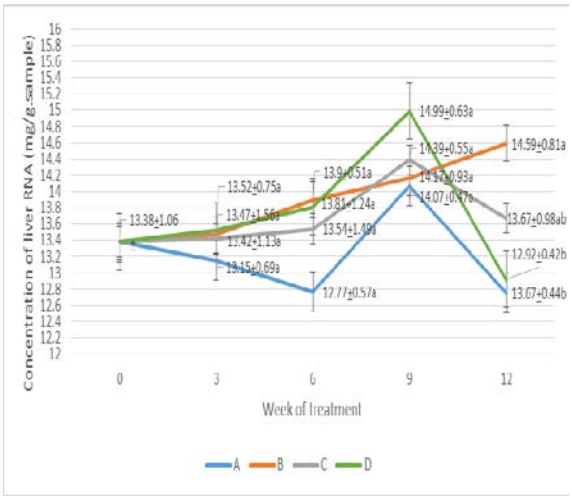

Figure 6. Concentrations of RNA in the liver tissues of experimental African catfish for 12 weeks of treatment with various combinations of curcumin and thyroxine. **A** (0 g curcumin kg^{-1}feed + 0 mg thyroxine kg^{-1}feed); **B** (5.0 g curcumin kg^{-1}feed + 0 mg thyroxine kg^{-1}feed); **C** (0 g curcumin kg^{-1}feed + 0.1 mg thyroxine kg^{-1}feed); **D** (5.0 g curcumin kg^{-1}feed + 0.1 mg thyroxine kg^{-1}feed). Means ± standard deviation with different superscripts indicate a significant difference ($p<0.05$).

4. Discussion

Liver plays an important role during reproduction of fish because as it functions as a main organ for synthesis of vitellogenin. Vitellogenin is an egg yolk precursor synthesized in the liver under the stimulation of estradiol-17β. During the reproduction period, the liver will continuously synthesize the vitellogenin to fulfill the requirement of each growing oocytes (Cerda *et al.* 1996). During the vitellogenesis, liver tissues showed the formation of many vacuoles in the liver cells (Dewi, 2018). The vacuole contains fats, the component of vitellogenin, synthesized by liver cells (Kasiyati *et al.* 2016a). The vitellogenin will be released into the circulation system and transported to the gonads. In this study, the presence of vitellogenin in the circulation has been detected since the beginning of the observation (**Figure 1**). According to Dewi *et al.* (2018), supplementation of turmeric powder in Siam catfish increased vitellogenin synthesis.

In this study the concentration of vitellogenin in the circulation was almost the same for all groups. However, the group that supplemented by curcumin and thyroxine showed the increase of vitellogenin in the circulation. According to Cerda et al. (1996), the concentrations of vitellogenin in the plasma were basically constant throughout the reproductive cycle, except that there was more activity in taking vitellogenin by a growing population of eggs that decreased the level of vitellogenin in the plasma. According to Kasiyati *et al.* (2016b) increased in vitellogenin synthesis in ducks supplemented with curcumin was not associated with the high estradiol concentrations but with the capacity and function of hepatocytes to synthesize vitellogenin. Vitellogenin is not always stored in the liver cells, but secreted directly after being synthesized and then deposited into the developing oocyte. Therefore, the concentration of vitellogenin in the circulation is a result of the rate of vitellogenin synthesis and secretion into the circulation and the rate of

vitellogenin transport and deposits into the developing oocytes (Nath and Sundararaj, 1979; Kasiyati *et al*. 2016b).

The results of the present study on African catfish showed that supplementation of catfish with curcumin and thyroxine resulted in decreased MDA concentrations in the liver tissues (three and six weeks post treatments) and serum SGPT concentrations (after nine and twelve weeks) as indicators of the improved conditions and functions of liver cells. Catfish without curcumin and thyroxine supplementation had the highest MDA concentrations in the liver tissue (after three and six weeks) and highest serum SGPT concentrations (after nine and twelve weeks). This result indicated the liver protection of curcumin and thyroxine. Therefore, curcumin and thyroxine supplementations improved physiological conditions of the liver that could maintain the optimum cell number, synthetic capacity as it was indicated by the increased vitellogenin synthesis.

The role of liver as an organ for synthesis of various compounds needed by the body makes it very susceptible to the exposure to free radicals as intermediate products formed in various processes of reactions and metabolism. MDA is a final product of lipid peroxidation. The observation of catfish for 12 weeks of maintenance showed the development of fish gonads. Along with the development of the gonads, liver activity also increases in synthesizing vitellogenin as an egg yolk precursor. Observation of MDA concentrations of catfish liver for 12 weeks showed a significant effect indicated by curcumin and thyroxine supplementations decreased the MDA levels in the liver. The fluctuation of MDA occurred during this study could be related to the reproductive activities that were currently occurring in the experimental catfish. This study showed that supplementation of curcumin can reduce the MDA level in liver, it indicated that curcumin play a role as hepato-protector agent. Observation conducted by Manju *et al*. (2013) showed the increase in endogenous antioxidant in hepatocytes cells and glutathione concentrations in *Anabas testudineus* (Bloch) supplemented with curcumin in 40% protein ration. Curcumin directly plays a role in the scavenging of free radicals, stimulating the pathways of antioxidant enzymes and increasing the antioxidant level in the cells (Manju *et al*. 2012; Iqbal *et al*. 2003; Sharma *et al.* 2005). A study conducted by Dewi *et al.* (2018) showed that supplementation of turmeric powder decreased the MDA level of the Siam catfish liver. In this study, the addition of thyroxine showed a decrease in MDA concentrations of catfish liver at the third and sixth weeks of treatment. The hepatoprotective activity with thyroxine supplementation in this study occurred because of an increase in endogenous antioxidant. Research conducted by Baskol *et al*. (2007) showed that the addition of thyroxine reduced the serum MDA levels in patients with hypothyroidism. Meanwhile, Siam catfish supplemented with turmeric and thyroxine powder for eight weeks showed a significantly lower liver MDA concentration than controls (Dewi, 2018).

This study also showed that the addition of curcumin and thyroxine in the feed of catfish can reduce SGPT concentrations at ninth and twelfth weeks but did not affect SGOT concentrations. Park *et al*. (2000) reported that giving curcumin significantly reduced liver damage and decreased SGOT and SGPT concentrations in the blood. The increased levels of SGPT and SGOT in the blood occurred along with the increasing age of fowl (Biswas *et al*. 2010). Chattopadhyay *et al*. (2004) suggested that curcumin acts as an antioxidant by activating macrophages to inhibit reactive oxygen species (ROS). Research conducted by Kasiyati *et al*. (2016a) showed that administration of curcumin protected hepatocytes from cell damage caused by free radicals characterized by the reduced levels of SGPT and SGOT in ducks supplemented with curcumin. Curcumin has been reported to induce nucleus translocation of NRF2 and increase the expression of a number of detoxifications of reactive oxygen species (ROS) and antioxidant genes in hepatocytes (Zhao *et al.* 2011). Therefore, supplementation of curcumin improved the status of cellular antioxidants, such as glutathione peroxidase, glutathione reductase, glucose-6-phosphate dehydrogenase, and catalase, which is also accompanied by the increase in Phase II-metabolizing enzymes, namely glutathione s-transferase and quinone reductase in the liver and kidney (Iqbal *et al*. 2003), thereby reducing ROS (reactive oxygen species) activity (Sharma *et al*. 2005).

The observations on the liver DNA concentrations as an indicator of the number and concentration of hepatocytes in the liver tissue showed that treatment of curcumin and thyroxine did not significantly affect the number of liver cells. This result is similar with the study conducted by Dewi *et al.* (2018). The fluctuation of DNA during this study was not associated with the curcumin and thyroxine supplementation, but this fluctuation could be related to the gonadal maturation of the experimental catfish, it stimulated the hepatocyte growth.

In this study, supplementation of curcumin and thyroxine showed an increase of RNA concentrations in liver tissue. Increasing level of RNA in liver tissue indicated the increase capacities of liver to produce vitellogenin during the reproductive period. According to Kasiyati *et al*. (2016b), supplementation of curcumin in ducks improved the functions of liver cells, so it increased the biosynthesis of egg yolk/vitellogenin precursors as indicated by the increase in RNA concentrations of liver tissue. Our study showed a decrease in MDA in line with an increase in RNA concentration. The protection of liver is very important to support the optimization of their productivity. Meanwhile thyroxine plays a role in protein synthesis by increasing the activity of mitochondria, which in turn increases the speed of formation of adenosine triphosphate (ATP) for cellular energy (Guyton and Hall 2006). Increase in RNA concentrations in the liver of experimental catfish supplemented with curcumin and thyroxine (Group D) is thought to occur because of an increase in glutathione production caused by the addition of curcumin (Manju *et al*. 2012), where the glutathione is a co-factor of deiodinases which are responsible for the conversion of thyroxine (T4) to triiodothyronine (T3) (Mancini *et al.* 2016; Visser, 1980). On the other hand, supplemented thyroxine could increase the concentration of triiodothyronine because thyroxine will be converted to triiodothyronine (Mancini et al. 2016)

5. Conclusion

Our study shows that curcumin and thyroxine supplementation could inhibit the liver oxidative damage of catfish by reducing liver MDA levels and serum concentrations of SGPT, so it can protect the liver and increase vitellogenin synthesis as indicated by the increased RNA concentrations in the liver. In this study, the Group D (catfish fed ration supplemented with 5.0 g curcumin kg^{-1}feed and 0.1 mg thyroxine kg^{-1}feed) showed the optimum result for concentration of vitellogenin in serum and liver protection.

Acknowledgements

This study was supported by BPPDN Scholarship from Ministry of Research, Technology, and Higher Education of the Republic of Indonesia. The authors are also thankful to National Freshwater Aquaculture Center, Sukabumi for allowing us to use the facilities to conduct the experiment.

References

Abdulbaqi NJ, Dheeb BI and Irshad R. 2018. Expression of biotransformation and antioxidant genes in the liver of albino mice after exposure to Aflatoxin B1 and an antioxidant sourced from turmeric (*Curcuma longa*). *Jordan J. Biol. Sci*, **11**(1):93-98.

Agusnimar and Rosyadi. 2015. Growth and survival of *Kryptopterus lais* treated with thyroxine hormone. *JAI*, **14**(1): 38-41

Akram M, Uddin S, Ahmed A, Usmanghani K, Hannan A, Mohiuddin E and Asif M. 2010. *Curcuma longa* and Curcumin: A Riview Article. *Rom J Biol-Plant Biol*, **55**(2):65-70.

Arukwe A and Goksoyr A. 2003. Eggshell and egg yolk proteins in fish : hepatic proteins for the next generation: oogenetic, population, and evolutionary implications of endocrine disruption. *Comp Hepatol*, **2**(4).

Baskol G, Atmaca H, Tanriverdi F, Baskol M, Kocer D and Bayram F. 2007. Oxidative stress and enzymatic antioxidant status in patients with hypothyroidism before and after treatment. *Exp Clin Endocrinol Diabetes*, **115**(8):522-526.

Biswas A, Mohan J, Venkata K and Sastry H. 2010. Age-Dependent Variation in Hormonal Concentration and Biochemical Constituents in Blood Plasma of Indian Native Fowl. *Vet Med In*: **737292**. 10.4061/2010/737292.

Cerda J, Calman BG, LaFleur GJ Jr and Limesan S. 1996. Pattern of Vitellogenesis and follicle maturational competence during the ovarian follicular cycle of *Fundulus heteroclitus*. *Gen Comp Endocrinol*, **103**(1):24-35.

Chattopadhyay I, Biswa K, Bandyopadhyay U and Banerjee RK. 2004. Turmeric and Curcumin: biological action and medicinal applications. Review article. *Curr Sci*, **87**(1): 44-53.

Dewi CD. 2018. Turmeric powder (*Curcuma longa)* supplementation, thyroxine and oodev in diet to improve the reproduction performance of catfish (*Pangasianodon hypophthalmus*). Dissertation, Bogor Agriculture University.

Dewi CD, Manalu W, Ekastuti DR and Sudrajat AO. 2018. The role of the turmeric powder supplementation in improving liver performance to support the production of siam catfish (*Pangasianodon hypophthalamus*). *Omni-Akuatika*, **144**(1):44-53.

Guyton AC, Hall JE. 2006. **Textbook of medical physiology,** *eleventh edition*. Elsevier Saunders. Pennsylvania.

Iqbal M, Sharma SD, Okazaki Y, Fujisawa M and Okada S. 2003. Dietary supplementation of curcumin enhances antioxidant and phase II metabolizing enzymes in ddY male mice: possible role in protection against chemical carcinogenesis and toxicity. *Pharmacol Toxicol,* **92**(1): 33-38.

Kohli K, Ali J, Ansari MJ and Raheman Z. 2005. Curcumin: Anatural anti-inflammatory agent. *Indian. J Pharmacol.* **37**(3):141-147.

Kasiyati, Manalu W, Sumiati and Ekastuti DR. 2016a. Efficacy of curcumin and monochromatic light in improving liver function of sexually mature Magelang ducks. *J Indonesian Trop Animal Agric*, **41**(3): 153-160.

Kasiyati, Sumiati, Ekasturi DR and Manalu W. 2016b. Roles of curcumin and monochromatic light in optimizing liver function to support egg yolk biosynthesis in Magelang duck. *Int J Poult Sci*, **15**:414-424.

Li Y, Ma QG, Zhao LH, Guo YQ, Duan GX, Zhang JY and Ji C. 2014. Protective efficacy of alpha-lipolic acid against aflatoxinB1-induced oxidative damage in the liver. Asian-Aus *J Anim.Sci*, **27**(6):907-915.

Luzbens E, Young G, Bobe J and Cerda J. 2010. Oogenesis in teleost: How fish eggs are formed. *Gen Comp Endocrinol*, **165**: 367-389.

Mancini A, Di Segni C, Raimondo S, Olivieri G, Silvestrini A, Meucci E and Curro D. 2016. Thyroid hormone, oxidative stress, and inflammation. Hindawi Publishing Corporation: *Mediators Inflamm*, **2016**:6757154.

Manju M, Vijayasree AS, Akbarsha MA and Oommen OV. 2013. Effect of curcumin supplementation on hepatic, renal and intestinal organization of *Anabas testudineus* (Bloch): Light and electron microscopic studies. *J Endocrinol Reprod*, **17**(2): 83-89

Manju M, Akbarsha MA and Oommen OV. 2012. In vivo protective effect of dietary curcumin in fish *Anabas testudineus* (Boch). *Fish Physiol Biochem*, **38**(2): 309-318.

Nath, P and B.I Sundararaj. 1979. Role of protein and steroid hormones in vitellogenesis in catfish, *Heteropneustes fossilis. Proc Indian Natl Sci Acad*, **45**:491-496.

Negi AS, Kumar JK, Luqman S, Shanker K, Gupta MM and Khanuja SPS. 2007. Recent Advances in Plant Hepatoprotectives: A Chemical and Biological Profile of Some Important Leads. *Med Res Rev*, 746-722.

Nowell MA, Power DM, Canario AVM, Llewellyn L and Sweeney GE. 2001. Characterization of a sea bream (*Sparus aurata*) thyroid hormone receptor-β clone expressed during embryonic and larva development. *Gen Comp Endocrinol*, **123**(1): 80-89.

Park EJ, Jeon CH and Ko G. 2000. Protective Effect of Curcumin in Rat Liver Injury Induced by Carbon tetrachloride. *J Pharm Pharmacol*, **52**:437-440.

Rahman K. 2007. Studies on free radicals, antioxidants, and co-factors. *Clin Interv Aging*, **2**(2):219-236.

Sewerynek E, Reiter RJ, Melchiorri D, Ortiz GG and Lewinski A. 1996. Oxidative damage in the liver induced by ischemia-reperfusion: protection by melatonin. *Hepato-gastroenterology*, **43**(10):898-905.

Sharma RA, Gescher AJ and Steward WP. 2005. Curcumin: The story so far. *Eur J Cancer*, **41**: 1955-1968.

Singh RP, Murthy KNC and Jayaprakasha GK. 2002. Studies on the antioxidant activity of pomegranate (*Punica granatum*) peel and seed extracts using in vitro models. *J Agric Food Chem*, **50**:81-86.

Sullivan CV and Yilmaz O. 2018. **Vitellogenesis and yolk proteins, fish**. *Encyclopedia of Reproduction, Second Edition*. Elsevier Inc.

Syano K, Saito T, Nagae M and Yamauchi K. 1993. Effect of thyroid hormone on gonadotropin-induced steroid production in medaka, *Oryzias latipes*, ovarian follicles. *Fish Physiol Biochem*, **11**: 265-272

Tata JR. 1979. Control by oestrogen of reversible gene expression: The vitellogenin model. *J Steroid Biochem* **11**:361-371.

Valko M, Leibfritz D, Moncol J, Cronin MT, Mazur M and Telser J. 2007. Free radicals and antioxidants in normal physiological functions and human disease. *In. J Biochem Cell Biol*, **39**(1):44-84.

Visser TJ. 1980. Deiodination of thyroid hormone and the role of glutathione. *Trends Biochem Sci*, **5**(8):222-224.

Watson RR. 2002. **Eggs and Health Promotion**. Iowa State Press.

Zhao SG, Li Q, Liu ZX, Wang JJ, Wang XX, Qin M and Wen QS. 2011. Curcumin attenuates insulin resistance in hepatocytes by inducing Nrf2 nuclear translocation.*Hepato-gastroenterology*, **58**(112):2106-2111.

JJBS

Volume 14, Number 1, March 2021
ISSN 1995-6673
Pages 129 - 135

Jordan Journal of Biological Sciences

Life History Traits of the Gangetic scissortail rasbora, *Rasbora rasbora* (Hamilton, 1822) in the Payra River, Southern Bangladesh

Newton Saha[1,*], Mohaiminul Haque Rakib[2], Md. Mahamudul Hasan Mredul[3], Md. Arifur Rahman[4] and Ferdous Ahamed[1]

[1]*Department of Fisheries Management, Patuakhali Science and Technology University, Dumki, Patuakhali-8602, Bangladesh,*[2]*Faculty of Fisheries, Patuakhali Science and Technology University, Patuakhali, Bangladesh,*[3]*Department of Aquaculture, Patuakhali Science and Technology University, Dumki, Patuakhali-8602, Bangladesh,*[4]*Department of Fisheries Biology and Genetics, Patuakhali Science and Technology University, Dumki, Patuakhali-8602, Bangladesh*

Received Feb 16, 2020; Revised July 25, 2020; Accepted July 25, 2020

Abstract

The near threatened gangetic scissortail rasbora, *Rasbora rasbora* (Hamilton, 1822), is an economically important, and nutritionally valuable freshwater food fish in south Asian countries. The present study provides the first inclusive explanation on life-history traits of *R. rasbora* in the Payra River, southern Bangladesh. This species invites research interest due to its nutritional demand and IUCN red list status. Sampling was carried out using different traditional fishing gears during July to December 2019. For each individual, total length (TL) and standard length (SL) were measured to the nearest 0.01 cm using digital slide caliper, while body weight (BW) was taken by an electronic balance with 0.01 g accuracy. A total of 215 specimens were measured ranging from 2.6-12.5 cm TL and 0.22- 10.65 g BW during this study. The 4.00 to 4.99 cm TL was numerically leading group of the total population. The allometric coefficient (*b*) of the length-weight relationships (*LWRs*) indicates negative allometric growth pattern (b<3.00) for *R. rasbora* in the Payra River. The results also indicate that the *LWRs* were highly significant (p<0.001) with r^2 values >0.963. In addition, The *LLR* (SL *vs.* TL) was highly significant (*p<0.0001*) with a coefficient of determination values of 0.988. The estimated form factor ($a_{3.0}$) was 0.007 indicating this fish is elongated in body shape and the size at first sexual maturity (L_m) for combined sexes of *R. rasbora* was calculated as 7.96 (~8.00) cm TL in the Payra River. The allometric condition factor (K_A) varied from 0.0063 to 0.0570 and Fulton′s condition factor (K_F) varied from 0.3933 to 4.1844. However, K_F tended to be lower after 9.0 cm for combined sexes, which may indicate the start of sexual maturation and therefore L_m could be around 8.0 cm TL for *R. rasbora*. The knowledge about the biological aspects of gangetic scissortail rasbora may be used for improved management tools in the future.

Keywords: *Rasbora rasbora*, Growth pattern, Conditions, Size at first sexual maturity, Payra River.

1. Introduction

Cyprinidae is the largest and most diverse fish family and the largest vertebrate animal family in general, with about 3,000 species of which only 1,270 remain extant, divided into about 370 genera (Froese and Pauly, 2015). The family belongs to the ostariophysian order Cypriniformes, of whose genera and species the cyprinids make up more than two-thirds. *Rasbora rasbora* (Hamilton, 1822) is a member of family Cyprinidae commonly known as Gangetic scissortail rasbora. Apparently, it is native to Bangladesh, India (Gangetic provinces and Assam), Myanmar, Pakistan and Thailand (Talwar and Jhingran, 1991). It is a surface feeder fish (IUCN Bangladesh, 2015). In Bangladesh, *R. rasbora* is commonly known as darkina/leuzzadarkina of the important small indigenous fish (SIS) species. Being a small indigenous fish species, *R. rasbora* is well-regarded as a quality food containing high amount protein, fat, carbohydrate, calcium and vitamins that helps to eliminate malnutrition, particularly for poor women and children in Bangladesh (Thilsted *et al*., 1997; Ross *et al.*, 2003). In addition, it can also be used as an aquarium fish (Froese and Pauly, 2015). The large numbers of small fish species are still available in southern water bodies amongst them, *R. rasbora* locally known as darkina/ kan chela is one of important ones. The Payra River (southern Bangladesh) is considered as an important natural spawning and nursery grounds for many commercially important fish species and a significant portion of the country's fisheries production is dependent on this coastal river (Islam *et al.*, 2015). Nonetheless, the untamed population of this species is waning due to overfishing, reckless fishing of larvae and juveniles, habitat destruction (siltation), pollution and other ecological changes to their surroundings (Islam *et al.*, 2015; Hossen *et al*., 2015; Hossain *et al.*, 2016, 2015) and afterward categorized as near threatened in Bangladesh (IUCN Bangladesh, 2015) although globally categorized as least concern (IUCN, 2019). Hence, there is an urgent need to manage and regulate its numerous

* Corresponding author e-mail: newtonsaha@pstu.ac.bd.

discrete stocks, which will require basic population dynamics information for the species (Santos *et al.*, 1995).

Usually, studies of length-frequency distribution (*LFD*) express the life-history traits and ecology of fishes (Ranjan *et al.*, 2005). In addition, length-weight relationships (*LWRs*) are considered as a useful tool in fisheries studies for the estimation of weight, biomass, and condition indices (Anderson and Gutreuter, 1983; Froese, 2006; Froese *et al.*, 2019). Moreover, condition factors assist evaluate the status of fish from which the present and future population success can be predetermined (Richter, 2007; Rypel and Richter, 2008).

This is believed to be the first report on biological aspects of this population in this region. However, sufficient information on this species is still now absent in the literature from Bangladeshi waters or elsewhere which attracted our attention. Therefore, the current study provides a complete and informative depiction of the life history traits of *R. rasbora* – including *LFD*, *LWRs*, *LLR*, form factor ($a_{3.0}$), size at first sexual maturity (L_m) and condition factors (allomatric, K_A; Fulton's, K_F; relative, K_R) from the Payra River, southern Bangladesh using many specimens of small to large sizes over a period of six months.

2. Materials and Methods

2.1. Study Area and Sampling:

The present study was carried out in the Payra River (Fig. 1), a southern coastal river of Bangladesh situated in the Patuakhali district (straddling 22º 35´ N and 90º 26´ E). A total of 215 specimens of *R. rasbora* were collected occasionally from that region over the period from July to December-2019, using different types of fishing gears; gill net (mesh size: 1.5–2.5 cm), square lift net (mesh size ~1.0 cm) and cast net (mesh size: 1.0–2.0 cm). Fish samples were quickly chilled in ice on site and then preserved in 10% buffered formalin in laboratory until examination. For each specimen, lengths (total length, TL and standard length, SL) were measured by digital slide caliper (Mitutoyo, CD-6"CSX), and the body weight (BW) was measured using an electronic balance (AND, FSH, Korea), to the nearest 0.01cm and 0.01 g precision, respectively.

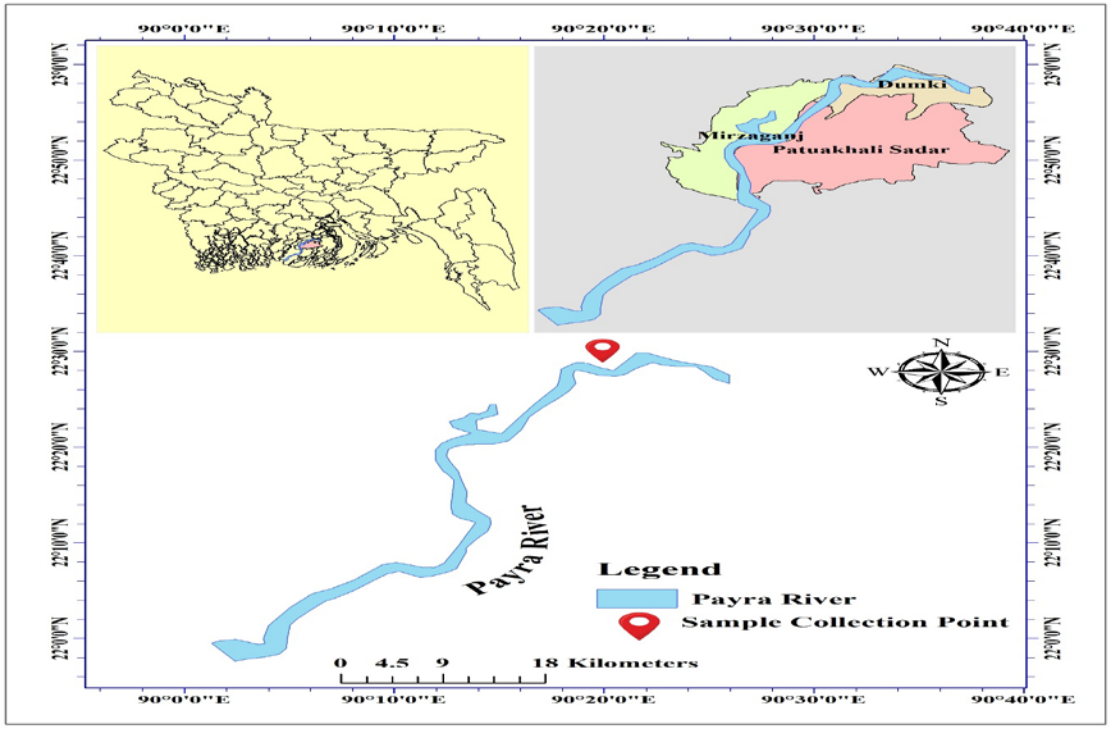

Figure 1. Map showing location of the study area for *R. rasbora* in the Payra River, southern Bangladesh.

2.2. Length Frequency Distribution (LFD):

LFD for total population of *R. rasbora* was constructed using 1.0 cm intervals of TL.

2.3. Length-weight Relationships and Length-length Relationship (LWRs and LLR):

The relationship between length and weight was calculated using expression: $W = aL^b$ (Le Cren, 1951) where the W is the whole body weight (g), L the total length (cm), *a* intercept of the regression and *b* is the regression coefficient (slope). The parameters *a* and *b* of the weight-length relationship will be estimated by linear regression analysis based on natural logarithms: ln (W) = ln (*a*) + *b* ln (L) (Frose, 2006; Hossain *et al.*, 2016a). According to Froese (2006), all extreme outliers were excluded from the analyses. A t-test was applied to determine significant differences from the isometric value (*b*= 3.0 for length-weight relationship and *b* = 1.0 for length-length relationship) (Sokal and Rohlf, 1987). Deviation of the *b* value from the theoretical isometric value indicates either positive (*b* > isometric value) or negative (*b* < isometric value) allometric growth. Analysis of covariance (ANCOVA) (Zar, 1984) was used to test for significant differences in slopes and intercepts among the relationships. Additionally, the *LLR* for SL *vs.* TL was estimated by linear regression analysis (Hossain *et al.*, 2006).

2.4. Form Factor ($a_{3.0}$):

The form factor ($a_{3.0}$) of *R. rasbora* was estimated using the equation of Froese (2006) as: $a_{3.0} = 10^{\log a - s(b-3)}$, where *a* and *b* are the regression parameters of *LWR*, and is the regression slope of *ln a vs. b*. The researchers used a mean slope S = -1.358 (Froese, 2006) for calculating the form factor because there was no available information on LWR for this species to estimate the regression (S) of *ln a vs. b*.

2.5. Size at First Sexual Maturity (L_m):

The size at first sexual maturity (L_m) of *R. rasbora* was calculated using the equation proposed by Binohlan and Froese (2009) as: $\log(L_m) = -0.1189 + 0.9157 \times \log(L_{max})$; where, L_m = size at first sexual maturity in TL, L_{max} = maximum length (TL) of *R. rasbora* in the present study. Furthermore, the maximum length of *R. rasbora* was obtained from available literature in the FishBase used to estimate L_m for water bodies throughout the world.

2.6. Condition Factor:

The allometric condition factor (K_A) was calculated by the equation of Tesch (1971): W/L^b, where *W* is the body weight (g), *L* is the TL (cm), and *b* is the LWR parameter. Fulton′s condition factor (K_F) was estimated using the equation of Fulton (1904): $K_F = 100 \times (W/L^3)$, where *W* is the body weight (g), and *L* is the TL in cm. The scaling factor of 100 was used to bring the K_F close to unit (Froese, 2006). In addition, the relative condition factor (K_R) was analyzed following the equation of Cren (1951): $K_R = W/(a \times L^b)$, where *W* is the body weight (g), *L* is the total length (cm), and *a* and *b* are *LWR* parameters.

2.7. Statistical Analysis:

For statistical analysis, Microsoft® Excel-add-in DDXL and GraphPad Prism 8 software were used. The Spearman rank-correlation test was applied to analyze the relationship of condition factors with TL and BW. All statistical analyses were considered significant at 5% ($p<0.05$).

3. Results

3.1. Length Frequency Distribution (LFD)

During the study period a total of 215 specimens of *R. rasbora* were collected from the Payra River, southern Bangladesh. The length frequency distribution of *R. rasbora* is shown in (Figure 2). Table 1 shows the descriptive statistics of maximum and minimum length and weight measurement of *R. rasbora*. *LFD* showed that the range of TLs was 2.6 to 12.5 cm (Fig. 2), and that body weight ranged from 0.22 to 10.65 g there. The 4.00 to 4.99 cm TL size group was numerically dominant and constituted 41.86% of the total population (Figure 2).

Table 1. Length (cm) and weight (g) measurements of combined sexes of *Rasbora rasbora* (Hamilton, 1822) from the Payra River, southern Bangladesh, July 2019 to December 2019.

Measurement	Total	Min	Max	Mean±SD
Total length (TL)		2.6	12.5	5.58±2.34
Standard length (SL)	215	2.4	10.5	4.40±1.99
Body weight (BW)		0.22	10.65	2.30±3.12

n, sample size; Min, minimum; Max; maximum and SD, standard deviation

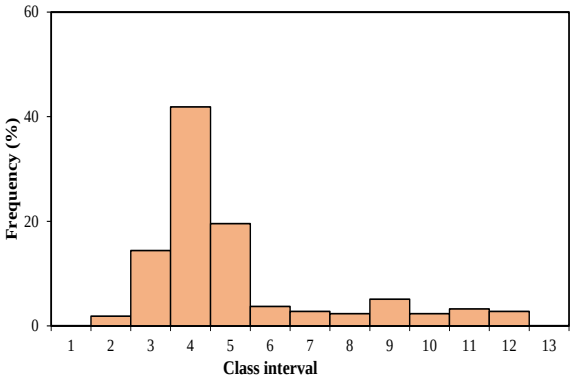

Figure 2. Total length frequency distribution of *R. rasbora* in the Payra River, southern Bangladesh.

3.2. Length -Weight Relationships (LWRs)

The sample size (*n*), regression parameter, 95% confidence interval of *a* and *b*, coefficient determination (r^2), and growth type (*GT*), of *R. rasbora* are shown in Table 2. In the present study, the calculated allometric coefficient (b=2.79) and t-test value (t_s=-7) of TL *vs.* BW indicates a negative allometric growth pattern (Figure 3), as did the SL-BW relationship (Table 2 and Figure 4) in the Payra River. The *LWRs* were highly significant ($p<0.0001$) with r^2 values >0.963.

Table 2. Descriptive statistics and estimated parameters of the length–weight and length-length relationships of *R. rasbora* (Hamilton, 1822) from the Payra River, southern Bangladesh.

Species	n	Regression parameters		95% CI of *a*	95% CI of *b*	r^2	GT
		a	b				
BW = $a*TL^b$	215	0.0120	2.79	0.011 to 0.014	2.726 to 2.862	0.969	A-
BW = $a*SL^b$		0.0290	2.66	0.026 to 0.032	2.604 to 2.747	0.963	A-
TL=$a+b*$SL		0.441	1.169	0.355 to 0.525	1.151 to 1.186	0.988	A+

n, sample size; TL, total length; SL, standard length; BW, body weight; *a*, intercept; *b*, slope; *CI*, confidence interval; r^2, coefficient of determination; GT, growth type; A-, negative allometric; A+, positive allometric.

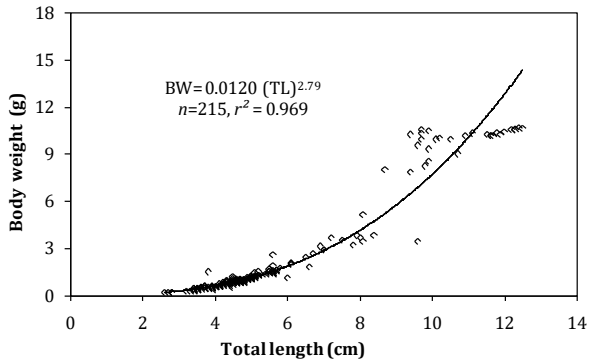

Figure 3. Total length-body weight relationship of *R. rasbora* in the Payra River, southern Bangladesh.

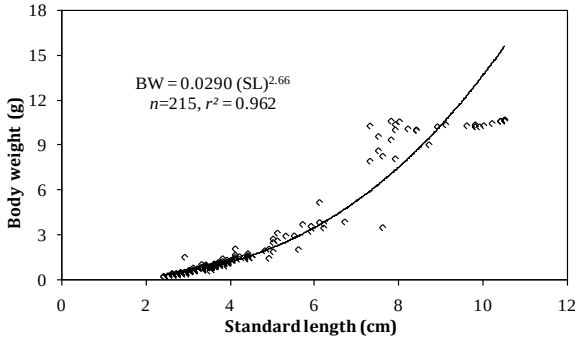

Figure 4. Standard length-body weight relationship of *R. rasbora* in the Payra River, southern Bangladesh.

3.3. Length-length Relationship (LLR)

The length-length relationship between TL and SL of *R. rasbora* along with the estimated parameters of the *LLR* and the coefficient of determination (r^2), are shown in Table 2 and Figure 5. During this study, the calculated allometric coefficent (b=1.16) and t-test value (t_s=20) of the *LLR* indicates positive allometric growth pattern. The *LLR* was highly significant ($p<0.0001$) with a coefficient of determination values of 0.988.

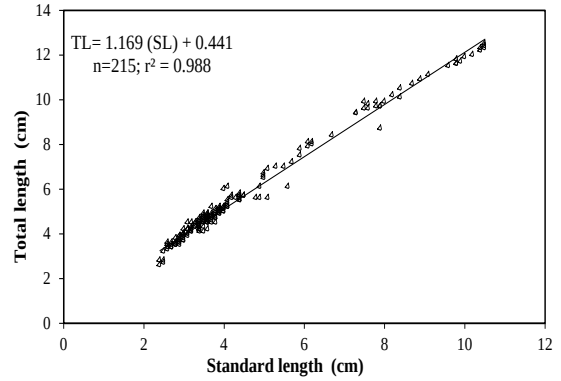

Figure 5. Total length-standard length relationship of *R. rasbora* in the Payra River, southern Bangladesh.

3.4. Form Factor ($a_{3.0}$)

The $a_{3.0}$ was calculated as 0.007 for combined sex of *R. rasbora* in the Payra River, southern Bangladesh, and this value indicates that this fish is elongated in shape.

3.5. Size at First Sexual Maturity (L_m)

Size at first sexual maturity for combined sex of *R. rasbora* was estimated as 7.96 (~8.00) cm TL in the Payra River.

3.6. Condition Factors

3.6.1. Allometric Condition Factor (K_A)

The estimated K_A of *R. rasbora* ranged from 0.0063-0.0570 (Mean ±SD, 0.0128±0.0040) (Table 3). According to Spearman rank-correlation tests, there was a significant relationship between BW *vs.* K_A (r_s= 0.2219, p = 0.0011), but not between TL *vs.* K_A (r_s= 0.0532, p = 0.4375) (Table 4).

Table 3. Condition factors of *R. rasbora* (Hamilton, 1822) in the Payra River (southern Bangladesh).

Condition factors	Min	Max	Mean±SD
Allometric condition factor (K_A)	0.0063	0.0570	0.0128±0.0040
Fulton's condition factor (K_F)	0.3933	4.1844	0.9110±0.2968
Relative condition factor (K_R)	0.5223	4.7535	1.0638±0.3329

Min, minimum; Max, maximum; SD, standard deviation

Table 4. Ralationships of condition factor with total length (TL) and body weight (BW) of *R. rasbora* (Hamilton, 1822) in the Payra River, southern Bangladesh.

Relationship	r_s value	95% CL of r_s	p values	Significance
TL *vs.* K_A	0.05322	-0.08511 to 0.1895	0.4375	*ns*
TL *vs.* K_F	-0.2354	-0.3614 to -0.1009	0.0005	***
TL *vs.* K_R	0.05312	-0.08522 to 0.1894	0.4384	*ns*
BW *vs.* K_A	0.2219	0.08682 to 0.3489	0.0011	**
BW *vs.* K_F	-0.0611	-0.1971 to 0.07726	0.3727	*ns*
BW *vs.* K_R	0.2218	0.08673 to 0.3488	0.0011	**

TL, total length; BW, body weight; K_A, allometric condition factor; K_F; Fulton′s condition factor; K_R, relative condition factor; r_S, Spearman rank-correlation values; CL, confidence limit; p, shows the level of significance; *ns*, not significant; * significant; ** highly significant; ***very highly significant.

3.6.2. Fulton's Condition Factor (K_F)

The calculated K_F ranged from 0.3933-4.1844 (Mean ± SD, 0.9110±0.2968) (Table 3). According to Spearman rank-correlation tests, there was a significant relationship between TL *vs.* K_F (r_s= -0.2354, p = 0.4375), but not between BW *vs.* K_F (r_s= -0.0611, p = 0.3727) (Table 4). The lowest K_F value was found in the size of 12 cm, whilst the highest in 2 cm for both sexes. Furthermore, the K_F value started decreasing after 9.0 cm TL (Figure 6).

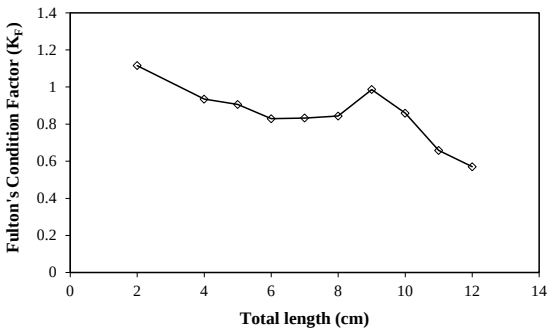

Figure 6. Fulton's condition factor (K_F) with regard to total length (cm) for *R. rasbora* in the Payra River, southern Bangladesh.

3.6.3. Relative Condition Factor (K_R)

The K_R of *R. rasbora* ranged from 0.5223-4.7535 (Mean ± SD, 1.0638±0.3329) during this study (Table 3). From Spearman rank-correlation tests, K_R showed a significant relationship with BW (r_s=0.2218, p =0.0011), but not with TL (r_s= 0.0531, p =0.4384) (Table 4).

4. Discussion:

According to the statement of the local fishers, this fish is mostly abundant during the summer (June-August) and autumn (September-October); other times they rarely found this species in the river which had made a great hindrance to collect fish sample from January to May. In our study, it was not possible to sample individuals of *R. rasbora* from January to May, for one or more of the following reasons: the biased selection of fishing gear or fishermen did not go where the fish were or possibly because of the fish's absence on the fishing grounds, and/or because fishermen discarded smaller fish (Rahman *et al.*, 2018) or the degradation of ecology of the Payra River, which signals the need for urgent measures to conduct extensive studies on these species to provide more information for their management and conservation.

In present study, it was not possible to collect the *R. rasbora* smaller than 2.6 cm, which was attributed to either the absence of small sized fishes (<2.6 cm TL) in the populations or the fishermen did not go where the smaller size exist (Azad *et al.*, 2018, Khatun *et al.*, 2018) or selectivity of fishing gears (Hossain *et al.*, 2012 a, b). Furthermore, the maximum length of *R. rasbora* within the Payra River was 12.5 cm TL which is slightly lower than the maximum recorded value of 13.0 cm TL (Froese and Pauly, 2019). Most likely, this growth differences can be attributed to differences in environmental factors, particularly water temperature and food availability (Ahamed and Othomi; 2012). Generally, maximum length is considered as a functional tool for fisheries resource planning and management, and is utmost for the determination of asymptotic length and growth coefficient of fishes (Hossain *et al.*, 2019; Khatun *et al.*,2019; Ahmed *et al.*, 2012; Hossain *et al.*, 2016b, 2017; Nawer *et al.*, 2017; Hossen *et al.*, 2016, 2018).

In the current study of *R. rasbora*, the estimated *b* values ranged from 2.67 to 2.79 for *LWRs* from the Payra River which were within the usual range (2.50 to 3.50) of *b* values for fishes (Carlander, 1969; Froese, 2006). To the best of our knowledge, no references dealing with *LWRs* for the studied species are available; thus it was not possible to compare the present results with previous references. Hence, the present study was compared with results from studies dealing with other species of the Cyprinid family. In this study, estimated *b* values of the *LWRs* (TL *vs.* BW; SL *vs.* BW) were <3 suggesting fish becomes more slender as the length increase for *R. rasbora* in the Payra River which was generally in agreement with results for fishes of same family and same genus (*R. daniconius*) obtained from the Sharavathi Reservoir, Karnataka (Kumar *et al.*, 2005). The length-weight relationship parameters (*a* and *b*) are influenced by a series of factors including season, habitat, gonad maturity, sex, diet, stomach fullness, health of the individuals in their natural habitats as well as the treatment of specimens and preservation techniques after sampling (Bagenal and Tesch, 1978; Tesch, 1971). However, *LLR* for the *R. rasbora* was highly correlated (r^2=0.988; $p<0.0001$). Since the current study is also the first assessment on LLR of *R. rasbora*, so lack of references dealing with *LLR* constrains the comparison of the present results with previous literature on the same population/ species.

Form factor ($a_{3.0}$) can help to determine whether the body profile of individuals in a particular population or species differs from others (Froese, 2006). The estimated $a_{3.0}$ for *R. rasbora* was within the limits 0.00775–0.00906 reported by Frose (2006); suggesting that this fish is elongated in shape in the Payra River. No references dealing with $a_{3.0}$ for this species are in the literature to make comparison across the water bodies.

Though most of the studies deal with single condition factor, we have, however, worked on three condition factors (K_A; K_F and K_R) to evaluate the physical and habitat status of *R. rasbora*. Furthermore, study on relative condition factor (K_R) in preference to the ponderal index (K) is recommended as the latter is generally influenced by many environmental and biological factors (Le Cren, 1951). The studied fish species has K_R >1, which indicates good general conditions of the fish (Le Cren, 1951). Generally, condition factor is influenced by many factors like sex, season, environmental factors, stress, gonadal development and availability of forage items (Lambert and Dutil, 1997; Zargar *et al.*, 2012; Ali *et al.*, 2014). Furthermore, the lowest K_F value was found in the size of 12 cm, whilst the highest in 2 cm for both sexes. The K_F with regard to length class showed a noticeable decrease after 9.0 cm for combined sexes, which might be attributed to the start of sexual maturation, as indicated in the present study, which recorded the size at first sexual maturity of *R. rasbora* as ~8.00 cm. Therefore, the size at first sexual maturity of *R. rasbora* could be around 8.0 cm TL in the Payra River, southern Bangladesh. Studies on L_m are very atypical (except Hossain et al., 2019, 2010, 2016a, 2017). This is the first study on size at first sexual maturity (L_m) for *R. rasbora* worldwide. Thus, our study will be the base for more thorough studies.

5. Conclusion:

The 4.00 to 4.99 cm TL size group (41.86%) was numerically dominant and fish becomes more slender as the length increases in the Payra River. The fish is elongated in body shape and ensures good general

conditions of the fish in the Payra River. The size at first sexual maturity of *R. rasbora* could be around 8.0 cm TL in the Payra River, southern Bangladesh. This study provides valuable information for the online Fish Base database, as well as providing an important baseline for future studies within the Payra River and surrounding ecosystems, as no information on the biological aspects of this species are currently available in the literature. Moreover, further detailed studies (with considering sampling period throughout the year) on spawning frequency and some other biological aspects, i.e. growth and abundance, are still necessary for the future management of this species.

Acknowledgements

We express our gratitude to (i) the local fishers of Payra (Patuakhali, southern Bangladesh) for collecting samples, and (ii) the Chairman (Department of Fisheries Management, Patuakhali Science and Technology University, Bangladesh) for use of the laboratory facilities.

Conflicts of Interest

The authors declare that there is no conflict of interest regarding the publication of this paper.

References

Ahamed F and Ohtomi J. 2012. Growth patterns and longevity of the pandalid shrimp *Plesionika izumiae* (Decapoda: Caridea). *J Crustacean Biol*. **32**:733 -740.

Ahmed ZF, Hossain MY and Ohtomi J. 2012. Modeling the growth of silver hatchet chela *Chela cachius* (Cyprinidae) from the Old Brahmaputra River in Bangladesh using multiple functions. *Zool Stud*, **51:** 336-344.

Ali S, Barat A, Kumar P, Sati J, Kumar R and Halder RS. 2014: Study of length weight relationship and condition factor for the Golden Mahseer, *Tor Putitora* from Himalayan rivers of India. *J. Environ. Biol.* **35(1):** 225-228.

Anderson RO and Gutreuter SJ. 1983. Length, weight, and associated structural indices. In: Nielsen L and Johnson D (Eds), **Fisheries Techniques**, Bethesda: American Fisheries Society. pp 284-300.

Azad MAK, Hossain MY, Khatun D, Parvin MF, Nawer F, Rahman O and Hossen MA. 2018. Morphometric relationships of the tank goby *Glossogobius giuris* (Hamilton, 1822) in the Gorai River using multi-linear dimensions. *Jordan J Biol Sci*, **11:** 81-85.

Bagenal TB and Tesch FW. 1978. **Age and growth. In methods for assessment of fish production in fresh waters,** 3rd ed. IBP Handbook No. 3, edited by Begenal, T. Oxford (UK): Blackwell Science Publications. pp. 101-136.

Binohlan C and Froese R. 2009. Empirical equations for estimating maximum length from length at first maturity. *J. Appl. Ichthyol.*, **25:**611-613.

Carlander KD. 1969. **Handbook of Freshwater Fishery Biology**. Vol:1. The Iowa State University Press. Ames, IA, 752 p.

Froese R and Pauly D, editors. 2019: Rasbora trilineata Steindachner, 1870. FishBase. Available: https://www.fishbase.de/summary/Rasbora-trilineata.html. (February 2019).

Froese R, Pauly D, eds. 2015: "Cyprinidae" in FishBase. July 2015 version.

Froese R. 2006. Cube law, condition factor and weight-length relationships: History, meta-analysis and recommendations. *J Appl Ichthyol*, **22**: 241-253.

Fulton TW. 1904. The Rate of Growth of Fishes. Twenty-second Annual Reports, Part III. Fisheries Board of Scotland, Edinburgh, 141-241 pp.

Hossain MY, Rahman MM, Miranda R, Leunda PM, Oscoz J, Jewel MAS, Naif A and Ohtomi J. 2012a. Size at first sexual maturity, fecundity, length– weight and length–length relationships of *Puntius sophore* (Cyprinidae) in Bangladeshi waters. *J. appl. Ichthyol.*, **28:** 818-822.

Hossain MY, Ahmed ZF, Islam ABMS, Jasmine S and Ohtomi J. 2010. Gonadosomatic index-based size at first sexual maturity and fecundity indices of the Indian River shad *Gudusia chapra* (Clupeidae) in the Ganges River (NW Bangladesh). *J Appl Ichthyol*, **26**: 550-553.

Hossain MY, Ahmed ZF, Leunda PM, Islam AKMR, Jasmine S, Scoz J, Miranda R and Ohtomi J. 2006. Length-weight and length-length relationships of some small indigenous fish species from the Mathabhanga River, southwestern Bangladesh. *J Appl Ichthyol*, **22**: 301-303.

Hossain MY, Hossen MA, Khatun D, Nawer F, Parvin MF, Rahman O and Hossain MA. 2017. Growth, condition, maturity and mortality of the Gangetic leaffish *Nandus nandus* (Hamilton, 1822) in the Ganges River (northwestern Bangladesh). *Jordan J Biol Sci*, **10:** 57-62.

Hossain MY, Islam R, Hossen MA, Rahman O, Hossain MA, Islam MA and Alam MJ. 2015. Threatened fishes of the world: *Mystus gulio* (Hamilton, 1822) (Siluriformes: Bagridae). *Croatian J. Fish.*, **73:** 43-45.

Hossain MY, Naser SMA, Bahkali AH, Yahya K, Hossen MA, Elgorban AM, Islam MM and Rahman MM. 2016a. Life History Traits of the Flying Barb *Esomus danricus* (Hamilton, 1822) (Cyprinidae) in the Ganges River, Northwestern Bangladesh. *Pakistan J. Zool.*, **48(2):** 399-408.

Hossain MY, Rahman MM and Abdallah EM. 2012b. Relationships between body size, weight, condition and fecundity of the threatened fish *Puntius ticto* (Hamilton, 1822) in the Ganges River, Northwestern Bangladesh. *Sains Malay.*, **41**: 803-814.

Hossain MY, Rahman MM, Bahkali AH, Yahya K, Arefin MS and Hossain MI. 2016b.Temporal variations of sex ratio, length-weight relationships and condition factor of *Cabdio morar* (Cyprinidae) in the Jamuna (Brahmaputra River distributary) River, northern Bangladesh. *Pakistan J Zool*, **48**: 1099-1107.

Hossen MA, Hossain MY, Pramanik MNU, Khatun D, Nawer F, Parvin MF, Arabi A and Bashar MA. 2018. Population Parameters of the Minor carp *Labeo bata* (Hamilton, 1822) in the Ganges River of northwestern Bangladesh. *Jordan J Biol Sci*, **11:** 179-186.

Hossen MA, Hossain MY, Pramanik MNU, Nawer F, Khatun D, Parvin MF and Rahman MM. 2016. Morphological characters of *Botia lohachata*. *J Coast Life Med*, **4:** 689-692.

Hossen MA, Hossain MY, Yahya K and Pramanik MNU. 2015. Threatened fishes of the world: *Labeo bata* (Hamilton, 1822) (Cypriniformes: Cyprinidae). Croatian J. Fish., **73:** 89-91.

Islam MA, Hossain MM, Ahsan ME and Nahar A. 2015. Status and current worries of fish diversity in the Payra River, Patuakhali, Bangladesh. *Int. J. Fish. Aquat. Stud*. **2(3):** 160-165.

IUCN 2019. **IUCN Red List of Threatened Species**. Version 2019-2. IUCN Red List of Threatened Species. Downloaded on 23 July 2019.

IUCN Bangladesh. 2015. **Red List of Bangladesh Volume 5: Freshwater Fishes.** IUCN, International Union for Conservation

of Nature, Bangladesh Country Office, Dhaka, Bangladesh, xvi+360 p.

Khatun D, Hossain MY, Parvin MF and Ohtomi J. 2018. Temporal variation of sex ratio, growth pattern and physiological status of *Eutropiichthys vacha* (Schilbeidae) in the Ganges River, NW Bangladesh. *Zool Ecol*., **28:** 343-354.

Khatun D, Hossain MY, Rahman MA, Islam MA, Rahman O, Azad MAK, Sarmin MS, Parvin MF, Haque ATU, Mawa Z and Hossain MA. 2019. Life-history traits of the climbing perch *Anabas testudineus* (Bloch, 1792) in a wetland ecosystem. *Jordan J Biol Sci*, **12**: 175-182.

Kumar KH, Kiran BR, Purushtham R, Puttaiah ET and Manjappa S. 2005. Length-weight relationship of cyprinid fish, *Rasbora daniconius* (Hamilton-Buchanan) from Sharavathi Reservoir, Karnataka. *Zoos Print J.*, **21(1):** 2140-2141.

Lambert Y and Dutil JD. 1997. Can simple condition indices be used to monitor and quantify seasonal changes in the energy reserves of Atlantic cod (*Gadus morhua*).*Can J Fish Aquat Sci*, **54 (1):** 104-112.

Le Cren ED. 1951. The Length-Weight Relationship and Seasonal Cycle in Gonad Weight and Condition in the Perch (*Perca fluviatilis*). *J Anim Ecol*, **20(2)**, 201-219.

Nawer F, Hossain MY, Hossen MA, Khatun D, Parvin MF, Ohtomi J and Islam MA. 2017. Morphometric relationships of the endangered ticto barb *Pethia ticto* (Hamilton, 1822) in the Ganges River (NW Bangladesh) through multi-linear dimensions. *Jordan J Biol Sci*, **10**: 199-203.

Rahman MM, Hossain MY, Jewel MAS, Billah MM and Ohtomi J. 2018. Population biology of the pool barb *Puntius sophore* (Hamilton 1822) (Cyprinidae) in the Padma River, Bangladesh. *Zool Ecol*, **28:** 100-108.

Ranjan JB, Herwig W, Subodh S and Michael S. 2005. Study of the length frequency distribution of sucker head, *Garragotyla gotyla* (Gray, 1830) in different rivers and seasons in Nepal and its applications. *Kathmandu Univ J Sci Eng and Technol*, **1:** 1-14.

Richter TJ. 2007. Development and evaluation of standard weight equations for bridgelip suckers and large scale suckers. *N Am J Fish Manag*, **27**: 936-939.

Ross N, Islam M and Thilsted SH. 2003. Small indigenous fish species in Bangladesh: contribution to vitamin A, calcium and iron intakes. *J. Nutr.* **133**:4021–4026.

Rypel AL and Richter TJ. 2008. Empirical percentile standard weight equation for the blacktail redhorse. *N Am J Fish Manag*, **28**: 1843-184.

Santos RS, Hawkins S, Monteiro LR, Alves M and Isidro EJ. 1995. Case studies and reviews. Marine research, resources and conservation in the Azores. Aquatic Conservation: Marine and Freshwater Ecosystem. **5**:311–354.

Sokal RR and Rohlf FJ. 1987. **Introduction to Biostatistics**, 2nd edn. Freeman Publication, New York, 225-227 pp.

Talwar PK and Jhingran AG. 1991. **Inland fishes of India and adjacent countries**, vol. 1. Oxford & IBH Publishing Co Pvt Ltd, New Delhi-Calcutta.pp. 542.

Tesch FW. 1971: **Age and growth. In Methods for Assessment of Fish Production in Fresh Waters,** edited by Rcker, W.E. Oxford: Balckwell Scientific Publications. pp. 99-130.

Thilsted SH, Roos N, Hasan N. 1997. The role of small indigenous fish species in food and nutrition security in Bangladesh. NAGA Newsletter, July–Dec. p. 13.

Zar JH. 1984. **Biostatistical Analysis,** 2nd Edn., Prentice-Hall Inc., Englewood Cliffs, New Jersey, USA.

Zargar UR, Yousuf AR, Mustaq B and Jain D. 2012. Length–weight relationship of the crucian carp, *Carassius carassius* in relation to water quality, sex and season in some lentic water bodies of Kashmir Himalayas. *Turk J Fish Aquat Sci.* **12:** 683–689.

JJBS

Volume 14, Number 1, March 2021
ISSN 1995-6673
Pages 137 - 146

Jordan Journal of Biological Sciences

Vegetative Morphological Variations within Some Egyptian *Amaranthus* L. Species

Wafaa K. Taia*, Azza A. Shehata, Manaser M. Ibrahim and Islam M. El-Shamy

[1]*Faculty of Science, Botany and Microbiology Department, Alexandria University, Alexandria, Egypt*

Received: November 8, 2019; Revised: January 14, 2020; Accepted: February 1, 2020

Abstract

Leaf and stem vegetative morphological characters have been studied in ten Egyptian *Amaranthus* species. Macro-and micro-morphological characters besides leaf venation and architecture have been studied. Twenty-seven main variable characters have been subjected as OTU's to numerical analysis. The resulted dendrograms (nearest neighbor, group average and farthest neighbor) divided the studied species into two categories with different subdivisions. From the most important morphological characters within the studied taxa are the places of red spot on the leaf surfaces and the type of leaf venation. These characters divided the studied taxa into two main groups: 1- the red spot; on the middle versus on the lower part of the leaf blades, 2- the leaf venation; reticulodromus versus brochidodromous.

Keywords : *Amaranthus*, Clustering analysis, Leaf characters, Macro-morphology, Micro-morphology, Stem characters, Venation.

1. Introduction

Genus *Amaranthus* L. is one of the widely distributed genera grown mainly in temperate and tropical climates, belonging to Amaranthaceae Juss., subfamily Amaranthoideae, tribe Amarantheae. Genus *Amaranthus* is the largest and has 70 annual or short lived perennial monoecious or dioecious species with worldwide distribution. It grows in roadsides, gardens and disturbed habitats with great morphological diversity between the species and even between individuals of the same species in response to environmental variables. *Amaranthus* has been faced with many opinions concerning species delimitation and identification since a long time ago. Thellung, (1914), Sauer, (1955), Aellen, (1961 and 1972), Cavaco, (1962) and Townsend, (1974 and 1985) have been faced with many difficulties in recognizing the different taxa while studying the morphological characters of the genus. Linnaeus, (1753) divided the genus into two groups; *Pentandri* and *Triandri* according to the number of stamens in the flower (which is the same as the number of perianth segments). This division of the genus has been accepted by Adanson, (1763) and Tournefort, (1794), while Dumortier, (1827) reclassified the *Amaranthus* species into two sections *Amaranthotypus* and *Blitopsis*, the former has monoecious plants with pentamerous flowers arranged in lax or dense spikes or panicles and circumscissile fruits. While section *Blitopsis* has dioecious plants with trimerous or pentamerous flowers arranged in axillary glomerules and has irregular ruptured indehiscent capsules.

Gordon, (1853) raised the inflorescence type to be a priori character in distinguishing the taxa under the genus and reclassified it into two subgenera; *Albersia* and *Euamaranthus.* And this reclassification has been accepted by both Kirschleger, (1857) and Bentham and Mueller, (1870), but they divided subgenus *Albersia* into three sections *Amblogyne*, *Euamaranthus*, and *Euxolus* according to the fruit whether bursts transversely or in an irregular manner or indehiscent. Afterward, Uline and Bray, (1894) classified the *Amaranthus* species into four groups; Amblogyne, Scleropus, Pyxidium, and Mega according to fruit characters. While Beck (1909) regrouped the *Amaranthus* species into three sections and Rouy, (1910) return back to the old classification of the species into two sections but renamed them *Euamaranthus* and *Pentrius*. Sauer, (1955), previously classified genus *Amaranthus* into two subgenera, differentiating only between monoecious and dioecious species, viz. *Amaranthus* and *Acnida* (L.) Aellen ex K. R. Robertson

The classification of *Amaranthus* is obscure due to the shortage of scrappy quantitative species-defining characteristics, besides the wide range of phenotypic flexibility, as well as introgression and hybridization involving weedy and crop species. This phenotypic variability led to nomenclature disorder and misapplication of names as seen in Mosyakin and Robertson, (1996), Costea *et al*., (2001) and Iamonico, (2009). Accordingly, the previous trials of classifications of the genus were faced with many difficulties in distinguishing and circumscription of the *Amaranthus* species. Mosyakin and Robertson, (1996) found that all the *Amaranthus* species must be divided into three subgenera; 1- *Acnida* (L.) Aellen ex K. R. Robertson with three sections; 2- *Albersia* (Kunth) Gren. and Godr. with four sections; and 3- *Amaranthus* with three sections and two subsections (Figure 1).

* Corresponding author e-mail: taia55taxonomy@hotmail.com.

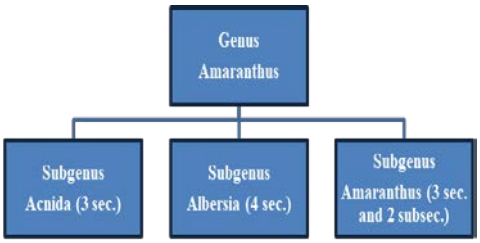

Figure 1. Mosyakin and Robertson (1996) division of *Amaranthus* species

Till now the classification of the genus is still a matter of controversy and faced with great arguments. This work has been carried out to investigate the variations within the *Amaranthus* species grown in Egypt. According to Täckholm, (1974) the genus was represented by fourteen annual species; El Hadidi and El Hadidi, (1980) reported 10 species with 5 subspecies and 5 varieties, while according to Boulos, (1999, 2009) the genus was represented by eleven annual, rarely perennial species and five subspecies. These taxa growing, either as weeds in the cultivated areas or wildly in the roadsides. Ten of these species can be obtained from the field and subjected to analysis in this study to increase knowledge about the morphological variability between the species in the local region.

2. Materials and Methods

Ten *Amaranthus* species were collected from the wild population in Alexandria and Cairo during the years 2015 and 2016. The ten studied species arranged according to the system of infra-generic classification of Mosyakin and Robertson, (1996), their different collection sources are cited in tables 1.and 2 The collected specimens were identified using Täckholm, (1974) and Boulos, (1999). Taxonomic authorities for Latin names and synonymy of the species investigated in this study were based on either the Australian plant name index (APNI), Gray card index (GCI) or Index Kewensis (IK). Voucher specimens were kept in the Faculty of Science, Alexandria University Herbarium (ALEX) for vegetative morphological measurements and any further inspection.

Table 1. *Infra-generic* classification of *Amaranthus* species used in the present study

Authors	Year	Characters	Ranks	Names	Further divisions
Linnaeus	1753	Perianth number	Groups	*Pentandri & Triandri*	--
Adanson	1763	Perianth number	Groups	*Pentandri & Triandri*	--
Tournefort	1794	Perianth number	Groups	*Pentandri & Triandri*	--
Dumortier	1827	Sex of plant	sections	*Amaranthotypus & Blitopsis*	--
Gorden	1855	Type of Inflorescence	Subgenera	*Albersia &Euamaranthus*	--
Kirschleger	1857	Type of Inflorescence & Fruit characters	Subgenera	*Albersia (3 sections) & Euamaranthus*	*Amblogene, Euamaranthus & Euxalus*
Bentham	1870	Type of Inflorescence & Fruit characters	Subgenera	*Albersia (3 sections) &Euamaranthus*	*Amblogene, Euamaranthus & Euxalus*
Uline and Bray	1894	Fruit	Sections	*Amblogyne, Scleropus, Pyxidium & Megea*	--
Beck	1909	Fruit	Sections	*Amblogene, Euamaranthus & Euxalus*	--
Rouy	1910	Perianth parts	Sections	*Euamaranthus & Pentrius*	--
Sauer	1955	Sex of plant	Subgenera	*Acnida & Amaranthus*	--
Mosyakin and Robertson	1996	Sex of plant & Inflorescence	Subgenera	*Acnida, Amaranthus* & *Albersia*	*Acnida* = 3 sections *Amaranthus* = 3 sections & 2 subsections *Albersia* = 4 sections

Table 2. Data of *Amaranthus* species collected in the present study and its taxonomic category after Mosyakin and Robertson, (1996)

No.	Species	Collection	Locations	Subgenus	Sections	Sub- Sections
1	*A. albus* L.	12 Jan. 2016,Wafaa Taia	Madinati,Cairo	*Albersia (Kunth) Gren. & Godr*	*Pyxdium oquin* in DC.	--
2	*A. blitiodes* S. Watson	11 Aug. 2015, Azza Shehata & Eslam El-Shamy	Fac. Agric., El-Shatby, Alexandria	*Albersia (Kunth) Gren. & Godr*	*Pyxdium oquin* in DC.	--
3	*A. caudatus* L.	11 Nov. 2015, Wafaa Taia	Madinet Nasr, Cairo.	*Amaranthus*	*Amaranthus*	*Amaranthus*
4	*A. graecizans* L.	12 Dec. 2015, Wafaa Taia	. Smouha, Alexandria	*Albersia (Kunth) Gren. & Godr*	*Pyxdium Moquin* in DC.	--
5	*A. hybridus* L.	15 Nov. 2015, Azza Shehata & Eslam El-Shamy	Fac. Of Sci., El-Shatby, Alexandria	*Amaranthus*	*Amaranthus*	*Hybrida*
6	*A. lividus* L.	1 Oct. 2015, Azza Shehata & Eslam El-Shamy	Fac. Of Sci., El-Shatby, Alexandria	*Albersia (Kunth) Gren. & Godr*	*Blitopsis Dumort*	--
7	*A. retroflexus* L.	14 Oct. 2015, Azza Shehata & Eslam El-Shamy	Fac. Of Sci., El-Shatby, Alexandria	*Amaranthus*	*Amaranthus*	*Amaranthus*
8	*A. spinosus* L.	22 Oct. 2015, Azza Shehata & Eslam El-Shamy	Al-Agamy, Alexandria	*Amaranthus*	*Centrusa Griseb*	--
9	*A. tricolor* L.	10 Jun. 2015, Wafaa Taia	Al-Saha Square, Madinet Nasr, Cairo.	*Albersia (Kunth) Gren. & Godr*	*Pyxdium Moquin* in DC.	--
10	*A. viridis* L.	1 Oct. 2015, Manaser Ibrahim	Smouha, Alexandria	*Albersia (Kunth) Gren. & Godr*	*Blitopsis Dumort*	--

Stem color and habits were noticed in the field. At least ten individuals were used in this study, for morphological measurements and examinations. The fourth interned leaves from ten individuals in each species were subjected to measurements. For epidermal cell investigation using LM, fresh leaves were collected from each plant samples, painted with fingernail polish on both the abaxial and adaxial surfaces and allowed to dry. After drying, short clear cellophane tape was firmly pressed over the dried nail polish on the surfaces according to the method of Mbagwu *et al.,* (2008). Epidermal strips were taken from the median portion of matured leaves stained in alcoholic safranin and mounted in 50% glycerin jelly for microscopic examination. Photographs of good preparations were taken at a magnification of X400 objective using the light microscope (Olympus CX 31 with its built in camera).

For leaf venation, fresh leaves were immersed in 70% ethyl alcohol for a few days with several changes of alcohol to remove chlorophyll pigments. Leaf samples were washed by water. Leaves were carefully brushed out to obtain leaf skeleton, examined and photographed using Olympus stereomicroscope. For SEM, dried leaves were fixed directly to the copper stub with double-sided adhesive tape at abaxial and adaxial surfaces and coated for 5 minutes with gold in polaron JFC-1100E coating unit, then examined and photographed with JEOL JSM-5300 SEM at the EM unit, Faculty of Science, Alexandria University. The terminology of the leaf was according to Stace, (1984), and Barthlot *et al.,* (1998) to describe the epidermal cell features and leaf venation.

The characters used for clustering analysis were chosen according to be of a fixed taxonomic value and not affected by any environmental conditions. Consequently, 27 characters represented in Appendix (1) have been subjected to this analysis using Systat 12 program.

3. Results

The general external morphology of the studied species was illustrated in plate 1. The results were summarized in tables 3, 4 and 5, plates 1, 2, 3 and 4. *Amaranthus* species are annuals; except *A. hybridus*, *A. lividus* and *A. viridis* are perennials. The stem takes different shades of green and sometimes tinged with pink; erect, procumbent or prostrate. The stem has different length and width, slender, angular or flattened with moderate to dense branches and either glabrous or covered with hairs in various densities (Table 3). The leaves are green, pale green or tinged with red or reddish purple; spiral or alternate. The leaves are ovate to lanceolate, with the broader part in the middle, except in both *A. hybridus A. lividus* and *A. viridis* the wider part in the lower part of the blade. All the studied species have hairy leaf surfaces with different densities; except *A. lividus* the leaves are glabrous. The hairs are mostly multicellular uniseriate glandular (Plate 4f), but in *A. blitoides* the hairs are multicellular uniseriate tabular (Plate 3e) and in *A. tricolor* the hairs are multicellular uniseriate pointed (Plate 4g). Multicellular biseriate hairs noticed in *A. retroflexus* only beside the multicellular uniseriate ones (table 4). The leaf blade venation is either reticulodromous or brochidodromous (Plate 2a and b), with different primary veins thickness. The secondary veins varied from 7 to 15, irregular or regular and in few species, they are wider at the leaf blade apex. The marginal veins are complete or incomplete with incomplete aeriolar veins except in *A. albus*, the aeriolar veins are closed (table 4).

Leaf micro-morphological characters were summarized in table 5. The epidermal cells as shown by LM and SEM have elongated and irregular shapes in the abaxial surfaces, while they are polygonal and irregular in the adaxial surfaces (plates 2, 3, and 4).

The anticlinal walls are straight and elevated in all the species, except in *A. graecizans*, *A. hybridus* and *A.*

tricolor the anticlinal walls are undulated (Plate 3g - j and Plate 4g and h). The ornamentation of the periclinal walls is mostly striate, rugate, wrinkled or papillate with few or dense epicuticular secretions, except in *A. graecizans*, *A. hybridus* and *A. lividus.* While in *A. blitoides* the periclinal walls are smooth with few granulate epicuticular secretions (Plate 3c and d). The stomata are anomocytic or anisocytic (Plate 2 c, d, f and g), raised in all the studied species in both the abaxial and adaxial surfaces, except in *A. blitoides* it is sunken in the adaxial surface (Plate 3d). Meanwhile, the stomata are diacytic (Plate 2e and h) and superficial in both the abaxial and adaxial surfaces in *A. lividus* (Plate 4a and b).

The most valuable morphological variations are subjected to numerical investigations by taking 27 characters as OUT's in the ten studies taxa and the obtained dendrograms showed that, the three dendrograms split the studied taxa into two groups (GI and GII) at dissimilarity matrix 3 in the farthest neighbor linkage (F.N.); 5.3 in group average (G.A.) and 3.5 in the nearest neighbor (N.N.). In the nearest neighbor linkage (Figure 2a) and farthest neighbor linkage (Figure 2c) the dendrograms coincide in the division of the taxa; as both of them gather the taxa number 5, 9, 7, 6, 10 and 3 in one group and the taxa number 2, 8, 1 and 4 in the second group at different dissimilarity matrices as shown in table 6. In group average linkage method (Figure 2b) the two taxa (9 and 5) were separated in a one group (GII) and the rest of the taxa in a second group (GI). The three dendrograms gathered both taxa (3 and 10) together at a similarity index 1.012. The F.N. and G.A. gathered the taxa 9 and 5 at dissimilarity index 1.745 and 2.292; and the taxa 2 and 8 at dissimilarity index 3.623 and 1.675, respectively (Table 6).

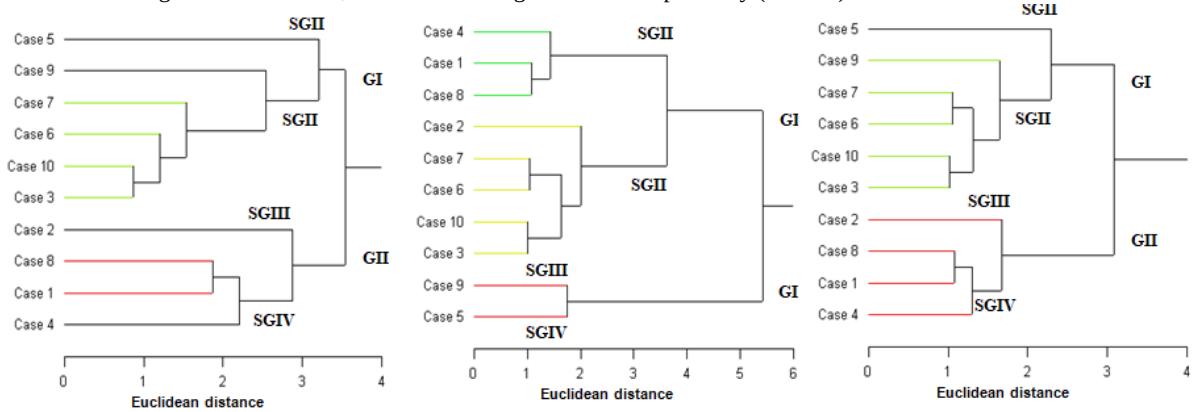

Figure 2a. Nearest neighbor linkage **Figure 2b.** Group average linkage **Figure 2c.** Farthest neighbor linkage

Figures 2a, b and c: Dendrograms showing the three possible relationships among the ten studied *Amaranthus* species using Euclidean distance method and; **a.** Nearest neighbor linkage, **b.** Group average linkage and **c.** Farthest neighbor linkage methods. Cases studied: 1. *A. albus* ; 2. *A. blitiodes* ; 3. *A. caudatus* ; 4. *A. graecizans* ; 5. *A. hybridus* ; 6. *A. lividus* ; 7. *A. retroflexus* ; 8. *A. spinosus* ; 9. *A. tricolor* and 10. *A. viridis.*

Table 3. Stem morphological characters of the studied *Amaranthus* species

No.	Species	Characters							
		Habit	Type	Length (cm)	Width (mm)	Shape	Color	Density of branches	Density of hairs
1	*A. albus*	Annual	Erect	17-30 (23.5±5.44)	0.2 – 0.4 (0.32±0.09)	Slender	Light green	Dense	Hairy
2	*A. blitiodes* Watson	Annual	Prostrate	25-35 (28.6±3.78)	0.1 - 0.2 (0.15±0.05)	Flattened	Greenish white	Moderate	Hairy
3	*A. caudatus*	Annual	Erect	30-40 (36.6±2.07)	0.2 - 0.5 (0.35±0.12)	Angular	Purple	Moderate	Hairy
4	*A. graecizans*	Annual	Procumbent	14-30 (20.5±6.8)	0.2 - 0.4 (0.3±0.08)	Angular	Red	Moderate	Sparsely hairy
5	*A. hybridus.*	Perennial	Erect	40-55 (47.4±7.16)	0.2 - 0.4 (0.32±0.09)	Angular	Green	Dense	Hairy
6	*A. lividus*	Perennial	Procumbent	20-39 (34.8±5.67)	0.1 - 0.3 (0.2±0.08)	Flattened	Green	Moderate	Hairy
7	*A. retroflexus*	Annual	Erect	35-40 (36.8±1.92)	0.2 - 0.4 (0.3±0.08)	Slender	Light Green	Moderate	Hairy
8	*A. spinosus*	Annual	Erect	15-30 (25±7.07)	0.3 - 0.6 (0.45±0.12)	Flattened	Green	Dense	Hairy
9	*A. tricolor*	Annual	Erect	39-45 (41±2.54)	0.2 - 0.3 (0.22±0.05)	Slender	Red	Moderate	Glabrous
	A. viridis	Perennial	Procumbent	27-40 (36.2±6.37)	0.2 - 0.4 (0.3±0.08)	Angular	Green or tinged purple	Moderate	Sparsely hairy

± = Standard deviation values

Table 4. Leaf macro-morphological characters of the studied *Amaranthus* species

No.	Species	Characters Arrangement	Color	Length (cm.)	Width (cm.)	Shape	Widest part	Spot	Surface	Hair type*
1	*A. albus*	Spiral	Pale Green	0.9-3.1 (2.25±1.02)	0.4-1.5 (0.97±0.45)	Lancolate	Middle	Middle	Sparsely hairy	MUG
2	*A. blitiodes* Watson	Alternate	Green with white spots	1-2.4 (1.94±0.65)	1-1.5 (1.32±0.16)	Ovate to Lancolate	Middle	Middle	Sparsely hairy	MUT
3	*A. caudatus*	Alternate	Green	4-4.5 (4.20±0.20)	1-2 (1.54±0.28)	Ovate to Lancolate	Middle	Middle	Hairy	MUG
4	*A. graecizans*	Alternate	Green tinged with red	1.8-3.8 (2.77±1.02)	1-1.9 (1.32±0.39)	Ovate to Lancolate	Middle	Middle	Sparsely hairy	MUG
5	*A. hybridus.*	Alternate	Green	2-5.9 (4.52±1.66)	1-4 (2.64±1.25)	Ovate	Lower	Lower	Wooly	MUG
6	*A. lividus*	Spiral	Green	1.5-4.5 (2.70±1.29)	1-3.5 (1.88±0.92)	Ovate	Lower	Lower	Glabrous	-
7	*A. retroflexus*	Alternate	Green tinged with red	3-3.5 (3.18±0.21)	1-1.5 (1.28±0.21)	Ovate to Lancolate	Middle	Middle	Hairy	MUG+ MBG
8	*A. spinosus*	Spiral	Green	2.5-6 (4.32±1.47)	2-3.8 (2.32±1.20)	Ovate to Lancolate	Middle	Middle	Hairy	MUG
9	*A. tricolor*	Alternate	Green or reddish purple	3-4 (3.54±0.36)	1-2 (1.54±0.36)	Ovate	Middle	Middle	Hairy	MUP
10	*A. viridis*	Alternate	Green tinged with purple	2-5.4 (3.60±1.47)	1-3.7 (2.58±0.94)	Ovate	Lower	Lower	Sparsely hairy	MUG

*****Hair types: MUG = Muticellular Uniseriate Glandular, MUT = Muticellular Uniseriate Tubular, MBG = Muticellular biseriate Glandular and MUP = Muticellular Uniseriate Pointed, ± = Standard deviation values.

Table 4 (Cont.) Leaf macro-morphological characters of the studied *Amaranthus* species

No.	Species	Characters					
		Types of venation	Size of 1^{ry} veins	Type of 2^{ry} veins		Marginal veins	Areolar Veins
				Spaces	No.		
1	*A. albus*	Reticulodromous	Moderate	Wide at apex	8	Incomplete	Closed
2	*A. blitiodes* Watson	Brochidodromous	Thin	Wide at apex	12	Incomplete	Incomplete
3	*A. caudatus*	Reticulodromous	Thick	Irregular	15	Incomplete	Incomplete
4	*A. graecizans*	Brochidodromous	Thick	Wide at base	7	Complete	Incomplete
5	*A. hybridus*	Brochidodromous	Thick	Wide at apex	11	Complete	Incomplete
6	*A. lividus*	Brochidodromous	Thick	Irregular	11	Incomplete	Incomplete
7	*A. retroflexus.*	Brochidodromous	Thick	Wide at apex	9	Complete	Incomplete
8	*A. spinosus*	Brochidodromous	Moderate	Irregular	11	Complete	Incomplete
9	*A. tricolor*	Reticulodromous	Thick	Irregular	8	Complete	Incomplete
10	*A. viridis*	Brochidodromous	Thick	Regular	14	Incomplete	Incomplete

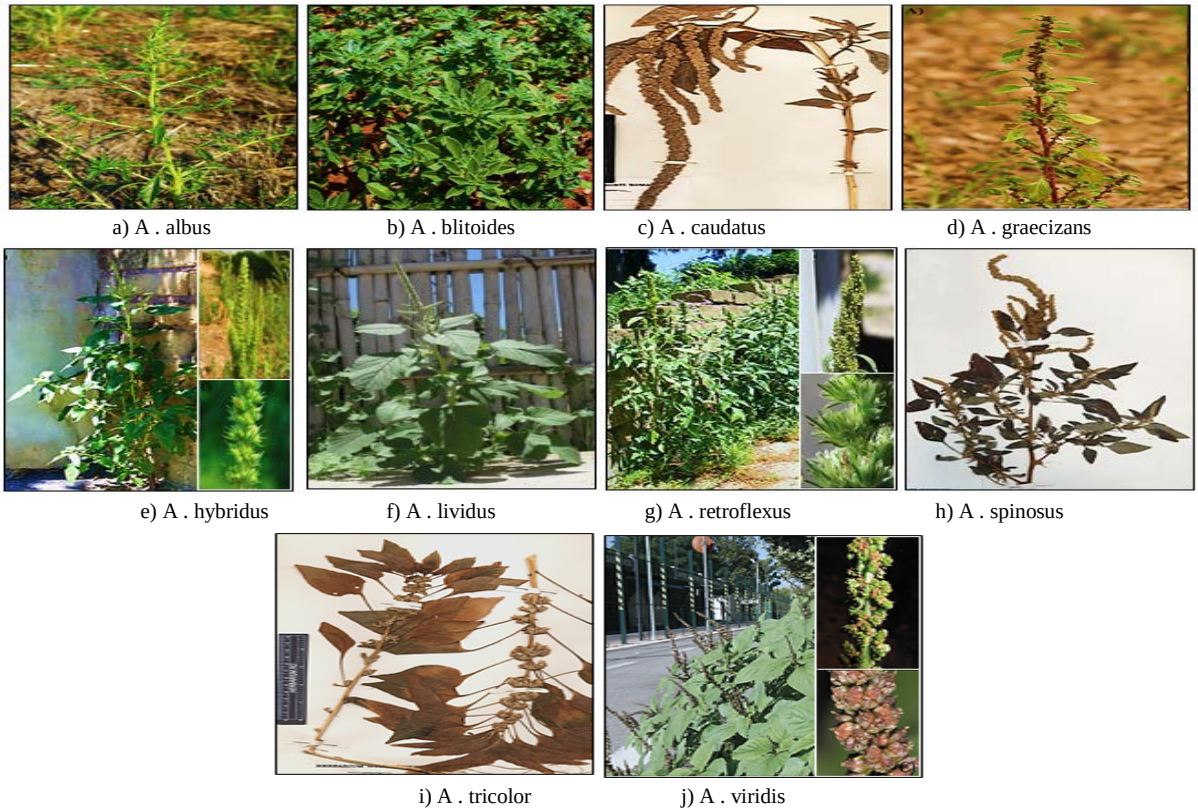

a) A . albus b) A . blitoides c) A . caudatus d) A . graecizans

e) A . hybridus f) A . lividus g) A . retroflexus h) A . spinosus

i) A . tricolor j) A . viridis

Plate 1. (a-j) Photo-micrographs showing the general external morphological features of the ten studied *Amaranthus* species; a) *A. albus*, b) *A. blitoides*, c) *A. caudatus*, d) *A. graecizans*, e) *A. hybridus*, f) *A. lividus*, g) *A. retroflexus*, h) *A. spinosus*, i) *A. tricolor*and and j) *A. viridis*, respectively.

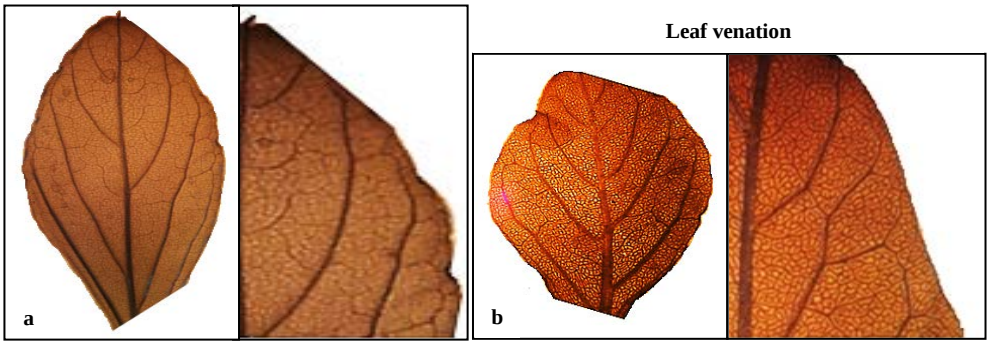

a) Reticulodromous venation b) Brochidodromous venation

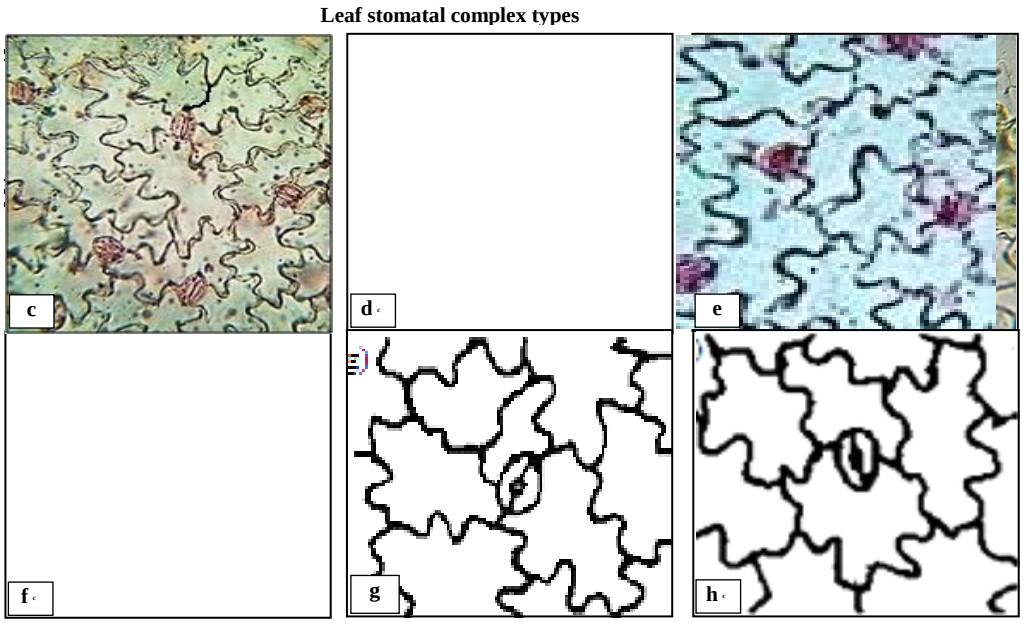

Anomocytic stomatal type Anisocytic stomatal type Diacytic stomatal type

Plate 2. (a and b) Photo-micrographs showing the types of the leaf venation, (c-e) Photo-micrographs, (f-h) drawings showing the types of the leaf stomatal complex for the studied *Amaranthus* species**.**

Table 5. Leaf micro-morphological characters of the studied *Amaranthus* species

No.	Species	Characters								
		Shape of epidermal cell		Epidermal wall pattern			Stomata type		Stomata level	
		Abaxial	Adaxial	Anticlinal wall	Periclinal wall	Epicuticuler secretion	Abaxial	Adaxial	Abaxial	Adaxial
1	*A. albus*	Elongated/ Irregular	Polygonal/ Irregular	Straight/ Elevated	Striate	Few granules	Anomo- Aniso- cytic	Anomo- Aniso-cytic	Raised	Raised
2	*A. blitiodes* Watson	Irregular	Polygonal/ Irregular	Straight/ Elevated	Smooth	Few granules	Anomo- Aniso- cytic	Anomo- Aniso-cytic	Raised	Sunken
3	*A. caudatus*	Sinuate/ Irregular	Polygonal/ Irregular	Straight/ Elevated	Rugate	Few granules	Anomo- Aniso- cytic	Anomo- Aniso-cytic	Raised	Raised
4	*A. graecizans*	Sinuate/ Irregular	Irregular	Undulate/ Elevated	Rugate	Absent	Anomo-cytic	Anomo-cytic	Raised	Raised
5	*A. hybridus*	Sinuate Irregular	Polygonal/ Irregular	Undulate/ Elevated	wrinkled	Absent	Anomo- Aniso- cytic	Anomo- Aniso- cytic	Raised	Raised
6	*A. lividus*	Elongated/ Irregular	Regular	Straight/ Elevated	Striate	Absent	Anomo- Aniso-Dia- cytic	Anomo- Aniso-Dia- cytic	Superficial	Superficial
7	*A. retroflexus*	Elongated	Isodiametric/ Irregular	Undulate/ Elevated	wrinkled	Dense granules	Anomo- Aniso-cytic	Anomo- Aniso- cytic	Raised	Raised
8	*A. spinosus*	Elongated	Polygonal/ Irregular	Undulate/ Elevated	Papillate	Dense granules	Anomo- Aniso-cytic	Anomo- Aniso- cytic	Raised	Raised
9	*A. tricolor*	Elongated/ Irregular	Elongated/ Irregular	Undulate/ Elevated	Striate	Dense granules	Anomo- Aniso-cytic	Anomo- Aniso- cytic	Raised	Raised
10	*A. viridis*	Elongated/ Irregular	Elongated/ Irregular	Straight/ Elevated	Striate	Few granules	Anomo- Aniso- cytic	Anomo- Aniso- cytic	Raised	Raised

Table 6. Joining Euclidean distances gathered for the ten studied *Amaranthus* species according to the linkage methods of data analysis using Systat 12 program

Nearest neighbor linkage method				Group average linkage method				Farthest neighbor linkage method			
Clusters Joining		Distance	No. of Members	Clusters Joining		Distance	No. of Members	Clusters Joining		Distance	No. of Members
Case 10	Case 3	1.012	2	Case 10	Case 3	1.012	2	Case 10	Case 3	1.012	2
Case 6	Case 10	1.043	3	Case 7	Case 6	1.049	2	Case 7	Case 6	1.049	2
Case 7	Case 6	1.049	4	Case 8	Case 1	1.081	2	Case 8	Case 1	1.081	2
Case 8	Case 1	1.081	2	Case 8	Case 4	1.302	3	Case 8	Case 4	1.437	3
Case 8	Case 4	1.167	3	Case 10	Case 7	1.313	4	Case 10	Case 7	1.632	4
Case 2	Case 8	1.297	4	Case 9	Case 10	1.653	5	Case 9	Case 5	1.745	2
Case 7	Case 9	1.357	5	Case 2	Case 8	1.675	4	Case 2	Case 10	2.011	5
Case 7	Case 2	1.432	9	Case 9	Case 5	2.292	6	Case 8	Case 2	3.623	8
Case 5	Case 7	1.745	10	Case 9	Case 2	3.088	10	Case 8	Case 9	5.422	10

Cases studied: 1. A . albus; 2. A . blitiodes; 3. A . caudatus; 4. A . graecizans; 5. A . hybridus; 6. A . lividus; 7. A . retroflexus; 8. A . spinosus; 9. A . tricolor and 10. A .viridis .

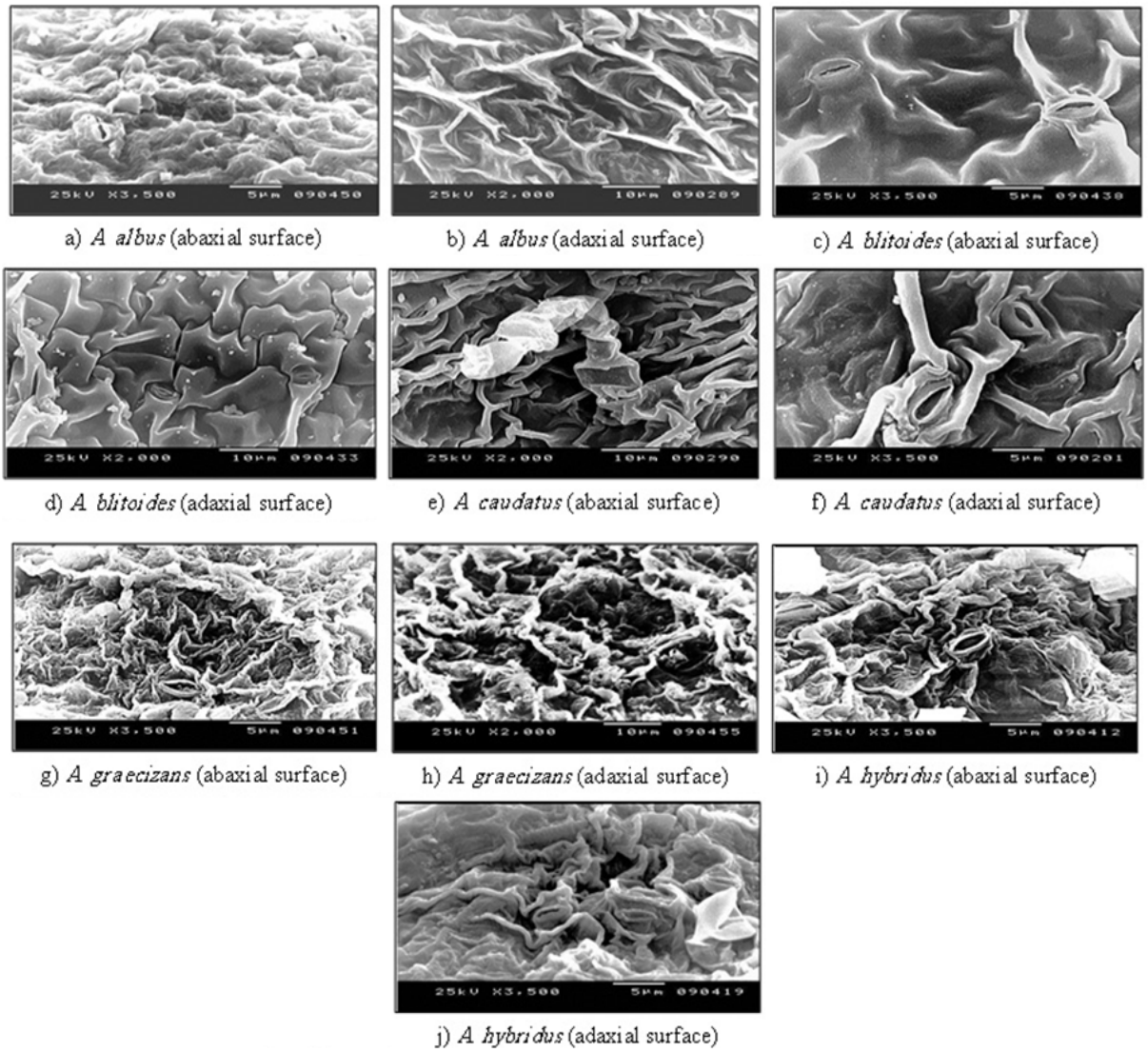

Plate 3. (a-j) SEM photo-micrographs showing types of stomata and shape of epidermal cells on both abaxial and adaxial surfaces of the leaf for *A. albus, A. blitoides, A. caudatus, A. graecizans,* and *A. hybridus***,** respectively.

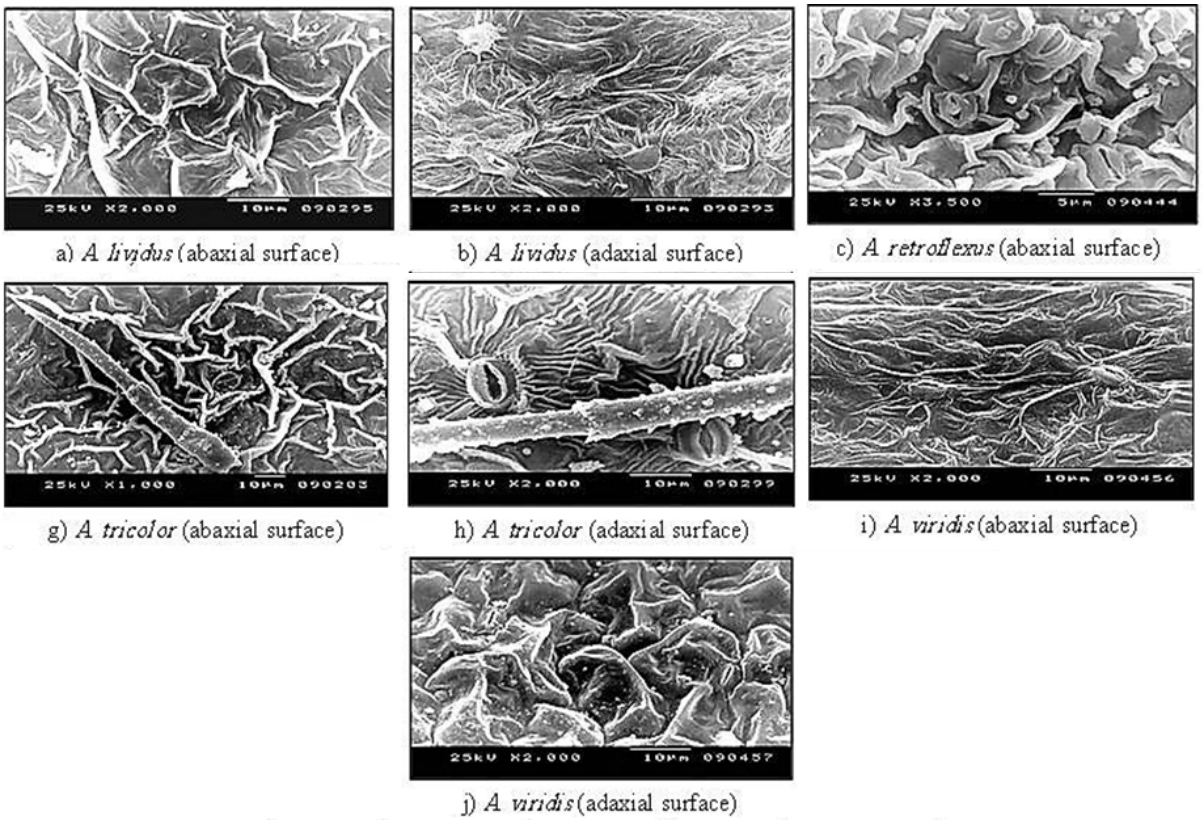

Plate 4. (a-j) SEM photo-micrographs showing types of stomata and shape of epidermal cells on both abaxial and adaxial surfaces of the leaf for *A. lividus, A. retroflexus, A. spinosus, A. tricolor* and *A. viridis*, respectively.

4. Discussion

Amaranthus is a cosmopolitan genus with annual monoecious or dioecious species. Species within this genus are under taxonomic investigations due to their high phenotypic variability (Mosyakin and Robertson, 2003; Iamonico, 2009 and 2015). The first comprehensive taxonomical division of the genus was that of Dumortier, (1827) who divided its species into two sections. Classification of the genus has been faced with many opinions and divisions afterward; from the most reasonable division is that of Mosyakin and Robertson, (1996). Accordingly, the vegetative morphological variation within the Egyptian *Amaranthus* has been investigated in this work. Davis and Heywood, (1973) pointed out that any stable character can be used in systematic. Subsequently, the most stable characters have been subjected to numerical analysis to investigate the relationship between the studied species.

According to Dumortier, (1827), the studied taxa were classified under the two sections; *Amaranthotypus* and *Blitopsis*; as follows: *A. caudus, A. hybridus, A. retroflexus,* and *A. spinosus* under section *Amaranthotypus*. While section *Blitopsis* includes *A. albus, A. blitoides, A. graecizans, A. lividus, A. tricolor* and *A. viridis*. The results found in the present study did not coincide with Dumortier's classification of the species. The obtained dendrograms divided the studied taxa into two groups in the three clustering methods (N.N., G.A. and F.N.). The three dendrograms put *A. albus* beside *A. spinosus* (1 and 8) at dissimilarity index 1.081, as well as *A. caudatus* beside *A. viridis* (3 and 10) at dissimilarity matrix 1.012. The species *A. lividus* and *A. retroflexus* (6 and 7) are closely met at dissimilarity matrix 1.049 in the three dendrograms. These gatherings of the species are logic due to the morphological similarities between every two species, in spite of gathering species between two different Dumortier's sections. This result may be in acceptance of Mosyakin and Robertson, (1996) who divided all the *Amaranthus* species into three subgenera; 1- *Acnida* (L.) Aellen ex K. R. Robertson with three sections; 2- *Albersia* (Kunth) Gren. and Godr. with four sections and 3- *Amaranthus* with three sections and two subsections.

As *Acnida* taxa were not represented in the flora of Egypt, accordingly the three resulted dendrograms revealed that the studied taxa can be divided into two subgenera, with many sections and *Acnida* is excluded. We can explain this division as it was according to the vegetative morphological characters only. From the most important morphological characters within the studied taxa are the places of red spot on the leaf surfaces and leaf venation, which divide the studied taxa into two groups, red spot on the leaf surfaces on the middle versus on the lower part of the leaf blades besides the leaf venation, reticulodromus versus brochidodromous. The species under these groups did not coincide with those of Dumortier, (1827). In spite of that, the results obtained were in partial acceptance with that of Waseltov *et al.*, (2018) who found that both *A. caudatus* and *A. hyvridus* were closed to each other in the phylogenetic tree, as well as *A. albus* and *A. blitoides*. Most of the taxonomical works on this genus were classified according to the floral characters and sex of the plants (Mosyakin and Robertson, 2003 and Iamonico, 2009 and 2015). As a conclusion the studied *Amaranthus* species can be divided into two main

groups based on their vegetative morphological characters only.

References

Adanson M. 1763. **Familles des Plantes.**, Vincent, Paris.

Aellen P. 1961, **Die Amaranthaceae Mitteleuropas**. Carl Hanser Verlag, München.

Aellen P. 1972. In: Rechinger K. (ed.), Amaranthaceae. **Flora Iranica 91**, Graz-Austria.

Barthlott W; Neinhuis C; Cutler D; Ditsch F; Meusel I; Theisen I and Wilhelmi H. 1998. Classification and terminology of plant epicuticular waxes. *Bot J Linn Soc*, **126**:237-260.

Beck GE. 1909**. Amaranthaceae**. In: Reichenbach, L.**,** and Reichenbach, HG (ed.), Icones Florae Germanicae et Helveticae. Lipsiae et Gerae pp. 91-174.

Bentham G. and Mueller F. 1870. **Flora Australiensis** vol.5. L. Reeve and co., London.

Boulos L. 1999. **Flora of Egypt**. Vol. 1. Azollaceae-Oxalidaceae, Al Hadara Publishing, Cairo, Egypt.

Boulos, L. 2009. Flora of Egypt. Checklist Al-Hadara Publishing, Cairo.

Cavaco A. 1962. **Les Amaranthaceae de l'Afrique au sud du tropique du Cancer et de Madagascar**. Mémoires du Muséum National d'Histoire Naturelle, sér. B, *Botanique* **13**: 1-254.

Costea M; Sanders A and Waines G. 2001. Notes on some little known *Amaranthus* taxa (Amaranthaceae) in the United States. *Sida*, **19**: 931-974.

Davis PH and Heywood VH. 1973. **Principles of Angiosperm Taxonomy**. Krieger, New York.

Dumortier, BCJB. 1827. **Florula Belgica Operis Majoris Prodromus**, Belgique.

El Hadidy, MN and El Hadidy AMH. 1980. Family 57. Amaranthaceae in M N. El Hadidi (Ed.). Flora of Egypt. *Taeckholmia add ser*.**1**:13-92.

Gordon D.1853. **Florula Juvenalis III** *Mém Acad Sci et Lettr de Montp*, .

Iamonico D. 2009. Invasive status and presence of *Amaranthus polygonoides* L. (Amaranthaceae) in Italy, with notes on its taxonomy and morphology. *Fl Medit.*, **19**: 233-239.

Iamonico D. 2015. Taxonomic revision of the genus *Amaranthus* (Amaranthaceae) in Italy. *Phytotaxa*, 199(1): 1-84.

Kirscleger F. 1857. **Flore d'Alsace et des contrées,** limitrophes Vol. 2, Les monochlamydées, Les monocotylées, Les cryptogames vasculaires.

Linneaus C. 1753. **Species Plantarum**. Vol. 2, Holmiae.

Mbagwu FN; Nwachukwu CU and Okoro OO. 2008. Comparative Leaf Epidermal Studies on *Solanum macrocarpon* and *Solanum nigrum*. *Res J Bot.*, **3**(1): 45-48.

Moquin-Tandon, CHBA (1849) **Amaranthaceae Juss**. In: De Candolle A (Ed.). Prodromus Systematis Regni Vegetabilis, Sumptibus Victois Masson, Parisiis, **13**(1): 231-424.

Mosyakin SL and Robertson KR. 1996. New infrageneric taxa and combinations in *Amaranthus* (Amaranthaceae). *Ann Bot Fenn*, **33**:275-281.

Mosyakin SL and Robertson KR. 2003. *Amaranthus*. In: **Flora of North America North of Mexico**, Vol. **4**, Oxford University Press.

Rouy G. 1910. **Flora of France ou description des plante vol. XII**, Paris.

Sauer JD. 1955. Revision of the dioecious *Amaranths*. *Madroño*, **13**: 5-46.

Stace CA. 1984. The taxonomic importance of the leaf surface. In: Heywood VH and Moore DM (eds.) **Current concepts in plant taxonomy**, Academic Press, London, U.K.

Täckholm V. 1974. **Students' Flora of Egypt**, second ed., Cairo University

Thellung A. 1914. *Amaranthus*. In: Ascherson P and Graebner P (eds.), **Synopsis der Mitteleuropaischen Flora 5**, Leipzg.

Tournefort JP. 1794. **Institutiones rei Herbariae**. Editio Altera, Paris.

Townsend CC. 1974. Amaranthaceae. In: Nasir E and Ali SI (Eds.) **Flora of West Pakistan** 7. Ferozsons Press, Rawalpindi

Townsend CC. 1985. Amaranthaceae **In: Polhill RM (ed.). Flora of Tropical East Africa**. Published on behalf of the East African Government.

Uline EB and Bray WL. 1894. A preliminary synopsis of the North American species of *Amaranthus*. *Bot Gaz.*, **19**: 313-320.

Waselkov KE; Boleda A and Olsen KM. 2018. A Phylogeny of the Genus *Amaranthus* (Amaranthaceae) Based on Several Low-Copy Nuclear Loci and Chloroplast Regions. *Syst Bot.*, **43**(2): 439-458.

Appendix 1. Types of characters (OTU's) used in the numerical analysis and its ranking

No.		Characters	Ranking of Multistated Qualitative					
			1	2	3	4	5	6
1	Stem characters	Habit	Annual	Perennial				
2		Type	Erect	Procumbent	Prostrate			
3		Length (cm)	Multistated Quantitative					
4		Width (mm)						
5		Shape	Flattened	Angular	Slender			
6		Color	Light Green	Greenish white	Green	Green tinged with purple	Purple	Red
7		Density of branches	Moderate	Dense				
8		Density of hairs	Glabrous	Sparsely hairy	Hairy			
9	Leaf macro-characters	Arrangement	Alternate	Spiral				
10		Color	Pale green	Green	Green with white spots	Green tinged with red	Green tinged with purple	Green or reddish purple
11		Length (cm)	Multistated Quantitative					
12		Width (cm)						
13		Shape	Ovate	Ovate to Lancolate	Lancolate			
14		Widest part	Middle	Lower				
15		Spot	Middle	Lower				
16		Surface	Glabrous	Sparsely hairy	Hairy	Wooly		
17		Hair type*	MUP	MUT	MUG	MUG+MBG		
18		Types of venation	Reticulodromous	Brochidodromous				
19		Size of 1^{ry} veins	Thin	Moderate	Thick			
20		Type of 2^{ry} veins space	Regular	Wide at apex	Wide at base	Irregular		
21		Number of 2^{ry} veins	Multistated Quantitative					
22	Leaf micro-characters	Marginal veins	Complete	Incomplete				
23		Areolar veins	Closed	Incomplete				
24		Abaxial epidermal cells	Irregular	Elongated/Irregular	Sinuate/Irregular			
25		Adaxial epidermal cells	Irregular	Elongated/Irregular	Polygonal/Irregular	Isodiametric/Irregular	Polygonal/regular	
26		Abaxial stomatal type	Anomo-cytic	Anomo-Aniso-cytic	Anomo-Aniso- Dia-cytic			
27		Marginal veins	Complete	Incomplete				

JJBS

Volume 14, Number 1, March 2021
ISSN 1995-6673
Pages 147 - 155

Jordan Journal of Biological Sciences

Rapid osmotic adjustment in leaf elongation zone during polyethylene glycol application: Evaluation of the imbalance between assimilation and utilization of carbohydrates

Mohamed Mahdid [1,*], Abdelkrim Kameli [1] and Thierry Simonneau [2]

[1] *Département des Sciences Naturelles, Ecole Normale Supérieure (ENS) de Kouba, BP 92, Vieux Kouba, 16308 Alger, Algeria,* [2] *Laboratoire d'Ecophysiologie des Plantes sous Stress Environnementaux (LEPSE), UMR 759, INRA-Montpellier, SupAgro, 2 Place Viala 34060 Montpellier cedex, France*

Received: March 25, 2020; Revised: August 7, 2020; Accepted: August 31, 2020

ABSTRACT

This work aims to study rapid osmotic adjustment, in order to simplify and follow this mechanism with the changes of various sugars and potassium in parallel with growth and photosynthesis measurements. Four durum wheat varieties of *Triticum turgidum* subsp. *durum* L. designated as: "Inrat-var", "MBB-var", "OZ-var", and "Waha-var" were growing in continuously aerated-nutrient-solutions. The kinetic of the leaf elongation for leaf 3 were measured by the linear variable differential transducer (LVDT); osmotic potential (OP), carbohydrates, and potassium (K^+) concentrations. Growth recovered rapidly after a sudden full after stress. A considerable difference was noted in the recuperation (%) of the leaf elongation rate (LER) under the four varieties. The variation in the partial recuperation of LER was, therefore, associated with the aptitude of osmotic adjustment in the elongation zone (EZ) of the leaf growth. Osmotic adjustment is associated with soluble sugars and potassium accumulation. Compared to the accumulation of these solutes in the mature zone (MZ) and the photosynthesis process, several ideas related to this accumulation mechanism can be assumed among them, this accumulation process cannot be considered as a direct result of the reduction of the growth. Rather, it might be as the result of their mobilization from the MZ of growing leaf or other expanded leaves. The accumulation of these sugars probably is uncoupled with direct photosynthesis activity.

Keywords: Leaf elongation rate, Recovery, Rapid osmotic adjustment, linear variable differential transducer, Photosynthesis, *Triticum turgidum* subsp. *durum* L.

1. Introduction

The osmotic adjustment may supposedly be favorable to survive below extreme aridity and desiccation, although at the same time, they approved that it can endorse improved soil moisture capture leading to enhanced recovery below lack stress. In reality, plant turgor repairs due to the osmotic adjustment in roots or shoots and its improvement of root-growth and soil dampness extraction has been frequently described (Kusaka *et al.,* 2004; Velázquez-Márquez *et al.,* 2015). The purpose of the study of rapid osmotic adjustment (within hours) is to simplify and follow its mechanism with other physiological and biochemical variables. A fast osmotic adjustment or water stress compulsory on plants by sodium chloride (NaCl) or polyethylene glycol (PEG) in medium begets for certain vegetation a rapid osmotic adjustment (Fricke and Peters, 2002; Fricke, 2004; Mahdid *et al.,* 2014). The osmotic adjustment mechanism occurs after stress application is speedily within 1-2 h; however, the growth recovery is very rapid too. Studying osmotic adjustment by the side of this stage might limit and make simpler the presence or absence of the hydraulic factors implicated in the plant responses following the osmotic stress. The later behavior may possibly guide to an enhanced understanding of these responses. In contrast, in long term, more complicated properties such as anatomical and morphological proprieties may interfere and intervene with physiological responses. This may complicate any evaluation of the growth diminution and its relation to osmotic adjustment. Through previous reports, the relationship between osmotic adjustment and turgor recovery, in synchronization with the restoration of growth stay evident, despite that growth in the short term, did not regain its full rate before the intervention of the stress.

During of the rapid saline stress (short term) case, the inorganic salt solutes of medium contributed robustly to accelerate the osmotic adjustment of tissues (Fricke, 2004) and at the long term (Chen *et al.,* 2019)**.** For the rapid water stress, the accumulation of sugars was noted, and little accumulation of potassium (K^+) was found compared to sugars (Mahdid *et al.,* 2014). During the stress, the concentration of K^+ increases in some varieties for a short period. Thereafter, it remains minor except for the MBB-var (~29%) which we are interested in to follow the accumulation and the source of contribution of soluble sugars. So, many questions have been raised about the source of accumulated solutes in the EZ compared with the MZ. If it is as a result of deviation of these sugars from the

* Corresponding author e-mail: mahdid_m@yahoo.fr.

growth process! Not using and not generating organic derivatives used for growth, or these accumulations as result of reduced growth after rapid stress؟

The current study tries to look into the varied involvement of sugars in a hasty osmotic adjustment of 4 varieties under osmotic stress. The greater part of previous works has not tried to scrutinize the relationship betwixt solutes accumulation and the decrease in growth following rapid stress, if this accumulation is a consequence of passive accumulation after growth inhibition. The work attempts to evaluate the balance between the assimilation of soluble carbohydrates; if the accumulation of carbohydrates for the first little hours of the water stress is compliant to the calculated reduction of growth. Consequently, it is imperative to control the relationship betwixt carbohydrates and photosynthetic yields and to reply to the question of whether an osmotic correction is an effect of accretion or translocation of photosynthates or an active accumulation method, e.g. a solutes mobilization or organic reserves utilize.

2. Materials and Methods

2.1. Growth conditions and rapid plant stress

Experiments were performed with 4 varieties of *Triticum turgidum* subsp. *durum* L.: Inrat-var, Mohamed Ben Bachir (MBB-var), Oued Zenati (OZ-var), and Waha-var, gained from the "Institut Technique des Grandes Cultures" (ITGC) in Algiers (Algeria) and chosen according to their growth analysis and degree of difference responses against water stress (Meziani *et al.*, 1992). Seeds were surface sterilized by NaCl (0.5%) for 15 min, washed three-folds with bidistilled water, and germinated on soaked-up filter paper in Petri dishes. After six-days, seedlings of like sizes were planted in ten-liter enclosed plastic basins including nutrient solutions. After that, plants were developed in a growth chamber, with a photoperiod of 14 h at photosynthesis photon flux density (PPFD) of 400 µmol/m^2/s and day/night temperature of 24/20°C as well as a vapor pressure deficit of 0.8-1 kPa as previously reported by the authors (Mahdid *et al.*, 2011).

The diluted nutrient solution, at pH 5.5, contained (in mM): calcium sulfate dihydrate: 0.5; potassium nitrate: 0.8; monopotassium phosphate: 0.3; magnesium sulfate heptahydrate: 0.2; ammonium nitrate: 0.4; Ferric-EDTA: 0.02; boric acid: 0.008; manganese sulfate monohydrate: 1×10^{-3}; sodium molybdate dihydrate: 0.1×10^{-3}; zinc sulfate heptahydrate: 0.2×10^{-3}; and copper(II) sulfate pentahydrate: 0.2×10^{-3}, was renewed periodically each four days. The measurement of the leaf elongation yield (LER) by means of LVDTs, in different conditions and PEG concentration was monitored as reported by the authors (Mahdid *et al.*, 2011).

2.2. Physiological ascertainment

The growth of the third leaf was released; the location of the EZ and the accurate distance of enlargement zone were established as reported elsewhere (Hu *et al.*, 2000). Then, it was confirmed by calculating the dislocation yields the length of the leaf axis with the stick in way (Schnyder *et al.*, 1987). The MZ is the rest of the leaf. The tissues were rapidly cut to little pieces set into microtubes having small plastic strainer, preserved, and speedily plunged into liquid nitrogen. The samples were defrosted and then spun in the centrifuge (10,000 rpm for 10 min). 20 µL of samples were collected and kept at -20 °C waiting for further experimental studies.

The potential of the osmotic adjustment was calculated and the relative water content (RWC) was ascertained as follows:

$$RWC = [(FW - DW) / (TW - DW)] \times 100 \quad \text{(Eq. 1)}$$

Where: FW, DW, and TW represent the fresh weight, the dry weight, and the turgid weight, respectively.

The osmotic potential or pressure (OP) at full plant turgor (π100) was calculated according to Wilson *et al.*, (1980) as follows:

$$OP = [\pi(RWC - 10)] / 90 \quad \text{(Eq. 2)}$$

The net photosynthetic rate (NPR) was calculated by a unique leaf chamber intended for durum wheat and linked to the Gas Analyzers from PP Systems (MA, USA) on four to six individual plants.

2.3. Biochemical determination

The total carbohydrates in a sample were estimated by the rapid colorimetric method of phenol-sulfuric-acid (Dubois *et al.*, 1956). The content of some carbohydrates e.g., glucose (Glu), fructose (Fru), and sucrose (Suc) were determined following enzymatic transformation to NADH (reducing agent), which is expected at the absorbance of 340 nm ($A_{340\ nm}$). The conversion of glucose was obtained via hexokinase (HK) to yield glucose-6-phosphate (G-6-P) which is changed with the G-6-P dehydrogenase (G6PDH) to yield NADH. The fructose conversion, however, requires the phospho-glucose-isomerase (PGI) which transforms the fructose-6-phosphate (F6P) to the G6P. The sucrose is the primary hydrolysis by means of β-fructosidase to yield Glu + Fru.

The oligo-fructans (DP1-DP7) were qualitatively estranged by thin-layer chromatography (TLC) as detailed elsewhere (Collins *et al.*, 1971). The obtained spots were visualized according to Wise *et al.*, (1956). The contents of carbohydrates in TLC-spots were determined to get an uneven approximation of the concentration of the fructan (Fig. 1). In the leaf sap, the concentration of potassium was calculated using a flame photometer. Every biochemical determination was made via the expressed sap extracted with liquid nitrogen (LN2).

2.4. Statistical analyses

The ANOVA unique factor betwixt groups was carried out under Microsoft Excel. The differences were deemed to be statistically significant at $p \leq 0.05$. The Student's t-tests were achieved by R software.

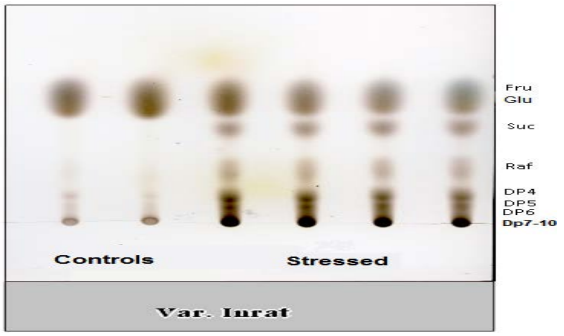

Figure 1. An image of obtained spots of the oligo-fructans from DP1 to DP10, as an example on experience; these spots were separated by TLC.

3. Results

3.1. Leaf growth recovery and rapid osmotic adjustment

Kinetics of short-term growth previous to and following the rapid stress is well-known (Mahdid *et al.*, 2014). Leaf elongation quickly finished within 2 minutes following the imposition of PEG 6000. Growth cessation continued for a few minutes in a steady rate for 2 h, growth stabilized to a new recovery rate below the pre-stress value (Fig. 2a). Data were used to estimate the rate of the leaf growth recuperation as denote steady LER in the previous phase of treatment connected to mean LER earlier than the stress. Significant difference was established betwixt varieties, the recovery achieved in MBB-var (72.72%) trail by Waha-var (62.51%). The lowly rate was reached in OZ-var (37.88 %) with a considerable difference (Fig. 2b).

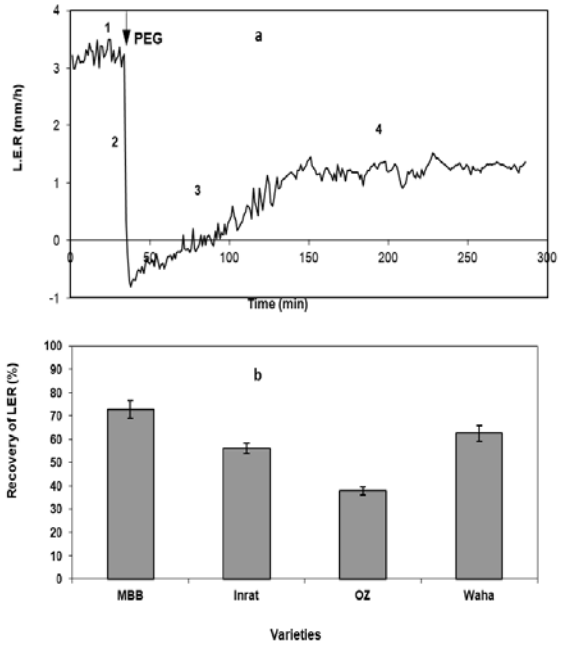

Figure 2. (a), LER kinetics (Four phases) calculated by LVDTs on the growing third *Triticum turgidum* subsp. *durum* L. as affected by water deficit imposed by adding PEG 6000 to the hydroponic's solution. (b), the percentage of leaf growth recovery represents the mean steady LER in the last phase (phase 4) of treatment related to the mean LER before stress (phase 1) in graph a.

The OP at full plant turgor (π100) at the same trend showed a dissimilar profile of reduces subsequent stress within four varieties. MBB-var showed constantly lower π100 from 1 h forward, attainment of 76 MPa (at 4 h) comparing to -1.24 MPa (control), Inrat-var, and Waha-var. By contrast, OZ-var showed no net decrease in π100 except a minor decrease 30 min after stress. Clearly, there are significant differences in the OP between the two zones (EZ + MZ), and the values of the osmotic adjustment at the finish of the stress period attained -0.52 (MBB-var) -37 (Inrat-var), and -0.33 (Waha-var). The OZ-var however, showed a small transient osmotic adjustment at 0.5-3 h (Fig. 3).

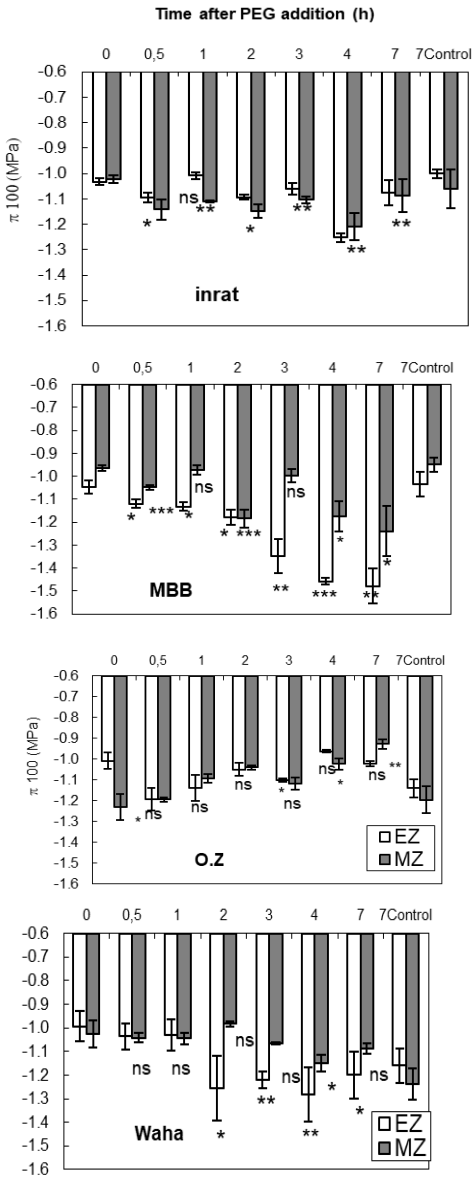

Figure 3. Modification in OP at full plant turgor (π100) of the bulk-tissue in elongation and both zones (EZ + MZ) of the third leaf of durum wheat previous before and after the supplementation of PEG 6000 to the root media. The data represents the average of at least 4 assays and ± SE are reported.

3.2. Rapid solute accumulation

3.2.1. Potassium

The increase in K^+ concentration occurred in all varieties through stress phase except OZ-var. The K^+ contribution to OP was important during and at the end of stress. This contribution to osmotic adjustment in other varieties was significantly towards the end of the stress period, between 29 and 56% except in Inrat-var, which occurred transiently. The results showed the predominance of this cation in the MZ compared to the EZ (Fig. 4).

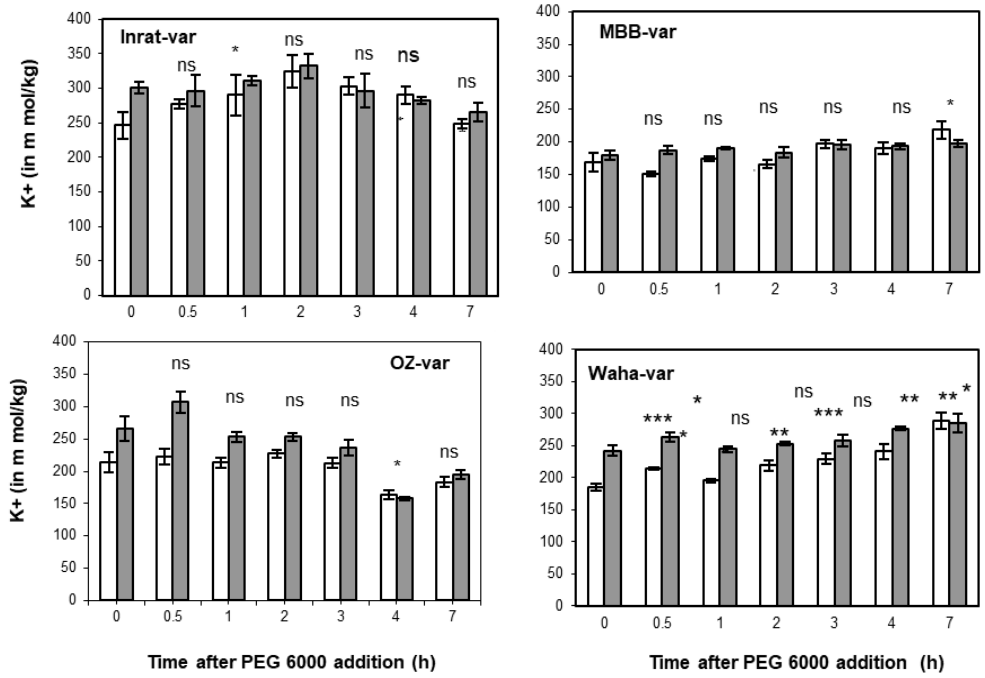

Figure 4. Modification in K^+ concentration at full plant turgor (π100) of bulk-tissue in the two zones (EZ + MZ) of third leaf of durum wheat previous to and next the supplementation of PEG 6000 to the root media. The data represents the average of at least 4 replicates ± SE.

3.2.2. Soluble sugars

The accretion of whole soluble carbohydrates was evidenced in the EZ and less in the mature one through the stress phase. The MBB-var demonstrated the highest accretion, followed by Inrat-var. However, the lowest accretion was achieved in OZ-var. The evaluation of individual carbohydrate concentrations by the enzymatic method exposed an augment in Glu, Fru, and Suc in both zones (EZ + MZ) of all varieties after the imposition of stress, and mainly in EZ (Table 1). In order to have an indication of the chemical (formula and range) of oligo-fructans as well as the comparison of sugars with the enzymatic method, data were obtained. The qualitative analyses of soluble carbohydrates allowed the determination of the degree of polymerization (Dp) from 3 to 7. The evaluation of total and individual sugar concentrations showed the presence of other sugars, especially oligo-fructans, with 22 and 56% of total sugars in EZ of the control and stressed, respectively, and to a smaller degree in MZ. The accretion of these carbohydrates was achieved in every variety excluding the OZ-var (Table 1).

The judgment of the reduction in the growth behind stress with the level of total carbohydrate accretion demonstrated no clear relationship betwixt the two variables, during the little-term stress until 7 h (Fig. 5). Similar deduction has been described between carbohydrate accumulation and photosynthetic rate during the stress (Fig. 6).

The photosynthesis rates graph indicated a slight decrease during stress and was not the same as the LER tendency during stress in all varieties (Fig. 7).

The judgment of the reduction in the growth behind stress with the level of total carbohydrate accretion demonstrated no clear relationship betwixt the two variables, during the little-term stress until 7 h (Fig. 5). Similar deduction has been described between carbohydrate accumulation and photosynthetic rate during the stress (Fig. 6).

The photosynthesis rates graph indicated a slight decrease during stress and was not the same as the LER tendency during stress in all varieties (Fig. 7).

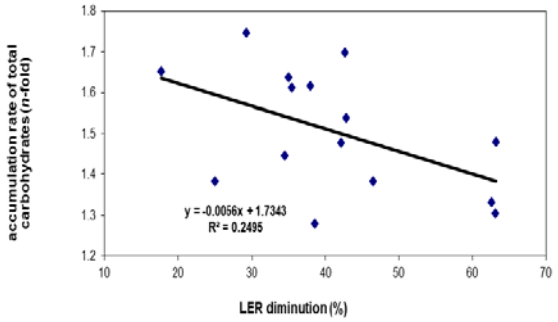

Figure 5. Correlation betwixt the accretion rate of the total sugars and the reduction of LER (%) at 7 h after stress in the four varieties of wheat. The data represents the average of at least 4 replicates.

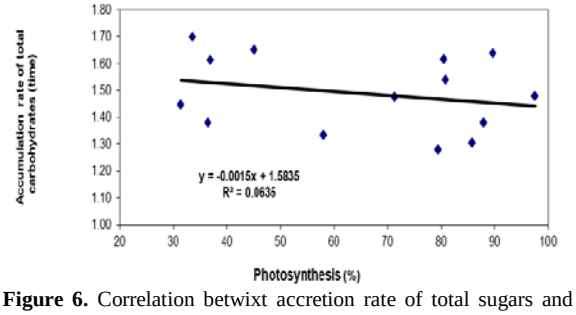

Figure 6. Correlation betwixt accretion rate of total sugars and photosynthesis decrease (%) at 7 h after stress in the four varieties of wheat. The data represents the average of at least 4 replicates

Table 1. Evaluation of total/other (g/kg) and individual (m.mol kg^{-1}) carbohydrate concentrations in EZ + MZ of MBB-var, Inrat-var, OZ-var, Waha-var of the last leaf of durum wheat calculated from the leaf sap tissue, behind the difference in concentrations betwixt two times (0 and 7 h). The data representing the average of at least 4 assays and ± SE are reported.

		Elongation zone (EZ)				Mature zone (MZ)			
		0h	7h	Difference		0h	7h	Difference	
MBB-var	Total Carbohydrates	53,05 ± 2,56	80,84 ± 5,38	27,79	***	37,76 ± 2,24	48,11 ± 1,29	10,3	**
	Glu	114,89 ± 2,62	158,36 ± 6,55	43,47	***	84,59 ± 7,05	98,87 ± 2,39	14,3	*
	Fru	33,19 ± 2,31	51,81 ± 4,16	18,62	**	19,71 ± 0,20	24,23 ± 2,02	4,52	*
	Suc	6,63 ±1,29	11,96 ± 1,32	5,33	**	7,97 ± 1,00	19,1 ± 0,23	11,1	***
	Other sugars	24,14 ± 2,18	38,92 ± 4,20	14,78	**	16,26 ± 1,14	19,41 ± 0,97	3,15	*
Inrat-var	Total Carbohydrates	31,89 ±2,43	45± 3,13	13,11	**	16,37 ± 1,19	29,13 ± 3,06	12,8	**
	Glu	61,94 ± 8,23	79,85 ± 5,25	17,91	*	30,55 ± 2,59	55,39 ± 7,70	24,8	**
	Fru	26,4 ± 3,26	38,8 ± 2,38	12,4	***	15,56 ± 1,84	20,55 ± 2,46	4,99	ns
	Suc	5,67 ± 1,59	4,8 ± 0,25	_	ns	4,85 ± 1,83	26,32 ± 4,36	21,5	***
	Other sugars	13,01 ± 3,11	25,88 ± 2,79	12,87	**	6,95 ± 1,73	13,91 ± 2,03	6,96	*
OZ-var	Total Carbohydrates	29,16 ± 1,08	38,92 ± 3,04	9,76	**	20,05 ± 0,52	21,13 ± 1,46	1,08	ns
	Glu	79,27 ± 2,22	106,34 ± 3,01	27,07	***	47,18 ± 1,17	56,32 ± 6,36	9,14	ns
	Fru	19,36 ± 1,60	29,15 ± 2,66	9,79	**	15,8 ± 1,10	24,21 ± 1,62	8,41	**
	Suc	2,65 ± 0,72	6,2 ± 1,68	3,55	*	4,53 ± 2,00	11,93 ± 4,11	7,4	ns
	Other sugars	10,50 ± 1,30	12,41 ± 1,92	1,91	ns	7,17 ± 0,45	2,55 ± 0,42	_	ns
Waha-var	Total Carbohydrates	25,71 ± 1,46	43,11 ± 2,89	17,4	***	9,76 ± 0,62	34,32 ± 1,81	24,6	***
	Glu	65,13 ± 4,32	96,22 ± 6,35	31,09	**	22,31 ± 2,33	46,41 ± 5,04	24,1	**
	Fru	23,15 ±1,59	35,61 ± 1,79	12,46	***	9,87 ± 0,41	23,04 ± 0,93	13,2	***
	Suc	3,07 ± 0,18	4,47 ± 0,27	1,4	**	5,82 ± 0,91	31,76 ± 5,30	25,9	***
	Other sugars	8,77 ± 0,51	17,85 ± 1,64	9,08	***	1,98 ± 0,41	10,95 ± 0,52	8,95	***

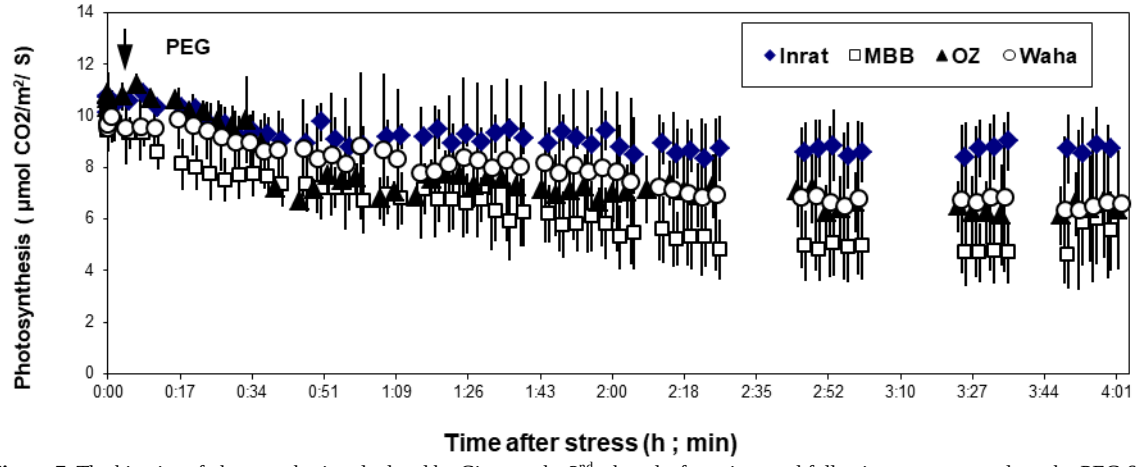

Figure 7. The kinetics of photosynthesis calculated by Ciras on the 2nd wheat leaf previous and following stress compulsory by PEG 6000 supplementation to the hydroponics solution.

4. Discussion

4.1. LER recuperation under prompt water insufficiency

Is very evident the reduction of the OP through the first rung of time hours in similar with the modifications of the LER. The source of the growth recuperation surely is linked to the water relations changes. The cells attuned osmotically inside 1 h, which designated that osmotic amendment is a speedy procedure produced by solute accretion. The continued reduction of OP behind 1 h resulted in a high recovery of the growth.

The osmotic adjustment in growing tissues gain water and thus turgor recovered immediately (Mahdid *et al.*, 2014), which the only explanation of LER changes due to turgor changes, where it turned out to be the reason for this is possibly owing to the vanishing of water possible gradient betwixt EZ cells and close to (mature) tissue and xylem due to the reduce in mature tissue and xylem water likely. Hence, this reduction shall ultimately result in minor water run and guide to the withering of the growing tissue (Mahdid *et al.*, 2011). The decrease of gradient water potential following the supplementation of PEG 6000 was pursued by a phase of rate of this gradient owing to the rapid reduce of the OP in the EZ.

The growth kinetics showed that the times' growth termination (little minutes) and recuperation (~1 h) may perhaps too rapid to generate the osmotic adjustment of lengthen tissue resulting to growth recuperation in the considered varieties. However, as in mainly earlier study, growth at time level hours did not recuperate to pre-stress levels, chiefly under conditions where elevated

concentrations of osmotic (PEG) or salt are current in the root medium, at least in the short-term (Munns *et al.*, 2000; Munns, 2002; Mahdid *et al.*, 2011). This perhaps owing to the modifications in biophysical characteristics of elongating cells, the hardening of the wall and the decrease of the extensibility provokes and leads to an additional turgor against wall hardness (Mahdid *et al.*, 2011). The osmotic adjustment collectively among cell wall extensibility regulates turgor in dehydration, where the previous is generally more efficient and widespread than the later (Bartlett *et al.*, 2012).

Considerable dissimilarity between the studied varieties was established in the amount of LER recuperation (%) at 2 h. Differences in the recuperation of LER (%) might not essentially signify the equal disparities in water stress acceptance between the varieties at the long-term. Other more complex responses, such as functional and structural responses may be implicated at a long-time scale.

The situation under sudden water stress is different, compared to saline stress. This situation may lead to variations in the metabolic procedures and fluctuations of endogenous solutes to rising zones transversely the plasma membrane. In this work, we attempt to match the differences in osmotic adjustment and growth recovery capacity between the four cultivars (Inrat-var, MBB-var, OZ-var, and Waha-var), that determine the velocity of osmotic adjustment in LER recovery at the short term under conditions of water stress. It also appears that the OP in the EZ is lower compared to the MZ. Dissimilarities in osmotic adjustment betwixt the varieties might be owing to the genetic variability. Thus, the degree of osmotic adjustment is correlated to the genetic potential of the plant. The osmotic mechanisms and possessions related with genotypic distinctions in osmotic adjustment have been elucidated in a lot of wheat research works (Morgan 1991; Blum, 2016; Morgan and Tan, 1996). This control behavior was maintained through another study. Indeed, the complex genetic control for osmotic adjustment has also been maintained through the quantitative trait locus (QTL) analysis in a population of sunflower plants in field environment, by the discovery of genomic regions related with water rank character and osmotic adjustment below water-stressed situations (Poormohammad Kiani *et al.*, 2007). We propose that a better considerate of this control at the physiological rank could help in propagation plants for arid and semi-arid conditions, and most important if we are looking at the impact of these mechanisms yield (Blum, 2016).

The magnitude of osmotic adjustment starting from 0.5 h may be due to the rapid accumulation of sugars and K^+, which indicates the accumulation so rapid of these solutes (especially sugars) in osmotic adjustment, particularly in the growing leaf tissue. Despite the small space occupied by vacuoles in growing cells, these rapid changes in K^+ concentration could be the result of increased mobilization and fluxes of endogenous solutes (including other ions) from MZ of grow athwart the plasma membrane, including potassium transporter channels (Osakabe *et al.*, 2013).

The phenol sulfuric way of full sugars does not permit the ascertainment of the DP of the accumulated sugars and consequently their involvements to osmotic adjustment. However, the enzymatic way applied for Glu, Fru, and Suc allowed the determination of the involvement of these regular sugars to osmotic adjustment.

The early accretion of whole sugars at 2 h gives considerable reduction in the OP (osmotic adjustment), attained betwixt 38 and 50% of osmotic adjustment at 7 h. The degree of whole sugars accretion illustrated a same outline in all varieties, e.g., MBB-var showed the highest accretion track by Inrat-var, Waha-var, and a lesser rate in OZ-var, which demonstrated the slightest rank of accretion. This outline was in accord with the modification in osmotic adjustment. Accumulation of sugars was primary announced in durum wheat but below long-term drought (Kameli and Lösel, 1995).

The outcome of this work designated a likely significant involvement of oligo-fructans to osmotic adjustment in every variety excluding the OZ-var. The function of oligo-fructan in lack resistance was further recommended by Hendry (1993), who declared that the emergence of fructan pro-suggest taxa matched with a climatological change on the way of cyclic drought and that the sharing of current fructan flora corresponds through areas of seasonal deficiency. Supplementary verification for a function of fructans in lack tolerance was given by the result in the genetically modified sugar beet, *Beta vulgaris*. Conversely, introduction of oligo-fructans in this non-fructan-producing species reconciles improved opposition to lack stress (Pilon-Smits *et al.*, 1999). Interestingly, the fructans enhance the growth in transgenic fructan-accumulating tobacco under water deficit (Pilon-Smits *et al.*, 1995). Was also considered as storage sugars of many species of grasses, and were given an important amount of cold tolerance (Livingston et al 2009).

More interestingly, many reports identify the opportunity that fructans might directly steady membranes below stress conditions (Hincha *et al.*, 2000).

The works examining the influence of fructan on liposomes showing that a straight relation betwixt membranes and fructan was promising. This novel field of investigation began to combine the fructan and its relationship by stress beyond simple association. This helps prevent leakage when water is isolated from the system either throughout drought (Livingston *et al.*, 2009).

The large accumulation of K^+, although its negligible concentration under the nutrient solution, it can indicate the physiological need of the plant to this cation. The involvement of K^+ to the osmotic adjustment has been exposed to increase with K^+ fertilization on the long-term in youthful durum wheat foliage below water stress (Damon *et al.*, 2011). As claimed by Fricke *et al.*, (2006); membrane potential is together a driving power and a probable monitor and is a significance of trans-membrane solute permeation and transport. This might propose that the rate in membrane possible agrees with growth recuperation and precedes solute accretion at osmotically considerable levels.

4.2. Balance betwixt carbohydrate accretion, photosynthesis, and LER throughout the stress

In terms of sugar stocks, we record here their levels in two periods of growth: The first, in normal conditions (before stress) followed by the second period of the stress response (osmotic adjustment). Data exposed no significant relationship betwixt the accretion of totality of carbohydrates and the reduction of LER throughout the stress, which might show that carbohydrate accretion, is not a direct result of growth decrease. This may be

associated with a complex development related to osmotic adjustment. These data maintain the active accumulation idea of solutes by the high permeability of sugars through the membrane or the hydrolysis of oligo-fructans or other sugars, as an osmotic reserve quite the passive accretion. It has been reported, that the water insufficiency usually augment the concentration of carbon in plant organs (Muller *et al.*, 2011), leading to an unbalance between expansion, the activity of organs, and photosynthesis. It seems, therefore, that metabolic processes and active accumulation of carbon depends on osmotic adjustment rather than on a passive accumulation of carbon as a result of the lack of growth during stress. In a second period, the growth recovery may be better associated with carbohydrate fluctuations introduced from the phloem and/or to carbohydrate gradients between the mature and elongating part of the growing leaf. The EZ has better osmotic adjustment and greater capacities to transport assimilate for growth, the same case for the fifth leaf of barley (Hein *et al.*, 2016).

In other studies, in reaction to the stress, abscisic acid (ABA) controls the activity of the β-amylase 1 (BAM1) and α-amylase 3 (AMY3) transcription via the ABA-dependent AREB/ABF-SnRK2 kinase-signaling pathway. A part of the released maltose from starch by the synergistic activity of amylases (BAM1 + AMY3) is export to the cytosol and metabolized into sucrose and free hexoses. The Suc is subsequently exported to the root or the buds to sustain osmotic adjustment. Hence, the creation of starch hydrolysis below abiotic stress shows to be an ordinary plant response as reported by Thalmann *et al.*, (2016) and Zanella *et al.*, (2016). Contrary to what was recorded in our previous results, starch levels were maintained or even elevated under long stress in barley leaves (Mahdid and Kameli, 1998). This led us to exclude the hypothesis of starch hydrolysis. We prefer here the mobilization of sugars to the EZ region across the membranes as an active transport.

. The insufficient recovery of growth despite the full recovery of turgor at short term stress may be signifying that additional mechanisms, probably concerning the cell wall rheology, growth, and cell function. As noted above (Bartlett *et al.*, 2012), and as detailed by Muller *et al.*, (2011), which suggested the possible implication of cell wall rheology or water flows to growing cells, override the role of C availability in sink organs such as mature leaves and take the lead on growth control.

The current research work does not specify also any relationship between the accretion of soluble carbohydrates and photosynthetic activity during stress which indicates that LER typically falls more quickly than photosynthetic revovery. Taking into consideration the transitive relationship between photosynthesis activity and LER diminution during stress, the accumulation of sugars by an osmotic adjustment is not a consequence of those intended for growth. The accretion of these carbohydrates is perhaps separated with direct photosynthesis activity. Muller *et al.*, (2011), mentioned this augment of the concentration of the carbon in plant organs may owe organ expansion (as a key carbon sink) being affected previously and more intensively than photosynthesis. The photosynthetic products (carbohydrates, etc.) can accrue to affect the osmotic adjustment when growth is initially condensed by water insufficiency whereas photosynthesis affected slightly. This reinforces the idea of the supply of these sugars from mature tissues, and this is evidenced by the increase in different soluble sugars in mature tissues

The inorganic solutes, e.g. potassium, are efficient in improving the osmotic adjustment. The maintenance of photosynthesis in water deficit is in line with other studies (Kaiser, 1987, Quick *et al.*, 1992; Bogeat-Triboulot *et al.*, 2007). As the data of Hasibeder *et al.*, (2015), who indicated that in drought conditions, the use of recent photosynthesis is shifted from metabolic activity to osmotic adjustment and storage compounds in grasses!

A partial stomatal aperture may allow the maintenance of photosynthesis through CO_2 supply, at least with low levels (Fig. 6). Hummel *et al.*, (2010), demonstrated that the rosette relative expansion yield of *Arabidopsis thaliana* is reduced further than photosynthesis in drought and that of the osmotic adjustment cost only a little percent of each day photosynthetic of the carbon fixation. This strengthens the suggestion of the recruitment of soluble carbohydrate or/and the employ of the carbon reserves for the osmotic adjustment of sink organs (old leaves or MZ).

As a conclusion, it is clear that the differences observed in the partial rate of LER are owing to the total plant turgor recovery (ΨP) caused by the fast osmotic adjustment. Nonetheless, the insufficient recovery of growth despite the magnitude of osmotic adjustment at short-term stress may propose that other mechanisms, may be relating to the cell wall rheology or wall extensibility changes. This fast osmotic adjustment occurs using chiefly entirety soluble sugars and potassium. We can consider the accumulation of total carbohydrates is uncoupled with direct photosynthesis or the reduction of the growth. Consequently, the increase of these carbohydrates possibly is undoing with direct activity of the photosynthesis. It is rather the mobilization of soluble carbohydrate or/and the exploit of the carbon reserves of nearby source organs in favor of EZ.

Acknowledgments

This study was financed by the “Direction Générale de la Recherche Scientifique et du Développement Technologique (DG-RSDT) in Algeria. The authors want to express their sincere gratitude to Mr. Gaëlle Rolland for her outstanding technical assistance in the applied behavior analysis and Miss Myriam Dauzat for her kind help in the photosynthesis measurement. The authors also want to sincerely acknowledge Dr. Issam Boudia (Université of M’Sila, Algeria) and Prof. Bassem Jaouadi (Centre of Biotechnology of Sfax, Tunisia) for language editing and polishing services as well as constructive proofreading.

Conflict of interest

The authors declare that they have no conflict of interest with this work and the preparation of the manuscript.

References

Bartlett MK, Scoffoni C and Sack L. 2012. The determinants of leaf turgor loss point and prediction of drought tolerance of species and biomes: A global meta-analysis. *Ecol Lett.,* **15**:393-405.

Blum A. 2016. Osmotic adjustment is a prime drought stress adaptive engine in support of plant production. *Plant Cell Environ,* 1-7.

Bogeat-Triboulot MB, Brosche M, Renaut J, Jouve L, Le Thiec D, Fayyaz P, Vinocur B, Witters E, Laukens K and Teichmann T. 2007. Gradual soil water depletion results in reversible changes of gene expression, protein profiles, ecophysiology, and growth performance in *Populus euphratica*, a poplar growing in arid regions. *Plant Physiol.,* **143**:876-892.

Chen T, Chen Y, Wang X and Zhang L. 2019. Osmotic adjustment in roots and leaves of two cotton cultivars with different tolerance to soil salinity. *Biomed J Sci Tech Res,* **15**:11249-11258.

Collins FW and Chandorkar KR. 1971. Thin-layer chromatography of fructooligosaccharides, *J Chromat.,* **56**:163-167.

Damon PM, Ma QF and Rengel Z. 2011. Wheat genotypes differ in potassium accumulation and osmotic adjustment under drought stress. *Crop Pasture Sci.,* **62**:550-555.

Dubois M, Gilles KA, Hamilton JK, Robers PA and Smith F. 1956. Calorimetric method for determination of sugars and related substances. *Annal Chem.,* **28**:350-356.

Fricke W and Peters WS. 2002. The biophysics of leaf growth in salt-stressed barley. A study at the cell level. *Plant Physiol,* **139**:374-388.

Fricke W. 2004. Rapid and tissue-specific accumulation of solutes in the growth zone of barley leaves in response to salinity. *Planta,* **219**:515-525.

Fricke W, Akhiyarova G, Wei W, Alexandersson E, Miller A, Kjellbom PO, Richardson A, Wojciechowski T, Schreiber L, Veselov D, Kudoyarova G and Volkov V. 2006. The short-term growth response to salt of the developing barley leaf. *J Exp Bot,* **57**:1079-1095.

Hasibeder R, Fuchslueger L, Richter A and Bahn M. 2015. Summer drought alters carbon allocation to roots and root respiration in mountain grassland. *New Phytologist,* **205**:1117-1127.

Hein JA, Sherrard ME, Manfredi KP and Abebe T. 2016.The fifth leaf and spike organs of barley (*Hordeum vulgare* L.) display different physiological and metabolic responses to drought stress. *BMC Plant Biol,* **16**:248.

Hendry GAF. 1993. Evolutionary origins and natural functions of fructans. A climatological, biogeographic and mechanistic appraisal, *New Phytologist,* **123**:3-14.

Hincha DK, Hellwege EM, Heyer AG and Crowe JH. 2000. Plant fructans stabilize phosphatidylcholine liposomes during freeze-drying. *Eur J Biochem,* **267**:535-540.

Hu Y, Camp, KH and Schmidhalter U. 2000. Kinetics and spatial distribution of leaf elongation of wheat (*Triticum aestivum* L.) under saline soil conditions. *Int J Plant Sci,* **161**:575-582.

Hummel I, Pantin F, Sulpice R, Piques M, Rolland G, Dauzat M, Christophe A, Pervent M, Bouteille M, Stitt M, Gibon Y and Muller B. 2010. *Arabidopsis thaliana* plants acclimate to water deficit at low cost through changes of C usage; an integrated perspective using growth, metabolite, enzyme and gene expression analysis. *Plant Physiol,* **154**:357-372.

Kaiser WM. 1987. Effects of water deficit on photosynthetic capacity, *Physiol Plant,* 71142-71149.

Kameli A and Lösel DM. 1995. Contribution of carbohydrates and other solutes to osmotic adjustment in wheat leaves under water stress. *J Plant Physiol,* **145**:363-366.

Kusaka M, Lalusin AC and Fujimura T. 2004. The maintenance of growth and turgor in pearl millet (*Pennisetum glaucum* [L.] Leeke) cultivars with different root structures and osmoregulation under drought stress. *Plant Sci,* **168**:1-14.

Livingston DP, Hincha DK and Heyer AG. 2009. Fructan and its relationship to abiotic stress tolerance in plants. *Cell Mol Life Sci,* **66**:2007-2023.

Mahdid M and Kameli A. 1998. A comparative study of water stress on osmotic adjustment in barley (*Hordeum vulgare*) and field bean (*Vicia faba*). *Rech. Agronom.,* **2**:67-80.

Mahdid M, Kameli A, Ehlert C and Simonneau T. 2011., Rapid changes in leaf elongation, ABA, and water status during the recovery phase following application of water stress in two durum wheat varieties differing in drought tolerance. *Plant Physiol Biochem.,* **49**:1077-1083.

Mahdid M, Kameli A, Ehlert C and Simonneau T. 2014. Recovery of leaf elongation during short term osmotic stress correlates with osmotic adjustment and cell turgor restoration in different Durum wheat cultivars. *Pak J Bot.,* **46**:1747-1754.

Meziani L, Bamoun A, Hamou N, Brinis L and Monneveux P. 1992. Essai de définition des caractères d'adaptation du blé dur dans différentes zones agroclimatiques de l'Algérie. In : Tolérance à la sécheresse des céréales en zones Méditerranéennes. Diversité et Amélioration Variétale. 191-203, INRA, Paris.

Morgan JM. 1991. A gene controlling differences in osmoregulation in wheat. *Aust J Plant Physiol,* **18**:249-257.

Morgan JM and Tan MK. 1996. Chromosomal location of a wheat osmoregulation gene using RFLP analysis. *Aust J Plant Physiol,* **23**:803-806.

Munns R, Passioura JB, Juo G, Chazen O and Cramer GR. 2000. Water relations and leaf expansion, importance of time scale. *J Exp Bot.,* **51**:350, 1495-1504.

Munns R. 2002. Comparative physiology of salt and water stress. *Plant Cell Environ.,* **25**:239-250.

Muller B, Pantin F, Gerard M, Turc O, Freixes S, Piques M and Gibon Y. 2011. Water deficits uncouple growth from photosynthesis, increase C content, and modify the relationships between C and growth in sink organs. *J Exp Botany,* **62**:1715-1729.

Osakabe Y, Arinaga N, Umezawa T, Katsura S, Nagamachi K, Tanaka H, Ohiraki H, Yamada K, Seo SU, Abo M, Yoshimura E, Shinozaki K and Yamaguchi-Shinozaki K. 2013. Osmotic stress responses and plant growth controlled by potassium transporters in *Arabidopsis*. *Plant Cell,* **25**:609-624.

Quick WP, Chaves MM, Wendler R, David M, Rodrigues ML, Passaharinho JA, Pereira JS, Adcock MD, Leegood RC and Stitt M. 1992. The effect of water stress on photosynthetic carbon metabolism in four species grown under field conditions. *Plant Cell Environ,* **15**:25-35.

Pilon-Smits EAH, Ebskamp MJM., Paul MJ, Jeuken MJW, Weisbeek PJ and Smeekens SCM. 1995. Improved performance of transgenic fructan-accumulating tobacco under drought stress. *Plant Physiol.,* **107**:125-130.

Pilon-Smits EAH, Terry N, Sears T and Van Dun K. 1999. Enhanced drought resistance in fructan-producing sugar beet. *Plant Physiol Biochem.,* **37**:313-317.

Poormohammad Kiani S, Talia P, Maury P, Grieu P, Heinz R, Perrault V, Nishinakamasu V, Hopp E, Gentzbittel L, Paniego N

and Sarrafi A. 2007. Genetic analysis of plant water status and osmotic adjustment in recombinant inbred lines of sunflower under two water treatments. *Plant Sci.*, **172**:773-787.

Schnyder H, Nelson CJ and Colts JH. 1987. Assessment of the spatial distribution of growth in the elongation zone of grass leaf blades. *Plant Physiol.*, **85**:290-293.

Thalmann M, Pazmino D, Seung D, Horrer D, Nigro A, Meier T, Kölling K, Pfeifhofer HW, Zeeman SC and Santelia D. 2016. Regulation of leaf starch degradation by abscisic acid is important for osmotic stress tolerance in plants. *Plant Cell*, **28**:1860-1878.

Velázquez-Márquez S, Conde-Martínez V, Trejo C, Delgado-Alvarado A, Carballo A, Suárez R and Trujillo AR. 2015. Effects of water deficit on radical apex elongation and solute accumulation in Zea mays L. *Plant Physiol Biochem.*, **96**:29-37.

Wilson JR, Ludlow MM, Fischer MJ and Schultz ED. 1980. Adaptation to water stress of leaf water relations characteristics of some tropical forage grasses and legume in semi-arid environment. *Aust J Plant Physiol*., **7**:207-220.

Wise CS, Dimler RJ, Davis HA and Rist CE. 1955. Determination of easily hydrolyzable fructose units in dextran preparations. *Anal Chem.*, **27**:33-36.

Zanella M, Borghi GL, Pirone C, Thalmann M, Pazmino D, Costa A, Santelia D, Trost P and Sparla F. 2016. β-amylase 1 (BAM1) degrades transitory starch to sustain proline biosynthesis during drought stress. *J Exp Botany*, **67**:1819-1826.

JJBS

Volume 14, Number 1, March 2021
ISSN 1995-6673
Pages 157 - 161

Jordan Journal of Biological Sciences

Utilization of Agro-industrial wastes as carbon source in solid-state fermentation processes for the production of value-added byproducts

Mahmoud W. Sadik[1], Moustafa M. Zohair[2,3,*], Ahmed A. El-Beih[2], Eman R. Hamed[2] and Mohamed Z. Sedik[1]

[1]*Microbiology Department, Faculty of Agriculture, Cairo University, Egypt,*[2]*Chemistry of Natural and Microbial Products Department. Pharmaceutical Industries Research Division, National Research Centre, Giza, 12311, Egypt,*[3]*Nanomaterial Investigation Lab., Central Laboratories Network, National Research Centre, Dokki, Giza, 12622, Egypt*

Received: March 30, 2020; Revised: July 5, 2020; Accepted: August 24, 2020

Abstract

Utilization of agro industrial wastes as solid support was evaluated in solid state fermentation (SSF) methods to produce value-added byproducts such as antioxidants and antimicrobial agents. Among these agricultural wastes added as a carbon source in SSF process are corn cobs, olive mill, wheat bran, rice straw, rice bran and sorghum. The biological activities of the extracts of ethyl acetate (EtOAc) of *Aspergillus pseudocaelatus* MG772677 and *Trichoderma gamsii* KX685665 strains were studied. The extract of ethyl acetate of *A. pseudocaelatus* cultured on medium containing sorghum as natural carbon source showed the highest inhibitory activity against tested microorganisms. The antioxidant activity results varied based on the used waste as a carbon source as well as the incubation period. The EtOAc extracts of *A. pseudocaelatus* and *T. gamsii* cultivated on different agricultural wastes media showed potent antioxidant activities of scavenging DPPH when compared to those cultivated on PDA media. The highest percentage of antioxidant activity (53.84%) for the EtOAc extract of *T. gamsii* was observed after 7 days of incubation period.

Keywords: Agro-industrial wastes *Aspergillus pseudocaelatus* MG772677, *Trichoderma gamsii* KX685665, Antimicrobial, Antioxidant and solid-state fermentation

1. Introduction

The manufacturing processing of agricultural raw materials generates a huge amount of wastes which are either burned or used for animal feeding. These wastes are usually rich in carbohydrates, proteins and minerals, and should be exploited as raw materials for other industries. Accumulation of agricultural wastes in huge quantities annually results not only in the environmental deterioration, but also in economic loss as these wastes can be utilized for production of high valuable products, for instance food, energy and chemicals producing (Singh, 2009). The carbon content, nutrient and moisture in these agricultural wastes offer favorable environment for the microbial growth, which opens up considerable potential for recycle in solid state fermentation (Mussato *et al.*, 2012).

The microbial species can exploit these collective wastes from agricultural industries, specially, fungi strains, which have the ability to produce hydrolytic enzymes such as chitinase and cellulose to ferment these wastes. The utilization of industrial agricultural waste in solid state fermentation is of particular importance because it is considered available and economic, as well as being an eco-friendly alternate for their discarding. The fermentation could be affected by some factors which could maximize the produced yields; these factors include the modifying of substrates size, moisture content, pH, temperature… etc. (Nigam and Pandey, 2009). In general, produced yield can be maximized by selecting an appropriate substrate or a combination of substrates with suitable conditions (Mussatto *et al.,* 2012). The large scale production of secondary metabolites requires studying the effective factors which include abiotic and biotic factors (Shentu *et al.*, 2013).

Fungi have been proven to be potent source for biologically active compounds with therapeutic potential (Hoeksma *et al.,* 2019) and has produced a number of compounds of medical importance, including penicillin, Lovastatin and caspofungin (Goler 2007; Keating and Figgitt, 2003; Vandermolen *et al.,* 2013). *Aspergillu*s and *Trichoderma* species are a valuable source of commercial enzymes used in the recycling of cellulose waste (Reino and Guerrero, 2008).

New and better techniques for the recovery of agricultural waste have been developed due to industrial innovation and high technology. These techniques contribute to maintaining resources efficiency, sustainable production, consumption and reduction of negative environmental impacts (Duque-Acevedo *et al.,* 2020). The aim of this research was to study the application of various industrial agricultural wastes as a carbon source or nutrient

* Corresponding author e-mail: moustafazohair@yahoo.com , Mo.zohair@nrc.sci.eg.

in SSF processes in order to produce antimicrobials and antioxidant agents.

2. Materials and Methods

2.1. Fungal strains

Two fungal strains, *Aspergillus pseudocaelatus* and *Trichoderma gamsii*, were recovered from rhizosphere area of medicinal plants (*Aloe vera*), Basil, (*Ocimum basilicum*), and Peppermint (*Mentha piperita*), planted in Sekem farm, Heliopolis University, Cairo, Egypt under organic farming regulations. The strains were maintained and stored on the surface of PDA slants at 4° C. They were identified on the basis of their morphological and microscopic characteristics as well as 18s rDNA (Zohair *et al.*, 2018).

2.2. Solid State Fermentation

Corncobs, olive mill pomace, rice bran, rice straw, sorghum and wheat bran wastes were obtained from the local fields in Giza governorate, Egypt, dried in oven at 55 °C for 48 h and ground to 40-mesh (400 um) were utilized as fermentation carbon sources. Three grams of the solid substrates were added to Erlenmeyer flasks (250 ml). The substrate moisture content was adjusted to 75% with solution of minerals (KH_2PO_4; 2.0 g/L, $CaCl_2$; 0.3 g/L, $MgSO_4$; 0.3 g/L, $FeSO_4$;0.11 g/L, $ZnSO_4$; 0.3 g/L). The pH of prepared solutions was adjusted to 6 then added to the solid substrate. The flasks contents were mixed well and autoclaved for 20 min at 121 ºC at 1 atm and then inoculated individually with 2discs each 6mm in diameter of *A. pseudocaelatus* or *T. gamsii* fungal strains grown on PDA fresh cultures. Incubation was carried out at 25-28 ºC up to 19 days. Flasks, incubated without inoculation, were used as a negative control, while flasks containing 100 ml of PDA medium inoculated with strains *A. pseudocaelatus* or *T. gamsii* strains were used as positive control.

2.3. Liquid culture and metabolite production

2.3.1. Extraction of crude extract

After different incubation period (7,11,15 and 19 days) cultivation medium and mycelial mats were soaked overnight in ethyl acetate (1:1, v/v), then were homogenized in ethyl acetate using an Ultra Sonic wave (*J.P selecta s.a* sonicator). The extraction process was carried out three times for complete extraction. All of the organic fractions were collected and dried using rotary evaporator at 40°C (180 rpm) under vacuum condition. The dried crude extract was subjected to biological activity evaluation (Zohair *et al.*, 2018).

2.3.2. Biological activity of the isolated fungal secondary metabolites

A. pseudocaelatus and *T. gamsii* ethyl acetate extracts were tested biologically using different bio-assays to determine antimicrobial activity using method of agar disc diffusion (El-Sawy *et al*., 2015; Yasser *et al.*, 2020) and antioxidant activity using DPPH assay (Hamed, 2009).

2.3.2.1. Antimicrobial activity

The antibacterial and antifungal activities were screened against different pathogenic strains through the agar disk diffusion methods (El-Sawy *et al*., 2015). Concentrations (1 mg/*5 µl*) of *A. pseudocaelatus* and *T. gamsii* ethyl acetate extracts were assessed against Gram positive bacteria such as *Bacillus subtilis* ATCC6633 and *Staphylococcus aureus* ATCC29213. It was also tested against Gram negative bacteria such as *Escherichia coli* ATCC25922, and *Salmonella enterica* ATCC25566. Also, it was tested against tested yeasts and fungal strains such as *Fusarium solani* NRC15 and *Aspergillus niger* NRC23, in addition to yeasts (*Candida albicans, Candida. trobicalis*). The concentration of tested fungi was 1×10^8 spores/ml. The concentration of the tested bacterial pathogens was 1×10^6 cfu/ml. The test was done within sterilized Petri dishes including 25 ml of sterilized PDA medium in case of fungi and in nutrient agar medium in case of bacteria. Thiophenicol and Treflucan antibiotics were used as positive controls for bacteria and fungi with concentration of 100 µg/disk. The Dimethyl sulfoxide antibiotic (DMSO) was used as a negative control. The prepared disks were loaded on Petri dishes containing the inoculated media then incubated for 24 hours at 30 °C for bacterial strains and 72 hours at 28 °C for fungal strains, respectively. The inhibition zones were measured.

2.3.2.2. In vitro determination of antioxidant activity

This assay was performed according to Hamed (2009) with some modifications. One mg of ethyl acetate fungal extract was dissolved in 1 ml of Dimethyl sulfoxide (DMSO) to prepare 1000 µg/ml stock solution. 2,2-Diphenyl-1-picrylhydrazyl (DPPH) (0.004 mg) was dissolved in 100 ml of methyl alcohol HPLC grade to make concentration 0.004% solution. Different concentrations (5-25 µg) of reference standard compounds such as Quercetin and Vitamin C were prepared. In a 96-wellplate, 20 µl of stock solutions (samples –or standard) was added into each well then 180 µl of methanol solution of DPPH (0.004%) was added to complete the final concentration of evaluated samples 100 µg/ml. After 30 min. of incubation, the plate was scanned at λ = 540 nm using microplate reader. In case of blank, 20 µl of dissolving agent (DMSO) were added instead of 20 µl of samples. The assay was repeated twice to confirm the records. The activity of radical scavenging could be determined based on the given equation:

Scavenging Activity (%) = $[(A_{Blank} - A_{Sample}) / A_{blank}] \times 100$

Where, A_{Blank} (Absorbance of mixture without sample "DPPH only"), A_{Sample} (Absorbance of test samples).

Samples that indicated 50% or higher antioxidant activity at 100 µg / ml concentration compared to control were considered active. The effect of scavenging on DPPH free radicals was estimated according to (Shimada *et al.*, 1992).

2.4. Data Analysis

The analysis of variance (ANOVA) was evaluated using MSTATC software. The differences of significance between means were compared based on the least significance differences (LSD) test at 5% significant level.

3. Results and Discussion

3.1. Activity of the fungal extract as Antimicrobial agents

A. pseudocaelatus EtOAc extract showed a strong antimicrobial activity as shown in (Table 1). It presented a

strong inhibitory activity against pathogenic tested yeasts and fungal strains (*Candida albicans, C. trobicalis, Fusarium solani, Rhizoctonia solani, Sclerotium rolfsii and Verticillium dahliae*) with zones of inhibition 13.5, 15.5, 14, 15, 7 and 8 mm diameter, respectively. For bacterial tested strains, *A. pseudocaelatus* extract has a significant effect against *B.subtilis* ATCC 6633, *E.coli* ATCC 25922, *S. aureus* ATCC 25923 and *S. enteric* ATCC 25566 with inhibition zones of 20, 19.5, 18.5 and 14.5 mm, respectively.

Table 1. Antimicrobial effect of *A. pseudocaelatus* extract.

Pathogenic		*A. pseudocaelatus* extract	Positive control
		Diameter of inhibition zone (mm)	
G+ve bacterial strains	*B.subtilis*	20±0.0	22.5±0.5
	S.aureus	13.5±0.5	18.5±0.5
G-ve bacterial strains	*E.coli*	18.5±0.5	11.5±0.5
	S.enterica	14.5±1.5	15±0.0
Yeast	*C.albicans*	13.5±0.5	7.5±0.5
	C.tropicalis	15.5±0.5	7±0.0
Fungi	*F.solani*	14±0.6	7±0.0
	R.solani	15±0.0	7±0.0
	S.rolfsii	7±0.0	7±0.0
	V.dahliae	8±.01	8.5±0.5

Notes: The inhibition zone measured as diameter expressed in (mm). (Values are mean ± S.D.)

Treflucan and Thiophenicol were applied with a concentration of 100 µg/disc as positive controls, DMSO was applied as negative control.

Extract of *T. gamsii* fungus resulted in a moderate activity against all yeasts and fungal pathogenic tested pathogens strains (*C.albicans*, *C.tropicalis*, *F.solani*, *R.solani*, *S.rolfsii* and *V.dahliae*) with inhibition zones of 8, 7, 8, 7, 7 and 7mm diameter, respectively. In parallel, the extract of *T. gamsii* had a moderate effect against *B. subtilis* ATCC6633, *S. aureus* ATCC 25923, *E. coli* ATCC 25922 and *S. enteric* ATCC 25566 with diameter of inhibition zone 12, 13.5, 9 & 7 mm, respectively as shown in (Table 2**).**

Table 2. Antimicrobial effect of *T. gamsii* extract.

Pathogenic		*T. gamsii* extract	Positive control
		Diameter of inhibition zone (mm)	
G+ve bacterial strains	*B.subtilis*	12±0.0	22.5±0.5
	S.aureus	13.5±0.5	18.5±0.5
G-ve bacterial strains	*E.coli*	9±0.0	11.5±0.5
	S.enterica	7±0.0	15±0.0
Yeast	*C.albicans*	8±0.0	7.5±0.5
	C.tropicalis	7±1	7±0.0
Fungi	*F.solani*	8±0.0	7±0.0
	R.solani	7±0.0	7±0.0
	S.rolfsii	7±0.0	7±0.0
	V.dahliae	7±0.0	8.5±0.5

Notes: The inhibition zone measured as diameter expressed in (mm). (Values are mean ± S.D.)

Treflucan and Thiophenicol were applied with a concentration of 100 µg/disc as positive controls, DMSO was applied as negative control.

Saleh *et al.* (2011) found that some of *Trichoderma* spp crude extract had an antibacterial effect against some bacterial pathogens with zones of inhibition fluctuating from (10 to 28 mm). Also**,** Vinale *et al.* (2006) indicated that *Trichoderma harzianum* fungal strains (T22 &T39) secondary metabolites showed an inhibition activity against plant pathogens *Pythium ultimum* and *R.solani*. From the above results, the *A. pseudocaelatus* ethyl acetate extract was more effective than the *T. gamsii* extract. These results were in agreement with Zohair *et al.*, (2018) who indicated that the biological activity of EtOAc extract of *A. pseudocaelatus* was more active than that of *T. gamsii*. It showed an effective inhibitory result against fungal test strains (*C.albicans, C.tropicalis, F.solani, R.solani, S.rolfsii & V.dahliae*).

Both fungi showed the capability of utilization of different agricultural industrial wastes used as carbon sources. As shown in Fig.1.

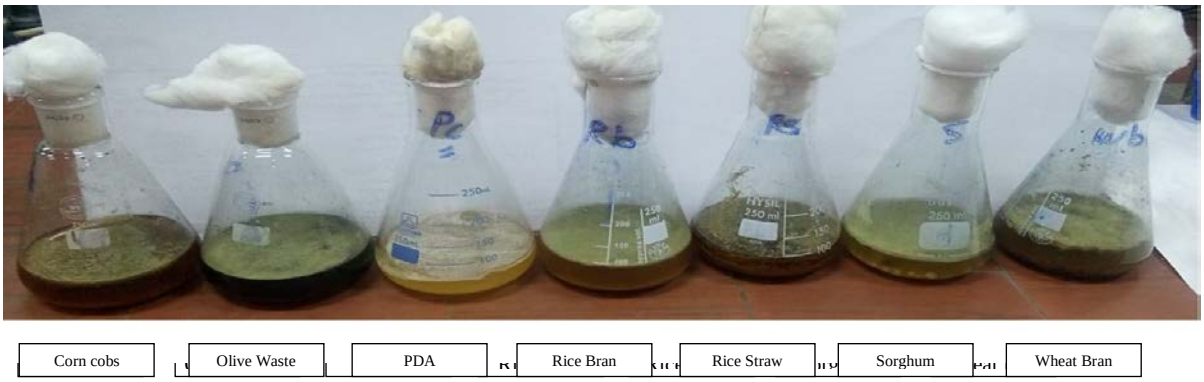

Figure 1. *A. pseudocaelatus* cultivated on media contain different agricultural industrial wastes as carbon sources

The most effective one as a medium was the agriculture waste, sorghum. The highest inhibition zone was obtained from *A. pseudocaelatus* cultivated on media containing sorghum as carbon sources after 15 days of incubation period. It exhibited antibacterial activity against both Gram-positive bacterial strains *B.subtilis* ATCC6633 and *S.aureus* ATCC25923 with inhibition zones of 26.0 and 22.5 mm diameter, respectively. Also, it exhibited antibacterial activity against Gram-negative bacterial strains *E. coli* ATCC25922 and *S.enterica* ATCC25566 with inhibition zones of 24.0 and 22.5 mm diameter, respectively as shown in (**Fig. 2**).

Many studies have suggested that sorghum and sorghum processing waste have a huge potential for the production of value added products due to its content of fermentable sugars (starch, sucrose, glucose and fructose),

and lignocelluloses feed stock. Makanjuola *et al.* (2019) reported that the high residual starch (up to 53% (w/w) in sorghum waste makes it rich medium for *Aspergillus awamori* growth for production of value added product.

The anti-yeast activity was 22.5 and 13.0 mm with *Candida albicans* ATCC 10321 and *Candida tropicalis* ATCC750, respectively, while the antifungal activity was 21.0 and 20.0 mm against *F. oxysporium* and *A. niger* as presented in (Fig. 2 & 3).

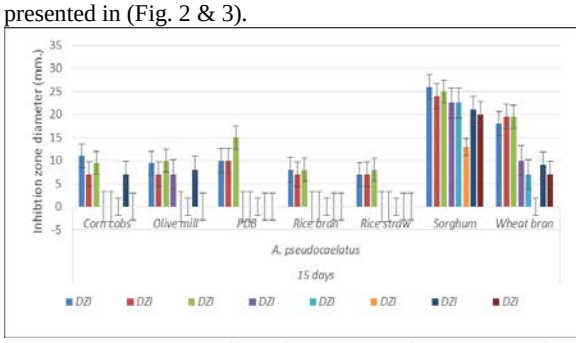

Figure 2. Antimicrobial effect of ethyl acetate fungal extract of *A. pseudocaelatus* using solid state fermentation after 15 days of incubation period.

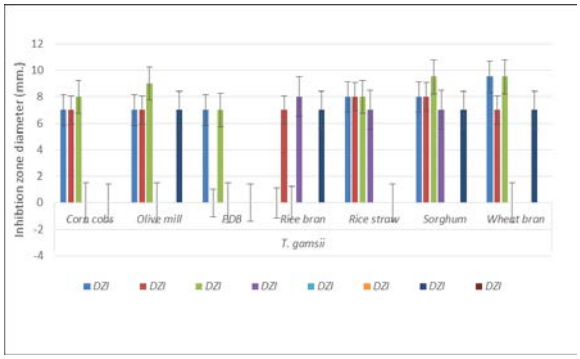

Figure 3. Antimicrobial effect of ethyl acetate fungal extract of *T. gamsii* using solid state fermentation after 15 days of incubation period.

Pandey *et al.* (2001) reported production of Cyclosporin A from *Tolypocladium infautum* using wheat bran and oxytetracycline antibiotic by *S. rimosus* using corn cob in solid state fermentation.

Ethyl acetate extract of *A. pseudocaelatus* on media containing sorghum as natural alternative carbon sources had the higher inhibitory activity against all tested microorganism than using PDA media. It showed antibacterial activity against both Gram-positive bacteria (*B. subtilis* ATCC6633 and *S. aureus* ATCC25923) and Gram-negative bacteria (*E.coli* ATCC25922 and *S. enterica* ATCC25566) with inhibition zones of 26.0, 22.5, 24.0 and 22.5 mm, respectively while the inhibition zone of EtOAc extract of *A. pseudocaelatus* growing on PDA media was 20, 19.5, 18.5 and 14.5 mm, against *B. subtilis* ATCC 6633, *S. aureus* ATCC 25923, *E.coli* ATCC 25922 and *S. enteric* 25566, respectively.

Also, the anti-pathogenic yeast activity was 22.5 and 13.0 mm with *C. albicans* ATCC 10321 and *C. tropicalis* ATCC 750, respectively using the sorghum as natural alternative carbon sources compared with 13.5 and 15.5mm diameter of ethyl acetate extract of *A. pseudocaelatus* fermented on PDA for 15 days of incubation**.**

3.2. In vitro antioxidant activity of ethyl acetate extract

The antioxidant capacity of the fungal isolates is shown in **Table 3**. The DPPH scavenging activity varied between the two fungal isolates ethyl acetate extracts. The *T. gamsii* extract showed a higher antioxidant activity than *A. pseudocaelatus extract.*

Table 3. Antioxidant potential of ethyl acetate (EtOAc) extract of *A. pseudocaelatus* and *T. gamsii* cultivated on PDA media

Ethyl acetate extract	Antioxidant activity %
A. pseudocaelatus	1.926
T. gamsii	14.788

The variation on the antioxidant activity can be attributed to the used waste as a carbon source and the incubation period. Both isolates showed differential utilization of the various carbon sources. The use of corn cobs waste as a carbon source enhanced the optimization of antioxidant activity percentage. The highest percentage of antioxidant activity observed was 53.84% for *T. gamsii* ethyl acetate extract after 7 days of incubation **(Table 4).**

Table 4. *In vitro* antioxidant activity (%) of *A. pseudocaelatus* and *T. gamsii* ethyl acetate extract cultivated on media containing different agricultural wastes and their different incubation periods (days).

Waste/ Incubation Period	7 days	11 days	14 days	19 days
	Ethyl acetate extract of *A. pseudocaelatus*			
Corn cobs	27.051	28.049	18.136	31.339
Olive meal	4.379	3.681	7.254	6.411
PDB	27.217	23.736	18.080	16.142
Rice bran	4.780	11.154	6.250	3.492
Rice straw	6.648	7.422	15.179	21.294
Sorghum	4.286	16.853	9.845	9.559
Wheat bran	4.478	18.080	8.930	9.134
	Ethyl acetate extract of *T. gamsii*			
Corn cobs	53.846	27.679	21.694	31.241
Olive meal	10.165	2.679	1.202	1.577
PDB	7.923	6.585	5.209	19.191
Rice bran	5.989	13.728	0.801	2.231
Rice straw	31.703	5.636	9.960	8.539
Sorghum	4.945	6.250	4.236	10.800
Wheat bran	7.418	14.286	6.926	9.015

The antioxidant effects of the *A. pseudocaelatus* and *T. gamsii* extracts ranged from 3.681 to 31.33% for olive waste and corncobs after 11 and 19 days incubation times, respectively. Meanwhile it ranged 1.20 and 53.84 % of DPPH scavenging, respectively with *A. pseudocaelatus and T. gamsii* cultivated on olive mill and corncobs after 14 days and 7 days, respectively. The fungal extracts of *A. pseudocaelatus* and *T. gamsii* cultivated on PDA showed antioxidant activity of 1.92 and 14.78 %, respectively.

Awad *et al.* (2018) reported that the volatile compound extracted from *Trichoderma viride* mycelia showed antioxidant effects by 29.62%, 63.12% and 70.37% at concentrations of 10, 50 and 100 µg, respectively. Moreover, other constituents such as carbohydrates, proteins could have remarkable antioxidant effects ranging from 3.70 - 33.00% for proteins and 3.00 - 23.00% for carbohydrates at concentrations of 10 - 100 µg, respectively.

The ability of the used fungal strains to produce hydrolytic enzymes could offer a promising chance for

exploiting these strains in waste conversion. Zohair *et al.* (2018) reported that *A. pseudocaelatus* exhibited a high hydrolytic ability to utilize carboxy methylcellulose and a moderate hydrolytic capacity of chitin (62.14 and 34.29 %), respectively, while *T. gamsii* had a high ability for hydrolyzing of carboxymethyl cellulose (CMC) and chitin 70.00 and 36.25 %, respectively. The use of hydrolytic enzymes to degrade agricultural wastes to fermentable sugar is highly recommended due to the specific nature of the enzymes and their ability to work at mild process conditions. The saccharification of lignocellulosic material requires the use of several enzymes with complementary activities as the endoglucanase, which attacks regions in the interior of linear cellulose chains, the exoglucanases or cellobiohydrolases, which hydrolyze cellobiose units from the ends of cellulose chains and β-glucosidase, which converts cello-oligosaccharides and cellobiose into glucose (Stichnothe *et al.*, 2016)

4. Conclusion

The ethyl acetate extract of *A. pseudocaelatus* cultured on medium containing sorghum as natural carbon sources showed higher inhibitory effect against the tested pathogenic microorganism than using PDA medium. In the same way, *T. gamsii* ethyl acetate extract of PDA medium showed the highest percentage of antioxidant activity 53.84% after 7 days of incubation period compared to 14.7 %. Exploiting of agro-industrial waste for the production of sustainable bio-resources and the conversion of these resources and wastes into valuable products should be initiated by implementing the biotechnological innovation perspective to establish economic sustainability

Acknowledgments

The authors would like to acknowledge National Research Centre (NRC), Egypt for financial support for the research project (No.11010103); "Production of some metabolic byproduct compounds which have biological activity from rhizospheric fungi."

Conflict of interest

The authors declare that there is no conflict of interest.

References

Awad NE, Kassem HA, Hamed MA, El- Feky AM., Mohamed AA, Mahmoud EK, et al. 2018. Isolation and characterization of the bioactive metabolites from the soil derived fungus *Trichoderma viride*. *Mycology* **9**: 70–80.

Duque-Acevedo M, Belmonte-Ureña LJ, Cortés-García FJ, Camacho-Ferre F, 2020. Agricultural waste: review of the evolution, approaches and perspectives on alternative uses. Glob. Ecol. Conserv. **22,** e00902.

https://doi.org/10.1016/j.gecco.2020.e00902.

El-Sawy WS, Mohamed NA, Kassem EM, EA. 2015. Synthesis of new benzofuran derivatives and evaluation of their antimicrobial activities. *Res J. Pharm. Biol. Chem. Sci*. **6**, 213–224

Gloer JB. In: The Mycota. Wicklow DT, Soderstrom BE, 2007. Applications of fungal ecology in the search for new bioactive natural products. Vol. 3. New York: Springer-Verlag.; pp. 257–283.

Hamed A. (2009). Investigation of multiple cytoprotective actions of some individual phytochemicals and plant extracts. (PhD Thesis Biomedical Sciences), Nottingham University, United Kingdom.

Hoeksma J, Misset T, Wever C. *et al.* 2019. A new perspective on fungal metabolites: identification of bioactive compounds from fungi using zebrafish embryogenesis as read-out. *Sci Rep* **9,** 17546. https://doi.org/10.1038/s41598-019-54127-9.

Keating G, Figgitt D. 2003. Caspofungin: a review of its use in *Oesophageal candidiasis*, invasive candidiasis and invasive aspergillosis. *Drugs*.; **3**:2235–2263.

Makanjuola O, Greetham D, Zou X, Du C. 2019, The Development of a Sorghum Bran-Based Biorefining Process to Convert Sorghum Bran into Value Added Products. *Foods*, **8**, 279.

Mussatto SI, Ballesteros LF, Martins S and Teixeira JA. 2012. Use of Agro-Industrial Wastes in Solid-State Fermentation Processes. In: Industrial Waste (K.-Y. Show & ISBN, eds.), 274; InTech Published.

Nigam PS, Ashok P.2009. Solid-state fermentation technology for bioconversion of biomass and agricultural residues. In: Nigam PS & Pandey A (Eds.), Biotechnology for Agro-Industrial Residues Utilisation. Springer Science + Business Media, Germany, pp. 197-221.

Pandey A, Soccol CR, Rodriguez-Leon JA and Nigam P (2001). Production of organic acids by solid state fermentation. In Solid state fermentation in Biotechnology-Fundamentals and Applications, Asitech Publishers N. Delhi, pp. 132–158

Reino J, Guerrero R, Hernández-Galán R, Collado, I. 2008. Secondary metabolites from species of the biocontrol agent *Trichoderma*. *Phytochemistry Reviews*. **7**. 89-123.

Saleh RM, Kabli SA, Al-garni SM, Mohamed SA. 2011. Screening and production of antibacterial compound from *Trichoderma* spp. against human-pathogenic bacteria. *Afr. J. Microbiol. Res*. **5**, 1619–1628.

Singh, P. 2009. Production of Bioactive Secondary Metabolites. In: *Biotechnology for Agro-Industrial Residues*, pp.129–145; Northern Ireland: Springer Science.

Shentu X, Liu W, Zhan X, Yu X, Zhang C. 2013. The Elicitation Effect of Pathogenic Fungi on Trichodermin Production by *Trichoderma brevicompactum*. *The Scientific World Journal*, vol. 2013, Article ID 607102.

Shimada K, Fujikawa K, Yahara K, Nakamura T. 1992. Antioxidative properties of xanthone on the auto oxidation of soybean in cylcodextrin emulsion *J. Agr. Food Chem.*, **40**, 945-948.

Stichnothe H, Storz H, Meier D, De Bari I, Thomas S. 2016 Development of second generation biorefineries P. Lamers, E. Searcy, J.R. Hess, H. Stichnothe (Eds.), 48 Developing the global bioeconomy - technical, market and environmental lessons from bioenergy Elsevier 10.1016/B978-0-12-805165-8.00002-1

Vandermolen KM, Raja HA, El-elimat T, Oberlies NH, 2013. Evaluation of culture media for the production of secondary metabolites in a natural products screening program, *AMB Express*. **3**; 3: 71, 1–7**.**

Vinale F, Marra R, Scala F, Ghisalberti EL, Lorito M, Sivasithamparam K, 2006. Major secondary metabolites produced by two commercial *Trichoderma* strains active against different phytopathogens. *Lett. Appl. Microbiol*. **43**, 143–148.

Yasser MM, Marzouk MA, El-Shafey NM. and Shaban SA. 2020. Diversity and Antimicrobial Activity of Endophytic Fungi from the Medicinal Plant *Pelargonium graveolens* (geranium) in Middle Egypt. *Jordan Journal of Biological Sciences* **13;** 2, 197 - 205.

Zohair MM, El-Beih AA, Sadik MW & Hamed EH, Sedik MZ. 2018. Promising biocontrol agents isolated from medicinal plants rhizosphere against root-rot fungi. *Biocatalysis and Agricultural Biotechnology*. **15**, 11-18.

JJBS

Volume 14, Number 1, March 2021
ISSN 1995-6673
Pages 163 - 171

Jordan Journal of Biological Sciences

Phytochemical study, nutritional evaluation and *in vitro* antiobesity potential of fruits pericarp and seeds of *Livistona carinensis* and *Thrinax parviflora*

Mohamed S. Hifnawy[a], Marwa Yousry Issaa[b], Hesham El-Seedi[b,c], Amr M. K. Mahrous[a,*], Rehab M. S. Ashour[a,*]

[a] *Pharmacognosy Department, Faculty of Pharmacy, Cairo University, Kasr El-Aini 11562, Egypt.*[b] *Chemistry Department, Faculty of Science, El-Menoufia University, 32512 Shebin El-Kom, Egypt.*[c] *Medicinal Chemistry Department, Division of Pharmacognosy, Uppsala University, Box 574, 75123 Uppsala, Sweden.*

Received: May 27, 2020; Revised: August 13, 2020; Accepted: August 21, 2020

Abstract

Overweight is a significant health hazard. It increases the risk of development of various diseases. The nutritional value, phytochemical composition and in-vitro antiobesity potential of the seeds and fruits pericarp of *Livistona carinensis* (*L. carinensis*) and *Thrinax parviflora* (*T. parviflora*) were assessed.

The phytochemical screening of both plants showed the presence of tannins, carbohydrates, sterols, flavonoids and anthraquinones. GLC (Gas liquid Chromatography) analysis of lipids allowed the identification of stigmasterol as the major phytosterol in seeds and pericarp of *L. carinensis* (9.01% and 10.81%), respectively while *β-sitosterol* is the major in seeds and pericarp of *T. parviflora* (13.79% and 9.19%), respectively. Palmitic acid was the major fatty acid methyl ester in the pericarp of *L. carinensis* (35.01%), followed by myristic acid in the pericarp of *T. parviflora* (20.68%). Concerning unsaturated fatty acids linoleic acid is the major in seeds of *T. parviflora* (53.93%) followed by seeds and pericarp of *L. carinensis* (18.49% and 11.10%), respectively, while oleic acid is the major in pericarp of *T. parviflora*. Quantitative estimation of constituents revealed that *L. carinensis* seeds showed the highest concentration of total polyphenolics (39.02±1.24 mg/g gallic acid equivalents), flavonoids (10.75±0.40 mg/g quercetin equivalent) and tannins (15.82±0.62 mg/g tannic acid equivalents). While the highest steroidal content is found in *T. parviflora* pericarp (11.51±0.44 mg/g *β-sitosterol* equivalent). Both plants pericarps possess higher content of carbohydrates than that of seeds while the protein content is higher in *T. parviflora*, pericarp and seeds than that of *L. carinensis*. Calcium and iron are found prominent in *T. parviflora* pericarp (6.47 and 2.07 mg/gm, respectively) while the highest concentration of potassium was found in *L. carinensis* pericarp (21.43 mg/gm). The free radicle scavenging activity using DPPH is found in the following order *T. parviflora* seeds (13.79 µg/ml) > *T. parviflora* pericarp (9.72 µg/ml) > *L. carinensis* pericarp (8.95 µg/ml) > *L. carinensis* seeds (7.37 µg/ml) compared to ascorbic acid as standard (7.80 µg/ml). In addition, seeds and pericarp of *L. carinensis* showed the highest *α*-glucosidase inhibitory activity with IC_{50} values 0.93 and 1.17 mg/ml, respectively followed by the seeds and pericarp of *T. parviflora* (IC_{50} =1.46 and 1.76 mg/ml, respectively), compared to acarbose (IC_{50} = 0.72 mg/ml). Moreover, seed extracts of *L. carinensis* and *T. parviflora* showed powerful inhibitory activity against pancreatic lipase (IC_{50} = 10.95 and 9.33 µg/ml, respectively) compared to orlistat (6.82 µg/ml).

In conclusion, seed extracts of *L. carinensis* and *T. parviflora* showed the most powerful *α*-glucosidase and lipase inhibitory activities, these recommend their incorporation in anti-obesity preparations. Their pericarps showed significant antioxidant activity with high calcium, iron and potassium contents in addition to their moderate *α*-glucosidase inhibitory activities which recommend their daily intake in weight control programs.

Keywords: *Livistona carinensis*, *Thrinax parviflora*, anti-obesity, *α*-glucosidase inhibition, pancreatic lipase.

1. Introduction

Obesity and its related diseases as type-II diabetes mellitus and coronary heart diseases possess a worldwide concern. It is now considered as a major lifestyle ailment specifically in developing countries due to several factors including fast food intake, reduction of physical activity and industrialization. Inhibition of fats and carbohydrates digestion through hinderance of pancreatic lipase and *α*-glucosidase enzymes with the purpose of reducing energy intake have been recently used in management of obesity (El-shiekh et al. 2019). *α*-glucosidase is the main enzyme that aids the digestion of carbohydrates. Hence, its inhibition can hinder the release of glucose from carbohydrates and delay the absorption of glucose, resulting in regulation of type II diabetes. Many phytoconstituents have been reported to inhibit *α*-glucosidase (Kumar et al. 2011). The free radical scavenging power is the main link to inhibit the oxidative stress related hyperglycemia. Some reports indicated that α-glucosidase inhibitory activity could be attributed to

* Corresponding author e-mail: Amrmkh@gmail.com, rehab.ashour@pharma.cu.edu.eg.

DPPH scavenging activity (Sekhon-Loodu,Rupasinghe 2019).

Moreover, pancreatic lipase inhibition has been widely used to assess natural drugs used as anti-obesity agents (Seyedan et al. 2015). Orlistat is a lipase inhibitor associated with numerous side effects as interference with the physiological process of gastrointestinal tract, disruption of the mineral and electrolyte balance system, affecting the absorption and pharmacokinetics of other medicaments regularly used by obese patients as sulfonylureas, oral contraceptives, statins, slow-released calcium channel blockers or drugs which have narrow therapeutic index and reduction of the liposoluble vitamins absorption (Qi 2018).

Based on previous studies, traditional medicinal plants have been used in management of obesity (El-shiekh et al. 2019, Kazemipoor et al. 2012). Natural anti-obesity agents can enhance weight loss through various mechanisms (Kazemipoor et al. 2012). The search for several natural sources to inhibit pancreatic lipase and α-glucosidase with the aim of overcoming obesity with less side effects is greatly indicated. Palm oil from fruits have been reported as a natural adipocyte differentiation inhibitor (Saad et al. 2017).

The potent inhibitory potential of seeds from several date palm (*Phoenix dactylifera*) varieties versus key enzymes affecting obesity and diabetes have been previously reported (Masmoudi-Allouche et al. 2016). Several members of family Palmae revealed significant antihyperlipidemic effect (Uroko, 2019 and Vembu, 2012). Family Palmae is considered among the largest plant families, both in terms of number of species and in abundance (Gonzàlez et al. 1995). Human use of palms is widely distributed as edible food, medicinal and ornamental importance (Ahmad et al. 2013). Chemical characteristics of family Palmae, include the accumulation of polyphenols, some simple alkaloids (especially pyridine derivatives) and fatty acids, as well as steroidal saponins, oil palm and sterols. The palm genus *Livistona*, comprises about 36 species, native to southern and southeastern Asia, Australia and the Horn of Africa. The biological activity of genus *Livistona* includes anticancer, anti-osteoporosis, antioxidant and antibacterial (Yuan et al. 2009, Zeng et al. 2014) . The palm genus *Thrinax* consists of four species, endemic to Cuba and Caribbean countries (Riffle et al. 2012) and traditionally used in treatment of skin injury, kidney stones and nervous disorders (Calvo-Irabién,Soberanis 2008).

Reviewing the available literature, there is no published data regarding the fruits pericarp and seeds of *L. carinensis* and *T. parviflora* growing in Egypt. Therefore, it was deemed of interest to study these plants. As phytochemical analysis revealed that the two plants contain a large variety of several components with different anti-obesity and anti-oxidant effects on body metabolism and fat oxidation, so the study of anti-obesity efficacy was needed.

2. Material & methods

2.1. Plant material

Fruits pericarp and seeds of *Livistona carinensis* and *Thrinax parviflora* were collected in summer of the years 2017-2019 from El-Zoharia and Orman Botanic Gardens, Egypt, respectively. The plants were identified by Mrs. Therese Labib, botanical specialist and consultant at Orman and Qubba Botanical Gardens. Voucher specimens numbered (28072019 & 11112019), were placed in the Pharmacognosy Department Museum, Faculty of Pharmacy, Cairo University.

2.2. Proximate analysis

Crude fiber, moisture, total ash and acid insoluble ash were evaluated (Feldsine et al. 2002). Each value was an average of three determinations.

2.3. Phytochemical screening

The powdered air-dried fruits pericarp and seeds of *L. carinensis* and *T. parviflora*, were subjected, separately, to preliminary phytochemical screening tests (Wagner et al. 2013).

2.4. Study of the lipid content

Two hundred grams of air-dried powdered fruits pericarp and seeds of the two plants were extracted, separately, till exhaustion with petroleum ether. Each extract was evaporated under vacuum to give 4.5 g and 2.8 g of the fruits pericarp and seeds of *L. carinensis*, respectively, while 0.8 g and 3.8 g were obtained from the fruits pericarp and seeds of *Thrinax parviflora*, respectively. The saponifiable and unsaponifiable fractions were obtained from the fraction of petroleum ether, then the produced fatty acids were subjected to methylation (Finar 1973; Furniss 1989). GLC conditions used for unsaponifiable matter (USM) were applied on a capillary column (30 m x 0.32 mm I.D. x 0.25 µm film), the column was packed with HP-5 (5% phenyl methyl siloxane), and 2 µl was the injection volume. Programmed temperature was used for the analysis, where the initial temperature used was 80 °C for 5 min. then the temperature increased by the rate of 8 °C/min. to reach 280 °C, and the temperatures for injector and detector (FID) were 240 °C and 300 °C, respectively. The flow rate of nitrogen was 20 ml/min. Fatty acid methyl ester (FAME) was analyzed with the same carrier gas but at flow rate of 30 ml/min and on the same column used for USM. The initial temperature was 120 °C increased by the rate of 4 °C/min. to 240 °C, the temperature of injector and detector (FID) were, respectively, 250 °C and 280 °C. Identification of compounds was done by comparing the retention times of their peaks with the retention times of the authentic compounds (Sigma Chemical Co. St. Louis, MO. USA) similarly analyzed. Peak area measurement using a computing integrator was used for quantification.

2.5. Total polyphenolics content

Total polyphenolics content was determined according to the procedure reported in the European Pharmacopeia, using Folin-Ciocalteau colorimetric method (Singleton et al. 1999). Standard gallic acid (Sigma Co., St. Louis, MO., USA) was used at concentrations 0.1 to 1 mg/ml, a calibration curve (R^2 =0.9449) was prepared. Total phenolics were expressed as mg of gallic acid equivalent (mg GAE), and three replicates were carried for each concentration.

2.6. Flavonoids content

Total flavonoid content was determined spectrophotometrically based on measuring the yellow

color intensity produced after aluminum chloride reagent was complexed with flavonoids (Geissman 1962). A standard calibration curve (R^2 =0.9767) was composed utilizing several dilutions of authentic quercetin (Sigma Co., St. Louis, MO., USA) equivalent to 0.025 to 1 mg/ml. Three replicates were carried out for each concentration.

2.7. Tannins content

Tannins content was determined according to the procedure reported in the European Pharmacopeia, by Folin-Denis colorimetric method (Earp et al. 1981) using tannic acid (Sigma Co., St. Louis, MO., USA) as standard. Using tannic acid concentrations ranging from 0.1-2 mg/ml, a standard calibration curve (R^2 =0.9925). The values of tannins content were expressed as mg of tannic acid equivalent (mg TAE). Three replicates were carried out for each concentration.

2.8. Steroids content

The total steroidal content was determined based on measuring the greenish color intensity generated after Libermann-Burchard's reagent complexes with steroidal compound using standard *β*-sitosterol (Daksha et al. 2010). Standard calibration curve (R^2 =0.9006) was established using several dilutions of standard *β*-sitosterol (E-Merk, Darmstadt, Germany) equivalent to 0.03-2 mg/ml. Three replicates were carried out for each concentration.

2.9. Nutritional evaluation

2.9.1. Determination of the carbohydrates, protein and minerals contents.

Determination of total carbohydrates was estimated using the phenol–sulphuric acid colorimetric method (Dubois et al. 1956). Concentrated sulphuric acid (5 mL) was added to the mixture of the sample (1 mL) and 1 mL phenol solution (5% w/v). The sample was left at room temperature for 30 min. before measuring absorbance at 485 nm utilizing a spectrophotometer. The total amount of carbohydrate was estimated based on a standard calibration curve prepared using different dilutions of glucose. Three replicates were done for each concentration

Determination of protein content was estimated using the Micro-Kjeldal method that includes oxidation or digestion of the sample with concentrated sulfuric acid. The rate of oxidation of organic matter is also increased under most conditions by addition of copper (Cu), or selenium (Se) that serves as catalysts. The reaction was followed by steam distillation. The ammonia which is formed at high PH was received in solution of 4% boric acid then titrated using 0.1N HCL.

Determination of minerals content: Advanced microwave digestion system was used for digestion of samples. The concentration of Ca and Fe in sample were determined by using Industry Coupled Plasma (ICP-AES), Thermo Sci, model: ICAP6000 series. Argon gas was used for excitation of the mineral atom. The blank values for each element were deduced from the sample values. Potassium: The concentration of K in sample was determined by using Atomic Absorption Spectrometry (Metcalfe 1987).

2.9.2. Vitamins:

The vitamins HPLC analysis was carried out using these conditions; the column hypersil-EDS-C_{18} (4.6 mm x 250 mm), methanol was used as mobile phase at 1 ml/min flow rate. The volume of injection was 5 µl. Vitamin A, E and C were estimated using UV detector at wavelength 325, 292 and 254 nm, respectively (Nöll 1996; Pyka,Sliwiok 2001; Romeu-Nadal et al. 2006).

2.10. In-vitro biological study

2.10.1. Preparation of plant material

One and half kg random samples of fruits pericarp and seeds of the two plants were collected, separately, air-dried in shade, reduced to fine powder (sieve number 36) and kept in tightly closed amber colored glass containers at low temperature then extracted using 70% ethanol.

2.10.2. DPPH assay

DPPH assay is non-enzymatic assay. It is well trusted and accepted tool to assess free radical scavenging activity. Assay is based on the decrease of the ethanolic DPPH solution (Sigma Co., St. Louis, MO., USA) in the presence of the antioxidant, which disturbs free radical chain oxidation to form a stable end product diphenyl-β-picrylhydrazyl (DPPH). This causes the purple-colored DPPH to lose its chromophore (α, α-diphenyl-β-picrylhydrazyl) (Gulati et al. 2012).

20 ul of different extracts (conc. 0.5 mg/ml) were added to 96-well plate, then, 280 µl of 0.5 mM DPPH was added. The mixture was strongly shaken and incubated for 30 minutes at room temperature in dark; after that the absorbance of control and ethanolic extracts were measured at 540 nm using a microplate reader UV-spectrophotometer. Vitamin C (Sigma Co., St. Louis, MO., USA) served as reference standard with conc. 100 µg/ml.

The reduction in the absorbance revealed an increase in DPPH radical-scavenging activity. The inhibition percent was determined using the equation:

DPPH radical scavenging (%) = (1 - AS/AC) X 100

Where AS = The absorbance of the sample

AC = The absorbance of the control

The experiment was repeated three times, and the mean values were calculated. IC_{50} values were calculated as the sample concentration required to scavenge 50% of DPPH free radicals. The lowest IC_{50} value indicates the strongest ability of the sample to act as DPPH radical scavenger.

2.10.3. α-glucosidase inhibitory assay

The *α*-glucosidase inhibitory activity was estimated using the standard method with minor modification (Shai et al. 2011). In a 96-well plate, reaction mixture including 50 µl phosphate buffer (100 mM, pH = 6. 8), 10 µl α-glucosidase (Sigma Co., St. Louis, MO., USA) (1 U/ml), and 20 µl of several concentrations of the two plants different extracts (0.1, 0.2, 0.3, 0.4, and 0.5 mg/ml) was preincubated at 37°C for 15 min. After that, 20 µl para-nitrophenyl-α-D-glucopyranoside P-NPG (5 mM) (Sigma Co., St. Louis, MO., USA) was added as a substrate and then incubated for 20 min. at 37°C. The reaction was stopped by the addition of 50 µl Na_2CO_3 (0.1 M). The released p-nitrophenol absorbance was measured at 405 nm using Multiplate Reader. Acarbose (Sigma Co., St. Louis, MO., USA) at different concentrations (0.1–0.5 mg/ml) was used as a standard drug (positive control). Negative control group was done concurrently without the addition of test substance and every experiment was done

three times. The results were calculated as percentage inhibition, using the formula,

$$\text{Inhibitory activity (\%)} = (1 - As/Ac) \times 100$$

Where, As: the test substance absorbance; Ac: the control absorbance.

2.10.4. Anti-lipase assay

Pancreatic lipase (PL) inhibitory activity was determined colorimetrically using ρ-nitrophenyl palmitate (PNPP) [10 mM, in isopropanol] as substrate and porcine pancreatic lipase (PPL) (Sigma Co., St. Louis, MO., USA) as described by (Kordel et al. 1991) with few modifications.

The solutions of enzyme were prepared prior to use, by suspending crude porcine PL type II (Sigma, EC 3. 1. 1. 3.) in Tris-HCl buffer (100 mMTris, PH 8) to produce a concentration of 2 mg/ml (200 unites/ml) and mixed gently. Methanolic extracts (1mg/ml) 25 µl were pre-incubated with 50 µl of PPL solution for 10 minutes at 37 ^{0}C in the absence of light before assaying the PPL activity. The reaction was then started by adding 10 µl solution of PNPP substrate (10 mM in isopropanol). Tris-HCl buffer was used to dilute the volume to 200 µl. After incubation for 20 min. at 37 ^{0}C, the absorbance was determined at 405 nm. The assay was accomplished using Orlistat (final concentration 100 µg/ml) as a positive control and 5% DMSO as blank, each experiment was performed in triplicates.

3. Results and discussion

The ethanolic extraction yield of fruits pericarp and seeds of *T. parviflora* (46.4 and 60.8 gm), respectively and *L. carinensis* (76.5 and 62.4 gm), respectively.

3.1. Proximate analysis

The quality and purity of crude drugs are determined by their ash values. The total ash values found in the seeds of *L. carinensis* and *T. parviflora* are 2.36±0.11 and 1.46±0.06, respectively. Results are consistent with that reported about the seeds of *L. chinensis* 1.31±0.01. Moreover, the results reported for *L. chinensis* fruits pericarp (6.92±0.01) are similar to those of *L. carinensis* fruits pericarp (7.17±0.33) while *T. parviflora* showed a higher value (12.89±0.62) (Nwosu et al. 2012). In addition, the total ash in both organs of the two plants is higher than the insoluble acid ash, indicating the presence of large amount of soluble crystals. In general the insoluble acid ash is used in the detection of calcium oxalate crystals (Priya et al. 2013). The total moisture content of fruits pericarp and seeds in *L. carinensis* are found to be 9.40±0.39, and 11.75±0.52, respectively, while in *T. parviflora* they are 13.99±0.68 and 10.16±0.43, respectively. These values are in accordance with that reported for *L. chinensis* pulp (11.14 ±0.02) while they are much lower than that reported for *L. chinensis* seeds (35.35±0.05) (Nwosu et al. 2012). The lower moisture content found the higher the stability as this lower the chances of microbial infections. Total crude fiber for fruits pericarp of *L. carinensis* and *T. parviflora* are 22.70±1.03 and 15.20±0.66%, respectively. This is much lower than the value reported for the pulp of *L. chinensis* 36.66±1.46% while that of the seeds of *L. carinensis* and *T. parviflora* are 49.20±2.36 and 58.60±2.39%, respectively (Nwosu et al. 2012). Results of pharmacopoeial constants of the fruits pericarp and seeds are tabulated in table 1. These variations in pharmacopoeal constants may be probably due to difference in plant species, origin and growth phase. These parameters were studied as they are helpful in identification and authentication of both plants.

Table 1. Pharmacopoeial constants of the fruits pericarp and seeds.

Analysis	g%			
	Pericarp		Seeds	
Plant	L. *carinensis*	T. *parviflora*	L. *carinensis*	T. *parviflora*
Moisture content	9.40±0.39	13.99±0.68	11.75±0.52	10.16±0.43
Total ash	7.17±0.33	12.89±0.62	2.36±0.11	1.46±0.06
Acid insoluble ash	3.90±0.17	4.15±0.19	1.45±0.06	1.10±0.05
Crude fiber	22.70±1.03	15.20±0.66	49.20±2.36	58.6±2.39

3.2. Phytochemical screening

The fruits pericarp and seeds of both species revealed the presence of tannins, carbohydrates, flavonoids and sterols while crystalline sublimate, steam volatile substances, alkaloids and cardiac glycosides are absent. Anthraquinones are present only in the fruits pericarp of both plants. Results of phytochemical screening are represented in table (2)

Table 2. Results of phytochemical screening of the fruits pericarp and seeds of *L. carinensis* and *T. parviflora*

Test	*Livistona carinensis*		*Thrinax parviflora*	
	Fruits pericarp	Seeds	Fruits pericarp	Seeds
Crystalline sublimate (Claus and Tyler, 1967)	-	-	-	-
Steam volatile substances (Wagner *et al.*, 1983)	-	-	-	-
Carbohydrates and/or glycosides (Coutts and Snail, 1973)	++	+	++	+
Tannins (Evans, 2002)	++	++	++	++
Flavonoids 1-Aglycones (Geissman, 1962)	±	+	+	-
2-Glycosides (Peach and Tracey, 1955)	+	+	+	±
Saponins (Walform*et al.*, 1940)	-	-	-	-
Sterols and/or Triterpenes (Leibermann and Burchard, 1890) (Salkowski, 1872)	±	++	+	±
Alkaloids (Evans, 2002)	-	-	-	-
Anthraquinones 1-Free (Borntrager, 1880)	+	±	+	±
2-Combined (Borntrager, 1880)	+	-	+	±
Cardiac glycosides (Feiser and Fieser, 1959)	-	-	-	-

+: Present ++: Strongly present -: Not detected ±: Trace

3.3. Lipid content

GLC analysis of lipids, revealed the identification of the unsaponified content in a 69.37% and 80.93% in the pericarp and seeds of *L. carinensis*, respectively, while 76.08% and 82.45% were identified in the pericarp and seeds of *T. parviflora*, respectively. Seeds of *T. parviflora* contained much higher percent of phytosterols (29.53%) and triterpenes (7.12%). Concerning the triterpenes, *α*-amyrin is the major triterpene of the unsaponified contents

(7.12 and 5.52% in the seeds of *T. parviflora* and *L. carinensis*, respectively). Stigmasterol is the major phytosterol in the fruits pericarp of *L. carinensis* representing 10.81% while β-sitosterol was the major in seeds (13.79%) and fruits pericarp (9.19%) of *T. parviflora*. *β-sitosterol* was previously reported as major compound in the unsaponifiable matter of *L. chinensis* pulp (43%) also stigmasterol and campsterol were detected (Kadry et al. 2009). The analysis of FAME (Fatty acid methyl ester) by GLC revealed the identification of 98.90% and 89.66% fatty acids of the total lipids of fruits pericarp and seeds of *L. carinensis*, correspondingly, while the total lipids displayed 99.30% of fruits pericarp and 99.29% of seeds of *T. parviflora*.

The saturated fatty acid palmitic acid constituted the highest percentage of FAME in the fruits pericarp of *L. carinensis* with a yield of 35.01%, followed by myristic acid in the fruits pericarp of *T. parviflora* by 20.68%. Concerning the unsaturated fatty acids; linoleic acid is the major constituent of the FAME with percent of 53.93% in the seeds of *T. parviflora* while in seeds of *L. carinensis* it is found to be 18.49%. Previous report on *L. decipiens* pulp showed that oleic acid was the major FAME constituting 53.40% of the total identified compounds while palmitic acid was the major in *L. chinensis* pulp 47.40%. On the other hand, linoleic acid concentration in *L. chinensis* pulp was found in relatively high concentration (12.16%) compared to that reported for *L. decipiens* (0.31%) (Kadry et al. 2009). The presence of the unsaturated fatty acids oleic and linoleic acid in *L. carinensis*, and *T. parviflora* is of great importance to help the reduction of the risk of heart diseases and lower cholesterol levels among other health benefits as anti-inflammatory and anti-cancer (de Morais et al. 2017). Results of GLC analysis of lipids were tabulated in tables (3&4)

Table 3. Results of GLC analysis of the identified unsaponified content of *L. carinensis* and *T. parviflora*

Authentic	RRt*	Percentage					
		L. carinensis			*T. parviflora*		
		Leaves	Pericarp	Seeds	Leaves	Pericarp	Seeds
n-Tridecane C-13	0.639	--	--	--	0.237	--	--
n-Tetradecane C-14	0.724	4.327	--	0.646	0.114	--	--
n-Pentadecane C-15	0.781	13.651	--	0.431	0.293	0.099	--
n-Hexadecane C-16	0.848	4.141	--	0.806	0.334	--	--
n-Heptadecane C-17	0.914	18.576	0.908	0.918	3.776	0.178	0.148
n-Octadecane C-18	1	24.680	1.150	0.721	1.757	0.113	1.423
n-Nonadecane C-19	1.058	5.858	5.740	3.174	2.718	1.111	3.481
n-Eicosane C-20	1.231	10.806	1.283	2.595	13.201	0.795	1.424
n-Henicosane C-21	1.254	3.760	16.537	6.337	7.810	1.497	10.450
n-Docosane C-22	1.349	1.826	4.120	2.741	2.711	1.625	2.288
n-Tricosane C-23	1.408	0.932	4.114	2.164	3.211	1.951	2.375
n-Tetracosane C-24	1.481	1.680	2.619	5.359	7.656	2.726	4.728
n-Pentacosane C-25	1.537	0.788	3.272	3.793	0.567	2.758	2.341
n-Hexacosane C-26	1.658	1.076	5.109	8.948	1.466	5.136	5.374
n-Heptacosane C-27	1.772	1.682	5.265	5.228	6.574	9.139	8.543
n-Octacosane C-28	1.868	1.042	--	9.414	4.283	17.615	3.231
n-Nonacosane C-29	1.948	--	--	3.288	--	5.502	--
Cholesterol	1.979	--	--	2.764	2.060	2.392	--
Campsterol	2.003	--	3.158	--	3.667	2.111	7.106
Stigmasterol	2.033	0.506	10.809	9.010	11.192	8.993	8.634
β-sitosterol	2.162	1.044	5.288	7.070	8.725	9.193	13.786
α-amyrin	2.362	0.753	--	5.522	0.828	3.144	7.121
% Total identified compounds		97.128	69.373	80.930	83.181	76.078	82.453
Percentage of total hydrocarbons		94.825	50.118	56.564	56.709	50.245	45.806
Percentage of total phytosterols		1.550	19.255	18.844	25.644	22.689	29.526
Percentage of total triterpenes		0.753	--	5.522	0.828	3.144	7.121

* RRt: Relative retention time to n-Octadecane C-18 with Rt= 14.597 min. -- : not detected

Table 4. Results of GLC analysis of the identified FAME of *L. carinensis* and *T. parviflora*

Authentic	RRt*	Percent					
		L. carinensis			*T. parviflora*		
		Leaves	Pericarp	Seeds	Leaves	Pericarp	Seeds
Caprylic acid (Octanoic acid) C_8 (0)	0.351	--		0.853	--	--	--
Capric acid (Decanoic acid) C_{10} (0)	0.401	--	1.146	1.473	3.840	--	--
Undecylic (Undecanoic acid) C_{11}	0.554	3.063	--	--	0.870	5.299	0.602
Lauric acid (Dodecanoic acid) C_{12} (0)	0.659	14.927	3.959	28.615	2.243	8.812	--
Tridecylic acid (Tridecanoic acid) C_{13}	0.749	28.003	8.535	--	--	2.497	14.598
Myristic acid (Tetradecanoic acid) C_{14} (0)	0.804	18.551	5.948	11.211	0.523	20.678	--
Pentadecylic (Pentadecanoic acid) C_{15} (0)	0.935	3.335	3.804	--	--	3.119	3.098
Palmitic acid C_{16} (0)	1	3.361	35.004	12.918	32.950	14.564	--
Palmitoleic acid C_{16} (1)	1.050	2.501	--	--	--	--	--
Heptadecanoic acid C_{17}(0)	1.071	3.643	2.308	--	--	15.521	--
Stearic acid C_{18} (0)	1.194	1.581	2.490	3.070	0.308	7.278	--
Oleic acid C_{18} (1)	1.232	1.322	9.771	12.363	34.371	10.827	24.258
Linoleic acid C_{18} (2)	1.267	1.318	11.106	18.485	14.697	6.886	53.925
α-Linolenic acid C_{18} (3)	1.313	3.849	10.977	0.676	6.408	3.818	2.813
Arachidic acid C_{20}(0)	1.367	1.547	3.849	--	--	--	--
Percentage of identified fatty acids		87.001	98.899	89.663	96.209	99.299	99.295
Percentage of unsaturated F.A.		8.990	31.855	31.524	55.476	21.531	80.997
Percentage of saturated F.A.		78.011	67.044	58.139	40.733	77.768	18.298

* RRt: Relative retention time to Palmitic acidC_{16}(0) with Rt= 21.176 min. --- : not detected.

3.4. Total polyphenolics, flavonoids, tannins and steroids

3.4.1. Spectrophotometric determination of total polyphenolics

L. carinensis seeds showed the highest concentration of total polyphenolics constituting 39.02±1.24 mg/g expressed in gallic acid equivalents followed by the *T. parviflora* seeds (30.45±0.97 mg/g) expressed in gallic acid equivalents. Our results are much higher than the results reported about *L. speciosa* seed polyphenolic content which was found to be 2.35 mg/g gallic acid equivalent (Takolpuckdee 2016). Results are shown in table (5).

Table 5. Total polyphenolics content in fruits pericarp and seeds of *L. carinensis* and *T. parviflora*.

Plant	Organ	Absorbance	Concentration mg/g expressed in gallic acid equivalents
Livistona carinensis	Pericarp	1.3937	20.97±0.83
	Seeds	1.7089	39.02±1.24
Thrinax parviflora	pericarp	1.3756	25.30±0.91
	Seeds	1.5593	30.45±0.97

Values are mean of triplicates ± Standard error M±S.E (n=3)
Mean values of significant variation at p <0.05

3.4.2. Total flavonoids content

The total flavonoids concentration, calculated as quercetin equivalent, was higher in *L. carinensis* seeds (10.75±0.40 mg/gm) than in the seeds of *Thrinax parviflora* (0.13±0.01 mg/gm), while that of fruits pericarp of *T. parviflora* (6.88±0.26 mg/gm) was greater than *L. carinensis*, fruits pericarp (1.13±0.04 mg/gm). On contrary of total polyphenolics reported on *L. speciosa* seed its total flavonoids content was found at very high concentration (39.27 mg/g rutin equivalent) much higher than that found on both species under study (Takolpuckdee 2016). Results of total flavonoids content are presented in table (6).

Table 6. Total flavonoids content in *L. carinensis* and *T. parviflora*, fruits pericarp and seeds.

Plant	Organ	Absorbance	Concentration mg/g expressed in quercetin equivalents
Livistona carinensis	Pericarp	0.0907	1.13±0.04
	Seeds	0.0984	10.75±0.40
Thrinax parviflora	Pericarp	0.0953	6.88±0.26
	Seeds	0.0899	0.13±0.01

Values are mean of triplicates ± Standard error M±S.E (n=3)
Mean values of significant variation at p <0.05

3.4.3. Tannins content

The *L. carinensis* seeds exhibited the highest tannins content with concentration of 15.82±0.62 mg of tannic acid equivalents / gram fresh weight while the concentration in fruits pericarp was 13.55±0.42 mg/gm. *T. parviflora*, fruits pericarp and seeds tannins contents are 11.92±0.47 and 11.05±0.33 mg/g, respectively. *L. speciosa* seed is reported to contain only 4.26 mg/g tannic acid equivalent (Takolpuckdee 2016). Results of total tannins content are presented in table (7).

Table 7. The tannins content in fruits pericarp and seeds of *L. carinensis* and *T. parviflora.*

Plant	Organ	Absorbance	Concentration mg of tannic acid equivalents per gram.
Livistona carinensis	Pericarp	2.3274	13.55±0.42
	Seeds	2.6310	15.82±0.62
Thrinax parviflora	Pericarp	2.1059	11.92±0.47
	Seeds	2.0022	11.05±0.33

Values are mean of triplicates ± Standard error M±S.E (n=3)
Mean values of significant variation at p <0.05

3.4.4. Steroidal content.

T. parviflora, pericarp were rich in steroidal content (11.51±0.44 mg/g) compared to the pericarp of *L. carinensis*, (0.82±0.03 mg/g), while the seeds of *L. carinensis*, (4.75±0.18 mg/g), were

higher than that of *T. parviflora*, (0.13±0.01 mg/g). Results of total steroidal content are presented in table (8).

Table 8. Total steroidal content in *L. carinensis* and *T. parviflora*, fruits pericarp and seeds.

Plant	Organ	Absorbance	Concentration mg/g expressed in β-sitosterol equivalents
Livistona carinensis	Pericarp	0.1892	0.82±0.03
	Seeds	0.2045	4.75±0.18
Thrinax parviflora	Pericarp	0.2308	11.51±0.44
	Seeds	0.1865	0.13±0.01

Values are mean of triplicates ± Standard error M±S.E (n=3)
Mean values of significant variation at p <0.05

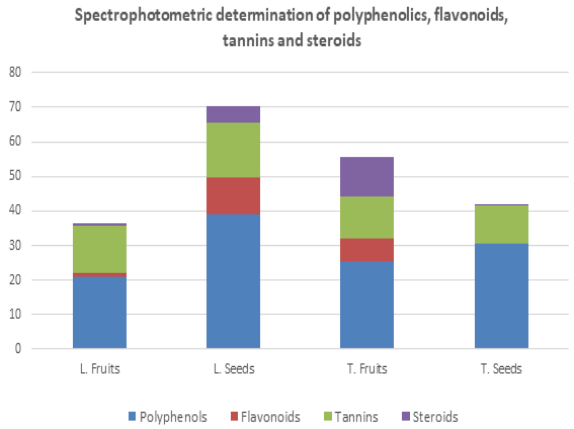

Figure 1. Spectrophotometric determination of total phenolics, flavonoids, tannins and steroids.

3.5. Nutritional evaluation

The worldwide mineral malnutrition is a serious issue in many countries especially in developing ones (Oyeyinka,Afolayan 2019). However, the potential of nutraceuticals to combat it has not been extensively studied. Fruits of *L. carinensis* and *T. parviflora* possess high content of total carbohydrates (30.22±1.19 and 32.08±0.98%, respectively) compared to that of the seeds (17.34±0.59 and 14.31±0.47%, respectively). This is in accordance with that previously reported about *L. chinensis* pulp (33.69 ± 0.05) and seeds (17.83 ± 0.03) (Nwosu et al. 2012), but the amount of carbohydrates is much lower than that reported for date pits that ranged from 70.9 - 86.9% (Hossain et al. 2014). In addition, the total protein content of edible plants is considered a measure of its nutritional value for herbivores (Al-Rowaily et al. 2019). The protein content showed significant variation, pericarp and seeds of *T. parviflora* (8.64±0.24 and 7.00±0.18%, respectively) comprises much more protein than that of *L. carinensis*, pericarp and seeds (0.13±0.01 and 0.27±0.01%, respectively). The results of protein content in *T. parviflora* seeds are higher than that previously reported about *L. chinensis* seed (4.44±0.16%) and *Phoenix dactylifera* seeds (5.64±0.21%), while the protein content of the pericarp are in accordance with that conveyed about *L. chinensis* pulp (9.04±0.03) (Nwosu et al. 2012).

Table 9. Mineral contents of *L. carinensis* and *T. parviflora*, fruits pericarp and seeds.

Mineral content (mg/100gm)	*L. carinensis*		*T. parviflora*		Daily needs**
	Pericarp	Seeds	Pericarp	Seeds	
Ca *	147.86 (14.786%)***	127.36 (12.736%)***	647.28 (64.728%)***	118.41 (11.841%)***	1000 mg
Fe *	10.27 (57.05%)***	14.62 (81.22%)***	207.31 (1151.72%)***	6.56 (36.44%)***	18 mg
K *	2143.28 (61.23%)***	614.79 (17.56%)***	1284.40 (36.69%)***	374.82 (10.70%)***	3500 mg

* Dry weight. ** The Daily Values are the nutrient amounts recommended per day for Americans 4 years of age or older (FDA Vitamins and Minerals Chart). *** % Percent of daily needs at consumption of 100 gm of crude powder.

There is a significant relation between obesity and several minerals intake including calcium, potassium and iron. Calcium regulates various cellular processes in the body as cell differentiation and proliferation in addition to bone formation. Moreover, the potent effect of dietary calcium supplementation in prevention or treatment of obesity has been reported (Zhang et al. 2019). Adequate daily potassium intake can in turn decrease the risk of obesity (Cai et al. 2016). Also, iron deficiency showed significant correlation (Sal et al. 2018).

The results of mineral contents are shown in table (9) and figure (2). Calcium and iron are found prominent in *T. parviflora*, fruits pericarp (6.47 and 2.07 mg/gm, respectively). While the highest concentration of potassium was found in *L. carinensis*, fruits pericarp (21.43 mg/gm).

This would recommend the use of the pericarp of both plants as a source of carbohydrates, calcium, potassium, and iron. In addition, the fruits pericarp and seeds of *T. parviflora* are also good protein sources.

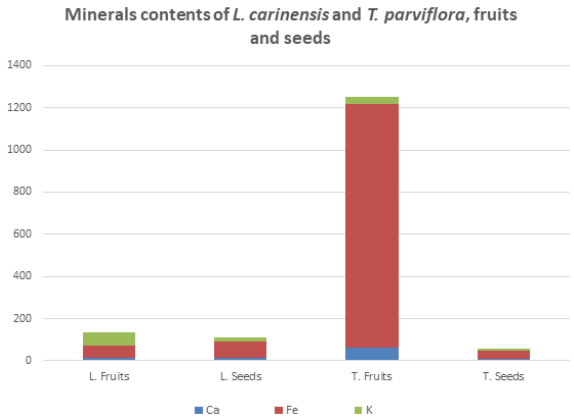

Figure 2. Mineral contents of *Livistona carinensis* and *Thrinax parviflora*, fruits and seeds.

3.6. DPPH assay

The results of the free radical scavenging activity are displayed in table (10). In the DPPH assay, the extracts (0.05- 1.0 mg/ml) scavenged the free radical in a concentration dependent pattern. The result also revealed

that at dose 1 mg/ml, *T. parviflora* fruits pericarp and seeds showed IC_{50} of 9.72 and 13.79 µg/ml, respectively while *L. carinensis* extracts, fruits pericarp and seeds inhibited DPPH radical by IC_{50} values 8.95 and 7.37 µg/ml, respectively compared to the standard, ascorbic acid IC_{50} = 7.80 µg/ml. The results are slightly higher when compared to the previously reported for *Phoenix dactylifera*, pulp and seeds (IC_{50} values 89.14 and 31.05 µg/ml, respectively) while the standard drug IC_{50} was 12.80 µg/ml (Masmoudi-Allouche et al. 2016).

3.7. α-glucosidase inhibitory assay

Seeds and fruits pericarp of *L. carinensis* showed the highest *α*-glucosidase inhibitory activity with IC_{50} values 0.93 and 1.17 mg/ml, followed by the seeds and fruits pericarp of *T. parviflora* (IC_{50} =1.46 and 1.76 mg/ml, respectively), compared to Acarbose IC_{50} = 0.72 mg/ml as standard drug. The results are in accordance with that previously reported about *Phoenix dactylifera*, pulp and seeds (IC_{50} equals 10.93 and 3.08 mg/ml, respectively) (Masmoudi-Allouche et al. 2016).

The potent *α*-glucosidase inhibitory activity of the seeds of *T. parviflora* may be attributed to the high content of linoleic acid (53.92%) and oleic acid (24.25%) which were previously reported to possess α-glucosidase inhibitory activity (Su et al. 2013).

3.8. Anti-lipase assay

The two plant extracts (0.5- 4.0 mg/ml) significantly inhibit the pancreatic lipase in a dose dependent pattern, at 4 mg/ml dose, the seeds extracts of *L. carinensis* and *T. parviflora* showed powerful inhibition activity against pancreatic lipase (PL) enzyme (IC_{50} = 10.95 and 9.335 µg/ml, respectively) compared to the standard drug Orlistat (0.1 mg/ml) with IC_{50} value 6.82 µg/ml. This is in accordance with that previously reported about *Phoenix dactylifera* seeds (IC_{50} ranging from 1.21 to 47.51 µg/ml) but for Orlistat, this is much higher than the previously reported (IC_{50} equals 0.92 µg/ml) due to the difference in substrates (Masmoudi-Allouche et al. 2016). Seeds extracts of *L. carinensis* and *T. parviflora* showed more powerful anti-lipase activity compared to the standard drug Orlistat.

The significant lipid lowering effect of *L. carinensis* and *T. parviflora* seeds may be due to their content of polyunsaturated fatty acids (linoleic acid).

Linoleic acid was reported to reduce body fat mass in specific regions in healthy, overweight and obese adults (Gaullier et al. 2007). Phenolic compounds derived from medicinal plants might be responsible for their lipase inhibitory potential (McDougall et al. 2009). Various natural products rich in polyphenolics have been reported as anti-obesity by inhibiting pancreatic lipase (McDougall et al. 2009, Yajima et al. 2005).

Table 10. IC_{50} values of *L. carinensis* and *T. parviflora*, fruits pericarp and seeds compared to standard drugs.

Parameter	Standard drug	*L. carinensis*		*T. parviflora*	
		Pericarp	**Seeds**	**Pericarp**	**Seeds**
DPPH	(Ascorbic acid) 7.80 µg/ml	8.95 µg/ml	7.37 µg/ml	9.72 µg/ml	13.79 µg/ml
α-glucosidase inhibitory	(Acarbose) 0.72 mg/ml	1.17 mg/ml	0.93 mg/ml	1.76 mg/ml	1.46 mg/ml
Anti-lipase	(Orlistat) 6.82 µg/ml	Nd	10.95 µg/ml	Nd	9.33 µg/ml

Nd: Not determined

There is no direct relation between the DPPH scavenging activity and the inhibition of *α*-glucosidase and pancreatic lipase enzymes. Further detailed *in vivo* studies are required to confirm the anti-obesity activity.

4. Conclusion

Seed extracts of *L. carinensis* and *T. parviflora* showed the most powerful α-glucosidase and lipase inhibitory activities which recommend their incorporation in anti-obesity preparations. While their fruits pericarp showed significant DPPH scavenging activity with high calcium, iron and potassium contents in addition to their moderate α-glucosidase and lipase inhibitory activities which recommend their daily intake in weight control programs.

References:

Ahmad, A., Soni Dutta, S., Varun Singh, K.,Santosh, M.K., (2013). *Phoenix dactylifera* Linn. (PIND KHARJURA): A REVIEW. International Journal of Research in Ayurveda & Pharmacy 4.

Al-Rowaily, S.L., Abd-ElGawad, A.M., Alghanem, S.M., Al-Taisan, W.a.A.,El-Amier, Y.A., (2019). Nutritional Value, Mineral Composition, Secondary Metabolites, and Antioxidant Activity of Some Wild Geophyte Sedges and Grasses. Plants 8, 569.

Cai, X., Li, X., Fan, W., Yu, W., Wang, S., Li, Z., Scott, E.M.,Li, X., (2016). Potassium and obesity/metabolic syndrome: a systematic review and meta-analysis of the epidemiological evidence. Nutrients 8, 183.

Calvo-Irabién, L.M.,Soberanis, A., (2008). Practices of Chit (*Thrinax radiata*) in Quintana Roo, Mexico.

Daksha, A., Jaywant, P., Bhagyashree, C.,Subodh, P., (2010). Estimation of sterols content in edible oil and ghee samples. Electron. J. Environ. Agric. Food Chem. 9, 1593-1597.

de Morais, S.M., do Nascimento, J.E.T., de Sousa Silva, A.A., Junior, J.E.R.H., Pinheiro, D.C.S.N.,de Oliveira, R.V., (2017). Fatty acid profile and anti-inflammatory activity of fixed plant oils. Acta Scientiae Veterinariae 45, 1-8.

Dubois, M., Gilles, K.A., Hamilton, J.K., Rebers, P.t.,Smith, F., (1956). Colorimetric method for determination of sugars and related substances. Analytical chemistry 28, 350-356.

Earp, C., JO, A., SH, R.,LW, R., (1981). Evaluation of several methods to determine tannins in sorghums with varying kernel characteristics.

El-shiekh, R., Al-Mahdy, D., Hifnawy, M.,Abdel-Sattar, E., (2019). In-vitro screening of selected traditional medicinal plants for their anti-obesity and anti-oxidant activities. South African journal of botany 123, 43-50.

Feldsine, P., Abeyta, C.,Andrews, W.H., (2002). AOAC International methods committee guidelines for validation of qualitative and quantitative food microbiological official methods of analysis. Journal of AOAC International 85, 1187-1200.

Finar, I., (1973). Chapter 4. Organic Chemistry, 119-120.

Furniss, B.S., (1989). Vogel's textbook of practical organic chemistry, Pearson Education India.

Gaullier, J.-M., Halse, J., Høivik, H.O., Høye, K., Syvertsen, C., Nurminiemi, M., Hassfeld, C., Einerhand, A., O'Shea, M.,Gudmundsen, O., (2007). Six months supplementation with conjugated linoleic acid induces regional-specific fat mass decreases in overweight and obese. British Journal of Nutrition 97, 550-560.

Geissman, T.A., (1962). The chemistry of flavonoid compounds, Macmillan.

Gonzȉez, R.B., Henderson, A.,Garcš, G.G., (1995). Field guide to the palms of the Americas, Princeton University Press.

Gulati, V., Harding, I.H.,Palombo, E.A., (2012). Enzyme inhibitory and antioxidant activities of traditional medicinal plants: potential application in the management of hyperglycemia. Bmc complementary and alternative medicine 12, 77.

Hossain, M.Z., Waly, M.I., Singh, V., Sequeira, V.,Rahman, M.S., (2014). Chemical composition of date-pits and its potential for developing value-added product-a review. Polish Journal of Food and Nutrition Sciences 64, 215-226.

Kadry, H., Shoala, S., Gindi, O.E., Sleem, A.A., Mosharrafa, S.,Kassem, M., (2009). Chemical characterization of the lipophilic fraction of *Livistona decipiens* and *Livistona chinensis* fruit pulps (Palmae) and assessment of their anti-hyperlipidemic and anti-ulcer activities. Natural product communications 4, 1934578X0900400220.

Kazemipoor, M., Radzi, C.W.J.W.M., Cordell, G.A.,Yaze, I., (2012). Potential of traditional medicinal plants for treating obesity: a review. arXiv preprint arXiv:1208.1923.

Kordel, M., Hofmann, B., Schomburg, D.,Schmid, R., (1991). Extracellular lipase of Pseudomonas sp. strain ATCC 21808: purification, characterization, crystallization, and preliminary X-ray diffraction data. Journal of bacteriology 173, 4836-4841.

Kumar, S., Narwal, S., Kumar, V.,Prakash, O., (2011). α-glucosidase inhibitors from plants: A natural approach to treat diabetes. Pharmacognosy reviews 5, 19.

Masmoudi-Allouche, F., Touati, S., Mnafgui, K., Gharsallah, N., El Feki, A.,Allouche, N., (2016). Phytochemical profile, antioxidant, antibacterial, antidiabetic and anti-obesity activities of fruits and pits from date palm (*Phoenix dactylifera* L.) grown in south of Tunisia. Journal of Pharmacognosy and Phytochemistry 5, 15.

McDougall, G.J., Kulkarni, N.N.,Stewart, D., (2009). Berry polyphenols inhibit pancreatic lipase activity *in vitro*. Food Chemistry 115, 193-199.

Metcalfe, E., (1987). Atomic absorption and emission spectroscopy, John Wiley & Sons Inc.

Nöll, G.N., (1996). High-performance liquid chromatographic analysis of retinal and retinol isomers. Journal of Chromatography A 721, 247-259.

Nwosu, J., Ezegbe, C., Omeire, G., Ahaotu, I., Owuamanam, C.,Udeozor, L., (2012). Evaluation of the Proximate properties of the Seed and Physicochemical properties of the Oil of Chinese Fan Palm (Livistona chinensis). IJBAS 1, 304-312.

Oyeyinka, B.O.,Afolayan, A.J., (2019). Comparative Evaluation of the Nutritive, Mineral, and Antinutritive Composition of Musa sinensis L.(Banana) and Musa paradisiaca L.(Plantain) Fruit Compartments. Plants 8, 598.

Priya, T., Kailash, T.,Amit, T., (2013). Pharmacognostic evaluation of fruit pulp of *Livistonia chinensis*. International Journal for Pharmaceutical Research Scholars 2.

Pyka, A.,Sliwiok, J., (2001). Chromatographic separation of tocopherols. Journal of Chromatography A 935, 71-76.

Qi, X., (2018). Review of the clinical effect of orlistat, p. 012063, IOP Publishing.

Riffle, R.L., Craft, P.,Zona, S., (2012). The encyclopedia of cultivated palms, Timber Press.

Romeu-Nadal, M., Morera-Pons, S., Castellote, A.,Lopez-Sabater, M., (2006). Rapid high-performance liquid chromatographic method for Vitamin C determination in human milk versus an enzymatic method. Journal of Chromatography B 830, 41-46.

Saad, B., Zaid, H., Shanak, S.,Kadan, S., (2017). Anti-diabetes and anti-obesity medicinal plants and phytochemicals. Springer Cham.

Sal, E., Yenicesu, I., Celik, N., Pasaoglu, H., Celik, B., Pasaoglu, O.T., Kaya, Z., Kocak, U., Camurdan, O.,Bideci, A., (2018). Relationship between obesity and iron deficiency anemia: is there a role of hepcidin? Hematology 23, 542-548.

Sekhon-Loodu, S.,Rupasinghe, H., (2019). Evaluation of antioxidant, antidiabetic and antiobesity potential of selected traditional medicinal plants. Frontiers in nutrition 6, 53.

Seyedan, A., Alshawsh, M.A., Alshagga, M.A., Koosha, S.,Mohamed, Z., (2015). Medicinal plants and their inhibitory activities against pancreatic lipase: a review. Evidence-based complementary and alternative medicine.

Shai, L., Magano, S., Lebelo, S.,Mogale, A., (2011). Inhibitory effects of five medicinal plants on rat α-glucosidase: Comparison with their effects on yeast α-glucosidase. Journal of Medicinal Plants Research 5, 2863-2867.

Singleton, V.L., Orthofer, R.,Lamuela-Raventós, R.M., (1999). Methods in enzymology, pp. 152-178, Elsevier.

Su, C.H., Hsu, C.H.,Ng, L.T., (2013). Inhibitory potential of fatty acids on key enzymes related to type 2 diabetes. Biofactors 39, 415-421.

Takolpuckdee, P., (2016). Chemical Compounds and Antioxidation Efficiency of Livistona speciosa Kurz. Seed Crude Extract. Thai Journal of Pharmaceutical Sciences (TJPS) 40.

Wagner, H., Bladt, S.,Zgainski, E.-M., (2013). Drogenanalyse: Dünnschichtchromatographische Analyse von Arzneidrogen, Springer-Verlag.

Yajima, H., Noguchi, T., Ikeshima, E., Shiraki, M., Kanaya, T., Tsuboyama-Kasaoka, N., Ezaki, O., Oikawa, S.,Kondo, K., (2005). Prevention of diet-induced obesity by dietary isomerized hop extract containing isohumulones, in rodents. International journal of obesity 29, 991-997.

Yuan, T., Yang, S.-P., Zhang, H.-Y., Liao, S.-G., Wang, W., Wu, Y., Tang, X.-C.,Yue, J.-M., (2009). Phenolic compounds with cell protective activity from the fruits of *Livistona chinensis*. Journal of Asian natural products research 11, 243-249.

Zeng, X., Tian, J., Cui, L., Wang, Y., Su, Y., Zhou, X.,He, X., (2014). The phenolics from the roots of Livistona chinensis show antioxidative and obsteoblast differentiation promoting activity. Molecules 19, 263-278.

Zhang, F., Ye, J., Zhu, X., Wang, L., Gao, P., Shu, G., Jiang, Q.,Wang, S., (2019). Anti-Obesity Effects of Dietary Calcium: The Evidence and Possible Mechanisms. International journal of molecular sciences 20, 3072.

Uroko, R. I., O. N. Uchenna, N. K. Achi, A. Agbafor, S. I. Egba and C. A. Orjiakor (2019). "The Effects of the Aqueous Extracts of *Elaeis guineensis* Fruits on the Lipid Profile and Kidney Function Indices of Male Wistar Albino Rats." Jordan Journal of Biological Sci.

Vembu, S., D. Sivanasan and G. Prasanna (2012). "Effect of *Phoenix dactylifera* on high fat diet induced obesity." J. Chem. Pharm. Res 4(1): 348-352.

JJBS

Volume 14, Number 1, March 2021
ISSN 1995-6673
Pages 173 - 177

Jordan Journal of Biological Sciences

New Approach for Biocontrolling Root-Knot Nematode, *Meloidogyne incognita* on Cowpea by Commercial Fresh Oyster Mushroom (*Pleurotus ostreatus*)

Mahmoud M.A.Youssef*, Wafaa M.A. El-Nagdi

Plant Pathology Department, Nematology Laboratory, National Research Centre, Dokki, Post code 12622, Cairo, Egypt.

Received: May 1, 2020; Revised: August 9 , 2020; Accepted: August 20, 2020

Abstract

For biocontrolling root-knot nematode, *Meloidogyne* incognita on cowpea**.** antagonistic fungi which considered among the main biological agents used are Basidiomycetes (Mushrooms). These are abundantly producing natural antibiotics in their secondary metabolites possess antimicrobial,nematicidal, antitumor, and antioxidant properties. In the laboratory, three aqueous extract concentrations of commercial fresh oyster mushroom (*Pleurotus ostreatus*) fruits at 5,10 and 15g /100ml distilled water were tested for their effect on the second stage juveniles (J_2) of root-knot nematode, *M. incognita*. They proved that there is positive relation between the tested concentrations and percentages net mortality of juveniles. Under screen house conditions, three rates of mashed fresh mushroom fruit residue at 5,10 and 15 g each per pot were applied for controlling *M. incognita* on cowpea. Using oyster mushroom at the highest rate (15g) achieved the highest percentages of reduction of nematode reproduction by 86.4% and galls by 92.4% compared to the control. The tested rates increased number of bacterial nodules. Also, they increased and improved plant growth and yield (pods and seeds) criteria coinciding with these rates. It could be concluded that commercial fresh mushroon as organic amendment could effectively affect *M. incognita* root-knot nematode and improve cowpea plant vegetative growth and yield parameters.

Keywords: Biocontrol, cowpea, oyster mushroom, root-knot nematode, *M.incognita*.

1. Introduction

As cited by Edwin and Jacob (2017), cowpea, *Vigna unguiculata* (L.) is considered to be an important cash and food crop with high nutritional value for poor farmers in some parts in the world. When there is shortage in animal proteins, cowpea becomes a source of dietary proteins. Infection by root-knot nematodes all over the world takes place to about 2000 plants exhibiting poor growth, a loss in quality and yield of the crop and breaking the resistance of host plant. Also, a high infection by root-knot nematode greatly affects utilization of water and fertilizers, resulting in additional losses for the farmers (Back *et al*., 2002; Castello *et al*., 2003; Manzanilla-Lopez and Bridge, 2004).

For evaluating alternative control strategies, biological control of root-knot nematodes is essential. In this context, biocontrolling phytoparasitic nematodes by the fungi are among the main used biological agents (Li *et al.*, 2007)), including *Meloidogyne* species (Swe *et al*., 2011; Degenkolb and Vilcinskas, 2016a,b) due to that they capture and parasitize nematodes (Goswami *et al*., 2006; Haseeb and Kumar 2006; Swe *et al*., 2011), through producing several antagonistic substances (Tranier *et al*.,2014; Degenkolb and Vilcinskas, 2016a). Basidiomycetes(Mushrooms) greatly produce natural antibiotics which possess antimicrobial, antitumor, and antioxidant properties (Sivanandhan *et al*., 2017). Among them, species of *Pleurotus* produce many substances with nematicidal properties including different fatty acids (Li *et al*., 2007); these fungi reduced galls on tomato plants as demonstrated by Putzke *et al.* (2007).In Egypt,there is one study recorded on the effect of commercial mushroom fungi on root-knot nematode,*M. incognita* (El-Sherbiny and Awd Allah, 2014).

Based on the previous information, this study aimed to evaluate the *in vitro* potential of different aqueous extract concentrations of commercial fresh oyster mushroom (*Pleurotus ostreatus*) fruits on *M. incognita* mortality and to evaluate the efficiency of its dfferent rates for *M. incognita* biocontrol on cowpea,and consequently on plant growth and yield under screenhouse conditions.

2. Materials and Methods

2.1. Aqueous extract of commercial fresh oyster mushroom fruits

In order to prepare aqueous extract concentrations, commercial mashed oyster mushroom of fruiting bodies was mixed in proportions of 5,10 and 15g/100ml distilled water.The mixtures were kept for 72 hours. Then, they were filtered through Whatman filter paper No.1.

2.2. Identification and preparing of root-knot nematode pure culture

The tested species of root-knot nematode, *M. incognita* was identified by using protocol described by Taylor and Sasser (1978) by using nematode adult female based on its

* Corresponding author e-mail: myoussef_2003@yahoo.com.

perineal pattern morphological characteristics. Pure culture of *M. incognita* was reared on tomato by a single egg-mass of this nematode inoculated to susceptible tomato cultivar in a screen house at 30 ± 5°C. Newly hatched second stage juveniles (J_2s) of nematode were used as inocula.

2.3. In vitro test

A population of the second stage juveniles(J_2) of *M. incognita* that was reared as pure culture on suseptible tomato plant was used. The population of J_2 from soil was extracted by using method referred to Barker (1985). For extraction of J_2 of *M.* nematode in roots, galled tomato roots bearing egg masses were washed thoroughly with tap water to avoid soil aggregation and debris and teased into small pieces. Then, they were incubated in plastic capsule filled with sufficient water to help egg hatching present in egg masses on roots. To prevent water evaporation, these capsules were covered and J2s collected every 24hrs (Young, 1954**).** *In vitro* test was applied by adding water filtrate at concentrations of 5**,** 10 and 15g fresh mushroom/100ml distilled water. One ml distilled water that contained 300 individuals in plastic capsule was added to 9ml of each mushroom filtrate. Mushroom filtrate was made by soaking each rate in distilled water for three days and filtered by using Whatman filter paper no.1.Equal number of juveniles was also added to equal number of plastic capsules filled with 9 ml distilled water served as control. There were 5 replicates for each treatment.

Under light microscope, numbers of dead and alive juveniles per each treatment were counted 24, 48 and 72 hrs after treatment. The J_2s were considered dead when they did not move when touched with a fine needle. The percentages of nematode mortality were calculated according to Abbott's Formula (1925) as follows:

$$\text{Juvenile mortality (\%)} = (m - n)/ (100 - n) \times 100$$

The percentages of mortality of juveniles in the treatment and control were represented by m and n, respectively. Each capsule containing nematodes after 72hr was filled with distilled water at the same volume replacing mushroom suspension concentration. % nematode recovery in distilled water was determined in which was subtracted from % total mortality after 72hr to obtain % nematode net mortality.

2.4. Effect of fresh mushroom fruit residue on the biocontrol of M. incognita in cowpea plant

To assess effect of different rates of commercial fresh mashed mushroom fruit residue on root-knot nematode,*M. incognita*, 5,10 and 15 g each were added to pots in screen house of Plant Pthology Department, National Research Centre (NRC).Three to four seeds of cowpea (*Vigna unguiculata* (L.) Walp.) cv. Baladi were sown in each pot (20-cm diameter) that contained 2 kg of solarized sandy loamy soil(1:1). One week after seed emergence, each pot was thinned to two plantlets and then, inoculated with 3,000 newly hatched second stage juveniles (J_2) added in four holes made around the plant. At the same time, cowpea plants were treated with the tested three mushroom filtrate concentrations and nematode only with distilled water served as untreated control. The compound, Okadean (containing nitrogen-fixing bacterium namely, *Bradyrhizobium* spp.) at recommended rate was added to pots in all treatments.A completely randomized design was used to arrange pots with 5 replicates for each treatment and control put on a bench and maintained at 30 ± 5 °C. Then, the plants were irrigated as needed.

Three months after the date of nematode inoculation (harvest stage of cowpea), plants of cowpea were carefully uprooted and roots were washed thoroughly as described previously. Then, roots were divided into two portions. Egg mass as well as gall numbers per plant were counted in one portion of roots. Then, the second portion of roots was processed as mentioned previously to extract second stage juveniles from egg masses. Also, number of J_2 in the soil per pot was extracted as mentioned previously. Number of bacterial nodules was recorded for each treatment.

The vegetative parameters of cowpea viz., shoot length (cm), fresh and dry weights of shoots and roots (g) were measured. Number of pods and seeds, and weights of pods and100 seeds (g) were recorded.

Means of total percentages of nematode reduction, plant growth and yield increases were calculated for each treatment as follows:

Mean of total percentages of each treatment (%) = Sum of the percentages of nematode reduction or plant growth and yield increases for each treatment/ number of these parameters ×100. This parameter was used to compare among treatments.

2.5. Statistical analysis

In this experiment, analysis of variance (ANOVA) procedures was performed for significance at 5% level of probability. For comparing among treatments, Duncan's Multiple Range Test by Snedecor and Cochran (1989) was used. This was done by Computer Statistical (COSTAT) software.

3. Results

3.1. Effect of the tested fresh oyster mushroom fruit residue filtrate on nematode mortality

As for mortality of nematode juveniles by using the tested filtrate concentrations of commercial fresh fruits of mushroom, it was noticed that this filtrate caused the nematode mortality depending on its concentration and exposure period, as the percentage of nematode mortality increased with increasing the mushroom filtrate concentration and time of exposure and vice versa. The highest concentration of 15g/100 ml induced the highest percentage net mortality (58%) after exposure period of 72 hrs followed by those of moderate (50%) and the lowest concentrations (40%) (Table 1).

Table 1. % mortality of second-stage juveniles (J_2s) of *Meloidogyne incognita* as affected by fresh oyster mushroom water filtrate concentrations under *in vitro* test.

Treatments	Concentration (g/100ml distilled water)	Nematode(J_2) mortality (%)			Nematode recovery(%)	Nematode net mortality (%)
		Exposure period				
		24h	48h	72h		
Mushroom	5	62	68	70	30	40
	10	70	72	78	28	50
	15	70	78	81	23	58
Distilled water	-	0	0	0	0	0

3.2. Effect of the tested fresh oyster mushroom fruit residue on nematode parameters

Fresh oyster mushroom fruit residue potential for biocontrolling root-knot nematode was proved in *the* present study in which it significantly($p \leq 0.05$) reduced the reproduction and galls of *M. incognita* and improved cowpea plant growth, bacterial nodulation and yield. Nematode biocontrol using mushroom fresh oyster fruit residue at the highest rate(15g) achieved the highest mean of total percentage of reduction of nematode parameters (86.4%) compared to the control.This was followed by 79.2 and 79.3% achieved by 10 and 5g fresh fruits of mushroom, respectively. The highest percentage of gall reduction(92.4%)was obtained by the higest rate of mushroom residue. However, the highest percentage bacterial nodule increase was achieved by the lowest rate of mushroom followed by the highest and moderate rates(Table 2).

Table 2.Effect of mushroom oyster fruit residue rates on root-knot nematode, *Meloidogyne incognita* infecting cowpea

treatments	Number and % reduction of nematode productive parameters and galls/pot or root system									No. of nodules/root system	% Inc.
	J_2 in soil/ Pot	% Red.	J_2 in roots	% Red.	Egg masses	% Red.	% mean of percentages of nematode red.	galls	% Red***.		
Control	8000a**	-	225a	-	95a	-	-	158a	-	15c	-
5g	4200b	47.5	63b	72.0	11b	88.4	69.3	15b	90.5	27a	35.0
10g	2800c	65.0	40c	82.2	9b	90.5	79.2	13b	91.8	18bc	20.0
15g	2380c	70.3	30d	96.3	7b	92.6	86.4	12b	92.4	20b	33.3

*-Each value is mean of 5 replicates. **-The same letter (s) following means of each column indicated that the treatments are not significantly different according to Duncan`s multiple range test at level ($p \leq 0.05$). ***-Red. = Reduction and Inc. =Increase.

3.3. Effect of the tested mushroom fruit residue on cowpea growth and yield

As for vegetative growth and yield criteria of cowpea plant, the means of total percentages of increases of the different plant growth and yield (pods and seeds) criteria were positively related the different rates, as higher mushroom residue rate, higher increase in the different criteria of plant growth and yields and vice versa. On this basis, the highest mean of increase (60.2%) was achieved by using the highest rate of mushroom residue followed by 24.8 and 5.6% increases occurred by moderate and the lowest rates, respectively (Tables 3 and 4).

Table 3. Effect of fresh oyster mushroom fruit residue rates on growth and yield criteria of cowpea as affected by root-knot nematode, *Meloidogyne incognita* infection.

Treatments	Shoot parameters			Root parameters		Pod parameters		Seed parameters		
	Length (cm)	Fresh w. (g)	Dry w. (g)	Fresh w. (g)	Dry w. (g)	N.***	W.*** (g)	N.of seeds/ pod	W. of seeds/ pod (g)	W. of 100 seeds (g)
control	51b**	40.0c	11.1b	7.6b	1.8b	4a	2.5b	6	0.63b	11.4a
5g	51b	41.7c	12.4b	6.8c	2.1b	4a	2.7b	6	0.72b	11.5a
10g	56ab	63.8b	13.9b	7.1c	2.5a	5a	3.0b	7	0.95a	11.6a
15g	60a	89.0a	15.6a	8.6a	2.8a	6a	4.1a	7	1.01a	11.8a

*-Each value is mean of 5 replicates. **-The same letter (s) following means in each column indicate that the treatments are not significantly different according to Duncan`s multiple range test at level ($p \leq 0.05$). ***-W. =weight and N= Number.

Table 4. % Increases of growth and yield parameters of cowpea infected by *Meloidogyne incognita* as affected by fresh oyster mushroom rates.

Treatments	increases (%)							Seed parameter increases (%)			
	Shoot parameters			Root parameters		Pod parameters					
	Length	Fresh	Dry w.	Fresh w.	Dry w.	N.*	W.**	N. of seeds/ pod	Seed W. / pod	W. of 100 seeds	Mean of increases (%)
control	-	-	-	-	-	-	-	-	-	-	-
5g	0.0	4.3	11.7	-	16.7	-	8.0	-	14.3	0.9	5.6
10g	9.8	59.5	25.2	-	38.9	25.0	20.0	16.7	50.8	1.8	24.8
15g	17.6	122.5	40.5	13.2	55.6	50.0	64.0	16.7	60.3	3.5	60.2

*-N =Number, **W=Weight.

4. Discussion

Aqueous filtrate of fruit fresh oyster mushroom in the present study reduced numbers of root-knot nematode,*M. incognita* by affecting juveniles motility under *in vitro* conditions. This resulted in the mortality and reducing of this parasitic nematode (Kulkarni and Sanget, 2000; Luo *et al.*, 2007; Wille *et al.*,2019). Nematodes became immobilized, paralyzed and straightened bodies as soon when they approached to the fungal colony, as reported by Palizi *et al.* (2009) on their work on oyster mushrooms.

In previous studies, Basidiomycete species proved to be effective in the control of root-knot nematode, *M. javanica* by using formulations produced from vegetative phase of fungi (mycelium) (Heydari *et al.*, 2006). However, fruiting bodies of fungi have higher activity, concentration and diversity of compounds in comparison with those found in mycelium (Tidke and Rai 2006; Ganeshpurkai and Jain, 2010). Besides, Barron and Thorne (1987)indicated that mushroom fungi can infect nematodes by secretory hyphal cells releasing toxins as droplets. This was confirmed by tiny droplets secreted on water agar by all tested strains of *Pleurotus* species (Barron and Thorne, 1987; Chitwood, 2002). Several compounds as polysaccharides were found in medicinal mushrooms which cause therapeutic activities of many fungal genera. These compounds have antoxidant, anticancer, antimicrobial and antiviral activities as shown by Elkhateeb *et al.* (2019). On this basis, mushroom oyster fruit residue used in this study was effective on *M. incognita* which corresponded with the results of El-Sherbiny and Awd Allah (2014). Also, our results are in agreement with those achieved by Goswami *et al.* (2006), Putzke *et al*. (2007) and Wille *et al.* (2019) on the effect of oyster mushroom on root-knot nematodes. Other investigators proved that the degree of decomposition of organic materials and consequently their suppressive effect against root knot nematode may be influenced by some factors, from which a very complete mixing of these materials with soil, enough soil moisture (Morra and Kierkegaard, 2002) and suitable soil temperature (Ploeg and Stapleton, 2001; López-Pérez *et al*., 2005).

From the present study, it was noticed that there is corresponding increase of cowpea plant growth and yield parameters with the percentage of nematode reduction at all cases, which may be due to that the improvement of plants exhibited by increases of shoot and root growth and consequently cowpea yield was favored by the reduction in nematode as shown by Wille *et al.* (2019). The consistent relation between population density of root-knot nematode and plant growth and yield in this study indicated its validity.

5. Conclusion

It could be concluded, based on the present study, that commercial mushroon as organic amendment could effectively reduce *M. incognita* root-knot nematode, and improve cowpea plant vegetative and yield. Also, these criteria were found to be positively related with the aqueous concentrations and rates of commercial oyster mushroom. Further studies are needed to investigate different kinds of mushrooms and factors affecting their decomposition in soil to biocontrol root-knot nematode and other nematodes.

References

Abbott WS. 1925.A method of computing the effectiveness of an insecticide. *J Econ Entomol*, **8**:265-267.

Back MA, Haydock PPJ and Jenkinson P. 2002. Disease complexes involving plant parasitic nematodes and soil borne pathogen. *Plant Pathol*, **51**: 683- 697.

Barker TR. 1985. Nematode extraction and bioassays. In: "An Advanced Treatise on *Meloidogyne"*: Vol. II. Methodology (Barker TR, Carter CC, Sasser JN, eds.). **North Carolina State University, USA, 19-35 pp.**

Barron GL and Thorne RG. 1987. Destruction of nematodes by species of *Pleurotus*. *Canad J Bot*, **65**: 774–778.

Castello P, Navas-Cortes JA, Goamar-Tinoco D, Di Vito M and Jimenez-Diaz RM 2003. Interactions between *Meloidogyne artiellia*, the cereal and legume root-knot nematodes and *Fusarium oxisporum* f.sp. *ciceris* race 5 in chickpea. *Phytopathology*, **93**:1513-1523.

Chitwood DJ. 2002. Phytochemical based strategies for nematode control. *Ann Rev Phytopathol*, **40**: 221–249.

Degenkolb T and Vilcinskas A. 2016a. Metabolites from nematophagous fungi and nematicidal natural products from fungi as an alternative for biological control. Part I: metabolites from nematophagous ascomycetes. *Appl Microbiol Biotechnol*, **100**: 3799-3812.

Degenkolb T and Vilcinskas A. 2016b. Metabolites from nematophagous fungi and nematicidal natural products from fungi as alternatives for biological control. Part II: metabolites from nematophagous basidiomycetes and non-nematophagous fungi. *Appl Microbiol Biotechnol*, **100**: 3813-3824.

Edwin IE and Jacob IE. 2017. Bio-insecticidal potency of five plant extracts against Cowpea weevil, *Callosobruchus maculates* (F.), on stored Cowpea, *Vigna unguiculata* (L.). *Jordan J Bio Sci*, **10**:311-32.

Elkhateeb WA, Daba GM, Thomas PW and Wen TC. 2019. Medicinal mushrooms as a new source of natural therapeutic bioactive compounds. *Egypt Pharm J*, **18**:88–101.

El-Sherbiny AA and Awd Allah SFA. 2014. Management of the root-knot nematode, *Meloidogyne incognita* on tomato plants by pre-planting soil biofumigation with harvesting residues of some winter crops and waste residues of oyster mushroom cultivation under field condition. *Egypt J Agronematol*, **13**: 189–202.

Ganeshpurkararai G and Jain AP. 2010. Medicinal mushrooms: towards a new horizon. *Pharm Rev*, **4**: 127-135.

Goswami BK, Pandey RK, Rathour KS, BhattaCharya C and Singh L. 2006. Integrated application of some compatible biocontrol agents along with mustard oil seed cake and furadan on *Meloidogyne incognita* infecting tomato plants. *J Zhejiang Univ Sci B*, **7:** 873-875.

Haseeb A and Kumar V. 2006. Management of *Meloidogyne incognita-Fusarium solani* disease complex in brinjal by biological control agents and organic additives. *Ann Plant Prot Sci*, **14**: 519-521.

Heydari R, Pourjam, E and Goltapeh EM. 2006. Antagonistic effect of some species of *Pleurotus* on the root-knot nematode, *Meloidogyne javanica in vitro*. *Plant Pathol J*, **5**: 173-177.

Kulkarni SM and Sanget AD. 2000. Cultivation of *Hohenbuehelia atrocaerulea* (Fr.) Sing. (Agaricomycetideae): a mushroom with nematicidal potential. *Int J Med Mush*, **2**: 161-163.

Li G, Zhang K, Xu J, Dong J and Liu Y. 2007. Nematicidal substances from fungi. *Recent Pat Biotechnol*, **1**: 212-223.

López-Pérez JA, Roubtsova T and Ploeg A. 2005. Effect of three plant residues and chicken manure used as biofumigants at three temperatures on *Meloidogyne incognita* infestation of tomato in greenhouse experiments. *J Nematol*, **37**: 489–494.

Luo H, Liu Y, Fang L, Li X, Tang N and Zhang K. 2007.*Coprinus comatus* damages nematode cuticles mechanically with spiny balls and produces potent toxins to immobilize nematodes. *Appl Environ Microbiol*, **73**: 3916-3923.

Manzanilla-Lopez RHEK and Bridge J. 2004. Plant diseases caused by nematodes. **CABI Publish. Beijing, China, pp.135-140.**

Morra M J and Kirkegaard JA. 2002. Isothiocyanate release from soil-incorporated Brassica tissues. *Soil Biol Biochem*,**34**: 1683–1690.

Palizi P, Goltapeh E M,Pourjam E and Safaie N. 2009. Potential of oyster mushrooms for the biocontrol of sugar beet nematode, *Heterodera schachtii*. *J Plant Prot Res*, **49**:27-33.

Ploeg AT and Stapleton JJ. 2001. Glasshouse studies on the effects of time, temperature and amendment of soil with broccoli plant residues on the infestation of melon plants by *Meloidogyne incognita* and *M. javanica*. *Nematology*, **3**: 855–861.

Putzke MTL, Matsumura ATS, Cavalcante MAQ and Cargnelutti Filho A. 2007. Taxonomia e importância das espécies de *Hohenbuehelia resupinatus* e *Pleurotus* no controle de *Meloidogyne javanica*. *Caderno de Pesquisa série Biologia Universidade de Santa Cruz do Sul*, **19**: 38-81.

Sivanandhan S , Khusro A , Paulraj MG, Ignacimuthu S and AL-Dhabi NA. 2017. Biocontrol Properties of Basidiomycetes: An overview. *J Fungi*, **3**:1-14.

Snedecor GW and Cochran WG. 1989. Statistical Methods. **8th ed. Ames, Iowa: Iowa State University Press.**

Swe A, Li J, Zhang, KQ, Pointang SB, Jeewon R and Hyde KD. 2011. Nematode-trapping fungi. *Cur Res Environ Appl Mycol*, **1**: 1-26.

Taylor AL, Sasser JN. 1978. Biology, identification and control of root-knot nematodes (*Meloidogyne* species). **Raleigh (NC): IMP, North Carolina State University Graphics.**

Tidke G and Rai M. 2006. Biotechnological potential of mushrooms: drugs and dye production. *Inter J Med Mush*, 8: 351-360.

Tranier MS, Gros P, Queiroz RC, Gonzalez CNA, Mateille T and Roussos S. 2014. Commercial biopesticides against plant parasitic nematodes. *Brazil Arch Biol Technol*, **57**: 831-841.

Wille CN, Gomes CB, Minotto E and Nascimento JS. 2019. Potential of aqueous extracts of basidiomycetes to control root-knot nematodes on lettuce. *Horti Brasil*, **7**: 54-59.

Young TW. 1954. An incubation method for collecting migratory-endoparasitic nematodes. *Plant Dis Reptr*, **38:**794-795.

JJBS

Volume 14, Number 1, March 2021
ISSN 1995-6673
Pages 179 - 186

Jordan Journal of Biological Sciences

Influence of Static Magnetic Field Seed Treatments on the Morphological and the Biochemical Changes in Lentil Seedlings (*Lens Culinaris* Medik.)

Amal M. Harb[1,*], Bar'a M. Alnawateer[1] and Ibrahim Abu-Aljarayesh[2]

[1] *Department of Biological Sciences,* [2]*Department of Physics, Faculty of Science, Yarmouk University, Irbid, Jordan*

March 19, 2020; Revised: September 7, 2020; Accepted: Oct 2, 2020

Abstract

The static magnetic field has been shown to affect the growth and the biochemical composition of different plant species such as rice and wheat. In this study, lentil seeds were exposed to static magnetic field in a systematic way from low intensity to high intensity to test its effect on lentil growth. After that, the effective magnetic treatments that stimulated or inhibited the growth of lentil seedlings were tested for biochemical changes in lentil seedlings. Lentil seeds were first exposed to a static magnetic field of 1,10, 20, 30, 40, 50, 60, 70, 80, 90, and 100 mT for 5, 10, 15, 20, 25, and 30 min. Then, the morphological changes in lentil seedlings were assessed. Some of the effective magnetic treatments were analyzed for the changes in lipid peroxidation and the activity of some antioxidant enzymes in lentil seedlings. The results showed that the effect of magnetic treatment on seedling growth is divided into three groups: growth improvement, growth inhibition and normal growth. Moreover, the magnetic treatment (50 mT for 30 min) that inhibited seedling growth showed a high level of oxidative stress in terms of lipid peroxidation (42.6 µmole malondialdhyde (MDA)/ g fresh mass compared to 20.20 µmole/ g fresh mass of the control). Whereas, the magnetic treatment (20 mT for 20 min) that improved the seedling growth showed the lowest level of lipid peroxidation (5.29 µmole malondialdhyde (MDA)/ g fresh mass compared to 20.20 µmole/ g fresh mass of the control). The magnetic treatment 20 mT for 25 min enhanced lentil growth without a significant lipid peroxidation but showed a significant increase in the activity of catalase and superoxide dismutase 0.57 and 1.09 unit/ mg protein compared to 0.15 an 0.40 unit/ mg protein of the control, respectively. Hence, the priming of lentil seeds with the right magnetic treatment could be an efficient, affordable, and eco-friendly approach for the enhancement of lentil growth.

Keywords: seedling growth; oxidative stress; lipid peroxidation; antioxidant enzymes.

1. Introduction

All living systems, humans, plants, animals, and microorganisms live within the geomagnetic field (GMF). The GMF is considered as a low magnetic field that ranges from 35 to 70 µT (microTesla) (Occhipinti et al. 2014). The magnetic field is a physical factor that can be used to enhance seed germination and plant growth without harming the environment (Pietruszewski and Martínez 2015; Rifna et al. 2019). Recently, many researchers are interested in the study of the effect of the magnetic field on plants' growth and productivity (Maffei et al. 2014). Seed germination was improved after the magnetic treatment of maize (*Zea mays* L.) grains with 125 and 250 milli Tesla (mT) for 1, 10, 20 min and 1 h (Flórez et al. 2007). The pretreatment of okra (*Abelmoschus esculentus*) seeds with a magnetic field of 99 mT for 3 and 11 min also enhanced seed germination (Naz et al. 2012). The magnetic treatment of wheat (*Triticum aestivum* L.) grains and bean (*Phaseolus vulgaris* L.) seeds with 4 and 7 mT for 7 days resulted in the enhancement of seedling growth (Cakmak et al. 2010). Seed germination and seedling growth were significantly improved after seed exposure of melon (*Cucumis melo* L.) to a magnetic field of 100 and 200 mT for 5-20 min (Iqbal et al., 2016a). The same effect was shown after seed exposure of bitter gourd (*Momordica charantia*) to a magnetic field of 25, 50, and 75 mT for 15, 30 and 45 min (Iqbal et al. 2016b). The exposure of soybean (*Glycine max*) seeds to a magnetic field of 50, 75 and 100 mT for 3 and 5 min also resulted in a significant improvement of seed germination and seedling growth (Asghar et al. 2017). The treatment of maize grains by a magnetic field of 100 and 200 mT for 1 and 2 h showed improved chlorophyll content, leaf area, yield, and fresh and dry mass (Anand et al. 2012). Seedling growth of soybean was also enhanced after seed exposure to a magnetic field of 200 mT for 1 h (Baghel et al. 2018). Seed germination and plant growth of Faba Bean (*Vicia faba*) were significantly increased after the magnetic pretreatment of the seeds with a magnetic field of 30 and 85 mT for 15 s (Podleśna et al. 2019). The pretreatment of wheat seeds with an electromagnetic field of 10 and 15 mT for 10 and 15 min resulted in enhanced seed germination, plant growth and productivity (Hussain et al. 2020).

The biochemical responses of plants to the magnetic field were studied in different plant species. A reduction in oxygen radicals was shown in the magnetically treated soybean seeds with 100 and 200 mT for 1 h (Baby et al. 2011). The magnetically treated cucumber seedlings with

* Corresponding author e-mail: aharb@yu.edu.jo.

200 mT magnetic field for 1 h showed an increase in superoxide radical and hydrogen peroxide (H_2O_2) (Bhardwaj et al. 2012). Lipid peroxidation and H_2O_2 was increased in shallot seedlings after their exposure to 7 mT magnetic field (Cakmak et al. 2012). A significant reduction in the activity of superoxide dismutase (SOD) in soybean seedlings after seed exposure to a magnetic field of 150 and 200 mT for 1 h was shown (Shine et al. 2012). The activity of the antioxidant enzymes: SOD, catalase (CAT), and guaiacol peroxidase was analyzed in 5-day-old radish seedlings exposed to a magnetic field of 185-650 μT (Serdyukov and Novitskii 2013). The activity of these enzymes was dependent on the intensity of the magnetic field; high intensity resulted in the activation of SOD and CAT. The growing of *Phaseolus vulgaris* L. seeds in a magnetic field of 130 mT for 14 days resulted in a significant increase in guaiacol peroxidase activity (GPOX) in the leaves (Mroczek-Zdyrska et al. 2016). The exposure of rice (*Oryza sativa*) grains to a magnetic field of 25 mT for 60 min resulted in an increased activity of CAT and peroxidase enzymes (Yadav et al. 2018).

Lentil (*Lens Culinaris* Medik.) is a member of family Fabaceae whose seeds are rich in protein. Indeed, lentil is an excellent protein source in poor and developing countries. The highest production of lentil worldwide is in Canada, and then comes India, Turkey, China, Nepal, and Syria (Andrews and McKenzie 2007). Lentil production is challenged by the changing environment and the consequent climate change. Therefore, it is of high importance to find ways to increase the production of this nutritious crop to meet the needs of the growing population, especially in the poor countries.

A few studies tested the effect of the magnetic field on lentil plants (Penuelas et al. 2004; Aladjadjiyan 2010). These studies showed enhancement of seedling growth after the magnetic treatment of lentil seeds. In these studies, only one or two intensities of the magnetic field (150 and 250 mT) were tested for a few selected exposure times (Penuelas et al. 2004; Aladjadjiyan 2010). Therefore, in this study the effect of different intensities of static magnetic field (1, 10, 20, 30, 40, 50, 60, 70, 80, 90, and 100 mT) for different exposure times (5, 10, 15, 20, 25, and 30 min) on the morphological changes in lentil seedlings will be tested. After that, the effective magnetic treatments that caused reduction or increase in lentil growth will be chosen to study the effect of magnetic treatment on some biochemical changes in lentil seedlings.

2. Materials and methods

The experiments of magnetic treatment were done in a biology research lab at Yarmouk University under controlled conditions of temperature, humidity, and light.

3. Plant material

Lentil seeds of genotype international legume lentil 10823 (ILL10823). Lentil seeds of this genotype were purchased from a local farmer of Irbid in the north of Jordan. The genotype of lentil seeds was determined by SSR analysis in the laboratory of Dr. Ayed Alabadallat, Department of Horticulture, Faculty Agriculture, Jordan University.

4. The magnet setup

The static magnetic field (H) was generated by an electromagnet that consists of identical Helmholtz coils (Fig. 1). The current was supplied to the coils by a power supply (HICKOK model number 5055, Hickok Electrical Instrument, Cleveland, OH). The intensity of the magnetic field was measured at several vertical and horizontal positions between the cabs, to find the place of a uniform magnetic field. The magnetic field was changed in two ways. The first way was by varying the current; at a fixed distance between the cabs. The second way was by adjusting the distance between the cabs in a symmetric way. The intensity of the magnetic field was measured in milli Tesla (mT) using magnetic meter model MG-3002 (Wenzhou, ZJ, China). The magnet setup and the magnetic treatments were under controlled laboratory conditions of humidity, temperature and with no interfering sources of radiations.

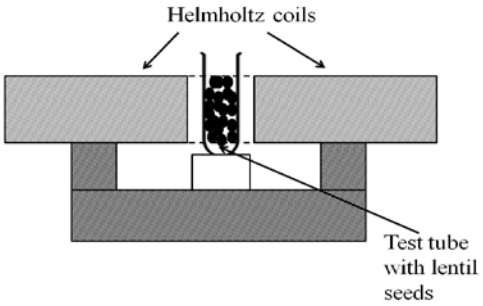

Figure 1. A schematic illustration of the electromagnet setup and the magnetization of lentil seeds.

5. Magnetic treatment of lentil seeds

For the magnetic treatment of lentil seeds, the magnetic field intensity of 1, 10, 20, 30, 40, 50, 60, 70, 80, 90, and 100 mT was tested. Each magnetic intensity was tested for an exposure time of 5, 10, 15, 20, and 30 min. For each magnetic treatment, three biological replications were treated at the same time. Each replication has 50 seeds in a glass tube. Magnetic treatment was done under controlled laboratory conditions at a temperature (22 ± 2ºC) and relative humidity of 60%.

6. Assessment of seedling growth after magnetic treatment

After magnetic treatment, lentil seeds were sown in a peatmoss: perlite mix (1:1) at 24°C, 70% humidity, 585 μmol m^{-2} s^{-1} light intensity and 16h light/16 h dark in a growth chamber. They pots were completely randomized in the growth chamber. After 7 days of growth in, 30 control lentil seedlings and 30 seedlings of magnetically treated seeds were sampled. Then, shoot length, root length, and seedling fresh mass were measured. After that, lentil plants were dried in the oven at 80 ºC for 1 day and then their dry mass was determined.

7. Analysis of biochemical changes in lentil seedlings under effective magnetic treatments

For the biochemical analyses, the magnetic treatments that resulted in an increase or decrease in the growth of

lentil seedlings (effective magnetic treatments) were selected (Table 1). The biochemical analyses in this study are the accumulation of malondialdhyde (MDA) and enzyme assay of some antioxidant enzymes: CAT (CAT 1.11.1.6), APX (APX 1.11.1.1), and SOD (SOD 1.15.1.1). For lipid peroxidation and antioxidant enzymes analyses, the shoots, and roots of 15 lentil seedlings were sampled separately. They were pooled into 3 biological replicates. All Plant samples were immediately frozen in liquid nitrogen.

Table. 1. Selected magnetic treatments for the biochemical analyses.

Magnetic treatment	Intensity of magnetic	Duration of
D1	20	20
D2	20	25
D3	40	30
D4	50	30
D5	70	5
D6	70	10
D7	70	25
D8	100	10
D9	100	25

8. Assessment of lipid peroxidation

Lipid peroxidation was determined by the quantification of MDA according to Heath and Packer (1968). Briefly, homogenization of samples in trichloroacetic acid (TCA) of 2.5 ml of 20% (w/v) was followed by centrifugation. The supernatant was mixed with thiobarbituric acid in TCA and boiled at 95ºC for 30 min. The reaction was stopped by cooling and centrifuged. Finally, the absorbance of the mixture was read at 532 nm and 600 nm. After subtracting the non-specific absorbance at 600 nm, the MDA concentration was determined by its extinction coefficient of 155 mM-1 cm-1.

9. Enzyme assay of CAT

The activity of CAT enzyme was determined according to Aebi (1984). In brief, the samples were homogenized in 1 ml extraction buffer Aebi 1984, and centrifuged. A volume of 20 µL of the shoot extract or 60 µL of the root extract was mixed with 50 mM potassium phosphate buffer (pH 7.0) and 15 mM H_2O_2. The reduction of H_2O_2 was then measured spectrophotometically at 240 nm for 2 min (UV-Visible Spectrophotometer-M51, Bell engineering S.R.L, Italy). The extinction coefficient of CAT is 43.6 $mM^{-1}cm^{-1}$.

10. Enzyme assay of APX

The activity of APX enzyme was determined according to Nakano and Asada (1981). The samples were homogenized in 1 ml extraction buffer (Nakano and Asada 1981) and then centrifuged. After that, the activity of APX was assayed by mixing 25 mM potassium phosphate buffer (pH 7.0), 0.1 mM EDTA, 0.25 mM ascorbate and 20 µL of the shoot extract or 60 µL of the root extract. The reaction was started by adding 1 mM H_2O_2 and APX activity was measured at 290 nm. The extinction coefficient of APX is 2.8 $mM^{-1}cm^{-1}$.

11. Enzyme assay of SOD

The activity of SOD enzyme was determined according to Beauchamp and Fridovich (1971). The samples were homogenized in 1 ml extraction buffer (Beauchamp and Fridovich 1971). The activity of SOD in the extract was assayed by mixing 50 mM potassium phosphate buffer (pH 7.8), 19.79 mM L-methonine, 0.025 % Triton X-100, 0.114 mM p- nitroblue tetrazolium (NBT) and 50 µL of the plant extract to a final volume of 1 ml. The reaction was started by adding 20 µL riboflavin solution (0.044 mg/ml). One unit of SOD activity is defined as the amount of enzyme that inhibits NBT reduction by half in comparison with the negative control (tubes lacking the enzyme).

12. Statistical analysis

The results of the morphological and biochemical changes in the control and the magnetically treated groups were statistically analyzed by One-way ANOVA and means were compared by Tukey's test at $p < 0.05$ using Minitab 17 (Minitab, LLC, USA). The results were expressed as the mean value ± standard deviation.

13. Results

The effect of the different magnetic treatments on the shoot and root length of lentil seedlings can be classified into 6 categories: a significant increase in both the shoot and root length, an increase in the shoot length without affecting the root length, no effect on the shoot length with an increase in the root length, a significant decrease in the shoot length with an increase in the root length, a significant increase in the shoot length with a decrease in the root length and a significant decrease in both the shoot and root length (Table 2). The highest increase in the shoot length was shown at 40 mT for 5 min (5.07 cm compared to 3.37 cm of the control). The highest root length was at 90 mT for 5 min (6.55 cm compared to 4.92 cm of the control).

Most of the magnetic treatments (1, 10, 20, 30, 40, 70, 90, and 100 mT) resulted in a significant decrease in the fresh mass of lentil seedlings for all or some of the exposure durations (Table 2). The magnetic field of 50 mT resulted in a highly significant increase in the fresh mass of lentil seedlings at an exposure time of 5, 15, 20, and 25 min (0.32, 0.39, 0.41, and 0.37 g compared to 0.20 g of the control, respectively). The magnetic field of 60 mT also resulted in a highly significant increase in the fresh mass of lentil seedlings at an exposure time of 5, 15, 20 and 30 min (0.30, 0.32, 0.33, and 0.27 g compared to 0.20 g of the control, respectively).

In general, the biomass (dry mass) of lentil seedlings was not significantly changed in response to most magnetic treatments (Table 2). The exposure of lentil seeds to 10 mT for 10, and 30 min showed a significant decrease in the biomass of lentil seedlings compared to the control seedlings (0.028 g compared to 0.034 g of the control). A significant decrease in the biomass was also shown in response to 50 mT for exposure time of 5, 20, 25, and 30 min (0.029, 0.028, 0.029, and 0.026 g compared to 0.034 g of the control, respectively).

Table 2. Morphological changes in lentil seedlings after seed exposure to different magnetic treatments.

Magnetic treatment					
Magnetic field intensity (mT)	Time of exposure (min)	Shoot length (cm)	Root length (cm)	Fresh mass (g)	Dry mass (g)
1	0	3.37 ± 1.11^{BC}	4.92 ± 2.10^{A}	0.20 ± 0.09^{A}	0.034 ± 0.010^{B}
	5	2.67 ± 0.79^{D}	2.60 ± 1.12^{C}	0.15 ± 0.03^{B}	0.034 ± 0.009^{AB}
	10	3.60 ± 1.40^{AB}	3.45 ± 1.76^{BC}	0.16 ± 0.03^{B}	0.032 ± 0.007^{B}
	15	2.75 ± 0.75^{CD}	2.73 ± 1.07^{BC}	0.15 ± 0.03^{B}	0.034 ± 0.008^{AB}
	20	3.33 ± 0.91^{ABCD}	3.83 ± 2.09^{BC}	0.17 ± 0.04^{AB}	0.035 ± 0.009^{AB}
	25	3.13± 1.29^{BCD}	3.05 ± 1.57^{BC}	0.16 ± 0.03^{B}	0.040 ± 0.012^{A}
	30	4.02 ± 1.32^{A}	4.13 ± 1.38^{AB}	0.16 ± 0.03^{B}	0.034 ± 0.010^{B}
10	0	3.37 ± 1.11^{A}	4.92± 2.10^{ABC}	0.20 ± 0.09^{A}	0.034 ± 0.009^{AB}
	5	3.20 ± 1.18^{A}	3.83 ± 1.48^{C}	0.16 ± 0.03^{B}	0.029 ± 0.01^{BC}
	10	3.40 ± 1.42^{A}	5.98 ± 2.13^{A}	0.17 ± 0.03^{AB}	0.028 ± 0.01^{C}
	15	3.63 ± 1.11^{A}	4.32 ± 1.47^{BC}	0.16 ± 0.04^{B}	0.031 ± 0.008^{ABC}
	20	3.55 ± 1.05^{A}	5.03 ± 1.74^{ABC}	0.17± 0.04^{AB}	0.038 ± 0.021^{A}
	25	3.84 ± 1.30^{A}	5.02 ± 2.04^{ABC}	0.18 ± 0.03^{AB}	0.031± 0.007^{ABC}
	30	3.92 ± 1.02^{A}	5.42 ± 2.05^{AB}	0.18 ± 0.05^{AB}	0.028 ± 0.007^{C}
20	0	3.37 ± 1.11^{C}	4.92 ± 2.10^{B}	0.20 ± 0.09^{A}	0.034 ± 0.009^{A}
	5	3.77 ± 1.15^{BC}	4.78 ± 1.36^{AB}	0.15 ± 0.03^{B}	0.035 ± 0.009^{A}
	10	4.18 ± 1.12^{B}	4.75 ± 1.65^{AB}	0.17 ± 0.04^{AB}	0.034 ± 0.006^{A}
	15	3.88 ± 0.10^{BC}	5.23 ± 1.69^{AB}	0.18 ± 0.04^{AB}	0.035 ± 0.009^{A}
	20	3.66 ± 1.23^{BC}	6.21 ± 1.64^{A}	0.17 ± 0.03	0.033 ± 0.008^{A}
	25	5.17 ± 1.24^{A}	5.09 ± 1.40^{AB}	0.16 ± 0.03^{B}	0.031 ± 0.010^{A}
	30	3.47 ± 0.94^{BC}	4.93 ± 1.71^{AB}	0.17 ± 0.03^{AB}	0.034 ± 0.009^{A}
30	0	3.37 ± 1.11^{D}	4.92 ± 2.10^{A}	0.20 ± 0.09^{A}	0.034 ± 0.009^{A}
	5	4.80 ± 1.42^{A}	3.22 ± 1.58^{BC}	0.16 ± 0.03^{B}	0.032 ± 0.010^{A}
	10	4.03 ± 0.93^{ABC}	3.05 ± 1.04^{BC}	0.15 ± 0.03^{B}	0.032 ± 0.006^{A}
	15	4.47 ± 1.49^{AB}	4.00 ± 1.49^{AB}	0.16 ± 0.03^{B}	0.032 ± 0.005^{A}
	25	3.30 ± 0.85^{CD}	2.58 ± 1.16^{C}	0.14 ± 0.03^{B}	0.030 ± 0.006^{A}
	30	4.38 ± 0.93^{AB}	2.32 ± 0.68^{C}	0.17 ± 0.03^{AB}	0.036 ± 0.007^{A}
40	0	3.37 ± 1.11^{C}	4.92 ± 2.10^{A}	0.20 ± 0.09^{A}	0.034 ± 0.009^{A}
	5	5.07 ± 1.30^{A}	3.87 ± 1.62^{ABC}	0.16 ± 0.03^{B}	0.032 ± 0.010^{A}
	10	3.63 ± 1.03^{BC}	4.87 ± 1.77^{AB}	0.15 ± 0.03^{B}	0.032 ± 0.006^{A}
	15	4.08 ± 1.57^{B}	2.57 ± 1.36^{CD}	0.15 ± 0.03^{B}	0.034 ± 0.009^{A}
	20	3.27 ± 1.28^{BC}	3.55 ± 1.51^{BCD}	0.16 ± 0.03^{B}	0.031 ± 0.007^{A}
	25	3.42 ± 1.01^{BC}	4.06 ± 1.45^{AB}	0.15 ± 0.03^{B}	0.031 ± 0.005^{A}
	30	2.20 ± 0.54^{D}	2.23 ± 0.72^{D}	0.12 ± 0.02^{B}	0.031 ± 0.007^{A}
50	0	3.37 ± 1.11^{A}	4.92 ± 2.10^{A}	0.20± 0.09^{C}	0.034 ± 0.009^{A}
	5	3.33 ± 0.93^{AB}	4.98 ± 1.88^{A}	0.32 ± 0.11^{B}	0.029 ± 0.007^{BC}
	10	2.97 ± 1.27^{AB}	6.15 ± 5.78^{A}	0.15 ± 0.03^{D}	0.033 ± 0.006^{AB}
	15	2.67 ± 0.86^{B}	4.28 ± 1.99^{A}	0.39 ± 0.07^{A}	0.032 ± 0.008^{ABC}
	20	3.15 ± 0.89^{AB}	5.95 ± 1.81^{A}	0.41 ± 0.07^{A}	0.028 ± 0.007^{BC}
	25	3.40 ± 0.82^{AB}	5.17 ± 2.00^{A}	0.37 ± 0.02^{AB}	0.029 ± 0.006^{BC}
	30	3.40 ± 1.73^{AB}	5.80 ± 1.60^{A}	0.18 ± 0.03^{CD}	0.026 ± 0.006^{C}
60	0	3.37 ± 1.11^{B}	4.92 ± 2.10^{A}	0.20 ± 0.09^{B}	0.034 ± 0.009^{A}
	5	4.27 ± 1.70^{A}	4.68 ± 1.82^{A}	0.30 ± 0.11^{A}	0.030 ± 0.006^{AB}
	10	3.38 ± 1.12^{B}	5.30 ± 1.73^{A}	0.16 ± 0.03^{B}	0.032 ± 0.006^{AB}
	15	3.40 ± 0.91^{AB}	4.63 ± 2.44^{A}	0.32 ± 0.11^{A}	0.031 ± 0.007^{AB}
	20	2.82 ± 1.19^{B}	4.10 ± 1.47^{A}	0.33 ± 0.12^{A}	0.029 ± 0.006^{B}
	25	3.58 ± 1.18^{AB}	5.25 ± 2.00^{A}	0.17 ± 0.07^{B}	0.032 ± 0.007^{AB}
	30	3.65 ± 1.08^{AB}	5.17 ± 1.76^{A}	0.27 ± 0.09^{A}	0.031 ± 0.007^{AB}
70	0	3.37 ± 1.11^{A}	4.92 ± 2.10^{A}	0.20 ± 0.09^{A}	0.034 ± 0.009^{A}
	5	2.50 ± 0.92^{B}	3.30 ± 1.95^{A}	0.14 ± 0.03^{B}	0.034 ± 0.010^{A}
	10	2.58 ± 1.10^{B}	4.68 ± 1.78^{A}	0.15 ± 0.04^{B}	0.037 ± 0.012^{A}
	15	2.60 ± 1.24^{B}	3.60 ± 1.68^{A}	0.15 ± 0.04^{B}	0.033 ± 0.010^{A}
	20	2.18 ± 1.05^{B}	5.25 ± 1.95^{A}	0.13 ± 0.03^{B}	0.030 ± 0.006^{A}
	25	2.17 ± 0.78^{B}	4.90 ± 1.95^{A}	0.14 ± 0.03^{B}	0.032 ± 0.006^{A}
	30	2.28 ± 0.63^{B}	5.08 ± 2.06^{A}	0.14 ± 0.03^{B}	0.034 ± 0.008^{A}
90	0	3.37 ± 1.11^{A}	4.92 ± 2.10^{B}	0.20 ± 0.09^{A}	0.034 ± 0.009^{A}
	5	2.58 ± 0.86^{B}	6.55 ± 2.15^{A}	0.17 ± 0.04^{AB}	0.033 ± 0.007^{A}
	10	2.62 ± 0.87^{B}	5.38 ± 2.25^{AB}	0.16 ± 0.03^{B}	0.032 ± 0.006^{A}
	15	2.10 ± 0.96^{B}	4.40 ± 2.18^{B}	0.16 ± 0.04^{B}	0.032 ± 0.007^{A}
	20	2.65 ± 1.52^{B}	6.07 ± 2.56^{AB}	0.17 ± 0.04^{AB}	0.035 ± 0.008^{A}
	25	2.17 ± 0.76^{B}	4.55 ± 2.52^{B}	0.16 ± 0.04^{B}	0.032 ± 0.007^{A}

	30	2.92 ± 1.49^{AB}	5.67 ± 2.86^{AB}	0.17 ± 0.04^{AB}	0.030 ± 0.005^{A}
100	0	3.37 ± 1.11^{A}	4.92 ± 2.10^{A}	0.20 ± 0.09^{A}	0.034 ± 0.009^{AB}
	5	2.63 ± 1.19^{B}	4.63 ± 1.65^{A}	0.16 ± 0.04^{AB}	0.037 ± 0.007^{AB}
	10	2.40 ± 1.21^{B}	4.03 ± 2.14^{A}	0.15 ± 0.04^{B}	0.031 ± 0.006^{BC}
	15	2.18 ± 0.73^{B}	4.40 ± 1.73^{A}	0.16 ± 0.04^{AB}	0.038 ± 0.011^{A}
	20	2.22 ± 0.78^{B}	4.43 ± 2.15^{A}	0.17 ± 0.03^{AB}	0.036 ± 0.006^{AB}
	25	1.85 ± 0.98^{B}	4.63 ± 2.03^{A}	0.16 ± 0.04^{AB}	0.029 ± 0.004^{C}
	30	2.27 ± 0.77^{B}	5.45 ± 2.20^{A}	0.16 ± 0.04^{AB}	0.032 ± 0.006^{ABC}

Different letters indicate statistically significant values following Tukey's test at $p < 0.05$. Each value represents the mean of thirty (n = 30) replicates ± standard deviation.

MDA in the shoot of lentil seedlings of the magnetically treated seeds was not significantly changed in most of the magnetic treatments (Table 3). MDA was significantly decreased in the root of lentil seedlings of the magnetically treated seeds with 20 mT for 20 min (D1) (5.29 µmole/ g fresh mass) compared to 23.93 µmole/ g fresh mass of the control. The root of lentil seedlings of the magnetically treated seeds with 50 mT for 30 min (D4) also showed a significant decrease in MDA concentration (10.44 µmole/ g fresh mass) compared to 23.93 µmole/ g fresh mass of the control. The magnetic treatment 50 mT for 30 min (D4) also resulted in a significant increase in MDA in the shoot of lentil seedlings (42.6 µmole/ g fresh mass) compared to 20.20 µmole/ g fresh mass of the control (Table 3).

The activity of CAT did not change significantly in the shoot of lentil seedlings of the magnetically treated seeds compared to the control seedlings (Table 3). The root of lentil seedlings of the magnetically treated seeds with 20 mT for 25 min (D2) showed significantly high CAT activity (0.57 unit/ mg protein) compared to 0.15 unit/ mg protein of the control (Table 3). The magnetic treatment 100 mT for 25 min (D9) also resulted in a significant increase in CAT activity in the root of lentil seedlings (0.30 unit/ mg protein) compared to 0.15 unit/ mg protein of the control.

The activity of APX activity was not significantly changed in the shoot of lentil seedlings of the magnetically treated seeds (Table 3). The magnetic treatment of lentil seeds with 70 mT for 5, 10, and 15 min (D5, D6, and D7) significantly increased APX activity in the root (9.18, 8.77, and 6.69 unit/ mg protein) compared to 2.46 unit/ mg protein of the control.

The activity of SOD was not significantly changed in the shoot of lentil seedlings from magnetically treated seeds (Table 3). The activity of SOD was significantly high in the root of lentil seedlings of the magnetic treatments D2 (20 mT for 25 min) and D3 (40 mT for 30 min) 1.09 and 1.00 unit/ mg protein compared to 0.40 unit/ mg protein of the control.

Table 3. Biochemical changes in lentil seedlings after seed exposure to effective magnetic treatments.

Magnetic treatment	**MDA (µmole/ g fresh mass)**		**CAT (unit/ mg protein)**		**APX (unit/ mg protein)**		**SOD (unit/ mg protein)**	
(Magnetic field (mT), time (min))	**Shoot**	**Root**	**Shoot**	**Root**	**Shoot**	**Root**	**Shoot**	**Root**
Control	20.20 ± 4.35^{B}	23.93 ± 5.10^{ABC}	0.16 ± 0.05^{AB}	0.15 ± 0.009^{C}	3.20 ± 0.43^{AB}	2.46 ± 1.13^{D}	0.32 ± 0.10^{ABC}	0.40 ± 0.17^{C}
D1 (20, 20)	20.70 ± 5.54^{B}	5.29 ± 0.27^{E}	0.20 ± 0.04^{AB}	0.08 ± 0.010^{C}	6.13 ± 0.79^{AB}	3.25 ± 1.39^{CD}	0.48 ± 0.17^{A}	0.27 ± 0.10^{C}
D2 (20, 25)	19.80 ± 2.95^{B}	23.50 ± 3.44^{ABC}	0.16 ± 0.01^{AB}	0.57 ± 0.050^{A}	3.56 ± 1.54^{AB}	4.05 ± 2.62^{CD}	0.46 ± 0.12^{A}	1.09 ± 0.33^{A}
D3 (40, 30)	23.37 ± 4.55^{AB}	31.57 ± 1.58^{A}	0.11 ± 0.04^{B}	0.16 ± 0.050^{C}	2.05 ± 1.46^{B}	5.47 ± 1.57^{ABCD}	0.39± 0.13^{ABC}	1.00 ± 0.37^{AB}
D4 (50, 30)	42.6 ± 20.8^{A}	10.44 ± 0.32^{DE}	0.33 ± 0.15^{A}	0.13 ± 0.05^{C}	2.13 ± 0.11^{A}	1.85^{D} ± 0.95	0.12 ± 0.09^{C}	0.21 ± 0.13^{C}
D5 (70, 5)	19.52 ± 1.68^{B}	17.00± 4.00^{CD}	0.08 ± 0.01^{B}	0.14 ± 0.006^{C}	5.39 ± 3.08^{AB}	9.18 ± 0.93^{A}	0.16 ± 0.04^{BC}	0.21 ± 0.02^{C}
D6 (70, 10)	20.20 ± 4.35^{B}	23.93 ± 5.10^{ABC}	0.11 ± 0.01^{B}	0.14 ± 0.03^{C}	8.11 ± 2.81^{A}	8.77 ± 2.54^{AB}	0.20± 0.04^{ABC}	0.25 ± 0.09^{C}
D7 (70, 25)	17.05 ± 3.52^{B}	19.56 ± 5.18^{BCD}	0.17 ± 0.02^{AB}	0.15 ± 0.010^{C}	7.24 ± 2.79^{AB}	6.69± 1.26^{ABC}	0.26± 0.02^{ABC}	0.47 ± 0.17^{BC}
D8 (100, 10)	10.57 ± 2.62^{B}	13.62 ± 4.79^{CDE}	0.18 ± .03^{AB}	0.09 ± 0.015^{C}	6.69 ± 3.82^{AB}	4.40 ± 0.37^{CD}	0.35± 0.05^{ABC}	0.48 ± 0.27^{BC}
D9 (100, 25)	21.83 ± 4.60^{AB}	30.11 ± 2.47^{AB}	0.28 ± 0.13^{AB}	0.30 ± 0.06^{B}	4.37 ± 2.92^{AB}	5.47 ± 1.77^{BCD}	0.41 ± 0.12^{AB}	0.39 ± 0.09^{C}

Different letters indicate statistically significant values following Tukey's test at $p < 0.05$. Each value represents the mean of three (n = 3) biological replicates ± standard deviation.

14. Discussion

In the present study, lentil seeds were exposed to different magnetic treatments and the seedling growth was assessed in terms of shoot and root length, seedling fresh and dry mass. The results revealed growth stimulatory, inhibitory, and neutral magnetic treatments. This is consistent with the results of the previous studies, which showed the enhancement and the inhibition of the growth of different plant species such as wheat, barley, maize, chickpea, sunflower, and lentil after seed exposure to a static magnetic field (Pittman 1977; Martinez et al. 2000 ; Flórez et al.,2004; Flórez et al. 2007; Vashisth and Nagarajan 2008; Martínez et al. 2009; Aladjadjiyan 2010; Vashisth and Nagarajan 2010; Asgharipour and Omrani 2011; Carbonell et al. 2011; Harb and Abu Aljarayesh 2013). Overall, there is an effective magnetic treatment in terms of the magnetic field intensity and the duration of exposure that results in the maximum enhancement of plant growth. Many factors determine this effective magnetic treatment. Plant species and its genotype, seed quality and its physical and physiological characters are major factors. In addition, the environmental conditions at

the time of magnetic treatment and even the time of the year are very crucial determinants of the magnetic effect (García Reina et al. 2001). The exact mechanism of growth changes in response to static magnetic field is not clear, but some biochemical changes such as the ROS and their scavengers might play an important role in plants' responses to magnetic treatment.

In general, most of the magnetic treatments in this study did not result in lipid peroxidation and the accumulation of MDA. But, one growth stimulatory magnetic treatment showed the lowest concentration of MDA in the root of lentil seedlings, and one inhibitory magnetic treatment has the highest concentration of MDA in the shoot of lentil seedlings. The effect of the static magnetic field on the accumulation of reactive oxygen species (ROS) and the oxidative stress were studied in a few plant species such as radish, soybean, and cucumber. The accumulation of ROS results in lipid peroxidation. Lipid peroxidation is mainly caused by Hydroxyl radical (OH•), which is produced from H_2O_2 by Fenton reaction (Gill and Tuteja 2010). Lipid peroxidation and the accumulation of MDA are indicative of oxidative stress, which at high concentrations has harmful effects on plant growth. Indeed, lipid peroxidation and the accumulation of MDA had negative impact on plants' resistance to different stresses such as drought and heat, due to the reduced ability of scavenging the accumulated ROS under stress (Liu and Huang 2000; Liang et al. 2003; Song et al. 2016). Therefore, the improvement of the seedling growth of lentil shown in this study for some magnetic treatments could be explained by the alleviation of the accumulation of ROS and the consequent oxidative stress. Indeed, reduced lipid peroxidation in the magnetically treated radish seedlings was a positive factor that enhanced the seedlings' growth (Novitskii et al. 2015). Moreover, the significant decrease in superoxide radical in soybean plants after seed exposure to 100 and 200 mT magnetic field for 1 h was suggested as an explanation for the enhanced plant growth (Baby et al. 2011). In contrast to this, the treatment of cucumber seedlings with 200 mT magnetic field for 1 h showed a significant increase in superoxide radical and H_2O_2, which was suggested as the cause of growth stimulation of cucumber seedlings (Bhardwaj et al. 2012). The discrepancy of the results could be explained by the different plant species that were tested, the method and the conditions of application of the magnetic field, the time of the day and the time of the year during which the magnetic treatment was applied. In addition, many other internal and external factors could play a role in the plant's response to magnetic treatment.

The activity of the antioxidant enzymes: APX, CAT and SOD was not changed in the shoot of lentil seedlings in response to magnetic treatments. But significant differences in the activity of these enzymes were shown in the root of lentil seedlings under many magnetic treatments. The activity of CAT was significantly increased in the root of lentil seedlings under one stimulatory and one inhibitory growth magnetic treatments. The activity of APX was significantly increased in the root in lentil seedlings under some growth inhibitory magnetic treatments. Yet, other stimulatory and inhibitory magnetic treatments showed no change in APX activity. APX is required for the fine scavenging of H_2O_2 under conditions of oxidative stress, whereas CAT is required for the bulk scavenging of H_2O_2 under the same conditions (Gill and Tuteja 2010). The changes in the activity of antioxidant enzymes under stress conditions are controversial (Abogadallah 2010). The high activity of antioxidant enzymes in the stress tolerant genotypes is a positive indicator of stress tolerance, whereas their high activity in the stress sensitive genotypes is an indicator of a significant oxidative stress. Therefore, in the present study, the high activity of CAT under the inhibitory magnetic treatments could be an indicator of elevated oxidative stress, whereas its high activity under the stimulatory magnetic treatments could be an indicator of alleviated oxidative stress. Our results showed high activity of SOD in the root of lentil seedlings under two magnetic treatments. The previous studies showed discrepancy in the effect of magnetic treatment on the activity of SOD. The activity of SOD was increased in the magnetically treated suspension-cultured tobacco cells (Sahebjamei et al. 2007), whereas it was reduced SOD in the magnetically treated maize and soybean plants (Shine and Guruprasad 2012; Asghar et al. 2017). Hence, changes in the activity of SOD after seed exposure to a magnetic field are dependent on the plant species and the intensity and the duration of magnetic treatment.

15. Conclusion

The results of this study showed three effects of the magnetic treatments on the growth of lentil seedlings: stimulatory, inhibitory, and neutral. In general, most of the effective magnetic treatments did not cause significant changes in the accumulation of MDA and the activity of antioxidant enzymes in the shoot of lentil seedlings. Most of the biochemical changes were shown in the root of lentil seedlings under magnetic treatments. One growth stimulatory magnetic treatment (20 mT for 20 min (D1)) significantly decreased the concentration of MDA and showed normal activity of antioxidant enzymes in the root of lentil seedlings. The pre-sowing treatment of lentil seeds with the effective magnetic treatment in terms of the magnetic field intensity and the duration of exposure could be an affordable and eco-friendly method for the improvement of lentil growth. Further detailed dissection of the interaction between the magnetic treatment and the growth of lentil seedlings at the molecular, biochemical, and physiological level is recommended.

Acknowledgments

This project was funded by the Deanship of Scientific Research at Yarmouk University fund No. 12/2014.

References

Abogadallah G. 2010. Antioxidative defense under salt stress. *Plant signal. and Behav*., **5**:369-374.

Aebi H. 1984. Catalase in vitro. *Methods Enzymol*., **105**:121-126.

Aladjadjiyan A. 2010. Influence of stationary magnetic field on lentil seeds. *Int. Agrophysics*, **24**:231-234.

Anand A, Nagarajan S, Verma A, Joshin D, Pathak P, Bhardwaj J. 2012. Pre-treatment of seeds with static magnetic field ameliorates soil water stress in seedlings of maize (*Zea mays* L). *Indian J. Biochem. Biophys*., **49**:63-70.

Andrews M, McKenzie BA. 2007. Adaptation and ecology. In: Yadav S, McNeil D, Stevenson P (Eds.), **Lentil an ancient crop for modern times**. Springer, Dordrecht, The Netherlands, pp. 23-32.

Asghar T, Iqbal M, Jamil Y, Haq Z, Nisar J, Shahid M. 2017. Comparison of He Ne laser and sinusoidal non-uniform magnetic field seed pre-sowing treatment effect on *Glycine max* (Var 90-I) germination, growth, and yield. *J. Photochem. Photobiol. B*, **166**:212-219.

Asgharipour M, Omrani M. 2011. Effects of seed pretreatment by stationary magnetic fields on germination and early growth of lentil. *Aust. J. Basic & Appl. Sci*., **5**: 1650-1654.

Baby S, Narayanaswamy G, Anand A. 2011. Superoxide radical production and performance index of photosystem in leaves from magneto primed soybean seeds. *Plant Signal. Behav*., **6**:1635-1637.

Baghel L, Kataria S, Guruprasad K. 2018. Effect of static magnetic field pretreatment on growth, photosynthetic performance and yield of soybean under water stress. *Photosynthetica*, **56**:718-730.

Beauchamp C, Fridovich I. 1971. Superoxide dismutase: improved assay and an assay applicable to acrylamide gels. *Anal. Biochem*., **44**:276-287.

Bhardwaj J, Anand A, Nagarajan S. 2012. Biochemical and biophysical changes associated with magnetopriming in germinating cucumber seeds. *Plant Physiol. Biochem*., **57**:67-73.

Cakmak T, Dumlupinar R, Erdal S. 2010. Acceleration of germination and early growth of wheat and beans seedlings grown under various magnetic field and osmotic conditions. *Bioelectromagnetics*, **31**:120-129.

Cakmak T, Cakmak E, Dumlupinar R, Tekinay T. 2012. Analysis of apoplastic and symplastic antioxidant system in shallot leaves: impacts of weak static electric and magnetic field. *J Plant Physiol*., **169**:1066-1073.

Carbonell V, Florez M, Martinez E, Mequeda R, Amaya J. 2011. Study of stationary magnetic field on initial growth of pea (*Pisum sativum* L.) seeds. *Seed Sci. Technol*., **39**:673-679.

Flórez M, Carbonell M, Martínez E. 2004. Early sprouting and first stages of growth of rice seeds exposed to a magnetic field. *Electromagn. Biol. Med*., **23**:157-166.

Flórez M, Carbonell M, Martĭnez E. 2007. Exposure of maize seeds to stationary magnetic fields: Effects on germination and early growth. *Environ. Exp. Bot*., **59**:68-75.

García Reina F, Arza Pascual L, Fundora Almanza I. 2001. Influence of a stationary magnetic field on water relations in lettuce seeds. Part II: Experimental results. *Bioelectromagnetics*, **22**: 596-602.

Gill S, Tuteja N. 2010. Reactive oxygen species and antioxidant machinery in abiotic stress tolerance in crop plants. *Plant Physiol. Biochem*., **48**:909-930.

Harb A, Abu-AlJarayesh I. 2013. The effect of exposure of dry and soaked grains of durum wheat (*Triticum durum* Desf.) to static magnetic field. *Intel. J. Biophys.*, **3**:26-32.

Heath R, Packer L. 1968. Photoperoxidation in isolated chloroplasts: I. Kinetics and stoichiometry of fatty acid peroxidation. *Arch. Biochem. Biophys.*, **125**:189-198.

Hussain M, Dastgeer G, Afzai A, Hussain S, Kanwar R. 2020. Eco-friendly magnetic field treatment to enhance wheat yield and seed germination growth. Environ. *Nanotechnol. Monit. Manag*., **14 (**doi.org/10.1016/j.enmm.2020.100299)

Iqbal M, Haq Z, Jamil Y, Nisar J. 2016a. Pre-sowing seed magnetic field treatment influence on germination, seedling growth and enzymatic activities of melon (*Cucumis melo* L.). *Biocatal. Agric. Biotechnol*., **6**:176-183.

Iqbal M, Haq Z, Malik A, Ayoub CM, Jamil Y, Nisar J. 2016b. Pre-sowing seed magnetic field stimulation: A good option to enhance bitter gourd germination, seedling growth and yield characteristics. *Biocatal. Agric. Biotechnol*., **5**:30-37.

Liang Y, Chen Q, Liu Q, Zhang W, Ding R. 2003. Exogenous silicon (Si) increases antioxidant enzyme activity and reduces lipid peroxidation in roots of salt-stressed barley (Hordeum vulgare L.). *J. Plant Physiol*., **160**: 1157-1164.

Liu X, Huang B. 2000. Heat stress injury in relation to membrane lipid peroxidation in creeping bentgrass. *Crop Sci*., **40**: 503-510.

Maffei M. 2014. Magnetic field effects on plant growth development and evolution. *Front. Plant Sci*., **5**:445-459.

Martinez E, Carbonell V, Amaya M. 2000. A static magnetic field of 125 mT stimulates the initial growth stages of barley (*Hordeum vulgare* L.). *Electro. Magnetobiol*., **19**:271-277.

Martinez E, Carbonell M, Flórez M, Amaya J, Maqueda R. 2009. Germination of tomato seeds (*Lycopersicon esculentum* L.) under magnetic field. *Int. Agrophys*., **23**: 45-49.

Mroczek-Zdyrska M, Tryniecki L, Kornarzyński K, Pietruszewski S, Gagoś M. 2016. Influence of magnetic field stimulation on the growth and biochemical parameters in *Phaseolus vulgaris* L. *J. Microbiol. Biotech. Food Sci*., **5**:548-551.

Nakano Y, Asada K. 1981. Hydrogen peroxide is scavenged by ascorbate specific peroxidase in spinach chloroplasts. *Plant Cell Physiol*., **22**:867-880.

Naz A, Jamil Y, Haq Z, Iqbal M, Ahmad M, Ashaf M, Ahmad R. 2012. Enhancement in the germination, growth and yield of Okra (*Abelmoschus esculentus*) using pre-sowing magnetic treatment of seeds. *Indian J. Biochem. Bio*., **49**:211-214.

Novitskii YI, Novitskaya G, Serdyukov Y, Kocheshkova T, Molokanov D, Dobrovolskii M. 2015. Influence of weak permanent magnetic field on lipid peroxidation in radish seedlings. Russ *J. Plant Physiol*., **62**:375-380.

Occhipinti A, Santis A, Maffei. M. 2014. Magnetoreception: an unavoidable step for plant evolution? *Trends Plant Sci*., **19**:1-4.

Penuelas J, Liusia J, Martinez B, Fontcuberta J. 2004. Diamagnetic susceptibility and root growth responses to magnetic field in *Lens Culinaris*, *Glysinesoja*, and *Triticum aectivum. Electromagn. Biol. Med*., **23**:97-112.

Pietruszewski S, Martínez E. 2015. Magnetic field as a method of improving the quality of sowing material: a review. *Int. Agrophys*., **29**:377-389.

Pittman U. 1977. Effects of magnetic seed treatment on yields of barely, wheat, and oats in southern Alberta. *Can. J. Plant Sci*., **57**:37-45.

Podleśna A, Bojarszczuk J, Podleśny J. 2019. Effect of pre-sowing magnetic field treatment on some biochemical and physiological processes in faba bean (*Vicia faba* L. spp. Minor*). J Plant Growth Regul*., **38**:1153–1160.

Rifna J, Ratish Ramanan K, Mahendran R. 2019. Emerging technology applications for improving seed germination. *Trends Food Sci. Technol*., **86**:95-108.

Sahebjamei H, Abdolmaleki P, Ghanati F. 2007. Effects of magnetic field on the antioxidant enzyme activities of suspension-cultured tobacco cells. *Bioelectromagnetics*, **28**:42-7.

Serdyukov YA, Novitskii YI. 2013. Impact of weak permanent magnetic field on antioxidant enzyme activities in radish seedlings. *Russ. J. Plant Physiol*., **60:**69-76.

Shine MB, Guruprased KN. 2012. Impact of pre-sowing magnetic field exposure of seeds to stationary magnetic field on growth, reactive oxygen species and photosynthesis of maize under field conditions. *Acta Physiol. Plant*, **34**:255-265.

Shine MB, Guruprasad KN, Anand A. 2012. Effect of stationary magnetic field strengths of 150 and 200 mT on reactive oxygen species production in soybean. *Bioelectromagnetics* **33**: 428-437.

Song X, Wang Y, Lv X. 2016. Responses of plant biomass, photosynthesis, and lipid peroxidation to warming and precipitation change in two dominant species (*Stipa grandis* and *Leymus chinensis*) from North China Grasslands. *Ecol. Evol*., **6**:1871-1882.

Vashisth A, Nagarajan S. 2008. Exposure of seeds to static magnetic field enhances germination and early growth characteristics in chickpea (*Cicer arietinuum*. L). *Bioelectromagnetics*, **29**:571-578.

Vashisth A, Nagarajan S. 2010. Effect on germination and early growth characteristics in sunflower (*Helianthus annuus*) seeds exposed to static magnetic field. *J. Plant Physiol*., **167**:159-156.

Yadav Y, Mahadik S, Dalvi V, Deogirikar A, Burondkar M, Vanave P. 2018. Effect of magnetic treatment on enzyme activation of paddy (*Oryza sativa* L.). *Int. J. Curr. Microbiol. App. Sci*., **7**:3573-3581.

JJBS

Volume 14, Number 1, March 2021
ISSN 1995-6673
Pages 187 - 189

Jordan Journal of Biological Sciences

Prevalence of *Helicobacter pylori* and Its seasonality in Ilam, Iran

Saeed Hemati[1,3], Arash Rahmatian[2], Ghasem Talee[2], Elham Bastani[2], Aryoobarzan Rahmatian[2], Morteza Shams[3*], Zahra Mahdavi[3*]

[1] *Department of Microbiology, School of Medicine, Tehran University of Medical Sciences, Tehran, Iran,*[2] *Faculty of Medicine, Ilam University of Medical Sciences, Ilam, Iran,*[3] *Zoonotic Diseases Research Center, Ilam University of Medical Sciences, Ilam, Iran.* *Received: April 5, 2020; Revised: July 25, 2020; Accepted: August 14, 2020*

Abstract:

The epidemiology of *Helicobacter pylori (H. pylori)* infection in Ilam city, Western Iran, is not well understood. We conducted the current research to determine the seroprevalence of *H. pylori* infection in this city. A total of 1102 individuals (661 females and 441 males) older than12 years old were enrolled in the study. The bacterium was detected by the *H. pylori* stool antigen (HpSA) test. The rate of *H. pylori* positivity in the sample population was 54.4% (n=600). No statistically significant association was found between gender and the prevalence of *H. pylori* (*P* value = 0.21). The highest *H. pylori* prevalence was observed in the summer (17.6%, n= 194); however, no statistically significant relationship was detected between seasonal changes and the incidence of *H. pylori* infection (*P value*= 0.30). According to our results, it seems that the prevalence of *H. pylori* infection is high, especially in summer, in the population of Ilam city. This may become a major health concern in the area.

Keyword: *Helicobacter pylori*, Stool antigen method, Gastrointestinal problems, Seasonality

1. Introduction

Helicobacter pylori (H. pylori) is an important Gram-negative bacterium categorized as a type 1 carcinogen due to its role in development of gastric cancer (Amin *et al*., 2019). Although the colonization of *H. pylori* in the stomach causes many gastrointestinal disorders, many infected individuals remain asymptomatic (Jafarzadeh *et al.*, 2013, Fakhre-Yaseri *et al.*, 2017). Because of different socioeconomic and living conditions, significant differences were observed in the prevalence of *H. pylori* infection between countries and within the same country. Different studies from various regions of Iran demonstrated a prevalence of *H. pylori* infection higher than 85% (Farshad *et al.*, 2010, Babatola *et al.*, 2019). Several studies suggested that some microorganisms such as *H. pylori* might have seasonal distribution (Yuan *et al*., 2015). Therefore, the present research was conducted to determine the prevalence of *H. pylori* infection across different seasons among the residents of Ilam city, western Iran.

2. Materials and Methods

2.1. Patients and samples:

Our study was performed on 1102 patients visiting our clinical laboratory (Khorshid Clinical Laboratory, Ilam, Iran) from February 2017 to January 2020. The *H. pylori* stool antigen (HpSA) test was performed for the patients. All the patients were older than 12 years. Stool samples were collected and kept at -20°C until use.

2.2. HpSA test:

The presence of *H. pylori* antigen in stool was checked using the HpSA test, a polyclonal ELISA assay (Generic Assays, Germany). First, all the components of the test were allowed to reach room temperature. Briefly, diluted stool samples (0.5 ml diluent+100 g stool) and antibody-biotin conjugates were added to wells and instantly incubated at room temperature for 60 minutes. Then the wells were decanted and washed before adding *streptavidin-HRP conjugate and again* incubated at room temperature *for* 30 minutes. *Afterwards, the wells were* decanted and washed, and chromogen substrate was added to each well. Finally, after adding the stop solution, the absorbance of samples was recorded at 450/620 nm by spectrophotometry (STAT FAX 4300, USA).

2.3. Statistical analysis

The Chi square and Fischer's exact tests were applied to check any association between the variables considering a *P value* of < 0.05 as the significance level.

3. Result

A total of 1102 individuals older than 12 years (661 females and 441 males) were investigated. *H. pylori* positivity was observed in 54.4% (n=600) while 45.6% (n=502) of the samples were negative. Gender was not significantly associated with the prevalence of *H. pylori* infection (*P* value= 0.21, table 1).

* Corresponding author e-mail: shamsimorteza55@gmail.com. and zahramahdavi9165@gmail.com

Table 1. Association between gender and prevalence of *H. pylori* infection

HpSA test	Sex		Total N=1102 n (%)	*P* value
	Female N=661 n (%)	Male N=441 n (%)		
Negative	291 (26.4%)	211 (19.1%)	502 (45.6%)	*P* value= 0.21
Positive	370 (33.6%)	230 (20.9%)	600 (54.4%)	
Total	661 (60%)	441 (40%)	1102 (100%)	

The highest rate of the infection was observed in the summer (17.6%, n=194); however, there was no statistically significant pattern in the seasonal distribution of the infection (*P* value= 0.30, table 2).

Table 2. The prevalence of *H. pylori* according to seasons

HpSA test	Season				Total	*P* value
	Spring	Summer	Autumn	Winter		
Negative	122 (11.1%)	158 (14.3%)	111 (10.1%)	111 (10.1%)	502 (45.6%)	
Positive	145 (13.2%)	194 (17.6%)	140 (12.7%)	121 (11%)	600 (54.4%)	*P* value= 0.30
Total	267 (24.2%)	352 (31.9%)	251 (22.8%)	232 (21.1%)	1102 (100%)	

4. Discussion

H. pylori infection can cause serious human disorders (Karimi *et al.*, 2013). It is estimated that *H. pylori* has already infected half of the world's population (Landarani *et al.*, 2014, Sedaghat *et al.*, 2014). Various noninvasive methods (e.g. *urea breath test*, HpSA, and highly accurate serological tests) are available for *H. pylori* diagnosis (Korkmaz *et al.*, 2015). Among these, the HpSA test is an easy, rapid, and inexpensive diagnostic method in clinical settings (Ceken *et al.*, 2011, Khalifehgholi *et al.*, 2013). The HpSA test directly detects the antigen of *H. pylori* in stool (Stefano *et al.*, 2018). Using this test, *H. pylori* frequency in our study was obtained 54.4%. Our observed prevalence was relatively high compared to the studies of Sharbatdaran *et al*. (2013, 37.7%) (Sharbatdaran *et al*., 2013), Dalla Nora *et al*. (2016, 49%) (Dalla Nora *et al*., 2016), Seid *et al*. (2018, 30.4 %) (Seid and Demsiss, 2018), Shiferaw *et al*. (2019, 36.8%) (Shiferaw and Abera, 2019), and Khoder *et al*. (2019, 41%) (Khoder *et al*., 2019). However, our result was similar to that of some other studies, for example Bashiri *et al*. (2019, 74%) (Bashiri *et al*., 2019), who reported a high frequency for *H. pylori* infection.

In the current study, the frequencies of *H. pylori* infection in females and males were 61.67% (n= 370/600) and 38.33% (n= 230/600), respectively. Agbor *et al*. (2018) reported an overall rate of 47.4% for *H. pylori* infection and respective frequencies of 47.0% and 47.5% in males and females. In the current study, there was no statistically significant association between gender and *H. pylori* infection. In this regard, our results were similar to those of Hajifattahi *et al*. (Hajifattahi *et al.*, 2015), Basir *et al*. (Ghasemi Basir *et al.*, 2017), and Tameshkel *et al*. (Tameshkel *et al.*, 2018) who reported no significant associations between gender and *H. pylori* infection.

Assessing the effects of seasonal patterns on the incidence of *H. pylori* infection, we observed no statistically significant association between *H. pylori* seroprevalence and seasons. Raschka *et al*. (1999) described a remarkable surge in *H. pylori* positive cases in October (i.e. fall); nevertheless, they reported that gender did not significantly influence the incidence of the infection. Moreover, Ibrahim *et al*. (2019) noted an elevated risk of *H. pylori* infection in January (winter).

In general, the discrepancies between our results and those of other studies may be due to (1) differences in the socio-economic and health status of participants (e.g. the availability of healthy sources of drinking water, and participants' knowledge about *H. pylori* transmission routes) (Wang *et al.*, 2019), (2) the presence of different bacterial strains in different geographical areas, may limit the diagnostic efficiency of some commercial diagnostic tests (Ghorbani *et al.*, 2009), and (3) other etiological and individual-specific features (for example dyspepsia) that can affect the prevalence of *H. pylori* infection (Suzuki *et al.*, 2011).

The HpSA test may deliver false-negative results in patients with low-intensity colonization and low fecal concentration of *H. pylori*. Also, false-positive results may occur due to cross-reactions with other *Helicobacter* species (Darma *et al.*, 2019). Nonetheless, this method can be used as a routine approach in clinical setting in Iran. In conclusion, the current study provided valuable information about the high prevalence of *H. pylori* infection, especially in summer season, in Ilam city that should be considered as a major health concern. Furthermore, this data can be useful for health decision makers and epidemiologists to conduct further studies.

Acknowledgments

We thank the staff of Khorshid Medical Laboratory and Zoonotic Diseases Research Center of Ilam University of Medical Sciences (Ilam, Iran) for laboratory assistance.

Funding: None

Conflicts of Interest:

The authors declare that there is no conflict of interest regarding the publication of this article.

References

Agbor N E, Esemu S N, Ndip L M, Tanih N F, Smith S I and Ndip R N. 2018. *Helicobacter pylori* in patients with gastritis in West Cameroon: prevalence and risk factors for infection. *BMC Res Note.*, **11,** 559.

Amin M, Shayesteh A A and Serajian A. 2019. Concurrent detection of cagA, vacA, sodB and hsp60 virulence genes and their relationship with clinical outcomes of disease in Helicobacter pylori isolated strains of southwest of Iran. Iran J Microbiol., 11, 198.

Babatola A O, Akinbami F O, Adeodu O O, Ojo T O, Efere M O and Olatunya O S. 2019. Seroprevalence and determinants of *Helicobacter pylori* infection among asymptomatic under-five children at a Tertiary Hospital in the South-Western region of Nigeria. *Afr Health Sci.,* **19,** 2082-2090.

Bashiri H, Esmaeilzadeh A, Vossoughinia H, Ghaffarzadegan K, Raziei H R and Bozorgomid A. 2019. Association Between Gastric Lymphoid Follicles (Precursor Of MALT Lymphomas) And *H. pylori* Infection At A Referral Hospital In Iran. *Clin Exp Gastroenterol.,* **12,** 409.

Ceken N, Yurtsever S G, Baran N, Alper E, Buyrac Z and Unsal B. 2011. Comparison of *Helicobacter pylori* antibody detection in stool with other diagnostic tests for infection. *Asian Pac J Cancer. Prev.,* **12,** 1077-1081.

Dalla Nora M, Horner R, De Carli D M, Rocha M P D, Araujo A F D and Fagundes R B. 2016. Is the immunocromatographic fecal antigen test effective for primary diagnosis of *Helicobacter pylori* infection in dyspeptic patients? *Arq Gastroenterol.,***53,** 224-227.

Darma A, Nugroho B S T, Yoanna V, Sulistyani I, Athiyyah A F, Ranuh R G and Sudarmo S M. 2019. Comparison of *Helicobacter pylori* stool antigen, salivary IgG, serum IgG, and serum IgM as diagnostic markers of *H. pylori* infection in children. *Iran J Microbiol.,* **11,** 206.

Fakhre-Yaseri H, Baradaran-Moghaddam A, Shekaraby M, Baradaran H R and Soltani-Arabshahi S K. 2017. Evaluating the relationship between serum immunoglobulin G (IgG) and A (IgA) anti-CagA antibody and the *cagA* gene in patients with dyspepsia. *Iran J Microbiol.,* **9,** 97.

Farshad S, Japoni A, Alborzi A, Zarenezhad M and Ranjbar R. 2010. Changing prevalence of *Helicobacter pylori* in south of Iran. *Iran J Clin Infect Dis.,* **5,** 65-69.

Ghasemi Basir H R, Ghobakhlou M, Akbari P, Dehghan A and Seif Rabiei M A. 2017. Correlation between the Intensity of *Helicobacter pylori* Colonization and Severity of Gastritis. *Gastroenterol Res Pract.,* **2017**.

Ghorbani D S, Kargar M, Doosti A, Abbasi P and Souod N. 2009. Optimization of real-time PCR method to assess the direct sensitivity of clarithromycin in *Helicobacter pylori*. *J Microbial World.,* **2,** 149-154.

Hajifattahi F, Hesari M, Zojaji H and Sarlati F. 2015. Relationship of halitosis with gastric *Helicobacter pylori* infection. *J Dent Tehran Iran.,* **12,** 200.

Ibrahim A, Ali Y B, Abdel-Aziz A and El-Badry A A. 2019. *Helicobacter pylori* and enteric parasites co-infection among diarrheic and non-diarrheic Egyptian children: seasonality, estimated risks, and predictive factors. *J Parasit Dis.,* **43,** 198-208.

Jafarzadeh A, Nemati M, Rezayati M T, Khoramdel H, Nabizadeh M, Hassanshahi G and Abdollahi H. 2013. Lower circulating levels of hemokine CXCL10 in *Helicobacter pylori*-infected patients with peptic ulcer: Influence of the bacterial virulence factor CagA. *Iran J Microbiol.,* **5,** 28.

Karimi A, Fakhimi-Derakhshan K, Imanzadeh F, Rezaei M, Cavoshzadeh Z and Maham S. 2013. *Helicobacter pylori* infection and pediatric asthma. *Iran J Microbiol.,* **5,** 132.

Khalifehgholi M, Shamsipour F, Ajhdarkosh H, Daryani N E, Pourmand M R, Hosseini M, Ghasemi A and Shirazi M H. 2013. Comparison of five diagnostic methods for *Helicobacter pylori*. *Iran J Microbiol.,* **5,** 396.

Khoder G, Muhammad J S, Mahmoud I, Soliman S S and Burucoa C. 2019. Prevalence of *Helicobacter pylori* and its associated factors among healthy asymptomatic residents in the United Arab Emirates. *Pathogens.,* **8,** 44.

Korkmaz H, Findik D, Ugurluoglu C and Terzi Y. 2015. Reliability of stool antigen tests: investigation of the diagnostic value of a new immunochromatographic *Helicobacter pylori* approach in dyspeptic patients. *Asian .Pac J Cancer Prev.,* **16,** 657-60.

Landarani Z, Falsafi T, Mahboubi M and Lameh-Rad B. 2014. Immunological detection of 34 KDa outer membrane protein as a functional form of OipA in clinical isolates of *Helicobacter pylori*. *Iran J Microbiol.,* **6,** 324.

Raschka C, Schorr W and Koch H J. 1999. Is there seasonal periodicity in the prevalence of *Helicobacter pylori*? *Chronobiol Int.,* **16,** 811-819.

Sedaghat H, Moniri R, Jamali R, Arj A, Zadeh M R, Moosavi S G A and Rezaei M. 2014. Prevalence of *Helicobacter pylori* vacA, cagA, cagE, iceA, babA2, and oipA genotypes in patients with upper gastrointestinal diseases. *Iran J Microbiol.,* **6,** 14.

Seid A and Demsiss W. 2018. Feco-prevalence and risk factors of *Helicobacter pylori* infection among symptomatic patients at Dessie Referral Hospital, Ethiopia. *BMC Infect Dis.,* **18,** 260.

Sharbatdaran M, Kashifard M, Shefaee S, Siadati S, Jahed B and Asgari S. 2013. Comparison of stool antigen test with gastric biopsy for the detection of *Helicobacter pylori* infection. *Pak J Med Sci.,* **29,** 68.

Shiferaw G and Abera D. 2019. Magnitude of *Helicobacter pylori* and associated risk factors among symptomatic patients attending at Jasmin internal medicine and pediatrics specialized private clinic in Addis Ababa city, Ethiopia. *BMC Infect Dis.,* **19,** 118.

Stefano K, Rosalia A, Chiara B, Federica G, Marco M, Gioacchino L, Fabiola F, Francesco D M and Gian L D A. 2018. Non-invasive tests for the diagnosis of *Helicobacter pylori*: state of the art. *Acta Bio Med Atene Parm.,***89,** 58.

Suzuki H, Matsuzaki J and Hibi T. 2011. What is the difference between *Helicobacter pylori*-associated dyspepsia and functional dyspepsia? *J Neurogastroenterol Motil.,* **17,** 124.

Tameshkel F S, Niya M H K, Kheyri Z, Azizi D, Roozafzai F and Khorrami S. 2018. The evaluation of diagnostic and predictive values of *Helicobacter pylori* stool antigen test in Iranian patients with dyspepsia. *Iran J Pathol.,* **13,** 38.

Wang W, Jiang W, Zhu S, Sun X, Li P, Liu K, Liu H, Gu J and Zhang S. 2019. Assessment of prevalence and risk factors of *Helicobacter pylori* infection in an oilfield Community in Hebei, China. *BMC Gastroenterol.,* **19,** 186.

Yuan X G, Xie C, Chen J, Xie Y, Zhang K H and Lu N H. 2015. Seasonal changes in gastric mucosal factors associated with peptic ulcer bleeding. *Exp Ther Med.,* **9,** 125-130.

JJBS

Volume 14, Number 1, March 2021
ISSN 1995-6673
Pages 191 - 197

Jordan Journal of Biological Sciences

Antibacterial and Anti virulence factors of Purified Dextran from *Lactobacillus gasseri* against *Pseudomonas aeruginosa*

Jehan Abdul Sattar Salman* and Ali Jumma Kareem

Department of Biology, College of Science, Mustansiriyah University, Baghdad-Iraq

Received: April 4, 2020; Revised: August 8, 2020; Accepted: August 12, 2020

Abstract

The objective of the current study is to purify and characterize dextran from *Lactobacillus gasseri* and to detect its anti-virulence factors against hemolysin, pyocyanin, and biofilm formation of clinical *Pseudomonas aeruginosa* isolated from wounds and burns. Purification and characterization of dextran were carried out by a Thin Layer Chromatography (TLC) and a Fourier Trans Infrared Spectroscopy (FTIR). Purified dextran obtained was white, granular, and easily soluble in water. TLC results showed that the purified dextran was composed of glucose only; while FTIR showed that dextran polysaccharide contained both (1-6) ∝- D glucan and (1-3) ∝- glucan. Antibacterial effect of purified dextran was determined against *P.aeruginosa* isolates using Minimum Inhibitory Concentration (MIC) with concentrations ranging between 0.39 to 200 mg/ml; the MIC was 50 mg/ ml for all isolates. On the other hand, the effect of dextran on the virulence factors of *P.aeruginosa* was evaluated. Dextran inhibited hemolysin production of *P.aeruginosa* and the highest inhibition recorded was 29.03%. Pyocyanin production by *P.aeruginosa* clinical isolates was inhibited by dextran and the concentration was recorded between 2.28-2.35 µg/ml compared with 3.31- 3.39 µg/ml for control. The effect of purified dextran on biofilm formation was studied at different incubation periods (24, 48 and 72 h), the highest biofilm inhibition was observed after 72 h was 71.42 %, while the lowest inhibition after 24 h was 37.66% compared to control, which recorded 0% in the absence of dextran. In conclusion, the purified and characterized dextran from local *L. gasseri* had an inhibitory effect on the growth and virulence factors of clinical *P. aeruginosa* isolated from wounds and burns.

Keywords: *Lactobacillus*, Dextran, Antibacterial, Antivirulence factors

1. Introduction

Dextran has a chemical formula of H- $(C_6H_{10}O_5)_n$-OH and is produced by the action of the microorganism's extracellular dextransucrase(Guzman *et al*.,2018). Dextran, such as that produced by *Leuconostoc* species and other dextran-producing lactic acid bacteria including *Streptococcus*, *Lactobacillus*, *Pediococcus* and *Weissella*, typically varied in their relative molecular mass, degree of branching, type of branching, and length of branched chains (Kothari *et al*., 2015). It is a hydrophilic, neutral, biodegradable and biocompatible polysaccharide (El-Meliegy *et al*., 2018). Dextran is used in food, chemical and pharmaceutical industries as emulsifier, stabilizer, adjuvant and carrier; also it is used in the field of drugs as blood plasma volume expander (Bhavani and Nisha, 2010) and as drug delivery with no toxic side effects (Huang and Huang, 2019).

Pseudomonas aeruginosa is a non-fermenting, motile, rod-shaped, Gram-negative bacterium belonging to the Pseudomonadaceae family (Alhazmi, 2015). It is responsible for acute infections commonly associated with burn wounds, colonization of host tissue. Host tissue damage facilitates adherence and colonization (Lovewell *et al*., 2014). This bacterial species has many virulence factors as a strategy for survival in the host (Feng *et al*., 2016). The nosocomial and toxicogenic *P. aeruginosa* is a highly adaptable opportunistic bacteria that prevalent in patients with immuno-compromised cystic fibrosis causing invasive infections (Kany *et al*., 2018); it is responsible of 10% of total infections in the hospitals (Fazeli *et al*., 2012). In burned patients *P. aeruginosa* is the causative agents of invasive infections, it is known as a resistant bacteria to a wide range of antimicrobial agents and the host immune system due to their ability in forming biofilms, causing difficulties in medical treatments (Alhazmi,2015). *P. aeruginosa* has been isolated from patient care equipment such as catheters, blood gas analyzers, breastfeeding bottles, from health care workers, and the environment such as sinks (Harnaen *et al*., 2015). The growth of *P. aeruginosa* could be strongly inhibited in the presence of dextran and the inhibition of growth reached 55.41% (Wang *et al*., 2010). A study by Wang *et al*. (2013) showed an inhibitory effect of dextran-coated by ceria nanoparticles (CeO_2) on the growth of *P.aeruginosa*; the dextran-coated may have promoted absorption of protein that inhibited bacterial growth. Therefore, this study aimed to examine the ability of dextran, purified from locally *L.gasseri* to inhibit growth and some virulence factors of *P.aeruginosa* isolated from burns and wounds.

* Corresponding author e-mail: Dr.Jehan Abdul Sattar Salman, jehanmmd.ja@gmail.com; Dr.jehan@uomustansiriyah.edu.iq.

2. Materials and Methods

2.1. Microorganisms

2.1.1. Lactobacillus gasseri

Lactobacillus gasseri was isolated from healthy women's vagina; vaginal swabs were placed in MRS medium, incubated anaerobically at 37 ^{o}C for (24-48) h. The isolate was identified using cultural, cellular, and biochemical tests as well as the Vitek 2 system.

2.1.2. Pseudomonas aeruginosa

A total of 20 clinical *Pseudomonas aeruginosa* were isolated from burns and wounds from Baghdad hospitals. All isolates were subjected to cultural, microscopic, and biochemical tests as well as to the Vitek 2 system. The virulence factors (hemolysin**,** pyocyanin**,** and biofilm formation) of all isolates were detected and 4 isolates that had the same virulence factors were chosen for further work (data not shown).

2.2. Dextran Production

This process was done according to the procedure described by Onilude *et al.* (2013) with minor modifications. Briefly, 100 ml of autoclaved dextran production medium (sucrose 150 g. peptone 5.0 g, K_2HPO_4 15.0 g, $MnCl_2.4H_2O$ 0.01 g, yeast extract 5.0 g, NaCl 0.01 g, $CaCl_2$ 0.05 g, added to 1 liter of distilled water, pH 7.0), was inoculated with 2% of the *L.gasseri* suspension (from MRS broth) at a concentration of 9 x 10^8 CFU/ml and incubated at 37 ˚C for 24 h.

2.3. Precipitation of Dextran

The total culture medium of dextran production was precipitated by using an equal volume of chilled ethanol, shaken, centrifuged for 15 min at 10,000 rpm and the supernatant was decanted. Precipitated dextran was dissolved in distilled water for the removal of impurities. The dextran slurry was again precipitated with an equal volume of chilled ethanol (Sarwat *et al*., 2008). This step was repeated two times. The precipitated dextran was dried in the oven (40C°) for 45 minutes.

2.4. Purification of Dextran Produced by L .gasseri

The precipitated dextran was dissolved in distilled water, then the suspension of dextran was precipitated with an equal volume of chilled ethanol. Re-dissolving, precipitation, and washing were repeated three times for cell debris elimination (Abedin *et al*., 2013). Purified dextran was dried using the oven (40C° for 45 min) then calculated on a dry weight basis.

2.5. Characterization of Dextran Purified from L. gasseri

2.5.1. Thin-Layer Chromatography (TLC)

The purified dextran from *L. gasseri* was analyzed and characterized by Thin-Layer Chromatography (TLC) to confirm its components. Dextran (0.01 gm.) was hydrolyzed in 5 % HCl (v/v) and heated for an hour in a water bath at 100ºC. Equal weights (0.01gm) of glucose, galactose, and fructose were dissolved in 1mL of 1% ethanol. TLC was performed using silica. The position and distance of the spots were determined, and the relative flow (Rf) was calculated according to the equation described by Radhi *et al*. (2013):

$$RF = \frac{\text{Distance moved by substance}}{\text{Distance moved by the solvent front}}$$

2.5.2. Fourier Transform Infrared Spectroscopy (FTIR)

Fourier transform infrared spectroscopy (FTIR) has been carried out in the Department of Chemistry / College of Science/ Mustansiriyah University / Baghdad, Iraq. The instrument operates in the wavelength range of 400 – 4000 cm^{-1} that measures the amount of IR radiation reflected or transmitted through a sample. The results were obtained in the form of a graphical chart, in which the X-axis represents the wavelength, while the Y-axis represents the transmittance %.

2.6. Antibacterial Activity of Purified Dextran against Pseudomonas aeruginosa Isolates

The antibacterial activity of dextran purified from *L. gasseri* against *P.aeruginosa* isolates was determined by the microdilution method in 96 – well flat-bottom microtiter plate based on minimum inhibitory concentration (MIC) values. The experiment was performed according to the procedures described by Salman *et al*. (2018). A stock solution of purified dextran in sterilized distilled water was diluted to a concentration ranging from 200 to 0.39 mg/ml. 125 µl of sterile Muller Hinton Broth was added in the first column of the 96 – well microplate, then 125 µl of dextran solution with a concentration of 200 mg/ml was added and mixed with the medium in the first column. Serially, 125 µl were transferred to subsequent wells and discarding 125 µl of the mixture in the last column, so that the final volume for each well was 125 µl. Control well contained 125 µl of Muller Hinton Broth only without dextran. The wells were inoculated with 2.5 µl of an overnight culture of *P.aeruginosa* isolates compared with the McFarland 0.5 ml. Microplates were covered and incubated at 37˚C for 24 h. The MIC was determined at a concentration in which no visible growth could be observed after subculturing on nutrient agar plates at 37C˚ for 24 h.

2.7. Effect of Dextran Purified from L. gasseri on P.aeruginosa Virulence Factors

2.7.1. Inhibition of Hemolysin Production

The inhibition of hemolysin production by dextran was detected using the procedure described by Lee *et al*. (2014), four *P.aeruginosa* isolates were grown in the absence and presence of dextran at sub MIC concentration, 20 µl of *P. aeruginosa* suspension compared to 0.5 McFarland was added to 80µl Nutrient broth mixed with 100 µl of dextran, while control contained only 180 µl of Nutrient broth and 20 µl of *P.aeruginosa* without dextran, incubated at 37˚C for 24 h.

Human red blood cells were prepared by centrifugation at 3000 rpm for 5 min and washed with PBS three times. The pellet diluted in PBS (330 µl red blood cells were added to 10 ml PBS).100 µl of bacterial (treated with dextran and control) was added to 10 ml red blood cells previously prepared and incubated at 37˚C for 1 hour. Centrifugation was applied at 12,000 rpm for 10 min to collect the supernatants, and then the optical densities were measured at 543 nm. Inhibition of hemolysin production percentage was calculated as the equation according to Lalitha *et al.* (2013) with some modification.

$$\% \text{ Inhibition of hemolysin production} = \frac{\text{O.D control} - \text{O.D treatment}}{\text{O.D control}} \times 100$$

2.7.2. Inhibition of Pyocyanin Production

The effect of purified dextran on pyocyanin production of *P.aeruginosa* isolates was evaluated using a pyocyanin quantitative assay described by Essar *et al*. (1990). The supernatant of *P.aeruginosa* grown in T-broth medium with dextran (sub MIC) at 37C° for 24 h was prepared by centrifugation at 1000rpm/10min. Control included supernatant of bacterial isolates grown in T-broth only without dextran. A volume of 7.5 ml of supernatant was extracted by 4.5 ml of chloroform, then vortexed for 10 sec (until the lower layer changed to blue color). Then two volumes of the blue layer were extracted by one volume of (0.2N) HCl and were mixed well for 10 sec to produced pink to deep red color. The absorbance of the acidic solution was measured at 520nm, using chloroform as blank. The concentrations expressed as micrograms of pyocyanin produced per milliliter of culture supernatant were calculated by the equation below,

O.D520 ×17.072= Conc. of Pyocyanin (µg/ml)

Inhibition of pyocyanin production percentage was calculated as the equation below,

$$\% \text{ Inhibition of pyocyanin production} = \frac{\text{Conc.of pyocyanin}\left(\frac{\mu g}{ml}\right)\text{control} - \text{Conc.of pyocyanin}\left(\frac{\mu g}{ml}\right)\text{treatment}}{\text{Conc.of pyocyanin}\left(\frac{\mu g}{ml}\right)\text{control}} \times 100$$

2.7.3 Inhibition of Biofilm Formation

The effect of dextran on the biofilm formation of *P.aeruginosa* was studied using 96 flat-bottom well microtiter plates according to the procedure described by Ali (2012). *P.aeruginosa* isolates were grown at 37 ºC for 24, 48, and 72 hours in the presence and absence of dextran at the sub MIC concentration. The inhibition percentage of the biofilm formation was calculated according to the equation described by Namasivayam *et al*. (2012).

$$\% \text{ Inhibition of biofilm formation} = \frac{\text{O.D control} - \text{O.D treatment}}{\text{O.D control}} \times 100$$

3. Results

3.1. Identification of Bacterial Isolates:

3.1.1. Lactobacillus gasseri

White to yellow, smooth, and round colonies of *L.gasseri* were observed on the surface of MRS *Lactobacillus* agar. Microscopical examination showed that the cells of *L.gasseri* were gram-positive, non–spore forming and short rods single or in pairs. Biochemical tests showed that *L.gasseri* isolate was catalase and oxidase negative. For Vitek 2 ANC ID card results, isolate showed positive results of D-Cellobiose, D-Glucose, D-Fructose, D-Galactose, D-Sucrose, Maltose, D-Mannose, Ala-Phe-Pro-arylamidase, L-pyrrolydonyl arylamidase, L-Proline arylamidase, Tyrosine arylamidase, Maltotriose, Leucine arylamidase, Phenylalanine arylamidase, N-acetyl –D-glucosamine, Arbutin and Esculin hydrolysis, while it gave negative results for remaining tests in the card.

3.1.2. Pseudomonas aeruginosa Isolates

Colonies of *P.aeruginosa* on MacConkey agar appeared as pale yellow, smooth round colonies, and gave grape-like odor, while on *pseudomonas* agar appeared green colony. Microscopically, *P. aeruginosa* isolates appeared as gram-negative very small straight rods that occurred as single or in pairs. All isolates gave positive results for catalase and oxidase tests. Identification of isolates by Vitek 2 GN ID card showed positive results of L-pyrrolydonyl arylamidase, Glutamyl arylamidase, D-Gamma glutamyl transferase, D-Glucose, D-Mannose,Beta-alanine arylamidase, Tyrosine arylamidase, Lipase, Citrate(sodium), Malonate, L-lactate alkalipisation, Succinate alkalipisation, Cormarate, O/129 Resistance (Comp.*Vibirio*), L-malate assimilation and L-lactate assimilation, while the isolates gave negative results for remaining tests in the card(L-Arabitol, D-Mannitol, D-Sorbitol, Saccharose/Sucrose, D-Trehalose, Urease, Phosphatase, Oriniythine Decarboxylase, and Lysine Decarboxylase).

3.2. Purification of dextran Produced by L .gasseri

Dextran was purified after production under optimum conditions (30 °C for 24 h. with 15% sucrose, 4% of inoculum size at pH 7.0 under aerobic conditions). The total dry weight of dextran produced from *L.gasseri* after purification was 1.12 g/L, which represents the yield of dextran. Purified dextran was characterized as whitish, granular, and highly soluble in water.

3.3. Characterization of Dextran Purified from L. gasseri

3.3.1. Thin-Layer Chromatography (TLC)

Purified dextran contents were analyzed by TLC to determine their components of monosaccharides to confirm that the purified polysaccharide is dextran. The Rf values of hydrolyzed dextran were identical or so close to the glucose. The Rf value of dextran was 0.33, while the Rf values of glucose, fructose, galactose were (0.33, 0.24, 0.53) respectively. This result indicated that purified dextran from *L.gasseri* was composed only of glucose which confirmed that purified polysaccharide was dextran (Figure 1).

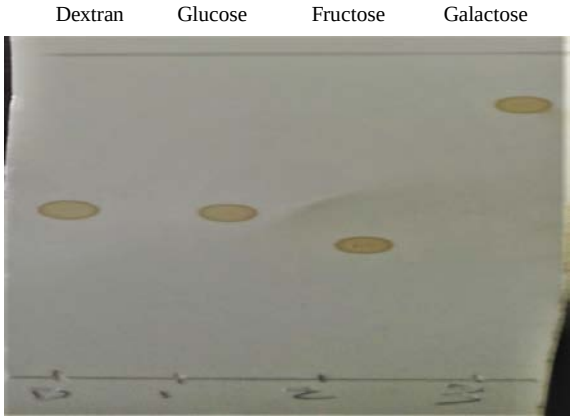

Figure 1. Thin – Layer Chromatography Analysis of Dextran Purified from *Lactobacillus gasseri*. Lane D: Dextran; Lane 1: Glucose; Lane 2: Fructose; Lane 3: Galactose

3.3.2. Fourier Transform Infrared Spectroscopy (FTIR)

FTIR- spectra analysis was applied to detect the functional groups of purified dextran from *L. gasseri* (Figures 2 and 3). The FTIR results of purified dextran showed that the bands in the region of 3275 and 3390.97 ^{cm} $^{-1}$ were due to the hydroxyl (O −H) stretching, while the band in region 2931.90 ^{cm} $^{-1}$ was due to (C −H) stretching vibration, the band region of 1633.78 and 1639.55 ^{cm} $^{-1}$ were due to bending vibration band of the (OH) group, while the band region found in the 1456.30 $^{cm-1}$ and 1375.29 $^{cm-1}$ were due to symmetrical stretching of carboxylic groups(confirming the polysaccharide nature of the compound), the band region of 1219.05^{cm} $^{-1}$ and 1043.52 ^{cm} $^{-1}$ were due to the (C −O) and (C −C) bonds, while the band region of 1028.09^{cm} $^{-1}$ was for ∝ (1,6) glycosidic acid bands (1-6)- ∝-D glucan, the band region 995 ^{cm} $^{-1}$ was the (1-3) ∝- glucan.

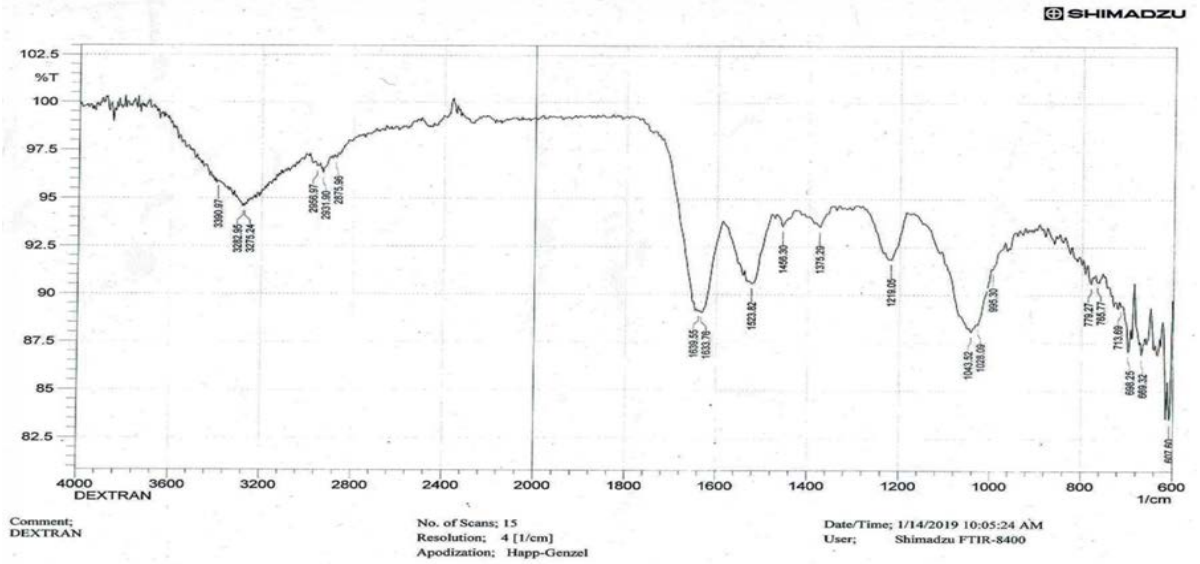

Figure 2. FTIR Spectra of Dextran Purified from *Lactobacillus gasseri*. T%: transmittance %; Wavelength range of 600 – 4000 cm^{-1}

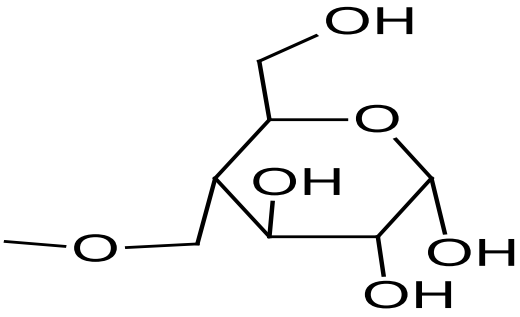

Figure 3. Suggested structure of purified dextran from *Lactobacillus gasseri* in the current study according to the functional groups of FTIR results

3.4. Antibacterial Activity of Purified Dextran against P.aeruginosa Isolates

The antibacterial activity of purified dextran from *L.gasseri* was examined against *P.aeruginosa* isolates by determination of the MIC of dextran at a concentration ranging from (200- 0.39) mg/ml. Results indicated that the MIC of dextran was 50 mg/ml against all twenty tested *P.aeruginosa* isolates compared to control, among them the four isolates included *P.aeruginosa*(Pb_2), *P.aeruginosa*(Pb_5), *P.aeruginosa*(Pw_{15}) and *P.aeruginosa*(Pw_{18}) that were chosen for subsequent experiences according to their virulence factors (Table 1).

Table 1. Minimum Inhibitory Concentration (MIC) of Dextran against *Pseudomonas aeruginosa* Isolates

Bacterial isolates	Dextran Concentration (mg/ml)										
	200	100	50	25	12.5	6.25	3.12	1.56	0.78	0.39	Control
P.aeruginosa(Pb_2)	-	-	- MIC	+	+	+	+	+	+	+	+
P.aeruginosa(Pb_5)	-	-	- MIC	+	+	+	+	+	+	+	+
P.aeruginosa(Pw_{15})	-	-	- MIC	+	+	+	+	+	+	+	+
P.aeruginosa(Pw_{18})	-	-	- MIC	+	+	+	+	+	+	+	+

"-" no growth of bacteria; "+" growth of bacteria; "Control" Muller Hinton broth only; "Pb" isolated from burns; "Pw" isolated from wounds; " MIC " Minimum Inhibitory Concentration

3.5. Effect of purified Dextran on virulence factors of P.aeruginosa isolates

3.5.1. Inhibition of Hemolysin Production

Purified dextran from *L.gasseri* had an inhibitory effect on hemolysin production of all *P.aeruginosa* isolated from both burns and wounds. Hemolysin production decreased in all *P.aeruginosa* isolates with no significant differences between isolates. The optical density of hemoglobin released from lysed erythrocyte ranged between 0.65 and 0.67 for treatment with dextran compared to 0.88 and 0.93 of control. Dextran inhibited hemolysin production with the inhibition of 27.17 % and 23.86 % for *P.aeruginosa* isolated from burns, and 26.96 %, and 29.03 % for *P.aeruginosa* isolated from wounds (Table 2). No

significant differences between *P. aeruginosa* isolates were observed.

Table 2. Inhibition of Hemolysin Production for *Pseudomonas aeruginosa* by Purified Dextran from *Lactobacillus gasseri*

Bacterial Isolates	O.D(543nm) of Hemoglobin		Hemolysin Inhibition %
	Control (without dextran)	Treatment (with dextran)	
Pseudomonas aeruginosa (Pb_2)	0.92	0.67	27.17
Pseudomonas aeruginosa (Pb_5)	0.88	0.67	23.86
Pseudomonas aeruginosa (Pw_{15})	0.89	0.65	26.96
Pseudomonas aeruginosa (Pw_{18})	0.93	0.66	29.03

Pb: isolated from burns; Pw: isolated from wounds; O.D: Optical density

3.5.2. Inhibition of Pyocyanin Production

In this study, purified dextran from *L. gasseri* showed an inhibitory effect on pyocyanin production against all tested *P.aeruginosa* isolates. The concentration of pyocyanin produced from *P.aeruginosa* isolates decreased after treatment of bacterial isolates with purified dextran (sub MIC) compared with control. The inhibition percentage recorded was 30.47% and 31.56% for *P.aeruginosa* isolated from burns, while 29.90 % and 31.32% for *P.aeruginosa* isolated from wounds (Table 3). No significant differences between *P. aeruginosa* isolates were observed.

Table 3. Inhibition of Pyocyanin Production for *Pseudomonas aeruginosa* by Purified Dextran from *Lactobacillus gasseri*

Bacterial Isolates	Pyocyanin Concentration(μg/ml)		Pyocyanin Inhibition %
	Control (without dextran)	Treatment (with dextran)	
Pseudomonas aeruginosa (Pb2)	3.38	2.35	30.47
Pseudomonas aeruginosa (Pb_5)	3.39	2.32	31.56
Pseudomonas aeruginosa (Pw_{15})	3.31	2.32	29.90
Pseudomonas aeruginosa (Pw_{18})	3.32	2.28	31.32

Pb: isolated from burns; Pw: isolated from wounds

3.5.3. Inhibition of Biofilm Formation

The biofilm formation of clinical *P.aeruginosa* isolated from burns and wounds were investigated by using the microtiter plate technique. This assay involved quantitation of the biofilm biomass attached to the walls of the microtiter plate. Purified dextran from *L. gasseri* had an inhibitory effect on biofilm formation of all *P.aeruginosa* isolates isolated from wounds and burns. Biofilm formation decreased in all *P.aeruginosa* isolates at different incubation periods (24, 48, 72) h compared to the control. The highest inhibition percentage for biofilm formation (71.42)% was recorded at 72 h for *P.aeruginosa* (Pw_{18}) isolated from wounds, while the lowest inhibition percentage (37.66)% was recorded at 24 h for *P.aeruginosa* (Pb_5) isolated from burns (Table 4).

Table 4. Inhibition Percentage of Biofilm Formation by Purified Dextran from *Lactobacillus gasseri* at Different Incubation Periods.

Bacterial Isolates	Inhibition of Biofilm (%)		
	Incubation Periods		
	24 h	48 h	72 h
Pseudomonas aeruginosa (Pb_2)	43.37	57.14	67.64
Pseudomonas aeruginosa (Pb_5)	37.66	48.83	58.94
Pseudomonas aeruginosa (Pw_{15})	44.87	59.34	64.94
Pseudomonas aeruginosa (Pw_{18})	47.61	60.00	71.42

Pb: isolated from burns; Pw: isolated from wounds

4. Discussion

Dextran is a homo-polysaccharide cationic polymer synthesized by dextransucrase enzyme; it consists of several α-glucans linked by α-(1-6) glycosidic bonds with branched linkages such as α-(1-3) linked as a single unit or lengthen side chain (Du *et al*., 2017). In this report, dextran was purified from local probiotic bacterium *L.gasseri* and characterized to detect the functional groups and the component of purified dextran. Indeed, we observed that *L.gasseri* produced dextran composed only of glucose from sucrose medium, which indicated that Lactobacillus isolate had dextransucrase. In FTIR spectra analysis we detected that dextran produced by *L.gasseri* contained both α (1, 6) and α (1-3) linkages indicating the glucan nature of purified dextran. The Rf value for dextran produced by *L. acidophilus* was identical to that of glucose which indicated that dextran was composed solely of glucose (Abedin *et al*., 2013). Salman and Salim (2016) reported that the dextran from *L.mesenteroides* ssp. *mesenteroides* was made of glucose and contained both α (1-6) and α (1 -3) linkages.

In the present study, dextran purified from *L.gasseri* showed antibacterial and anti-virulence factors such as biofilm, pyocyanin, and hemolysin of clinical *P.aeruginosa* isolated from burns and wounds; and we suggest that dextran may suppress the production of quorum sensing mediated virulence factors. The findings of the study suggested that dextran can be combined with antibiotics, and used as an effective skin sanitizer in both medical ointments and drugs used to treat burns and skin injuries. The inhibitory activity of the polysaccharide polymer may be due to the linking of the polysaccharide in the bacterial outer membrane (Aziz et al., 2012). Also, polysaccharide caused leakage of protein, DNA binding, and cytoplasmic membrane permeability (He *et al*., 2010). The modification of fluidity can increase membrane permeability (Wu et al., 2016). Protein leakage causes impairment of metabolic enzymes then leads to bacterial cell death (Shu *et al.*, 2019). The destruction of cell membrane permeability caused metabolic dysfunction, inhibited energy synthesis, and induction cell death (Zou *et al*., 2015). The other suggestion of the inhibitory effect of several polysaccharides is the trapping of cationic minerals or nutrients which can reduce the bioavailability of nutrients (Jun *et al.*, 2018).

The antibiofilm mode of action of polysaccharide hypotheses was reported. The most antibiofilm polysaccharides from probiotic bacteria act as surfactant molecules that modify the physical properties of bacterial cells. Also, polysaccharides may act as signaling molecules that modulate the gene expression of bacteria (Kim *et al*., 2009). *Lactobacillus* polysaccharide act as a signal that caused the down-regulation of several genes related to biofilm formation (Rendueles *et al*., 2013). The polysaccharides might block lectin dependent adhesion of *P. aeruginosa* or sugar-binding proteins present on the bacterial surface, or block tip adhesins of fimbriae and pili (Zinger-Yosovich and Gilboa-Garber, 2009). The competitive inhibition of multivalent carbohydrate-protein interactions is another possible mode of action of antibiofilm polysaccharide (Wittschier *et al*., 2007).

In the present study, dextran purified from *L.gasseri* showed an antibiofilm effect against *P. aeruginosa* isolates. Salman and Khudair (2019) showed that the purified polymer (homopolysaccharide) produced by *L. mesenteroides* had an inhibitory effect against several virulence factors of *Candida albicans*. Further, Li *et al*. (2014) showed that the exopolysaccharide purified from *L. helveticus* had inhibition activity against biofilm formation by pathogenic bacteria *S. aureus, P. aeruginosa,* and *E. coli*. The exopolysaccharide purified from *L. plantarum* exhibited strong inhibition against biofilm formation by pathogenic bacteria, including *P. aeruginosa*, *E. coli*, *S. typhimurium, and S.aureus* (Liu *et al*., 2017).

5. Conclusion

In conclusion, the purified and characterized dextran from local *Lactobacillus gasseri* had an inhibitory effect on the growth and some virulence factors of *P.aeruginosa* isolated from wounds and burns.

Acknowledgments

The authors would like to thank Mustansiriyah University in Iraq (www.uom ustansiriyah.edu.iq) for their support in the current work.

References

Abedin R M, El-Borai A M, Shall M A and El-Assar S A .2013. Optimization and statistical evaluation of medium components affecting dextran and dextransucrase production by *Lactobacillus acidophilus* ST76480.01. *Life Sci J*., **10**(**1**):1346-1353.

Alhazmi A .2015. *Pseudomonas aeruginosa* pathogenesis and pathogenic mechanisms. *Int J Biol*., **7**(**2**):44-67.

Ali OA. 2012. Prevention of *Proteus mirabilis* biofilm surfactant solution. *Egypt. Acad. J. Biol. Sci*., **4**(**1**):1-8.

Aziz MA, Cabral J A, Brooks H J L, Moratti S C and Hantona L R. 2012. Antimicrobial properties of a chitosan dextran-based hydrogel for surgical use. *Antimicrob Agents Ch*., **56** (**1**): 280 – 287.

Bhavani A L and Nisha J.2010.Dextran polysaccharide with versatile uses. *Int J Pharma.Bio.Sci*.,**1**(**4**):569-573.

Du R, Xing H, Yang Y, Jiang H, Zhou Z and Han Y. 2017. Optimization, purification and structural characterization of a dextran produced by *L. mesenteroides* isolated from Chinese sauerkraut. *J.Carpol*., **174**: 409-416.

El-Meliegy, Abu-Elsaad E N I, El-Kady A M and Ibrahim M A.2018. Improvement of physico-chemical properties of dextran-chitosan composite scafolds by addition of nano-hydroxyapatite. *Sci. Rep*., **8**(**12180**): 1-10.

Essar DW, Eberly L, Hadero A and Crawford I P. 1990. Identification and characterization of genes for a second anthranilate synthase in *Pseudomonas aeruginosa*: interchangeability of the two anthranilate synthases and evolutionary implications. *J. Bacteriol*., **172**(**2**): 884-900.

Fazeli H, Akbari R, Moghim S, Narimani T, Arabestani MR, Ghoddousi AR.2012. *Pseudomonas aeruginosa* infections in patients, hospital means, and personnel's specimens. *J Res Med Sci*., **17**(**4**):332-3372.

Feng L, Xiang Q, Ai Q, Wang Z, Zhang Y and Lu Q. 2016. Effects of quorum sensing systems on regulatory T cells in catheterrelated *Pseudomonas aeruginosa* biofilm infection rat models. *J. Mediators Inflamm.*, **2016**:4012912.

Guzman G Y F, Hurtado G B and Ospina S A. 2018. New dextransucrase purification process of the enzyme produced by *Leuconostoc mesenteroides* IBUN 91.2. 98 based on binding product and dextranase hydrolysis. *J. Biotech*., **265**: 8-14.

Harnaen E, Doctor T N and Malhotra A. 2015. Characteristics of *Pseudomonas aeruginosa* infection in a tertiary neonatal unit. *Int. J. Pediatr. Res.*, **1**:2-4.

Huang S and Huang G. 2019. Preparation and drug delivery of dextran-drug complex. *Drug Deliv*., **26**(**1**): 252-261.

He F, Yang Y, Yang G and Yu L. 2010. Studies on antibacterial activity and antibacterial mechanism of a novel polysaccharide from *Streptomyces virginia* H03. *Food Control*., **21**(**9**):1257-1262.

Jun JY, Jung MJ, Jeong IH, Yamazaki K, Kawai Y and Kim BM.2018. Antimicrobial and Antibiofilm Activities of Sulfated Polysaccharides from Marine Algae against Dental Plaque Bacteria. *Mar. Drugs*., **16(301):**1-13.

Kany A M, Sikandar A , Haupenthal J , Yahiaoui S , Maurer C K, Proschak E and Hartmann R W. 2018. Binding Mode Characterization and Early in Vivo Evaluation of Fragment-Like Thiols as Inhibitors of the Virulence Factor LasB from *Pseudomonas aeruginosa*. *ACS Infect. Dis*., **4**(**6**): 988-997.

Kim Y, Oh S, Kim SH .2009. Released exopolysaccharide (r-EPS) produced from probiotic bacteria reduce biofilm formation of enterohemorrhagic *Escherichia coli* O157:H7. *Biochem Biophys Res Commun*., **379**:324–329.

Kothari D, Das D, Patel S and Goyal A. 2015. Dextran and food application. In: Ramawat K., Mérillon JM. (eds). **Polysaccharides**. Springer, Cham. pp.735-752.

Lalitha A, Subbaiya R and Ponmurugan P. 2013. Green synthesis of silver nanoparticles from leaf extract Azhadirachta indica and to study its anti-bacterial and antioxidant property. *Int J Curr Microbiol App Sci*., **2**(**6**): 228-235.

Lee J H, Kim Y G, Cho M H and Lee J. 2014. ZnO nanoparticles inhibit *Pseudomonas aeruginosa* biofilm formation and virulence factor production. *Microbiol Res*., **169**(**12**): 888-896.

Li W, Ji J, Rui X , Yu J, Tang W, Chen X and Dong M. 2014. Production of exopolysaccharides by *Lactobacillus helveticus* MB2-1 and its functional characteristics in vitro. *LWT-Food Sci Technol*., **59**(**2**): 732-739.

Liu Z , Zhang Z , Qiu L, Zhang F, Xu X, Wei H and Tao X. 2017. Characterization and bioactivities of the exopolysaccharide from a probiotic strain of *Lactobacillus plantarum* WLPL04. *J Dairy Sci*., **100**(**9**): 6895-6905.

Lovewell R R, Patankar Y R and Berwin B. 2014. Mechanisms of phagocytosis and host clearance of *Pseudomonas aeruginosa*. *Am J Physiol Lung Cell Mol Physiol*., **306**(**7**):L591-L603.

Namasivayam S K R , Preethi M , Bharani A R S , Robin G and Latha B. 2012. Biofilm inhibitory effect of silver nanoparticles coated catheter against Staphylococcus aureus and evaluation of its synergistic effects with antibiotics. *Int J Biol Pharm Res*., **3**(**2**):259 -265.

Onilude A A, Olaoye O, Fadahunsi I F, Owoseni A Garuba E O and Atoyebi T. 2013. Effect of cultural conditions on dextran production by Leuconostoc spp. *Int Food Res J*., **20**(**4**):1645 - 1651.

Radhi SN, Hasan S S and Alden SB. 2013. Production of levan from Paenibacillus polymyxa in Date Syrup and analyzing of levan composition by TLC. Proceeding of the first Scientific Conference the Collage of Sciences. Kerbala University. Kerbala, Iraq.

Rendueles O, Kaplan JB, and Ghigo JM.2013. Antibiofilm polysaccharides. *Environ Microbiol*.,**15**(**2**): 334–346.

Salman J A S, Ajah, H A, and Khudair AY. 2019. Analysis and Characterization of Purified Levan from *Leuconostoc mesenteroides* ssp. *cremoris* and its Effects on *Candida albicans* Virulence Factors. *J J B S*., **12**(**2**): 243 - 249.

Salman J A S and Salim M Z. 2016.Production and characterization of dextran from *Leuconostoc mesenteroides* ssp. *mesenteroides* isolated from Iraqi fish intestine. *European J. Biomed. Pharm. Sci***., 3**(**8**): 62-69.

Salman J A S, Kadhim A A and Haider A J. 2018. Biosynthesis, characterization and antibacterial effect of ZnO nanoparticles synthesized by Lactobacillus sp. *J Global Pharma Technol*., **10**(**03**):348-355.

Sarwat F, Qader S A U, Aman A and Ahmed N .2008.Production and characterization of a unique dextran from an indigenous *Leuconostoc mesenteroides* CMG713. *Int. J.Biol.Sci*., **4**(**6**): 379 - 386.

Shu H , Chen H, Wang X, Hu Y , Yun Y , Zhong Q, Chen W and Chen W.2019. Antimicrobial Activity and Proposed Action Mechanism of 3-Carene against *Brochothrix thermosphacta* and *Pseudomonas fluorescens. Molecules.*, **24**(**3246**):1-18.

Wang H K, Dong C, Chen Y F, Cui L M, and Zhang H P. 2010. A new probiotic cheddar cheese with high ACE-inhibitory activity and γ-aminobutyric acid content produced with koumiss-derived Lactobacillus casei. *Food Technol Biotech*., **48**(**1**): 62-70.

Wang Q, Perez J M and Webster T J. 2013.Inhibited growth of *pseudomonas aeruginosa* by dextran –and polyacrylic acid – coated ceria nanoparticles. *Int J Nanomed*., **8**:3395.

Wittschier N, Lengsfeld C, Vorthems S, Stratmann U, Ernst JF, Verspohl EJ and Hensel A. 2007. Large molecules as anti-adhesive compounds against pathogens. *J Pharm Pharmacol*., **59**:777–786.

Wu Y , Bai J , Zhong K, Huang Y, Qi H , Jiang Y and Gao H.2016.Antibacterial Activity and Membrane-Disruptive Mechanism of 3-p-trans-Coumaroyl-2-hydroxyquinic Acid, a Novel Phenolic Compound from Pine Needles of *Cedrus deodara*, against *Staphylococcus aureus*. *Molecules.*,**21(1084**):1-12.

Zinger-Yosovich KD and Gilboa-Garber N. 2009.Blocking of *Pseudomonas aeruginosa* and *Ralstonia solanacearum* lectins by plant and microbial branched polysaccharides used as food additives. *J Agric Food Chem*., **57**:6908–6913.

Zou L, Hu YY, Chen and W X. 2015.Antibacterial mechanism and activities of black pepper chloroform extract. *J. Food Sci. Technol.*, **52**:8196–8203.

Subscription

Jordan Journal of Biological Sciences

An International Peer – Reviewed Research Journal

Published by the Deanship of Scientific Research, The Hashemite University, Zarqa, Jordan

Name: ..... الاسم:

Specialty: ..... التخصص:

Address: ..... العنوان:

P.O. Box: ..... صندوق البريد:

City &Postal Code:..... المدينة: الرمز البريدي:

Country: ..... الدولة:

Phone: ..... رقم الهاتف

Fax No.: ..... رقم الفاكس:

E-mail: ..... البريد الإلكتروني:

Method of payment: ..... طريقة الدفع:

Amount Enclosed: ..... المبلغ المرفق:

Signature: ..... التوقيع:

Cheque should be paid to Deanship of Research and Graduate Studies – The Hashemite University.

I would like to subscribe to the Journal

For

- ☐ One year
- ☐ Two years
- ☐ Three years

One Year Subscription Rates

	Inside Jordan	Outside Jordan
Individuals	JD10	$70
Students	JD5	$35
Institutions	JD 20	$90

Correspondence

Subscriptions and sales:

The Hashemite University
P.O. Box 330127-Zarqa 13115 – Jordan
Telephone: 00 962 5 3903333
Fax no. : 0096253903349
E. mail: jjbs@hu.edu.jo

المجلة الأردنية للعلوم الحياتية
Jordan Journal of Biological Sciences (JJBS)

http://jjbs.hu.edu.jo

المجلة الأردنية للعلوم الحياتية: مجلة علمية عالمية محكمة ومفهرسة ومصنفة، تصدرعن الجامعة الهاشمية وبدعم من صندوق دعم البحث العلمي والإبتكار – وزراة التعليم العالي والبحث العلمي.

ترسل البحوث الى العنوان التالي:

رئيس تحرير المجلة الأردنية للعلوم الحياتية
الجامعة الهاشمية
ص.ب , 330127 , الزرقاء, 13115 , الأردن
هاتف: 0096253903333
E-mail: jjbs@hu.edu.jo, Website: www.jjbs.hu.edu.jo

المملكة الأردنية الهاشمية

المجلة الأردنية

للعلوم الحياتية

مجلة علمية عالمية محكمة

تصدر بدعم من صندوق دعم البحث العلمي و الابتكار

http://jjbs.hu.edu.jo/